

Investigations on 1,2-oxaphosphetane complexes

Dissertation

zur

Erlangung des Doktorgrades (Dr. rer. nat.)

der

Mathematisch-Naturwissenschaftlichen Fakultät

der

Rheinischen Friedrich-Wilhelms-Universität Bonn

vorgelegt von

Andreas Wolfgang Kyri

aus

Bonn

Bonn, 2017

Angefertigt mit Genehmigung der Mathematisch-Naturwissenschaftlichen Fakultät
der Rheinischen Friedrich-Wilhelms-Universität Bonn

1. Gutachter: Prof. Dr. R. Streubel

2. Gutachter: Prof. Dr. R. Glaum

Tag der Promotion: 16.10.2017

Erscheinungsjahr: 2017

Der Unterschied zwischen Genie und Wahnsinn definiert sich lediglich aus dem Erfolg.

James Bond 007 – Der Morgen stirbt nie

Teilergebnisse aus dieser Arbeit wurden mit Genehmigung der Mathematisch-Naturwissenschaftlichen Fakultät der Universität Bonn vorab veröffentlicht.

- (1) "Synthesis of Li/OR phosphinidenoid complexes: on the evidence for intramolecular O-Li donation and the effect of cation encapsulation" R. Streubel, A. W. Kyri, L. Duan, G. Schnakenburg, *Dalton Trans.* **2014**, 43, 2088 - 2097.
 - (2) "Synthesis and Reaction of the First 1,2-Oxaphosphetane Complexes" A. W. Kyri, V. Nesterov, G. Schnakenburg, R. Streubel *Angew. Chem. Int. Ed.* **2014**, 53, 10809 - 10812.
 - (3) "C-Trifluoromethyl-Substituted 1,2-Oxaphosphetane Complexes: Synthetic and Structural Study" A. W. Kyri, G. Schnakenburg, R. Streubel, *Organometallics* **2016**, 35, 563 - 568.
 - (4) "A novel route to C-unsubstituted 1,2-oxaphosphetane and 1,2-oxaphospholane complexes" A. W. Kyri, G. Schnakenburg, R. Streubel, *Chem. Commun.* **2016**, 52, 8593 - 8595.
 - (5) "Synthesis of a monomolecular anionic FLP complex" A. W. Kyri, R. Kunzmann, G. Schnakenburg, Z.-W. Qu, S. Grimme, R. Streubel, *Chem Commun.* **2016**, 52, 13361 - 13364.
 - (6) "Synthesis and Deprotonation of Aminophosphane Complexes: First K/N(H)R Phosphinidenoid Complexes and Access to a Complex with a P₂N-Ring Ligand" P. Kumar Majhi, A. W. Kyri, A. Schmer, G. Schnakenburg, R. Streubel, *Chem. Eur. J.* **2016**, 22, 15413 - 15419.
 - (7) "Ring opening of a sterically crowded 1,2-oxaphosphetane complex" A. W. Kyri, P. Brehm, G. Schnakenburg, R. Streubel, *Dalton Trans.* **2017**, 46, 2904 - 2909.
 - (8) "1,1'-Bifunctional Aminophosphane Complexes via N-H Bond Insertion of a Li/Cl Phosphinidenoid Complex and First Studies on N/P Mono Functionalizations" R. Streubel, A. Schmer, A. W. Kyri, G. Schnakenburg, *Organometallics* **2017**, 36, 1488 - 1495.
-

Tagungsbeiträge:

- (1) A. Kyri, T. Heurich, R. Streubel, 10th European Workshop on Phosphorus Chemistry, Regensburg/Germany, March 18th - 20th, **2013**: “*Searching for phosphanyl and phosphoxyl complexes*” (poster contribution).
 - (2) A. Kyri, R. Streubel, MHC-6 PhD Workshop, Bonn/Germany, April 5th – 7th, **2013**: “*Synthesis and reactions of new Li/OR phosphinidenoid complexes*” (oral contribution).
 - (3) T. Heurich, A. Kyri, R. Streubel, Z.-W. Qu, S. Grimme, S. Saeidpour, O. Schiemann SFB 813 Workshop, Trier/Germany, September 25th – 27th, **2013**: “*Targeting Phosphoxyl and Phosphanyl Complexes*” (poster contribution).
 - (4) A. Kyri, R. Streubel, 15. Anniversary of the Tokitoh workgroup, Kyoto/Japan, June 7th, **2014**: “*First synthesis and reactions of 1,2-oxaphosphetane complexes* ” (poster contribution) and “*Synthetic chemistry using Li/Cl phosphinidenoid complexes*“ (poster contribution).
 - (5) A. Kyri, R. Streubel, 9th International Conference on Inorganic Chemistry (AGICHEM) Edinburgh/ Scotland, July 30th – August 1st, **2014**: “*First synthesis and reactions of 1,2-oxaphosphetane complexes* ” (poster contribution).
 - (6) A. Kyri, R. Streubel, MHC-7 PhD Workshop, Freiberg/Germany, September 19th - 21st, **2014**: “*Synthesis and reactions of the first 1,2-oxaphosphetane complexes* ” (oral contribution).
 - (7) A. W. Kyri, R. Streubel, 12th European Workshop on Phosphorus Chemistry, Kassel/Germany, March 16th – 18th, **2015**: “*Insertion reactions of phosphinidenoid complexes*” (oral contribution).
 - (8) A. W. Kyri, R. Streubel, 10th Organoelement Chemistry Seminar, Kyoto University, Kyoto, Japan, June 8th, **2015**: “*Synthesis of 1,2-Oxaphosphetane Complexes and Reactions with Brønsted acids*” (poster contribution).
 - (9) V. Nesterov, A. Kyri, T. Heurich, T. Wasano, T. Agou, T. Sasamori, N. Tokitoh, R. Streubel, 11th International Conference on Heteroatom Chemistry, Caen, France, June 14th – 19th, **2015** “*Attempted synthesis of silyl substituted phosphasilenes*” (poster contribution).
 - (10) A. W. Kyri, R. Streubel, 50th Meeting of Young Chemists, Hiroshima/Japan, July 29th - 31st, **2015**: “*Synthesis and reactions of 1,2-oxaphosphetane complexes – New building blocks*” (poster contribution).
 - (11) R. Kunzmann, A. W. Kyri, R. Streubel, 13th European Workshop on Phosphorus Chemistry, March 7th - 9th, **2016**: Berlin, Germany, “*Synthesis of polyfunctional phosphane complexes having a P-O-E bonding motif*” (poster Contribution).
-

-
- (12) A. Kyri, R. Streubel, 13th European Workshop on Phosphorus Chemistry, March 7th - 9th, **2016**: Berlin-Germany, "*1,2-Oxaphosphetane complexes: first reactivity studies*" (poster Contribution).
- (13) A. Kyri, R. Streubel, MHC-8 PhD Workshop, Kassel/Germany, March 11th - 13st, **2016**: "*Synthesis and first reactions of 1,2-oxaphosphetane complexes*" (oral contribution).
- (14) P. K. Mahji, T. Sasamori, A. Kyri, T. Agou, Y. Mizuhata, J.-D. Guo, S. Nagase, V. Nesterov, R. Streubel, N. Tokitoh 96th Annual Meeting of the Chemical Society of Japan, Kyoto, Japan, March 24th – 27th **2016**: "*Synthesis of 2-Chlorophosphasilene coordinated by an N-Heterocyclic Carbene*" (poster contribution).
- (15) R. Kunzmann, A. W. Kyri, R. Streubel, 21st International Conference on Phosphorus Chemistry, June 5th - 10th, **2016**: Kazan, Russia, "*Polyfunctional phosphane complexes containing P-O-E motifs as potential precursors for novel strained three-membered P-ligands*" (poster contribution).
- (16) A. W. Kyri, R. Streubel, 21st International Conference on Phosphorus Chemistry, June 5th-10th, **2016**: Kazan, Russia, "*1,2-Oxaphosphetane complexes: syntheses and reactions*" (oral contribution).
- (17) A. Kyri, P. Brehm, R. Streubel, 3rd European Conference on Smart Inorganic Polymers, Porto, Portugal, September 12th - 14th, **2016**: "*1,2-Oxaphosphetane complexes: novel precursors for P-containing polymers?*" (poster contribution).
-

Die vorliegende Arbeit wurde im Zeitraum von November 2012 bis Mai 2017 im Arbeitskreis von Prof. Dr. R. Streubel am Institut für Anorganische Chemie der Rheinischen Friedrich Wilhelms-Universität in Bonn angefertigt.

Hiermit versichere ich, dass ich diese Arbeit selbst verfasst und keine anderen als die angegebenen Quellen und Hilfsmittel verwendet habe.

Bonn, den 11. Mai 2017

Danksagung:

An dieser Stelle möchte ich mich bei all jenen bedanken die mich während der letzten Jahre in meinem Werdegang begleitet und mir zur Seite gestanden haben.

Vor allem **Prof. Dr. Rainer Streubel** danke ich, nicht nur für die Möglichkeit diese Arbeit in seiner Forschungsgruppe durchzuführen, sondern auch für die vielen fruchtbaren Gespräche, die Möglichkeiten der aktiven Teilnahme an viele Konferenzen und das Ermöglichen zweier Auslandsaufenthalte.

Prof. Dr. Robert Glaum danke ich für die Übernahme der Aufgabe des Zweitgutachters. Zudem danke ich sowohl **Prof. Dr. Dirk Menche** als fachnahem als auch **Prof. Dr. Diana Imhof** als fachfremdem Mitglied der Prüfungskommission.

Prof. Dr. Norihiro Tokitoh und **Prof. Dr. Takahiro Sasamori** von der Universität Kyoto (Japan) danke ich für die Aufnahme in die Forschungsgruppe während meiner zwei Forschungsaufenthalte dort in den Jahren 2014 und 2015. Hierbei möchte ich auch allen aktuellen und ehemaligen Mitarbeitern der Forschungsgruppe Tokitoh für die herzliche Aufnahme und deren große Hilfe danken. Vor allem **Dr. Tomohiro Agou** bedarf hier einer extra Nennung für die viele Hilfe im Labor und für die vielen Orte in Japan die ich durch ihn gesehen habe.

Bedanken will ich mich bei den Mitarbeitern der Analytikabteilung der Universität Bonn ohne deren Hilfe diese Arbeit nicht möglich gewesen wäre. Hierbei will ich vor allem **Dr. Gregor Schnakenburg** und **Charlotte Rödde** für das Vermessen und Lösen der zahlreichen Einkristallstrukturen namentlich erwähnen. **Frau Karin Prochnicki** danke ich für die Aufnahme der zahlreichen NMR-Spektren und der Durchführung der NMR-Sondermessungen, sowie Frau **Dr. Senada Nozinovic** für die fruchtbaren Diskussionen. Ebenso danke ich Frau Hannelore Spitz und Frau Ulrike Weynand für die Aufnahme von NMR Spektren. Für die Aufnahme von MS Spektren danke ich Frau Christine Sondag, Frau Karin Peters-Pflaumbaum, Frau Nora Schocher und **Frau Dr. Marianne Engeser**. Frau Anna Martens danke ich für die Durchführung der Elementaranalysen sowie Frau Kerstin Kühnel-Lysek für die Vorbereitung der empfindlichen Proben.

Des Weiteren möchte ich mich ganz herzlich bei **Dr. Melina Klein** bedanken, für die anregenden Diskussionen, die gute Atmosphäre in Labor 1.013 und die morgendlichen Kaffeerunden, ebenso **Jan Faßbender** für dies alles. Dann **Dr. Maren Bode** und **Dr. Carolin Albrecht** für die gute Atmosphäre im Labor und all diesen für die Diskussionen und das was ich von ihnen gelernt habe.

Für Betreuung und sehr gute Hinweise zum Arbeiten im Labor danke ich **Dr. Vitaly Nesterov**. Und **Abhishek Koner** vor allem für abendliche Diskussionen.

Für Unterstützung im Labor danke ich noch all denen die mit mir und unter meiner Leitung im Labor den Anfang ihrer beruflichen Laufbahn gestartet haben:

Mein Dank geht daher an die Studenten die ich während ihrer Abschlussarbeiten im Rahmen des Masterstudiums oder Diplomstudiums (**Niklas Künemund, Robert Kunzmann, Alexander Schmer, Philip Junker**) sowie Bachelorstudiums (**Philipp Brehm, Florian Gleim**) mitbetreuen durfte. Ich habe ihnen hoffentlich nicht nur einiges beibringen können sondern auch immer selber von ihnen gelernt.

Als Auszubildenden, den ich in der letzten Phase seiner Ausbildung betreuen durfte, danke ich **Christof Grimmeling** für seine Unterstützung bei den alltäglichen Aufgaben im Labor und vor allem der Hilfe bei der Synthese etlicher Ausgangsverbindungen für die Gruppe.

Zudem danke ich Johanna Salz für ihr Vertrauen in mich als Betreuer für ihr Schülerpraktikum.

Und zuletzt danke ich meiner Familie: meinen Eltern, meinen beiden Schwestern und meinem Zwillingbruder. Ihnen allen habe ich in den schweren Zeiten der letzten Jahre viel zu verdanken und ohne sie würde ich heute nicht da stehen wo ich nun bin.

Table of contents

Table of contents	1
Numbering and abbreviations.....	7
1 General introduction - from phosphorus to phosphinidenoid complexes	10
1.1 Phosphorus, the precious element.....	10
1.2 Development of novel building blocks: From carbenes to phosphinidenoid complexes	12
2 Objective of the thesis	20
3 Insertion reactions into N-H bonds	21
3.1 Introduction to aminophosphane complexes.....	21
3.2 Insertion reactions using R ₂ NH	26
3.3 Insertion reactions using RNH ₂	31
4 Insertion reactions into strained heterocycles	37
4.1 Introduction.....	37
4.2 Insertion reactions of Li/Cl phosphinidenoid complexes into cyclopropanone.....	41
5 Synthesis of 1,2-oxaphosphetane complexes by insertion into epoxides	44
5.1 Introduction to small-sized O,P-heterocycles	44
5.2 Synthesis of <i>P</i> -bis(trimethylsilyl)methyl-substituted 1,2-oxaphosphetane derivatives	50
5.2.1 The reactions with monosubstituted epoxides	50
5.2.2 Discussion of the origins of isomerisms	64
5.3 Synthesis of <i>P</i> -C ₅ Me ₅ and <i>P</i> -CPh ₃ -substituted 1,2-oxaphosphetane complexes	71
5.3.1 <i>P</i> -C ₅ Me ₅ -substituted derivatives	71
5.3.2 <i>P</i> -CPh ₃ -substituted derivatives.....	74
5.3.3 Attempts to synthesize bis-1,2-oxaphosphetane complexes	78
5.4 Some conclusions on 1,2-oxaphosphetane complexes	81
5.5 Proposed mechanism for the 1,2-oxaphosphetane complex formation.....	85
6 A novel route to C-unsubstituted O,P-containing heterocycles.....	89
7 Reactions of Li/Cl phosphinidenoid complexes with aziridines and thiiranes	102
8 Reactions of 1,2-oxaphosphetane complexes	107
8.1 Introduction – general reactivity of epoxides, oxetanes and tetrahydrofuranes.....	107
8.2 Ring opening reactions with HCl or HBF ₄ ·OEt ₂	108
8.3 Hydrolysis and decomposition reaction using triflic acid and water	118
8.4 Ring expansion reactions using the system triflic acid/triethylamine in the presence of nitriles.....	120
8.5 Ring opening reactions with catechol(chloro)borane	124
8.6 Lewis acid induced ring opening reactions.....	126
8.7 Fluoride mediated hydrolytic ring opening reaction.....	132
9 Summary	137
10 Experimental section	146
10.1 General part.....	146
10.2 Analytical Methods	147

10.2.1 Melting point determination	147
10.2.2 NMR spectroscopy	147
10.2.3 Mass spectrometry	148
10.2.4 IR spectroscopy	148
10.2.5 Elemental analysis.....	148
10.2.6 Single crystal X-ray diffraction studies	148
10.2.7 Used chemicals	149
10.2.8 Waste disposal	151
11 Syntheses and analytical data.....	152
11.2.1 Preparation of Li/Cl phosphinidenoid complexes 2.1-2.3 at low temperature.....	152
11.2.2 Syntheses of aminophosphane complexes.....	153
11.2.2.1 Pentacarbonyl[diethylamino(triphenylmethyl)phosphane- κP]tungsten(0) [6.3a].....	153
11.2.2.2 Pentacarbonyl[cyclohexylamino(triphenylmethyl)phosphane- κP]tungsten(0) [9.3a]	154
11.2.2.3 Pentacarbonyl[1-methylethylamino(triphenylmethyl)phosphane- κP]tungsten(0) [9.3b]	155
11.2.2.4 Pentacarbonyl[1,1-dimethylethylamino(triphenylmethyl)phosphane- κP]tungsten(0) [9.3c]	156
11.2.3 Attempted reactions of Li/Cl phosphinidenoid complex 2.3 with diisopropylamine and dicyclohexylamine.....	157
11.2.4 Synthesis of lithium(1,4,7,10-tetraoxacyclododecane) pentacarbonyl[diethylamino(triphenylmethyl)phosphanido- κP]tungsten(0) [7.3]	158
11.2.5 Synthesis of pentacarbonyl[chloro(triphenylmethyl)phosphane- κP]tungsten(0) [10.3]....	158
11.2.6 Synthesis of pentacarbonyl[1-(1,2,3,4,5-pentamethylcyclopenta-2,4-dien-1-yl)-3,4-diphenyl-1 <i>H</i> -phosphet-2-on- κP]tungsten(0) [14.2]	159
11.2.7 Synthesis of pentacarbonyl{2-[bis(trimethylsilyl)methyl]-3-phenyl-1,2-oxaphosphetane- κP }tungsten(0) [16.1]	161
11.2.8 Syntheses of 4-substituted 1,2-oxaphosphetane complexes:.....	163
11.2.8.1 Pentacarbonyl{4-methyl-2-[bis(trimethylsilyl)methyl]-1,2-oxaphosphetane- κP }tungsten(0) [21.1a _w].....	164
11.2.8.2 Synthesis of pentacarbonyl{4-methyl-2-[bis(trimethylsilyl)methyl]-1,2-oxaphosphetane- κP }tungsten(0) [21.1a _w] using R(+)-propylene oxide	166
11.2.8.3 Pentacarbonyl{4-methyl-2-[bis(trimethylsilyl)methyl]-1,2-oxaphosphetane- κP }molybdenum(0) [21.1a _{Mo}].....	166
11.2.8.4 Pentacarbonyl{4-methyl-2-[bis(trimethylsilyl)methyl]-1,2-oxaphosphetane- κP }chromium(0) [21.1a _{Cr}]	168
11.2.8.5 Pentacarbonyl{4-ethyl-2-[bis(trimethylsilyl)methyl]-1,2-oxaphosphetane- κP }tungsten(0) [21.1b].....	170
11.2.8.6 Pentacarbonyl{4-(1-methylethyl)-2-[bis(trimethylsilyl)methyl]-1,2-oxaphosphetane- κP }tungsten(0) [21.1c]	172
11.2.8.7 Attempted synthesis of pentacarbonyl{4-(1,1-dimethylethyl)-2-[bis(trimethylsilyl)methyl]-1,2-oxaphosphetane- κP }tungsten(0) [21.1d].....	174
11.2.8.8 Pentacarbonyl{4-(chloromethyl)-2-[bis(trimethylsilyl)methyl]-1,2-oxaphosphetane- κP }tungsten(0) [21.1e].....	174
11.2.8.9 Pentacarbonyl{4-epoxy-2-[bis(trimethylsilyl)methyl]-1,2-oxaphosphetane- κP }tungsten(0) [21.1f].....	176

11.2.8.10 Pentacarbonyl{4-(trifluoromethyl)-2-[bis(trimethylsilyl)methyl]-1,2-oxaphosphetane- κP }tungsten(0) [21.1g]	178
11.2.8.11 Pentacarbonyl{4,4-dimethyl-2-[bis(trimethylsilyl)methyl]-1,2-oxaphosphetane- κP }tungsten(0) [25.1a]	179
11.2.8.12 Pentacarbonyl{[(2-methyl-2-propenyl)oxy][bis(trimethylsilyl)methyl]phosphane- κP }tungsten(0) [4.1d]	181
11.2.8.13 Pentacarbonyl{4,4-bis(trifluoromethyl)-2-[bis(trimethylsilyl)methyl]-1,2-oxaphosphetane- κP }tungsten(0) [25.1b]	182
11.2.8.14 Pentacarbonyl{4-methyl-2-(1,2,3,4,5-pentamethylcyclopenta-2,4-dien-1-yl)-1,2-oxaphosphetane- κP }tungsten(0) [21.2a]	184
11.2.8.15 Pentacarbonyl{4-chloromethyl-2-(1,2,3,4,5-pentamethylcyclopenta-2,4-dien-1-yl)-1,2-oxaphosphetane- κP }tungsten(0) [21.2e]	184
11.2.8.16 Pentacarbonyl{4-(trifluoromethyl)-2-(1,2,3,4,5-pentamethylcyclopenta-2,4-dien-1-yl)-1,2-oxaphosphetane- κP }tungsten(0) [21.2g]	185
11.2.8.17 Pentacarbonyl{4,4-bis(trifluoromethyl)-2-(1,2,3,4,5-pentamethylcyclopenta-2,4-dien-1-yl)-1,2-oxaphosphetane- κP }tungsten(0) [25.2b]	186
11.2.8.18 Pentacarbonyl{4-methyl-2-(triphenylmethyl)-1,2-oxaphosphetane- κP }tungsten(0) [21.3a]	187
11.2.8.19 Attempted synthesis of pentacarbonyl{4-(1,1-dimethylethyl)-2-(triphenylmethyl)-1,2-oxaphosphetane- κP }tungsten(0) [21.3d]	189
11.2.8.20 Pentacarbonyl{4-(trifluoromethyl)-2-(triphenylmethyl)-1,2-oxaphosphetane- κP }tungsten(0) [21.3g]	189
11.2.8.21 Pentacarbonyl{4,4-bis(trifluoromethyl)-2-(triphenylmethyl)-1,2-oxaphosphetane- κP }tungsten(0) [25.3b]	191
11.2.9 Attempted reactions of Li/Cl phosphinidenoid complex 2.1 with 1,3-butadiene diepoxide and 1,5-hexadiene diepoxide	192
11.2.10 Synthesis of 1,4-bis[(pentacarbonyl{2-[bis(trimethylsilyl)methyl]-1,2-oxaphosphetane-4-yl}- κP }tungsten(0)]butane [29.1c]	192
11.2.11 Synthesis of pentacarbonyl{(2-iodoethoxy)[bis(trimethylsilyl)methyl]phosphane- κP }tungsten(0) [33.1 _w]	194
11.2.12 Synthesis of pentacarbonyl{2-[bis(trimethylsilyl)methyl]-1,2-oxaphosphetane- κP }tungsten(0) [34.1 _w]	195
11.2.13 Synthesis of pentacarbonyl{2-[bis(trimethylsilyl)methyl]-1,2-oxaphosphetane- κP }molybdenum(0) [34.1 _{Mo}]	196
11.2.14 Synthesis of pentacarbonyl{2-[bis(trimethylsilyl)methyl]-1,2-oxaphosphetane- κP }chromium(0) [34.1 _{Cr}]	198
11.2.15 Synthesis of pentacarbonyl{2-(1,2,3,4,5-pentamethylcyclopenta-2,4-dien-1-yl)-1,2-oxaphosphetane- κP }tungsten(0) [34.2]	199
11.2.16 Attempted synthesis of pentacarbonyl{2-(triphenylmethyl)-1,2-oxaphosphetane- κP }tungsten(0) [34.3]	200
11.2.17 Synthesis of lithium(1,4,7,10-tetraoxacyclododecane) pentacarbonyl{[bis(trimethylsilyl)methyl]phosphanoxido- κP }tungsten(0) [36.1]	201
11.2.18 Synthesis of {(4-bromopropoxy)[bis(trimethylsilyl)methyl]phosphane- κP }pentacarbonyltungsten(0) [39.1]	201
11.2.19 Synthesis of pentacarbonyl{2-[bis(trimethylsilyl)methyl]-1,2-oxaphospholane- κP }tungsten(0) [19.1]	203

11.2.20 Synthesis of pentacarbonyl{catecholboranoxo[bis(trimethylsilyl)methyl]phosphane- κP }tungsten(0) [41.1]	204
11.2.21 Attempted reactions of Li/Cl phosphinidenoid complexes 2.1 and 2.3 with aziridines 42a or 42b	205
11.2.22 Attempted synthesis of pentacarbonyl{4-methyl-2-[bis(trimethylsilyl)methyl]-1,2-thiaphosphetane- κP }tungsten(0) [46.1]	205
11.2.23 Synthesis of pentacarbonyl[4-methyl-2-(triphenylmethyl)-1,2-thiaphosphetane- κP]tungsten(0) [46.3]	206
11.2.24 Acid induced ring opening reactions of 1,2-oxaphosphetane complexes	207
11.2.24.1 Pentacarbonyl{chloro(2-hydroxyethyl)[bis(trimethylsilyl)methyl]phosphane- κP }tungsten(0) [47.1a]	208
11.2.24.2 Pentacarbonyl{chloro(2-hydroxypropyl)[bis(trimethylsilyl)methyl]phosphane- κP }tungsten(0) [47.1b]	209
11.2.24.3 Pentacarbonyl{chloro(3,3,3-trifluoro-2-hydroxypropyl)[bis(trimethylsilyl)methyl]phosphane- κP }tungsten(0) [47.1c]	210
11.2.24.4 Pentacarbonyl{fluoro(3,3,3-trifluoro-2-hydroxypropyl)[bis(trimethylsilyl)methyl]phosphane- κP }tungsten(0) [48.1a]	212
11.2.24.5 Pentacarbonyl{[3,3,3-trifluoro-2-(trifluoromethyl)-2-hydroxypropyl][bis(trimethylsilyl)methyl]phosphane- κP }tungsten(0) [48.1b]	214
11.2.24.6 Pentacarbonyl{fluoro[3,3,3-trifluoro-2-(trifluoromethyl)-2-hydroxypropyl](1,2,3,4,5-pentamethylcyclopenta-2,4-dien-1-yl)phosphane- κP }tungsten(0) [48.2b]	215
11.2.25 Synthesis of 1,2-oxaphosphetane complex (21.1a _w) from pentacarbonyl{chloro(2-hydroxypropyl)[bis(trimethylsilyl)methyl]phosphane- κP }tungsten(0) (47.1b)	216
11.2.26 Synthesis of [3,3,3-trifluoro-2-(trifluoromethyl)-2-hydroxypropyl][bis(trimethylsilyl)methyl]phosphane-oxide [52]	216
11.2.27 Synthesis of pentacarbonyl{6-methyl-4-[bis(trimethylsilyl)methyl]-2-phenyl-1-oxa-3-aza-5,6-dihydrophosphinine- κP }tungsten(0) [54.1]	218
11.2.28 Optimized synthetic protocol for the acid induced ring expansion with nitriles:	219
11.2.28.1 Pentacarbonyl{2-methyl-4-[bis(trimethylsilyl)methyl]-1-oxa-3-aza-5,6-dihydrophosphinine- κP }tungsten(0) [55.1a]	220
11.2.28.2 Pentacarbonyl{4-[bis(trimethylsilyl)methyl]-2-phenyl-1-oxa-3-aza-5,6-dihydrophosphinine- κP }tungsten(0) [55.1b]	221
11.2.28.3 Pentacarbonyl{2-(1,1-dimethylethyl)-4-[bis(trimethylsilyl)methyl]-1-oxa-3-aza-5,6-dihydrophosphinine- κP }tungsten(0) [55.1c]	222
11.2.29 Synthesis of pentacarbonyl{[2-(catecholboranoxo)ethyl]chloro[bis(trimethylsilyl)methyl]phosphane- κP }tungsten(0) [56.1]	223
11.2.30 Synthesis of lithium(1,4,7,10-tetraoxacyclododecane) pentacarbonyl{[3,3,3-trifluoro-2-hydroxypropyl](triphenylmethyl)phosphanoxido- κP }tungsten(0) [57.3a]	224
11.2.31 Synthesis of lithium(1,4,7,10-tetraoxacyclododecane) pentacarbonyl{[3,3,3-trifluoro-2-(trifluoromethyl)-2-hydroxypropyl](triphenylmethyl)phosphanoxido- κP }tungsten(0) [57.3b]	226
11.2.32 Synthesis of pentacarbonyl[6,6-bis(trifluoromethyl)-2,2-dimethyl-4-triphenylmethyl-1,3,4,2-dioxaphosphasilinan- κP]tungsten(0) [60.3a]	227
11.2.33 Synthesis of pentacarbonyl[6,6-bis(trifluoromethyl)-2,2-dimethyl-4-triphenylmethyl-1,3,4,2-dioxaphosphagerminan- κP]tungsten(0) [60.3b]	228
11.2.34 Synthesis of tetrabutylammonium pentacarbonyl[(2-hydroxyethyl)methylphosphanoxido- κP]tungsten(0) [61]	230

11.2.35 Synthesis of pentacarbonyl(2,2-dimethyl-4-methyl-1,3,4,2-dioxaphosphasilinan- κP)tungsten(0) [66].....	231
Literature.....	232
12 X-ray crystallographic data.....	237
12.1 Pentacarbonyl[diethylamino(triphenylmethyl)phosphane- κP]tungsten(0) [6.3a].....	237
12.2 Pentacarbonyl[cyclohexylamino(triphenylmethyl)phosphane- κP]tungsten(0) [9.3a]	242
12.3 Pentacarbonyl[1-methylethylamino(triphenylmethyl)phosphane- κP]tungsten(0) [9.3b]	245
12.4 Pentacarbonyl[1,1-dimethylethylamino(triphenylmethyl)phosphane- κP]tungsten(0) [9.3c]....	249
12.5 Pentacarbonyl[chloro(triphenylmethyl)phosphane- κP]tungsten(0) [10.3]	252
12.6 Pentacarbonyl[1-(1,2,3,4,5-pentamethylcyclopenta-2,4-dien-1-yl)-3,4-diphenyl-1 <i>H</i> -phosphet-2-on- κP]tungsten(0) [14.2].....	255
12.7 Pentacarbonyl{2-[bis(trimethylsilyl)methyl]-3-phenyl-1,2-oxaphosphetane- κP }tungsten(0) [16.1]	258
12.8 Pentacarbonyl{4-methyl-2-[bis(trimethylsilyl)methyl]-1,2-oxaphosphetane- κP }tungsten(0) [21.1a _W].....	261
12.9 Pentacarbonyl{4-methyl-2-[bis(trimethylsilyl)methyl]-1,2-oxaphosphetane- κP }molybdenum(0) [21.1a _{Mo}].....	264
12.10 Pentacarbonyl{4-methyl-2-[bis(trimethylsilyl)methyl]-1,2-oxaphosphetane- κP }chromium(0) [21.1a _{Cr}]	267
12.11 Pentacarbonyl{4-ethyl-2-[bis(trimethylsilyl)methyl]-1,2-oxaphosphetane- κP }tungsten(0) [21.1b].....	269
12.12 Pentacarbonyl{4-(1-methylethyl)-2-[bis(trimethylsilyl)methyl]-1,2-oxaphosphetane- κP }tungsten(0) [21.1c]	272
12.13 Pentacarbonyl{4-(chloromethyl)-2-[bis(trimethylsilyl)methyl]-1,2-oxaphosphetane- κP }tungsten(0) [21.1e]	274
12.14 Pentacarbonyl{4-epoxy-2-[bis(trimethylsilyl)methyl]-1,2-oxaphosphetane- κP }tungsten(0) [21.1f].....	277
12.15 Pentacarbonyl{4-(trifluoromethyl)-2-[bis(trimethylsilyl)methyl]-1,2-oxaphosphetane- κP }tungsten(0) [21.1g].....	280
12.16 Pentacarbonyl{4,4-dimethyl-2-[bis(trimethylsilyl)methyl]-1,2-oxaphosphetane- κP }tungsten(0) [25.1a].....	283
12.17 Pentacarbonyl{[(2-methyl-2-propenyl)oxy]-[bis(trimethylsilyl)methyl]phosphane- κP }tungsten(0) [4.1d].....	285
12.18 Pentacarbonyl{4,4-bis(trifluoromethyl)-2-[bis(trimethylsilyl)methyl]-1,2-oxaphosphetane- κP }tungsten(0) [25.1b]	287
12.19 Pentacarbonyl[4-(trifluoromethyl)-2-(1,2,3,4,5-pentamethylcyclopenta-2,4-dien-1-yl)-1,2-oxaphosphetane- κP]tungsten(0) [21.2g]	294
12.20 Pentacarbonyl[4,4-bis(trifluoromethyl)-2-(1,2,3,4,5-pentamethylcyclopenta-2,4-dien-1-yl)-1,2-oxaphosphetane- κP]tungsten(0) [25.2b]	296
12.21 Pentacarbonyl[4-methyl-2-(triphenylmethyl)-1,2-oxaphosphetane- κP]tungsten(0) [21.3a] ..	300
12.22 Pentacarbonyl[4-(trifluoromethyl)-2-(triphenylmethyl)-1,2-oxaphosphetane- κP]tungsten(0) [21.3g].....	303
12.23 Pentacarbonyl[4,4-bis(trifluoromethyl)-2-(triphenylmethyl)-1,2-oxaphosphetane- κP]tungsten(0) [25.3b]	306

12.24 1,4-Bis[(pentacarbonyl{2-[bis(trimethylsilyl)methyl]-1,2-oxaphosphetane-4-yl}- κP)tungsten(0)]butane [29.1c]	311
12.25 Pentacarbonyl{(2-iodoethoxy)[bis(trimethylsilyl)methyl]phosphane- κP }tungsten(0) [33.1 _w]	315
12.26 Pentacarbonyl{2-[bis(trimethylsilyl)methyl]-1,2-oxaphosphetane- κP }tungsten(0) [34.1 _w]	317
12.27 Pentacarbonyl{2-[bis(trimethylsilyl)methyl]-1,2-oxaphosphetane- κP }molybdenum(0) [34.1 _{Mo}]	319
12.28 Pentacarbonyl{2-[bis(trimethylsilyl)methyl]-1,2-oxaphosphetane- κP }chromium(0) [34.1 _{Cr}]..	321
12.29 Pentacarbonyl{2-[bis(trimethylsilyl)methyl]-1,2-oxaphospholane- κP }tungsten(0) [19.1]	324
12.30 Pentacarbonyl{catecholboranoxo[bis(trimethylsilyl)methyl]phosphane- κP }tungsten(0) [41.1]	326
12.31 Pentacarbonyl[4-methyl-2-(triphenylmethyl)-1,2-thiaphosphetane- κP]tungsten(0) [46.3]	329
12.32 Pentacarbonyl{chloro(2-hydroxyethyl)[bis(trimethylsilyl)methyl]phosphane- κP }tungsten(0) [47.1a]	335
12.33 Pentacarbonyl{chloro(2-hydroxypropyl)[bis(trimethylsilyl)methyl]phosphane- κP }tungsten(0) [47.1b]	340
12.34 Pentacarbonyl{chloro(3,3,3-trifluoro-2-hydroxypropyl)[bis(trimethylsilyl)methyl]phosphane- κP }tungsten(0) [47.1c]	344
12.35 Pentacarbonyl{fluoro(3,3,3-trifluoro-2-hydroxypropyl) [bis(trimethylsilyl)methyl]phosphane- κP }tungsten(0) [48.1a]	346
12.36 Pentacarbonyl{[3,3,3-trifluoro-2-(trifluoromethyl)-2-hydroxypropyl][bis(trimethylsilyl)methyl]phosphane- κP }tungsten(0) [48.1b]	349
12.37 Pentacarbonyl{fluoro[3,3,3-trifluoro-2-(trifluoromethyl)-2-hydroxypropyl](1,2,3,4,5-pentamethylcyclopenta-2,4-dien-1-yl)phosphane- κP }tungsten(0) [48.2b]	351
12.38 Pentacarbonyl{6-methyl-4-[bis(trimethylsilyl)methyl]-2-phenyl-1-oxa-3-aza-5,6-dihydrophosphinine- κP }tungsten(0) [54.1]	356
12.39 Pentacarbonyl{2-methyl-4-[bis(trimethylsilyl)methyl]-1-oxa-3-aza-5,6-dihydrophosphinine- κP }tungsten(0) [55.1a]	359
12.40 Pentacarbonyl{4-[bis(trimethylsilyl)methyl]-2-phenyl-1-oxa-3-aza-5,6-dihydrophosphinine- κP }tungsten(0) [55.1b]	361
12.41 Pentacarbonyl{2-(1,1-dimethylethyl)-4-[bis(trimethylsilyl)methyl]-1-oxa-3-aza-5,6-dihydrophosphinine- κP }tungsten(0) [55.1c]	364
12.42 Lithium(1,4,7,10-tetraoxacyclododecane) pentacarbonyl{[3,3,3-trifluoro-2-hydroxypropyl](triphenylmethyl)phosphanoxido- κP }tungsten(0) [57.3a]	367
12.43 Lithium(1,4,7,10-tetraoxacyclododecane) pentacarbonyl{[3,3,3-trifluoro-2-(trifluoromethyl)-2-hydroxypropyl](triphenylmethyl)phosphanoxido- κP }tungsten(0) [57.3b]	373
12.44 Pentacarbonyl[6,6-bis(trifluoromethyl)-2,2-dimethyl-4-triphenylmethyl-1,3,4,2-dioxaphosphasilinan- κP]tungsten(0) [60.3a]	379
12.45 Pentacarbonyl[6,6-bis(trifluoromethyl)-2,2-dimethyl-4-triphenylmethyl-1,3,4,2-dioxaphosphagerminan- κP]tungsten(0) [60.3b]	383
12.46 Tetrabutylammonium pentacarbonyl[(2-hydroxyethyl)methylphosphanoxido- κP]tungsten(0) [61]	386

Numbering and abbreviations

Due to the huge amount of derivatives, especially in case of the metal complexes, a specific numbering scheme was developed for clarity.



The numbering consists of the following parts:

- X a consecutive number describing the type of compound
- Y a number describing the substituents at phosphorus:
 - 1 for $\text{CH}(\text{SiMe}_3)_2$ (bis(trimethylsilyl)methyl)
 - 2 for C_5Me_5 (1,2,3,4,5-pentamethylcyclopenta-2,4-dien-1-yl)
 - 3 for CPh_3 (triphenylmethyl)
- a alphabetic character for further organic substituents at the complex (for each case a closer description is given in the corresponding schemes)
- M element symbol of the metal in the pentacarbonyl substituent (not given if only the tungsten complex was prepared)
 - W for tungsten
 - Mo for molybdenum
 - Cr for chromium
- n denotes the presence of isomers for the compound and is given as number for each one, starting from the one with the strongest deshielded signal in the ^{31}P NMR spectrum (not given if only one isomer was observed)

Å	Ångström ($1 \cdot 10^{-10}$ m)	T	temperature
°	angle in degree	^t Bu	<i>tert</i> -butyl
Ar	aromatic substituent	t/tert	tertiary
ATR	Attenual Total Reflexion	ESI	electrospray ionization
au	Atomic unit	Et ₂ O	diethyl ether
br	broad signal	Et	ethyl
calc.	calculated	eV	electron volt
°C	degree Celsius	FWHM	full width at half maximum
cat	catechol	g	gram
C ₆ D ₆	deuerated benzene	h	height or hour
CDCl ₃	deuterated chloroform	HMBC	Heteronuclear Multiple Bond Correlation
cm	centimeter	HMDS	hexamethyldisilazide
C ₅ Me ₅	1,2,3,4,5-pentamethyl-cyclopenta-2,4-dien-1-yl	HMPT	hexamethylphosphoramide
CSD	Cambridge Structural Database	HMQC	Heteronuclear Multiple Quantum Correlation
Cy	cyclohexyl (C ₆ H ₁₁)	Hz	Hertz
Cp	cyclopenta-2,4-dien-1-yl	ⁱ Pr	iso-propyl
12-crown-4	1,4,7,10-tetraoxacyclododecane	IR	infrared
d	days	ⁿ J _{X,Y}	coupling constant (between the elements X,Y over n bonds) in Hz
δ	chemical shift in ppm	K	Kelvin
Δ	thermal reaction	L	ligand
∅	diameter	m	medium
Δδ	chemical shift difference	m	multiplett
DBU	1,8-diazabicyclo[5.4.0]undec-7-ene	M	metal or molar weight in g/mol
dec.	decomposition	<i>m</i> -CPBA	meta-chloroperoxybenzoic acid
DEPT	Distortionless Enhancement by Polarization	Me	methyl (CH ₃)
EA	elemental analysis	mg	milligram

EI	electron impact ionization	min	minutes
eq.	equivalent	mL	millilitre
ML _n	transition metal fragment bearing n ligands	THF	tetrahydrofuran
mmol	millimol	TfOH	trifluoromethanesulfonic acid
MS	mass spectrometry	THF-d ₈	deuterated tetrahydrofuran
m/z	mass to charge ratio	TMEDA	Tetramethylethylenediamine
<i>n</i>	normal	toluene-d ₈	deuterated toluene
ⁿ Bu	<i>n</i> -butyl	$\tilde{\nu}$	wave number
nm	nanometre	vs	very strong
NMR	nuclear magnetic resonance	VT-NMR	Variable Temperature NMR
%	percent	w	weak
PE	petroleum ether	X	halogen or leaving group
Ph	phenyl (C ₆ H ₅)		
ppm	parts per million		
q	quartet		
quin	quintet		
R, R', R''	organic substituent		
r.t.	room temperature		
s	singlet		
sat	satellites		
solv	solvent		
t	triplett or time		

1 General introduction - from phosphorus to phosphinidenoid complexes

1.1 Phosphorus, the precious element

Regarding the recent developments around the world, *i.e.* a higher living standard, and with this the higher consumption of resources, it is necessary for chemistry to concentrate on novel synthetic strategies. These novel strategies should help to preserve the priceless resources of our planet for future generations.

One of the most precious elements, which is often one of the first referred to in discussions about our resources, is phosphorus.^[1] The biggest suppliers today are China, Africa and the USA, but their stocks are not endless. There is indeed a lot of phosphorus dissolved in the surface water on earth, either deriving from soil erosion or from sewage but this can, to date, not be mined efficiently.^[2]

The high value of phosphorus for humanity is hereby not only based on its limited resources but also on the scope of its high-end applications, *e.g.* in ligands for enantioselective catalysis^[3] or in flame retardant materials,^[4,5] besides its basic use as fertilizer.^[6]

Phosphorus,^[7] as 15th element of the periodic system, is one of the essential elements for all life on earth and found in the living nature in form of phosphorus esters or phosphates. As ATP and ADP it forms parts of the DNA and is essential for the energy cycle of cells. Additionally it can be found as hydroxyl- or fluoroapatite ($\text{Ca}_5\text{X}(\text{PO}_4)_3$, X = OH, F) in the bones and teeth of mammals.

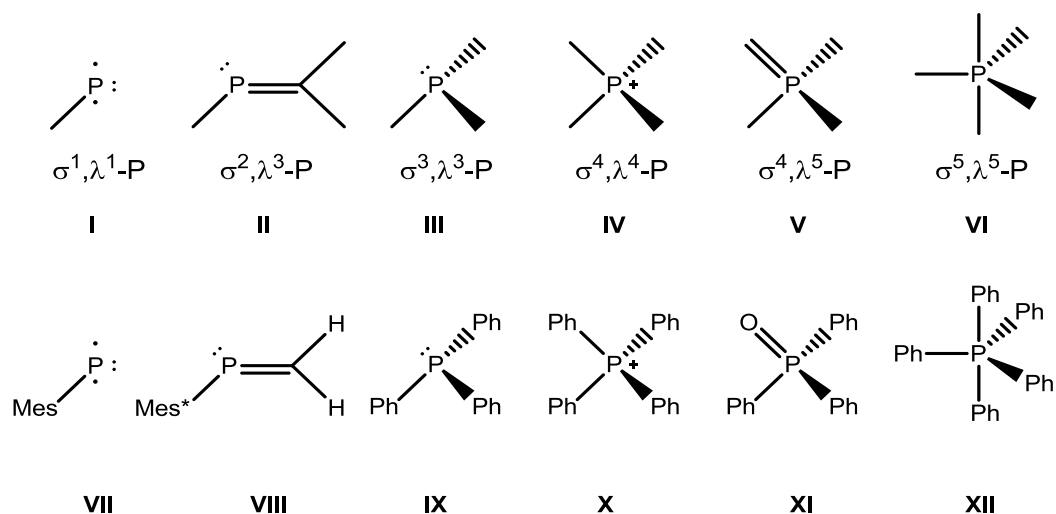
For phosphorus, all oxidation states between -III (*e.g.* in PH_3) and +V (*e.g.* in H_3PO_4 , phosphorus acid) are known. P^{V} compounds play a substantial role in nature, but the “true” synthetic potential of phosphorus is based on compounds bearing a free electron pair at the phosphorus centre. These, mainly P^{III} , compounds, *e.g.* Ph_3P , can be used widely, for example as ligands in organic catalysis or as starting materials for the Wittig reaction.

Due to its high reactivity, especially towards oxygen, all phosphorus compounds found in nature are in oxidation state +V. Usually phosphorus is obtained in form of apatites, less common is the mining of other phosphates (*e.g.* iron- or aluminium phosphate). After reduction of phosphates with carbon, the phosphorus is obtained as P_4 molecules (formed by condensation of P_2 molecule containing gas). P_4 , the so called white phosphorus, is the most reactive allotrope and, despite being starting point of all phosphorus chemistry, only one of

several allotropic modifications. If white phosphorus is heated under exclusion of oxygen it yields red phosphorus with a polymeric structure. The transformation can be catalysed by iodine. Other allotropic forms are for example violet phosphorus (Hittorf's phosphorus, obtained from red phosphorus by prolonged heating above 550 °C, composed of polymeric phosphorus chains) and black phosphorus (obtained by heating white phosphorus under high pressures (about 1.2 giga pascals)), which contains layers of corrugated P₆-rings, connected in a manner similar to graphene.

Most phosphorus is subsequently oxidized with air to produce phosphorus pentoxide and from this hydrolysed to give phosphoric acid. Some part of the synthesized phosphorus is first oxidized by Chlorine to PCl₃, the most common starting point for phosphorus organic chemistry.

Several descriptors were developed due to the variety of different bonding situations that phosphorus can adopt. While the σ^n -descriptor gives the number of σ bonds and with this the coordination number of the phosphorus atom, the λ^n -descriptor gives (implicitly) information about the number of all bonds (σ and π).^[8] Metal fragments coordinated by the free electron pair of a phosphorus atom are not taken into account with these descriptors.



Scheme 1.1: Important bonding motifs of phosphorus in different chemical environments (I-VI) and some examples (VII-XII).^[8]

The κ -descriptor specifies the atom of a ligand that is coordinating to the metal centre as illustrated in XIII (figure 1.1).^[9]

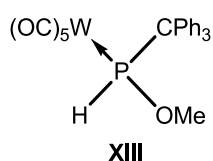
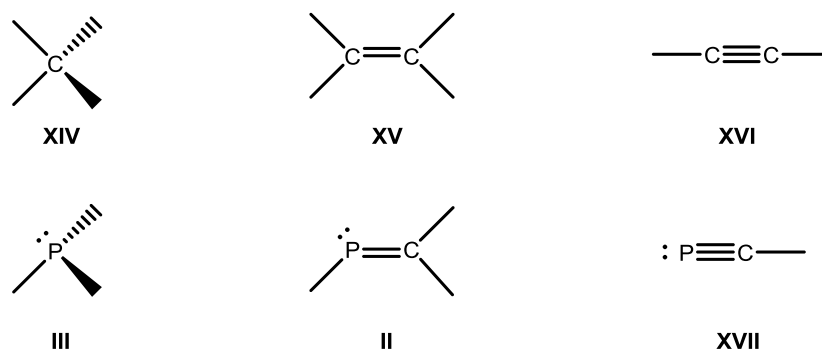


Figure 1.1: Pentacarbonyl[σ^3, λ^3 -methoxy(triphenylmethyl)phosphane- κ P]tungsten(0)^[10]

Phosphorus shows a diagonal relationship to carbon. This relation means that an element is, in specific reactions and structures, closer to an element of a different group and period than to its heavier and lighter homologues. For phosphorus and carbon many similar structural motifs and reactions are known. Important examples can be found especially in modern synthesis and use of phosphorus or carbon in low coordination states. Therefore, phosphorus was also referred to as “the carbon copy”.^[11] The known phosphalkenes **II** and phosphalkynes **XVII** can be mentioned as examples of such similar behaviour (scheme 1.2).



Scheme 1.2: Generalized examples of carbon compounds and their isolobal P^{III} analogues.^[11]

1.2 Development of novel building blocks: From carbenes to phosphinidenoid complexes

A breakthrough in carbon chemistry was the development of a special kind of highly reactive low-coordinated carbon compounds, the so called carbenes, which can be used as versatile building blocks, either as transient species or as stable derivatives.^[12] In general carbenes, carbon compounds possessing an electron sextet at the C-centre, show a broad reactivity.^[13] For example, insertion reactions into different σ -bonds or addition reactions to π -systems are known. Depending on the electronic nature of the substituents as well as on the generation method, carbenes can be formed in two different electronic states. They are classified as singlet (having both electrons paired, most often in the same orbital as well as one empty p-orbital) or triplet (having two unpaired electrons in different orbitals) carbenes.^[13] Methods to synthesize carbenes involve, to just name two, the decomposition of chloro(organo)mercury compounds^[3] or the N₂-release from diazo compounds, e.g from CH₂N₂.^[14] Several such reactions were investigated over the last decades and allow the use of carbenes, as such as well as in transition metal-catalysed reactions.

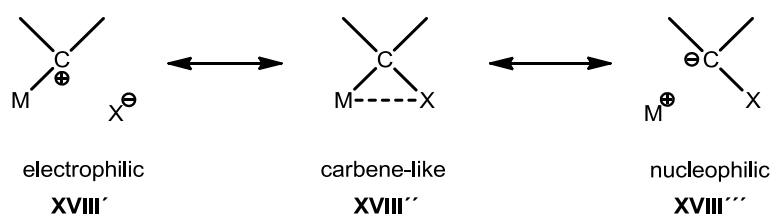
A second breakthrough was the synthesis of some of the first stable heterocyclic carbenes by Arduengo in 1991 and the first structural verification by an X-ray diffraction study.^[15] These N-heterocyclic carbenes (NHCs, singlet carbenes) can be isolated, stored and have

subsequently been used to stabilize many novel structural motifs or as ligands in catalysis. Earlier, push-pull-substituted derivatives were described by Bertrand. The true nature of these carbenes was strongly discussed as the P-C bond showed multiple bond character, but these compounds showed also typical carbene type reactivity (e.g. cyclopropanation reaction with alkenes or epoxide formation with aldehydes).^[16] Since that time, several more stable derivatives could be synthesized, e.g. the mixed substituted cyclic alkyl amino carbenes (CAACs).^[17]

In contrast to NHCs and other acyclic, donor-substituted carbenes, stabilization of carbenes can also be achieved by coordination to a transition metal centre.^[18,19] Due to the high variability of possible coordination modes, only terminal carbene complexes shall be briefly mentioned. Again the reactivity is strongly influenced by the electronic nature of the carbene ligand and the complexes can be separated into two types. The first ones are known as Fischer-type carbene complexes^[18] (electrophilic carbene complexes, that can be formally described as composed of a singlet-singlet combination of the carbene fragment and the metal fragment^[20]) and the latter ones as Schrock-type carbene complexes^[19] (nucleophilic carbene complexes, having a triplet-triplet combination^[20]). Both types of complexes have been used in novel synthetic strategies, catalytically as well as stoichiometric.^[20] Carbene complexes, unfortunately, show (very often) a different reactivity than free carbenes but could be used as carbene transfer reagents.^[20]

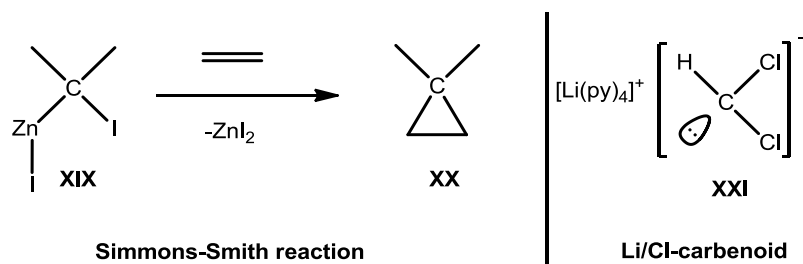
Due to their extremely high reactivity, non-stabilized carbenes are in most cases problematic to handle. Therefore, a new strategy was necessary to achieve carbene-like reactions. One strategy is the synthesis and use of so called carbenoids **XVIII**. Carbenoids^[21,22] feature an electropositive metal (M) and a good leaving group (most often a halogen atom X) at the same carbon atom, so that under formal elimination of MX a carbene could be formed. As the reaction mechanism usually does not involve free carbenes, this often leads to a high(er) selectivity by reducing the number of side reactions.

Noteworthy is, that carbenoids can show several different types of reactivity, based on their ambiphilic nature (scheme 1.4). This means that, besides allowing addition or insertion reactions (in analogy to carbenes), they also allow electrophilic and nucleophilic substitution, as can be illustrated by their electronic resonance structures (scheme 1.3).^[21]



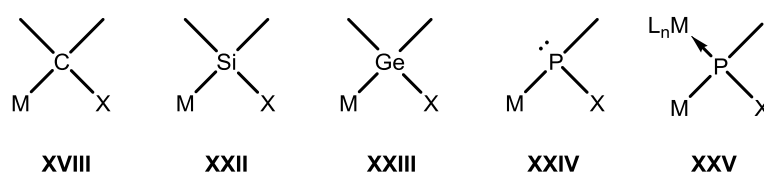
Scheme 1.3: Simplified canonical electronic resonance structures of carbenoids.

One of the best described examples for carbenoid chemistry is the Simmons-Smith reaction (scheme 1.4), where, starting from alkenes, a zinc/iodine carbenoid **XIX** is used in cycloaddition reactions to yield cyclopropanes **XX**.^[23] A second well known example of carbenoid formation is the reaction between dichloromethane and strong bases to form a dichlorocarbenoid, which could even be isolated by separating the cation with pyridine ligands (**XXI**, scheme 1.4).^[24]



Scheme 1.4: Zn/I-carbenoid in the Simmons-Smith reaction^[23] (left) and an example for an isolated Li/Cl carbenoid^[24] (right).

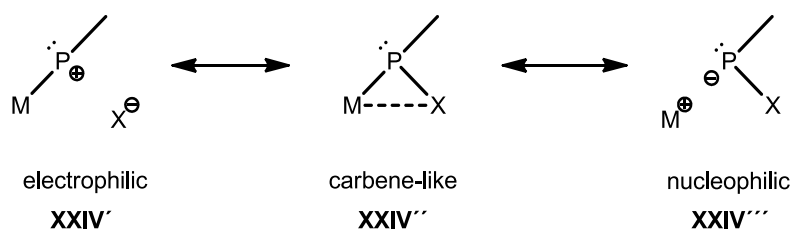
Over the last years, beside carbenoids^[25] **XVIII** also silylenoids^[26] **XXII** and germylenoids^[27] **XXIII** were described, broadening the scope of possible group 14 “-enoid” chemistry.



M = electropositive metal, X = good leaving group

Scheme 1.5: Generalized structures of a carbenoid **XVIII**, silylenoid **XXII**, germylenoid **XXIII**, phosphinidenoid **XXIV** and phosphinidenoid complex **XXV**

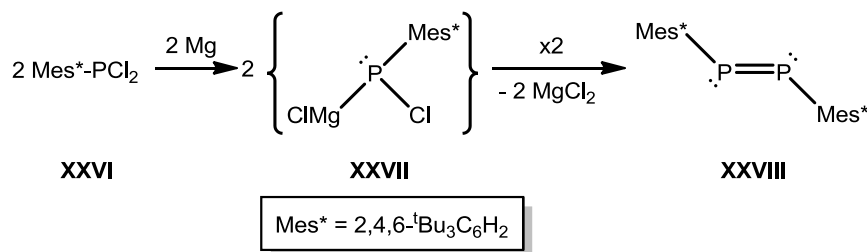
A priori, the phosphinidenoids, being related to carbenoids, should show similar ambiphilic behaviour and similar electronic resonance structures (scheme 1.6).



Scheme 1.6: Generalized electronic resonance structures of phosphinidenoids.

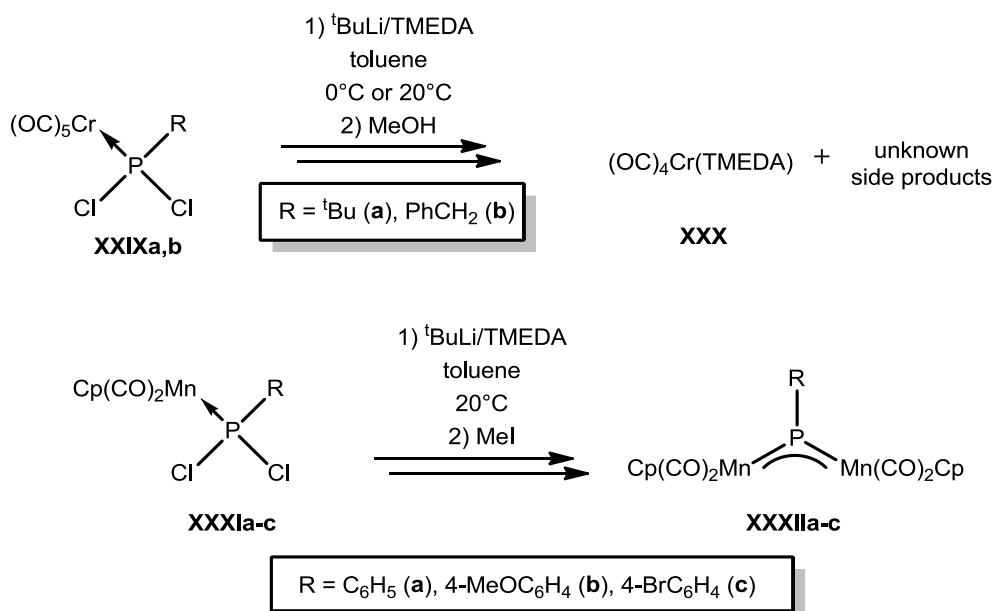
The existence of phosphinidenoids **XXIV**, being examples of group 15 “-enoids”, has not been proven to date. They were proposed as plausible intermediates in several reactions but

never detected by spectroscopic means: Yoshifuji reported the reduction of dichloro-(organo)phosphane **XXVI** with magnesium to form the first *E*-diphosphene **XXVIII** (scheme 1.7).^[28] Yoshifuji also suggested formation of the intermediate **XXVII** and proposed the name “phosphinidenoid” for the first time.^[29]



Scheme 1.7: Synthesis of diphosphene **XXVIII** via a proposed Mg/Cl phosphinidenoid by Yoshifuji.^[29]

If the lone pair of the phosphorus atom is coordinated to a transition metal fragment (e.g. W(CO)₅), phosphanido complexes can be synthesized that should show close similarity to carbenoids, structurally and in their reactivity. A first attempt to create these so called M/X phosphinidenoid complexes (**XXV**) was published by Huttner *et al* in 1985.^[30] Yet, after the (assumed) Li/halogen exchange in dichlorophosphane complexes, only decomposition products of **XXIXa,b** or, in case of **XXXIa-c**, bridged dinuclear phosphinidene complexes (**XXXIIa-c**) were isolated (scheme 1.8).

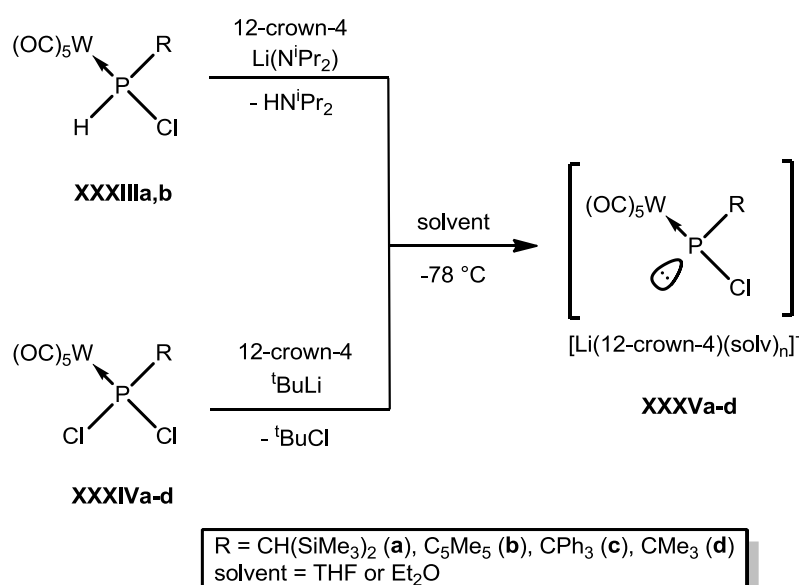


Scheme 1.8: First attempts to obtain Li/Cl phosphinidenoid complexes by Huttner.^[30]

A solution to the problem was presented by Streubel in 2007,^[31] when the first characterised derivative of the class of phosphinidenoid complexes was stabilized by separation of the cation from the anion using a crown ether (12-crown-4) (scheme 1.9). The ion separation was essential for thermal stabilization and, hence, allowed for their synthetic

use at low temperature. During the following years, investigations revealed the potential of the Li/Cl phosphinidenoid complexes as interesting building blocks as well as several similarities to the carbenoid chemistry (scheme 1.10 and 1.11).

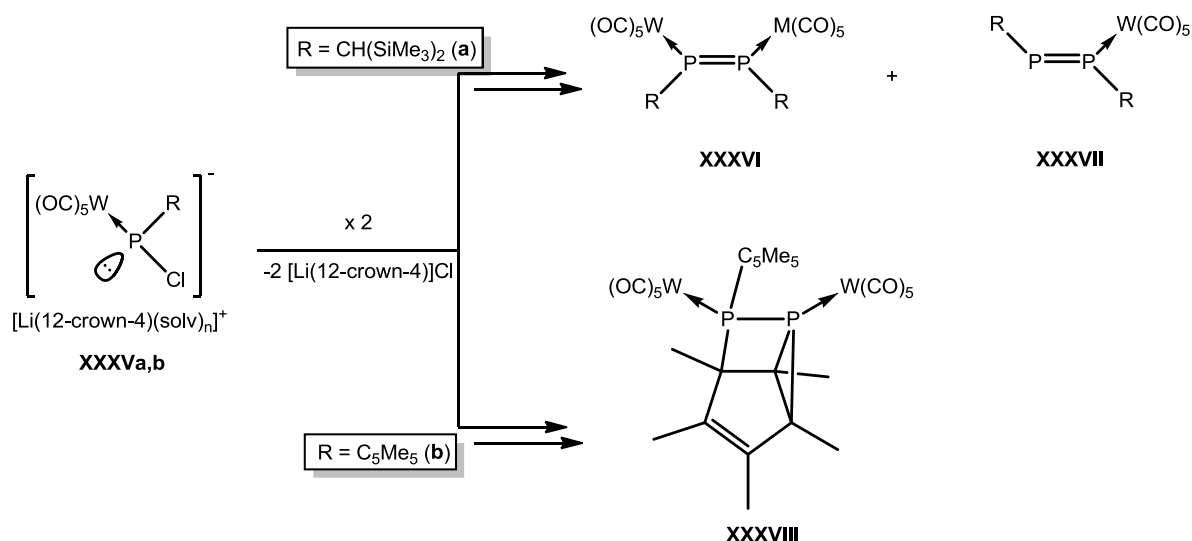
The synthesis of Li/X phosphinidenoid complexes **XXXVa-d** was performed by deprotonation of chloro(organo)phosphane complexes **XXXIIIa,b** using LDA or by Li/Cl exchange starting from the corresponding dichloro(organo)phosphane complexes **XXXIVa-d** using ^tBuLi (scheme 1.9) in the presence of 12-crown-4.^[31–33] Due to the high reactivity and, in most cases, the decomposition below ambient temperature, the complexes are normally generated and reacted *in situ* at low temperature. The solid state molecular structures were obtained for **XXXVa**^[34] and **XXXVc**,^[35] showing well separated ion pairs having a [Li(12-crown-4)₂] cation.^[34,35] In case of a more stable Li/F phosphinidenoid complex, which is even stable at ambient temperature for several hours, a molecular structure was presented having only one molecule of crown ether coordinated to lithium, but also an additional diethyl ether molecule. Studies revealed separated ions also in solution.^[36]



Scheme 1.9: Generation of Li/Cl phosphinidenoid complexes **XXXVa-d** by Streubel.^[31–33]

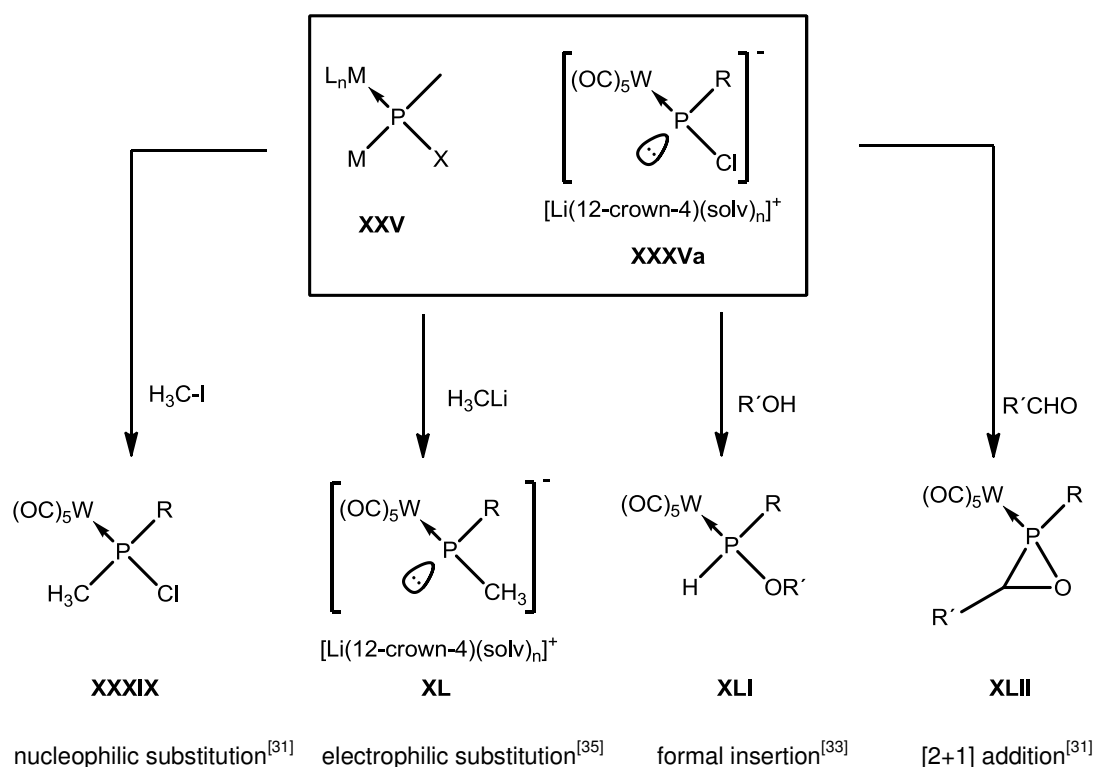
Nowadays the synthesis starting from the chloro(organo)phosphane complexes **XXXIIIa,b** is not used anymore due to the more time-efficient synthetic protocol using the dichloro-(organo)phosphane complexes **XXXIVa-d**. In addition, the deprotonation protocol formed diisopropyl amine which was found to influence the reaction outcome in several cases. *I.e.* it can lead to subsequent reactions such as protonation or deprotonation of other reactive intermediates.^[31,37,38]

A set of Li/Cl phosphinidenoid complexes was described by Streubel *et al.* having different group 6 metal fragments ($P\text{-}M(\text{CO})_5$ with $M = \text{Cr}, \text{Mo}, \text{W}$).^[39,40] as well as different $P\text{-}R$ groups, ranging from extremely reactive complexes with small substituents ($R = \text{}^t\text{Bu}$)^[41] to complexes with moderate ($R = \text{C}_5\text{Me}_5$,^[32] $\text{CH}(\text{SiMe}_3)_2$ ^[31]) and sterically demanding substituents ($R = \text{CPh}_3$).^[33] The stabilisation by the bulky CPh_3 substituent was remarkable as it led to a phosphinidenoid complex which was even stable for about one day at ambient temperature, while all other Li/Cl derivatives started to decompose at significant lower temperatures (normally above $-50\text{ }^\circ\text{C}$). Especially for the $P\text{-}\text{CH}(\text{SiMe}_3)_2$ and the $P\text{-}\text{C}_5\text{Me}_5$ derivatives these decomposition pathways were well investigated (scheme 1.10), allowing often qualitative and semi-quantitative evaluations of the reactions due to the specific ^{31}P NMR data of the side products.



Scheme 1.10: Decomposition reactions of Li/Cl phosphinidenoid complexes **XXXVa**^[31] and **XXXVb**.^[32]

Extensive studies over the past decade by the research group of Streubel demonstrated that phosphinidenoid complexes are very useful building blocks in phosphorus chemistry, comparable to carbenoids in carbon chemistry (scheme 1.11) The Li/Cl phosphinidenoid complexes show nucleophilic reactions^[31], electrophilic reactions^[35] as well as formal insertion into OH bonds^[10,33] and 1,2-addition to different π -systems,^[31,42] the latter being comparable to the cyclopropanation reaction of carbenoids.

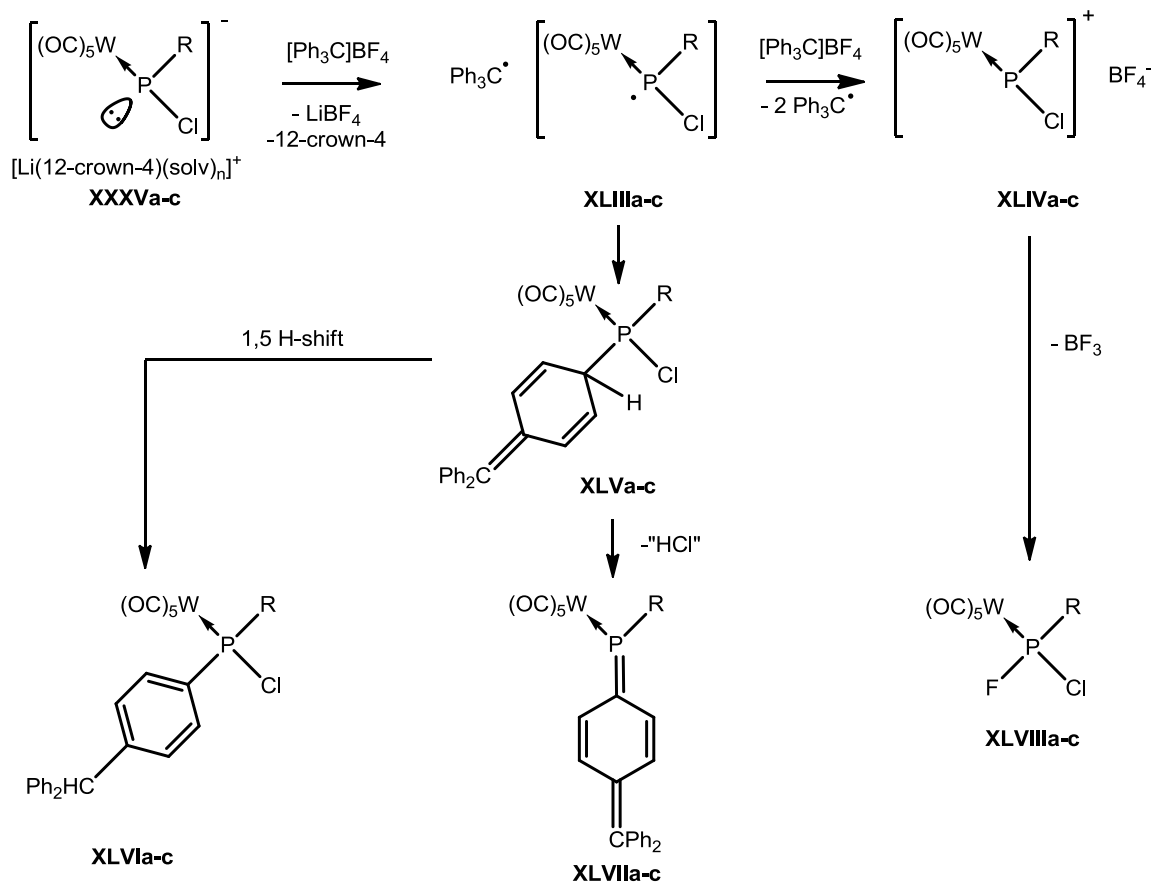


Scheme 1.11: Examples for the reactivity of Li/Cl phosphinidenoid complexes (R = CH(SiMe₃)₂, R' = variable organic substituent).

The last type of reaction that shall be mentioned is the oxidative single electron transfer (SET) reaction of Li/Cl phosphinidenoid complexes **XXXVa-c** (scheme 1.12). In case of [Ph₃C]BF₄ as the oxidant two important steps were identified.^[43] The first step consists of the formation of solvent-caged (close) radical pairs **XLIIa-c** which can recombine to form “hetero-Gomberg” dimers **XLVa-c**. Depending on the nature of the substituent at phosphorus and the conditions, hydrogen shift to give complexes **XLVIa-c**, or HCl elimination to yield *para*-phosphachinomethane complexes **XLVIIa-c** were observed.

While in the beginning complexes **XLVa-c** were proposed only as intermediates, they could be isolated and unambiguously identified just recently.^[44] It was shown that moderately strong N-bases induce a 1,5-hydrogen shift, thus enabling rearomatisation. In contrast, addition of stronger bases such as KHMDS led to formal HCl abstraction and formation of the *para*-phosphaquinomethane complex derivative.

A second oxidation step may occur, as well, requiring excess of the oxidant Ph₃C⁺ and yielding the P-F derivatives **XLVIIIa-c** as final products. The reaction may involve phosphonium complexes **XLIVa-c** as reactive intermediates that, due to their high Lewis acidity, abstract fluoride from the BF₄⁻ anion.^[43]



Scheme 1.12: Examples for oxidative SET reactions of Li/Cl phosphinidenoid complexes **XXXVa-c**.^[43]

2 Objective of the thesis

The research in this PhD work was focused on reactions of Li/Cl phosphinidenoid complexes with a variety of different substrates having N-H bonds or strained heterocyclic rings, to study the hitherto scarcely investigated formal insertion reactions of a P_1 -fragment into different polar E-E'-bonds. In case of the strained rings, the focus was on epoxides.

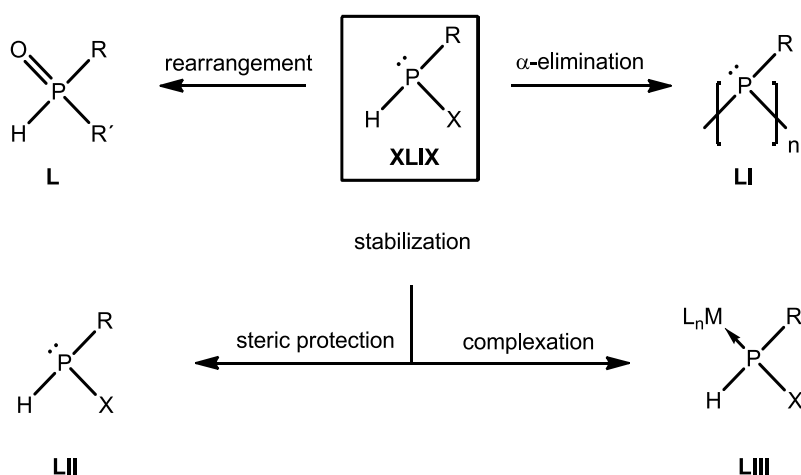
Furthermore, the chemistry of the new product complexes was to be investigated towards their own potential as molecular building blocks to form novel P-ligands.

3 Insertion reactions into N-H bonds

3.1 Introduction to aminophosphane complexes

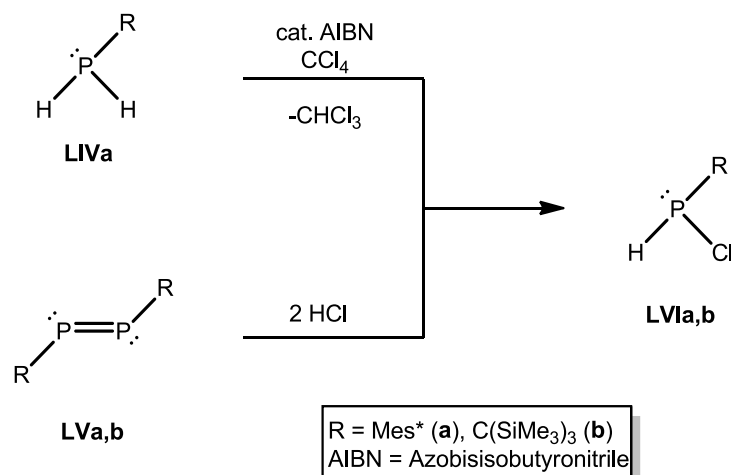
Phosphanes bearing a hydrogen atom together with an electronegative substituent (**XLIX**, $X = \text{OR}, \text{NHR}, \text{NR}_2, \text{halogen}$) on the same phosphorus atom are scarce. On one hand they can undergo rearrangement reactions, *e.g.* to yield phosphane oxides (**L**),^[45,46] on the other hand they can undergo formal α -elimination^{[47][48]} to initiate rearrangement reactions, dimerizations, oligomerizations or insertion reactions, thus yielding products of transient (or formal) phosphinidenes, *e.g.* **LI**. Therefore they are complicated to synthesize.

Stabilization of compounds **XLIX** was mainly achieved in two ways: the kinetic protection by applying sterically demanding *P*-substituents (**LIIa,b** (*e.g.* $R = \text{Mes}^*$ ^[49] or CPh_3 ^[50])) or the complexation to a transition metal fragment (**LIII**).^[48]



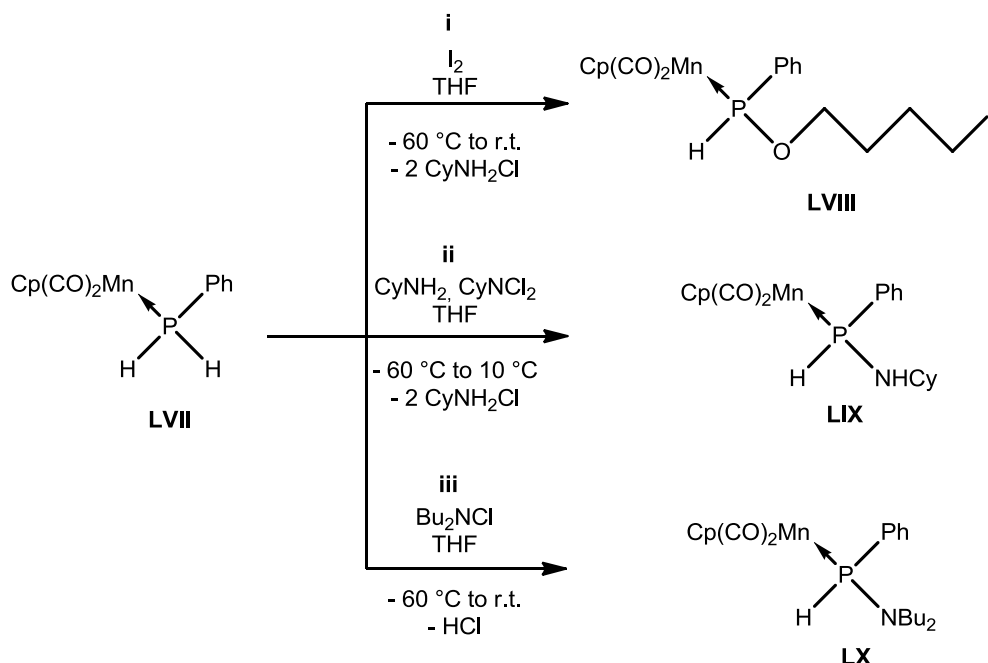
Scheme 3.1: Typical reactions and stabilisation of secondary phosphanes bearing electronegative substituents ($X = \text{OR}, \text{NHR}, \text{NR}_2, \text{halogen}$, $L_nM = \text{transition metal fragment}$).

An example for steric protection is the $\text{Mes}^*\text{P}(\text{H})\text{Cl}$ **LVla**. This compound was synthesized via different routes, namely the radical mediated chlorination of the corresponding phosphane **LIV**^[49] or the splitting of a diphosphene **LVa** with $\text{HCl}_{(\text{g})}$,^[51,52] reported by Cowley *et al.* in 1983. The second route was later expanded to another diphosphene derivative bearing the $\text{C}(\text{SiMe}_3)_3$ substituent **LVb**.^[52]



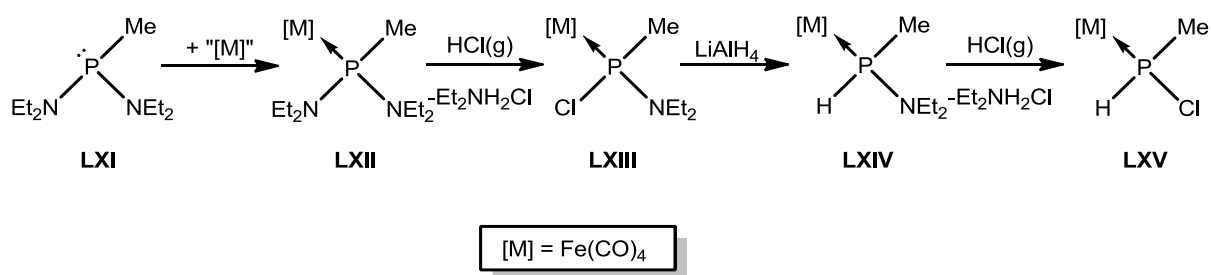
Scheme 3.2: Synthetic strategies to the unligated chlorophosphanes **LVia,b**^{[49],[51,52]} ($\text{Mes}^* = 2,4,6\text{-}^t\text{Bu}_3\text{C}_6\text{H}_2$).

The stabilization by complexation was described first by Huttner *et al.* for phosphinite complex **LVIII** and the aminophosphane complexes **LIX** and **LX**, all having the combination of a PX and PH motif.^[48] They were obtained by oxidation of the corresponding primary phosphane complex **LVII** with iodine in the presence of THF (**i**), the reaction of **LVII** with a mixture of cyclohexylamine and *N,N*-dichlorocyclohexylamine (**ii**) or the reaction with Bu_2NCl (**iii**). All three complexes are air stable at ambient temperature and no α -elimination was observed, even under harsh conditions.



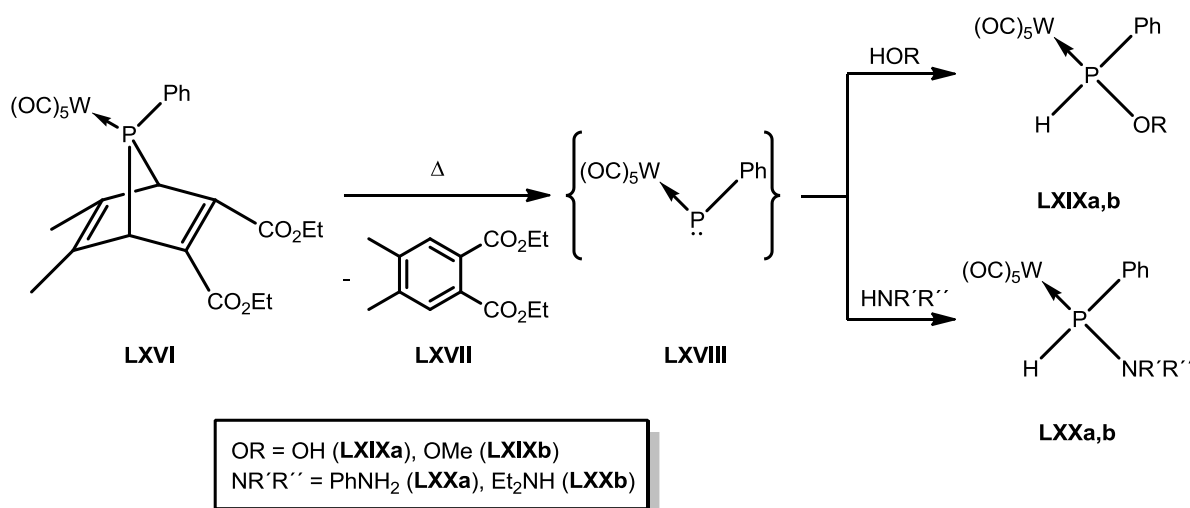
Scheme 3.3: Syntheses of the first phosphinite complex **LVIII** and the first aminophosphane complexes **LIX** and **LX** by Huttner.^[48]

Due to the problematic synthesis of suitable precursors, the complexation of free H/X phosphanes is usually not feasible and/or advantageous. Therefore, a step-wise *P*-ligand conversion including protection and deprotection of the phosphorus centre was developed by Vahrenkamp in 1983^[53] for an iron tetracarbonyl complex bearing a diethylamino-(organo)phosphane ligand. The reaction sequence was investigated for a broader set of group 6 metal complexes ($[M] = \text{Cr}(\text{CO})_5, \text{Mo}(\text{CO})_5, \text{W}(\text{CO})_5$) and *P* substituents ($R = \text{}^t\text{Bu}, \text{Cy}, \text{Ph}, (-)\text{Men}$) by Lorenzen *et al.* in 1990.^[46] In the first step, diamino(organo)phosphane **LXI** was coordinated and then converted with $\text{HCl}_{(\text{g})}$ to the asymmetrically substituted amino(chloro)phosphane complex **LXIII**. Subsequent reduction with LiAlH_4 , yielded the aminophosphane complex **LXIV**. The exchange of the amino by a chloro substituent could again be achieved using $\text{HCl}_{(\text{g})}$ (**LXV**).



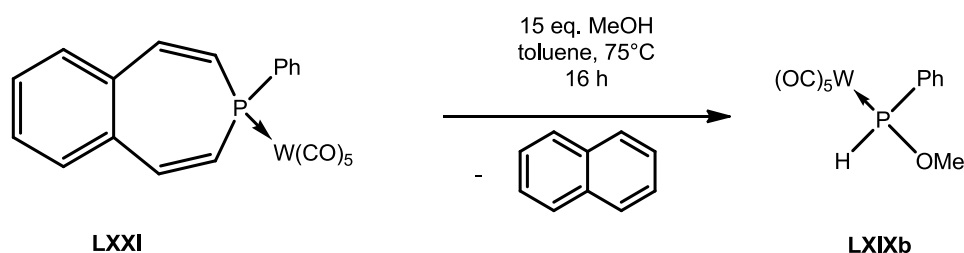
Scheme 3.4: Step wise synthesis of aminophosphane complexes **LXV** by Vahrenkamp^[53].

A different route was presented in 1982 by Mathey *et al.* showing that phosphinite complexes **LXIXa,b** and aminophosphane complexes **LXXa,b** can be synthesized via thermal decomposition of phosphanorbornadiene complex **LXVI** in the presence of the respective amine or alcohol.^[47] Here the insertion reaction of an *in situ* formed electrophilic terminal phosphinidene complex **LXVIII** into the NH or OH bonds led to the desired products. A drawback of these syntheses are especially the reaction conditions, while NH functional substrates reacted already in boiling toluene, temperatures above 120 °C in a high pressure vessel were necessary for most OH functional substrates. In addition, the syntheses of phosphanorbornadiene complexes bearing sterically demanding substituents at *P* (e.g. 9-fluorenyl^[54]) are quite complicated. The necessary Diels-Alder reaction for the formation of the norbornadiene motif can be suppressed by the steric demand so that these complexes usually need several more reaction steps in the synthesis than those bearing smaller substituents like Me or Ph.



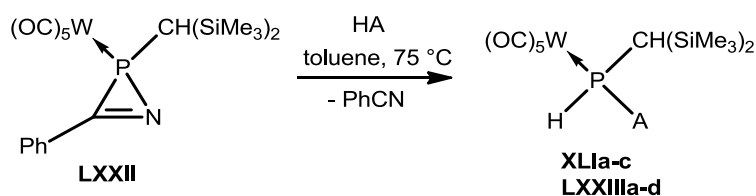
Scheme 3.5: Thermal synthesis of PH functional phosphane complexes **LXIXa,b** and **LXXa,b** using 7-phosphornorbornadiene complex **LXVI** by Mathey.^[47,54]

A somewhat similar route to phosphinite complexes was described by Lammertsma, who started from a phosphepine complex, but only the reaction of complex **LXXI** with methanol has been described so far (scheme 3.6).^[55]



Scheme 3.6: Synthesis of phosphinite complex **LXIXb** by Lammertsma.^[55]

The third thermal route was presented by Streubel in 2010. Here, the decomposition of 2*H*-azaphosphirene complex **LXXII** at elevated temperature was used to generate the transient electrophilic phosphinidene complex that subsequently reacted either with alcohols to form phosphinite complexes **XLIa-c**^[56] or with different primary or secondary amines to form aminophosphane complexes **LXXIIIa-d**.^[57]

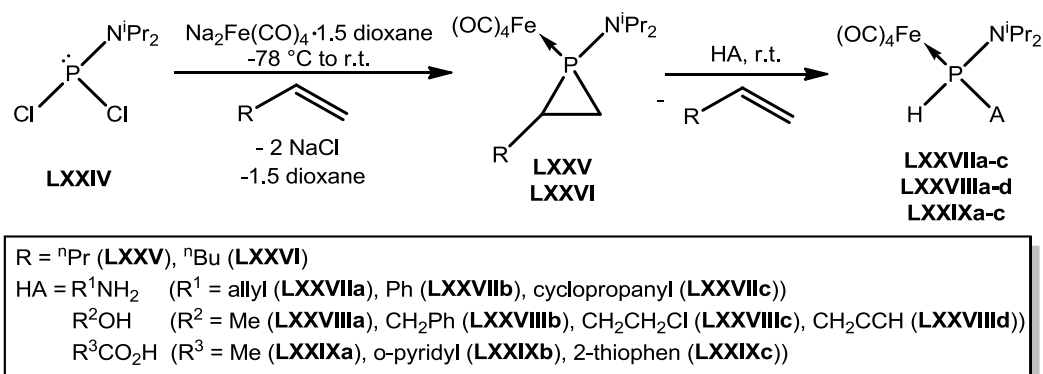


phosphinite complexes (**XLI**):
 HA = ⁿBuOH (**a**), MeOH (**b**), MeO(CH₂)₂OH (**c**)

aminophosphane complexes (**LXXIII**):
 Me₂NH (**a**), Et₂NH (**b**), PhNH₂ (**c**), ⁱPrNH₂ (**d**)

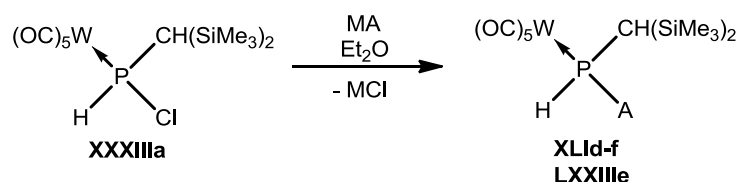
Scheme 3.7: Syntheses of phosphinite and amino phosphane complexes by Streubel.^[56,57]

The most recent published reaction sequence, involving again a terminal electrophilic phosphinidene complex, was presented by Lammertsma.^[58] Starting from dichloro-(diisopropylamino)phosphane **LXXIV** and Collman's reagent ($\text{Na}_2\text{Fe}(\text{CO})_4 \cdot 1.5\text{-dioxane}$), a phosphinidene complex was generated in a double salt elimination reaction. This phosphinidene complex is, in 1-pentene or 1-hexene as solvent, in an equilibrium with the corresponding phosphiranes **LXXV** or **LXXVI**, respectively, and the term "bottled phosphinidene complex" was used by Lammertsma to emphasize its reactivity. In the presence of protic compounds (such as amines or alcohols), a clean conversion to the corresponding aminophosphane **LXXVIIa-c** or phosphinite complexes **LXXVIIIa-d** was observed. This reaction has the advantage to yield amino-substituted Fe complexes. The latter can easily be further functionalized at phosphorus and the iron centre at ambient temperature, meaning that possible thermal decomposition of the products is suppressed.



Scheme 3.8: Syntheses of tetracarbonyliron-substituted phosphinite and aminophosphane complexes by Lammertsma.^[58]

Another route to phosphinite^[56] and aminophosphane^[57] complexes was presented by Streubel using a post-functionalization strategy, *i.e.* using chloro(organo)phosphane complex **XXXIIIa** and sodium alkoxides or sodium amides in salt elimination reactions (scheme 3.9). A drawback in these reactions were the possible deprotonation of the starting chloro(organo)phosphane complex, leading in the end to the formation of diphosphene complexes (**XXXVI** and **XXXVII**) via transient phosphinidenoid complexes (for more information on the diphosphene complexes see chapter 1.2) and the laborious multi-step synthesis of the chloro(organo)phosphane complex **XXXIIIa**.



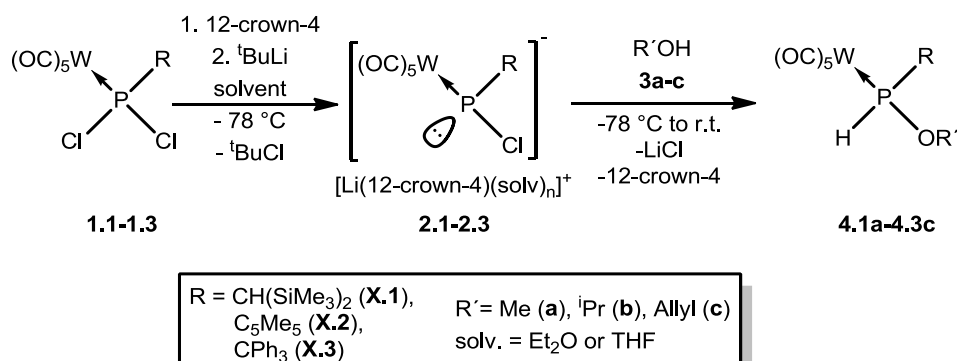
phosphinite complexes (XLI) A = OPh (d), NaO(2,6-Me ₂ C ₆ H ₃) (e), AgO ₂ CCH ₃ (f)	aminophosphane complexes (LXXIII) A = NPh ₂ (e)
M = Na (XLId , XLIf , LXXIIIe), Ag (XLIf)	

Scheme 3.9: Syntheses of phosphane complexes via salt elimination reactions by Streubel.^[56,57]

The analogous reactions in main-group “-enoid” chemistry have attracted considerable attention in the past owing to the versatile construction of useful building blocks. Those are the insertion reactions of metallocarbenoids, which are derived from diazocarbonyl compounds, into X-H bonds of main-group compounds (X = C, N, P, O, S, etc.).^[59,60] A similar reactivity for phosphinidenoid complexes would be of high interest for the synthesis of P-containing building blocks.

3.2 Insertion reactions using R₂NH

Although being similar to electrophilic phosphinidene complexes in their reactivity, the true potential of Li/Cl phosphinidenoid complexes was not fully unveiled, yet. First investigations towards the formal insertion reactions of the Li/Cl phosphinidenoid complexes into the OH-bond of alcohols were just recently presented by Streubel.^[10,33] *E.g.* warming up a *P*-CPh₃-substituted Li/Cl phosphinidenoid complex **2.3** containing solution in the presence of isopropanol **3b** selectively yielded the phosphinite complex **4.3b**.^[33]

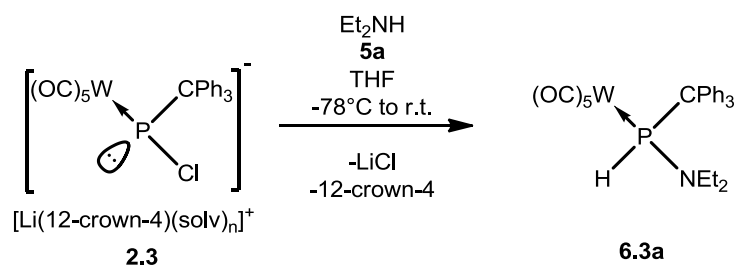


Scheme 3.10: Synthesis of phosphinite complexes **4.1a-4.3c** by formal insertion of phosphinidenoid complexes **2.1-2.3** in OH-bonds of different alcohols **3a-c**.^[33]

To broaden the scope of such formal insertion reactions the reagents were changed to the easiest accessible pentel analogues of the alcohols, the amines. In this research field, problems depending on the different reactivity (especially the lower acidity of the proton) as

well as the steric influence of a second organic substituent and, in this regard, the possibility of double insertion reactions due to more hydrogen-nitrogen bonds in the primary amines were of great interest. To avoid possible problems by such multiple insertion reactions, the investigation was started with secondary amines.

A first successful product formation was observed for the reaction of **2.3** with diethylamine **5a** (scheme 3.11). The aminophosphane complex showed a resonance signal at 74.4 ppm with a doublet splitting in the ^{31}P NMR spectrum due to the directly bonded hydrogen atom, thus having a $^1J_{\text{P,H}}$ coupling constant of 352.2 Hz; satellite signals from the coupling to the ^{183}W nucleus ($^1J_{\text{W,P}} = 252.1$ Hz, natural abundance of $^{183}\text{W} = 14.3\%$) were also observed.



Scheme 3.11: Synthesis of aminophosphane complex **6.3a** using diethylamine **5a** and the *P*-CPh₃-substituted Li/Cl phosphinidenoid complex **2.3**.

Using other substrates, the reaction was found to be strongly dependent on the steric demand of the amine substituents. When the steric demand is too high, the reaction is slowed down significantly and no product formation is observed, *i.e.* the reactions with diisopropylamine (**5b**) as well as dicyclohexylamine (**5c**) were unselective. These unselective reactions showed several side products, of which the phosphinidenoid complex **2.3** at 252.1 ppm ($^1J_{\text{W,P}} = 77.6$ Hz)^[33], and a product at 12 ppm, that corresponds to a formal insertion reaction of the phosphinidenoid complex into a *para*-CH bond of Ph₃CH [(OC)₅W{P(CPh₃)(*para*-(CHPh₂)C₂H₄)H}], could be identified as not substrate specific product.^[61] The mechanism to yield the second product is so far not clear. A reaction between Li/Cl phosphinidenoid complex **2.3** and Ph₃CH did not show a clean conversion.

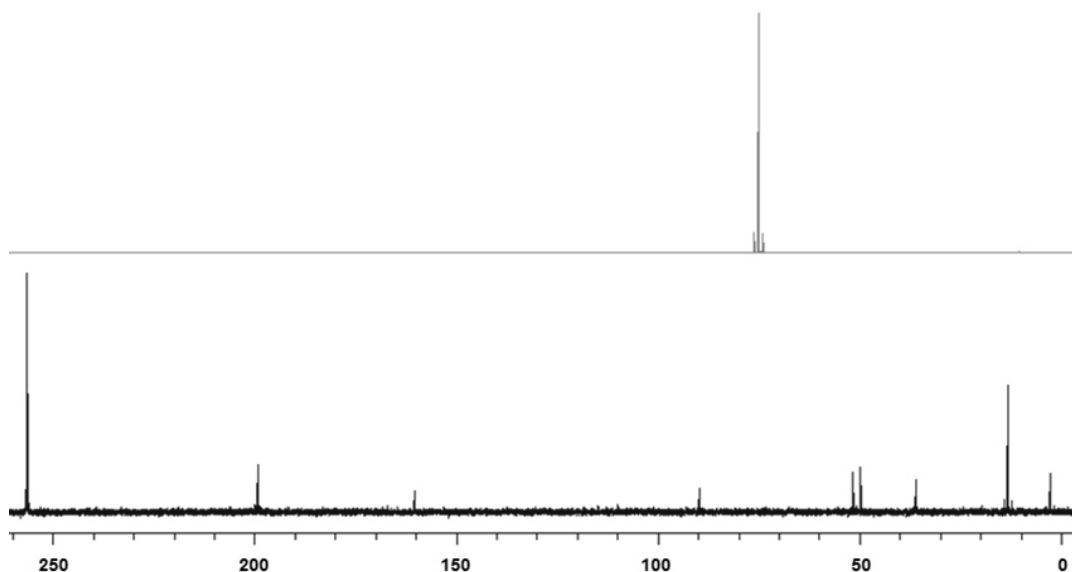


Figure 3.1: $^{31}\text{P}\{^1\text{H}\}$ NMR spectra for the reaction solution of Li/Cl phosphinidenoid complex **2.3** with diethylamine (**5a**, top) and diisopropylamine (**5b**, bottom).

Based on the results presented herein, Schmer could show in his MSc thesis that the reaction was found to yield aminophosphane complexes only when the α -C atom is bearing just one *C*-substituent, *e.g.* the reaction with dibenzylamine (**5d**) was possible. A set of acyclic (dimethylamine (**5e**), dibenzylamine (**5d**)) and cyclic (piperidine (**5f**), pyrrolidine (**5g**)) secondary amines was used by Schmer and the prepared complexes were completely characterised, including ^1H , $^{13}\text{C}\{^1\text{H}\}$ and ^{31}P NMR, mass spectrometry, elemental analysis and single crystal diffraction studies.^[62]

The biggest advantages of this novel route were found especially in the yields and the easy work-up by simple filtration over SiO_2 in most cases. Previous routes gave lower yields according to Duan (10-50 %)^[57], while in the present cases they were moderate and good (45 – 82 %) and starting from the easier accessible dichloro(organo)phosphane complexes as starting materials.

Table 3.1: ^{31}P NMR data (in CDCl_3) and yields of complexes **6.3a-e**.

	R_2	$\delta^{31}\text{P}$ [ppm]	$^1J_{\text{W,P}}$ [Hz]	$^1J_{\text{P,H}}$ [Hz]	yield [%]
6.3a	Et_2	74.4	252.1	352.2	81
6.3d	$(\text{PhCH}_2)_2$ ^[62]	77.3	254.5	354.6	52
6.3e	Me_2 ^[62]	82.6	254.9	349.8	82
6.3f	$(\text{CH}_2)_5$ ^[62]	58.4	254.5	346.1	62
6.3g	$(\text{CH}_2)_4$ ^[62]	81.9	254.6	345.9	45

Single crystals of **6.3a**, suitable for X-ray diffraction studies, were obtained from a saturated diethyl ether solution. The complex shows a planar geometry at the nitrogen atom with a sum of bond angles of 359° and 359.6° (for two independent molecules), presumably due to steric effects of the bulky CPh_3 and $\text{W}(\text{CO})_5$ groups. All other structural parameters are in good accordance with the ones found for complexes **9.3a-f** (cf. chapter 3.3) and similar to those described in the literature^[57] and shall therefore not be discussed further.

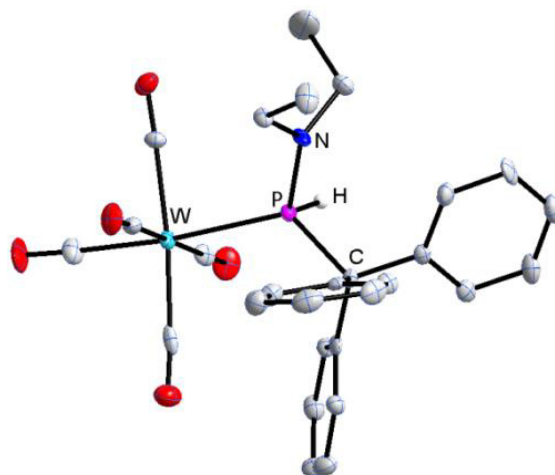
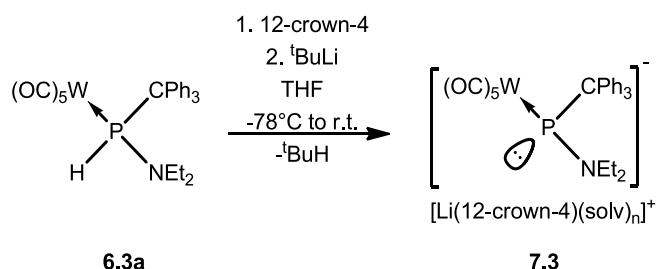


Figure 3.2: DIAMOND plot of the molecular structure of complex **6.3a** in the solid state; the thermal ellipsoids are set at 50 % probability level and all hydrogen atoms except at phosphorus are omitted for clarity. Only one of two independent molecules in the unit cell is shown for clarity. Both sets of data for the two independent molecules are given (molecule 1/molecule2), selected bond lengths in Å and angles in $^\circ$: P-W 2.5540(18)/2.5509(17), P-N 1.673(6)/1.678(6), P-C 1.957(7)/1.954(6), W-P-C 123.1(2)/123.1(2), W-P-N 115.9(2)/115.6(2), C-P-N 109.7(3)/110.3(3).

For aminophosphane complex **6.3a**, bearing two organic substituents at N, a deprotonation at the PH functionality could be achieved by the addition of $^t\text{BuLi}$. This deprotonation led selectively to the *P*-amino-substituted phosphinidenoid complex **7.3** (scheme 3.12).



Scheme 3.12: Synthesis of Li/ NEt_2 phosphinidenoid complex **7.3**.

The successful formation of phosphinidenoid complex **7.3** could be deduced from the ^{31}P NMR spectrum, and no side-products were observed. This outcome is in stark contrast to the one for the corresponding *P*- $\text{CH}(\text{SiMe}_3)_2$ -substituted complex, where a deprotonation led to a fast decomposition of the complex with partial decomposition to unknown products, even below ambient temperature.^[57] A low field shifted resonance signal was observed for

complex **7.3** at $\delta^{31}\text{P} = 160.3$ ppm with a small coupling constant between phosphorus and tungsten ($^1J_{\text{W,P}} = 102.6$ Hz), both are typical for known phosphinidenoid complexes.^{[31][10,33]} Unfortunately, the complex decomposed after a short time at ambient temperature, yielding mainly the starting material **6.3a** as well as a small amount of un-identified products (figure 3.3).

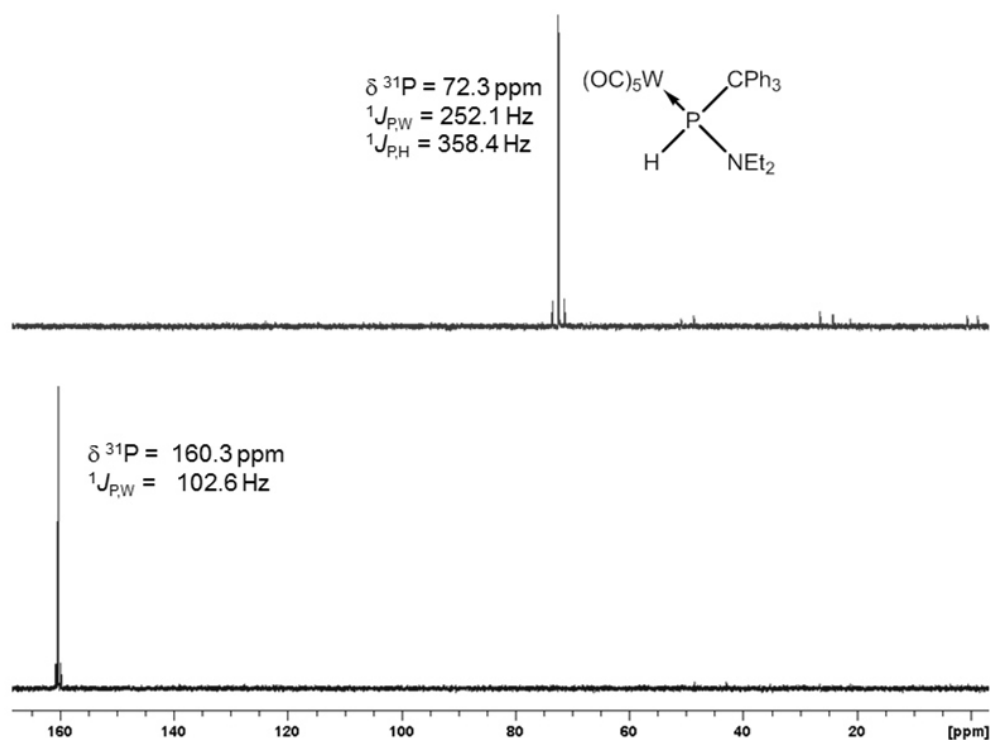
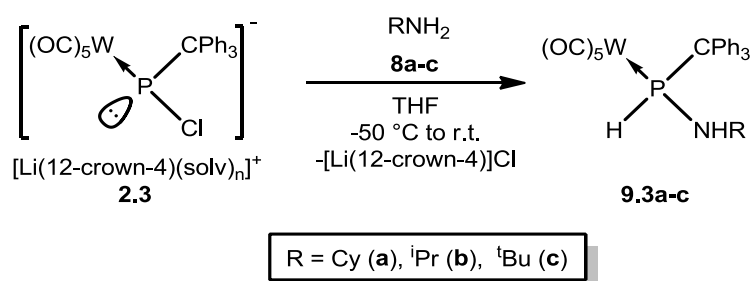


Figure 3.3: $^{31}\text{P}\{^1\text{H}\}$ NMR of Li/ NEt_2 phosphinidenoid complex **7.3** in the reaction mixture after 20 minutes (bottom) and after one day at ambient temperature (top).

3.3 Insertion reactions using RNH₂

The reaction of phosphinidenoid complexes **2.1-2.3** with primary amines might in principle be problematic due to the possibility to form products from mono-insertion and bis-insertion reactions.

Nevertheless a selective reaction to 1,1'-bifunctional aminophosphane complexes was achieved using the *P*-CPh₃-substituted Li/Cl phosphinidenoid complex **2.3**. The observation of only one signal in the ³¹P{¹H} NMR spectrum for each complex proved that only the mono-insertion product is formed, presumably due to the high steric demand of the *P*-CPh₃ substituent.



Scheme 3.13: Syntheses of aminophosphane complexes **9.3a-c** using the formal P₁-insertion reaction of Li/Cl phosphinidenoid complex **2.3** in the presence of primary amines **8a-c**.

A set of reactions using primary amines, having slightly different steric demand for the substituents at the N-centre (CyNH₂ (**8a**), ⁱPrNH₂ (**8b**) and ^tBuNH₂ (**8c**), scheme 3.13), was performed and the obtained aminophosphane complexes **9.3a-c** were unambiguously characterised by multinuclear NMR, IR and MS measurements as well as elemental analysis and single crystal X-ray diffraction studies.

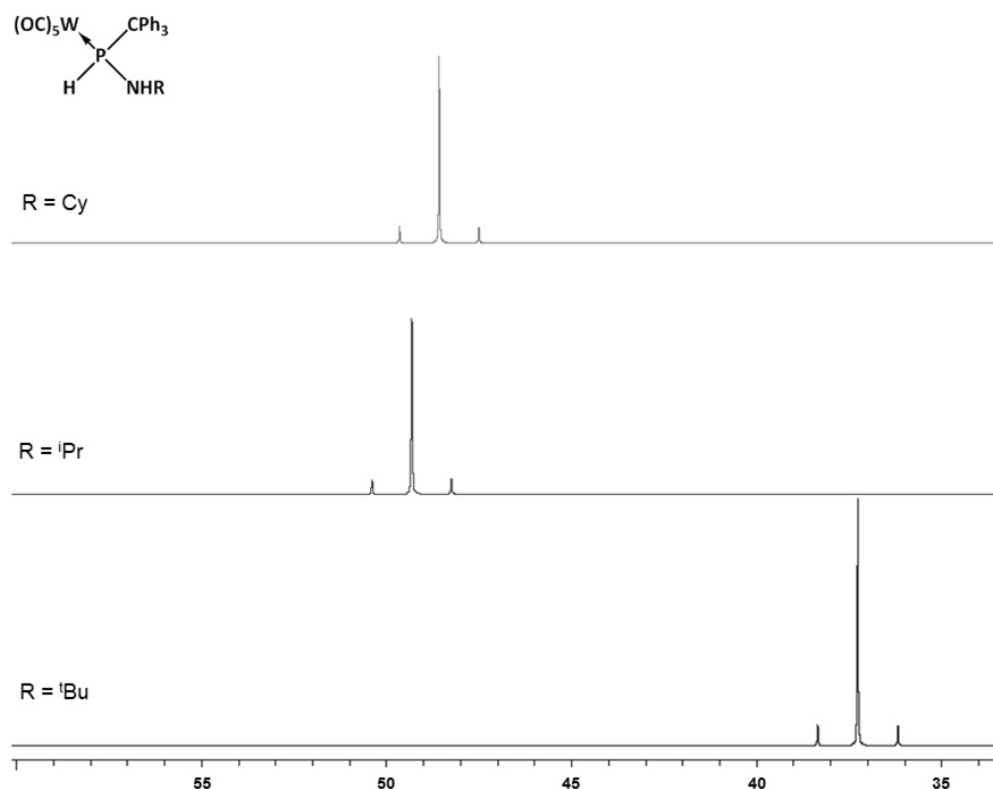


Figure 3.4: $^{31}P\{^1H\}$ NMR spectra of aminophosphane complexes **9.3a-c**.

Around the same time, several other derivatives were prepared by Mahji^[63] (R = Me (**9.3d**), Ph (**9.3e**) and Schmer^[62] (R = Et (**9.3f**)) using this strategy. It is also worthwhile to mention that Schmer could observe a selective reaction with ammonia under the same conditions, leading to the *P*-NH₂-substituted organophosphane complex, the second known derivative having this substitution pattern.^[47]

Complexes **9.3a-f** displayed resonances in the range of 37 to 58 ppm ($^1J_{W,P} = 258.4 - 264.5$ Hz and $^1J_{P,H} = 332.6 - 346.5$ Hz, selected NMR spectroscopic data are given in table 3.2). The resonance signals are significantly shifted towards lower field, compared to the resonance signals of complexes bearing the *P*-CH(SiMe₃)₂ substituent which were described by Duan ($\delta^{31}P = 5.3 - 46.1$ ppm, $^1J_{W,P} = 249.2 - 263.2$ Hz, $^1J_{P,H} = 320.2 - 357.7$ Hz).^[57]

Table 3.2: ^{31}P NMR data (in CDCl₃) and yields of complexes **9a-f**.

	R	$\delta^{31}P$ [ppm]	$^1J_{W,P}$ [Hz]	$^1J_{P,H}$ [Hz]	yield [%]
9.3a	Cy	48.6	260.4	333.0	77
9.3b	ⁱ Pr	49.4	260.5	332.6	71
9.3c	^t Bu	37.3	263.7	342.3	84
9.3d	Me ^[63]	57.4	258.4	346.1	83
9.3e	Ph ^[63]	54.6	264.5	342.0	79
9.3f	Et ^[62]	53.7	258.8	346.5	84

Comparison of **9.3a-f** to complexes **6.3a-e**, shows that *N,N*-disubstituted complexes possess smaller $^1J_{\text{P,H}}$ coupling constants (approximately 7 Hz) and smaller $^1J_{\text{W,P}}$ coupling constants (approximately 5 Hz). The ^{31}P resonance signals are also significantly low-field shifted (e.g. $\delta^{31}\text{P} = 74.4$ ppm for complex **6.3a**) in comparison to those of complexes obtained with primary amines (e.g. $\delta^{31}\text{P} = 53.7$ ppm for complex **9.3f**). The stronger shielding by introducing more hydrogen substituents at the N-centre was also described by Duan for *P*-CH(SiMe₃)₂-substituted aminophosphane complexes^[57].

High-field shifted resonances were observed with increase of the steric demand of the amino group ($\delta^{31}\text{P}$ for Me>ⁱPr>^tBu), consistent with the trend observed for phosphinite complexes.^[56] The P-H bond stretching vibrations are in line with reported values, being between 2310 and 2370 cm⁻¹ in the IR spectra of complexes **9.3a-f**.

Single crystals of **9.3a-c** suitable for X-ray diffraction studies could be obtained from saturated diethyl ether solutions. Complexes **9.3a** and **9.3c** crystallized in the space group P2₁/c and complex **9.3b** in P $\bar{1}$. The molecular structures are displayed in figure 3.5.

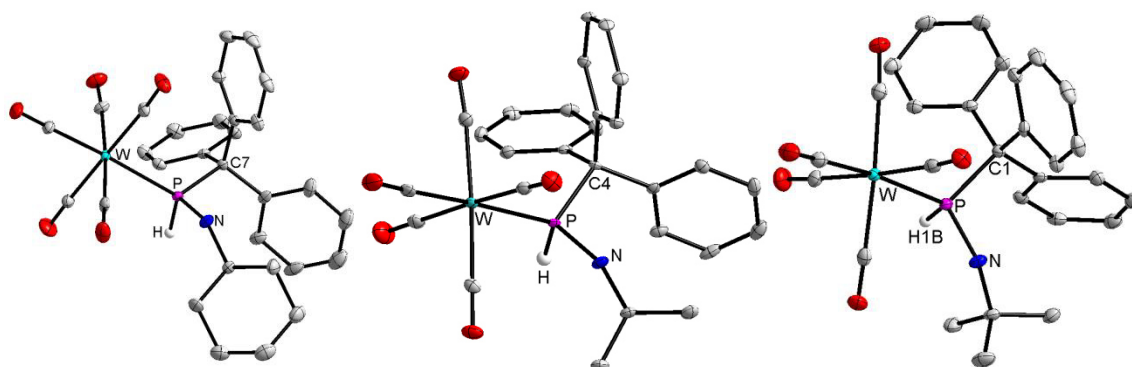


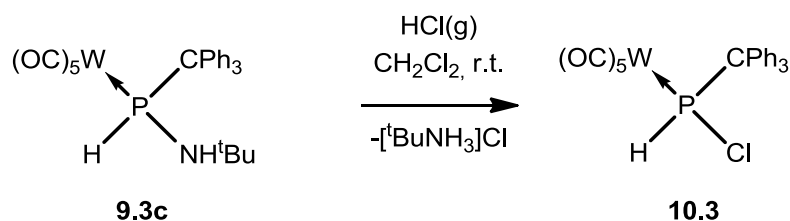
Figure 3.5. DIAMOND plot of the molecular structures of complexes **9.3a-c** (from left to right) in the solid state; the thermal ellipsoids are set at 50 % probability level and all hydrogen atoms except at phosphorus are omitted for clarity. In case of **9.3b** only one of two independent molecules in the unit cell is shown for clarity.

The phosphorus centres, including the W(CO)₅ fragment and not the P-H unit, display a trigonal geometry with a bond angle sum of about 340°, similar to those found in phosphinite complexes.^[10] All complexes show a significant bond elongation for the P-C bonds and P-W bond lengths similar compared to the ones found for *P*-CH(SiMe₃)₂-substituted aminophosphane complexes.^[57] The P-C bond elongation has been reported as a feature of all *P*-CPh₃-substituted phosphane complexes as well as unligated *P*-CPh₃-substituted phosphanes. In the past it was often attributed to the repulsive interaction induced by the bulky triphenylmethyl group. This explanation is rather questionable as no further elongation could be observed by complexation to the bulky W(CO)₅ group and it still demands to be seen by calculation what causes this effect.

Table 3.3: Selected bond lengths in Å and angles in ° for complexes **9.3a-c**. Both sets of data for the independent molecules are given for **9.3b** (molecule 1/molecule 2).

	P-W	P-C	P-N	C-P-N	C-P-W
9.3a	2.5210(5)	1.912(2)	1.6652(18)	106.64(9)	121.53(6)
9.3b	2.5361(8)/	1.924(3)/	1.663(3)/	104.13(13)/	116.54(10)/
	2.5344(8)	1.927(3)	1.674(3)	107.54(13)	122.75(9)
9.3c	2.5324(6)	1.918(2)	1.670(2)	110.24(10)	110.99(7)

To gain access to the *P*-CPh₃-substituted chlorophosphane complex **10.3**, representing an interesting molecular building block, aminophosphane complex **9.3c** was reacted with HCl_(g) in dichloromethane (scheme 3.14). The reaction showed a clean conversion of the starting material to the desired product, whereas neither a reaction with HCl_(g) in Et₂O nor a reaction with PCl₃ in CH₂Cl₂ led to any significant exchange reaction.



Scheme 3.14: Synthesis of the *P*-CPh₃-substituted chlorophosphane complex **10.3**.

Isolation of complex **10.3** was performed by removal of all volatiles and subsequent extraction with diethyl ether to separate the product from the formed ammonium salt. The resonance signal shows typical values for chloro(organo)phosphane complexes in the ³¹P NMR spectrum (in CDCl₃) with 70.7 ppm, ¹J_{W,P} = 270.8 Hz and a P-H coupling (¹J_{P,H} = 343.7 Hz) as well as an absorption in the IR spectrum due to the P-H bond vibration at 2351 cm⁻¹. A small splitting of the resonance signal was observed, *i.e.* two signals in a ratio of 2:1 were assigned to the ³⁵Cl and ³⁷Cl isotopomers (³⁵Cl: δ³¹P = 71.22 ppm, ¹J_{W,P} = 270.95 Hz, ³⁷Cl: δ³¹P = 71.20 ppm, ¹J_{W,P} = 270.93 Hz). These ³¹P NMR data are similar to the ones observed for the corresponding *P*-C₅Me₅-substituted derivative **10.2**^[64] (³⁵Cl: δ³¹P = 76.75 ppm, ¹J_{W,P} = 274.2 Hz; ³⁷Cl: δ³¹P = 76.73 ppm, ¹J_{W,P} = 273.9 Hz). The ratio of the two isotopomers represents the natural abundance of the ³⁵Cl and ³⁷Cl isotopes and their electronic influence in the P-Cl bond exerts a small effect on the shielding of the phosphorus nucleus, but the effect is quite small and no other data of complex **10.3** are influenced by this effect.

A molecular structure in the single crystal could be determined, too, showing the constitutional P(H)Cl motif (figure 3.6).

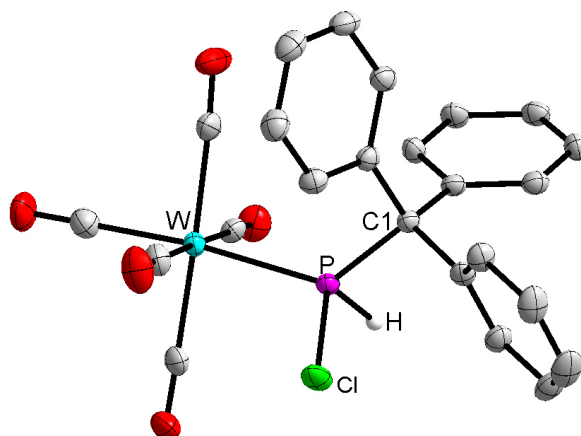
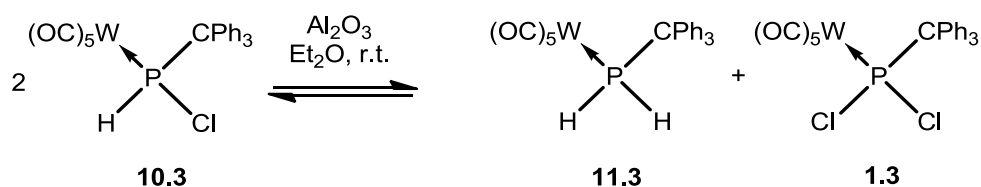


Figure 3.6: DIAMOND plot of the molecular structure of complex **10.3** in the solid state; the thermal ellipsoids are set at 50 % probability level and all hydrogen atoms except at phosphorus are omitted for clarity. Selected bond lengths in Å and angles in °: P-W 2.4868(9), P-C1 1.917(3), P-Cl 2.0596(11), Cl-P-W 107.55(5), C1-P-Cl 104.19(10), C1-P-W 128.54(10).

The molecular structure of **10.3** shows a slight shortening of the P-C bond compared to the corresponding *P*-CPh₃-substituted dichlorophosphane complex **1.3**^[33] (1.917(3) Å vs 1.955(2) Å in **1.3**) as well as a slight elongation of the P-W bond (2.4868(9) Å vs 2.4685(6) Å in **1.3**).

Research performed with derivatives of chlorophosphane complex **10.3** bearing the CH(SiMe₃)₂ group (**10.1**) or C₅Me₅ group (**10.2**), had already shown that deprotonation with weakly nucleophilic bases like LDA leads to Li/Cl phosphinidenoid complexes **2.1**^[31] or **2.2**.^[32] Also substitution reactions of the chloride were performed, to yield for example phosphinite complexes^[56] or aminophosphane complexes.^[57] Therefore, bearing the sterically more demanding CPh₃ substituent, **10.3** could lead to a variety of new applications in the future.

An interesting observation was made when a diethyl ether solution of complex **10.3** was treated with aluminium oxide, or when work-up procedures involving aluminium oxide as solid phase material for filtration or column chromatography were tried (scheme 3.15). Both conditions led to an H/Cl exchange between two molecules of **10.3** (“scrambling” or “dismutation”), forming the dichloro(organo)phosphane complex **1.3** and the primary phosphane complex **11.3**, which could easily be identified due to their literature known ³¹P resonance signals at 166.2 ppm (¹J_{W,P} = 319.7 Hz) for dichloro(organo)phosphane complex **1.3**^[33] and -41.2 ppm (¹J_{P,H} = 329.3 Hz, ¹J_{W,P} = 225.1 Hz) for the phosphane complex **11.3**^[33]. No complete conversion was found even after prolonged reaction time (ratio (**1.3** : **10.3** : **11.3**) after 1 day: 3:88:9, ratio after 7 days 6:78:16), indicating an equilibrium between the three complexes.



Scheme 3.15: Dismutation reaction of **10.3** in the presence of Al_2O_3 .

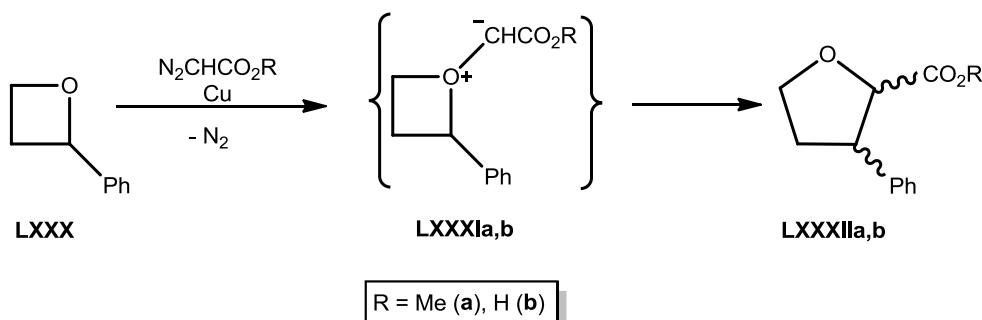
A similar dismutation reaction was described previously by Mathey for the *P*-Ph-substituted derivative of **10**; the stronger Lewis acid AlCl_3 catalysed the reaction in dichloromethane and led to an almost quantitative conversion to the corresponding dichloro- and primary phosphane complexes.^[47] No such dismutation was described for the *P*- $\text{CH}(\text{SiMe}_3)_2$ or *P*- C_5Me_5 -substituted derivatives (**10.1** and **10.2**), yet.

While the obtained aminophosphane complexes are of great interest as building blocks for further phosphane complexes due to the presence of the P-H and the N-H functionalities, the problem with decomposition and reprotonation hampered further research (c.f. scheme 3.12 and figure 3.3). A solution to this problem was found by the group of Streubel, *i.e.* Majhi showed that the stability of such phosphinidenoid complexes is significantly enhanced when the cation is changed to $[\text{K}(18\text{-crown-6})]^+$.^[63] First reactivity studies on the K/N(H)R phosphinidenoid complexes were done by Majhi and Schmer.^[62] Majhi could prove that under double deprotonation conditions a reaction with PhPCl_2 led to an azadiphosphiridine complex. Schmer could additionally show that a selective functionalization either at the P or the N centre is possible.^[62]

4 Insertion reactions into strained heterocycles

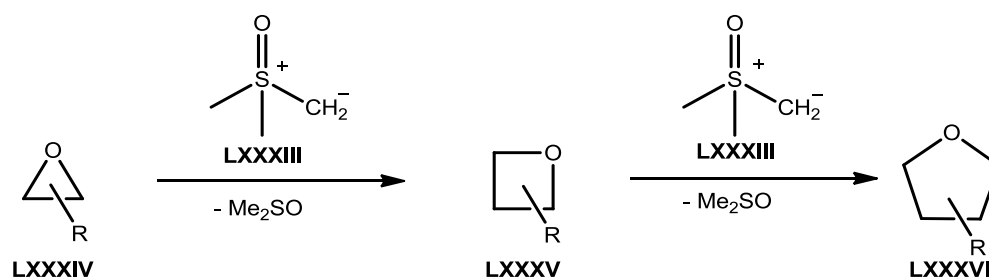
4.1 Introduction

To overcome problems observed for carbenes, due to their high reactivity and therefore often low selectivity, several carbene transfer reagents were developed and subsequently used for ring expansion and insertion reactions. Examples for these reagents are diazo organo compounds in the presence of transition metals, which can mimic carbene reactivity in ring expansion reactions.^[59] This was presented for example by Nozaki and *co-workers* in 1986 in the reactions of phenyloxetane **LXXX** to give substituted tetrahydrofuranes **LXXXIIa,b**.^[65] Formation of oxonium-ylides **LXXXIa,b** from the oxetane with diazoalkanes in the presence of copper and a subsequent [1,2]-C-shift was proposed as mechanism for the ring expansion reaction (scheme 4.1).



Scheme 4.1: Copper catalyzed ring expansion reaction of an oxetane by Nozaki *et al.*^[65]

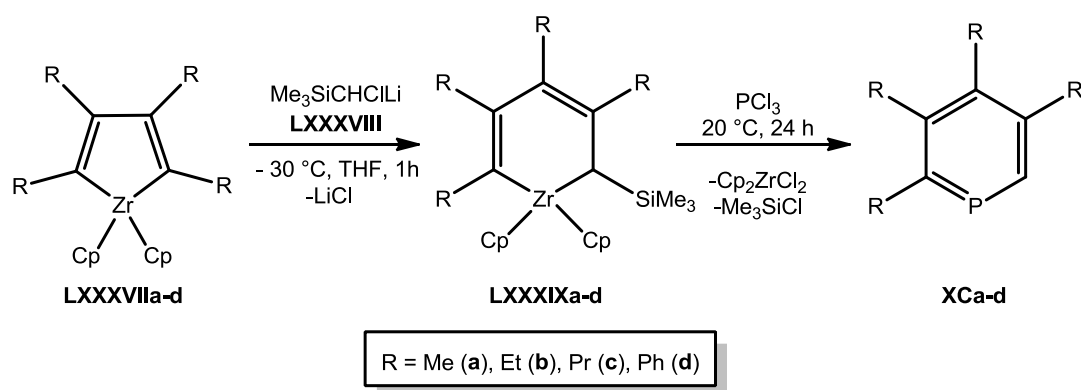
To avoid the use of reactive carbenes or explosive and toxic diazoalkanes, several more systems to transfer carbene fragments, *e.g.* methylene (CH_2), were developed. One of these systems is a mixture of trimethylsulfoxonium iodide ($[\text{Me}_3\text{SO}]\text{I}$) and KO^tBu in $^t\text{BuOH}$ as solvent.^[66] Similarly, a deprotonation of the trimethylsulfoxonium iodide with NaH can be used to generate the reactive dimethylsulfoxoniummethylid **LXXXIII**.^[67] These systems, using sulfur-ylides, allow easy access to epoxides **LXXXIV** from ketones, oxetanes **LXXXV** from epoxides and tetrahydrofuranes **LXXXVI** from oxetanes (scheme 4.2).^[68]



Scheme 4.2: Stepwise heterocyclic ring expansion reactions using dimethylsulfoxonium-methylid as methylene source (Johnson-Corey-Chaykovsky reaction, R = variable substituents).^[68]

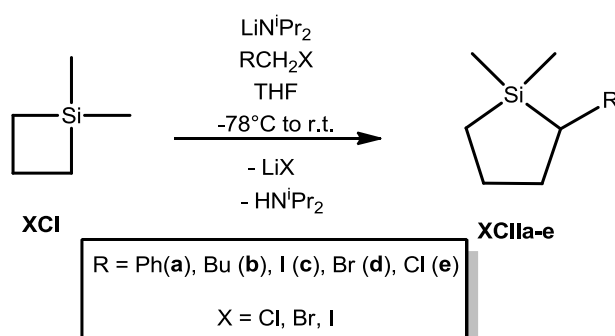
The implementation of non-transition metal carbenoids to mimic the reactivity of carbenes in the preparation of heterocycles is still extremely scarce. The Simmons-Smith reaction, which can efficiently be used in cyclopropanation reactions or epoxide formation reactions,^[23] was rarely used in ring expansion reactions, so far. To the best of my knowledge (SciFinder search from 10th of May 2017), reactions of zirconium carbenoids with epoxides have not been described.

Newer developments involve the use of Li/Cl carbenoids, easily accessible by deprotonation of the corresponding halo alkanes with strong bases (e.g. LDA), for the ring expansion of different heterocycles.^[69–71] Three of those reactions shall be shown exemplarily. The reaction of zirconacycles **LXXXVIIa-d** with the sila-neopentyl Li/Cl carbenoid **LXXXVIII** led to valuable precursors (**LXXXIXa-d**) for the synthesis of phosphinines **XCa-d**.^[69]



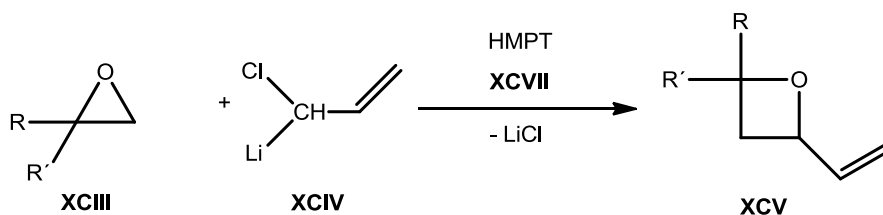
Scheme 4.3: Carbenoid ring expansion and subsequent phosphinine formation using zircona-cyclopentadienes **LXXXVIIa-d**.^[69]

The second example is the ring expansion reaction of silacyclobutane **XCI** with Li/X carbenoids to yield silacyclopentanes **XCIla-e**.^[70]



Scheme 4.4: Ring expansion of 1,1-dimethylsilacyclobutane **XCI** with different Li/halogen carbenoids.^[70]

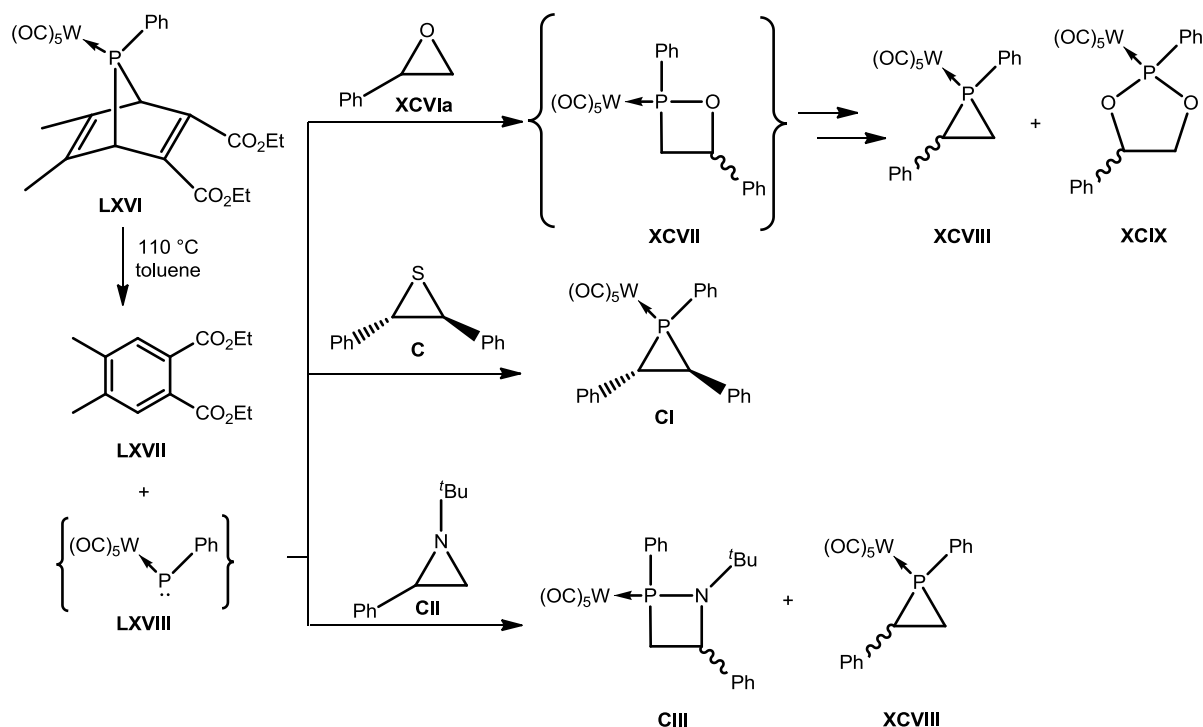
Li/Cl carbenoid **XCIV** was used in ring expansion reactions of different 1,1'-disubstituted epoxides **XCIII**, which was described by Migniac in 1985.^[71]



Scheme 4.5: Ring expansion reaction of epoxides using Li/Cl carbenoids **XCIV** (R, R' = various organic substituents).^[71]

In contrast to the insertion reactions of carbene equivalents in carbon chemistry, only two attempts towards ring expansion reactions of epoxides utilizing terminal phosphinidene complexes being isolobal to carbenes were published prior to this work.^{[72][73]}

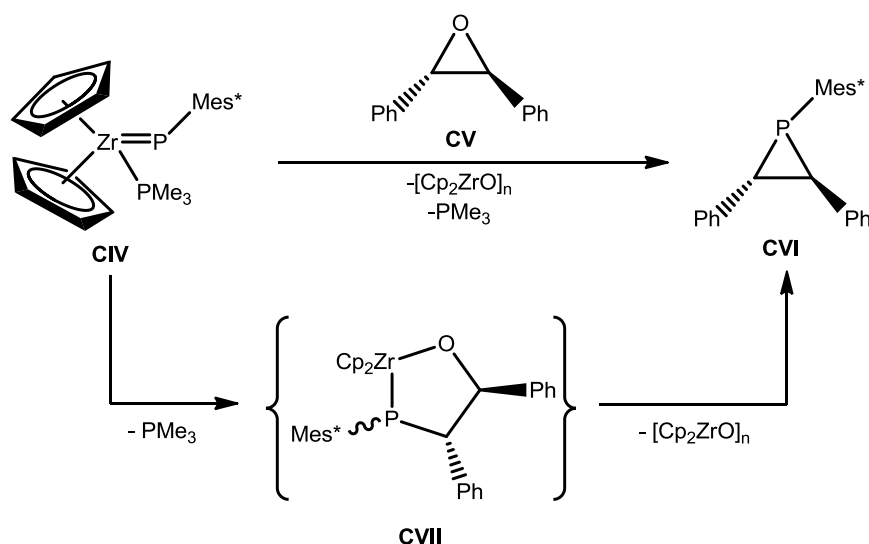
The first such ring expansion reaction to a 1,2-oxaphosphetane complex **XCVII** was proposed by Mathey *et al.* 1987 to occur in the thermal reaction of a 7-phosphanorbornadiene complex (**LXVI**) with styrene oxide **XCVIa** (scheme 4.6)^[72] but only a mixture of a phosphirane (**XCVIII**, 9 % isolated yield) and a 1,3-dioxaphospholane complex (**XCIX**, 46 % isolated yield) was obtained. It should be emphasized here that, while the comparable reaction with a thiirane (**C**) only led to the corresponding phosphirane complex **CI**, the reaction with an aziridine derivative (**CII**) gave a 1,2-azaphosphetane complex as insertion product (**CIII**, 40 % isolated yield, obtained as mixture of isomers).



Scheme 4.6: Reactions of a transient, terminal electrophilic phosphinidene complex **LXVIII** with different three membered heterocycles, published by Mathey *et al.* in 1987.^[72]

Because the reaction of the terminal electrophilic phosphinidene complex developed by Mathey was only performed at elevated temperatures, it is worthwhile to compare it to the described reaction of *trans*-stilbene oxide (**CV**) with the isolable, terminal nucleophilic phosphinidene complex **CIV** (scheme 4.7). This comparison illustrates several problems, e.g. the nature of the metal complex fragment coordinated to the phosphorus centre which has to be tuned accordingly.

The reaction reported by Stephan *et al.* showed, that the nucleophilic terminal phosphinidene complex **CIV** does not yield the product of an insertion reaction but phosphirane **CVI** in a formal exchange of the O atom for a PR unit.^[73] This formal exchange proves the close relation between nucleophilic phosphinidene complexes and the electronically comparable and similarly reacting Schrock-type carbene complexes.

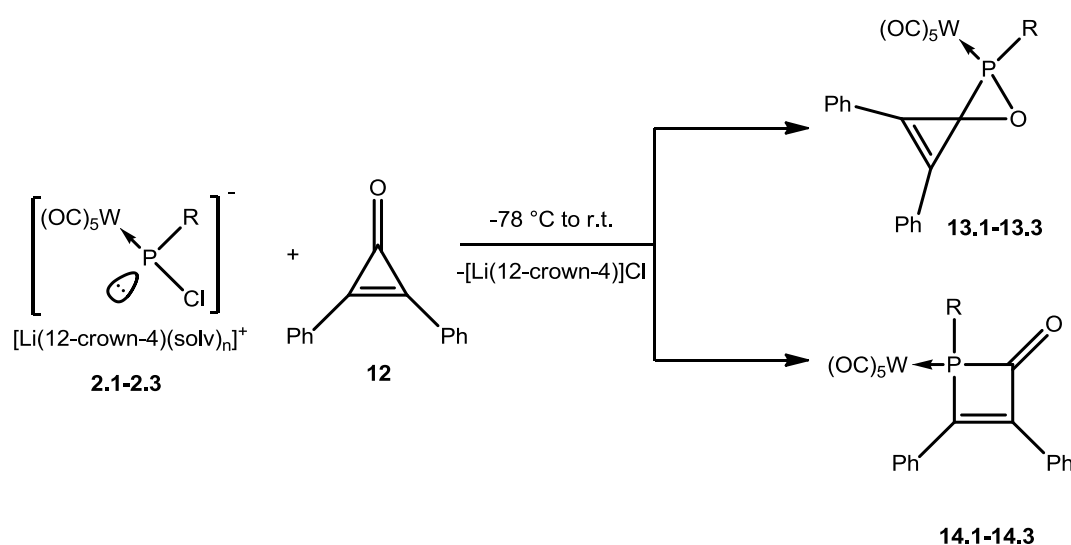


Scheme 4.7: Reactions of transient terminal nucleophilic phosphinidene complex **CIV** with *trans*-stilbene oxide (**CV**) by Stephan *et al.*^[73]

In comparison to the well-established carbene transfer reagents, it would be of interest to have a phosphinidene-transfer reagent that is able to perform ring expansion reactions. In this regard, a good alternative to the only transiently formed electrophilic phosphinidene complexes are often Li/Cl phosphinidenoid complexes (see chapter 1.2), allowing for a better control of the reaction while preserving the reactivity. Advantageous is that these complexes can be generated and used at low temperature, so that Lewis acid or thermally induced follow-up reactions are suppressed.

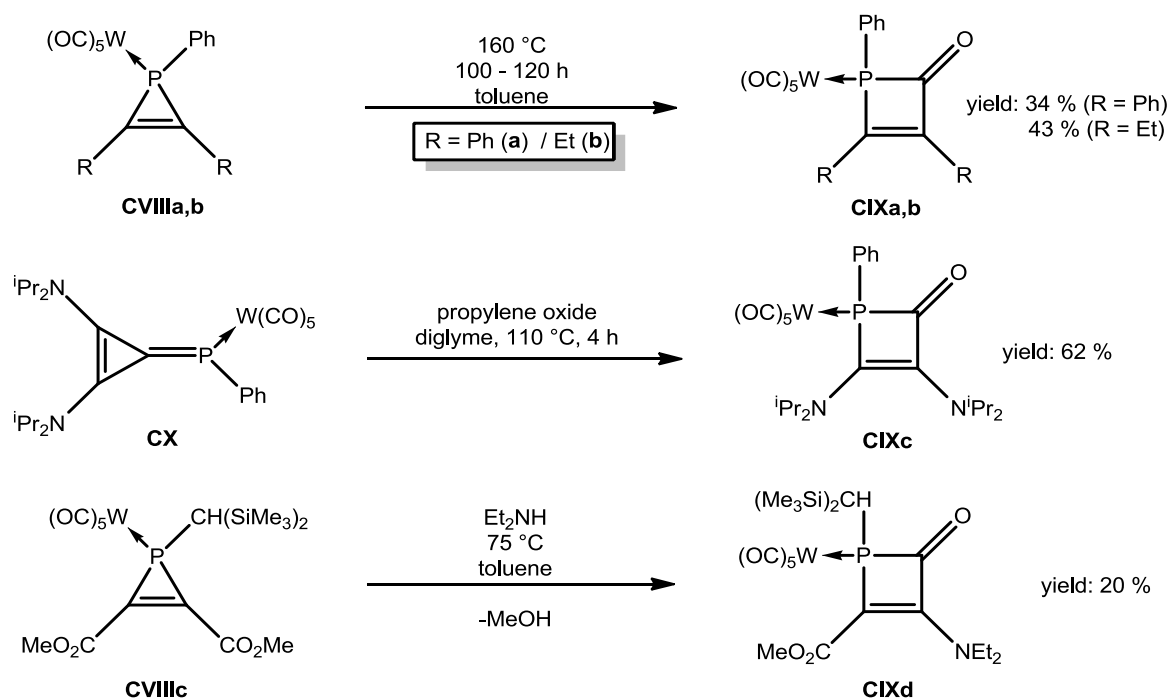
4.2 Insertion reactions of Li/Cl phosphinidenoid complexes into cyclopropenone

Previous work in the research group of Streubel only provided one example of a formal insertion of a P₁ fragment, originating from Li/Cl phosphinidenoid complexes, into a strained heterocycle:^[74] the reaction of Li/Cl phosphinidenoid complex **2.1** with diphenylcyclopropenone **12** did not yield the expected spirocyclic oxaphosphirane complex **13.1**. Instead, 1,2-dihydrophosphet-2-one complex **14.1**, a phosphorus analogue of unsaturated β-lactams was formed by the formal insertion of a phosphinidene fragment into a C-C bond of the three-membered ring, was obtained (scheme 4.8).



Scheme 4.8: Ring expansion reaction of diphenylcyclopropenone to 1,2-dihydrophosphet-2-one complexes **14.1-14.3** using different Li/Cl phosphinidenoid complexes.

It should be noted that such 1,2-dihydrophosphet-2-one complexes (**CIXa-d**) have been prepared previously by three other methodologies (scheme 4.9): The intramolecular ring expansion of 1*H*-phosphirene complexes **CVIIIa,b** with carbon monoxide,^[75] the oxidation of phosphalkene complex **CX** with propylene oxide,^[76] and the ring expansion of 1*H*-phosphirene complex **CVIIIc** in combination with an aminolysis.^[77] All three methodologies required tediously prepared starting materials and, especially in the first two cases, harsh reaction conditions. Despite the multi-step preparation of these complexes, a first reactivity study was presented by Mathey in 1985 showing the synthetic potential of these complexes by oxidative decomplexation,^[75] hydrolysis under basic conditions, aminolysis and the reduction of the C=O unit with NaBH₄ or LiAlH₄.^[78]



Scheme 4.9: Previously described syntheses of 1,2-dihydrophosphet-2-one complexes **CIXa,b**,^[75] **CIXc**^[76] and **CIXd**.^[77]

To exploit and compare the results obtained by Klein, the reaction of diphenylcyclopropanone **12** with the *P*-C₅Me₅-substituted Li/Cl phosphinidenoid complex **2.2** was performed.

The reaction yielded selectively one complex that could be isolated by extraction from the reaction mixture with *n*-pentane and assigned to the corresponding 1,2-dihydrophosphet-2-one complex **14.2**. The resonance signal in the ³¹P NMR spectra at 111.0 ppm as well as the ¹J_{W,P} coupling constant of 233.5 Hz are in good accordance to the ones described before by Klein ($\delta^{31}\text{P} = 91.5$ ppm, ¹J_{W,P} = 230.2 Hz) and a second derivative prepared by Mathey showed similar values (e.g. R = R' = R'' = Ph, M = W, $\delta^{31}\text{P} = 86.9$, ¹J_{W,P} = 231.9 Hz).^[75]

Finally, support for the proposed molecular structure of **14.2** could be obtained from a single crystal diffraction study (figure 4.1).

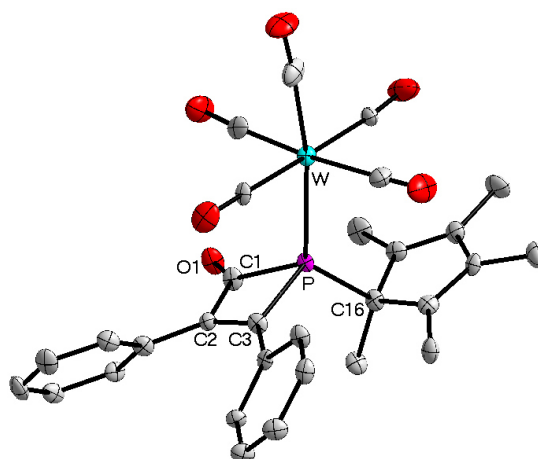


Figure 4.1: DIAMOND plot of the molecular structures of 1,2-dihydrophosphet-2-one complexes **14.2** in the solid state; the thermal ellipsoids are set at 50 % probability level and all hydrogen atoms are omitted for clarity. Selected bond lengths in Å and angles in °: W-P 2.5004(17), P-C1 1.905(7), P-C3 1.857(6), P-C16 1.877(7), C2-C3 1.362(9), C3-P-C1 70.9(3).

The data for the molecular structure (figure 4.1) show consistency compared to the complex obtained by Klein.^[74] The ring system is characterized by the C2-C3 bond length of 1.362(9) Å.

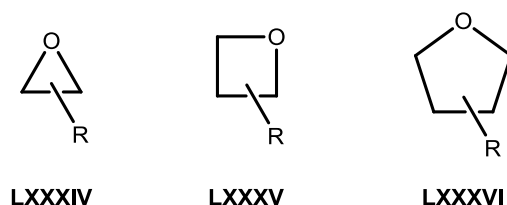
The corresponding complex, bearing the *P*-CPh₃ substituent was synthesized recently by Junker, showing similar NMR and bonding parameters.^[79]

The observations made for these first insertion reactions gave rise to the fundamental question, if strained heterocycles in general can be used in such ring expansion reactions and, hence, providing access to novel four-membered E,P-heterocyclic ligands. The results of these investigations will be presented and discussed in the following chapters.

5 Synthesis of 1,2-oxaphosphetane complexes by insertion into epoxides

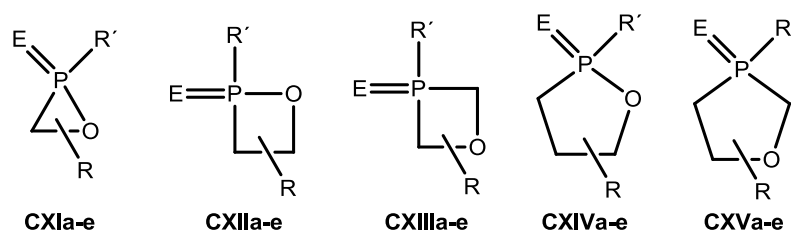
5.1 Introduction to small-sized O,P-heterocycles

Ethylene oxide (oxirane, R = H), as the most important single derivative of the oxiranes (**LXXXIV**, scheme 5.1), and other small-sized O-heterocycles are amongst the most useful building blocks in organic chemistry and material science.^[80] Therefore, oxiranes are fine chemicals produced in a scale of several million tons per year. Activation and polymerization reactions can not only be used for oxiranes but also for the less reactive, larger heterocycles such as oxetanes **LXXXV** and tetrahydrofuranes **LXXXVI** (scheme 5.1).^[81]



Scheme 5.1: Oxiranes **LXXXIV**, oxetanes **LXXXV** and tetrahydrofuranes **LXXXVI** (R = various substituents).

Similar to those rings, phosphorus- and oxygen-containing heterocycles gained more and more interest over the last years due to their industrial use in several high-end applications, e.g. the use as additives in flame retardant materials.^[4,5] Therefore the search for new heterocyclic phosphorus-containing building blocks became a desirable task.

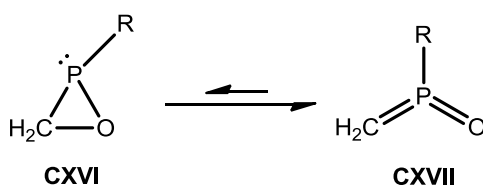


e.g. E = W(CO)₅ (a), O (b), NR' (c), lone pair (d) or R'₂ (e)

Scheme 5.2: Oxaphosphiranes **CXIa-e**, 1,2-oxaphosphetanes **CXIIa-e**, 1,3-oxaphosphetanes **CXIIIa-e**, 1,2-oxaphospholanes **CXIVa-e** and 1,3-oxaphospholanes **CXVa-e** (R, R' = variable organic substituents).

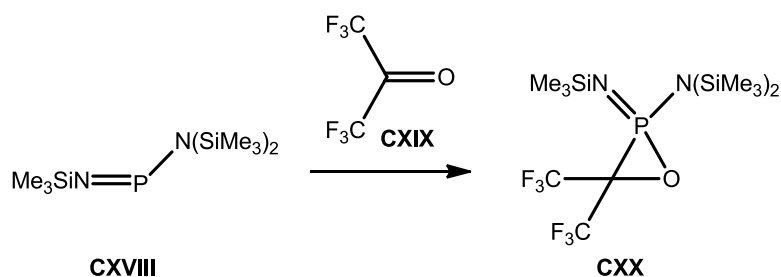
Based on the high importance of the small oxygen-containing saturated heterocycles in carbon chemistry it surprises that most σ^4, λ^5 -P and σ^5, λ^5 -P derivatives of the O,P-heterocycles are still poorly investigated and almost no σ^3, λ^3 -P derivatives are known. Several problems for the syntheses of such ring systems were described in the literature, but also some stable derivatives thereof. For the σ^3, λ^3 -oxaphosphiranes (**CXId**), problems in the

syntheses of suitable precursors and in adaptation of the reactions used for the syntheses of oxiranes were hampering research for a long time. For example oxidation of unligated phosphalkenes with *m*-CPBA does not yield oxaphosphiranes but the corresponding phosphalkene *P*-oxides (= alkylidene(oxo)phosphoranes).^[82,83] In addition, the three-membered σ^3, λ^3 -phosphorus heterocycles are prone to ring opening under valence isomerization. First such predictions, based on theoretical calculations of ring systems having a symmetric PA_2 constitution, led to the assumption that the equilibrium for oxaphosphiranes is on the side of the open form isomer (scheme 5.3).^[84] Very recently, a new theoretical study provided first insights into the situation of oxaphosphiranes and transition metal complexes thereof.^[85]



Scheme 5.3: Postulated valence isomerization of σ^3, λ^3 -oxaphosphiranes (R = H, CH₃, F, NH₂)^[84]

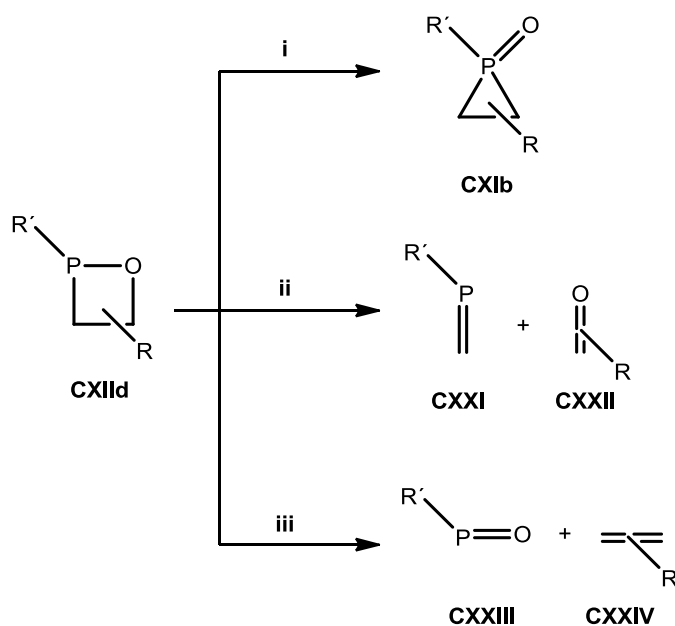
Only very few derivatives of P^V -oxaphosphiranes were reported so far.^[86,87] In one case an equilibrium between the oxaphosphirane and its dimer was found,^[88] making further investigations of its specific reactivity impossible. An isolable σ^4, λ^5 -oxaphosphirane (**CXX**) was presented by Röschenthaler and Schmutzler in 1978, obtained from the reaction of iminophosphane **CXVIII** with hexafluoroacetone **CXIX** (scheme 5.4). The rearrangement is prevented by the double bonded P-substituent and dimerization is suppressed by introduction of sterically demanding substituents.



Scheme 5.4: Synthesis of the first σ^4, λ^5 -oxaphosphirane derivative^[86]

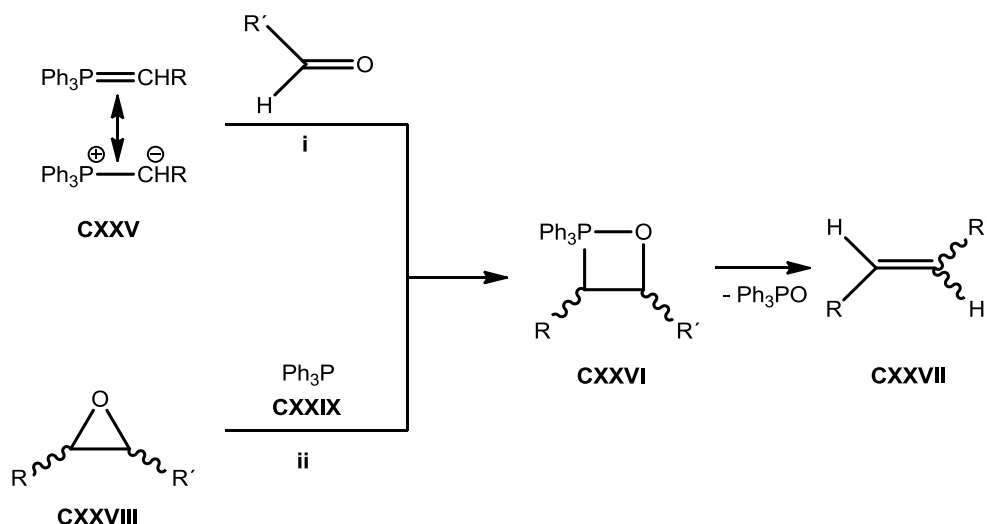
No σ^3, λ^3 -oxaphosphetanes are known to date which is somewhat surprising. A retrosynthetic analysis leads to various scenarios (scheme 5.5): an isomerization to a three-membered σ^4, λ^5 -phosphirane oxide **CXib** (i) could occur, which, due to the existence of such a phosphirane oxide,^[89] seems to be feasible (but isomerization is unknown). Other possibilities would be [2+2] retroaddition reactions forming phosphalkenes **CXXI** and carbonyl derivatives **CXXII** (ii) or to form phosphinidene oxides **CXXIII** and corresponding

alkene derivatives **CXXIV** (iii). Both types of reactions have not been described, but the inverse reaction of **ii** was tried and in the reaction of hexafluoroacetone with a phosphalkene in a ratio of 2:1, a 1,3,2-dioxaphospholane was formed.^[90]



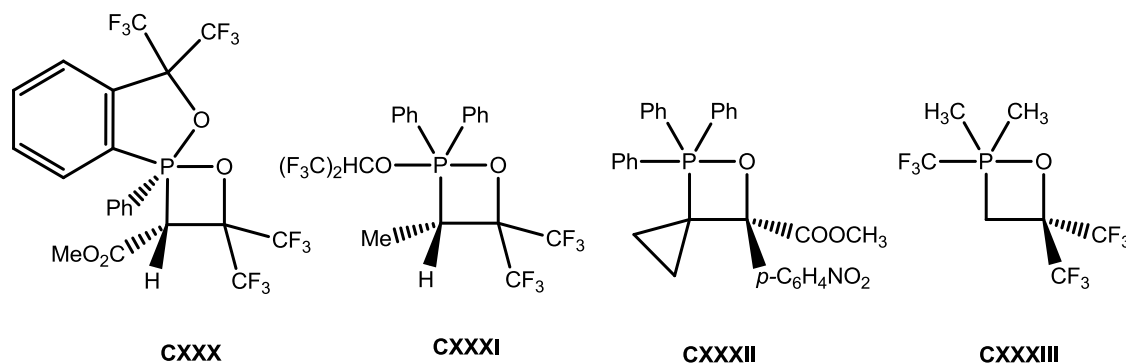
Scheme 5.5: Hypothetical rearrangement and decomposition pathways of 1,2 σ^3 , λ^3 -oxaphosphetanes.

In contrast, 1,2 σ^5 , λ^5 -oxaphosphetanes already had a great impact on phosphorus chemistry in the past and were investigated in great detail. The reaction between aldehydes or ketones and phosphonium ylides **CXXV** which led to alkene formation was first presented by Wittig in 1953,^[91,92] representing a fundamental breakthrough in the use of strained phosphorus heterocycles in organic synthesis.^[93] Great effort was invested to clarify the reaction mechanism and 1,2 σ^5 , λ^5 -oxaphosphetanes **CXXVI** were proposed as key intermediates in the reaction (scheme 5.6),^[94] and their formation was verified by ^{31}P NMR measurements. During the past decades several derivatives could be isolated and characterized, including single crystal X-ray results (scheme 5.7).^[95–97] Nevertheless, also betaines and several equilibria between stereoisomers of the 1,2-oxaphosphetanes are involved in the reaction mechanism proposed today.^[13]



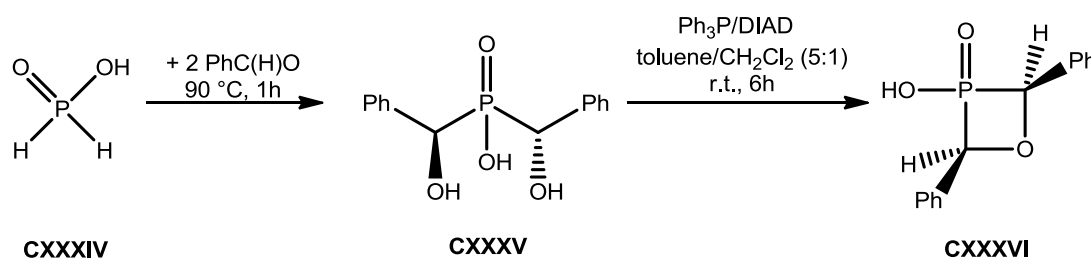
Scheme 5.6: 1,2 σ^5 , λ^5 -oxaphosphetane rings in the simplified mechanism for the Wittig reaction (i)^[91,92] and in the deoxygenation of epoxides with triphenylphosphane (ii).^[98]

Interestingly, such 1,2 σ^5 , λ^5 -oxaphosphetanes were also proposed as intermediates in the deoxygenation reactions of epoxides using σ^3 , λ^3 -phosphanes.^[98] This would be a remarkable similarity to the formal ring expansion reaction by insertion of carbenes into epoxides.



Scheme 5.7: Examples of by single crystal X-ray diffraction studies characterized 1,2 σ^5 , λ^5 -oxaphosphetanes (CXXX^[95], CXXXI^[97], CXXXII^[96], CXXXIII^[99]).

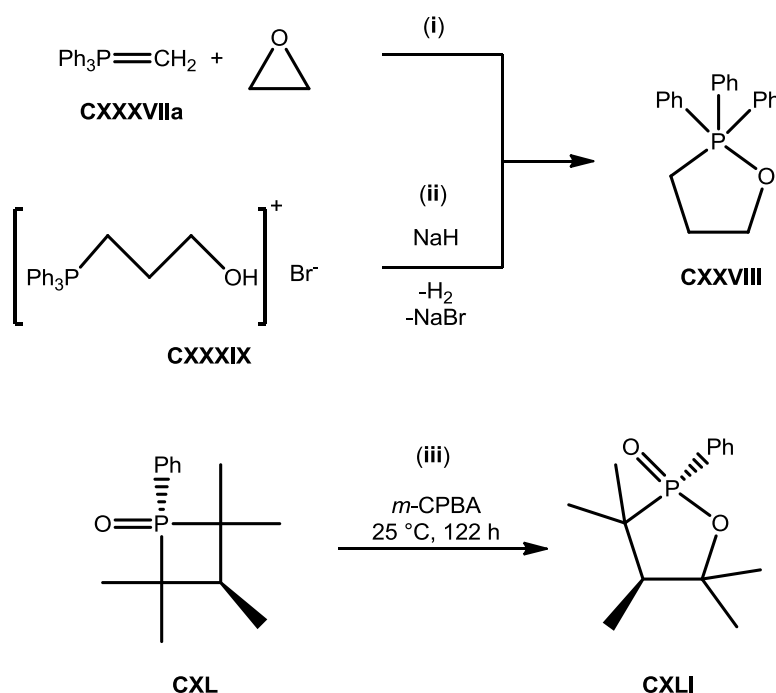
It is also noteworthy that regioisomeric 1,3 σ^4 , λ^5 -oxaphosphetanes, e.g. **CXXXVI**, were synthesized by an intramolecular Mitsunobu reaction (scheme 5.8).^[100]



Scheme 5.8: Example of the synthesis of 1,3 σ^4 , λ^5 -oxaphosphetanes^[100] (DIAD = diisopropyl azodicarboxylate)

Similar to the situation of oxaphosphetanes, 1,2- as well as 1,3-oxaphospholanes are possible regioisomers for this five-membered ring system. Several synthetic strategies were developed for the synthesis of 1,2 σ^5, λ^5 -oxaphospholanes **CXXXVIII**. These involve insertions of ylides (e.g. **CXXXVII**) into epoxides (**i**, scheme 5.9),^[101] the reaction of triphenylphosphane with 3-bromopropanol and ring closing by subsequent dehydrohalogenation from the phosphonium salt **CXXXIX** (**ii**, scheme 5.9)^[102] or the oxidation of a phosphetane-oxide (**CXL**) with *m*-CPBA to the corresponding Bayer-Villiger product **CXLI** (**iii**, scheme 5.9).^[103]

In contrast to the three- and four-membered heterocycles, also 1,2 σ^3, λ^3 -oxaphospholane derivatives are known.^[104] Surprisingly, the 1,3-oxaphospholanes are even less investigated, which might be due to their missing synthetic accessibility, as only very few multi-step syntheses were described so far.^[105]



Scheme 5.9: Synthetic routes to 1,2 σ^5, λ^5 -oxaphospholane (**CXXXVIII**)^{[101][102]} and a 1,2 σ^4, λ^5 -oxaphospholane (**CXLI**).^[103]

Of special interest for further functionalization are the derivatives containing a P-O bond, as rings containing only C-O or P-C bonds (1,3-oxaphosphetanes and 1,3-oxaphospholanes) are reacting very similar to their carbon derivatives, while the phosphorus atom mainly plays a spectator role. Therefore focus of this work was placed on the P-O containing ring systems.

As the background picture suggested, blocking of the phosphorus lone pair could suppress decomposition and, hence, allow for the synthesis and isolation of the first derivatives of 1,2 σ^3, λ^3 -oxaphosphetanes, e.g. by coordination to a transition metal. In particular, as there is

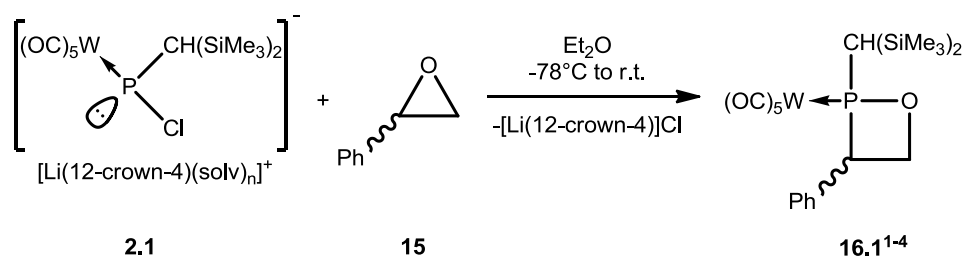
ample precedence from oxaphosphirane chemistry as research by Mathey^[82] and Streubel^{[31][106]} has revealed. The development of synthetic strategies to and investigation of the reactivity of oxaphosphirane complexes **CXIa** have been longstanding areas of research.^[107–110] In contrast, no 1,2-oxaphosphetane complexes **CXIIa** and only two examples of 1,2-oxaphospholane complexes **CXIVa** were described so far.^[111,112]

5.2 Synthesis of *P*-bis(trimethylsilyl)methyl-substituted 1,2-oxaphosphetane derivatives

5.2.1 The reactions with monosubstituted epoxides

As discussed before (see chapter 4.1), formal ring expansion reaction of epoxides using a terminal phosphinidene complex fragment (P_1 fragment) could lead to 1,2-oxaphosphetane complexes, but only one unsuccessful attempt has been described so far.^[113] Based on the previous successful ring expansion reaction of a cyclopropanone derivative (see chapter 4),^[74] a novel method for the synthesis of 1,2-oxaphosphetane complexes was envisaged: the reaction of Li/Cl phosphinidenoid complexes with oxirane derivatives.

In an early study, Bode has speculated that in the thermal reaction of a *P*-CH(SiMe₃)₂-substituted 2*H*-azaphosphirene complex with styrene oxide or propylene oxide 1,2-oxaphosphetane complexes are formed, besides several other products.^[113] More recently, Nesterov gained further evidence for the targeted complexes using **2.1** and styrene oxide **15** (scheme 5.4) and, although these reaction showed a significantly increased selectivity compared to the one previously described by Bode, isolation and full characterization of the products was not achieved; furthermore, the assignment of the unusual ³¹P chemical shift of the products could not be asserted. Nevertheless, the continued progress in Li/Cl phosphinidenoid complex chemistry provided further stimulus to start a detailed investigation.



Scheme 5.10: Reaction of Li/Cl phosphinidenoid complex **2.1** with styrene oxide (**15**).

Hereafter, the in-depth study on the formation of 1,2-oxaphosphetane complexes will be presented. Firstly, the reaction from Nesterov was repeated under different conditions (figure 5.1). Changing the solvent from THF to Et_2O showed a first slight increase in selectivity. A little excess of the epoxide (up to 2.8 equivalents) could be effectively used to suppress the formation of diphosphene complexes (derived from self-reactions of **2.1**) in most cases.^[31] Addition of Cu(I)Cl (1 equivalent) as additional Lewis acid, to activate the epoxide via a proposed Cu-O coordination, showed only a negligible influence on the selectivity. The highest selectivity was observed if an excess of 12-crown-4 was employed, but unfortunately the excess crown ether was extremely difficult to separate during further work-up. Therefore,

the isolation of the complex was attempted using standard reaction conditions (one equivalent ^tBuLi, one equivalent 12-crown-4 and diethyl ether as solvent, figure 5.1).

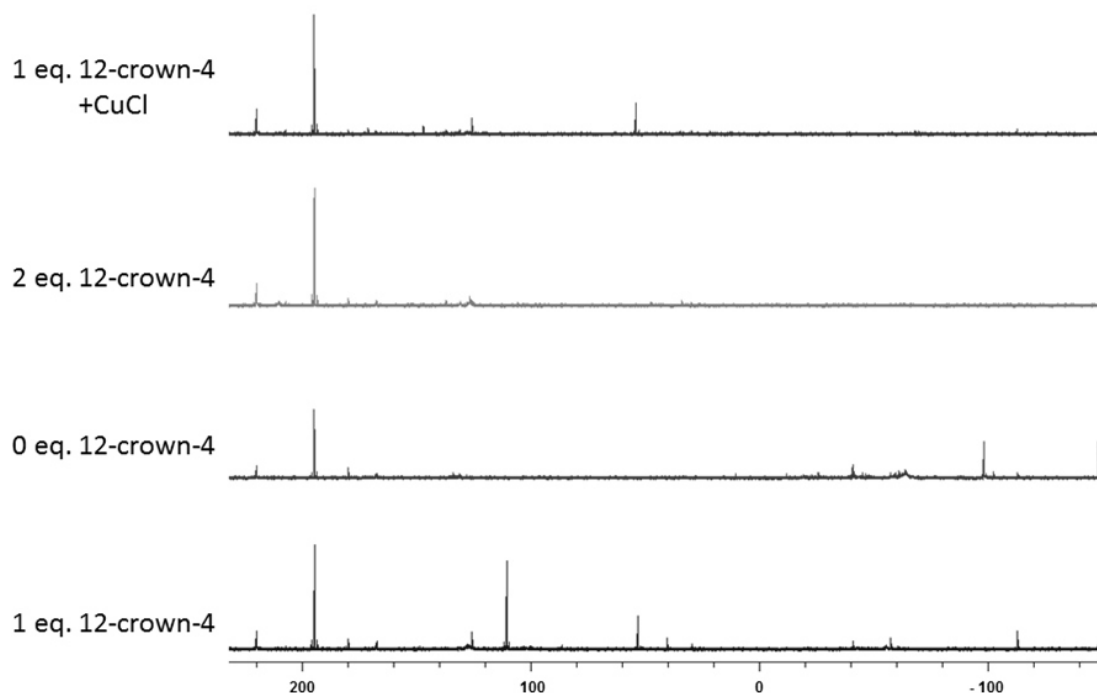


Figure 5.1: ³¹P{¹H} NMR spectra for the reaction mixtures of Li/Cl phosphinidenoid complex **2.1** and styrene oxide in Et₂O under different reaction conditions.

After optimization of the conditions, it was achieved to obtain complexes **16.1** as mixture of isomers. The complexes showed a surprisingly high thermal stability, *i.e.* a very slow, unselective decomposition of a mixture of isomers (ratio 40:4:53:3) was observed starting at 100 °C.

Four signals with similar ³¹P{¹H} NMR spectroscopic parameters were observed (Figure 5.2 and table 5.1).

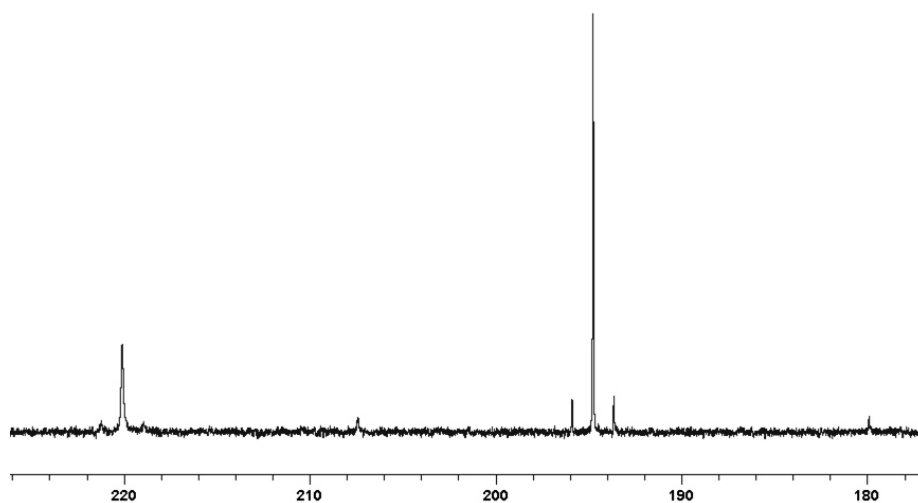
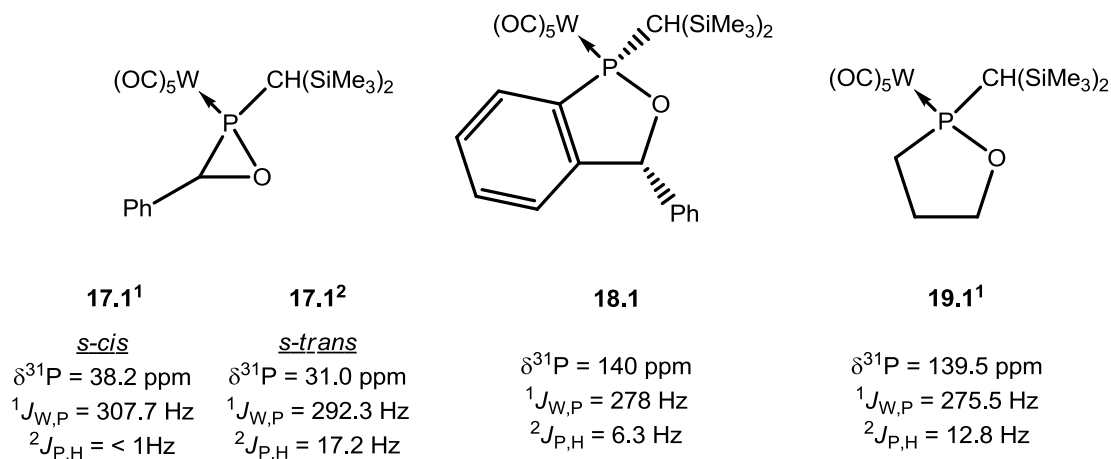


Figure 5.2: ³¹P{¹H} NMR spectrum for complexes **16.1**¹⁻⁴ after isolation from the reaction mixture (in CDCl₃).

NMR spectroscopic measurements revealed that the four signals could be assigned to four isomers of the corresponding 1,2-oxaphosphetane complexes **16.1**¹⁻⁴, showing ³¹P resonance signals at much lower field than it would be anticipated based on data of oxaphosphirane complexes **17.1**^{1[106]} and **17.1**^{2[114]} and 1,2-oxaphospholene complex **18.1**^[115,116] or 1,2-oxaphospholane complex **19.1**¹ (scheme 5.11, for complex **19.1**¹ see chapter 6).



Scheme 5.11: Examples of different O,P-heterocyclic ligands, ³¹P NMR data as well as the exocyclic ²J_{P,H} couplings for oxaphosphirane complexes **17.1**^[106] and **17.1**^[114], oxaphospholene complex **18.1**^[115,116] and 1,2-oxaphospholane complex **19.1**¹ (all measured in CDCl₃).

The most interesting NMR feature is the magnitude of the exocyclic ²J_{P,H} coupling constant. Two of the isomers (**16.1**^{3,4}) showed coupling constants of approximately 19.5 Hz while the other two (**16.1**^{1,2}) showed far lower coupling constant magnitudes of approximately 5 Hz. This is an indication that the mixture contains two types of atropisomers, one in which the CH-proton of the CH(SiMe₃)₂ substituent is oriented towards the metal fragment (*s-cis*) and one in which the proton is oriented in the opposite direction (*s-trans*). This dependency was observed several times before in oxaphosphirane complex chemistry and the correlation between the orientation and coupling constant was proven by Peréz via independent synthesis of the two atropisomeric complexes **17.1**^{1[106]} and **17.1**^{2.[114]} Complex **16.1**¹ was obtained in almost pure form (98% of **16.1**¹) by extraction of the other isomers with *n*-pentane and recrystallization from diethyl ether, containing only small amounts of **16.1**³.

Table 5.1: Selected NMR characteristics of the isomers of the first isolated 1,2-oxaphosphetane complexes. (measured in CDCl₃, [a] broadened signal, [b] not observed due to low signal/noise ratio)

	³¹ P{ ¹ H} NMR		¹ H NMR (P-CH(SiMe ₃) ₂)		ratio 1:2:3:4
	δ [ppm]	¹ J _{W,P} [Hz]	δ [ppm]	² J _{P,H}	
16.1 ¹	220.2	275.4	2.25	6.4	40
16.1 ²	210.7 ^[a]	- ^[b]	1.70	4.0	4
16.1 ³	195.1	273.1	2.59	19.4	53
16.1 ⁴	179.7	281.1	2.29	19.5	3

Mass spectrometric measurements confirmed the molecular composition of the mixture of **16.1**¹⁻⁴ as C₂₀H₂₇O₆PSi₂W and an elemental analysis using the isomer mixture was performed, and the result was in accordance with the elemental composition. Based on this, the successful insertion of the P₁-fragment into the epoxide was proposed and the ring constitution was finally confirmed by a single crystal X-ray diffraction study (Figure 5.3).

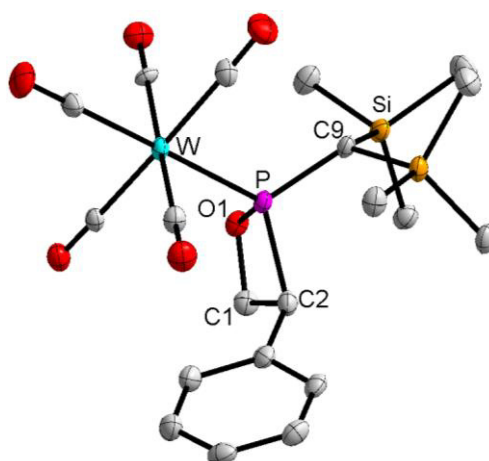
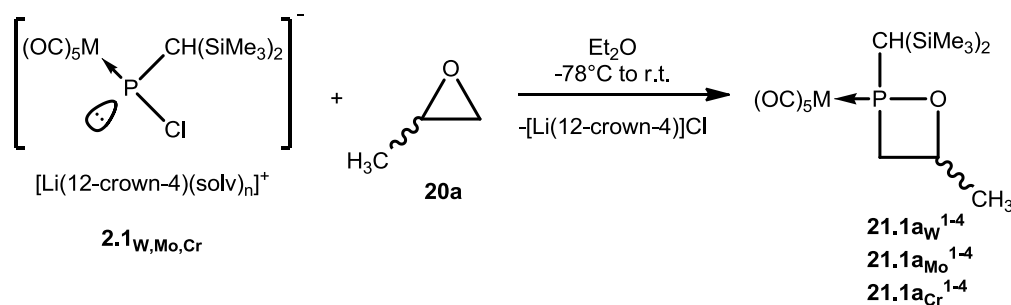


Figure 5.3: DIAMOND plot of the molecular structure of 1,2-oxaphosphetane complex **16.1** in the solid state; the thermal ellipsoids are set at 50 % probability level and all hydrogen atoms are omitted for clarity. Selected bond lengths in Å and angles in °: W-P 2.4749(11), P-O1 1.677(3), P-C2 1.894(5), P-C9 1.820(4), C1-C2 1.537(6), C1-O1 1.458(5), C2-P-O1 79.20 (18), P-C2-C1 84.5(3), C2-C1-O1 99.2(3), C1-O1-P 95.3(3), C9-P-O1 107.28, C2-P-C9 109.76(19), O1-P-W 111.47(11), C2-P-W 124.78(14), C9-P-W 116.91(15).

The molecular structure of **16.1** shows the non-planar four-membered POCC-ring as main ligand motif and proves that the reaction took place at the benzylic position of the styrene oxide, yielding the corresponding 3-regioisomer of the 1,2-oxaphosphetane complex. This is in contrast to the expected attack at the least hindered side of the epoxide, but typical for styrene oxide as the benzylic position is the most electrophilic one.^[117]

All bond lengths, also for the bonds in the ring, are in the expected range for single bonds and show neither a significant elongation nor shortening. The bond angles in the ring represent the four membered heterocycle with the sum of all four ring angles equals 358.2° being almost exactly the geometrically expected, but bond angles between 79.2 and 99.2° were found. In addition, the ring shows a slight folding with a folding angle of 14.2°.

Surprisingly, the selectivity of the reactions increased drastically when alkyl-substituted epoxides were used. For example, the reaction of the *P*-CH(SiMe₃)₂-substituted Li/Cl phosphinidenoid complex **2.1** with propylene oxide (**20a**) in diethyl ether led to a mixture of four isomers of the 1,2-oxaphosphetane complex **21.1a_w** in high selectivity (ratio see table 5.2). A minor side-product with a resonance signal at 103 ppm (less than 1 % by ³¹P NMR-integration) was observed; the nature of the side product and its formation will be discussed in chapter 5.2.2.



Scheme 5.12: The reaction of Li/Cl phosphinidenoid complexes **2.1_w**, **2.1_{Mo}** and **2.1_{Cr}** with propylene oxide **20a**.

To broaden the scope of the reaction, a set of 1,2-oxaphosphetane complexes was synthesized using the homologous Li/Cl phosphinidenoid complexes **2.1_w**, **2.1_{Mo}** and **2.1_{Cr}**, bearing the different group 6 metal pentacarbonyl fragments. A selective reaction was observed in all cases, but a drop in yield for the Mo and Cr complexes was found, compared to **21.1a_w** (table 5.2).

Complexes **21.1a_{w-Cr}** showed similar analytic characteristics and only a small influence of the metal fragment on the isomeric ratio was observed. The amount of **21.1a_{Cr}¹** and **21.1a_{Cr}³** is slightly reduced (about 10 %) in favour of isomer **21.1a_{Cr}⁴** (table 5.2). A typical shift of the resonance signal to lower field is observed when comparing the W, Mo and the Cr derivatives ($\Delta\delta$ W/Mo \sim 32 ppm, $\Delta\delta$ Mo/Cr \sim 25 ppm).

Table 5.2: ³¹P{¹H} NMR data (CDCl₃) and yields for the *C*-Me-substituted 1,2-oxaphosphetane complexes **21a_w-21a_{Cr}** (^[a] not determined due to low signal/noise ratio).

	³¹ P [ppm] (¹ J _{W,P} [Hz])				ratio [1:2:3:4]	yield [%]
	Isomer 1	Isomer 2	Isomer 3	Isomer 4		
21.1a_w¹⁻⁴	176.4 (273.4)	169.2 - ^[a]	164.5 (267.8)	164.4 (268.7)	30:4:19:47	58
21.1a_{Mo}¹⁻⁴	209.8	201.0	196.2	195.7	30:6:46:18	27
21.1a_{Cr}¹⁻⁴	233.1	226.7	222.6	221.0	23:3:14:60	11

A similar, typical influence was observed for the CO resonance signals in the $^{13}\text{C}\{^1\text{H}\}$ NMR spectra, *i.e.* the resonance signals are shifted towards lower field in going from W to Mo and Cr ($\Delta\delta$ W/Mo \sim 8 ppm (*cis*-CO) and \sim 11 ppm (*trans*-CO), $\Delta\delta$ Mo/Cr \sim 11 ppm (*cis*-CO) and \sim 11 ppm (*trans*-CO)). A typical influence on the magnitude of the $^2J_{\text{P,C}}$ coupling constant was also observed, in which the coupling constants are quite similar for W and Mo complexes ($^2J_{\text{P,C}}$ (*cis*-CO) \sim 8 Hz (W) / 10 Hz (Mo), $^2J_{\text{P,C}}$ (*trans*-CO) \sim 24 Hz (W) / 27 Hz (Mo)) and the coupling constants for Cr complexes are significantly different ($^2J_{\text{P,C}}$ (*cis*-CO) \sim 15 Hz (Cr), $^2J_{\text{P,C}}$ (*trans*-CO) \sim 7 Hz (Cr)). While most signals for the ligand systems are similar, a slight influence on the magnitude of the $^1J_{\text{P,C}}$ coupling constants for the P-CH₂ group was observed: in contrast to the data found for the M(CO)₅ unit, the Cr and Mo complexes are quite similar and only the W complexes show slightly higher coupling constants ($\Delta^1J_{\text{P,C}}$ \sim 3-7 Hz).

While the ^1H NMR data are almost identical, a small but significant influence was found for the P-CH(SiMe₃)₂ proton, which experienced a slight highfield-shift in going from W to Cr to Mo ($\Delta\delta$ \sim 0.1 ppm per each derivative) with the magnitudes of the $^2J_{\text{P,H}}$ coupling constants being similar for Cr and W and being significantly smaller for Mo ($\Delta^2J_{\text{P,H}}$ \sim 2-3 Hz, table 5.3). The signals for the W complex are magnified in figure 5.4 to show the observable difference in the coupling constants for the *s-cis* and *s-trans* configured complexes.

Table 5.3: Selected ^1H NMR data (CDCl₃) for the P-CH(SiMe₃)₂ proton of the C-Me-substituted 1,2-oxaphosphetane complexes **21.1a_W**-**21.1a_{Cr}** (^[a] very weak signal, ^[b] not determined due to low signal/noise ratio).

	$\delta^1\text{H}$ [ppm] ($^2J_{\text{P,H}}$ [Hz])			
	Isomer 1	Isomer 2	Isomer 3	Isomer 4
21.1a_W ¹⁻⁴	1.99 (6.2)	2.46 (\sim 19) ^[a]	2.24 (19.5)	1.93 (6.0)
21.1a_{Mo} ¹⁻⁴	1.78 (3.8)	- ^[b]	1.72 (3.3)	1.96 (18.1)
21.1a_{Cr} ¹⁻⁴	1.88 (6.8)	2.30 (20.3)	2.09 (20.0)	1.84 (6.1)

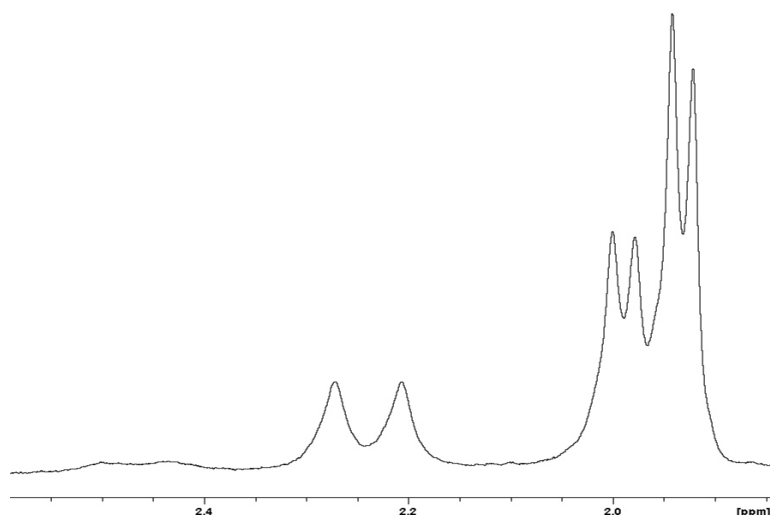


Figure 5.4: Zoom in on the $P\text{-CH}(\text{SiMe}_3)_2$ signals in the ^1H NMR spectrum of complexes **21.1a_w**¹⁻⁴ as example of the signal pattern.

Single crystals that were suitable for X-ray diffraction studies could be obtained for the three complexes from saturated *n*-pentane solutions. All three complexes crystallized in the space group $P2_12_12_1$. The three molecular structures (figure 5.5) show the heterocyclic ligands and similar data for the bond lengths and angles.

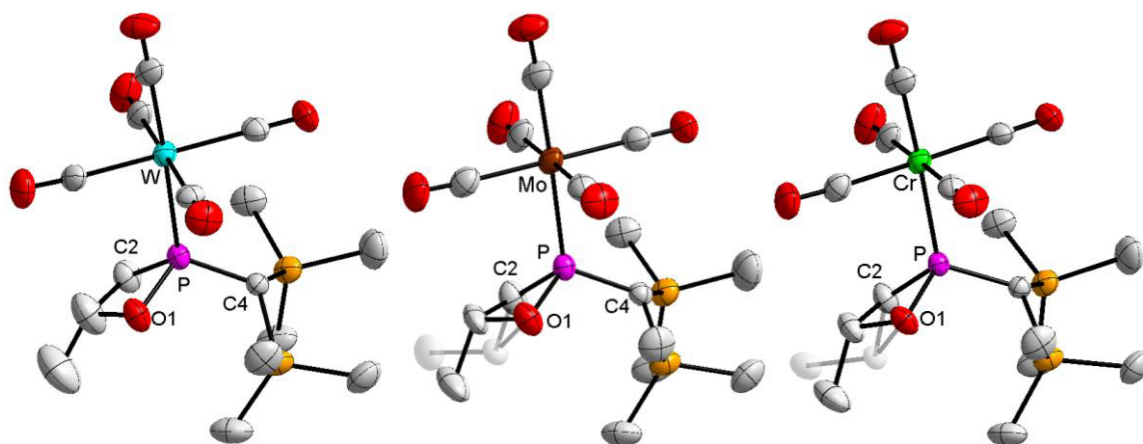


Figure 5.5: DIAMOND plot of the molecular structures of 1,2-oxaphosphetane complexes **21.1a_w**, **21.1a_{Mo}** and **21.1a_{Cr}** (from left to right) in the solid state; the thermal ellipsoids are set at 50 % probability level and all hydrogen atoms are omitted for clarity. The split-site (1:1) for the Me-C unit is represented using a transparent mode for clarity.

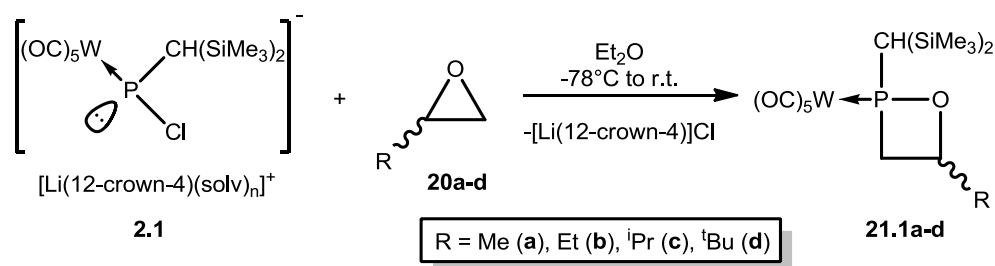
The three molecular structures are isostructural and only the P-M bond for the case $M = \text{Cr}$ is slightly shorter due to the smaller Cr atom. Of special interest are the molecular structures of **21.1a_{Cr}** and **21.1a_{Mo}** as they show that two isomers co-crystallized (substituent at the ring oriented towards or away from the $\text{M}(\text{CO})_5$ fragment). Depending on the orientation of the

C-substituent of the isomer, the ring folds in the opposite direction to reduce the steric interaction of the C-substituent and the P-substituent or the metal fragment (table 5.4).

Table 5.4: Selected bond lengths in Å and angles in ° for 1,2-oxaphosphetane complexes **21.1a_W**-**21.1a_{Cr}** (folding angles are given for solid/transparent part of the splitting).

	P-C2	P-C4	P-M	C2-P-O1	folding angle
21.1a_W	1.827(5)	1.800(5)	2.4846(14)	79.7(2)	21.9
21.1a_{Mo}	1.817(3)	1.806(3)	2.4883(8)	80.03(14)	33.09/16.2
21.1a_{Cr}	1.830(3)	1.807(3)	2.3412(8)	79.90(13)	27.3/20.6

To obtain further insight into the effect of different substituents and the scope of the ring forming reaction, the specifics including the steric demand of the C-substituent at the epoxide was changed stepwise. Therefore the reaction of **2.1** was performed with butylene oxide **20b**, 1,2-epoxy-3-methylbutane **20c** and 3,3-dimethylbutylene oxide **20d** (scheme 5.13).



Scheme 5.13: Syntheses of 1,2-oxaphosphetane complexes **21.1a-d** bearing different sterically demanding C-substituents.

While the reaction was very selective using propylene oxide **20a**, and still quite selective in case of butylene oxide **20b**, first problems were observed in case of 1,2-epoxy-3-methylbutane **20c**. Finally, the reaction with 3,3-dimethylbutylene oxide **20d** led mainly to the diphosphene complexes **22** and **23** and, besides some unknown side products, only in traces to the 1,2-oxaphosphetane complexes **21.1d**¹⁻⁴. Direct comparison of the four reaction spectra clearly shows how the selectivity is influenced by the steric demand of the substituent R at the epoxide ring (figure 5.6).

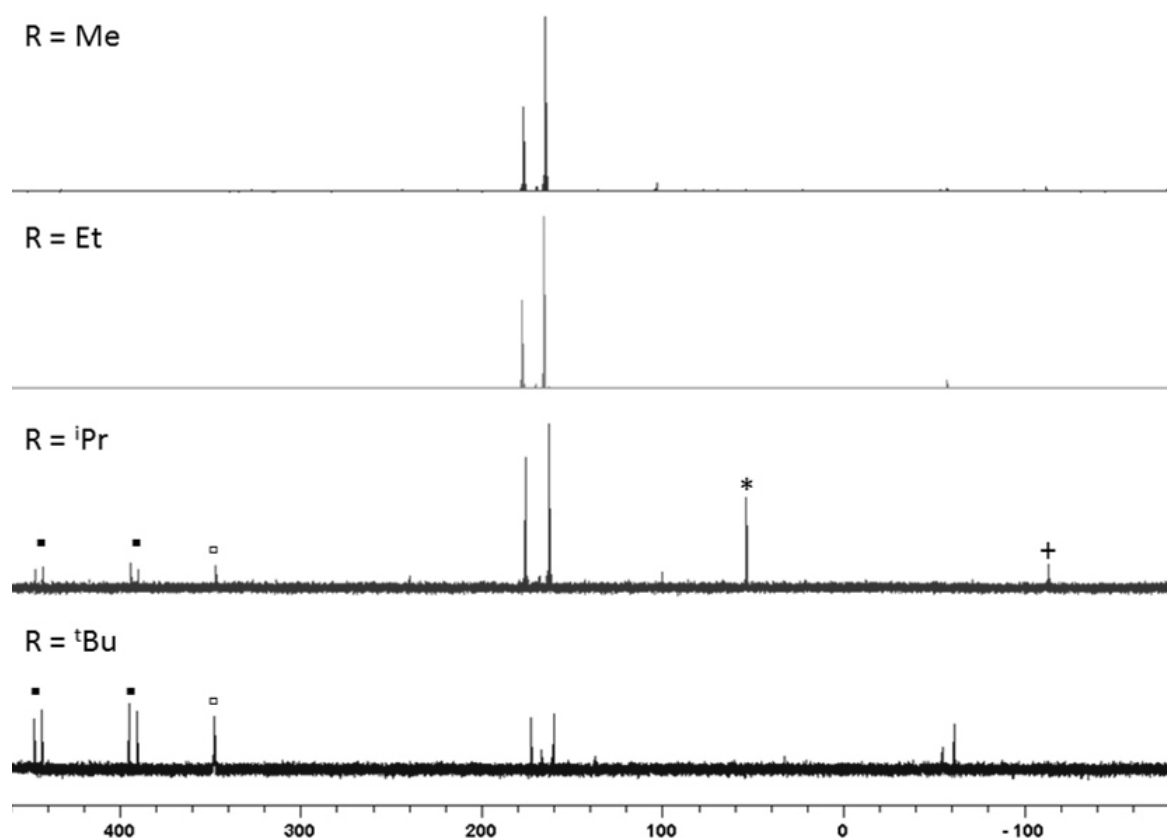
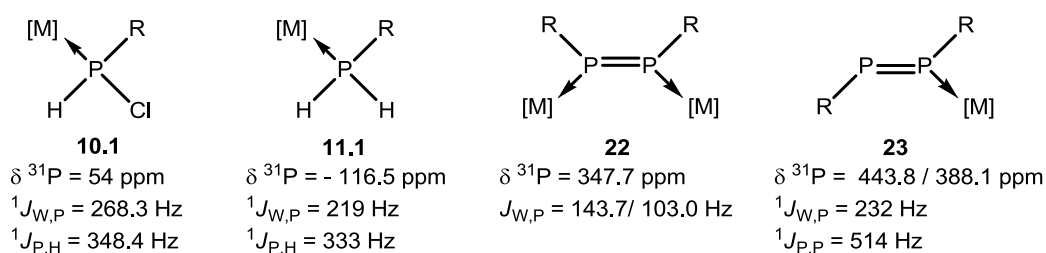


Figure 5.6: $^{31}\text{P}\{^1\text{H}\}$ NMR spectra for the reaction mixtures of the syntheses of 1,2-oxaphosphetane complexes with different steric demanding C-substituents R.

The formation of diphosphene complexes (**22** \square , **23** \bullet), formed due to decomposition of the Li/Cl phosphinidenoid complex as a competing reaction pathway, as well as small amounts of the chloro(organo)phosphane complex (**10.1**, \square) and phosphane complex (**11.1**, \bullet) were observed. They were assigned using their typical NMR data (scheme 5.14).



Scheme 5.14: ^{31}P NMR data for the chlorophosphane complex **10.1**^[118] (CDCl_3), phosphane complex **11.1**^[119] (C_6D_6) and the diphosphene complexes **22**^[31] and **23**^[20] ($\text{R} = \text{CH}(\text{SiMe}_3)_2$ and $[\text{M}] = \text{W}(\text{CO})_5$).

While these reactions showed a clear trend with regard to reactivity, no significant influence was observed on the isomeric ratio (table 5.5). A good comparison for the case $\text{R} = \text{tBu}$ is not possible due to the low amount of 1,2-oxaphosphetane complexes formed (9.5% of the reaction mixture by ^{31}P NMR integration) and, therefore, the bad signal to noise ratio in the $^{31}\text{P}\{^1\text{H}\}$ NMR spectrum and a larger error in the ^{31}P NMR integration.

Table 5.5: $^{31}\text{P}\{^1\text{H}\}$ NMR data (CDCl_3) and yields for the C^4 -R-substituted 1,2-oxaphosphetane complexes **21.1a_w**-**21.1d** and their isomers ^[a] not determined due to low signal to noise ratio, measurement in Et_2O .

	R (yield [%])	$\delta^{31}\text{P}$ [ppm] ($^1J_{\text{W,P}}$ [Hz])				ratio [1:2:3:4]
		Isomer 1	Isomer 2	Isomer 3	Isomer 4	
21.1a_w ¹⁻⁴	Me (58 %)	176.4 (273.4)	169.2 - ^[a]	164.5 (267.8)	164.4 (268.7)	30:4:19:47
21.1b ¹⁻⁴	Et (31 %)	177.1 (274.8)	169.8 (271)	165.1 (268.4)	165.0 (268.8)	29:4:23:44
21.1c ¹⁻⁴	ⁱPr (20 %)	174.7 (274.8)	167.1 (274)	162.6 (268.6)	161.7 (268.7)	29:5:24:42
21.1d ¹⁻⁴	^tBu (not isolated)	172.2 - ^[a]	166.5 - ^[a]	not observed - ^[a]	159.8 - ^[a]	35:21:0:43

Complexes **21.1b**¹⁻⁴ and **21.1c**¹⁻⁴ could be isolated and characterized by all means necessary. The yield of complexes **21.1c**¹⁻⁴ was quite low (20 %) due to the formation of the side-products. No further discussion of the NMR or IR data will be done as there are no significant differences to the previously described complexes.

Single crystals suitable for X-ray diffraction studies could be obtained for complexes **21.1b** and **21.1c** from saturated *n*-pentane solutions. Both complexes show two co-crystallized isomers by a split-site of the ring, due to the relative orientation of the *C*-substituent to the metal fragment (figure 5.7). No significant influence of the *C*-substituent could be observed on the bond lengths and angles when comparing the three complexes bearing the Me, Et and ⁱPr substituents (table 5.6).

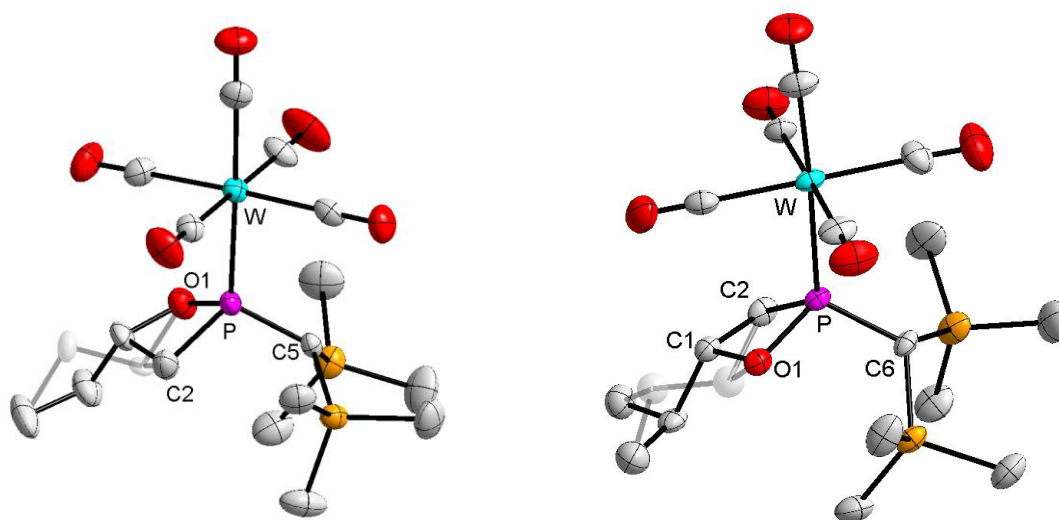
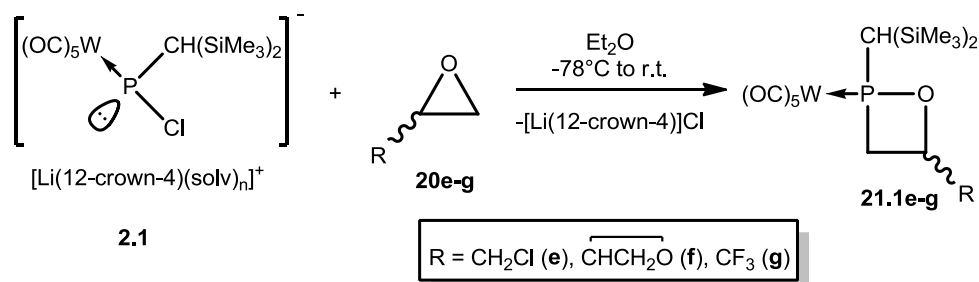


Figure 5.7. DIAMOND plot of the molecular structures of 1,2-oxaphosphetane complexes **21.1b** (left) and **21.1c** (right) in the solid state; the thermal ellipsoids are set at 50 % probability level and all hydrogen atoms are omitted for clarity. The split-sites (1:1) for the R-C units are represented using a transparent mode for clarity.

Table 5.6: Selected bond lengths in Å and angles in ° for 1,2-oxaphosphetane complexes **21.1a**–**21.1c** (folding angles are given for solid/transparent part of the splitting).

	P-CH ₂	P-CH	P-W	P-O	CH ₂ -P-O1	folding angle
21.1a_w	1.827(5)	1.800(5)	2.4846(14)	1.672(4)	79.7(2)	21.9
21.1b	1.800(5)	1.809(4)	2.4789(12)	1.668(3)	79.7(2)	26.5 /19.7
21.1c	1.846(6)	1.808(6)	2.4818(15)	1.668(5)	79.6(3)	24.3/19.1

The next part of the investigations using complex **2.1** focused on the quest of functional group tolerance, as functional groups in the epoxide could lead to side reactions or might even activate the epoxide for the reaction. Especially the last aspect could provide further insight into the possible reaction mechanism. Also the influence of the substitution on the spectroscopic data, like the NMR chemical shifts or the magnitudes of the different coupling constants as well as the isomeric ratio should be checked.

**Scheme 5.15:** Reaction of Li/Cl phosphinidenoid complex **2.1** with different functionalized epoxides (**20e-g**).

Using epichlorohydrin (**20e**) it could be shown that the reaction is not disturbed by the presence of an additional halogen atom at the epoxide substituent. Employing 1,3-butadiene diepoxide (**20f**) it could further be proven that not even an additional epoxy substituent changes the reaction outcome (scheme 5.15). In case of **21.1f** more than the typical four signals for the isomers were observed in the reaction mixture, but all additional signals in less than 1% (figure 5.8). These signals might correspond to complexes where a subsequent reaction took place at the second epoxy-ring, as they are found in larger amounts if the reaction was performed with an excess of the Li/Cl phosphinidenoid complex (cf. chapter 5.3.3). Nevertheless the formation of only four isomers is counter-intuitive as one more stereogenic centre is introduced in the molecule with the epoxy substituent.

To increase the reactivity while maintaining a steric demand of the substituent similar to the ^tBu group, the reaction with the CF₃-substituted epoxide (**20g**) was performed, leading to 1,2-oxaphosphetane complexes **21.1g**¹⁻⁴ in a selective reaction.

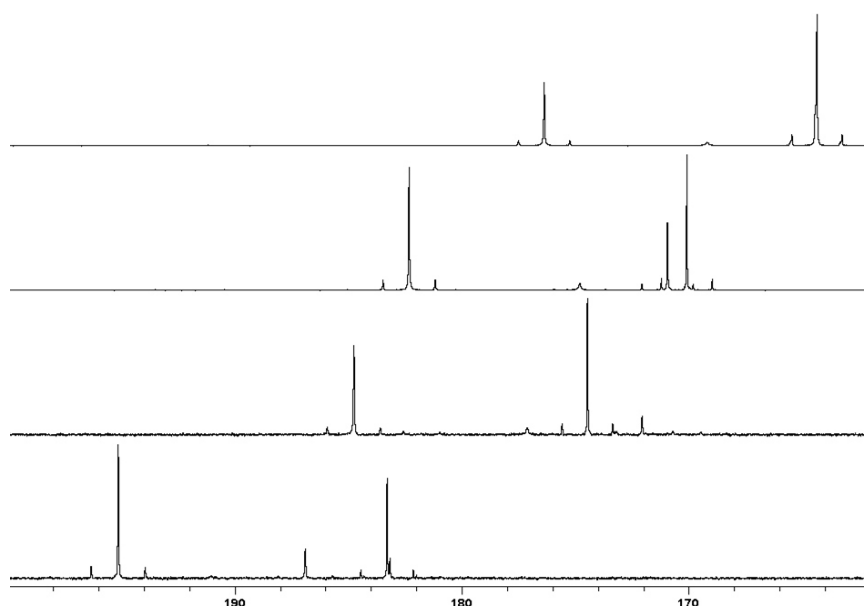


Figure 5.8: $^{31}\text{P}\{^1\text{H}\}$ NMR spectra for the reactions of Li/Cl phosphinidenoid complex **2.1** with propylene oxide (**20a**), epichlorohydrin (**20e**), 1,3-butadiene diepoxide (**20f**) and 1,1,1-trifluoro-2,3-propylene oxide (**20g**) (from top to bottom).

All products could be isolated in moderate to good yields (35 – 61 %). A strong influence of the substituent was found especially on the ^{31}P NMR data if the electronic nature of the C-substituent is changed stepwise from weakly electron-donating (CH_3) to strongly electron-withdrawing (CF_3). Not only do the signals show a deshielding of the phosphorus nucleus but also an increase in the magnitude of the $^1J_{\text{W,P}}$ coupling constant (table 5.7). This is unexpected, as in other heterocyclic phosphane complexes, *e.g.* oxaphosphirane complexes, C-substituents only showed a rather small influence on the NMR spectroscopic data, especially the $^1J_{\text{W,P}}$ couplings. Nevertheless a comparable effect of electron withdrawing substituents at phosphorus on the chemical shift and the coupling to tungsten was described before.^[121]

The ratio of isomers seems to be only slightly influenced by the introduction of the electron-withdrawing groups. Formation of the isomer with the resonance signal at lowest field is more favoured than in case of the Me, Et and ^iPr -substituted complexes, but no further trend could be observed by changing the substituent.

Table 5.7: $^{31}\text{P}\{^1\text{H}\}$ NMR data, yields and isomeric ratios for complexes **21.1a_w** and **21.1e-g**.

	R (yield [%])	$\delta^{31}\text{P}$ [ppm] ($^1J_{\text{W,P}}$ [Hz])				ratio [1:2:3:4]
		Isomer 1	Isomer 2	Isomer 3	Isomer 4	
21.1a_w ¹⁻⁴	CH₃ (58 %)	176.4 (273.4)	169.2 - ^[a]	164.5 (267.8)	164.4 (268.7)	30:4:19:47
21.1e ¹⁻⁴	CH₂Cl (61 %)	182.4 (278.6)	174.8 (281.0)	171.0 (274.4)	170.1 (271.3)	44:7:19:30
21.1f ¹⁻⁴	Epoxy (49 %)	184.8 (283.9)	177.1 - ^[a]	174.5 (271.4)	172.1 (273.9)	41:7:44:8
21.1g ¹⁻⁴	CF₃ (35 %)	195.1 (289.5)	186.9 (292.5)	183.3 (279.6)	183.2 (283.2)	49:14:31:6

Single crystals of the three new derivatives could be obtained from saturated *n*-pentane solutions at 4 °C, and the molecular structures prove the constitution of all three 1,2-oxaphosphetane complexes including unchanged *C*-substituents at the rings (figure 5.9).

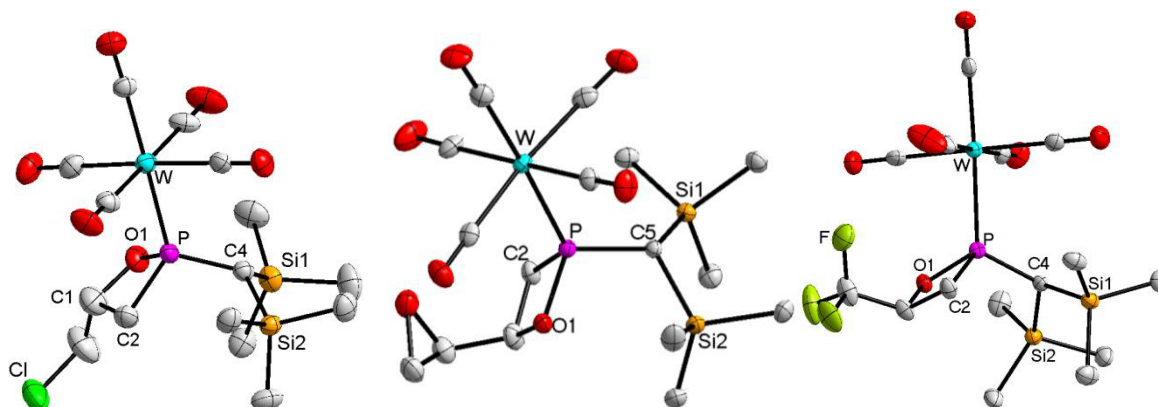


Figure 5.9: DIAMOND plot of the molecular structures of 1,2-oxaphosphetane complexes **21.1e**, **21.1f** and **21.1g** (from left to right) in the solid state; the thermal ellipsoids are set at 50 % probability level and all hydrogen atoms are omitted for clarity.

All data for the bond lengths and angles are in the expected range, similar to other 1,2-oxaphosphetane complexes and they show only small differences that can be neglected (table 5.8).

Table 5.8: Selected bond lengths in Å and angles in ° for 1,2-oxaphosphetane complexes **21.1a** and **21.1e-g**.

	P-CH ₂	P-CH	P-W	P-O	CH ₂ -P-O1	folding angle
21.1a_w	1.827(5)	1.800(5)	2.4846(14)	1.672(4)	79.7(2)	21.9
21.1e	1.835(4)	1.813(4)	2.4726(10)	1.693(3)	80.35(18)	22.3
21.1f	1.841(4)	1.809(4)	2.4914(10)	1.679(3)	79.79(16)	2.2
21.1g	1.858(4)	1.802(4)	2.4672(11)	1.687(3)	78.83(17)	1.9

An especially interesting feature of the 1,2-oxaphosphetane complexes was found: the ring geometry of complexes **21.1** was highly flexible with respect to the folding angle (figure 5.10), describing a range from almost planar (**21.1g**, folding angle: 1.9°) to strong folded, with almost 25° folding (**21.1e**, folding angle 22.3°).

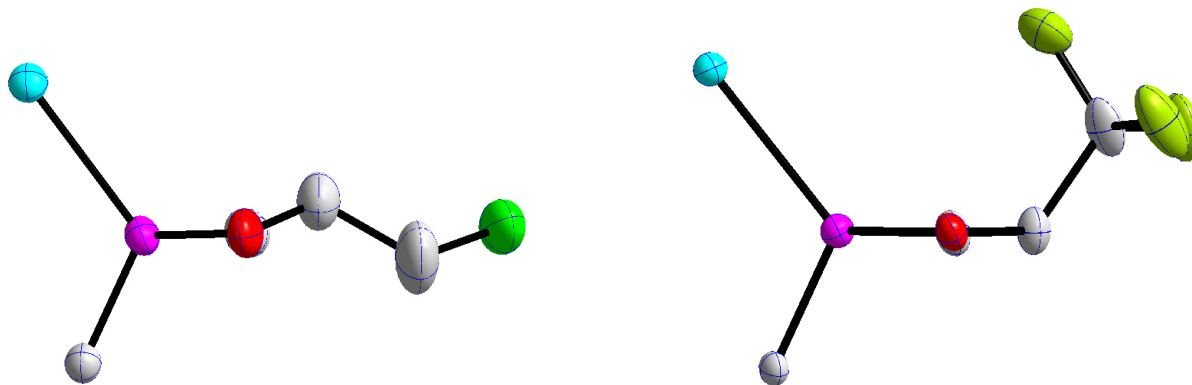
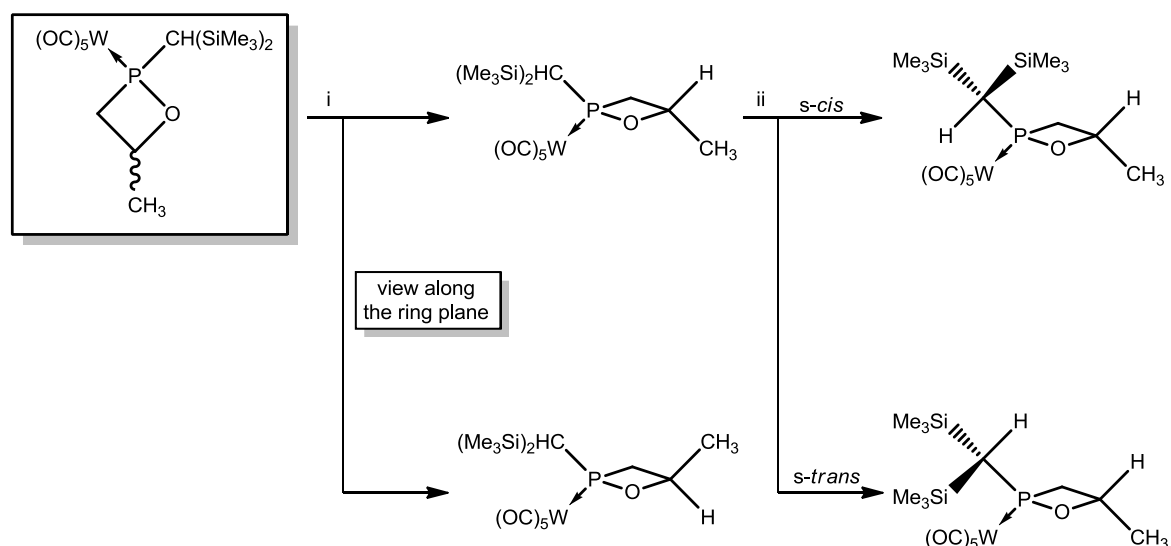


Figure 5.10: Side view along the 1,2-oxaphosphetane rings in the molecular structures of complexes **21.1e** (left) and **21.1g** (right) (the thermal ellipsoids are set at 50 % probability level, hydrogen atoms as well as the CO and SiMe₃ groups are omitted for clarity).

As no influence of the steric demand on the folding angle was found in case of the Me, Et and ⁱPr-substituted complexes (**21.1a-c**), it can be proposed that the change in the electronic structure plays the dominant role here. But the statistical platform comprising only a small number of derivatives doesn't allow for a final conclusion, yet. A theoretical study could provide further insights.

5.2.2 Discussion of the origins of isomerisms

As in all studies described above four isomers of 1,2-oxaphosphetane complexes were found, a more detailed study on the origins of the isomerisms deemed necessary, although molecular structures and the NMR characteristics of complexes **21.1a-21.1g** had provided first hints to one origin: the orientation of the *C*-substituent relative to the metal fragment (i, scheme 5.16) and the additional problem of the orientation of the CH-proton of the CH(SiMe₃)₂ group (ii, scheme 5.16) pointing to (*s-cis*) or away (*s-trans*) from the W(CO)₅ fragment. This was already proposed for the *C*-Ph-substituted 1,2-oxaphosphetane complex **16.1**, and was envisaged as reason for the formation of four isomers (scheme 5.16). The possible formation of different regioisomers (*C*-substitution in 3- or 4-position) was neglected due to the usually very high regioselectivity found in nucleophilic reactions of epoxides and phosphanides^[122] alongside the clear-cut assignment of all ring-CH₂ groups as part of *P*-CH₂ units by ¹³C{¹H} NMR, except for **16.1**.



Scheme 5.16: Illustration of the proposed situations for the isomerism in 1,2-oxaphosphetane complexes.

So far, all reactions were performed using racemic mixtures of epoxides which was done mainly for cost efficiency as the enantiomerically pure epoxides are quite expensive. Therefore, it was necessary to rule out an influence of the initial stereochemical information on the reaction outcome. Using enantiomerically pure R(+)-propylene oxide, no significant change on the reaction selectivity or the ratio of the formed isomers was observed (figure 5.11), proving that the formation of the isomers is independent from the configuration of the epoxide used. An enantiomeric excess was not determined as separation of the isomers was considered to be of minor interest for the problem investigated herein.

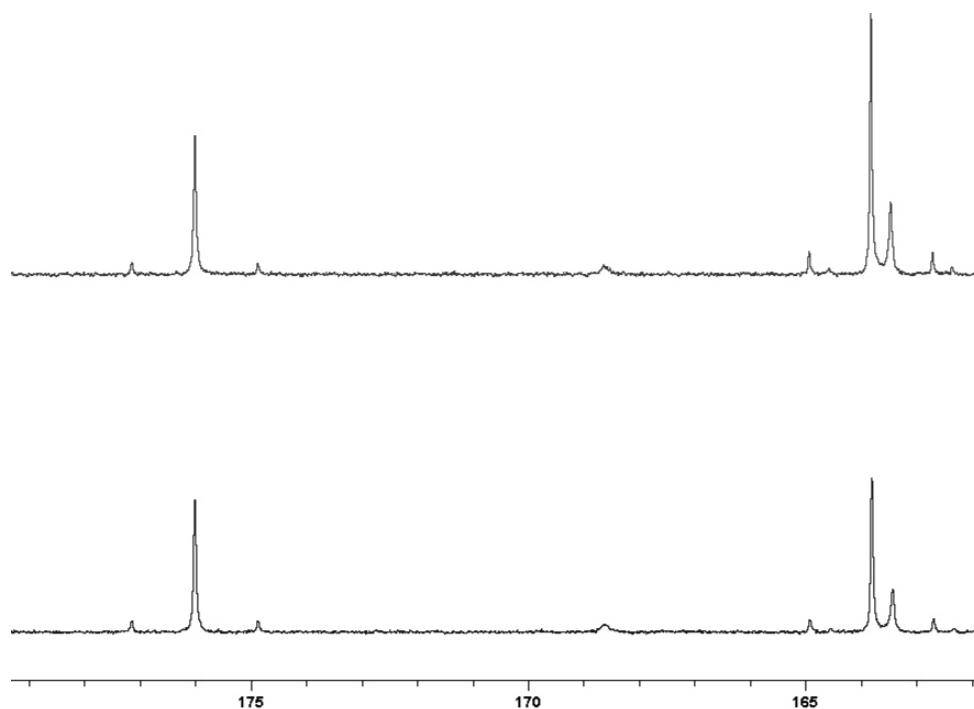
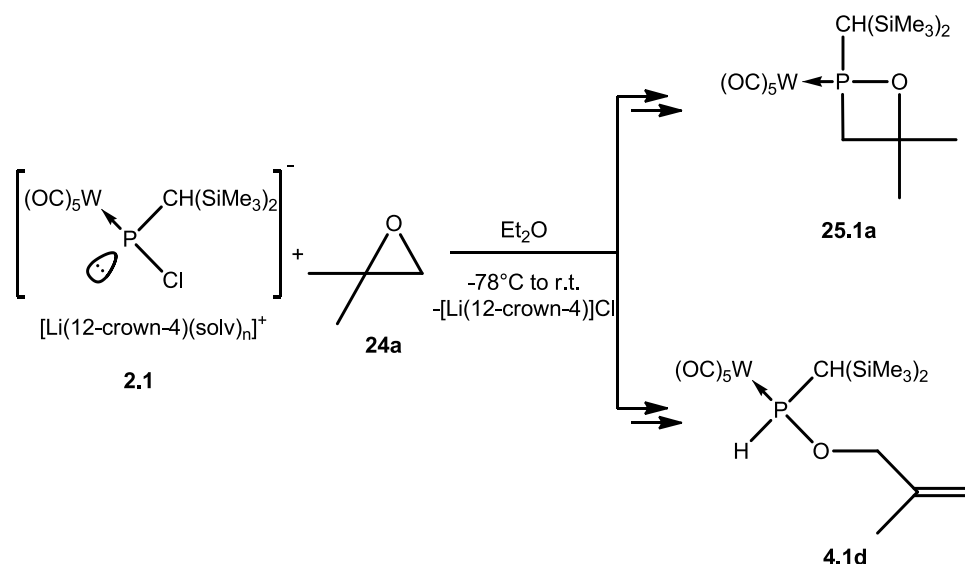


Figure 5.11: $^{31}\text{P}\{^1\text{H}\}$ NMR spectra from the reaction mixtures of the reactions of **2.1** and propylene oxide, as racemic mixture (top) and enantiomerically pure R(+)-propylene oxide (bottom).

After steric and electronic effects on the isomeric ratio were studied, further investigations on a stepwise conceptual elimination of stereogenic centres in the rings were started.

As first step the “removal” of the stereogenic carbon centre was envisaged via employment of symmetrically 1,1-disubstituted epoxides while preserving all other reaction conditions.

Using the simplest 1,1-disubstituted epoxide, namely the 1,1-dimethyloxirane **24a**, a reaction was observed that did not only lead to the isomeric 1,2-oxaphosphetane complexes **25.1a**¹⁻², but also to a novel side-product (**4.1d**) in significant amounts (ratio (**25.1a** : **4.1d**): 47:53, scheme 5.17). This side-product contained a P-H bond, as evidenced through the coupling in the ^{31}P NMR spectrum ($^1J_{\text{P,H}} = 322.3$ Hz). Furthermore, the resonance signal of **4.1d** at 103.6 ppm ($^1J_{\text{W,P}} = 268.1$ Hz) appeared in the range of phosphinite complexes, obtained via formal insertion of a phosphinidene fragment into OH bonds (compare chapter 1.2).^[10]



Scheme 5.17: Reaction of Li/Cl phosphinidenoid complex **2.1** with 1,1-dimethyloxirane **24a**.

While the formation of complex **4.1d** as side product was unexpected, the reduction of stereogenic centres in the epoxide led to the proposed reduction of the number of isomers observed for 1,2-oxaphosphetane complex **25.1a**. Only two isomers were observed instead of four, formed in a ratio of almost 1:2 (table 5.9). In addition the typical dependency of the $^2J_{P,H}$ coupling constants for two orientations of the $CH(SiMe_3)_2$ proton was observed ($^2J_{P,H}$ (Isomer 1) = 4.6 Hz, $^2J_{P,H}$ (Isomer 2) = 18.9 Hz).

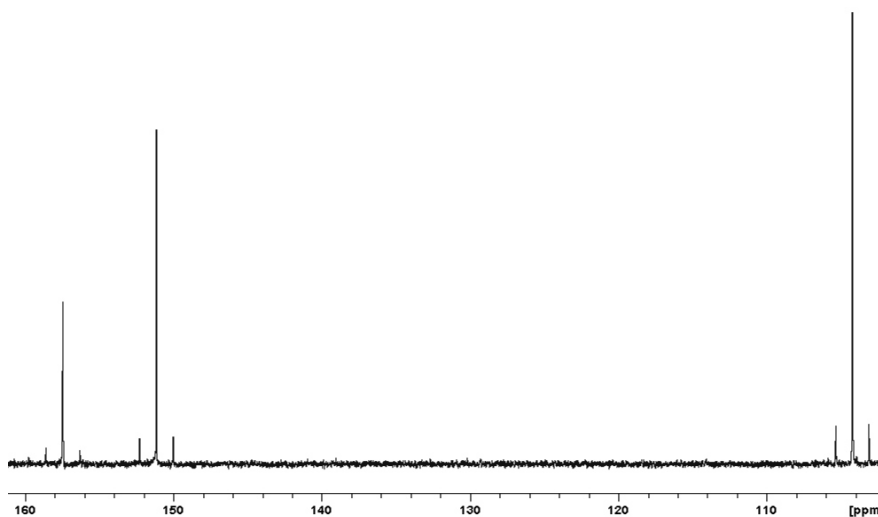


Figure 5.12: $^{31}P\{^1H\}$ NMR spectrum of the reaction mixture from Li/Cl phosphinidenoid complex **2.1** and 1,2-dimethyloxirane **24a**, measured in diethyl ether.

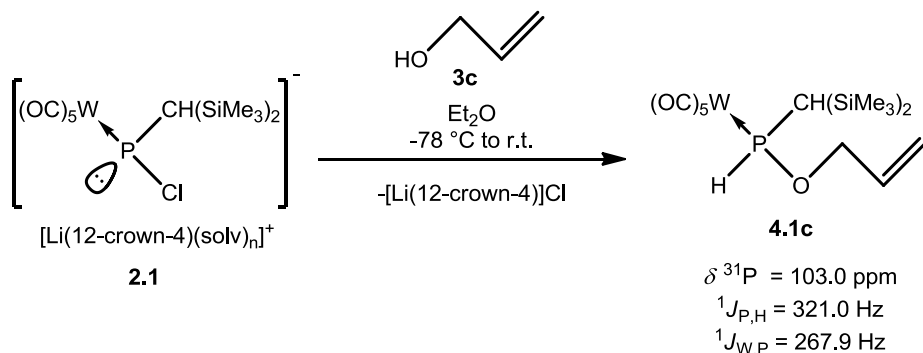
Both isomers display comparable NMR data sets for all other atoms, also the chemical shifts for the resonances of the quaternary $C(CH_3)_2$ carbon atoms in the $^{13}C\{^1H\}$ NMR are nearly identical for both isomers (85.5 and 85.6 ppm). This strong deshielding proves the C-O connection, so that the presence of two different regioisomers (substitution in 3 and 4 position) can again be ruled out.

Table 5.9: ^{31}P NMR data and yields for complexes **25.1a**¹⁻² and **4.1d**.

	$\delta^{31}\text{P}$ [ppm]	$^1J_{\text{W,P}}$ [Hz]	$^1J_{\text{P,H}}$ [Hz]	yield [%]	ratio
25.1a ¹	157.5	277.5	-	17	36
25.1a ²	151.1	276.0	-		64
4.1d	103.6	268.1	322.3	7	-

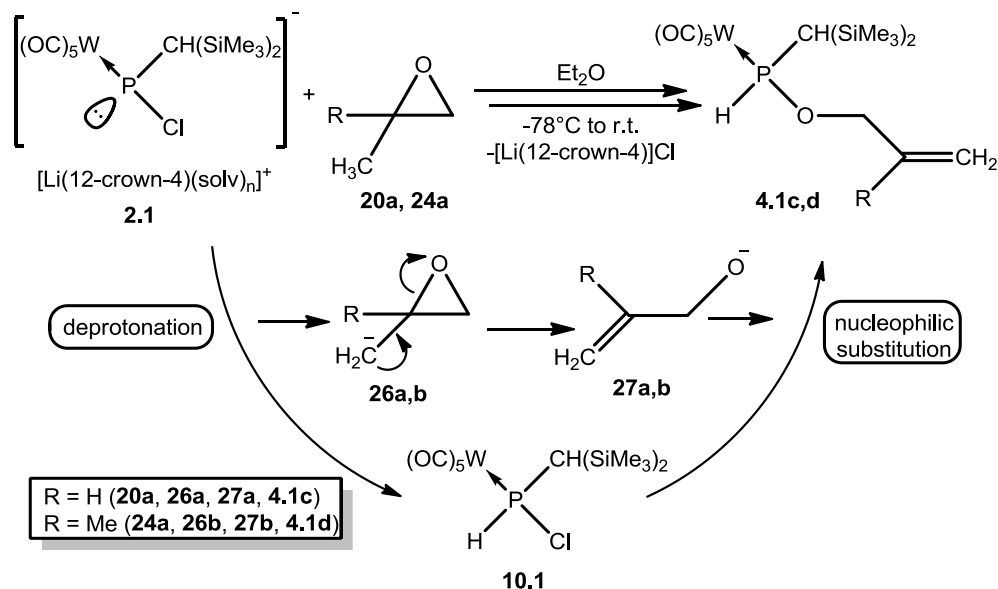
The ^{31}P NMR data show some interesting features compared to those observed for *C*-mono-substituted 1,2-oxaphosphetane complexes. The resonance signals showed a significant highfield-shift which is just the opposite effect to the situation found for oxaphosphirane complexes. The $^1J_{\text{W,P}}$ coupling constant shows only a slightly higher magnitude than the one for the *C*-methyl-substituted complex **21.1a_w**.

Renewed inspection of the ^{31}P NMR reaction spectra of the reaction solution of complex **21.1a_w** (chapter 5.2.1) revealed that a side product, similar to **4.1d**, was already observed when propylene oxide was used. Despite being less than 1 % of the reaction mixture, by integration of the signals in the ^{31}P NMR, the resonance signal could easily be assigned to the allyl-substituted phosphinite complex **4.1c**.^[10] This complex was already prepared and characterized using the formal insertion reaction of Li/Cl phosphinidenoid complex **2.1** in the OH bond of allyl alcohol **3c** (scheme 5.18) and, hence, could be employed here as authentic sample to prove the identity of the resonance signal.

**Scheme 5.18:** Synthesis and ^{31}P NMR data (CDCl_3) for complex **4.1c**.^[10]

The formation of complexes **4.1c** and **4.1d** can be explained by a different initial reaction step (scheme 5.19). While the first step for the formation of 1,2-oxaphosphetane complexes **21.1a_w** and **25.1a** is supposed to be a nucleophilic attack on the epoxide ring, a deprotonation at the C^α -position could lead to chloro(organo)phosphane complex **10.1** and carbanions **26a,b** which can rearrange in a ring opening reaction to give the unsaturated alkoxides **27a,b**. This deprotonation and rearrangement is a well-known reaction sequence for CH_3 -substituted epoxides,^[123] e.g. as first step in the anionic polymerization of propylene

oxide initiated by strong bases.^[124] A nucleophilic substitution yields the complexes **4.1c,d** in a reaction similar to the synthesis of phosphinito complexes described by Duan.^[56]



Scheme 5.19: Formation of phosphinite complexes **4.1c,d** by deprotonation and rearrangement of the CH_3 -substituted epoxides **20a** and **24a**.

Complex **4.1d** and a mixture of isomeric complexes **25.1a¹** and **25.1a²** were separated by low temperature column chromatography. The formation of phosphinite complex **4.1d** and the 1,2-oxaphosphetane complexes **25.1a¹⁻²** was also proven by single crystal X-ray diffraction studies (figure 5.13).

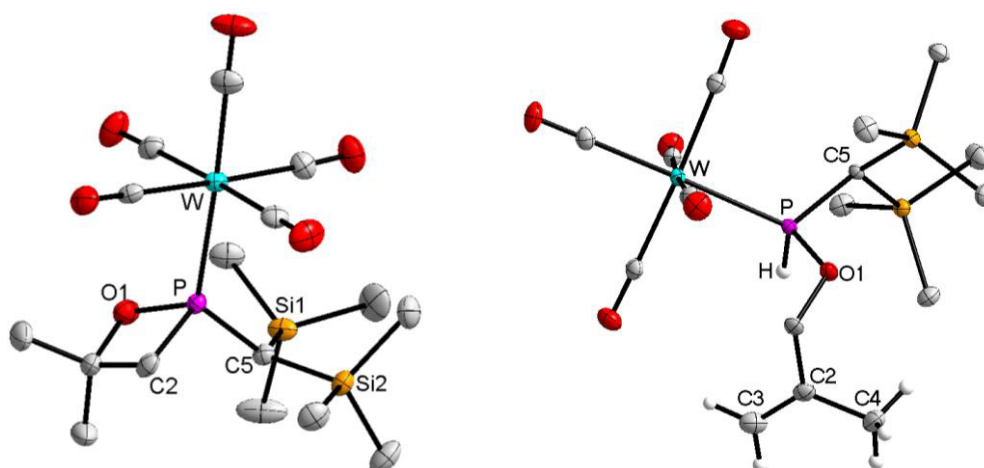


Figure 5.13: DIAMOND plot of the molecular structures of complexes **25.1a** (left) and **4.1d** (right) in the solid state; the thermal ellipsoids are set at 50 % probability level and all hydrogen atoms except at phosphorus and at the $H_2C=C-CH_3$ subunit are omitted for clarity.

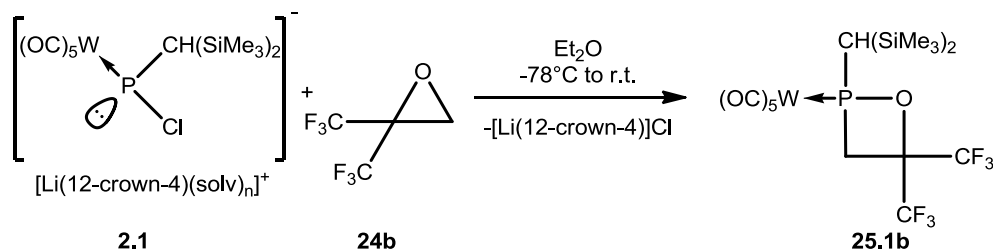
Except for a shortening of the P- CH_2 bond, compared to the 4-mono and other 4,4-disubstituted 1,2-oxaphosphetane complexes, all data obtained were close to previously described derivatives of both classes of compounds. Interestingly, the molecular structure of

complex **25.1a** showed the *s-trans* conformation of the W-P-C-H motif for the first time for an 1,2-oxaphosphetane complex. This could explain the small differences in the structural data, but is of special interest as it proves the existence of the two relative orientations of the P-CH(SiMe₃)₂ group for this ligand system. The ring folding angle of complex **25.1a** is quite small (folding angle 2.2°), presumably due to the missing option to avoid steric interactions between the C-methyl groups and the bulky substituents at the phosphorus centre (the W(CO)₅ and CH(SiMe₃)₂ groups). The latter was discussed to be the reason for the strong ring folding in the case of C-mono-substitution, e.g. **21.1a_w**.

Table 5.10: Selected bond lengths in Å for complexes **21.1a**, **25.1a** and **4.1c,d**.

	P-CH ₂	P-CH	P-W	C=C	P-O
21.1a_w	1.827(5)	1.800(5)	2.4846(14)	-	1.672(4)
25.1a	1.804(3)	1.809(3)	2.4879(7)	-	1.664(2)
4.1d	-	1.8087(18)	2.4849(4)	1.323(3)	1.6242(13)
4.1c^[10]	-	1.804(3)	2.4750(7)	1.309(6)	1.626(2)

To avoid the side reactions, described for the 1,1-dimethylepoxide **24a**, the bis-CF₃-substituted epoxide **24b** was employed (scheme 5.20).



Scheme 5.20: Synthesis of 1,2-oxaphosphetane complex **25.1b**.

Surprisingly, the reaction proceeded fast, despite having two bulky CF₃ substituents (compare chapter 5.2.1), and a very selective reaction occurred leading to (only) two isomers of the 1,2-oxaphosphetane complex **25.1b**^{1,2}; the formation of one isomer was largely preferred (ratio 96:4). This clearly serves as an impressive example of electronic substrate activation for Li/Cl phosphinidenoid complex reactions.

Table 5.11: $^{31}\text{P}\{^1\text{H}\}$ and selected ^1H NMR data for complexes **25.1b**¹ and **25.1b**² (**25.1b**¹ in CDCl_3 , **25.1b**² in toluene- d_8).

	$^{31}\text{P}\{^1\text{H}\}$ NMR	^1H NMR (P-CH)	ratio	
	δ [ppm] ($^1J_{\text{W,P}}$ [Hz])	δ [ppm] ($^2J_{\text{P,H}}$ [Hz])	initial	after heating*
25.1b ¹	198.2 (297.6)	2.25(4.0)	96	7
25.1b ²	191.5 (295.0)	2.70(19.5)	4	93

* 85 °C, 3 days

Interestingly, the $^2J_{\text{P,H}}$ coupling constants revealed the typical values for the *s-cis* and *s-trans* isomers ($^2J_{\text{P,H}}$ (**25.1b**¹) = 4.0 Hz, $^2J_{\text{P,H}}$ (**25.1b**²) = 19.5 Hz), and the isomer ratio was changed by heating the product in toluene- d_8 at 85 °C for three days (the ratio changed from 96:4 to 7:93). This is a clear indication that the present case is due to atropisomerism caused by the hindered rotation around the *exo*-P-C bond. Unfortunately, also slight decomposition occurred over time, so that the second isomer was only characterized from the mixture by multinuclear NMR spectroscopy.

The molecular structure of **25.1b** (figure 5.14), obtained from a single crystal X-ray diffraction study using crystals obtained from a saturated *n*-pentane solution, proves the 1,2-oxaphosphetane ligand ring motif, but it was also strongly disordered in several atoms and groups. Therefore, it just serves as constitutional proof, but the data will not be discussed further (see appendix, chapter 12.17 for further details on the disordering).

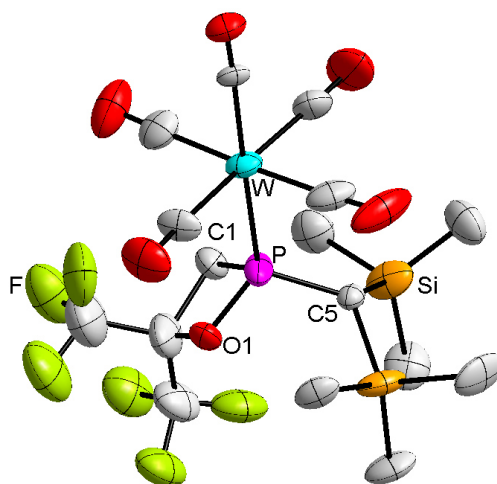


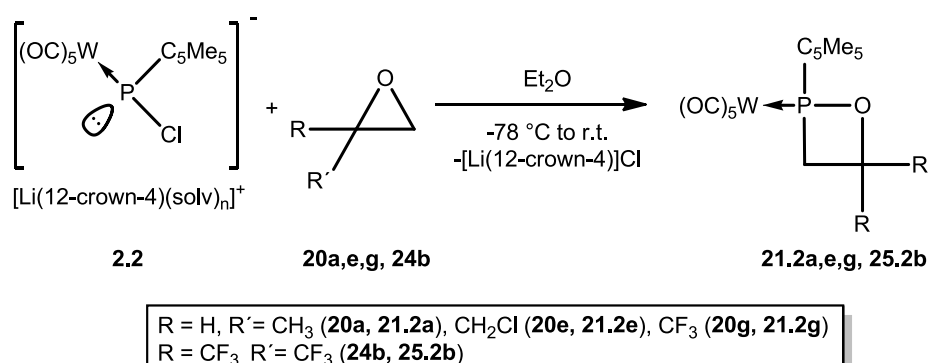
Figure 5.14: DIAMOND plot of the molecular structure of 1,2-oxaphosphetane complex **25.1b** in the solid state; the thermal ellipsoids are set at 50 % probability level and all hydrogen atoms are omitted for clarity. The disordering of several groups is not shown for clarity. Selected bond lengths in Å and angles in °: P-W 2.4562(19), P-O1 1.568(12), P-C1 2.04(2), P-C5 1.805(7), C1-P-O1 76.5(7).

5.3 Synthesis of *P*-C₅Me₅ and *P*-CPh₃-substituted 1,2-oxaphosphetane complexes

In the past years, two more substituents were implemented in phosphinidenoid chemistry, the CPh₃^[33] and the C₅Me₅^[32] substituent. The *P*-C₅Me₅-substituted complexes offered new reactivity by involvement of the ring system in follow-up reactions whereas the *P*-CPh₃ substituent introduces more steric bulk into the molecule, allowing to access other novel structural motifs, e.g. chloroformylphosphane complexes.^[37] Another advantage of these substituents is the suppression of atropisomers that were found in case of the *P*-CH(SiMe₃)₂-substituted derivatives.

5.3.1 *P*-C₅Me₅-substituted derivatives

The *P*-C₅Me₅-substituted Li/Cl phosphinidenoid complex is slightly less thermally stable (decomposition starts at -40 °C in solution)^[125] than the *P*-CH(SiMe₃)₂-substituted one (decomposition starts at -30 °C)^[126] and the influence of this was observed especially in the reaction with propylene oxide (scheme 5.21). The reaction could be performed in small scale to obtain the ³¹P NMR data, but the product could not be obtained in large amounts due to faster thermal decomposition of the Li/Cl phosphinidenoid complex. The subsequent formation of several inseparable side products (especially complex **XXXVIII**) made isolation impossible, especially when the size of the reaction was scaled-up. Nevertheless, using *C*-CF₃-substituted epoxides the isolation of *P*-C₅Me₅-substituted 1,2-oxaphosphetane complexes (**21.1g** and **25.2b**) was possible.



Scheme 5.21: Syntheses of *P*-C₅Me₅-substituted 1,2-oxaphosphetane complexes.

As proposed, and in contrast to the reactions observed for the *P*-CH(SiMe₃)₂-substituted complex, formation of only two isomers was observed when using mono-substituted epoxides (propylene oxide **20a**, epichlorohydrin **20e** and 1,1,1-trifluoro-2,3-propylene oxide **20g**, figure 5.15). A small influence on the isomeric ratio was observed by introducing the

steric more demanding CF_3 substituent (table 5.12), changing the ratio from around 1:1 to almost 2:1.

The reaction with hexafluoro isobutene oxide led to only one observable signal for complex **25.2b** in the $^{31}\text{P}\{^1\text{H}\}$ NMR spectrum, proving the proposed diminishing of the isomers by elimination of all stereogenic centres, besides at the phosphorus atom itself.

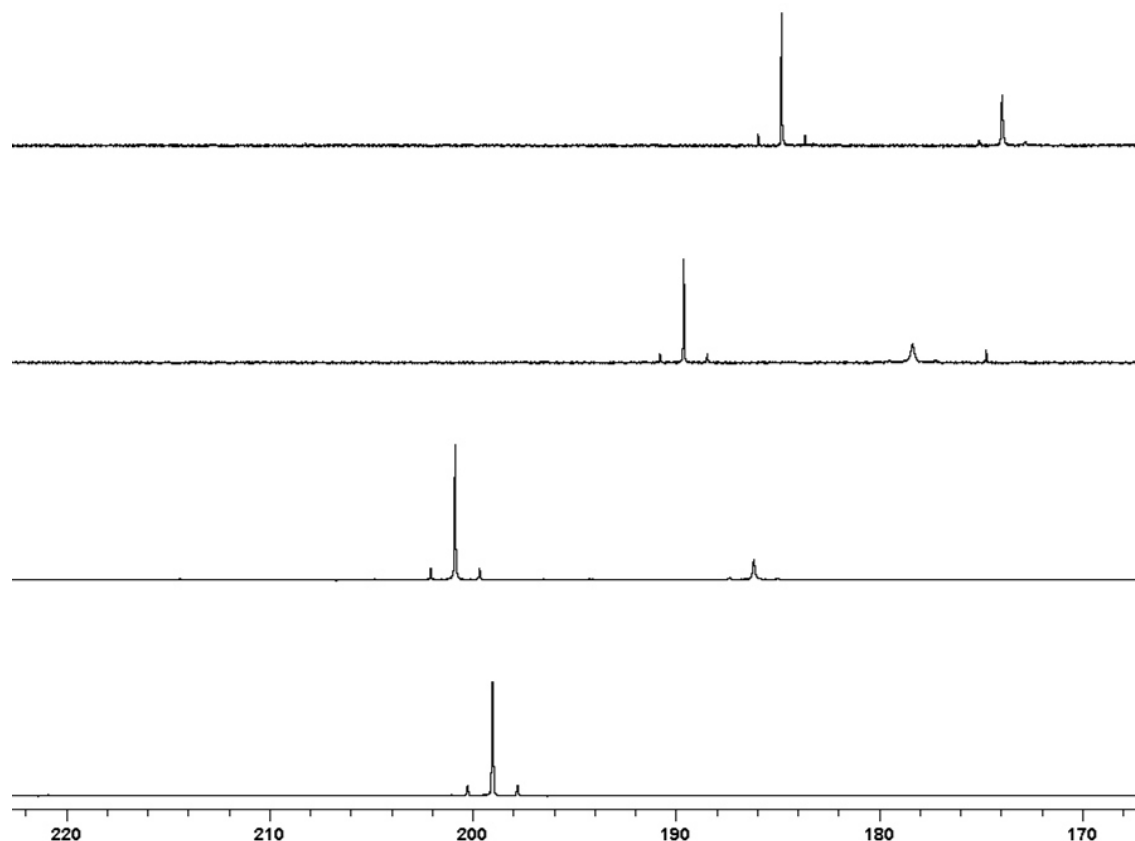


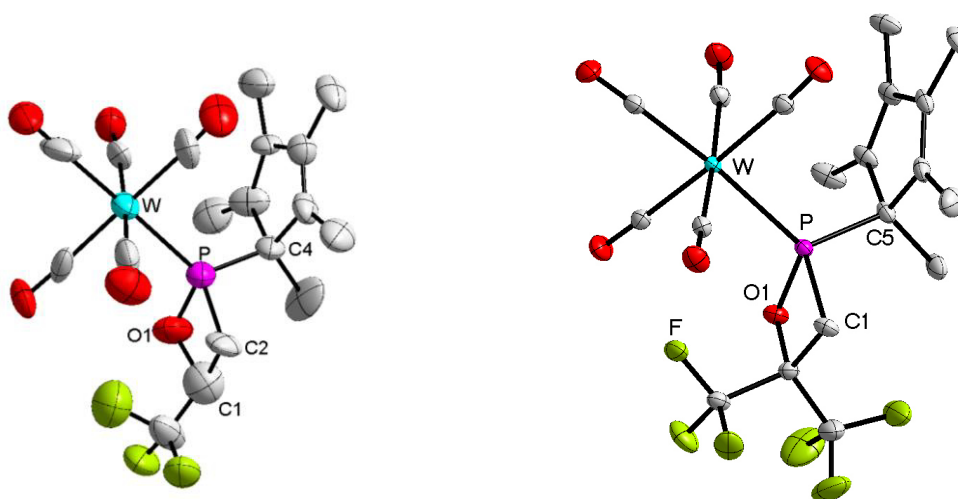
Figure 5.15: $^{31}\text{P}\{^1\text{H}\}$ NMR spectra for the reaction mixtures of Li/Cl phosphinidenoid complex **2.2** and propylene oxide (**20a**), epichlorohydrin (**20e**), 1,1,1-trifluoro-2,3-propylene oxide (**20g**) and hexafluoroisobutene oxide (**24b**) (from top to bottom).

The $^{31}\text{P}\{^1\text{H}\}$ NMR data of all $P\text{-C}_5\text{Me}_5$ -substituted 1,2-oxaphosphetane complexes are in a similar range as those found for the $P\text{-CH}(\text{SiMe}_3)_2$ -substituted complexes. Nevertheless a slight shift to lower field was observed, that is common when comparing complexes bearing these two P -substituents.

Table 5.12. $^{31}\text{P}\{^1\text{H}\}$ NMR data and yields for complexes **21.2a**, **21.2e**, **21.2g** and **25.2b** (^[a] not isolated).

	R, R'	$\delta^{31}\text{P}$ [ppm] ($^1J_{\text{P,W}}$ [Hz])		ratio [1:2]	yield [%]
		Isomer 1	Isomer 2		
21.2a ¹⁻²	Me, H	184.8 (279.5)	174.0 (273.6)	53:47	– ^[a]
21.2e ¹⁻²	CH ₂ Cl, H	189.6 (283.6)	178.4 (280.0)	53:47	– ^[a]
21.2g ¹⁻²	CF ₃ , H	200.8 (292.3)	186.1 (284.0)	73:27	36 %
25.2b	CF ₃ , CF ₃	199.0 (295.1)		–	45 %

Single crystals suitable for X-ray diffraction studies were obtained from saturated *n*-pentane solutions for complexes **21.2g** and **25.2b** (figure 5.16).

**Figure 5.16:** DIAMOND plot of the molecular structures of complexes **21.2g** (left) and **25.2b** (right) in the solid state; the thermal ellipsoids are set at 50 % probability level and all hydrogen atoms are omitted for clarity.

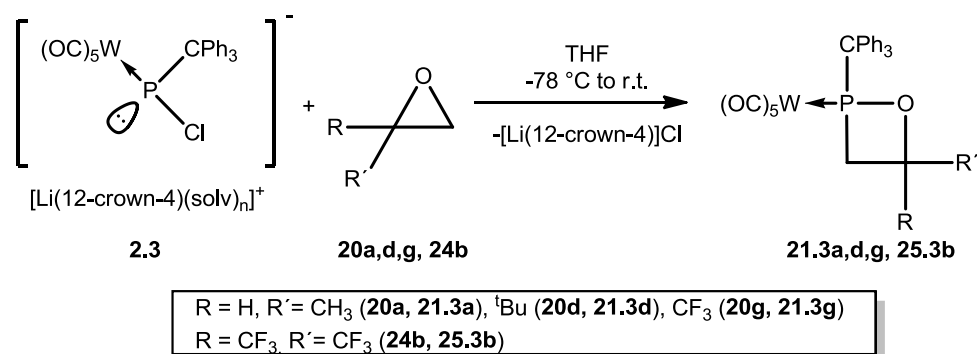
The data showed typical values for the bond lengths and angles, compared to previously presented 1,2-oxaphosphetane complexes. Unfortunately the structure of complex **21.2g** was of low quality, so that a further discussion based on direct comparison of the data for both complexes is not possible.

Table 5.13. Selected bond lengths in Å and angles in ° for complexes **21.2g** and **25.2b**.

	P-CH ₂	P-C4	P-W	CH ₂ -P-O1	folding angle
21.2g	1.95(2)	1.96(2)	2.554(7)	79.1(8)	14.2
25.2b	1.835(2)	1.849(2)	2.4768(6)	77.70(9)	10.1

5.3.2 *P*-CPh₃-substituted derivatives

With the *P*-CPh₃-substituted Li/Cl phosphinidenoid complex **2.3**,^[33] being stable up to ambient temperature, no problems were found in most reactions with mono-substituted epoxides (scheme 5.22 and figure 5.17).



Scheme 5.22: Reaction of Li/Cl phosphinidenoid complex **2.3** with different epoxides.

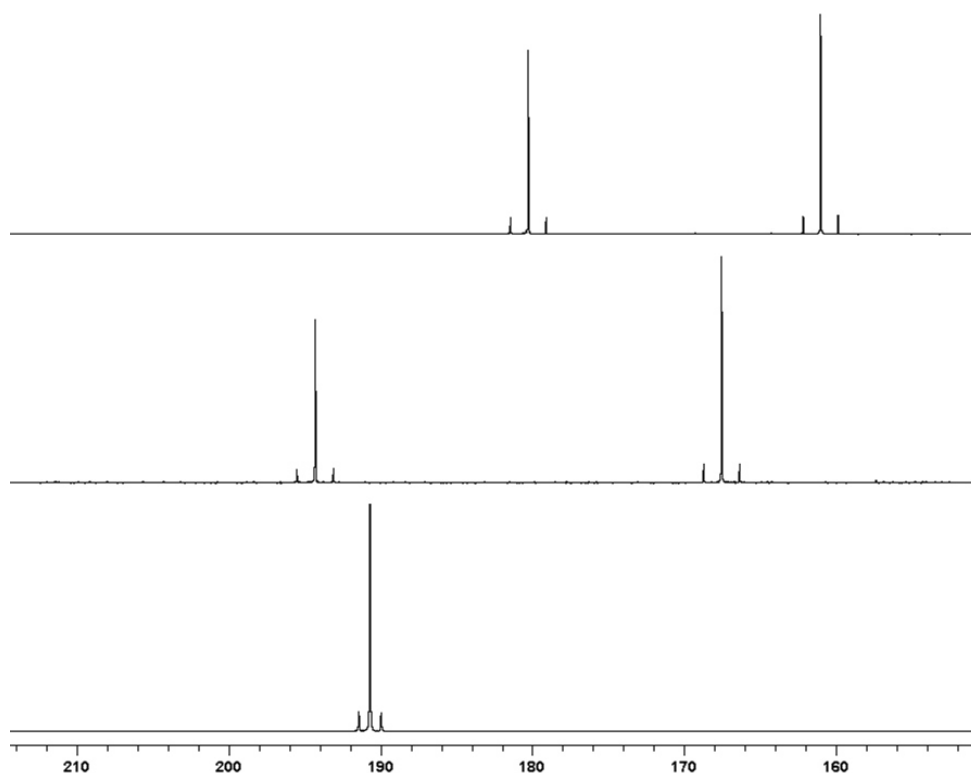


Figure 5.17: ³¹P{¹H} NMR spectra for the reactions of Li/Cl phosphinidenoid complex **2.3** with propylene oxide (**20a**, top), 1,1,1-trifluoro-2,3-propylene oxide (**20g**, middle) and hexafluoroisobutene oxide (**24b**, bottom), measured in CDCl₃.

Similar to the reactions using the *P*-C₅Me₅-substituted Li/Cl phosphinidenoid complex, only two isomers were found for the mono-substituted epoxides and only one isomer for the bis-CF₃-substituted derivative **25.3b**.

Table 5.14: $^{31}\text{P}\{^1\text{H}\}$ NMR data and yields for complexes **21.3a,g** and **25.3b**.

	R, R'	$\delta^{31}\text{P}$ [ppm] ($^1J_{\text{P,W}}$ [Hz])		ratio	yield [%]
		Isomer 1	Isomer 2		
21.3a ^{1,2}	Me, H	180.2 (283.1)	161.0 (278.3)	47:53	46 %
21.3g ^{1,2}	CF ₃ , H	194.3 (295.3)	167.5 (287.1)	42:58	32 %
25.3b	CF ₃ , CF ₃	190.7 (299.0)	-	-	32 %

The reactions using propylene oxide and 1,1,1-trifluoro-2,3-propylene oxide showed selective conversions to the 1,2-oxaphosphetane complexes. As expected, only two isomers were observed for these two cases, **21.3a**^{1,2} in a ratio of 47:53 and **21.3g**^{1,2} in a ratio of 42:58 (table 5.14).

All resonance signals show similarities to the ones found for the *P*-C₅Me₅ and *P*-CH(SiMe₃)₂-substituted complexes as far as chemical shift and coupling constants are concerned. While only a small influence of the *P*-substituent was found on most NMR data, the sterically demanding *P*-CPh₃ substituent leads to a stronger differentiation of the two isomers in the ^{31}P NMR spectra: a $\Delta\delta$ value of about 20-30 ppm for the *P*-CPh₃-substituted complexes, but only about 10-15 ppm for the derivatives bearing the other two *P*-substituents was found.

The reaction with hexafluoro isobutene oxide was still very selective but the work-up had to be done under complete exclusion of water, as long as the Lewis acidic salt [Li(12-crown-4)]Cl^[127] was present. This is in stark contrast to previously described 1,2-oxaphosphetane complexes, which showed no significant tendency to react with water under similar conditions. A surprisingly high stability was found when complex **25.3b** was in a salt free solution. No reaction with water could be observed in THF, even at elevated temperature ($T = 60\text{ }^\circ\text{C}$).

The resonance signal of complex **25.3b** in the $^{31}\text{P}\{^1\text{H}\}$ NMR spectrum (190.7 ppm, $^1J_{\text{W,P}} = 299.0$ Hz) is in the range found for similar 1,2-oxaphosphetane complexes (191.5 – 199.0 ppm, $^1J_{\text{W,P}} = 295.1 – 297.6$ Hz). All NMR characteristics are in accordance with the ones for *P*-C₅Me₅ and *P*-CH(SiMe₃)₂-substituted ring systems.

Single-crystal X-ray diffraction studies confirmed the 1,2-oxaphosphetane ring structure as the important feature of complexes **21.3a,g** and **25.3b** (Figure 5.18).

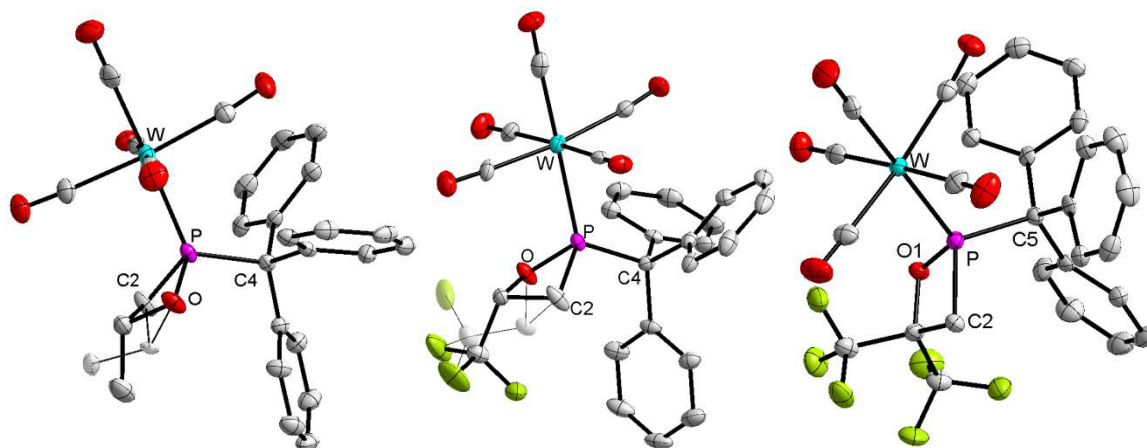


Figure 5.18: DIAMOND plot of the molecular structures of the *P*-CPh₃-substituted 1,2-oxaphosphetane complexes **21.3a** (left), **21.3g** (middle) and **25.3b** (right) in the solid state; the thermal ellipsoids are set at 50 % probability level and all hydrogen atoms are omitted for clarity. The split-sites (1:1) for the Me-C and F₃C-C units are represented using a transparent mode for clarity.

For the three complexes all structural parameters are in the expected range, but an elongation of the exocyclic bonds was observed, compared to similar complexes bearing the *P*-C₅Me₅ (**25.2b**: P-W: 2.4768(6) Å, P-C: 1.849(2) Å) or the *P*-CH(SiMe₃)₂ substituent (**25.1b**: P-W: 2.4562(19) Å, P-C: 1.805(7) Å).

Table 5.15: Selected bond lengths in Å and angles in ° for the *P*-CPh₃-substituted 1,2-oxaphosphetane complexes **21.3a**, **21.3g** and two independent molecules of **25.3b** (folding angles are given for solid/transparent part of the splitting).

	P-CH ₂	P-C ^{exo}	P-W	P-O	CH ₂ -P-O1	folding angle
21.3a	1.843(4)	1.905(4)	2.4926(12)	1.656(3)	80.49(18)	30.7/14.9
21.3g	1.841(4)	1.885(4)	2.4695(9)	1.681(2)	79.20(14)	34.4/21.1
25.3b	1.843(4)/	1.914(4)/	2.5017(11)/	1.706(3)/	78.41(15)/	10.2/
	1.800(4)	1.913(4)	2.4915(11)	1.713(3)	77.60(16)	10.5

The higher thermal stability of the Li/Cl phosphinidenoid complex, compared to the ones bearing the CH(SiMe₃)₂ and C₅Me₅ substituents, allowed the reaction with the ^tBu-substituted epoxide. Remarkable is, that no reaction was observed below ambient temperature. After warming up the Li/Cl phosphinidenoid complex was found as main product, first, but a slow and selective reaction was observed over time at ambient temperature. The data for complexes **21.3d**^{1,2} are in the expected range (**21.3d**¹: δ³¹P = 181.0 ppm (¹J_{W,P} = 285.2 Hz), **21.3d**² δ³¹P = 155.2 ppm (¹J_{W,P} = 279.9 Hz)) and the two isomers are formed in a ratio of 52 : 48 (figure 5.19).

Unfortunately no isolation was possible due to decomposition of the complexes during work up.

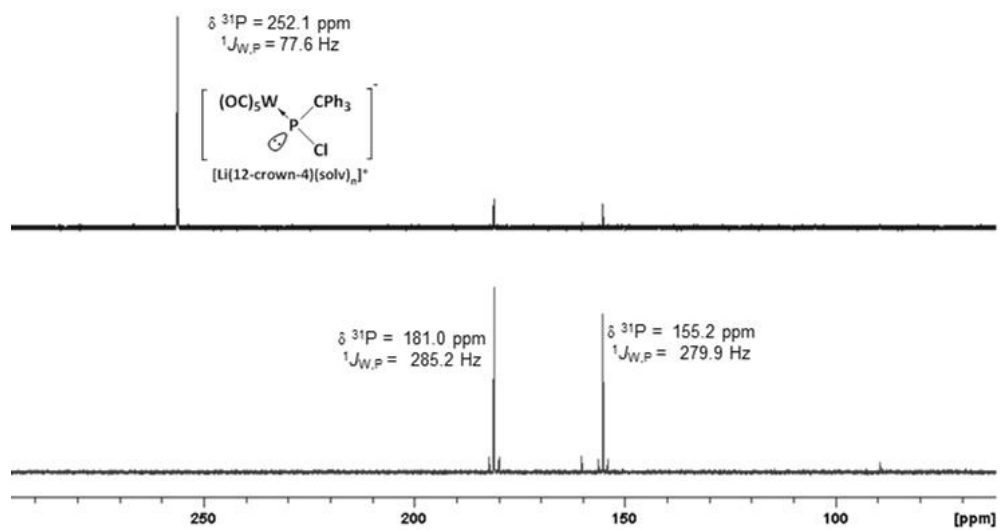
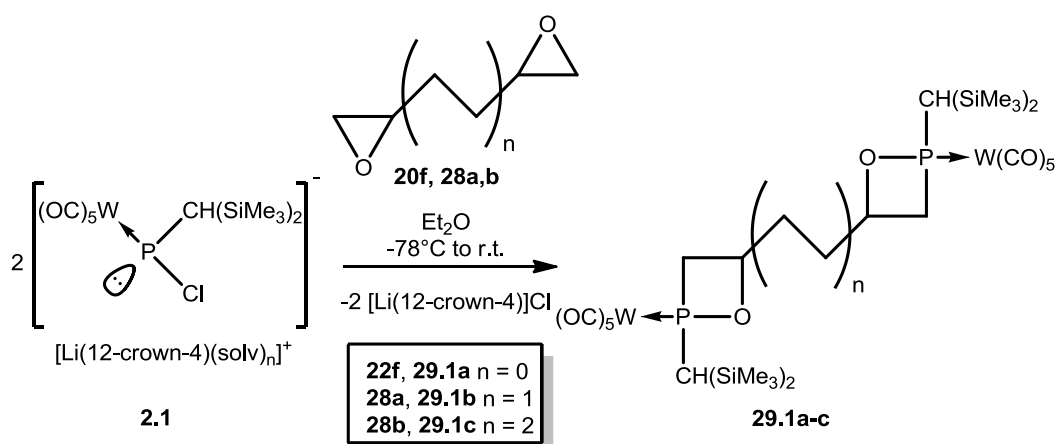


Figure 5.19. $^{31}\text{P}\{^1\text{H}\}$ NMR spectra of the reaction mixture of **2.3** with $t\text{Bu}$ -substituted epoxide (**20d**) (measured in THF) after 30 minutes at ambient temperature (top) and after 24 h at ambient temperature (bottom).

5.3.3 Attempts to synthesize bis-1,2-oxaphosphetane complexes

Polymers made from small heterocycles, *i.e.* oxiranes, oxetanes or tetrahydrofuranes, play a vital role in material science.^[81] Therefore, future research might be focused on the target to obtain similar polymers from related phosphorus ligands such as oxaphosphiranes, oxaphosphetanes or oxaphospholanes. In general, polymers can be prepared from two types of monomers: mono- or bifunctional monomers like alkenes, alkynes and epoxides. In the second case two possibilities exist: the combination of two (same or different) functional groups in one monomer and a second component having also two functional groups which are added for the polymerization.

Therefore, the fundamental question for the present case was: is a bis-1,2-oxaphosphetane complex accessible using the new protocol? To study this Li/Cl phosphinidenoid complex **2.1** and symmetric diepoxides (**20f**, **28a,b**) were applied. Taking into account that the stoichiometric reaction of 1,3-butadiene diepoxide was already explored (see chapter 5.2.1), *i.e.*, the mono ring expansion was clearly preferred but also significant amounts of side products (up to 50 % per integration in the ³¹P{¹H} NMR spectra) were observed in case of the reaction with **20f**.



Scheme 5.23: Strategy for the synthesis of bis-1,2-oxaphosphetane complexes **29.1a-c**.

Therefore, reaction of **2.1** and two other bis-epoxides having a variable chain length in-between the two epoxide rings, namely 1,5-hexadiene diepoxide (**28a**) and 1,7-octadiene diepoxide (**28b**), was studied (scheme 5.23). In case of 1,5-hexadiene diepoxide reaction to 1,2-oxaphosphetane complexes was only observed as minor reaction pathway, and the main products were the diphosphene complexes **22** and **23** (figure 5.20, middle). In contrast a selective reaction was observed for 1,7-octadiene diepoxide. Here, besides 6 % of diphosphene complexes (presumably due to the weight measuring error in such a small scale reaction), several resonance signals in the typical range of 1,2-oxaphosphetane

complexes were observed. As expected not only four but a larger number of different isomers were observed. Nevertheless, it was found that even in this case the typical signal pattern for 3-4 sets of isomers could be observed that was found for all mono-substituted 1,2-oxaphosphetane complexes bearing the $P\text{-CH}(\text{SiMe}_3)_2$ group (see chapter 5.2.1).

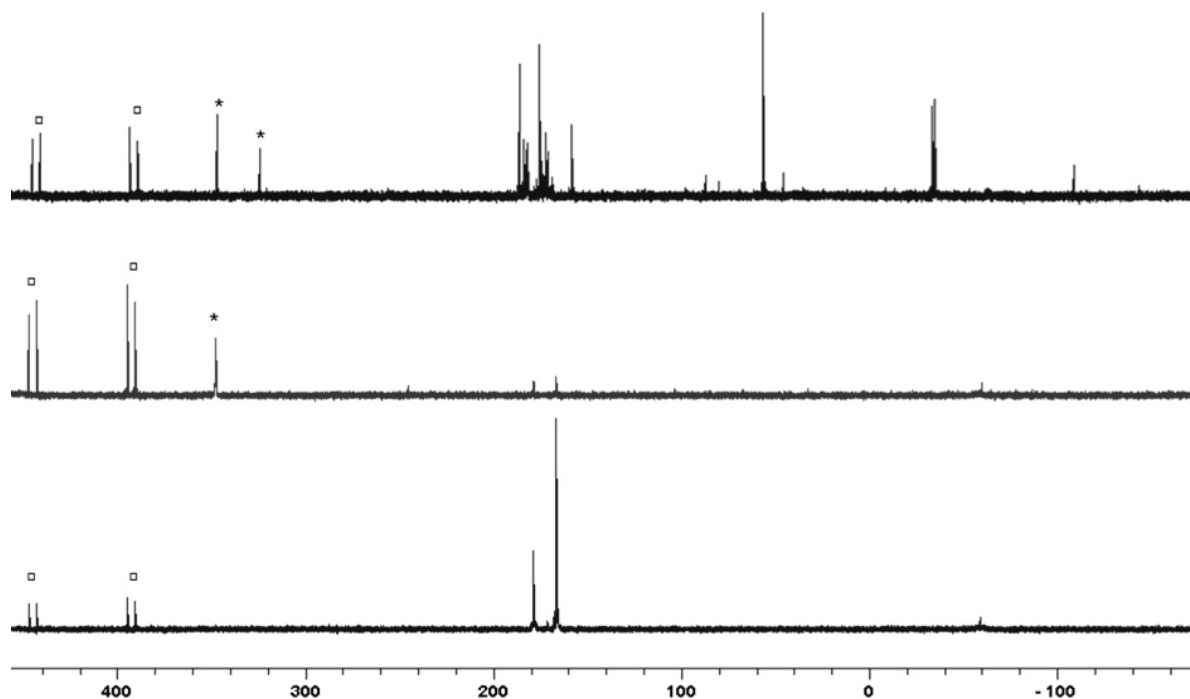


Figure 5.20: $^{31}\text{P}\{^1\text{H}\}$ NMR spectra for the performed test reactions using 1,3-butadiene diepoxide (**20f**, top), 1,5-hexadiene diepoxide (**28a**, middle) and 1,7-octadiene diepoxide (**28b**, bottom) (* and \square describe diphosphene complexes with two (*, **22**) and one $\text{W}(\text{CO})_5$ unit (\square , **23**)).

Due to the large number of isomers (figure 5.21) –the number of isomers could not be determined – no further NMR spectroscopic characterization could be performed. But the nature of the products was proven by other techniques, *i.e.* the MS experiment (EI, 70 eV) showed the signal for the molecular ion of **29.1c** (calc. for $\text{C}_{32}\text{H}_{52}\text{O}_{12}\text{P}_2\text{Si}_4\text{W}_2$) at m/z 1170.1; the subsequent loss of 10 CO molecules was found to be the preferred fragmentation pathway in this case.

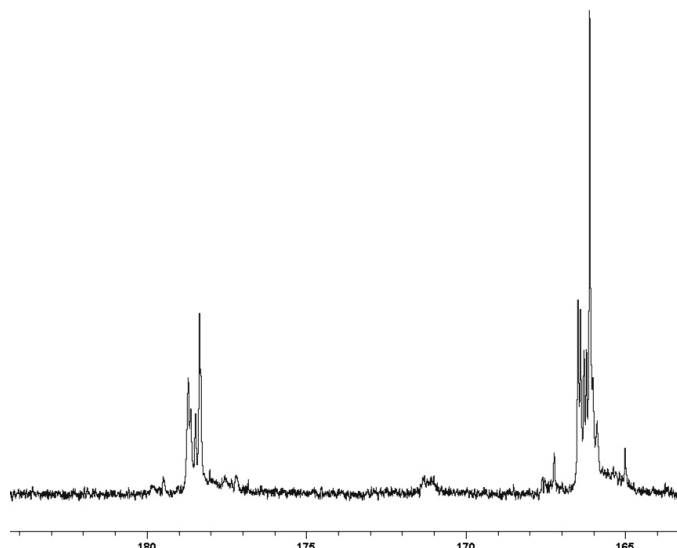


Figure 5.21: $^{31}\text{P}\{^1\text{H}\}$ NMR spectrum of the isolated complex **29.1c**. Visible are groups of the different isomer signals and the typical isomeric pattern found also for other *C*-mono-substituted 1,2-oxaphosphetane complexes.

The elemental analysis of the mixture of **29.1c** (calc. for $\text{C}_{32}\text{H}_{52}\text{O}_{12}\text{P}_2\text{Si}_4\text{W}_2$: C 32.83 %, H 4.48 %; found C 33.08 %, H 4.56 %) lend further support to the proposed molecular composition of the products. Finally, a single crystal suitable for an X-ray diffraction study could be obtained from a saturated *n*-pentane solution at 4 °C thus confirming the proposed ligand structure (figure 5.22).

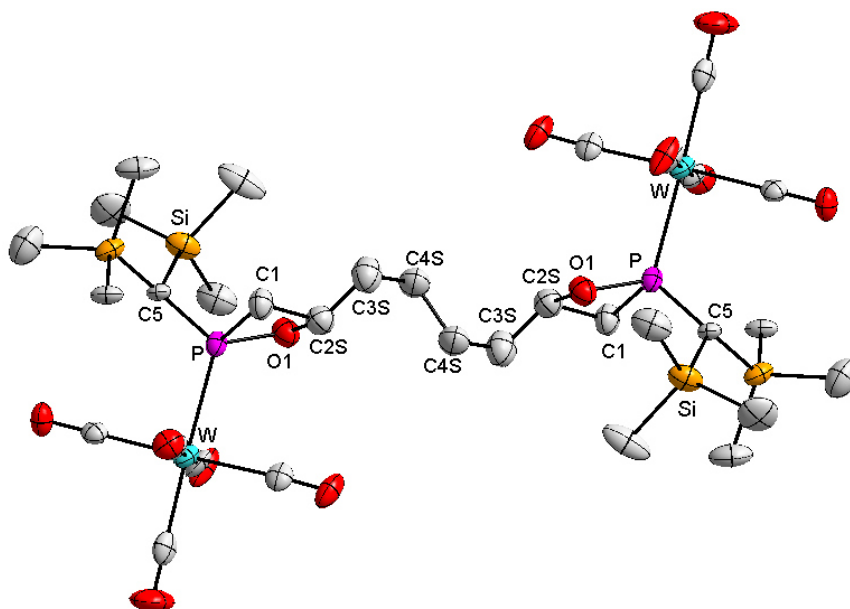


Figure 5.22: DIAMOND plot of the molecular structure of complex **29.1c** in the solid state; the thermal ellipsoids are set at 50 % probability level and all hydrogens are omitted for clarity. Only the main orientation of the bridging C_4 -unit and the ring folding is shown for clarity (split ratio 82:18). Selected bond lengths in Å and angles in °: W-P 2.480(3), P-C5 1.809(12), P-C1 1.824(14), P-O1 1.689(9), O1-P-C1 79.1(5), C5-P-W 116.7(4).

5.4 Some conclusions on 1,2-oxaphosphetane complexes

Comparison of the newly synthesized 1,2-oxaphosphetane complexes led to the following noteworthy aspects:

Most reactions proceeded with high selectivity and the formation of regioisomers was rarely observed, *i.e.* complex **16.1** represents the only 3-substituted 1,2-oxaphosphetane complex, so far. The reactivity of epoxides bearing sterically demanding substituents could be significantly enhanced by the introduction of strongly electron-withdrawing groups at the ring *C*-atom; *e.g.*, reaction of *P*-CH(SiMe₃)₂-substituted Li/Cl phosphinidenoid complex **2.1** with *C*-CF₃-substituted epoxides (**20g** or **24b**) was possible while the corresponding *C*-^tBu derivative (**20d**) showed almost no reaction.

All isolated 1,2-oxaphosphetane complexes showed a high thermal stability, so that no or only slow decomposition was found in boiling toluene (111 °C). In several cases, even the transition to the gas phase could be performed without problems, *i.e.* complex **34.2** (cf. chapter 6) could even be evaporated for the purpose of purification without decomposition. In addition, a very low sensitivity towards water and oxygen was observed for the purified complexes. Of high interest for the purification was the solubility of the complexes: those complexes bearing the *P*-C₅Me₅ and the *P*-CH(SiMe₃)₂ substituent showed a good solubility in *n*-pentane or petroleum ether at ambient temperature. In contrast, the *P*-CPh₃-substituted derivatives were almost insoluble under similar conditions and significantly better soluble in diethyl ether and chlorinated solvents (CHCl₃, CH₂Cl₂).

Problems appeared due to the relative orientation of the *C*-substituent, either facing towards the M(CO)₅ substituent or away from it, therefore at least two isomers were formed for all *C*-monosubstituted derivatives. In addition, atropisomerism was found for *P*-CH(SiMe₃)₂-substituted complexes, giving rise to the problem of proper signal assignments in case of the minor isomers due to a bad signal-to-noise ratio. Consequently, further comparison of analytical data was hampered and, therefore, these 1,2-oxaphosphetane complexes were discussed separately in chapters 5.2 and 5.3.

Especially the ³¹P{¹H} NMR data were found to be strongly influenced by the *C*-substituents. If for easier comparison between the derivatives the mean values of the isomers are taken a clear trend towards lower field shifted signals as well as higher ¹J_{W,P} coupling constants was observed when electron withdrawing *C*-substituents were introduced. A change of the *P*-substituent only resulted in small changes of below 20 ppm, dependent on the derivatives that are compared. The strongest shielding was observed for

P-CH(SiMe₃)₂-substituted complexes and the strongest deshielding for the *P*-C₅Me₅-substituted derivatives.

Comparison of the molecular structures obtained from X-ray diffraction studies were also hampered by problems due to the isomerism. Here, some structures were determined possessing either two isomers (co-crystallized) or only one of the possible isomers. Most structures were obtained showing the *s-cis* conformation for the *P*-CH(SiMe₃)₂ substituent, but also one example for the *s-trans* conformation could be observed (**25.1a**). No significant changes of the ring bond lengths and angles were observed upon changes of the *P*-substituents and no clear-cut trend was observed for electronic or sterical effects of the *C*-substituent.

Comparison of 16 structures led to the observation that the ring itself is almost invariant to the substitution pattern and mean values are given in figure 5.23. The structure of the 3-substituted derivative **16.1** as well as **29.1c** and the structures of **21.2g** and **25.1b**, having low quality, were not taken into account for this comparison. Also split layers were not taken into account due to significantly higher standard deviations and only one of two independent molecules of **25.3b**.

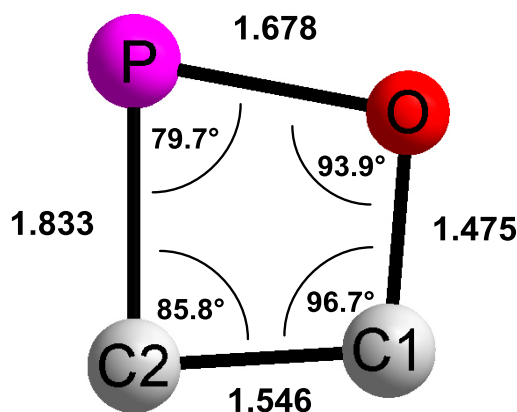


Figure 5.23: Average bond lengths and angles for the ring system in 1,2-oxaphosphetane complexes.

Surprisingly no significant influence was found by the changed relative orientation of the C-R group and the metal fragment in case of complexes **21.1g** and **21.1f**.

A small influence was observed on the P-O bond length by introducing CF₃ groups in the molecules. Going from the *C*-Me to the *C*-CF₃ and *C*(CF₃)₂-substituted derivatives a slight elongation of this bond was observed, while the other bonds show no significant difference. This is observable especially in case of the *P*-CPh₃-substituted derivatives with values for the bond lengths of 1.656(3)Å (**21.3a**) < 1.681(2)Å (**21.3g**) < 1.706(3)/1.713(3) (**25.3b**) and could be either due to the steric demand of the CF₃ groups or their electronic influence.

Table 5.16: Ranges for bond lengths in Å and angles in ° for 1,2-oxaphosphetane complexes and σ^5, λ^5 -oxaphosphetanes (CXXX^[95], CXXXI^[97], CXXXII^[96], CXXXIII^[99]).

	1,2-oxaphosphetane complexes	CXXX-CXXXIII
P-O	1.663(2) - 1.7272(17)	1.781(6) - 1.851(1)
P-C2	1.800(5) - 1.858(4)	1.822(2) - 1.831(3)
O-C1	1.433(4) - 1.527(6)	1.36(2) - 1.404(3)
C1-C2	1.518(3) - 1.603(7)	1.520(5) - 1.55(1)
C2-P-O	77.70(9) - 81.08(12)	73.30(9) - 75.5(6)
P-O-C1	91.8(3) - 96.1(2)	94.7(2) - 97.0(5)
O-C1-C2	94.4(4) - 98.5(3)	97.0(7) - 100.5(14)
C1-C2-P	82.7(3) - 88.44(15)	88.1(11) - 93.0(1)

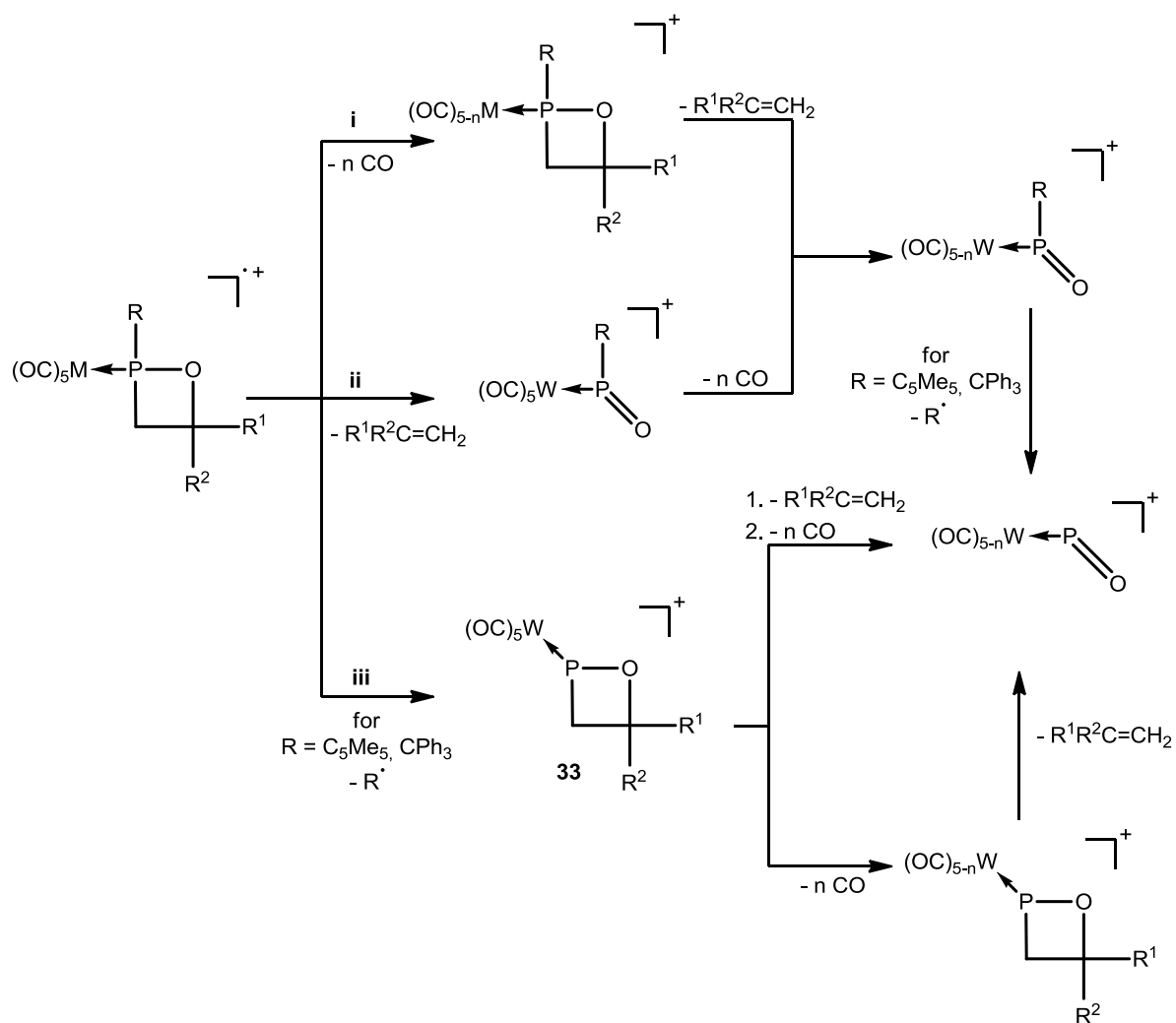
Comparison to the σ^5, λ^5 -P derivatives, known in the literature, revealed several significant differences for bond lengths and angles (table 5.16): The P-O bond length is shortened in the complexes and the O-C bond is elongated. In contrast neither the P-C nor the C-C bonds show any significant difference. Although the O-P-C angle is increased in the complexes by an average of approximately 4.5° all other angles are smaller so that the overall sum of bond angles is not varying much.

In addition, a stronger influence of the substitution pattern was found on the folding angle of the ring, *i.e.* some derivatives with *P*-CH(SiMe₃)₂ substituents have almost planar rings while most possess strongly folded rings with folding angles between 10° and 30° (cf. chapter 5.2.1 and figure 5.10).

The IR spectra of the complexes showed three absorption bands for the carbonyl groups, as expected for an M(CO)₅L fragment,^[128] stemming from two A₁ and an E symmetric vibration. The signals are almost the same for all complexes, independent of the substitution pattern. An almost negligible influence was observed showing a slight shift to higher wave numbers for all three absorption bands with introduction of electron withdrawing substituents as well as by comparison of the *C*-mono-substituted and *C*-disubstituted complexes.

Especially the mass spectrometric data allow a closer comparison between all the obtained derivatives. All 1,2-oxaphosphetane complexes showed mass spectrometric fragmentation (EI, 70 eV) which can be divided into three typical decomposition pathways, mainly depending on the substituent at phosphorus. The first step was in most cases either found to be the splitting of a metal carbon bond with loss of different numbers of CO (**i**) or, to a minor part, the loss of an alkene unit (**ii**), similar to the oxaphosphetane decomposition in the Wittig reaction. The two pathways **i** and **ii** can happen in different order until all CO groups and the alkene are lost. For complexes where R = C₅Me₅ or CPh₃, a third pathway was found (**iii**),

which, in case of C_5Me_5 , was even the preferred one. Here, splitting of the exocyclic P-C bond with loss of the *P*-substituent was found, either before or after loss of CO and the alkene unit, in the latter case, complexes of the type $[(OC)_{5-n}W\{PO}]^{[129]}$ are formed. For most 1,2-oxaphosphetane complexes bearing the $P-CH(SiMe_3)_2$ substituent the formation of a phosphinidene oxide complex ($[(Me_3Si)_2HCRP(O)W]$) after complete loss of all five CO and the alkene was found.

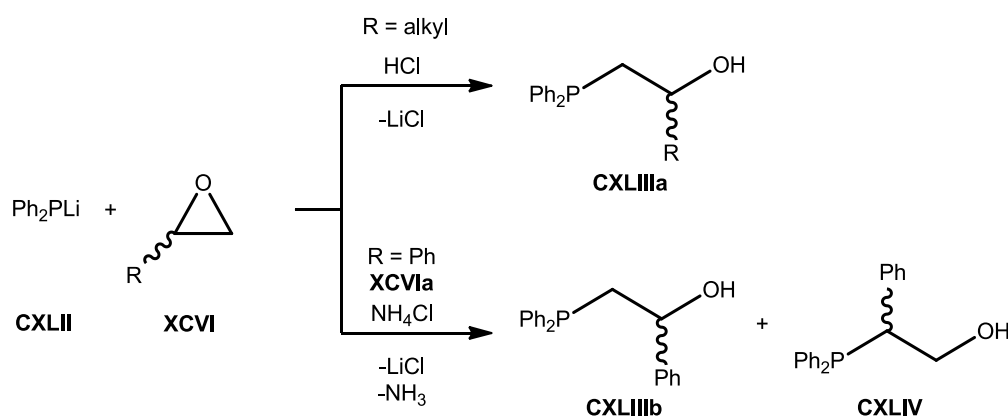


Scheme 5.24: Main mass spectrometric fragmentation pathways of 1,2-oxaphosphetane complexes under EI conditions (70 eV).

5.5 Proposed mechanism for the 1,2-oxaphosphetane complex formation

A proposal for a reaction mechanism was developed based on investigations on the reactivity of Li/Cl phosphinidenoid complexes towards epoxides.

Earlier studies on ring opening reactions of epoxides **XCVI** with alkali metal phosphanides **CXLII** have shown a preference for nucleophilic attack at the least hindered side of the epoxide ring, yielding 1,2-phosphanyl alcohols **CXLIII** as final products (scheme 5.25).^[122] Further studies showed that, in case of aryl substituents, a mixture of two regioisomeric products can be observed, resulting from the reaction either at the benzylic position or the least hindered side (e.g. R = Ph, ratio (**CXLIIIb**: **CXLIV**) 70:30).^[117]

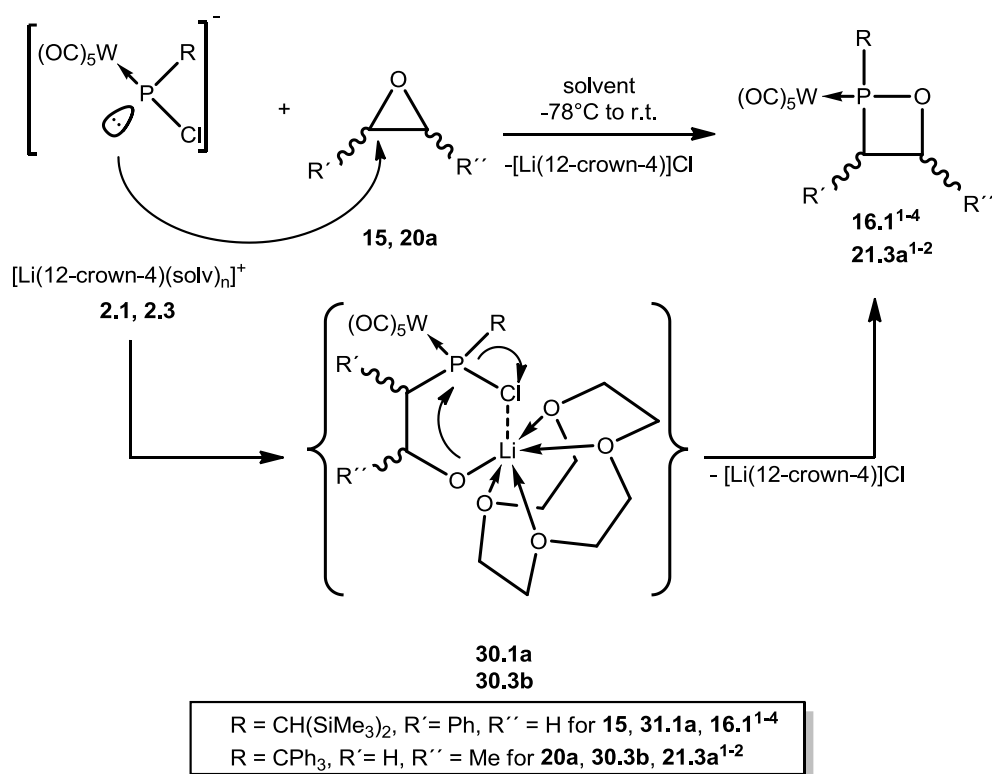


Scheme 5.25: Ring opening reactions of mono-substituted epoxides with lithium diphenylphosphanide.^{[122][117]}

The observed reaction of alkyl-substituted epoxides and Li/Cl phosphinidenoid complexes at the least hindered side as well as the activation of epoxides by electron-withdrawing substituents increasing the electrophilicity support this interpretation. Of special interest and, hence, crucial for the understanding of the mechanism is the regiochemical differentiation that was observed in case of styrene oxide (chapter 5.2.1). In aryl-substituted epoxides, the ring carbon atom that is located at the benzylic position is the most electrophilic one and, therefore, often the preferred site of attack in nucleophilic ring opening reactions. In contrast to this, a reaction of a terminal electrophilic phosphinidene complex would be expected to take place preferably at the least hindered side.

Here an ionic mechanism was proposed based on these observations (scheme 5.26). The acyclic intermediate **30** is formed after an initial nucleophilic ring opening by the Li/Cl phosphinidenoid complex **2**, followed by an intramolecular nucleophilic substitution that is facilitated by the close proximity of both reactive centres. A preorientation of the ring because of a Li/Cl interaction might also be assumed. Similar interactions were described previously, e.g. in the decomposition of alkoxyphosphinidenoid complexes.^[10] Somewhat similar

intermediates were proposed for the formation of oxaphosphirane complexes by Klein,^[34] which were also supported by DFT calculations performed by Espinosa.^[130]



Scheme 5.26: Proposed reaction mechanism for the formation of 1,2-oxaphosphetane complexes, examples are given for the formation of **16.1¹⁻⁴** and **21.3a¹⁻²**.

To obtain additional evidence for the formation of intermediates, a variable temperature ³¹P{¹H} NMR study (-60 °C to 25 °C in steps of 10 °C, figure 5.24) was performed to investigate the reaction of *P*-CPh₃-substituted Li/Cl phosphinidenoid complex **2.3** and propylene oxide **20a**.

The reaction starts at -60 °C and is finished after reaching -10 °C. This observation again supports the ionic mechanism, as no decomposition of the *P*-CPh₃-substituted Li/Cl phosphinidenoid complex can be observed up to ambient temperature in the absence of a substrate.^[33] An intermediate formation and subsequent reaction of a terminal phosphinidene complex can therefore be excluded.

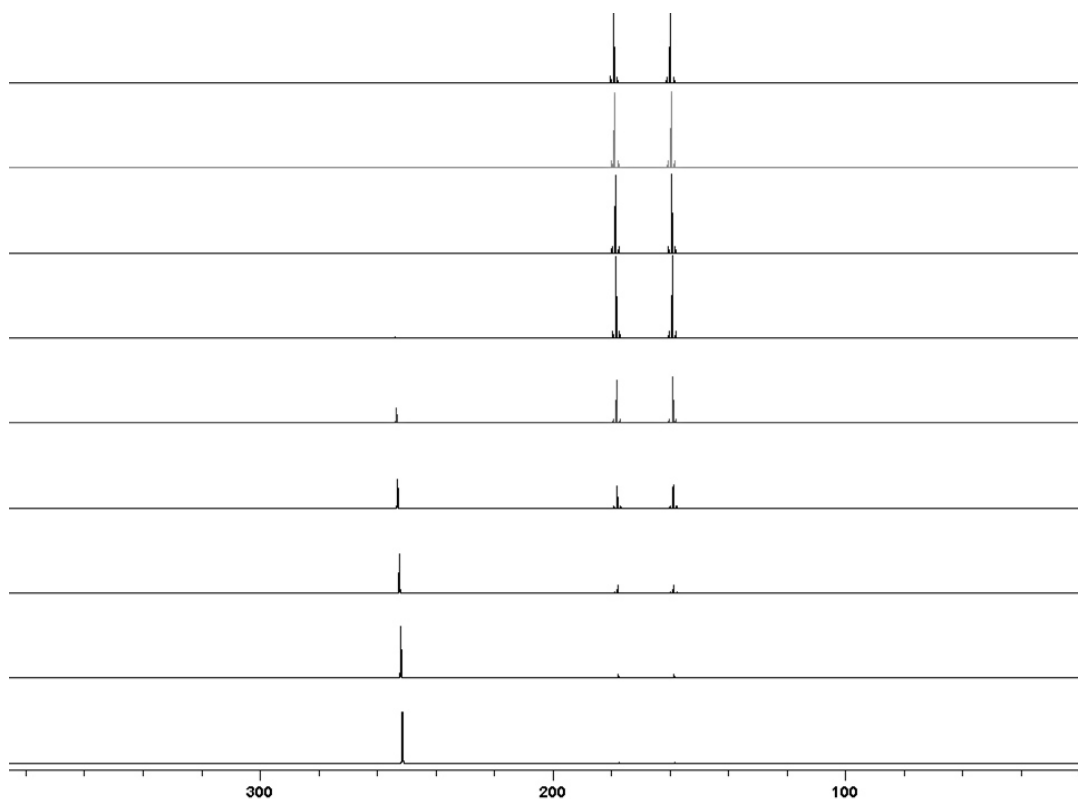


Figure 5.24: Low temperature $^{31}\text{P}\{^1\text{H}\}$ NMR monitoring of the reaction between **2.1** and propylene oxide **20a** in THF. Shown are the spectra obtained from $-60\text{ }^\circ\text{C}$ (bottom) to $20\text{ }^\circ\text{C}$ (top) in steps of $10\text{ }^\circ\text{C}$ difference.

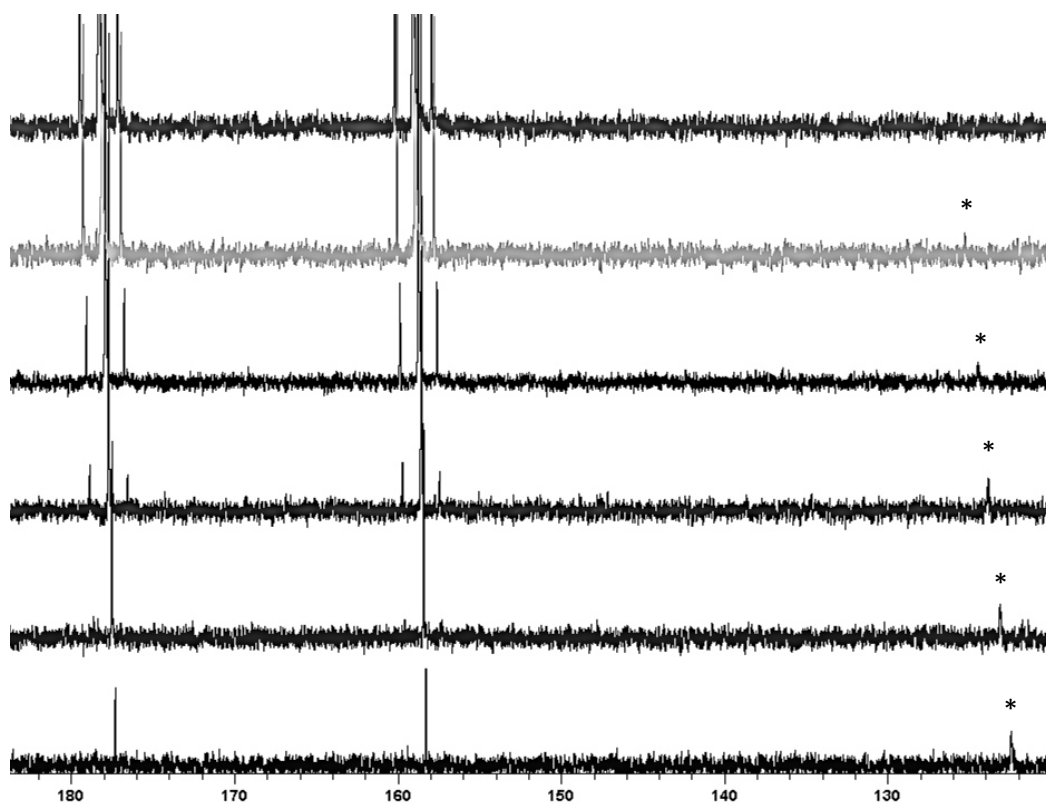


Figure 5.25: Zoom in on the low temperature $^{31}\text{P}\{^1\text{H}\}$ NMR monitoring of the reaction between **2.3** and propylene oxide **20a**. Shown are the spectra obtained from $-60\text{ }^\circ\text{C}$ (bottom) to $-10\text{ }^\circ\text{C}$ (top) (steps of $10\text{ }^\circ\text{C}$).

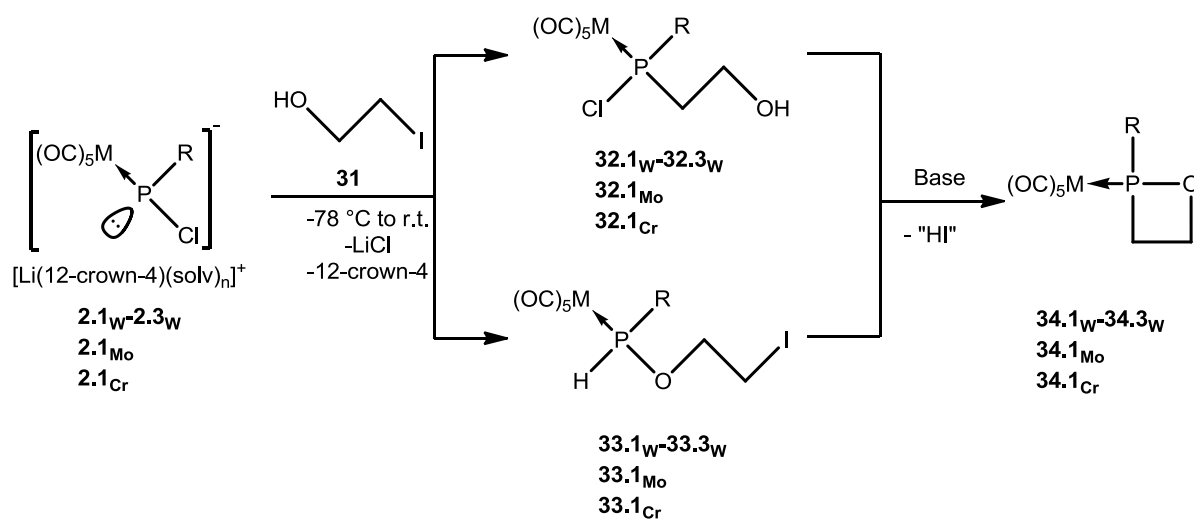
The $^{31}\text{P}\{^1\text{H}\}$ NMR spectra of the low temperature monitoring (figure 5.24) show mainly the resonance signals for the Li/Cl phosphinidenoid complex at 252.1 ppm with a typical small magnitude for the $^1J_{\text{W,P}}$ coupling constant (77.6 Hz) and two signals for the isomeric 1,2-oxaphosphetane complexes at 180.2 ppm ($^1J_{\text{W,P}} = 283.1$ Hz) and 161.0 ppm ($^1J_{\text{W,P}} = 278.3$ Hz). Nevertheless, closer inspection of the area between 100 and 200 ppm at low temperature revealed an additional resonance signal at approximately 125 ppm that is present as long as the reaction proceeds (*, figure 5.25). Assuming the nucleophilic ring opening reaction to be the rate determining step thus leading to a small and quasi-stationary concentration of the intermediate **30.3b** would explain the low intensity of the resonance signal.

A $P\text{-CH}(\text{SiMe}_3)_2$ -substituted chloro(2-hydroxypropyl)phosphane complex **47.1b**¹⁻² that is structurally closely related to the proposed intermediate could be synthesized (see later on chapter 8.2) and shows a similar shift in the ^{31}P NMR spectrum to the observed resonance signal (**47.1b**¹: $\delta^{31}\text{P} = 119.8$ ppm, $^1J_{\text{W,P}} = 276.0$ Hz, **47.1b**²: $\delta^{31}\text{P} = 115.1$ ppm, $^1J_{\text{W,P}} = 274.2$ Hz). Deprotonation of this complex, formally leading to a similar intermediate, and the subsequent formation of 1,2-oxaphosphetane complexes further support the proposed mechanism (see chapter 8.2).

6 A novel route to C-unsubstituted O,P-containing heterocycles

A novel synthetic strategy to O,P-containing heterocycles was developed in order to clarify if substitution at the ring carbon atoms is crucial for the ^{31}P NMR spectroscopic characteristics as well as for the thermal stability of these complexes.

The proposed synthetic strategy was the formation of an acyclic intermediate followed by a ring closing reaction in the second step. The first reaction step, the reaction of Li/Cl phosphinidenoid complexes with α,ω -halogenoalcohols (e.g. 2-iodoethanol, **31**), could lead to two types of products: the one formed by formal insertion into the OH bond of the alcohol (e.g. **33**) or the product of the nucleophilic substitution at the C-halogen centre (e.g. **32**) (scheme 6.1). Examples for both reactions, using only non-functionalized alcohols (methanol, *iso*-propanol, allyl alcohol) or electrophiles (methyl iodide), are known from previous studies. The knowledge about reactions with alcohols profits from results previously obtained in my MSc thesis, *i.e.* from the experience obtained for non-functionalized alcohols (chapter 1.2). Apart from that the envisaged study would also examine the functional group tolerance of the formal P_1 insertion reaction into an O-H bond.

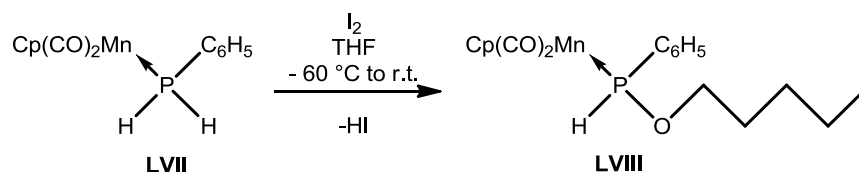


Scheme 6.1: Proposed synthetic strategy to different C-unsubstituted 1,2-oxaphosphetane complexes.

Both initially formed complexes could lead to the desired ring systems via an intramolecular nucleophilic substitution after deprotonation by a suitable base. This reaction sequence offers several advantages to the previously described one: the probable elimination of regio- and stereoisomers due to loss of the C-substitution (chapter 5), the avoidance of toxic heterocycles like ethylene oxide gas by substituting them with α,ω -halogenoalcohols, e.g. 2-iodoethanol, as synthetic equivalents.

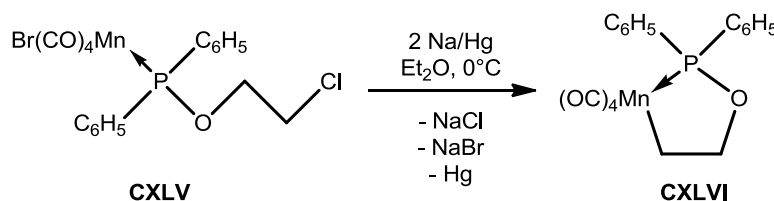
It is remarkable that no similar ring closing reaction has been described to date, especially as Huttner had already reported in 1975 on the formation of an α,ω -substituted phosphinite

complex, representing the first stable derivative of this class of compounds. The alkoxy substituent in **LVIII** was hereby formed by ring opening of THF with *in situ* generated HI (scheme 6.2).^[48]



Scheme 6.2: Synthesis of the first phosphinite complex by Huttner.^[48]

One more related reaction has to be mentioned. Lindner utilized a similar reaction procedure to form metallacycle **CXLVI**,^[131] although no ring closing reaction to a heterocyclic phosphane ligand was described (scheme 6.3).



Scheme 6.3: Ring closing reaction of a chloroethoxyphosphane complex.^[131]

The first attempted reaction sequence with α,ω -halogenoalcohols was aiming at the synthesis of a C-unsubstituted 1,2-oxaphosphetane complexes **34**.

The reaction between **2.1** and 2-iodoethanol (**31**) led selectively to the 2-iodoethylphosphinite complex **33.1_w**, as the ³¹P NMR spectrum of the reaction mixture showed only one signal at 106.7 ppm with a direct coupling to one hydrogen atom (¹J_{P,H} = 321.4 Hz) and satellites due to the coupling to the ¹⁸³W nucleus (¹J_{W,P} = 270.3 Hz) and thus a quantitative conversion. These parameters are in good accordance and lie within the range of known phosphinite complexes bearing the *P*-CH(SiMe₃)₂ substituent ($\delta^{31}\text{P}$ = 91 - 109 ppm, ¹J_{W,P} = 266 - 274 Hz).

Complex **33.1_w** was obtained as yellow oil via extraction from the reaction mixture with *n*-pentane which partially solidified while standing at 4 °C. Tiny single-crystals could be obtained after several weeks, so that, in addition to multinuclear NMR and MS measurements, the molecular structure of the product could be confirmed by single crystal X-ray diffraction studies (Figure 6.1).

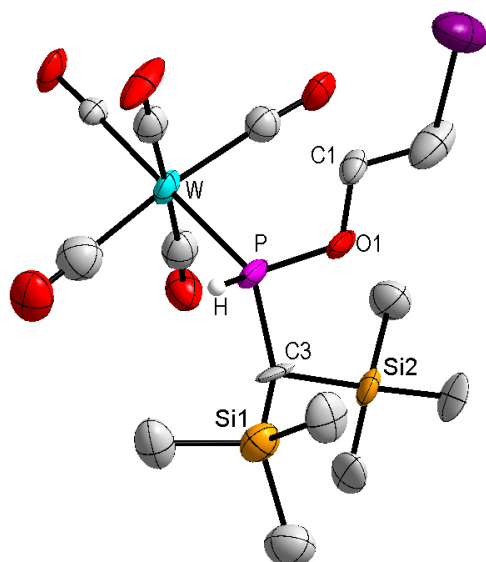
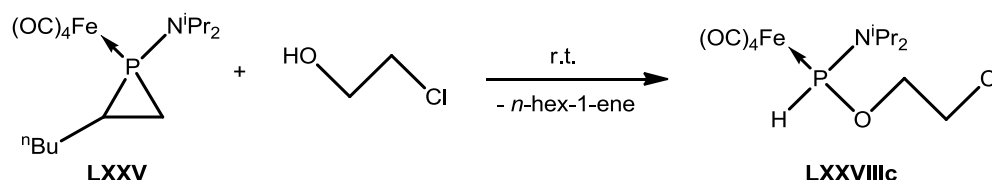


Figure 6.1: DIAMOND plot of the molecular structure of 2-iodoethylphosphinite-complex **33.1_w** in the solid state; the thermal ellipsoids are set at 50 % probability level and all hydrogen atoms except at phosphorus are omitted for clarity.

A related result was reported by Lammertsma at the time this research was performed. Iron complex **LXXVIIIc** was obtained by insertion of tetracarbonyl-[(diisopropylamino)phosphinidene]iron(0) into the OH bond of 2-chloroethanol (scheme 6.4),^[58] showing a similar shift for the resonance signal in the ³¹P NMR spectrum ($\delta^{31}\text{P} = 136.5$ ppm) and structural similarities to **33.1_w**. But no further investigations on its reactivity have been described, yet.

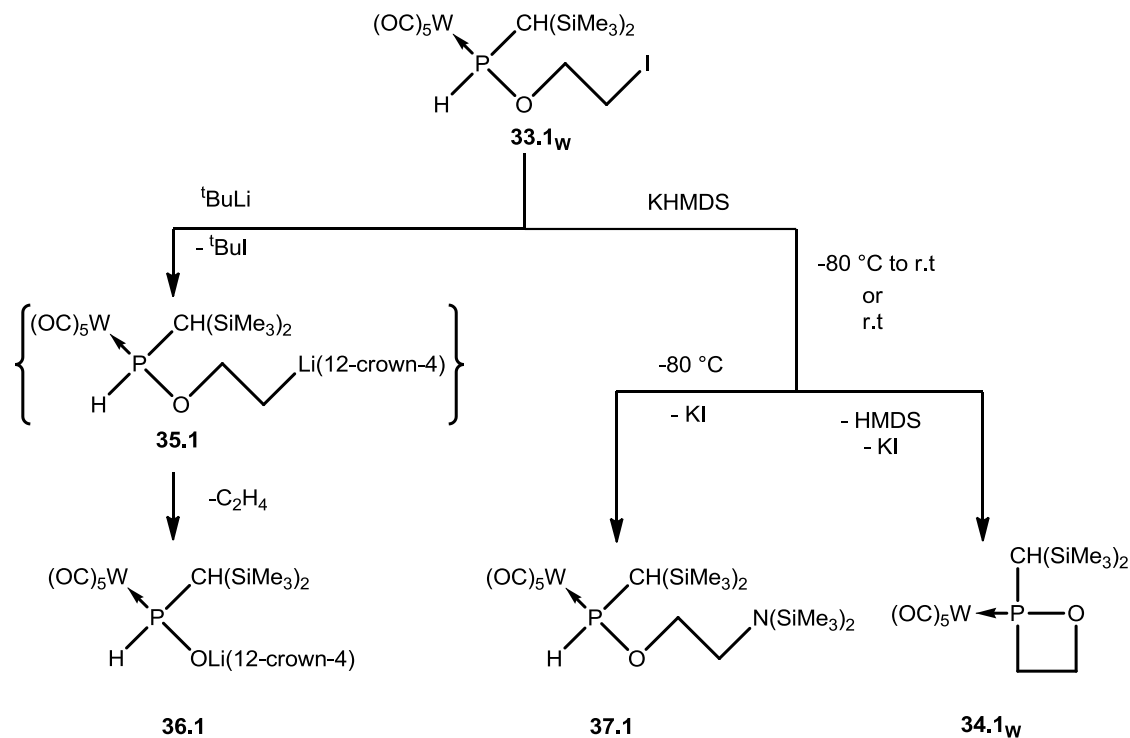


Scheme 6.4: Synthesis of **LXXVIIIc** by Lammertsma.^[58]

Surprisingly, complex **33.1_w** showed several base- and temperature-dependent reaction pathways, not only the proposed formal HCl elimination and cyclization. When *tert*-butyllithium in the presence of 12-crown-4 was used, an interesting result was obtained: not the expected 1,2-oxaphosphetane, but a phosphinito complex was formed (**36.1**, scheme 6.5). A selective lithium/iodine exchange, as typical reaction for lithium organic reagents, took place instead of the expected P-deprotonation, yielding **35.1**, followed by an elimination of ethylene to yield phosphinito complex **36.1** as final product (scheme 6.5).

Complex **36.1** was described before, and for the first time by Duan in 2011.^[132] However, the novel synthetic access is superior due to the fact that the previous route was more time-consuming and more expensive as silver acetate had to be used. Starting from

dichloro(organo)phosphane complex **1.1** (isolated yield up to 75 %) this new route enabled easy access towards synthetic studies of phosphinito complex **36.1** as building block for novel phosphane ligands bearing a POE motif. First reactions and results using this building block will be discussed at the end of this chapter.



Scheme 6.5: Base- and temperature-dependent reactions of 2-iodoethylphosphinite complex **33.1_w**.

Two different reaction pathways were observed when the less nucleophilic base $\text{KN}(\text{SiMe}_3)_2$ (KHMDS for short) was used for the deprotonation (scheme 6.5). When the reaction was performed at low temperature ($-80\text{ }^\circ\text{C}$), even with an excess of KHMDS (molar ratio 1 : 1.25) a mixture of two compounds was observed by ^{31}P NMR spectroscopy; both could be separated via low temperature column chromatography.

One product showed a resonance signal at 105.2 ppm with a direct coupling to the P-bound hydrogen atom ($^1J_{\text{P,H}} = 320\text{ Hz}$) and satellites from the coupling to the ^{183}W nucleus ($^1J_{\text{W,P}} = 267.6\text{ Hz}$); this is similar to the data obtained for the starting material **33.1_w** (106.7 ppm, $^1J_{\text{P,H}} = 321.4\text{ Hz}$, $^1J_{\text{W,P}} = 270.3\text{ Hz}$). The small influence on the ^{31}P NMR characteristics for this first reaction product implies a change in the molecular structure further away from the phosphorus centre; therefore, complex **37.1** can be proposed as product of a nucleophilic substitution. The isolation of this complex was unfortunately not possible due to decomposition during column chromatography.

The second compound (complex **34.1_w**) showed a resonance signal in the ^{31}P NMR spectrum at 190.3 ppm with a $^1J_{\text{W,P}}$ coupling constant of 267.7 Hz and no direct coupling to a proton. These data are in the typical range found for other 1,2-oxaphosphetane complexes

(see chapter 5). Isolation from the mixture, obtained at low temperature, was possible via low temperature column chromatography, but only in low yields (29 %).

When the reaction was performed at ambient temperature, a significant increase in selectivity was observed, yielding 1,2-oxaphosphetane complex **34.1_w** via an intramolecular nucleophilic substitution reaction (scheme 6.5) in good overall yields (up to 60 % starting from dichlorophosphane complex **1.1**).

Surprisingly, no isomerism due to the orientation of the CH group of the CH(SiMe₃)₂ substituent, that presented a significant problem in the characterization of other derivatives, was observed for complex **34.1_w**. A similar observation, regarding the selective formation of only one isomer, was found for the class of oxaphosphirane complexes by Pérez.^[114] There, the ring opening reaction with HCl, followed by a base-induced ring closing reaction, only led to the formation of only one of two possible isomers.

For further comparison the reaction was repeated using the Mo(CO)₅ and Cr(CO)₅-substituted 2-iodoethyl phosphinite complexes **33.1_{Mo}** and **33.1_{Cr}** under otherwise identical conditions and the corresponding 1,2-oxaphosphetane complexes **34.1_{Mo}** and **34.1_{Cr}** could be isolated in reasonable yields via column chromatography and subsequent recrystallization or precipitation from *n*-pentane (see table 6.1).

Table 6.1: Selected NMR data (CDCl₃) and yields for the C-unsubstituted 1,2-oxaphosphetane complexes **34.1_{w-cr}**.

	³¹ P NMR	¹³ C{ ¹ H} NMR (P-CH)	¹ H NMR (P-CH)	yield [%]
	δ [ppm] (¹ J _{M,P} [Hz])	δ [ppm] (¹ J _{P,C} [Hz])	δ [ppm] (² J _{P,H} [Hz])	
34.1_{Cr}	250.2	39.0 (18.6)	1.99 (8.2)	32
34.1_{Mo}	225.6 (151.7)	38.7 (19.9)	1.96 (7.3)	27
34.1_w	191.4 (268.5)	38.7 (14.2)	2.10 (8.7)	65

An outstanding feature, found for all 1,2-oxaphosphetane complexes, is the electronic differentiation of the ring-CH₂ protons, leading to quite complicated coupling patterns (figure 6.2).

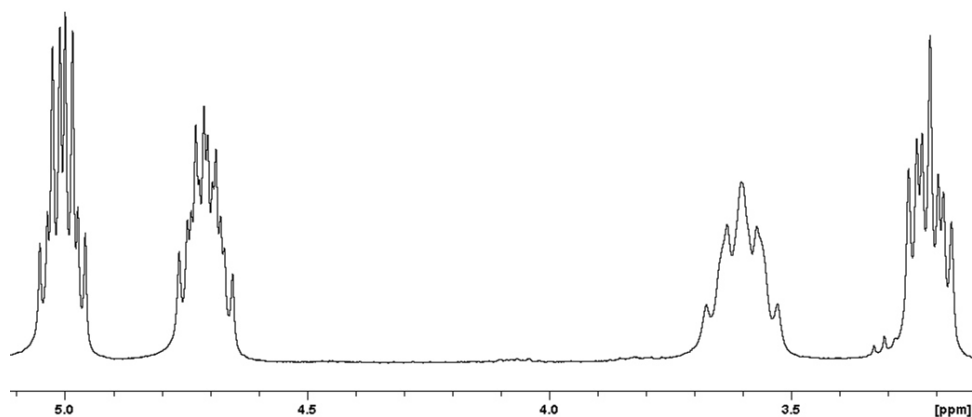


Figure 6.2: Zoom in on a part of the ^1H NMR spectrum of the $\text{W}(\text{CO})_5$ -1,2-oxaphosphetane complex **34.1_W**. The region for the resonance signals of the ring protons is shown exemplarily.

All three complexes crystallized well from *n*-pentane and the molecular structures in single crystals could be obtained by X-ray diffraction studies, proving again the formation of the C-unsubstituted complexes (figure 6.3).

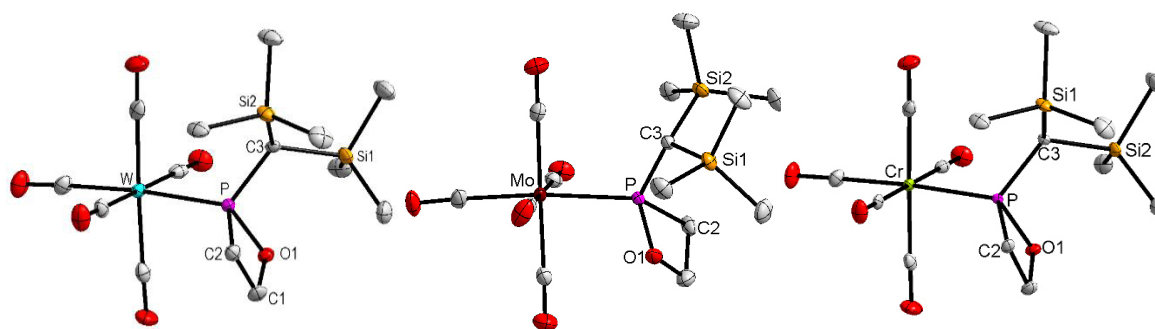


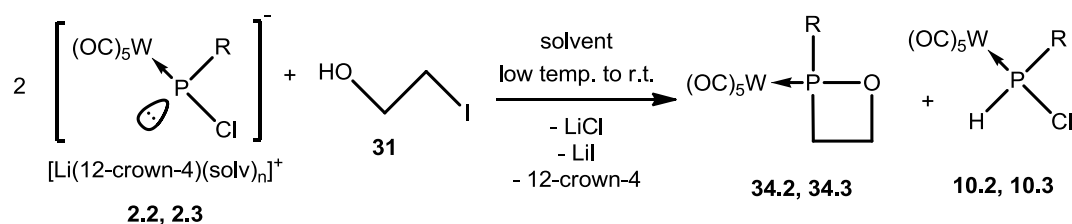
Figure 6.3: DIAMOND plot of the molecular structures of 1,2-oxaphosphetane complexes **34.1_W** (left), **34.1_{Mo}** (middle) and **34.1_{Cr}** (right) in the solid state; the thermal ellipsoids are set at 50 % probability level and all hydrogen atoms are omitted for clarity.

All three complexes **34.1_W**, **34.1_{Mo}** and **34.1_{Cr}** are isostructural but the structure of the Mo complex shows the other enantiomer. It has to be noted that while the flack parameters were 0.126(5) for **34.1_W** and 0.05(3) for **34.1_{Cr}**, it was 0.52(3) for **34.1_{Mo}**. This indicates that the W and Mo-derivative crystallized as racemic twins, containing 12.6 % of the second enantiomer in case of **34.1_W** and an almost 1:1 ratio for the enantiomers of **34.1_{Mo}**. The single crystal data show no significant difference between the three complexes. Just the typical differences for the M-P bond were observed in going from Cr to W. Comparison to the C-Me derivatives shows an additional shortening of the P-M bond lengths, presumably due to the reduced steric demand of the ring; the folding angles were also significantly smaller.

Table 6.2: Selected bond lengths in Å and angles in ° for 1,2-oxaphosphetane complexes **34.1_w**, **34.1_{Mo}** and **34.1_{Cr}**.

	P-C3	P-C2	P-M	C2-P-O1	folding angle
34.1_{Cr}	1.808(3)	1.838(3)	2.3183(8)	80.11(11)	15.1
34.1_{Mo}	1.809(2)	1.833(2)	2.4768(6)	80.40(11)	14.1
34.1_w	1.810(4)	1.830(5)	2.4654(13)	80.5(2)	15.4

In sharp contrast to the straightforward reaction and the observations for the $P\text{-CH}(\text{SiMe}_3)_2$ -substituted complexes, the reactions of the $P\text{-C}_5\text{Me}_5$ and $P\text{-CPh}_3$ -substituted phosphinidenoid complexes **2.2** and **2.3** with 2-iodoethanol **31** did not yield 2-iodoethylphosphinite complexes. In both reactions, performed under typical Li/Cl phosphinidenoid complex conditions, an almost 1:1 mixture of the 1,2-oxaphosphetane complexes **34.2** or **34.3** and the chloro(organo)phosphane complexes **10.2** or **10.3**, respectively, was formed (see scheme 6.6 and figure 6.4). Based on this observation, a reaction sequence can be assumed, in which one equivalent of the Li/Cl phosphinidenoid complex *in-situ* acts as a base towards the initially formed phosphinite complex and, hence, induces ring closure to **34.2** or **34.3**, while forming the chloro(organo)phosphane complex **10.2** or **10.3** as side-products.



X.2 R = C₅Me₅ (solvent = Et₂O, low temp. = -78 °C)
X.3 R = CPh₃ (solvent = THF, low temp. = -50 °C)

Scheme 6.6: Reaction of the $P\text{-CPh}_3$ and $P\text{-C}_5\text{Me}_5$ -substituted phosphinidenoid complexes **2.2** and **2.3** with 2-iodoethanol (**31**).

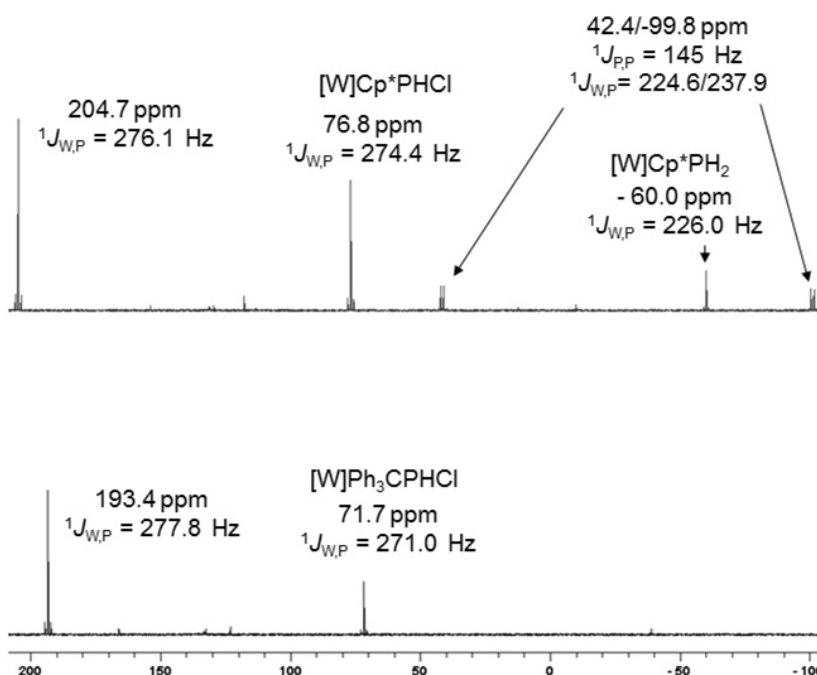


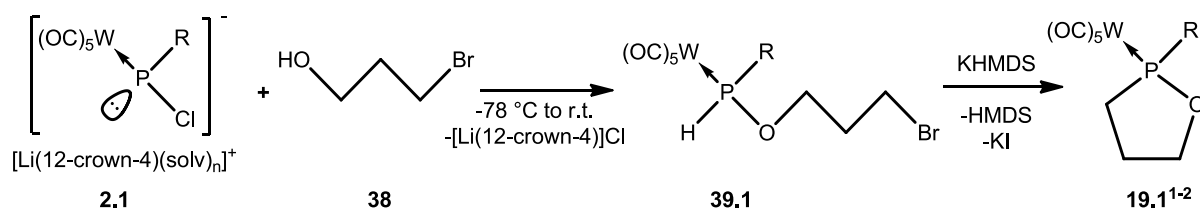
Figure 6.4: $^{31}\text{P}\{^1\text{H}\}$ NMR spectra of the reaction mixtures of **2.2** (top) and **2.3** (bottom) with 2-iodoethanol **31**.

Isolation of the *P*- CPh_3 -substituted derivative was not possible due to the similar solubility and column chromatography retention times of the two reaction products (the 1,2-oxaphosphetane complex **34.3** and chlorophosphane complex **10.3**).

In contrast, a somewhat troublesome separation via low temperature column chromatography and an additional sublimation of the 1,2-oxaphosphetane complex **34.2** rendered the isolation of the *P*- C_5Me_5 derivative possible. The sublimation was performed to separate the product from small amounts of a formed decomposition product of the Li/Cl phosphinidenoid complex (the self-reaction product **XXXVIII**). Separation was therefore only possible due to the high thermal stability of the 1,2-oxaphosphetane complex. The yield was below 50% (yield for **34.2**: 20 %) as expected from the reaction stoichiometry.

Complex **34.2** could be unambiguously characterised using multinuclear NMR spectroscopy, high resolution mass spectrometry and elemental analysis. The complex shows typical values for the ^{31}P NMR resonance signal (204.8 ppm, $^1J_{\text{W,P}} = 275.5$ Hz); the latter being close to the values observed for the *P*- $\text{CH}(\text{SiMe}_3)_2$ -substituted complex **34.1_w**.

To provide first evidence that the synthetic method described beforehand has a broader applicability in the synthesis of new, differently sized heterocyclic phosphorus ligands, an additional reaction was performed. Starting from Li/Cl phosphinidenoid complex **2.1** and 3-bromopropane-1-ol **38**, a phosphinite ligand **39.1** bearing a C_3 spacer between the oxygen and halogen atom was synthesized (scheme 6.7).



Scheme 6.7: Synthesis of the 1,2-oxaphospholane complexes **19.1**¹⁻² (R = CH(SiMe₃)₂).

In analogy to the reaction with 2-iodoethanol, a selective insertion of the P₁-fragment (from **2.1**) into the OH bond of the alcohol was observed. Nevertheless, some minor impurities were present that may arise from deprotonation of the alcohol by the Li/Cl phosphinidenoid complex. These side products (the chloro(organo)phosphane complex **10.1** and the primary phosphane complex **11.1**) could be separated by sublimation *in vacuo* at elevated temperatures (130 °C, 2 · 10⁻² mbar).

The ³¹P NMR spectrum of **39.1** showed typical values for phosphinite complexes with a resonance signal at 104.7 ppm (¹J_{W,P} = 268.1 Hz, ¹J_{P,H} = 321.5 Hz) without any significant differences compared to previously reported ones. Unfortunately **39.1** was obtained as an oil that, in contrast to **33.1**, did not solidify over time.

Deprotonation of **39.1** with KHMDS at ambient temperature finally led to the formation of the isomeric 1,2-oxaphospholane complexes **19.1**¹⁻² in a selective reaction.

In the ³¹P NMR spectrum complexes **19.1**¹⁻² showed two resonance signals. The resonance signal of the major isomer (**19.1**¹, 99.5% by integration) was observed at 139.5 ppm, showing a strong broadening (FWHI (h_{1/2}) = 760 Hz), whereas the minor isomer (**19.1**², 0.5% by integration) appeared as a sharp signal at 125.2 ppm (¹J_{W,P} = 267.1 Hz). Similar broadened signals were observed before, *i.e.* for 1,3,2-dioxaphospholene complexes.^[133]

A variable temperature NMR study (figure 6.5) revealed some sharpening of the resonance signal for **19.1b**¹ at elevated temperature, but no splitting, allowing to observe the tungsten satellites with a ¹J_{W,P} of approximately 275.5 Hz (δ³¹P (60°C) = 138.4 ppm). It is assumed that the origin of the signal broadening is due to an interaction between the CH proton from the CH(SiMe₃)₂ group and the oxygen atom in the five-membered ring. The ²J_{P,H} coupling constant magnitude is, with 12.8 Hz, significantly higher than it is expected for an *s-cis* conformation. An *s-trans* conformation would also be in accordance with the necessary orientation for this interaction. Surprisingly the determined molecular structure (figure 6.6) showed the *s-cis* configuration so that the interaction may be disfavoured in the solid state.

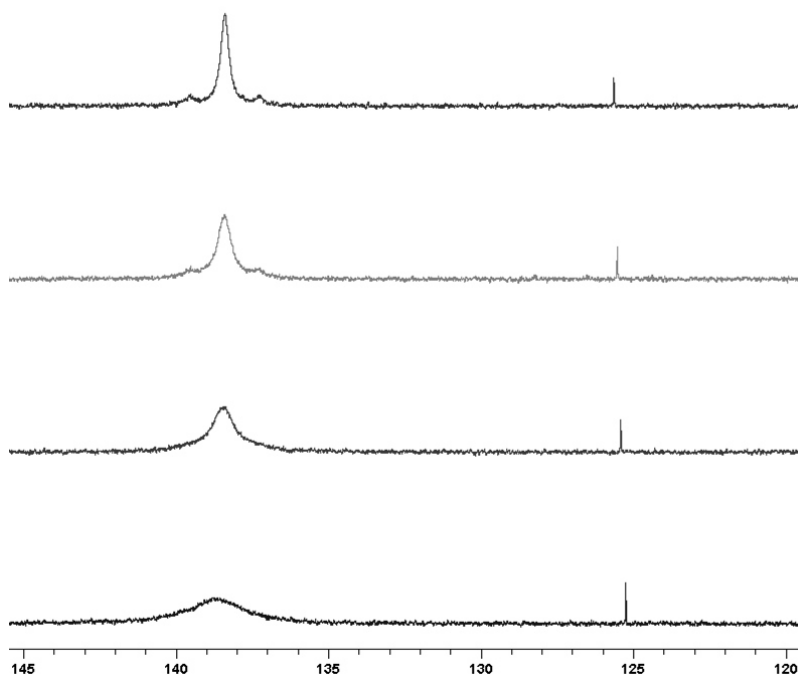


Figure 6.5: Variable temperature $^{31}\text{P}\{^1\text{H}\}$ NMR measurement of **19.1**¹⁻² at 25 °C, 40 °C, 50 °C and 60 °C (from bottom to top) in CDCl_3 .

The heterocyclic ligand structure was confirmed by a single crystal X-ray diffraction study of **19.1** (figure 6.6). Most structural data are similar to those obtained for the 1,2-oxaphosphetane complex **34.1_w**, but an (expected) increase from 80.5(2)° (**34.1_w**) to 93.4(3)° (**19.1**) was observed for the endocyclic OPC angle.

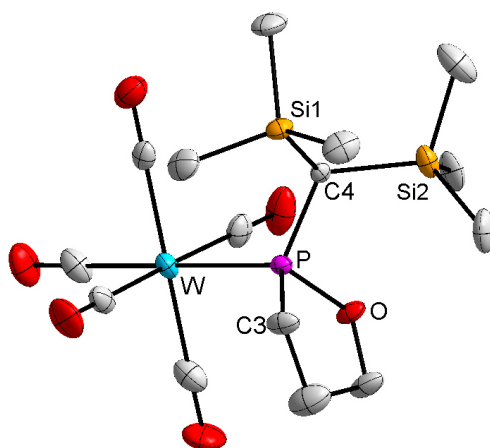


Figure 6.6: DIAMOND plot of the molecular structure of the first 1,2-oxaphosphetane complex **19.1** in the solid state; the thermal ellipsoids are set at 50 % probability level and all hydrogen atoms are omitted for clarity. Selected bond lengths in Å and angles in °: W-P 2.4937(17), P-C3 1.835(7), P-O 1.640(5), P-C4 1.816(6), W-P-C3 119.8(3), W-P-C4 116.5(2), C3-P-O 93.4(3), and O-P-C4 105.7(3).

A similar 1,2-oxaphospholane complex was described by Mathey in 1982, synthesized by the oxidative desulfurization of the corresponding 1,2-oxaphospholane sulfide with $\text{Fe}(\text{CO})_5$.^[112] While no structural data were described, the ^{31}P NMR resonance signal ($\delta^{31}\text{P}(\text{CDCl}_3) = 173.7$ ppm) was found low field shifted in comparison to the ones found for **19.1**. This is in accordance with the expected difference based on the different metal fragment (e.g. $(\text{OC})_4\text{Fe}(\text{PPh}_3)$ ^[134]: $\delta^{31}\text{P}(\text{CD}_2\text{Cl}_2) = 71.7$ ppm vs. $(\text{OC})_5\text{W}(\text{PPh}_3)$ ^[135]: $\delta^{31}\text{P}(\text{CD}_2\text{Cl}_2) = 20.95$ ppm).

Structural proof obtained from X-ray diffraction studies was given for a σ^5, λ^5 1,2-oxaphospholane **CXLVII**,^[101] showing similar data for bond lengths and the bond angles in the ring (figure 6.7, table 6.3). Interestingly the biggest difference between the two structures is found at the bond lengths and angles around the phosphorus atom. The complex shows a significant shorter P-O bond, a slight elongation of the O-C bond as well as a significant bigger intra-ring angle at the phosphorus.

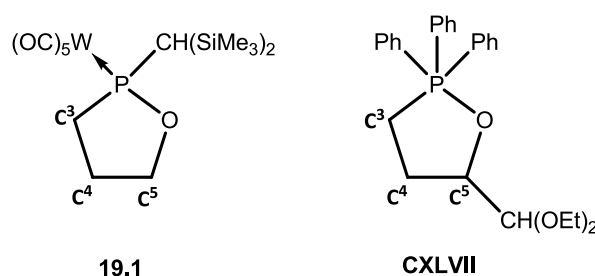


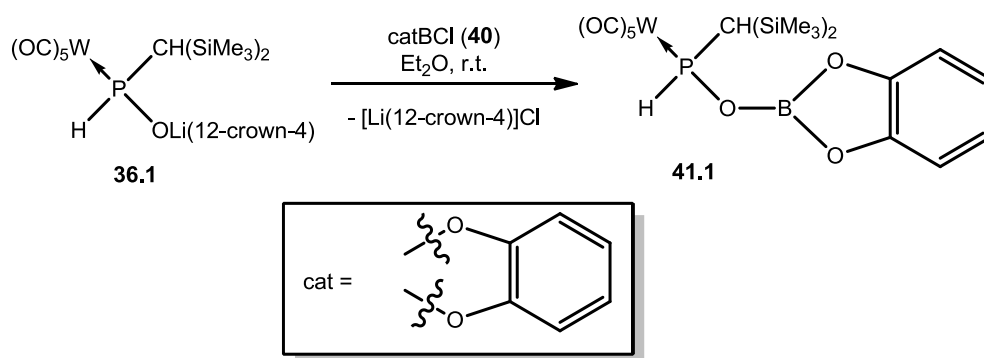
Figure 6.7: Lewis-structures of **19.1** and **CXLVII**^[101] and assignment of the ring carbon atoms.

Table 6.3: Selected bond lengths in Å and angles in ° for 1,2-oxaphospholane complex **19.1** and σ^5, λ^5 1,2-oxaphospholane **CXLVII**.

	P-O	P-C ³	O-C	C ³ -C ⁴	C ⁴ -C ⁵	O-P-C	P-O-C	O-C-C
19.1	1.640(4)	1.835(7)	1.449(8)	1.499(11)	1.520(9)	93.4(3)	114.3(4)	109.2(6)
CXLVII ^[101]	1.789	1.855	1.399	1.508	1.515	87.1	111.7	110.9

As shown in chapter 3.1, phosphanes of the general formula R_2POR' tend to rearrange to the corresponding phosphane oxides and phosphanes bearing a hydrogen atom together with the alkoxy substituent can in addition undergo formal α -eliminations.^{[47][48]} One way to stabilize the phosphanes was achieved by coordination of the electron pair to a transition metal fragment, but no general synthetic procedure of these complexes was developed so far. Therefore a complex that allows the easy synthesis of a variety of such derivatives would be of great interest for further investigations.

Phosphinito complex **36.1**, obtained from the reaction of **33.1_w** with $tBuLi$, can act as oxygen-centred nucleophile and due to the large amount of possible electrophiles it can be seen as a general building block for complexes bearing a P-H function as well as a P-O-E motif in the ligand. While Duan could already show that phosphinito complex **36.1** does not react with typical carbon nucleophiles like MeI or $tBuCl$, it did react with the oxophilic electrophile Me_3SiCl . Based on the observation for Me_3SiCl , a first reaction was performed using the oxophilic catechol(chloro)borane (**40**) which is easy to access and handle. The reaction yielded complex **41.1**, bearing a POB unit, selectively (scheme 6.8).



Scheme 6.8: Reaction of phosphinito complex **36.1** with catechol(chloro)borane.

In the ^{31}P NMR spectrum, complex **41.1** shows a highfield-shifted resonance signal in comparison to most of the previously described phosphinite complexes (**41.1**: $\delta^{31}P = 97.7$ ppm, $^1J_{W,P} = 277.1$ Hz, $^1J_{P,H} = 331.6$ Hz). The difference in the chemical shift is explainable due to the electron deficient Boron centre connected to the oxygen atom. This highfield shift is comparable to the one found for an acyl-substituted complex, described by Duan in 2011, $[(OC)_5W\{PCH(SiMe_3)_2(H)OC(O)CH_3\}]$, $\delta^{31}P = 88.6$ ppm, $^1J_{W,P} = 275.8$ Hz, $^1J_{P,H} = 354.2$ Hz).^[132]

The molecular structure of **41.1** (figure 6.8) was confirmed by a single-crystal X-ray diffraction study. The boron bonding environment has the expected trigonal planar geometry ($\sum \angle B = 360^\circ$), but as geometrical data of complex **41.1** revealed similar bond lengths and angles similar to known phosphinite complexes^[10,56,132] further discussion is not necessary.

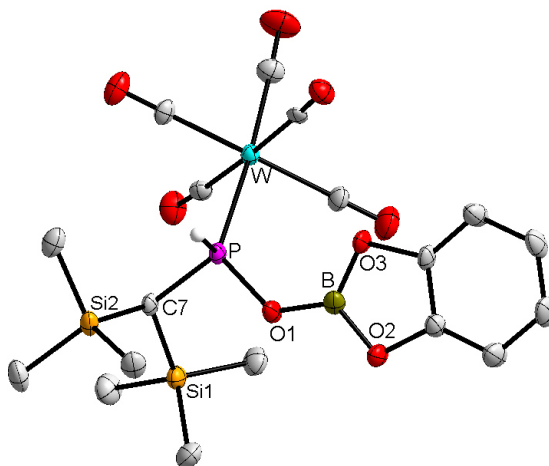
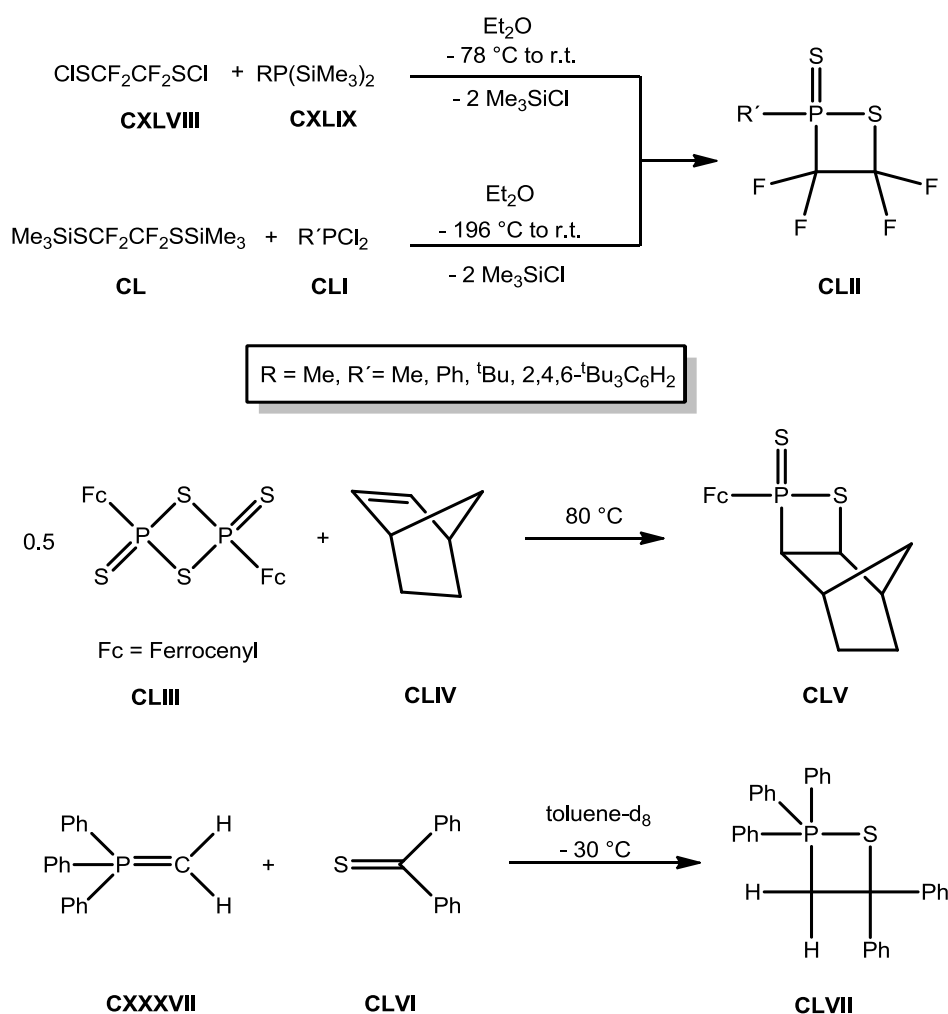


Figure 6.8: DIAMOND plot of the molecular structure of complex **41.1** in the solid state; the thermal ellipsoids are set at 50 % probability level and all hydrogen atoms except at phosphorus are omitted for clarity. Selected bond lengths in Å and angles in °: W-P 2.4695(9), P-C7 1.798(4), P-O1 1.656(3), O1-B 1.353(5), P-O1-B 127.2(3), $\sum \angle B = 360^\circ$.

Further investigations towards the potential of **36.1** as building block for phosphorus ligands were performed by R. Kunzmann, focussing on group 14 and 15 element electrophiles. Here the case of Cy_2BCl deserves special mention as the reaction product was used as precursor for the first monomolecular, anionic FLP complex.^[136]

A different behaviour was observed in the reaction of these Li/Cl phosphinidenoid complexes and propylene sulphide (methyl-thiirane). It is noteworthy to mention that, in contrast to the well-established $1,2\sigma^5, \lambda^5$ and $1,2\sigma^4, \lambda^5$ -oxaphosphetane chemistry, the chemistry of the corresponding 1,2-thiaphosphetanes is rather underdeveloped. Three synthetic strategies to access 1,2-thiaphosphetanes are described, two of which led to thiaphosphetane sulfides,^[142,143] starting either from fluorinated alkanes **CXLVIII** and **CL**^[143] or a modified Lawesson's reagent **CLIII**^[142]. A third synthetic strategy employed the [2+2]-addition of phosphorus ylides (*e.g.* **CXXXVII**) and thiobenzophenone **CLVI**,^[144] in analogy to the Wittig reaction (scheme 7.2).



Scheme 7.2: Examples for the syntheses of P^{V} 1,2-thiaphosphetanes.^{[142,143][144]}

The 1,2-thiaphosphetanes show strong similarities to 1,2-oxaphosphetanes, *e.g.* a solvent dependant equilibrium between the thiaphosphetane and a betain-type structure as well as a decomposition pathway leading to phosphane sulfides by elimination of the corresponding alkene.^[145]

NMR signals show a high-field-shift of approximately 43 ppm, indicating the presence of the less electronegative sulphur instead of the oxygen atom.

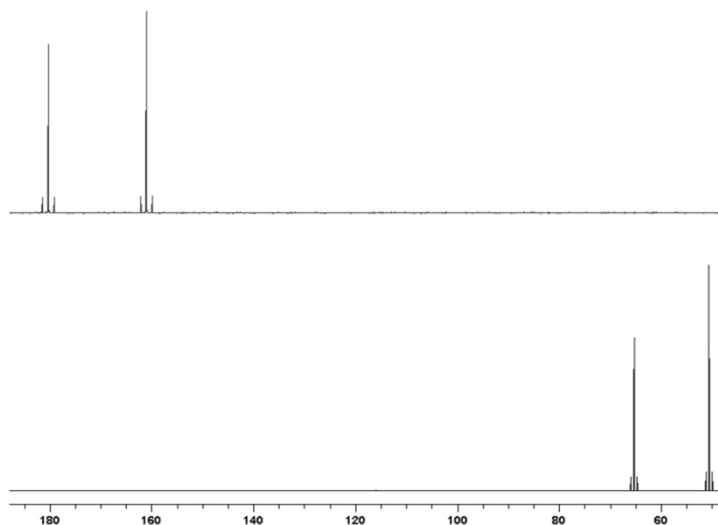


Figure 7.1: Comparison of the $^{31}\text{P}\{^1\text{H}\}$ NMR spectra of 1,2-oxaphosphetane complexes **21.3a**¹⁻² (top) and 1,2-thiaphosphetane complexes **46.3**¹⁻² (bottom), both spectra measured in CDCl_3 .

The molecular structure of the first 1,2-thiaphosphetane complex **46.3** proves the four-membered ring ligand structure (figure 7.2). Suitable single crystals for the X-ray diffraction study were obtained by slow evaporation of a saturated diethyl ether solution at 4 °C. Three independent molecules were found in the unit cell and selected data for all are given in table 7.1. No significant differences were observed comparing the data of the three independent molecules. Compared to **21.3a**, the P-S and the C-S bonds are elongated due to the larger sulfur atom. Also the P-W and the exocyclic P-C bonds are elongated (table 8.1). Surprisingly, no significant increase of the C(1)-P-S angle was observed.

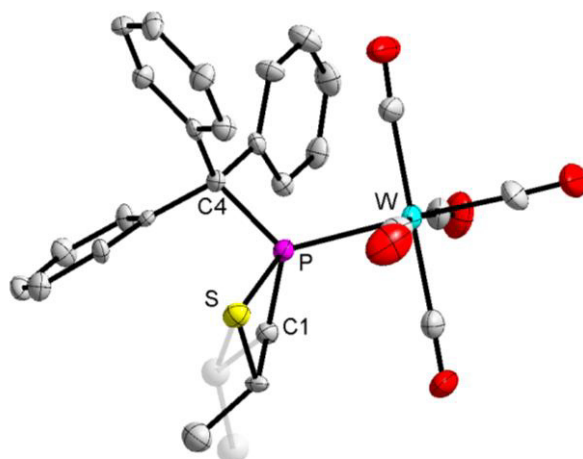


Figure 7.2: DIAMOND plot of the molecular structure of complex **46.3** in the solid state; the thermal ellipsoids are set at 50 % probability level and all hydrogen atoms are omitted for clarity. Only one of three independent molecules in the unit cell is shown for clarity. The split-site (1:1) for the C-Me unit is represented using a transparent mode for clarity.

Like in case of the 1,2-oxaphosphetane complex **21.3a** two orientations were found for the C-Me group, leading to two folding angles at the ring. Both folding angles are in the range found for the 1,2-oxaphosphetane complexes (24.3°/25.7°/26.8° (C-Me oriented towards the CPh₃ substituent) and 18.1°/15.2°/11.3° (C-Me orientated towards the W(CO)₅ fragment)).

Table 7.1: Selected bond lengths in Å and angles in ° for 1,2-oxaphosphetane complex **21.3a** and the three independent molecules of 1,2-thiaphosphetane complex **46.3**.

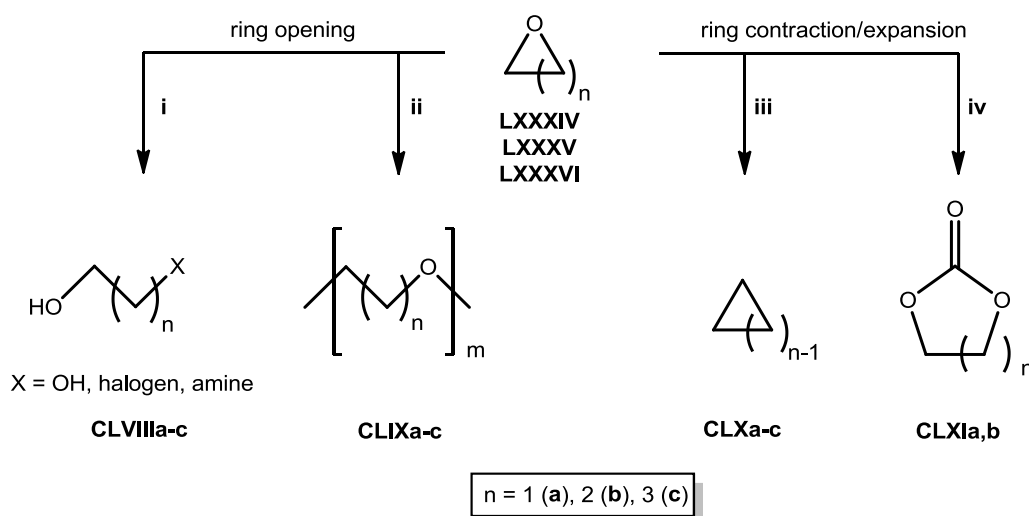
	P-W	P-C ^{ring}	P-C ^{exo}	P-chalcogen	CH-chalcogen	chalcogen-P-C ^{ring}
21.3a	2.4926(12)	1.843(4)	1.905(4)	1.656(3)	1.515(8)	80.49(18)
46.3	2.5158(18)	1.861(7)	1.922(7)	2.125(3)	1.876(10)	80.8(2)
	2.5060(18)	1.856(7)	1.920(7)	2.132(2)	1.901(11)	80.6(2)
	2.539(2)	1.872(8)	1.936(7)	2.115(3)	1.832(16)	81.8(3)

To check the influence of the chalcogen on the reactivity two exemplary reactions were tested: the ring opening reaction using HBF₄·OEt₂ and an acid induced ring expansion reaction with HOTf and acetonitrile, as both of which showed selective reactions for 1,2-oxaphosphetane complexes (see later on chapter 8). Surprisingly, in both cases no reaction was observed for **46.3**, even at elevated temperatures. In addition to this low reactivity, complex **46.3** showed a high thermal stability; no decomposition was observed in toluene up to the boiling point.

8 Reactions of 1,2-oxaphosphetane complexes

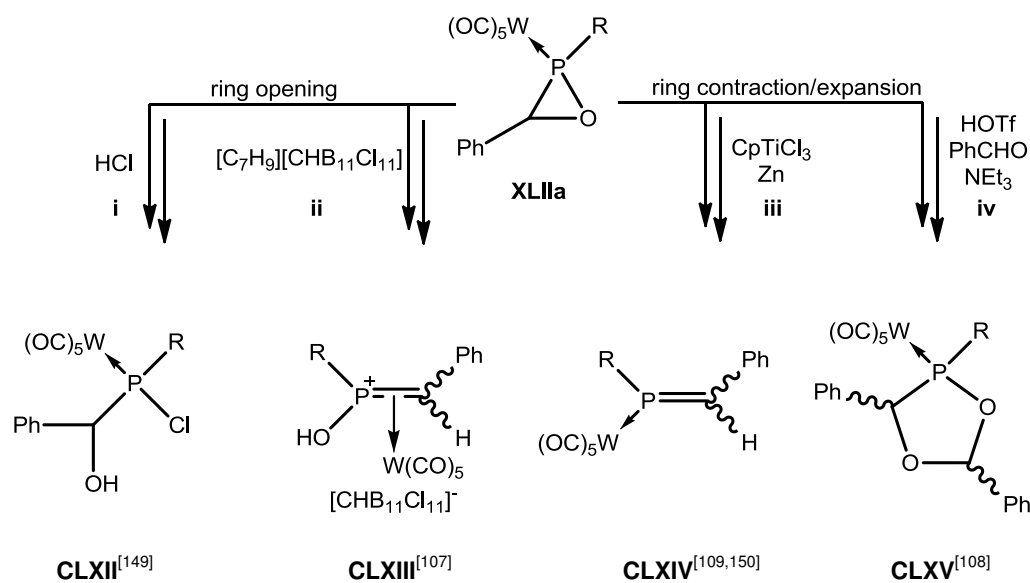
8.1 Introduction – general reactivity of epoxides, oxetanes and tetrahydrofuranes

Hydrolytic or acidic ring opening, ring opening polymerizations, deoxygenation reactions, ring expansion reactions, and subsequent reactions, *e.g.* of, by hydrolysis, formed α,ω -diones, led to the immense importance of small heterocycles as building blocks in Organic Chemistry and material science. Oxiranes are by far the best investigated derivatives of the heterocyclic ring systems, but also larger and less reactive heterocycles such as oxetane (scheme 8.1 $n = 2$) and tetrahydrofuran (scheme 8.1, $n = 3$) can be used as raw material for numerous high-end applications.^[80] The reactivity of the oxygen-containing heterocycles can mainly be separated into two formal reaction patterns, based on the products obtained: formal ring opening reactions, *e.g.* with electrophiles or nucleophiles (**i**)^[80] or in polymerization reactions (**ii**),^[124] or change of the ring size by a sequential bond breaking and bond forming process, *e.g.* the deoxygenation of epoxides (**iii**) or the reaction with CO_2 to cyclic carbonates (**iv**).^[148]



Scheme 8.1: Examples for ring opening and ring expansion or contraction reactions of small-sized oxygen containing heterocycles.

Oxaphosphirane ligands, *e.g.* in complex **CLXIV**, are the phosphorus analogues of epoxides, and due to their synthetic potential the Streubel research group has shown a longstanding interest in the development of their synthesis and the investigation of their reactivity. A set of typical reactions such as Brønsted acid-induced ring opening reactions, leading to halophosphane complexes (**i**)^[149] or side-on bonded phosphalkene complexes (**ii**),^[107] deoxygenation reactions (**iii**),^[109,150] being a form of “ring contraction”, as well as ring expansion reactions (**iv**)^[108] could be developed over the past decade (scheme 8.2).

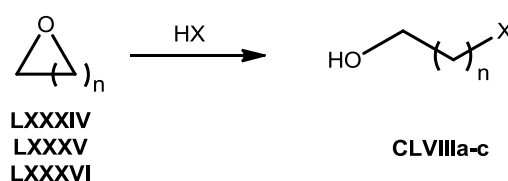


Scheme 8.2: Typical reactions of oxaphosphirane complexes as the smallest O,P-heterocyclic complexes (R = CH(SiMe₃)₂).

After the development of synthetic routes for 1,2-oxaphosphetane complexes, the potential of this new phosphorus heterocycle should be investigated. Here, particular emphasis was on the discovery of reactivity similarities compared to oxaphosphirane ligands. The results will be presented in the following chapters.

8.2 Ring opening reactions with HCl or HBF₄·OEt₂

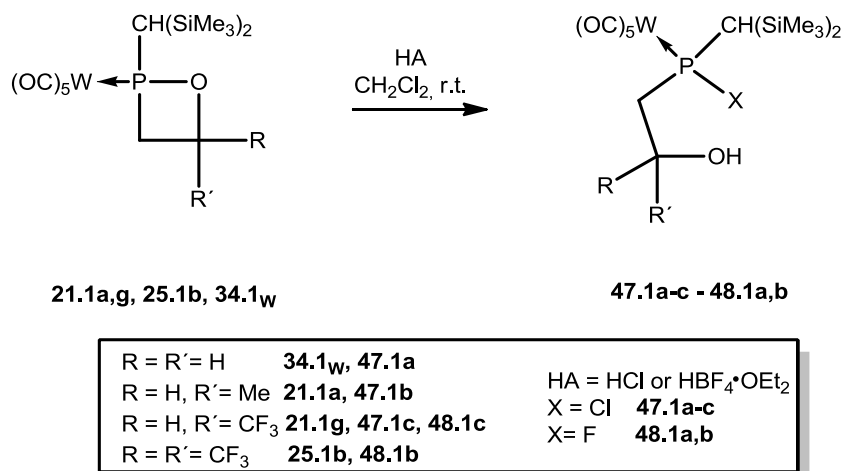
The reaction of small oxygen-containing heterocycles like oxiranes, *e.g.* propylene oxide^[151], oxetanes, *e.g.* 2-methyloxetane^[152], and tetrahydrofuranes^[153] with most Brønsted acids in the absence of water leads to asymmetric α,ω -substituted alcohols, as shown in scheme 8.3.



Scheme 8.3: Ring opening reactions of oxygen containing heterocycles with Brønsted acids (X = variable, *e.g.* F, Cl, Br, I; n = 1-3).

In the present case, surprisingly, no reaction of 1,2-oxaphosphetane complexes with hydrogen chloride in diethyl ether was observed, possibly due to the low basicity of the O-centres in these complexes, which prevents the initial protonation as the solvent is preferably protonated. By changing the solvent to dichloromethane and using HCl_(g) this

problem could be overcome, allowing a first regioselective ring opening of 1,2-oxaphosphetane complexes at the P-O bond (scheme 8.4).



Scheme 8.4: Ring opening reactions of 1,2-oxaphosphetane complexes with Brønsted acids.

In case of **34.1w** a complete conversion was observed using HCl_(g) (after less than 30 minutes). The product was isolated by evaporation of the solvent and had to be, due to the oily nature at that point, recrystallized from *n*-pentane. The complex **47.1a** showed a resonance signal 79.9 ppm high-field-shifted in the ³¹P NMR spectrum, compared to the starting 1,2-oxaphosphetane complex ($\delta^{31}\text{P} = 191.4$, $^1J_{\text{W,P}} = 268.5$ Hz) with the magnitude of the $^1J_{\text{W,P}}$ coupling increased by 4.4 Hz (table 8.1).

Table 8.1: ³¹P{¹H} NMR data in CDCl₃ and yields of complexes **47.1a-c** and **48.1a,b**.

	R/R'/X	$\delta^{31}\text{P}$ in ppm ($^1J_{\text{W,P}}$ [Hz]) { $^1J_{\text{P,F}}$ [Hz]}		isomeric ratio	yield [%]
		Isomer 1	Isomer 2		
47.1a	H / H / Cl	111.5 (272.9)	-	-	71
47.1b	Me / H / Cl	119.8 (276.0)	115.1 (274.2)	25:75	100
47.1c	CF ₃ / H / Cl	113.4 (br)	110.6 (281.3)	12:88	33
48.1a	CF ₃ / H // F	194.0 (290.0) {823.0}	185.6 (294.0) {821.8}	26:74	39
48.1b	CF ₃ / CF ₃ / F	180.4 (302.1) {852.4}	-	-	70

A single crystal suitable for X-ray diffraction studies could be obtained for **47.1a** from an *n*-pentane solution. The molecular structure showed four independent molecules in the unit cell and an additional water molecule for two molecules of **47.1a**. Nevertheless, the structural motif and, with this, the regioselective reaction was proven (figure 8.1).

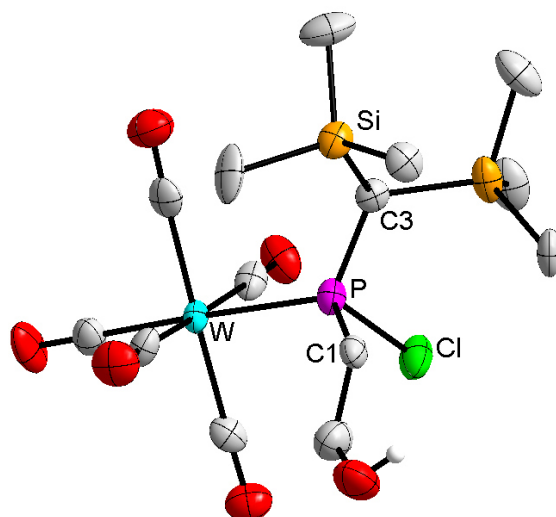


Figure 8.1: DIAMOND plot of the molecular structure of complex **47.1a** in the solid state; the thermal ellipsoids are set at 50 % probability level and all hydrogen atoms except the OH and a quarter of an equivalent of water are omitted for clarity. Only one of the four independent molecules in the unit cell is shown for clarity.

Table 8.2: Selected bond lengths in Å and angles in ° for complex **47.1a**. The data of all four independent molecules in the unit cell are given.

Independent molecule	P-W	P-C1	P-X	W-P-C1	Cl-P-C1
1	2.491(3)	1.842(11)	2.082(4)	118.8(4)	97.7(4)
2	2.494(3)	1.823(10)	2.101(4)	121.1(3)	97.6(3)
3	2.501(2)	1.816(9)	2.085(3)	122.2(4)	96.8(4)
4	2.490(2)	1.836(9)	2.090(3)	118.9(3)	97.6(3)

In case of **21.1a**, bearing the *C*-Me substituent, the reaction with $\text{HCl}_{(g)}$ also led to the same outcome in a highly selective reaction and less than an hour reaction time. Work-up was performed similar to the procedure described above for **47.1a**.

An interesting strong decrease of the reactivity was observed using different *C*-substituted 1,2-oxaphosphetane complexes and introduction of electron withdrawing CF_3 substituents. When complex **21.1g**, bearing one CF_3 substituent, was used in the reaction a significant slower reaction with $\text{HCl}_{(g)}$ was observed. To check the dependency of the reaction progression on different acids $\text{HBF}_4 \cdot \text{OEt}_2$ was used; the $\text{HBF}_4 \cdot \text{OEt}_2$ acted here formally as a source of HF. The reaction of **21.1g** and **25.1b** with $\text{HBF}_4 \cdot \text{OEt}_2$ yielded almost instantaneously the products **48.1a** and **48.1b**, respectively. This is in contrast to the case of **25.1b**, bearing two CF_3 groups, and $\text{HCl}_{(g)}$ in which the reaction was completely suppressed.

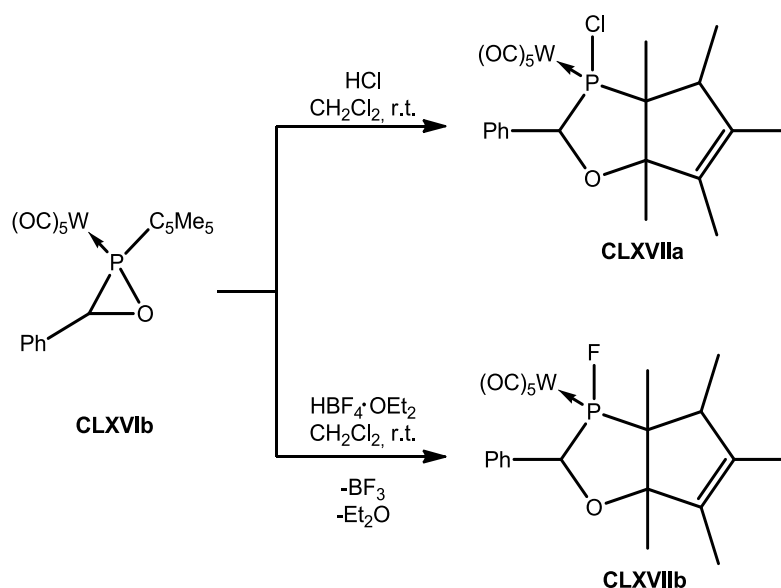
$^{31}\text{P}\{^1\text{H}\}$ NMR spectroscopic data of chloro(organo)phosphane complexes **47.1a-c** and fluoro(organo)phosphane complexes **48.1a,b** are given in table 8.1. The $^{31}\text{P}\{^1\text{H}\}$ NMR resonances of chloro(organo)phosphane complexes **47.1a-c** are observed in a chemical shift range between 110 and 120 ppm with $^1J_{\text{W,P}}$ constants between 272 and 281 Hz, which is in good accordance with the ones observed for other $P\text{-CH}(\text{SiMe}_3)_2$ -substituted chlorophosphane complexes, e.g. $[(\text{OC})_5\text{W}\{\text{P}(\text{CH}_3)\text{CH}(\text{SiMe}_3)_2(\text{Cl})\}]$ ($\delta^{31}\text{P} = 105.4$ ppm, $^1J_{\text{W,P}} = 273.4$ Hz).^[31] Complexes **48.1a,b**, possessing P-F bonds, show significantly downfield-shifted values at around 180-195 ppm and a coupling to the fluoride. The changes in chemical shifts and coupling constants are in accordance with the higher electronegativity of the P-bound halogens (F vs Cl) in these cases, which is also reflected by the tungsten-phosphorus couplings.^[121] The fluorophosphane complex **48.1b**, bearing two CF_3 substituents, displays the largest coupling constants in this series (table 1), accordingly.

In the IR spectra the absorption due to O-H valence bond stretching vibrations of **47.1b,c** and **48.1a,b** were found around 3600 cm^{-1} . In case of **47.1a** a broad absorption band at 3298 cm^{-1} was found, which indicates the presence of hydrogen bonding.

Single crystals could be obtained of all complexes and X-ray diffraction studies proved the high regioselectivity of the reactions. All bond lengths and angles, apart from the expected difference in the P-X bond lengths for $X = \text{Cl}$ and $X = \text{F}$, are very similar and shall therefore not be discussed further (table 8.3).

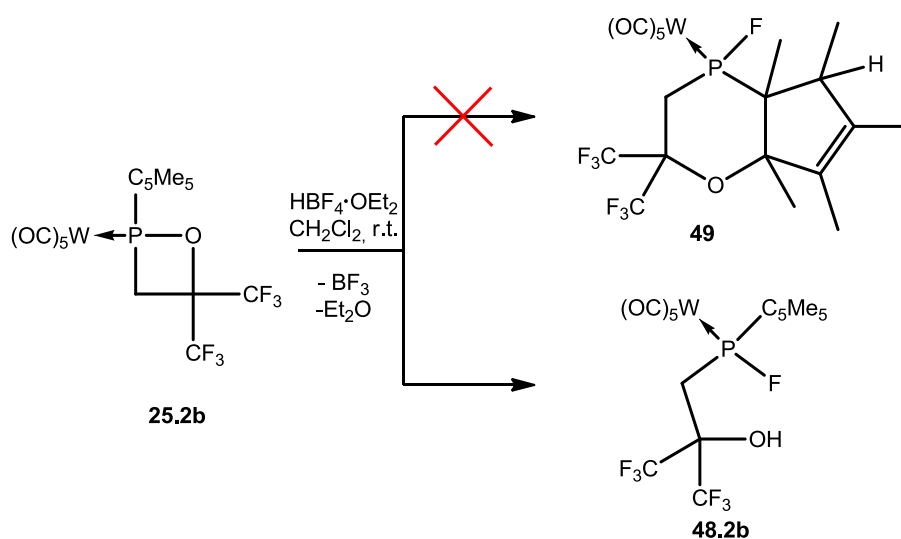
Table 8.3: Selected bond lengths in Å and angles in ° for complexes **47.1b** to **48.1b**.

	P-W	P-C1	P-X	W-P-C1	X-P-C1
47.1b	2.503(5)/ 2.504(5)	1.84(2)/ 1.796(19)	2.098(7)/ 2.117(6)	122.2(6)/ 117.8(6)	108.0(2)/ 105.9(6)
47.1c	2.4872(4)	1.8463(16)	2.0969(5)	123.67(5)	96.28(5)
48.1a	2.4682(9)	1.835(4)	1.614(2)	123.32(13)	108.53(9)
48.1b	2.4767(9)	1.844(4)	1.600(2)	125.75(12)	109.63(9)



Scheme 8.5: Reactions of *P*-C₅Me₅-substituted oxaphosphirane complex **CLXVIb** with HCl^[149] or HBF₄·OEt₂.^[39]

The reaction of complex **25.2b** with HBF₄·OEt₂ was performed and led to only one product in a clean conversion.



Scheme 8.6: Proposed and found acid-induced ring opening reaction of the *P*-C₅Me₅-substituted 1,2-oxaphosphetane complex **25.2b**.

A broad resonance signal was observed for **48.2b** in the ³¹P{¹H} NMR spectrum ($\delta^{31}\text{P} = 190.3$ ppm, FWHI ($h_{1/2}$) = 440 Hz), exhibiting a $^1J_{\text{P,F}}$ coupling constant of 830 Hz. These ³¹P NMR data are similar to the ones found for the *P*-CH(SiMe₃)₂-substituted derivative **48.1b** ($\delta^{31}\text{P} = 180.4$ ppm ($^1J_{\text{P,F}} = 852.4$ Hz, $^1J_{\text{W,P}} = 302.1$ Hz)). Due to the presence of all 4 expected signals of the C=C bonds of the C₅Me₅ group in the ¹³C{¹H} NMR spectrum, a ring expansion reaction similar to the one for oxaphosphirane complexes could already be ruled out. The nature of the proposed ring opening reaction product was further confirmed by a single

crystal X-ray diffraction study (figure 8.3). All structural data are similar to the ones observed for **48.1b** and shall therefore not be discussed further.

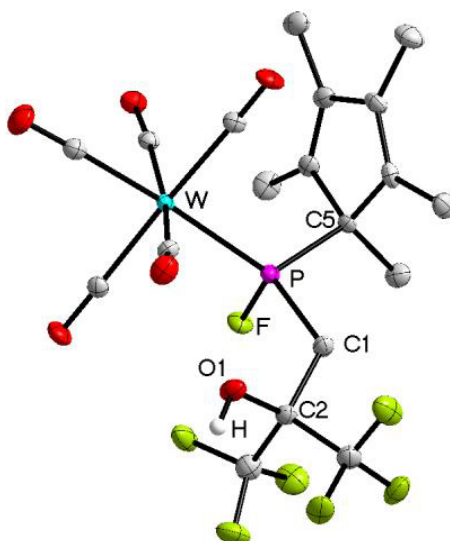


Figure 8.3: DIAMOND plot of the molecular structure of complex **48.2b** in the solid state; the thermal ellipsoids are set at 50 % probability level and all hydrogen atoms except at the OH group are omitted for clarity. Only one of two independent molecules is shown, both sets of data are given (molecule1/molecule2). Selected bond lengths in Å and angles in °: W-P 2.5014(15)/2.4793(16), P-F 1.600(4)/1.598(4), P-C1 1.849(6)/1.840(7), P-C5 1.872(6)/1.862(6), F-P-C1 99.8(2)/100.5(3).

Besides the typical bond lengths and angles one aspects of the molecular structures of **47.1a-c** and **48.1a,b** deserve closer inspection: All obtained structures are dominated by hydrogen bond interactions of the C-OH groups. In case of **47.1a** the packing is dominated by hydrogen bridging between the OH groups of the molecule and the water molecules present. The molecules form a structure with one molecule of water in the centre, coordinated by one C-OH from each side. These C-OH-O-OH-C moieties are then connected to a second C-OH unit by a hydrogen bond (figure 8.4). Further elongation of this hydrogen bridging network is suppressed, presumably by steric effects.

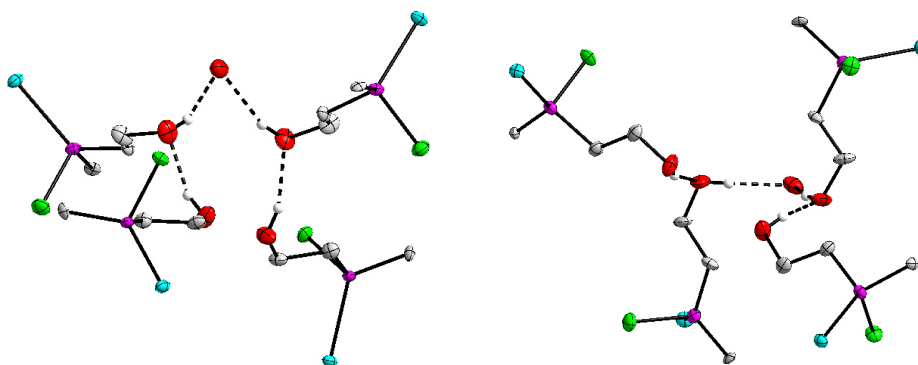


Figure 8.4: DIAMOND plots, indicating the OH-OH-O-HO-HO unit (hydrogen bonds as dashed lines) in the molecular structure of complex **47.1a** in the solid state; the thermal ellipsoids are set at 50 % probability level. All hydrogen atoms except at the C-OH groups and parts of the P-substituents are omitted for clarity. The view from top (left) and from the side (right) of the unit is shown.

Two different types of interaction were observed in the structure of complex **47.1b**. Here, a hydrogen bridge between two C-OH groups was observed (figure 8.5, left side). However, this bridge was only observed for one of two independent molecules as the second one shows an intramolecular hydrogen bridge to the chlorine atom (figure 8.5, right side).

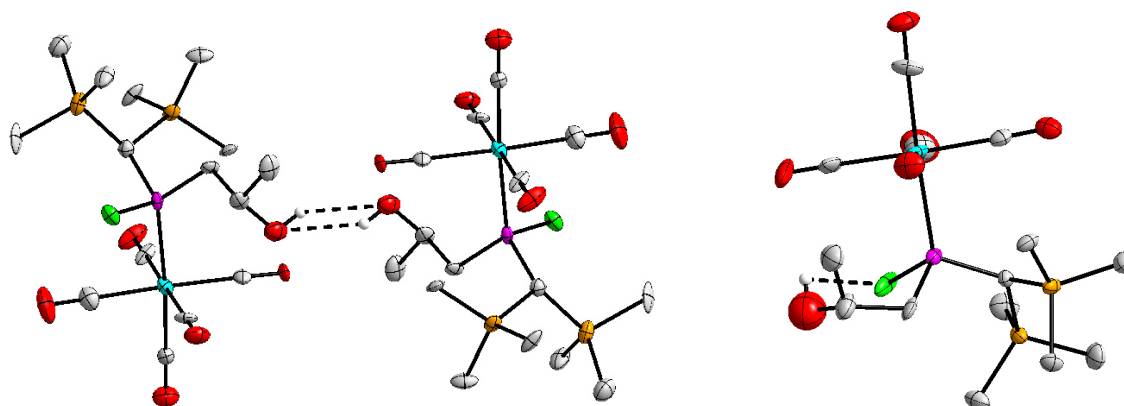


Figure 8.5: DIAMOND plots, indicating the OH-HO unit (left) and the intramolecular hydrogen bridge (right) (hydrogen bonds are depicted as dashed lines) in the molecular structure of complex **47.1b** in the solid state; the thermal ellipsoids are set at 50 % probability level. All hydrogen atoms except at the C-OH groups are omitted for clarity.

In the molecular structures of complexes **47.1c**, **48.1a,b** and **48.2b** no hydrogen bridging between the OH and the P-F group was observed. Weak interactions between the OH group and one of the *cis*-CO groups of the metal fragments were present, thus leading to coordination dimers in the solid state. Figure 8.6 shows the sixteen-membered rings that are formed by this interaction for complexes **48.1d** and **48.2b**. In case of **47.1c** and **48.1a** this interaction is only observed for one of the two split sites shown in figure **8.2** (shown as solid part in both cases).

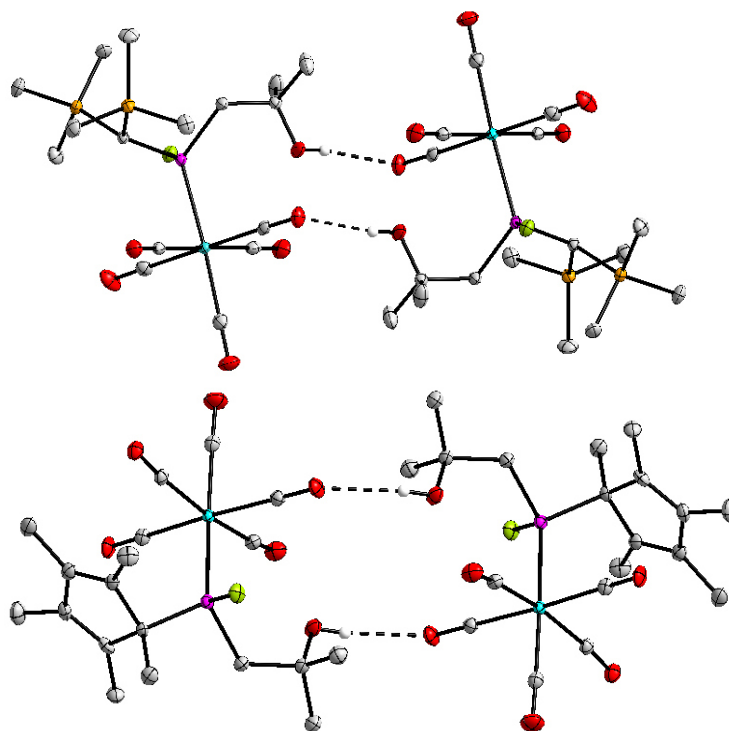
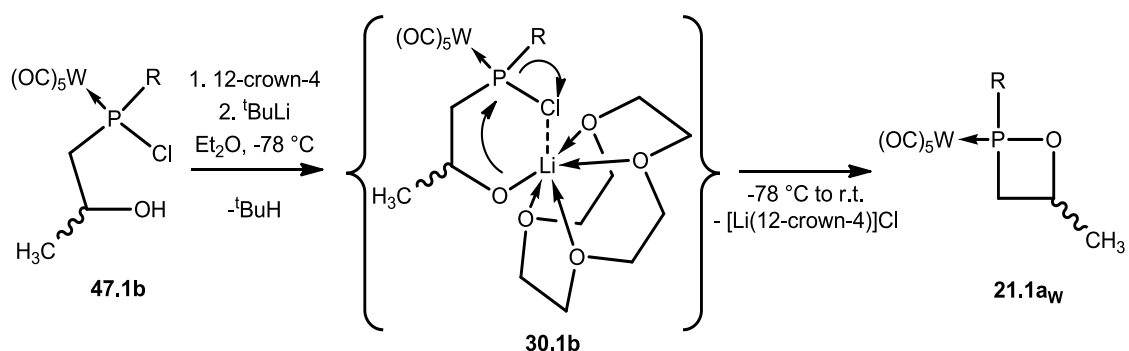


Figure 8.6: DIAMOND plots, indicating the OH-OCW interaction (dashed line) in the molecular structures of complex **48.1b** and **48.2b** in the solid state; the thermal ellipsoids are set at 50 % probability level and all hydrogen atoms except at the OH group, as well as the fluorine atoms of the CF₃ groups are omitted for clarity. Only one of two independent molecules is shown for **48.2b**.

A strong influence of the substitution pattern on this effect, especially the presence of the electron-withdrawing CF₃ groups can be assumed based on the obtained structures. Unfortunately no assignment to the nature of this hydrogen bond can be presented at this point, and calculations would be very helpful in this regard. However, such non-bonding interactions between the CO groups of the W(CO)₅ unit and electron deficient groups were described just recently by Streubel.^[154]

After the ring opening was successfully performed, it was examined if the ring closing reaction is possible, too, by applying typical phosphinidenoid-type conditions, *i.e.* using $t\text{BuLi}$ and 12-crown-4. This reaction is of great importance as it would also represent an independent route to synthesize intermediate **30.1c**, proposed in the reaction mechanism for the reaction of Li/Cl phosphinidenoid complexes with epoxides (chapter 5.5).



Scheme 8.7: Synthesis of complexes **21.1a_W**¹⁻⁴ via deprotonation of complex **47.1b** using $t\text{BuLi}$ /12-crown-4.

The reaction is selective according to the $^{31}\text{P}\{^1\text{H}\}$ NMR spectrum (figure 8.7), but showed a significant change of the ratio of the isomeric products (original synthesis: 29:4:48:19, this route: 10:0:60:30). This is similar to a case previously observed for an oxaphosphirane complex; there, the stepwise ring opening and ring closing reaction even featured a complete conversion of the *s-cis* into the *s-trans* isomer.^[114]

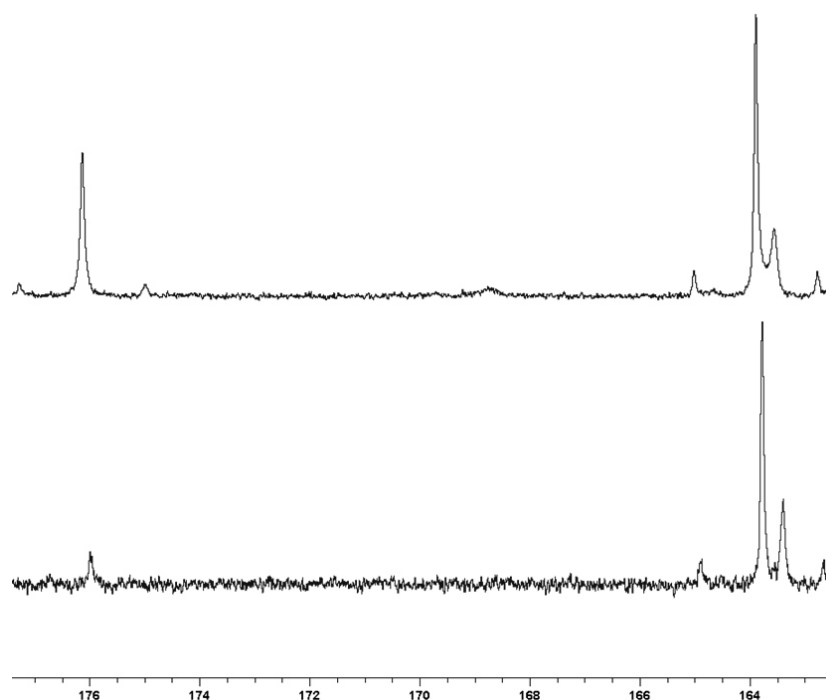
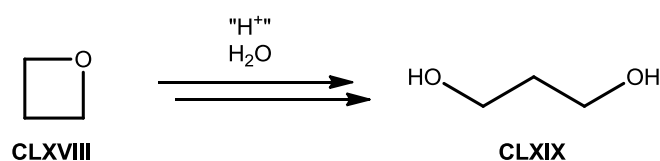


Figure 8.7: $^{31}\text{P}\{^1\text{H}\}$ NMR spectra of the reaction mixture for the syntheses of **21.1a_W**¹⁻⁴ using the Li/Cl phosphinidenoid complex **2.1** and propylene oxide **20a** (top) and of the reaction using complex **47.1b** and $t\text{BuLi}$ /12-crown-4 (bottom), both measured as reaction mixture in Et_2O .

8.3 Hydrolysis and decomposition reaction using triflic acid and water

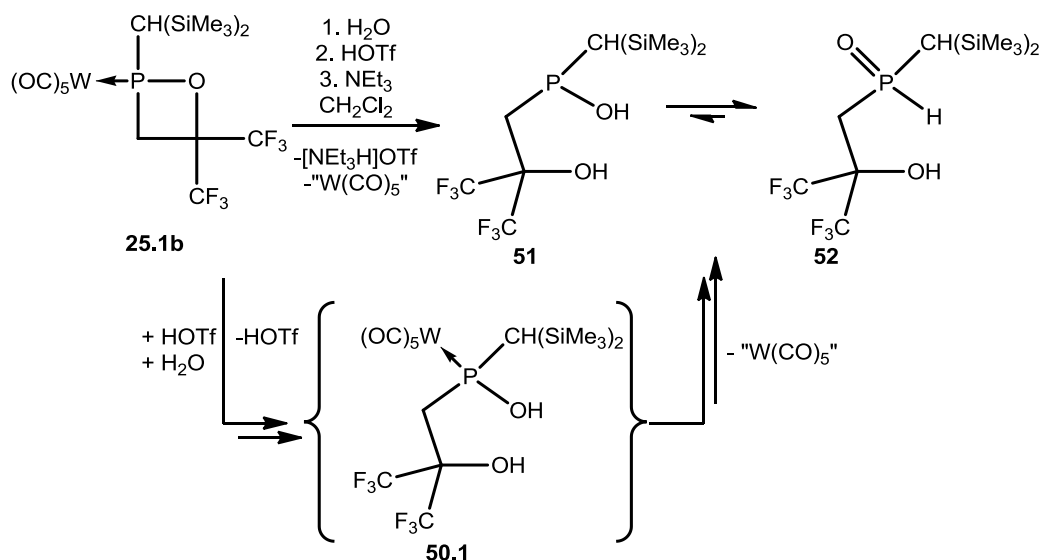
Although the ring opening reaction of oxiranes with water is slow, it is often observed. In contrast to this, it is normally not observed for oxetanes or tetrahydrofuranes. Nevertheless, an activation of the ring (via additional interactions of the heteratom) can lead to a fast(er) reaction which is usually achieved for example by addition of Brønsted acids. Therefore reaction of epoxides, oxetanes or tetrahydrofuranes with acids in the presence of water leads to the corresponding α,ω -dioles; this is illustrated for oxetane in scheme 8.8.^[155]



Scheme 8.8: Acid-catalyzed hydrolysis of oxetane.^[155]

In order to mimic this α,ω -diol formation, the reaction of 1,2-oxaphosphetane complex **25.1b** with H_2O in presence of HOTf (scheme 8.9) was performed. The hydrolysis took place, but unexpectedly loss of the $\text{W}(\text{CO})_5$ fragment was observed, additionally. This loss was surprising, as complexes bearing a POH motif were described before as stable derivatives, e.g. $[(\text{OC})_5\text{W}\{\text{PH}(\text{OH})(\text{Ph})\}]$ ^[47] or even $[(\text{OC})_5\text{M}\{\text{P}(\text{OH})_3\}] \cdot n \text{H}_2\text{O}$ ($\text{M} = \text{Cr}$ ($n = 1$),^[156] $\text{M} = \text{Mo}$ ($n = 2$)^[157]).

For the present case, the proposed mechanism consists of the formation of hydrolysis product **50.1**, presumably after intermediate protonation of the 1,2-oxaphosphetane complex for activation, which then loses the metal fragment under the reaction conditions. The initially formed phosphinic acid **51** is thereby in equilibrium with the phosphane oxide and rapidly rearranges to the thermodynamically more favoured product **52**.



Scheme 8.9: Acid-induced hydrolysis of 1,2-oxaphosphetane complex **25.1b**.

Phosphane oxide **52** could be purified by addition of water, acidification of the solution and extraction with dichloromethane. The tungsten complex **50.1** decomposed under these conditions yielding $W(CO)_6$ and unidentified metal compounds in the aqueous phase. The $W(CO)_6$ was separated by sublimation at elevated temperature (0.014 mbar and 55 °C), and the purification of **52** was monitored by IR spectroscopic measurements, *i.e.* following the intensity decrease of the CO absorption in the IR spectrum.

The ^{31}P NMR spectrum of phosphane oxide **52** revealed only one resonance signal at $\delta^{31}P = 34.3$ ppm ($^1J_{P,H} = 486.8$ Hz) indicating the loss of the P-W bond by absence of ^{183}W satellites (figure 8.8). The resonance signal is strongly shielded in comparison to the starting material (**25.1b**^{1,2}: $\delta^{31}P = 198.2/191.5$ ppm) and in a typical range for phosphane oxides.

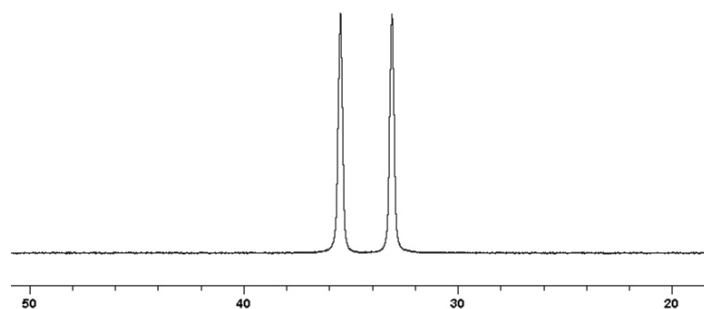


Figure 8.8: Zoom in on the ^{31}P NMR spectrum of **52**.

Absence of carbonyl resonance signals in the $^{13}C\{^1H\}$ NMR spectrum (figure 8.9) as well as the MS measurement and an elemental analysis further verified the loss of the $W(CO)_5$ moiety.

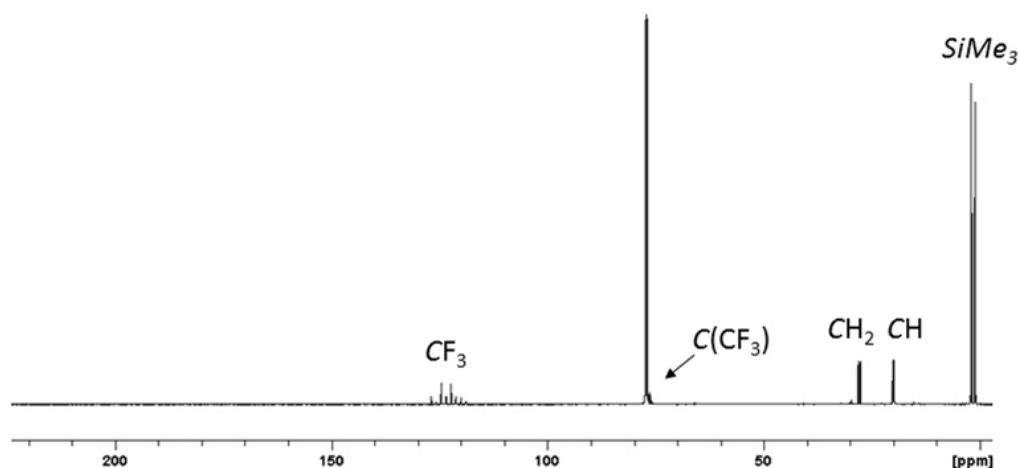
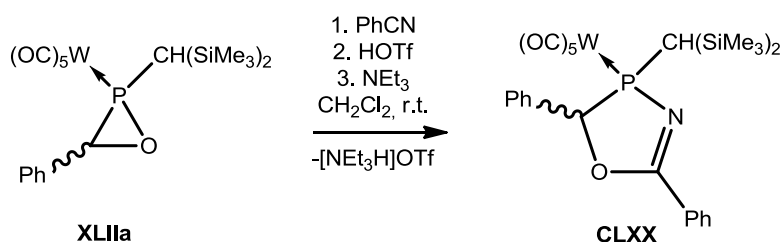


Figure 8.9: $^{13}\text{C}\{^1\text{H}\}$ NMR spectrum of **52**.

The hydrolysis was also proven by the presence of an OH resonance signal at 7.53 ppm in the ^1H NMR spectrum as well as an absorption band for the OH group in the IR spectrum at 2961 cm^{-1} .

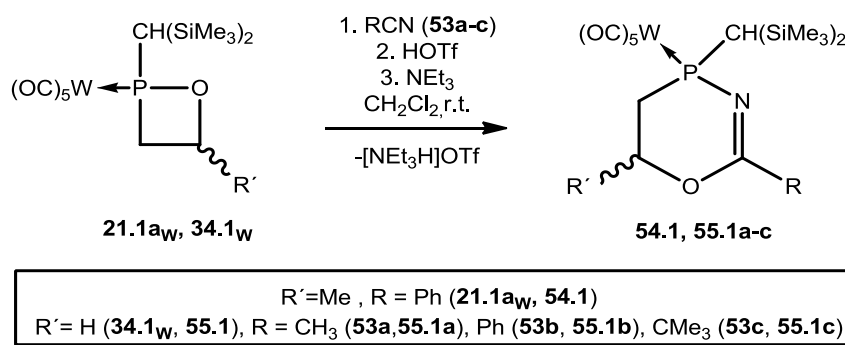
8.4 Ring expansion reactions using the system triflic acid/triethylamine in the presence of nitriles

A further possible 1,2-oxaphosphetane ring activation was tested, based on a reaction procedure developed in the research group of Streubel for oxaphosphirane complexes. In the presence of triflic acid (HOTf, trifluoromethanesulfonic acid), containing the weakly coordinating anion OTf⁻, the regioselective insertion of nitriles was observed into the PO bond of the oxaphosphirane complex **XLIIa** (scheme 8.10).^[158]



Scheme 8.10: Acid induced ring expansion reaction of oxaphosphirane complex **XLIIa**.^[158]

A P-O bond-selective ring expansion took also place when a methylene chloride solution of complexes **21.1a_w**¹⁻⁴ (30:4:19:47) was treated with $\text{CF}_3\text{SO}_3\text{H}$ (HOTf) at ambient temperature in presence of benzonitrile (**53b**), followed by addition of triethylamine. The reaction of **21.1a_w** with benzonitrile (**53b**) (in the presence of triflic acid) yielded a mixture of isomers (ratio 93:7) of 1,3,4-oxazaphosphacyclohex-2-ene complex **54.1** (scheme 8.11).



Scheme 8.11: Ring expansion reactions of 1,2-oxaphosphetane complexes **21.1a_w** and **34.1_w** with different nitriles.

In case of **54.1**, the major isomer (**54.1**¹) was isolated in pure form by column chromatography; the minor isomer could not be obtained. Complex **54.1**¹ displays a ³¹P{¹H} NMR resonance at $\delta = 40.0$ ppm ($^1J_{\text{W,P}} = 258.8$ Hz) while the minor product was observed at $\delta = 31.0$ ppm. Yellow single crystals of **54.1**¹ were obtained by subsequent recrystallization from a diethyl ether solution and, hence, X-ray diffraction studies were possible to establish the regiochemistry of the ring expansion product (Figure 8.10).

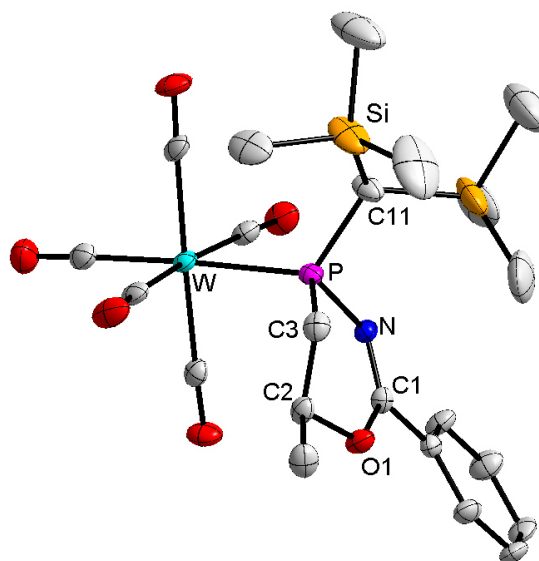


Figure 8.10: DIAMOND plot of the molecular structure of complex **54.1**¹ in the solid state; the thermal ellipsoids are set at 50 % probability level and all hydrogen atoms are omitted for clarity. Selected bond lengths in Å and angles in °: W-P 2.4989(10), P-N 1.703(3), P-C3 1.828(4), P-C11 1.821(4), C3-P-N 99.80(16), C11-P-N 104.83(17), C11-P-C3 105.63(18), N-P-W 107.06(11), C3-P-W 118.70(13), C11-P-W 118.40(15).

Afterwards, an in-depth study including an optimization of the reaction conditions was performed using the C-unsubstituted 1,2-oxaphosphetane complex **34.1_w** to suppress the formation of isomers.

Table 8.4: Selected NMR data (in CDCl₃), IR data and yields for complexes **55.1a-c**.

	$\delta^{31}\text{P}$ [ppm] ($^1J_{\text{W,P}}$ [Hz])	$\delta^{13}\text{C}\{^1\text{H}\}$ (C=N) [ppm] ($^2J_{\text{P,C}}$ [Hz])	IR ($\nu(\text{C}=\text{N})$) [cm^{-1}]	yield [%]
55.1a	34.1 (259.2)	160.0 (13.7)	1642	99
55.1b	36.1 (259.6)	156.9 (12.6)	1626	99
55.1c	34.2 (260.9)	168.8 (14.7)	1631	99/43*

* after recrystallization

The $^{31}\text{P}\{^1\text{H}\}$ NMR spectra showed only a small influence of the C-substituent on the NMR characteristics and all data are in good accordance with the ones described for the C-Me-substituted derivative **54.1**¹. In the $^{13}\text{C}\{^1\text{H}\}$ NMR measurement a resonance signal for the C=N motif was observed in all cases between 156.9 and 168.8 ppm and could be further confirmed by the typical absorptions between 1626 and 1642 cm^{-1} in the IR spectra (table 8.4).

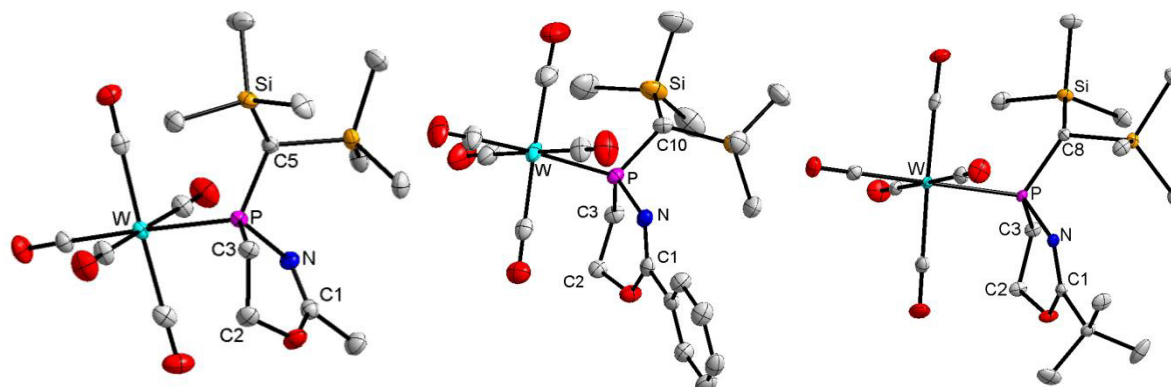


Figure 8.11: DIAMOND plot of the molecular structures of complexes **55.1a**, **55.1b** and **55.1c** (from left to right) in the solid state; the thermal ellipsoids are set at 50 % probability level and all hydrogen atoms are omitted for clarity. In case of **55.1c** only one of two independent molecules is shown for clarity.

Single crystals suitable for X-ray diffraction studies (figure 8.11) could be obtained from saturated diethyl ether solutions. The C1-N bond shows typical values for a C=N double bond in all three cases and only the exocyclic C-C bond is slightly elongated in case of **55.1c** as result of the sterically more demanding ^tBu substituent.

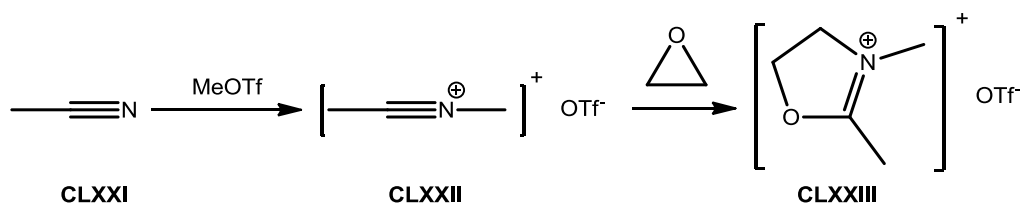
Table 8.5: Selected bond lengths in Å and angles in ° for complexes **55.1a-c**.

	P-W	P-C3	P-N	C1-N	C1-C ^{exo}	C3-P-N
55.1a	2.5089(12)	1.835(5)	1.700(4)	1.268(6)	1.497(7)	98.8(2)
55.1b	2.5171(8)	1.833(3)	1.696(3)	1.272(4)	1.485(4)	100.12(15)
55.1c	2.5084(8)/ 2.5030(8)	1.830(3)/ 1.826(3)	1.702(3)/ 1.705(3)	1.270(4)/ 1.265(4)	1.526(4)/ 1.532(4)	99.46(14)/ 99.04(14)

Two reaction pathways are possible for these ring expansion reactions. The first one is initiated by protonation of the 1,2-oxaphosphetane complex, followed by a nucleophilic attack of the nitrile at the now more electrophilic P-centre. This leads to a breaking of the P-O bond and the subsequent ring expansion. This first reaction pathway would be in accordance to the previously calculated mechanism for oxaphosphirane complexes.^[158]

Another possibility is the initial protonation of the nitrile and a subsequent nucleophilic attack of the ring-O-atom at the electrophilic carbon centre. A similar reaction is known from carbon chemistry (scheme 8.12): the reaction of methyl triflate with acetonitrile **CLXXI** leads to nitrilium salt **CLXXII** which can be isolated; subsequently it reacts with ethylene oxide to the *N*-alkylated oxazolium salt **CLXXIII**.^[159]

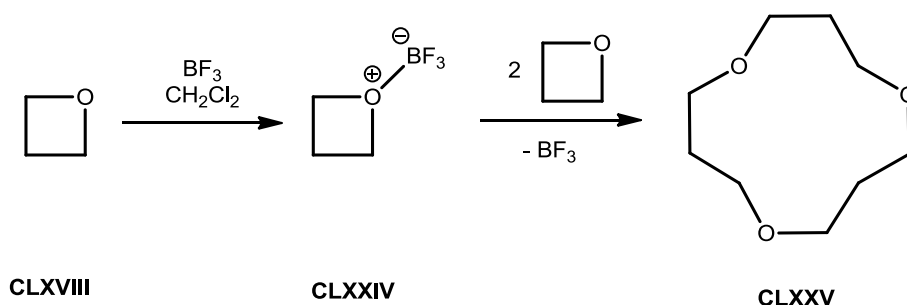
Unfortunately no clear-cut assignment to one or the other reaction pathway was possible with the data at hand.



Scheme 8.12. Ring expansion reaction of ethylene oxide using nitrilium salt **CLXXII**.^[159]

8.5 Ring opening reactions with catechol(chloro)borane

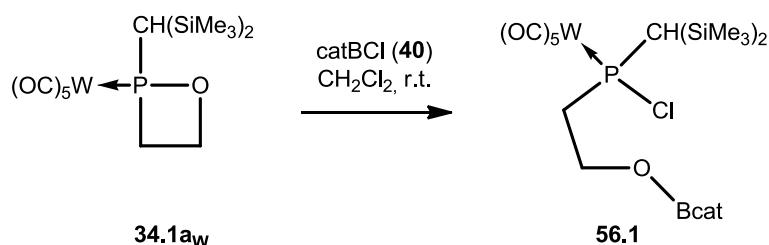
Another example of activation of the heterocycles is the ring opening polymerization (ROP) or oligomerization in the presence of haloboranes. For example, the reaction of oxetane with BF_3 in methylene chloride leads to 1,5,9-trioxacyclododecane as the main product (scheme 8.13). The initiation of this reaction is the coordination of BF_3 to an electron pair of the oxygen atom, thus forming a more electrophilic carbon centre in α -position where a second equivalent of the epoxide can attack. Under other reaction conditions, and especially in the presence of water, the formation of linear polymers is favoured.^[160]



Scheme 8.13: Cyclotrimerization of oxetane in the presence of BF_3 as catalyst.^[160]

No reactions of boranes with oxaphosphirane complexes were described so far, but first calculations regarding the ring opening reactions of oxaphosphiranes by borane complexation and migration of borane substituents were presented just recently by Espinosa and Streubel.^[161]

Catechol(chloro)borane **40** was used, instead of BF_3 , to investigate first reactions between 1,2-oxaphosphetane complexes and haloboranes. The presence of two oxygen substituents and only one chloro functionality was chosen to reduce the amount of possible side reactions, e.g. the multiple substitution reaction that could occur at the boron halogen bonds in BX_3 ($\text{X} = \text{Cl}, \text{F}$).



Scheme 8.14: Ring opening reaction of 1,2-oxaphosphetane complex **34.1_{aw}** with catechol(chloro)borane **40**.

A full and selective conversion of **34.1_{aw}** to **56.1** was observed in a slow reaction (7 days) (scheme 8.14). All volatiles were removed in *vacuo* and the product subsequently analysed (figure 8.12).

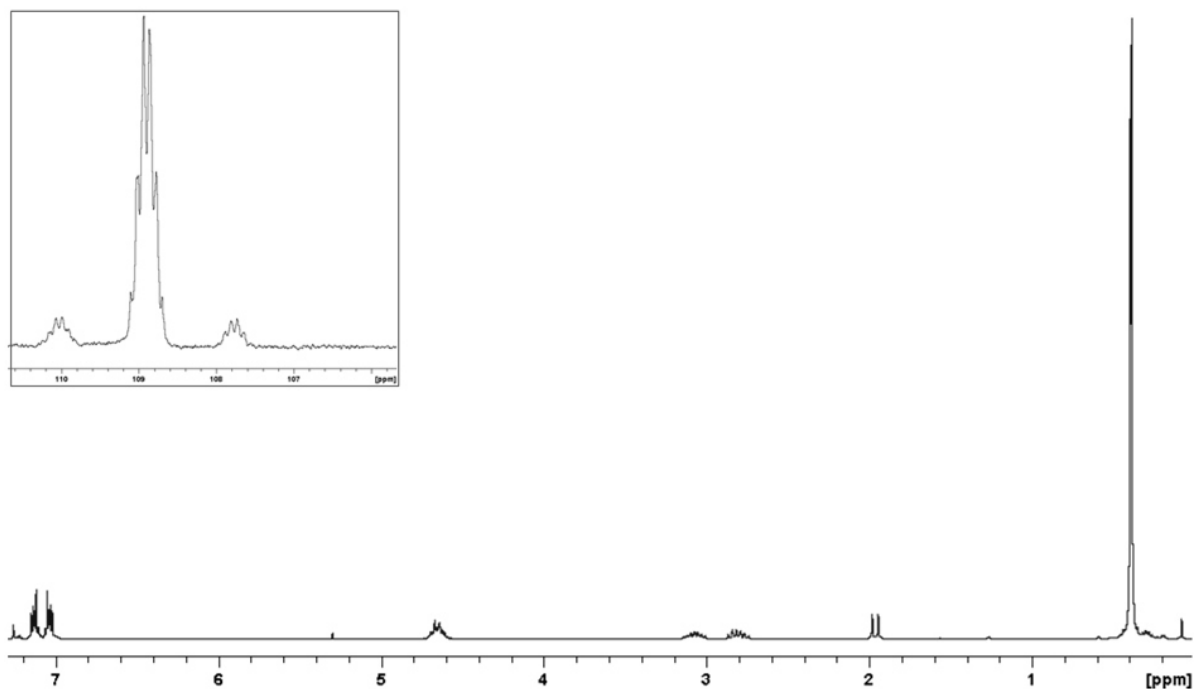


Figure 8.12: ^{31}P NMR spectrum (in the box) and ^1H NMR spectrum of **56.1**.

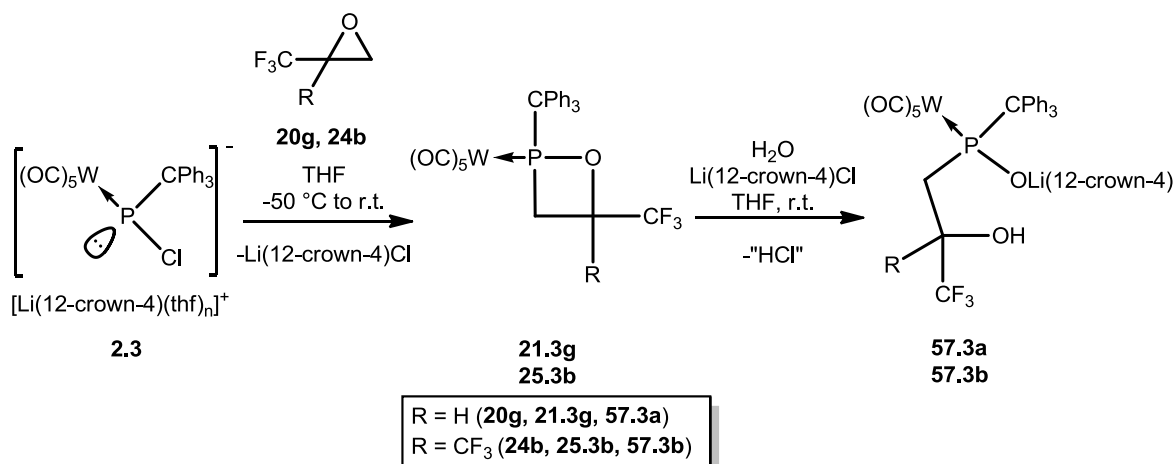
Complex **56.1** showed ^{31}P NMR spectroscopic characteristics similar to the data of complex **47.1a** ($\delta^{31}\text{P} = 115.5$ ppm, $^1J_{\text{W,P}} = 272.9$ Hz), obtained by reaction of **34.1a_w** with $\text{HCl}_{(\text{g})}$. Only a slight shift to higher field and a 1.4 Hz larger coupling constant (**56.1**: $\delta^{31}\text{P} = 108.9$ ppm, $^1J_{\text{W,P}} = 274.3$ Hz) were observed.

Additional support for the successful reactions was obtained from the $^{11}\text{B}\{^1\text{H}\}$ NMR spectrum, here a resonance signal at 23.3 ppm for **56.1** was observed, which is in the expected range, compared to $\text{R}_2\text{P}(\text{O})\text{-OB}(\text{OR})_2$ compounds.^[162]

8.6 Lewis acid induced ring opening reactions

As already pointed out in the introduction of chapter 8, Lewis acid-induced activation is an interesting option for small-ring heterocycles. Therefore, the effect of the abundant Li(12-crown-4)-cation, often present in solution was tested. Whereas for most of the syntheses described beforehand, no significant interaction between this cation and the ring P-ligands could be detected, an interesting reaction was observed in case of **21.3g** and **25.3b**. Here, P-O bond-selective ring opening was achieved, using a one-pot reaction protocol. As comparison of **25.3b** to **21.3g** revealed, steric crowding at the phosphorus centre, induced by the bulky CPh₃ group, and the CF₃ groups, combined with the electron-withdrawing influence of the latter played a crucial role. In case of the corresponding complexes bearing the *P*-CH(SiMe₃)₂ substituent as well as the *P*-C₅Me₅ substituent no reaction was observed with water, even at elevated temperature. In contrast, addition of water to the reaction mixture of **25.3b** yielded the novel 1,3-functional phosphinito complex **57.3b** (scheme 8.15); the formally generated HCl might be consumed by the solvent THF,^[153] this wasn't further investigated. The exact same protocol only led to traces of product in case of **21.3g** and a conversion of only 55 % was observed even after 5 days at ambient temperature. Nevertheless, full conversion was achieved after 16 h by slight heating (40 °C), providing more evidence for the influence of the CF₃ substituents.

In order to proof the importance of solvated lithium cations, the following test was undertaken: addition of water to a THF solution of complex **25.3b** in the absence of the lithium salt did not lead to any observable reaction, even at elevated temperatures (up to 65 °C). The activation therefore requires the presence of a Lewis acid and not only the steric crowding. It should be noted here that ring opening of penta-coordinated 1,2-oxaphosphetanes and formation of betaine-type structures was observed in the presence of lithium salts as it was stated by Schlosser in 1967.^[163] Although the involvement of compounds with betain structure in the stereoselectivity of the Wittig reaction especially in salt free reactions is still discussed today.^[164]



Scheme 8.15: Syntheses and Lewis acid-induced hydrolytic ring opening reactions of 1,2-oxaphosphetane complexes **21.3g** and **25.3b**.

Starting from an isomeric mixture of complexes **21.3g**¹ and **21.3g**² (ratio 42:58), a mixture of two isomers was observed for **57.3a**. The resonance signals were observed in the ³¹P{¹H} NMR (in CDCl₃) at 116.7 ppm (¹J_{W,P} = 283.7 Hz) and 109.2 ppm (¹J_{W,P} = 284.9 Hz) and in a ratio of 47:53.

For complex **57.3b** a resonance signal was observed in the ³¹P{¹H} NMR spectrum at $\delta = 125.6$ ppm (¹J_{W,P} = 300.9 Hz). The signal shows a slight deshielding compared to the mono-CF₃-substituted derivatives **21.3g**^{1,2}. In addition, hydrogen bridging in solution was indicated by the strongly deshielded signal for the C-OH proton at 9.41 ppm; this is similar to the situation found for enolic OH protons in 1,3-diketones.^[165]

The molecular structures of **21.3g** and **57.3b** in the single crystal (Figure 8.13, suitable crystals were obtained from diethyl ether solutions) show PO-Li interactions and the 12-crown-4 units coordinate the Li-cations from the far side. Orientation of the C-OH group towards the PO moiety indicates the proposed bridging O-H-O unit.

A comparable complex bearing the P-O-Li motif and an OMe group instead of the alcohol substituent ([Li(12-crown-4)][(OC)₅W{P(O)(CPh₃)(OMe)}]) was presented just recently.^[10] A similar deshielded signal at $\delta = 140.1$ ppm (¹J_{W,P} = 314.0 Hz) was described. The P-O-Li angle of **57.3b** was found to be, with an average of 160.5°, smaller than in that complex (P-O-Li angle: 170.2(4)°). Also the data for *P*-CH(SiMe₃)₂-substituted phosphinito complexes [Li(12-crown-4)][(OC)₅W{P(CH(SiMe₃)₂)F(O)}]^[166] (P-O-Li angle = 165.3(9)°) and [Li(12-crown-4)][(OC)₅W{PH(CH(SiMe₃)₂)(O)}]^[132] (P-O-Li angle = 166.7(5)°) showed a more linear geometry at the oxygen atom. The stronger deviation from the linear geometry in **57.3b** is presumably due to the hydrogen bridging in the OH-O unit.

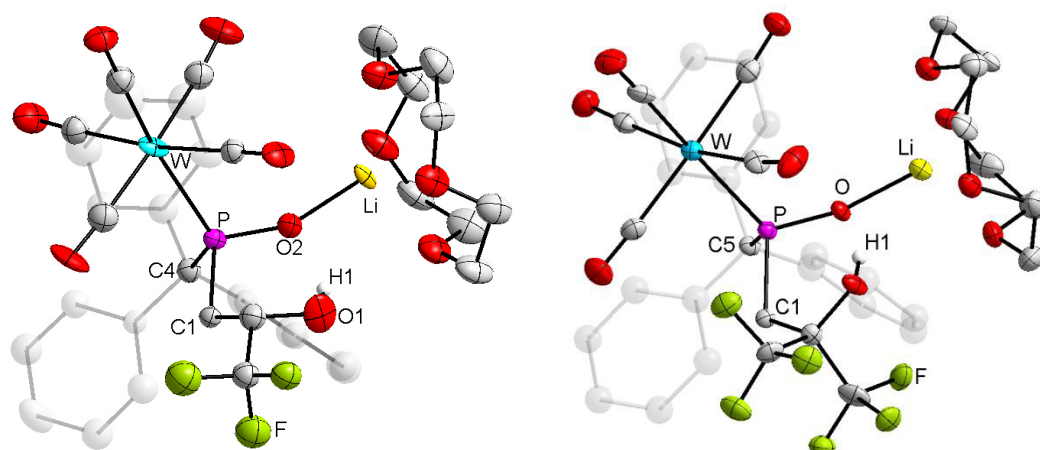


Figure 8.13: DIAMOND plot of the molecular structures of complexes **57.3a** (left) and **57.3b** (right) in the solid state; the thermal ellipsoids are set at 50 % probability level and all hydrogen atoms are omitted for clarity. Only one of two independent molecules is shown for both complexes and the phenyl rings of the CPh₃ unit are represented using a transparent mode for clarity.

Table 8.6: Selected bond lengths in Å and angles in ° for complexes **57.3a** and **57.3b**. In both cases two sets of data for two independent molecules in the unit cell are given (molecule 1/molecule 2)

	P-W	P-C1	P-CPh ₃	P-O	C1-P-O	P-O-Li
57.3a	2.553(4)/	1.856(16)/	1.965(18)/	1.547(13)/	102.3(7)/	156.7(12)/
	2.569(4)	1.88(2)	1.943(17)	1.556(12)	103.6(8)	164.6(13)
57.3b	2.5759(16)/	1.892(5)/	1.952(6)/	1.542(4)/	103.3(2)/	160.4(4)/
	2.5633(15)	1.903(6)	1.948(6)	1.542(4)	103.0(2)	160.6(4)

To test the potential of complex **57.3b** as synthetic building block for novel phosphorus heterocyclic ligands a preliminary study were investigated exemplarily, *i.e.* the ring closing reactions using dichloro-tetrel derivatives Me₂ECl₂ (E = Si (**58a**), Ge (**58b**)). Addition of Me₂SiCl₂ to a THF solution of **57.3b** showed a clean reaction and a conversion of 89 % after 4.5 h with a good selectivity. Further tests revealed that addition of DBU as a nitrogen base to the reaction mixture, to achieve HCl elimination, increased the reaction rate significantly (full conversion was observed in less than three hours).

If the reaction of complex **57.3b** with Me₂GeCl₂ was performed under base free conditions a set of broad resonance signals was observed in the ³¹P{¹H} NMR spectrum after 21 h (δ = 124.7 ppm, 34 %, h_{1/2} = 65 Hz and δ = 123.6 ppm, 46 %, h_{1/2} = 55 Hz), in addition to 20 % of the final product (figure 8.14). The intermediate was selectively converted to complex **60.3b** after addition of triethylamine to enhance the reaction progression.

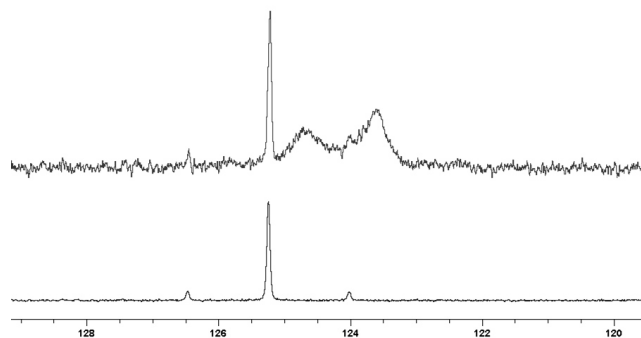
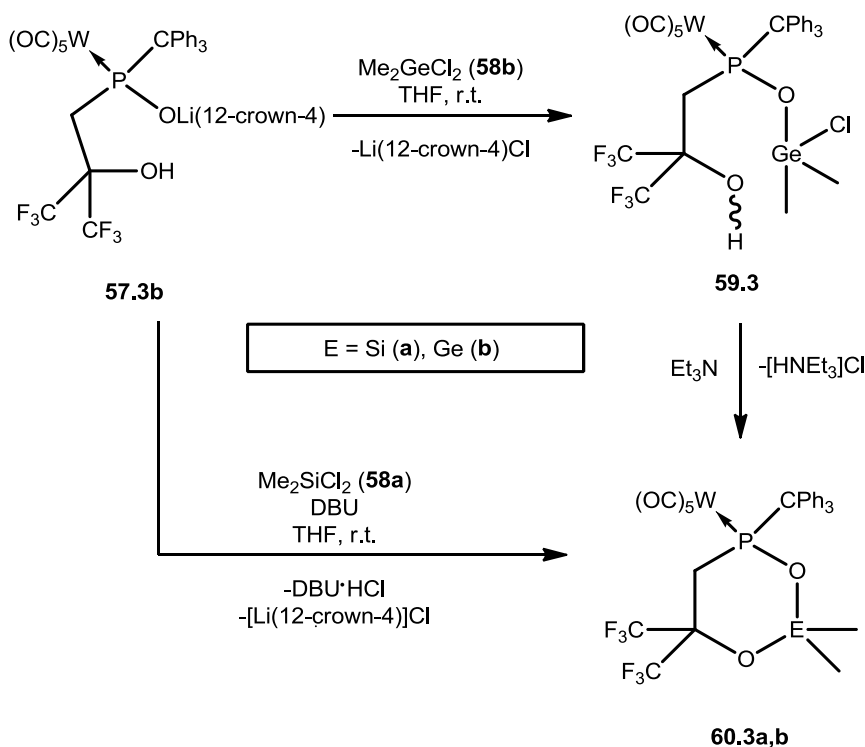


Figure 8.14: $^{31}\text{P}\{^1\text{H}\}$ NMR spectra before (top) and after addition of Et_3N (bottom) for the reaction of **57.3b** with Me_2GeCl_2 (**58b**).

Weak intra- and/or intermolecular interactions of the hydroxyl groups of intermediates **59.3** (scheme 8.16) are likely to be the reason for the broadening observed for the signals.



Scheme 8.16: Ring closing reactions of complex **57.3b** using Me_2ECl_2 (E = Si, Ge).

60.3a could be isolated by filtration and recrystallization (yield 54%). The presence of the Me_2Si unit in the ring was clearly established by the observation of a signal with a $^2J_{\text{P,Si}}$ -coupling of 9.6 Hz in the $^{29}\text{Si}\{^1\text{H}\}$ NMR spectrum. Surprisingly, only a very small influence of the Me_2Si linker on the $^{31}\text{P}\{^1\text{H}\}$ NMR parameters were observed. The ring closing results only in a slight low-field shift and a 4.8 Hz bigger $^1J_{\text{W,P}}$ coupling constant ($\delta = 123.8$ ppm, $^1J_{\text{W,P}} = 295.0$ Hz, in THF for **57.3b**, and 125.2 ppm, $^1J_{\text{W,P}} = 299.8$ Hz in THF for **60.3a**).

Complex **60.3b** showed a similar chemical shift for the resonance signal in the $^{31}\text{P}\{^1\text{H}\}$ NMR spectrum ($\delta = 126.2$ ppm, $^1J_{\text{W,P}} = 299.0$ Hz) and the influence of the Me_2Ge linker was again rather negligible.

Similar ^1H NMR and $^{13}\text{C}\{^1\text{H}\}$ NMR spectroscopic parameters to **60.3a** were observed for **60.3b** and the only notable difference was observed in case of the methyl groups bound to the group 14 elements. Strong deshielding was observed for the resonance signals of the E- CH_3 groups in the ^1H and $^{13}\text{C}\{^1\text{H}\}$ NMR spectra when going from the Si derivative **60.3a** to the Ge derivative **60.3b**.

Single-crystals suitable for X-ray diffraction studies could be obtained from saturated diethyl ether solutions at 4 °C for the Si- and Ge-containing complexes (Figure 8.15).

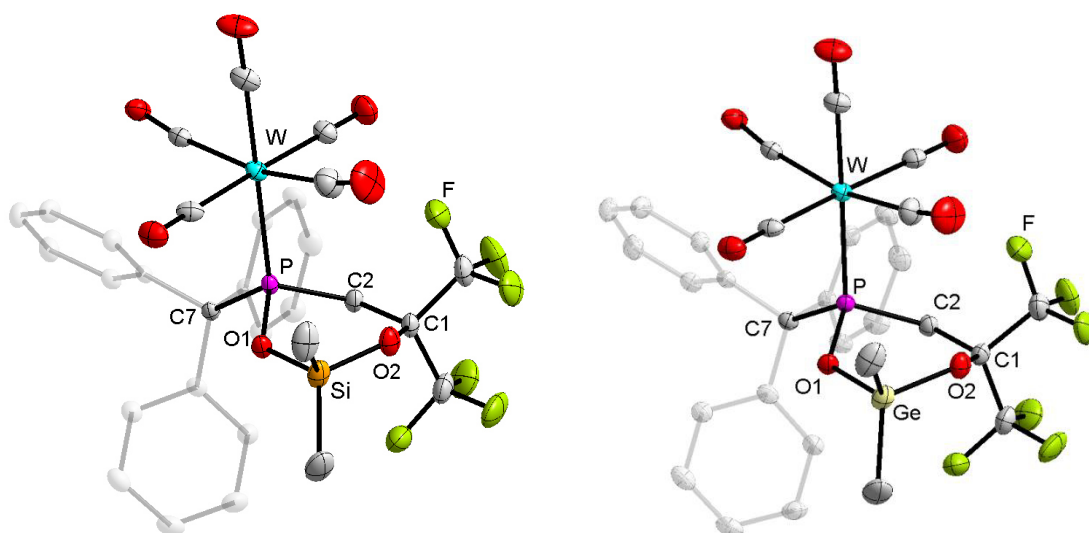


Figure 8.15: DIAMOND plot of the molecular structures of complex **60.3a** (left) and complex **60.3b** (right) in the solid state; the thermal ellipsoids are set at 50 % probability level and all hydrogen atoms are omitted for clarity. The phenyl rings of the CPh_3 units are represented using a transparent mode for clarity.

Table 8.7: Selected bond lengths in Å and angles in ° for complexes **60.3a** and **60.3b**.

	P-W	P-O1	P-C2	P-C7	C2-P-O1
60.3a	2.5376(7)	1.623(2)	1.869(3)	1.957(3)	101.81(11)
60.3b	2.5439(7)	1.613(2)	1.875(3)	1.959(3)	103.45(12)

In the solid state complexes **60.3a** and **60.3b** show a boat conformation of the distorted six-membered rings. All differences in the bond lengths and angles show the expected changes due to the atom size difference between the Si and Ge atoms (table 7.8, figure 8.16), e.g. a bigger O-E-O angle and longer O-E bonds for E = Ge.

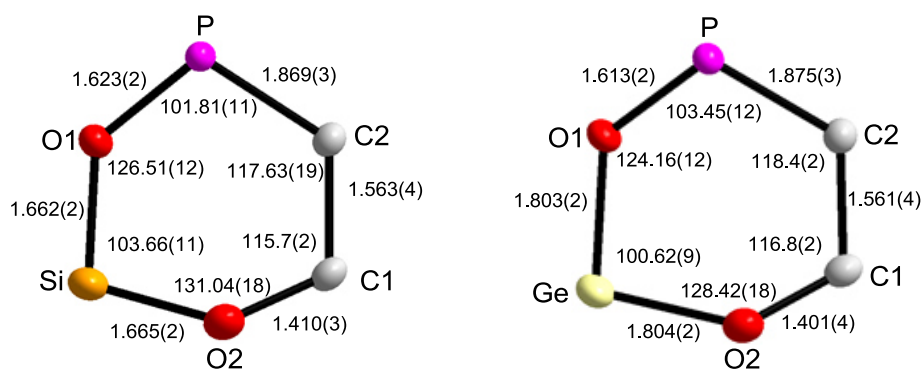
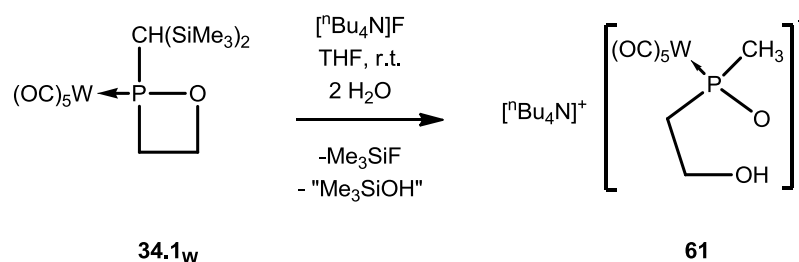


Figure 8.16: Bond lengths in Å (outside the rings) and angles in ° (inside the rings) of the six membered heterocyclic rings of complexes **60.3a** (left) and **60.3b** (right). The atoms are displaced as ellipsoids, set at 50% probability level and all substituents are omitted for clarity.

8.7 Fluoride mediated hydrolytic ring opening reaction

The reactions of epoxides or oxetanes with nucleophiles are of great importance in carbon chemistry, leading to many useful products in ring opening reactions. So for example the hydrolytic ring opening to diols utilizing metal hydroxides^[167] or opening of epoxides to halohydrines, *e.g.* with tetrabutylammonium fluoride in THF.^[168] In contrast, only very few examples of reactions using nucleophiles are known for the phosphorus analogues, the oxaphosphirane complexes or the oxaphosphetanes. In case of the oxaphosphirane complexes, mainly decomposition of the ring systems by formal simultaneous splitting of the P-O and P-C bond were observed, *e.g.* leading to secondary phosphane complexes in the reaction with Grignard reagents, after protonation of the intermediately formed phosphanido complexes.^[169] As there are only very few isolable oxaphosphetanes their reactivities have been only poorly investigated in this regard. Some ring openings by nucleophilic reagents, *e.g.* with NaOH,^[170] were described. Also deprotonation of the ring and subsequent reaction with electrophiles without destruction of the cyclic structure were shown, proving the low reactivity of 1,2-oxaphosphetanes.^[95]

First insight into the reaction of nucleophiles with 1,2-oxaphosphetane complexes was obtained when $[\text{nBu}_4\text{N}]\text{F}$ was added to a THF solution of 1,2-oxaphosphetane complex **34.1_w**. This complex was chosen as a case in point to avoid problems with isomerism, as often caused by C-substitution.



Scheme 8.17: Fluoride mediated hydrolysis of 1,2-oxaphosphetane complex **34.1_w**.

Surprisingly, not the nucleophilic ring opening of the 1,2-oxaphosphetane complex was observed. Instead a hydrolytic ring opening and an additional desilylation of the *P*-CH(SiMe₃)₂ substituent, presumably caused by contamination of the used $[\text{nBu}_4\text{N}]\text{F}$ solution with water, was observed (scheme 8.17).

Selective conversion of **34.1_w** to **61** was proven by only one observable signal in the ³¹P{¹H} NMR spectrum ($\delta = 67.2$ ppm, $^1J_{\text{W,P}} = 233.9$ Hz). These data are comparable to those observed for phosphinito complex **36.1** ($\delta = 46.0$ ($^1J_{\text{W,P}} = 244.1$ Hz)), indicating the anionic PO motif. The stronger deshielding, by 23.2 ppm, is in accordance with the expectation for

signal in the ^{29}Si NMR spectrum. No such problem was observed in CDCl_3 after recondensing and all signals were in accordance to literature known values.^[171]

A variable temperature NMR experiment was performed and revealed that, already at $-70\text{ }^\circ\text{C}$, no signal in the range of 1,2-oxaphosphetane complexes (between 150 and 220 ppm) was observed. Instead several signals close to the resonance signal of the final product were detected (figure 8.18).

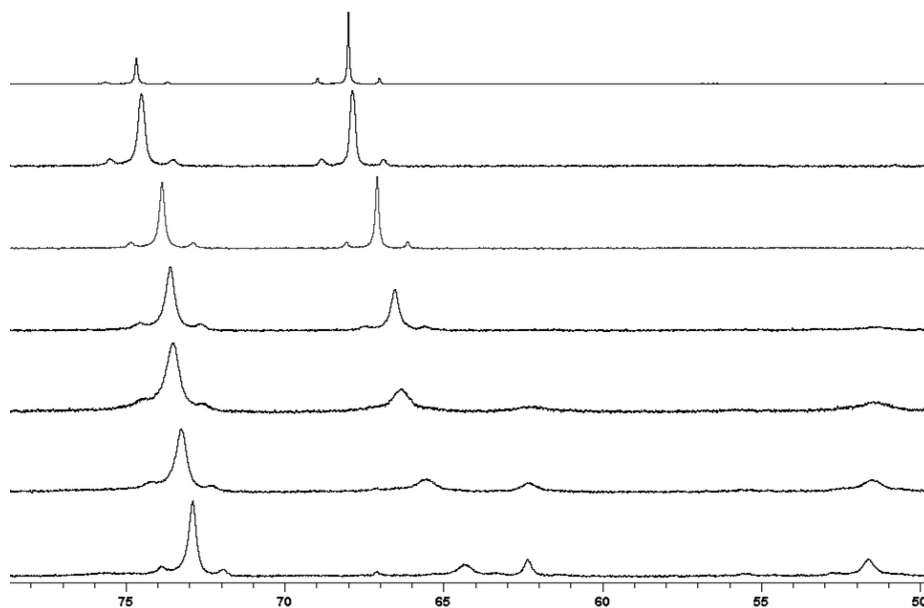
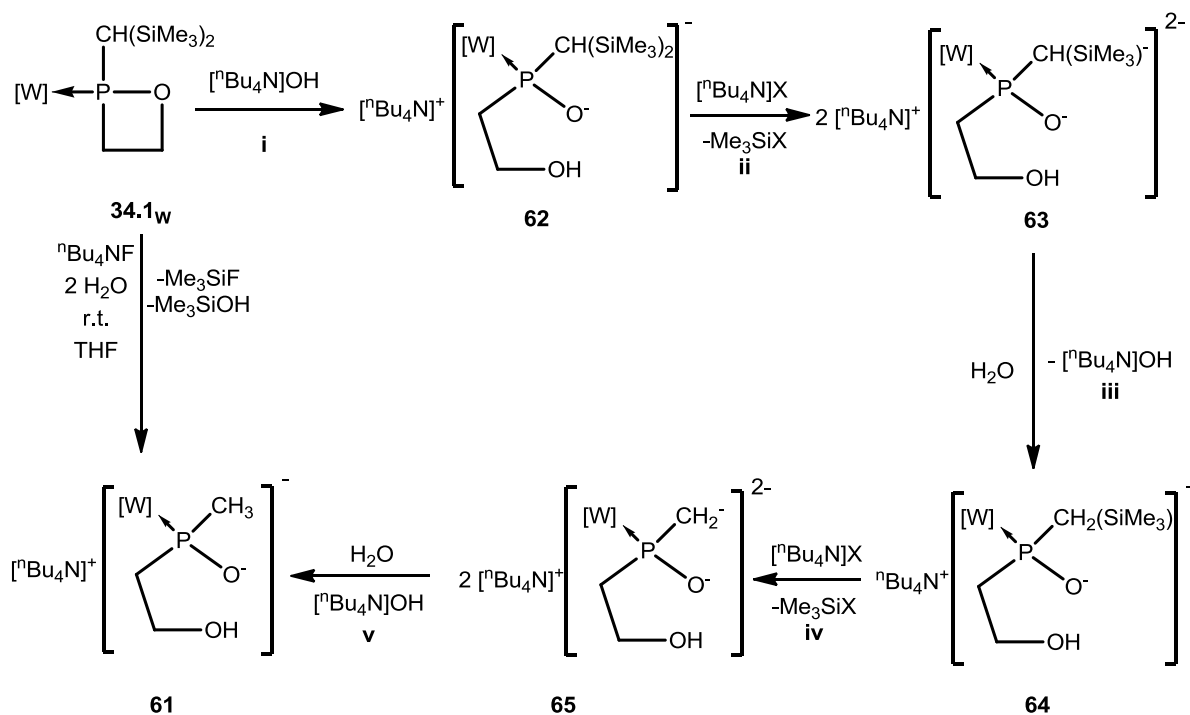


Figure 8.18: Variable temperature NMR measurement of the reaction between **34.1w** and $[\text{nBu}_4\text{N}]\text{F}$. Shown are the $^{31}\text{P}\{^1\text{H}\}$ NMR spectra at $-70\text{ }^\circ\text{C}$, $-60\text{ }^\circ\text{C}$, $-50\text{ }^\circ\text{C}$, $-40\text{ }^\circ\text{C}$, $-20\text{ }^\circ\text{C}$, $0\text{ }^\circ\text{C}$ and at room temperature (from bottom to top).

Based on this result, a stepwise mechanism was proposed for the product formation (scheme 8.18): a hydrolytic ring opening of the 1,2-oxaphosphetane complex **34.1w** by $[\text{nBu}_4\text{N}]\text{OH}$ takes place as the initial step (i). The complex then undergoes a desilylation reaction at the $\text{CH}(\text{SiMe}_3)_2$ group, forming the dianionic complex **63** (ii). The carbanion subsequently deprotonates water, forming the *P*-sila-neopentyl-substituted phosphinito complex **64** as well as one equivalent of $[\text{nBu}_4\text{N}]\text{OH}$ (ii). A second desilylation step forms dianion **65** (iii). The carbanion can deprotonate one more equivalent of water, liberating a second equivalent of $[\text{nBu}_4\text{N}]\text{OH}$ (v), forming the phosphinito complex **61**, as final product. Only catalytic amounts of $[\text{nBu}_4\text{N}]\text{OH}$ are necessary to initiate the reaction, as it is regained in the last step of the reaction sequence.

An initial desilylation reaction by the $[\text{nBu}_4\text{N}]\text{F}$ was excluded as reaction mechanism. The subsequent stepwise degradation of the $\text{CH}(\text{SiMe}_3)_2$ group to the CH_3 group and a hydrolytic ring opening in the last step would yield resonance signals in the ^{31}P NMR spectrum in a region very close to the one of the starting material.

Two aspects are of greater importance. In one of the desilylation steps (**ii** or **iv**) the fluoride salt has to react, as Me_3SiF was found as reaction product. Unfortunately, no differentiation can be made between the steps based on the products. Also, the reaction only requires the presence of 1.5 equivalents of water, as two molecules Me_3SiOH condensate to $(\text{Me}_3\text{Si})_2\text{O}$, liberating half an equivalent of water.

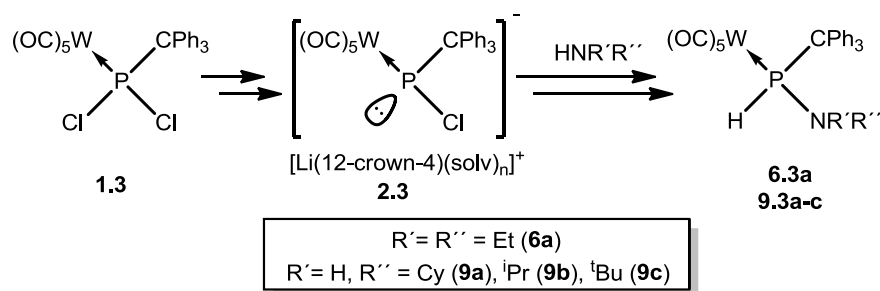


Scheme 8.18: Proposed mechanism for the fluoride mediated hydrolysis of 1,2-oxaphosphetane complex **34.1_w** ($[\text{W}] = \text{W}(\text{CO})_5$, $\text{X} = \text{F}, \text{OH}$).

9 Summary

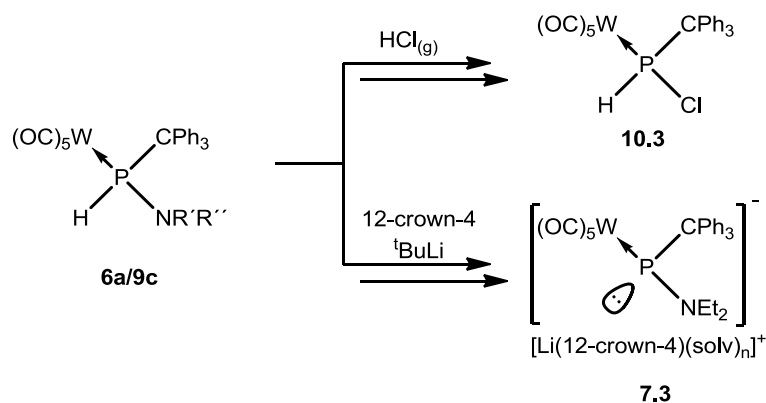
The research in this thesis focused on the formal insertion reaction of Li/Cl phosphinidenoid complexes into polar E-E' bonds of alcohols, amines and strained heterocycles, in particular epoxides. The obtained new and novel complexes were characterized by multinuclear NMR and infrared spectroscopy, mass spectrometry and elemental analysis, as well as single crystal X-ray diffraction studies in most cases. Furthermore, focused investigations towards the potential of some products as novel building blocks in P-ligand complex chemistry were performed.

In the first part of the thesis, research on the reactions of Li/Cl phosphinidenoid complexes with primary and secondary amines was performed. First examples of highly efficient insertion reactions of the P₁-fragment into N-H bonds yielded 1,1'-bifunctional amino-phosphane complexes in very good isolated yields (**6a**: 81%, **9a**: 77 %, **9b**: 71 %, **9c**: 84%) (scheme 9.1).



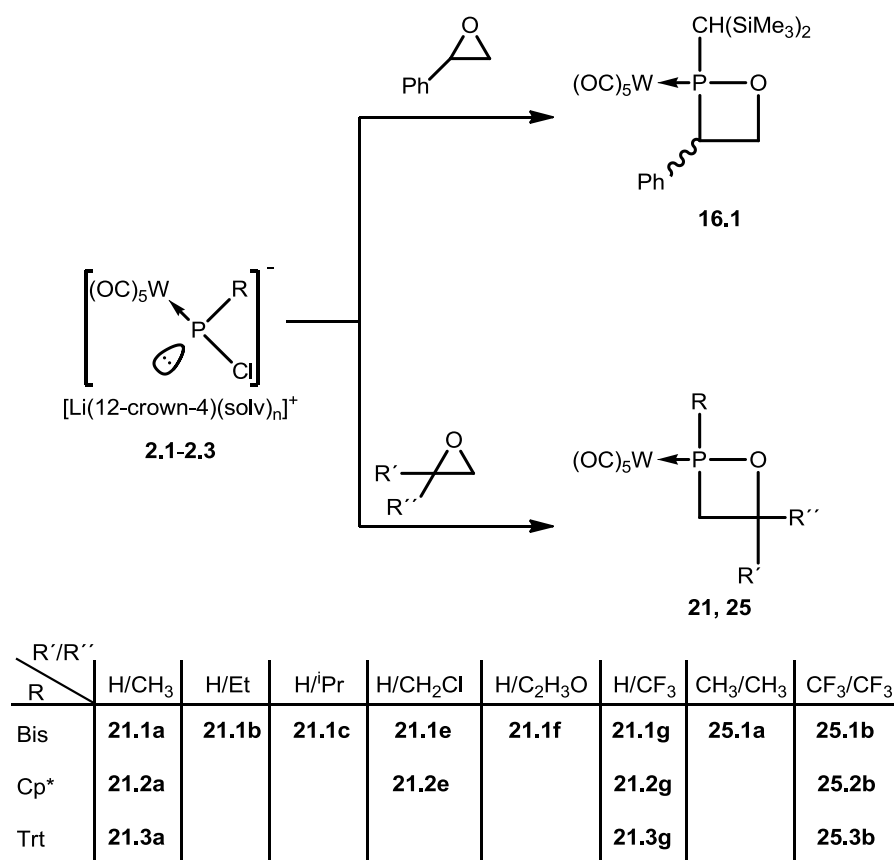
Scheme 9.1: Formal insertion reaction of Li/Cl phosphinidenoid complexes into N-H bonds.

The substitution reaction of the amino group by Cl using HCl_(g) in dichloromethane yielded the corresponding chlorophosphane complex **10.3**. Furthermore, a P-H deprotonation reaction using ^tBuLi in presence of 12-crown-4 proved that synthesis of Li/NEt₂ phosphinidenoid complex **7.3** is also possible; the latter represents the first stable derivative.



Scheme 9.2: First reactions of aminophosphane complexes by amino/chloro exchange and deprotonation.

In the second part of this thesis, synthetic routes to 1,2-oxaphosphetane complexes and reactions thereof were investigated. The first route used the formal insertion reaction of Li/Cl phosphinidenoid complexes into the C-O bond of different epoxides (scheme 9.3).



Scheme 9.3: Syntheses of 1,2-oxaphosphetane complexes using the formal insertion reaction of Li/Cl phosphinidenoid complexes into the CO bond of epoxides.

While the reaction with styrene oxide led selectively to 3-substituted 1,2-oxaphosphetane complex **16.1** (figure 9.1), C-alkyl-substituted epoxides led exclusively to 4-substituted 1,2-oxaphosphetane complexes in selective reactions. In the latter cases the nucleophilic attack at the least hindered side of the epoxide was identified as the initial reaction step.

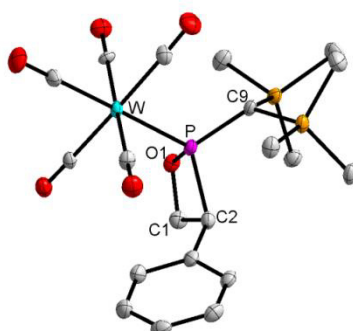


Figure 9.1: Molecular structure of the first isolated 1,2-oxaphosphetane complex in the solid state (all hydrogen atoms are omitted for clarity).

Most complexes were obtained in good yields (up to 61 %) either via extraction/separation from the formed salt and subsequent precipitation from *n*-pentane or diethyl ether at low temperature or by low temperature column chromatography. In case of CH(SiMe₃)₂ as the phosphorus substituent, a particular problem was observed: the formation of atropisomers arising from the relative orientation of the CH(SiMe₃)₂ proton with respect to the P-metal bond. This results in two isomers (*s-cis* and *s-trans*) due to a hindered rotation around this (exocyclic) P-C bond, which was studied in detail.

Apart from the regiochemistry aspect, stereoelectronic effects were investigated, using complex **2.1** as a case in point with a special focus on alkyl-derived C-substituted epoxides. While linear aliphatic derivatives furnished the corresponding products selectively, the C-ⁱPr-substituted epoxide led to a mixture of 1,2-oxaphosphetane complexes **21.1c** and diphosphene complexes (**22**, **23**). In addition almost no reaction occurred with the C-^tBu epoxide. Contrary, reactions proceeded with epoxides bearing sterically demanding and electron-withdrawing groups, *i.e.* with one or two CF₃ groups, thus illustrating substrate activation towards a nucleophilic attack.

Additional studies on the functional group tolerance showed that C-substitution of epoxides with a CH₂Cl, CF₃ and even an epoxy substituent did neither influence the selectivity of the ring formation in a negative way nor was the ratio of the formed isomers affected. Formation of two isomers was found for all C-monosubstituted derivatives, based on the relative orientation of the C-substituent of the ring either towards or away from the metal fragment. Indications of these isomers were often found as a split site in the molecular structure as they co-crystallised. In addition, a high flexibility was found for the ring itself, adapting folding angles in the range of approximately 2 to 35°.

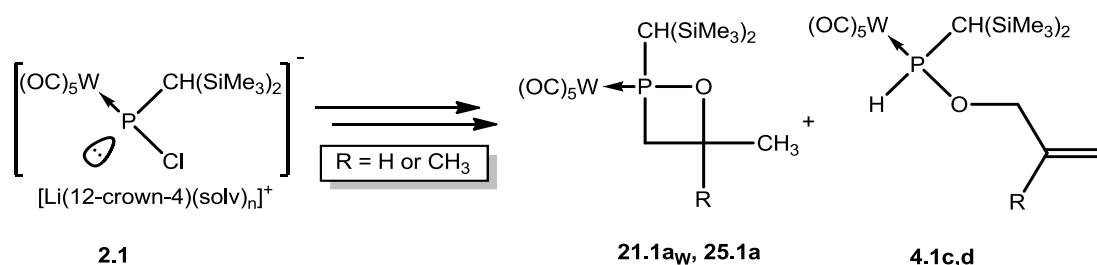
In addition, derivatives of **21.1a**, bearing not only the W(CO)₅ but also the Mo(CO)₅ and Cr(CO)₅, were synthesized. The change of the metal did neither influence the reaction outcome nor most of the analytical data. Significant but typical changes were only observed in the ¹³C{¹H} and ³¹P{¹H} NMR for the atoms directly bonded to the metal and for the metal phosphorus bond in the molecular structure.

A striking difference between the 1,2-oxaphosphetane complexes and 1,2σ⁵,λ⁵- or 1,2σ⁴,λ⁵-oxaphosphetanes is the high thermal stability which was found for all derivatives. Only slow and unselective decomposition was observed in toluene solutions at temperatures above 100 °C for most derivatives.

A significant influence of the C-substituent on the ³¹P NMR spectroscopic data was observed. ³¹P NMR resonances were observed in the range of 150 to 200 ppm with ¹J_{W,P} of 260 - 300 Hz, whereby a stronger deshielding as well as higher magnitudes for the coupling

constants were observed with the introduction of electron-withdrawing groups. This is of special interest as no such influence is known for the smaller heterocycles, the oxaphosphirane complexes. The other NMR and IR data as well as crystallographic parameters for all 1,2-oxaphosphetane complexes presented in this work are close to invariant.

1,2-Oxaphosphetane complexes bearing different *P*-substituents as well as 4,4-disubstituted complexes were prepared in a detailed study to evaluate the influence of the substitution pattern on the number of isomers formed and the general synthetic applicability. Change of the epoxides to either isobutylene oxide or hexafluoroisobutylene oxide showed a reduction to two isomers in case of the *P*-CH(SiMe₃)₂-substituted 1,2-oxaphosphetane complexes.



Scheme 9.4: Reaction of Li/Cl phosphinidenoid complex **2.1** with *C*-Me-substituted epoxides **20a** and **24a**.

During the studies phosphinite complexes **4.1a** and **4.1d** could be identified as side products in the reaction of Li/Cl phosphinidenoid complex **2.1** with *C*-Me-substituted epoxides. **4.1d** was isolated and characterized in case of the reaction with isobutylene oxide. Of particular interest was not only the formation of this side product but also the molecular structure of the corresponding 1,2-oxaphosphetane complex **25.1a**, as it showed the *s-trans* conformation of the *P*-CH(SiMe₃)₂ substituent for the first time.

In case of complex **25.1b** the presence of atropisomers by a hindered rotation could be proven by thermal change of the ratio between both complexes.

A reduced number of isomers was also observed using derivatives having the *P*-C₅Me₅ or the *P*-CPh₃ substituent, *i.e.* two isomers were observed for the 4-monosubstituted complexes (R = C₅Me₅: **21.2a,e,g**; R = CPh₃: **21.3a,g**). Consequently, only one isomer was observed in cases of the 4,4-disubstituted complexes **25.2b** and **25.3b**.

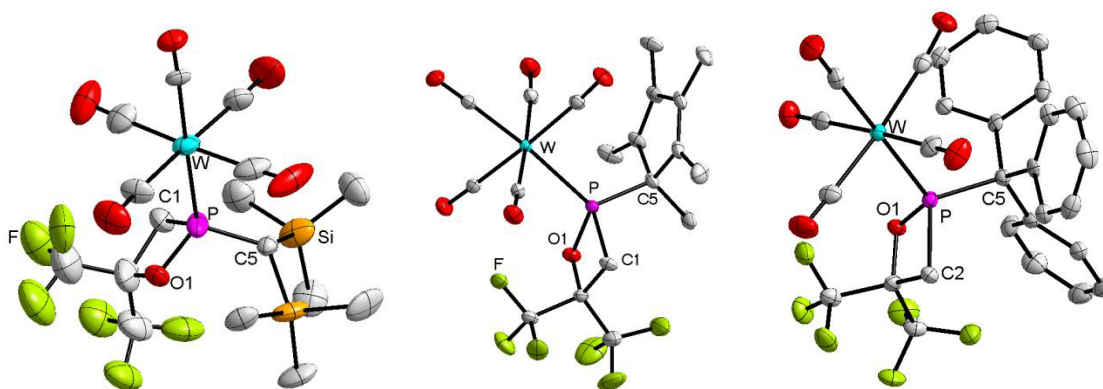


Figure 9.2: Molecular structures of bis- CF_3 -substituted 1,2-oxaphosphetane complexes **25.1b-25.3b** in the solid state (all hydrogen atoms are omitted for clarity).

An investigation on the synthetic accessibility of bis-oxaphosphetane complexes revealed a strong influence of the chain lengths of the used bis-epoxide on the reaction outcome. A selective reaction of **2.1** was only observed in the reaction with 1,7-octadiene diepoxide. Isolation of the first bis-oxaphosphetane complex was achieved and the product unambiguously characterized (figure 9.3).

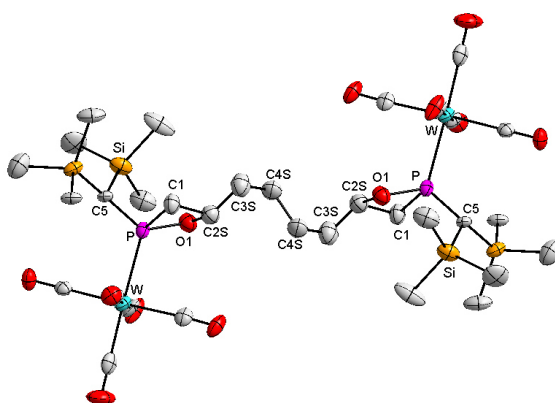
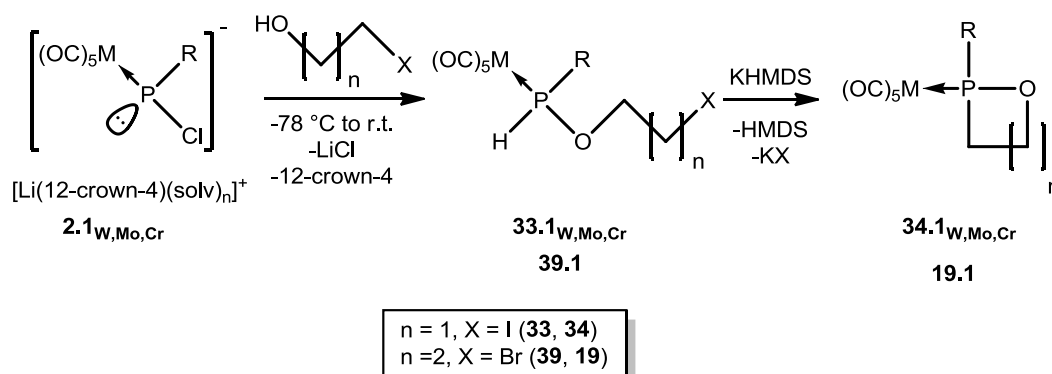


Figure 9.3: DIAMOND plot of the molecular structure of complex **29.1c** in the solid state; the thermal ellipsoids are set at 50 % probability level and all hydrogens are omitted for clarity. Only the main orientation of the bridging C_4 -unit and the ring folding is shown for clarity.

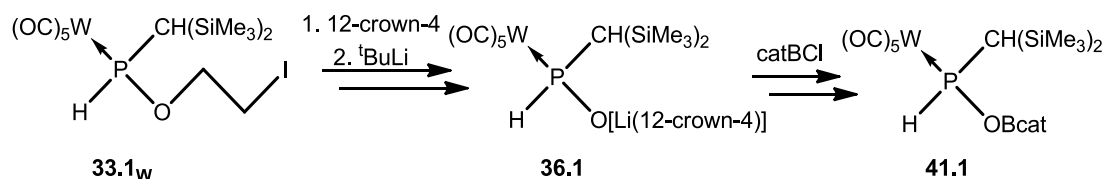
The second synthetic route to 1,2-oxaphosphetane complexes and a novel route to a 1,2-oxaphospholane complex was developed starting from the selective insertion reaction of Li/Cl phosphinidenoid complexes into the O-H bond of α,ω -bifunctional alcohols, *i.e.* 2-iodoethanol or 3-bromopropan-1-ol. Using the $P\text{-CH}(\text{SiMe}_3)_2$ -substituted Li/Cl phosphinidenoid complex **2.1** and the subsequent deprotonation with KHMDS and HI or HBr elimination in **33.1** or **39.1**, opened access to the novel C-unsubstituted O,P heterocyclic ligands in **19.1** and **34.1_{W,Mo,Cr}**. In addition, formation of only one isomer of the C-unsubstituted 1,2-oxaphosphetane complexes **34.1_{W,Mo,Cr}** allowed to broaden further reactivity studies due the simplification of otherwise unnecessarily complicated spectra.



Scheme 9.5: Syntheses of C-unsubstituted 1,2-oxaphosphetane complexes ($n = 1$, $M = Cr, Mo, W$, $X = I$) and a 1,2-oxaphospholane complex ($n = 2$, $M = W$, $X = Br$).

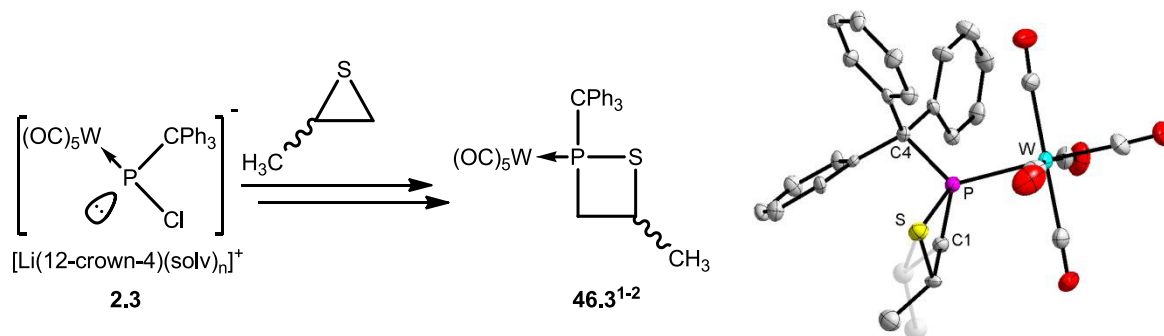
In the reactions of the $P-C_5Me_5$ and $P-CPh_3$ -substituted Li/Cl phosphinidenoid complexes **2.2** and **2.3** with 2-iodoethanol the formation of 1,2-oxaphosphetane complexes as well as chloro(organo)phosphane complexes **10.2** and **10.3**, respectively were observed in a 1:1 ratio. Nevertheless, the $P-C_5Me_5$ -substituted complex **34.2** could be isolated and unambiguously characterized.

A different result was obtained when *tert*-butyl lithium in the presence of 12-crown-4 instead of KHMDS was used in the reaction with 2-iodoethylphosphinite complex **33.1_W**. Not the P-H deprotonation, but a lithium/iodine exchange with subsequent elimination of ethylene to yield phosphinito complex **36.1** was observed. The complex was described by the group of Streubel before, but the previous route was too laborious and expensive to be fully exploited. With a far better yield (75 %) it was now possible to investigate further reactivity: In a first test, complex **36.1** could be used as synthetic building block for the preparation of complex **41.1**, being the first example of a complex bearing a P-ligand with the structural POB motif.



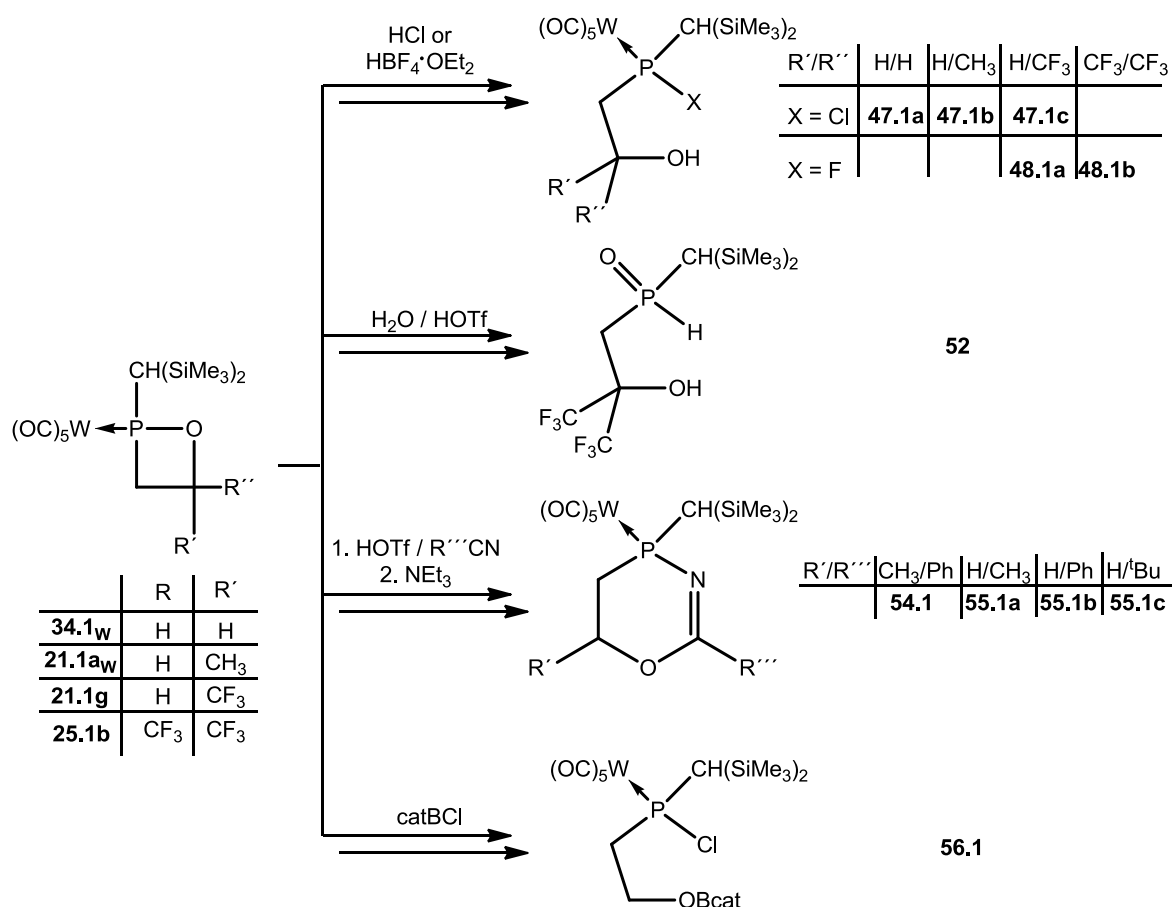
Scheme 9.6: Syntheses of phosphinito complex **36.1** and phosphinite complex **41.1**.

Before this work was started, the heavier homologues of the 1,2-oxaphosphetane complexes were unknown. A first investigations towards the reaction of Li/Cl phosphinidenoid complex **2.3** with propylene sulfide showed that also 1,2-thiaphosphetane complexes are accessible using the strategy developed for the synthesis of 1,2-oxaphosphetane complexes. Complexes **46.3**¹⁻² were formed selectively in form of two isomers and showed high-field shifted resonance signals in the $^{31}P\{^1H\}$ NMR spectra with smaller $^1J_{W,P}$ coupling constants compared to the otherwise similar complexes **21.3a**.



Scheme 9.7: Synthesis and molecular structure of 1,2-thiaphosphetane complex **46.3**.

In chapter 8 the chemical behaviour of 1,2-oxaphosphetane complexes was presented with the special focus on an acid-induced reactivity.



Scheme 9.8: Acid-induced reactions of 1,2-oxaphosphetane complexes (R = CH(SiMe₃)₂).

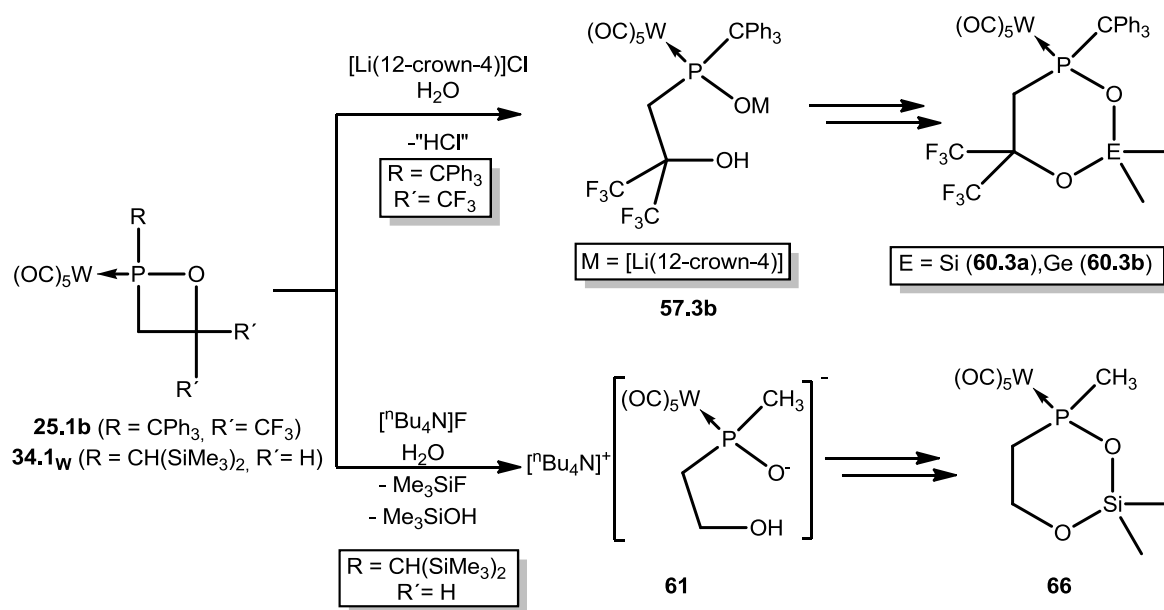
Brønsted acid-induced ring opening reactions were achieved using either HCl_(g) or tetrafluoroboric acid diethyl ether complex (HBF₄·OEt₂) in dichloromethane, yielding the corresponding chloro(organo)phosphane complexes **47.1a-c** or fluoro(organo)phosphane complexes **48.1a,b**, respectively. The reaction with HCl_(g) was found to be dependent on the C-substituent as introduction of one CF₃ group reduced the reaction speed noticeably and introduction of a second CF₃ group completely suppressed the reaction. In contrast to reactions of oxaphosphirane complexes, where the C₅Me₅ group is involved in the reaction

with Brønsted acids, the analogous reaction of a *P*-C₅Me₅-substituted 1,2-oxaphosphetane complex **25.2b** yielded the fluoro(organo)phosphane complex **48.2b** by simple ring opening.

Of particular interest was the activation of 1,2-oxaphosphetane complexes using triflic acid. In the presence of water, hydrolysis of the ring and loss of the W(CO)₅ moiety was observed to form phosphane oxide **52** as the single P-containing product. In the presence of nitriles, a ring expansion reaction yielding 1-oxa-3-aza-5,6-dihydrophosphinines **54.1** and **55.1a-c** was achieved using a subsequent treatment with triflic acid and triethylamine. Optimization of the reaction conditions led to the isolation of complexes **55.1a-c** in almost quantitative yields.

In a preliminary study, reaction of the 1,2-oxaphosphetane complex **34.1_w** with catechol(chloro)borane as Lewis acid afforded the chloro(diorgano)phosphane complex **56.1** in a ring opening reaction, being similar to the one observed with HCl_(g).

A hydrolytic ring opening reaction was observed in case of the sterically crowded 1,2-oxaphosphetane complex **25.1b** in presence of Li(12-crown-4)Cl. The reaction led selectively to phosphinito complex **57.3b**. Interestingly, no reaction was observed in the absence of the lithium salt, *i.e.* an additional activation by this Lewis acid was necessary.



Scheme 9.9: Hydrolytic ring opening reactions of 1,2-oxaphosphetane complexes and their use in medium sized P-ligand formation.

A somewhat similar product was observed by an [ⁿBu₄N]F-mediated hydrolysis in case of the *P*-CH(SiMe₃)₂-substituted 1,2-oxaphosphetane complex **34.1_w**. Surprisingly, a desilylation was observed in case of **34.1_w**, leading to complex **61**. Analysis of the molecular structures in the solid state showed a preformed ring by a hydrogen bond between the OH and the PO moiety in the ligand framework.

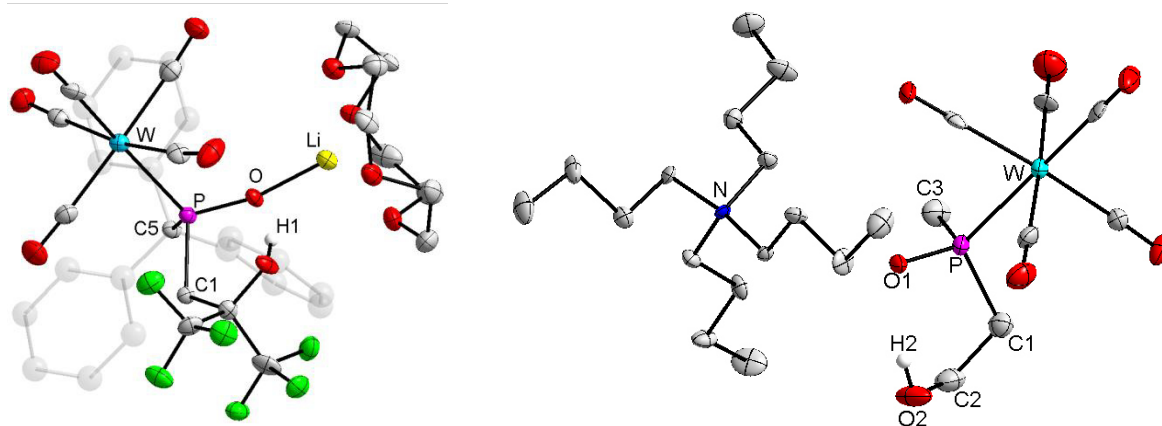


Figure 9.4: Molecular structures of phosphinito complexes **57.3b** and **61**.

The synthetic potential of phosphinito complexes **57.3b** was illustrated by reactions with Me_2SiCl_2 and Me_2GeCl_2 and in case of **61** with Me_2SiCl_2 in ring closing reactions, thus leading to novel 6-membered heterocyclic ligands in **60a,b** and **66**.

10 Experimental section

10.1 General part

All reactions were performed under strict exclusion of moisture and oxygen using standard Schlenk or glove box techniques under an atmosphere of deoxygenated and dried argon. The used argon gas was commercially received with a purity of > 99.999 % and purified by passing through a system of three columns, one for deoxygenating using the BTS copper catalyst (BASF AG, 100 – 130 °C), one for drying, filled with phosphorus pentoxide and one with silica gel. The glove box (build by MBRAUN) was maintained under an argon atmosphere (O₂ content below 0.1 ppm and H₂O content below 0.1 ppm) with an excess pressure of 1.5 mbar.

All solvents were dried by standard procedures:^[173] THF and Et₂O over benzophenone and sodium-wire, *n*-pentane, petroleum ether and toluene over sodium wire and dichloromethane over CaH₂. The solvents were refluxed for several days and either distilled prior to use or distilled and kept in brown glass bottles with Argon inlet over sodium wire or 4 Å molecular sieves. Solvents used for the preparation of extremely air and moisture sensitive compounds were degassed and recondensed from either potassium or CaH₂ prior to use.

The transfer of solvents or solutions was performed using stainless steel cannulas that were dried prior to use in an oven at 75 °C for at least one hour and facilitated by positive argon pressure at one side and a pressure relieve valve at the side of the receiving flask. For filtration either a Schlenk-frit or a stainless steel filtration cannula with an attached filtration head was used. For the filtration with the stainless steel cannula either standard filter paper or Whatmann glass filter paper was used, depending on the sensitivity of the material, which was fixed at the filtration head with Teflon tape. In both cases the filter paper and cannula were dried at 75 °C in the oven for at least an hour prior to use. The cannulas were cleaned after use with acetone, water, diluted hydrochloric acid, water and again acetone.

All glassware was cleaned by storage in a KOH/water bath, containing some NaClO for oxidation of all metal contaminations. The glassware was stored in the bath for at least two days and subsequently washed with tap water/soap, diluted HCl_(aq) and finally with acetone and petroleum ether to remove all traces of grease. All clean glassware was dried overnight in an oven at 75 °C.

Prior to use all joints were greased with OKS grease type 1112. The glassware was heated under active vacuum (0.02 mbar) to 400-500 °C, filled with argon while it was still hot, evacuated, again heated, allowed to cool down to ambient temperature under active vacuum to remove adsorbed water from the surface and refilled with argon.

Low temperatures (< 0 °C to -100 °C) were achieved using either a petroleum ether or ethanol bath and liquid nitrogen.

Several compounds were purified using low temperature column chromatography. The chromatographic columns were equipped with an integrated cooling mantle, cooled with a connected cryostat and ethanol (technical grade) as cooling medium for constant cooling of the column material as well as a vacuum mantle to avoid ice formation on the surface. Neutral Silica (Merck 60-200) or aluminum oxide (Merck 90 neutral) was used as stationary phase. The column's dimensions (diameter x length), the used stationary phase and eluents are given in the experimental details for each case.

10.2 Analytical Methods

10.2.1 Melting point determination

Melting points were determined on a Büchi 535 Type S melting point apparatus in both sided clothed glass tubes; the values are not corrected.

10.2.2 NMR spectroscopy

All NMR spectra were recorded on a Bruker Avance DMX-300, DPX-300, DPX-400 or DMX-500 spectrometer. The ^1H NMR resonance signals and the $^{13}\text{C}\{^1\text{H}\}$ NMR resonance signals were referenced to the solvent residual signals. Deuterated solvents (CDCl_3 , THF- d_8 or C_6D_6) were dried using literature procedures and used for the multi nuclear NMR characterizations and the chemical resonances are given relative to Tetramethylsilane (^1H , ^{13}C , ^{29}Si NMR), 1 M LiCl in D_2O (^7Li NMR), 15 % $\text{BF}_3\cdot\text{OEt}_2$ in CDCl_3 (^{11}B NMR), CFCl_3 (^{19}F NMR) or 85% H_3PO_4 (^{31}P NMR), respectively. The chemical shift is given in parts per million, ppm. Magnitudes of coupling constants are abbreviated as $^nJ_{X,Y}$, where X and Y denote the coupling nuclei (ordered by decreasing atomic number, the nuclear numbers are omitted), and n denotes the number of bonds that separate X and Y; only absolute values were determined.

Table 10.1: Chemical shifts of the deuterated solvents and multiplicity of the residual signals used for the calibration.^[174]

Solvent	^1H NMR (δ in ppm)	$^{13}\text{C}\{^1\text{H}\}$ NMR (δ in ppm)
CDCl_3	7.62 (s)	77.16 (3)
C_6D_6	7.16 (br)	128.06 (3)
THF-d_8	1.72 (br)	25.31 (5)
	3.58 (br)	67.21
toluene-d_8	2.08 (5)	20.43 (7)

Signals are characterized by the following abbreviations: for their form and multiplicities s = singlet, d = doublet, t = triplet, q = quartet, quin = quintet, sept = septet, m = multiplet and br

= broad signal. The ^1H NMR and $^{13}\text{C}\{^1\text{H}\}$ NMR signals of all compounds were assigned by a combination of HMQC, HMBC and DEPT experiments.

All measurements were performed, as long as not specified otherwise, at 298 K.

10.2.3 Mass spectrometry

Mass spectrometric data were recorded on a Bruker Daltonik micrOTOF-Q using ESI (+/-), a Thermo Finnigan MAT 90 sector instrument equipped with a LIFDI ion source (Linden CMS) or MAT 95 XL Finnigan using EI (70 eV). Only selected data are given for the detected ions (mass to charge ratio, relative intensity in percent). Assignments of the ionic molecule fragments is based on plausibility and on the observed isotopic distributions; for compounds containing several isotopes the given m/z values refer in each case to the most intense peak according to the combination of elements each with the highest abundance.

10.2.4 IR spectroscopy

Infrared spectra were recorded of the pure solids on a Thermo IR spectrometer with an attenuated total reflection (ATR) attachment or on a Bruker Alpha Diamond ATR FTIR spectrometer at room temperature. A selection of the registered bands is given for each compound where the intensity is marked with the following abbreviations: vs = very strong, s = strong, m = medium, w = weak, vw = very weak, sh = shoulder.

10.2.5 Elemental analysis

Elemental analysis was performed with an Elementar Vario Micro elemental analyser by the micro analysis laboratory of the Chemical Institute of the University of Bonn. The mean value of at least three measurements is given.

10.2.6 Single crystal X-ray diffraction studies

Suitable single crystals were separated from the supernatant solution at the temperature of the crystallization and covered with Formblin[®] Y lubricant to protect them from air and moisture. A crystal suitable for measurement was selected on a microscope and transferred to the diffractometer. The data were collected on a Bruker D8-Venture, Bruker X8-KappaApexII, Bruker APEX-II CCD, Nonius KappaCCD or STOE IPDS 2T diffractometer equipped with a low-temperature device (Cryostream, Oxford Cryosystems) using graphite monochromated Mo-K_α radiation ($\lambda = 0.71073 \text{ \AA}$) or Cu-K_α radiation ($\lambda = 1.54178$). The absorption correction, structure solution was performed by Patterson methods or direct methods (SHELXS-97^[175]) and structure refinement by full-matrix least squares on F^2 (SHELXL-97^[176], SHELXL-2015^[177] or OLEX2^[178]) programs. All non-hydrogen atoms were refined anisotropically, the hydrogen atoms were included isotropically using the riding model on the bound carbon atoms.

Data analysis and preparation of the pictures of the molecular structures were prepared using the program DIAMOND 3.0. Details on the structure solutions presented in this thesis are included in the appendix.

10.2.7 Used chemicals

The following chemicals were purchased and purified or distilled prior to use according to literature procedures:^[173]

• acetonitrile	VWR
• aluminium oxide Merck 90 neutral (70-230 mesh ASTM)	Merck
• benzene-d ₆	deutero
• benzonitrile	Merck
• boron trichloride	Acros
• 3-bromopropan-1-ol	abcr
• 1,3-butadiene diepoxide	Alfa Aeser
• 1,2-butylene oxide	TCI
• calcium chloride (anhydrous)	VWR
• chloroform-d ₁	deutero
• chlorotrimethylsilane	Aldrich
• chromium hexacarbonyl	Aldrich
• 12-crown-4	Acros
• cyclohexylamine	Chimica
• dichloromethane	Fisher
• diethylamine	Acros
• diethyl ether	VWR
• dichlorodimethylgermane	Fluorochem
• dichlorodimethylsilane	Alfa Aeser
• 2,3-diphenylcyclopropenone	Alfa Aeser
• epichlorohydrin	Acros
• 1,2-epoxy-3-methylbutane	Alfa Aeser
• hexafluoro isobutylene oxide	abcr
• 1,5-hexadiene diepoxide	abcr
• hydrochloric acid (35%)	Acros
• isobutylene oxide	Acros
• isopropylamine	Acros
• 2-iodoethanol	Acros or Alfa Aeser
• KHMDS (potassium hexamethyldisilazide)	Aldrich

• molybdenum hexacarbonyl	Aldrich
• <i>n</i> -pentane	VWR
• 1,7-octadiene diepoxide	Alfa Aeser
• petroleum ether 40/60	Hoesch
• phosphorus pentoxide (SICAPENT®)	Merck
• phosphorus trichloride	Acros
• propylene oxide	Aldrich
• R(+)-propylene oxide	Alfa Aeser
• propylene sulfide	Aldrich
• Silica gel Merck 60 (0.063 – 0.2 mm, pH = 6.5 – 7.5)	Merck
• styrene oxide	Merck
• <i>tert</i> -butyllithium (1.7 M in <i>n</i> -pentane)	Aldrich
• <i>tert</i> -butylamine	Acros
• tetrabutylammonium fluoride (1 M in THF)	Alfa Aeser
• tetrafluoroboric acid diethyl ether complex	Aldrich
• tetrahydrofurane	Fisher
• tetrahydrofurane-d ₈	deutero
• toluene	VWR
• toluene-d ₈	Euriso-top
• triethylamine	Acros
• 1,1,1-trifluoro-2,3-propylene oxide	abcr
• trifluoromethanesulfonic acid	Aldrich or Acros
• trimethylacetonitrile	Acros
• trimethylamine-N-oxide dihydrate	Alfa-Aeser
• tungsten hexacarbonyl	Aldrich or abcr

The following starting materials were synthesized according to described procedures

- acetonitrile(pentacarbonyl)tungsten(0)^[179]
- acetonitrile(pentacarbonyl)molybdenum(0)^[179]
- acetonitrile(pentacarbonyl)chromium(0)^[179]
- dichloro[bis(trimethylsilyl)methyl]phosphane^[180]
- dichloro(triphenylmethyl)phosphane^[181]
- dichloro(1,2,3,4,5-pentamethylcyclopenta-2,4-dien-1-yl)phosphane^[182]
- pentacarbonyl[dichloro(triphenylmethyl)phosphane-κP]tungsten(0)^[33]
- pentacarbonyl{dichloro[bis(trimethylsilyl)methyl]phosphane-κP}tungsten(0)^[114]
- pentacarbonyl{dichloro[bis(trimethylsilyl)methyl]phosphane-κP}molybdenum(0)^[114]

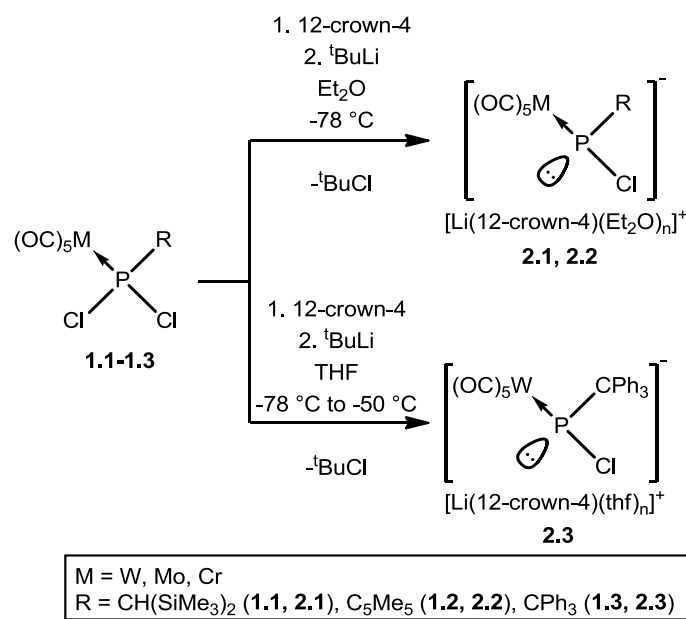
- pentacarbonyl{dichloro[bis(trimethylsilyl)methyl]phosphane- κ P}chromium(0)^[114]
- pentacarbonyl[dichloro(1,2,3,4,5-pentamethylcyclopenta-2,4-dien-1-yl)phosphane- κ P]tungsten(0)^[125]
- pentacarbonyl{(2-iodoethoxy)[bis(trimethylsilyl)methyl]phosphane- κ P}molybdenum(0)^[183]
- pentacarbonyl{(2-iodoethoxy)[bis(trimethylsilyl)methyl]phosphane- κ P}chromium(0)^[183]
- 1-(1-methylethyl)-2-phenyl-aziridine^[140]
- 1-(phenylmethyl)-2-(trifluoromethyl)-aziridine^[141]

10.2.8 Waste disposal

The waste disposal was performed according to the institutes waste disposal policy. Single use syringes and cannulae, solvents, column material and other contaminated materials were collected in special containers. Alkaline metals were first treated with isopropanol, using appropriate safety measurements, to obtain the corresponding salts and subsequently disposed. All contaminated waste was submitted to the department 4.2 "Arbeits und Umweltschutz" of the University of Bonn for further handling and disposal.

11 Syntheses and analytical data

11.2.1 Preparation of Li/Cl phosphinidenoid complexes 2.1-2.3 at low temperature



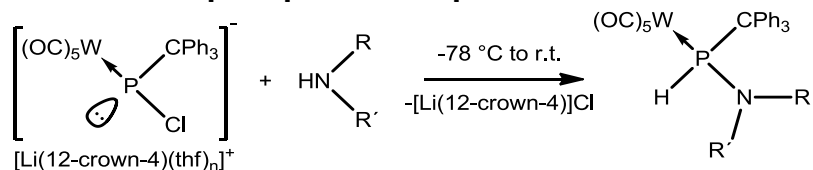
11.2.1.1 Preparation of **2.1**^[31] and **2.2**^[32]

One equivalent of dichlorophosphane complex [(OC)₅M{PCl₂(R)}] **1.1** (R = CH(SiMe₃)₂, M = Cr, Mo, W) or **1.2** (R = C₅Me₅) and one equivalent of 12-crown-4 are dissolved in diethyl ether (20 mL per mmol of reagent) in an appropriate Schlenk tube (approximately twice the volume of the solvent). The solution is cooled to -78 °C and subsequently 1.05 equivalents of *tert*-butyllithium (1.7 M solution in *n*-pentane) are added dropwise. The solution is stirred for 10 minutes at -78 °C to ensure complete conversion to the Li/Cl phosphinidenoid complexes **2.1** or **2.2**, respectively.

11.2.1.2 Preparation of **2.3**^[33]

One equivalent of the dichlorophosphane complex [(OC)₅W{PCl₂(CPh₃)}] (**1.3**) and one equivalent of 12-crown-4 are dissolved in THF (12 mL per mmol) in an appropriate Schlenk tube (approximately twice the volume of the used solvent). The solution is cooled to -78 °C and subsequently 1.05 equivalents of *tert*-butyllithium (1.7 M solution in *n*-pentane) are added dropwise. The solution is allowed slowly warming up to -50 °C (ca. 1 h) to ensure complete conversion to the Li/Cl phosphinidenoid complex **2.3**.

11.2.2 Syntheses of aminophosphane complexes

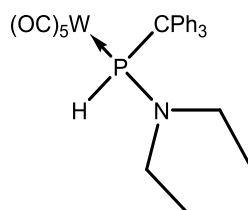


A solution of Li/Cl phosphinidenoid complex **2.3** was prepared as described in chapter 11.2.1, starting from $[(OC)_5W\{P(Cl)_2(CPh_3)\}]$ (**1.3**). The solution was cooled subsequently to $-78\text{ }^\circ\text{C}$ and the corresponding amine was added. The solution was allowed slowly warming up to $0\text{ }^\circ\text{C}$ before removing the cooling bath. Formation of a white precipitate was observed during the warm up period and the solution was stirred for at least 30 more minutes at ambient temperature. (In case of **9.3c** the solution was kept on stirring overnight.)

Table 11.1: Amounts of used dichloro(organo)phosphane complex **1.3** and amines.

	R	R'	m (1.3) [mg]	n (1.3) [mmol]	amine	V (amine) [mL]	n (amine) [mmol]
6.3a	Et	Et	333.5	0.50	5a	0.06	0.57
9.3a	H	Cy	167.0	0.25	8a	0.03	0.26
9.3b	H	ⁱ Pr	167.0	0.25	8b	0.03	0.35
9.3c	H	^t Bu	669.0	1.00	8c	0.06	1.10

11.2.2.1 Pentacarbonyl[diethylamino(triphenylmethyl)phosphane- κP]tungsten(0) [**6.3a**]



Purification: All volatiles were removed in *vacuo* (ca. 0.02 mbar). The product was extracted from the formed salt with two times 15 mL of diethyl ether and one time 10 mL of diethyl ether. The product was obtained as yellow solid after evaporation of all volatiles in *vacuo* (ca. 0.02 mbar).

Molecular formula: $C_{28}H_{26}NO_5PW$

Molecular weight: 671.324 g/mol

Melting point: $151\text{--}152\text{ }^\circ\text{C}$

Yield: 271.1 mg (0.404 mmol, 81 %).

^1H NMR (300.1 MHz, $CDCl_3$): $\delta = 0.88$ (t, 6H, $^3J_{H,H} = 7.08$ Hz, CH_3), 2.71 – 2.90 (m, 2H, N- CH_2), 2.82 – 3.10 (m, 2H, N- CH_2), 7.28 – 7.44 (m, 15H, CPh_3), 7.25 (d, 1H, $^1J_{P,H} = 352.2$ Hz, P- H).

$^{13}\text{C}\{^1\text{H}\}$ NMR (75.5 MHz, $CDCl_3$): $\delta = 12.9$ (d, $^3J_{P,C} = 1.9$ Hz, CH_3), 47.0 (d, $^2J_{P,C} = 4.2$ Hz, N- CH_2), 64.0 (d, $^1J_{P,C} = 1.9$ Hz, P- C), 127.2 (d, $^5J_{P,C} = 1.9$ Hz, *para*- CH_{Ar}), 127.1 (s, CH_{Ar}), 130.8 (d, $^3J_{P,C} = 6.8$ Hz,

CH_{Ar}), 142.2 (d, $^2J_{\text{P,C}} = 1.9$ Hz, *ipso-C*), 197.1 (d, $^2J_{\text{P,C}} = 6.6$ Hz, $^1J_{\text{W,C}} = 126.7$ Hz, *cis-CO*), 198.9 (d, $^2J_{\text{P,C}} = 28.1$ Hz, *trans-CO*).

^{31}P NMR (121.5 MHz, CDCl_3): $\delta = 74.4$ (dquin_{sat}, $^1J_{\text{P,W}} = 252.1$ Hz, $^1J_{\text{P,H}} = 352.2$ Hz, $^3J_{\text{P,H}} = 9.5$ Hz).

MS (EI, 70 eV, ^{184}W , selected data): m/z (%) = 671.0 (0.01) $[\text{M}]^{++}$, 614.0 (0.02) $[\text{M} - \text{C}_4\text{H}_9]^+$, 428.0 (0.04) $[\text{M} - \text{CPh}_3]^+$, 400.0 (0.02) $[\text{M} - \text{CPh}_3 - \text{CO}]^+$, 243.3 (100) $[\text{CPh}_3]^+$, 165.1 (60) $[\text{CPh}_3 - \text{C}_6\text{H}_6]^+$.

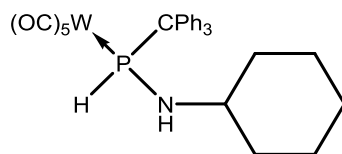
IR (ATR Diamond, $\tilde{\nu}$ [cm^{-1}], selected data): 2069 (s, $\nu(\text{CO})$), 1979 (m, $\nu(\text{CO})$), 1907 (vs, $\nu(\text{CO})$).

Elemental analysis:

calc.:	C	50.10	H	3.90	N	2.09
found:	C	49.78	H	3.92	N	2.00

Single crystal measurement: GSTR317, twin5-merg

11.2.2.2 Pentacarbonyl[cyclohexylamino(triphenylmethyl)phosphane- κP]tungsten(0) [9.3a]



Purification: All volatiles were removed in *vacuo* (ca. 0.02 mbar) and the crude product was extracted from the formed salt with 3 times 15 mL of diethyl ether, followed by evaporation of the diethyl ether in *vacuo* (ca. 0.02 mbar) and low temperature column chromatography (Al_2O_3 , -20 °C, eluent: petroleum ether, petroleum ether/dichloromethane 10:1). The product was obtained as an oil from the second fraction after evaporation of all volatiles in *vacuo* (ca. 0.02 mbar). The product was subsequently recrystallized by slow evaporation of a saturated diethyl ether solution at 4 °C to yield a yellow crystalline material.

Alternatively a separation by filtration with diethyl ether over aluminium oxide ($\varnothing = 2$ cm, $h = 3$ cm) and subsequent washing with *n*-pentane was performed, giving similar yield.

Molecular formula:	$\text{C}_{30}\text{H}_{28}\text{NO}_5\text{PW}$
Molecular weight:	697.361 g/mol
Melting point:	142 °C
Yield:	134.5 mg (0.190 mmol, 77 %)

^1H NMR (300.1 MHz, CDCl_3): $\delta = 1.20 - 1.40$ (m, 1H, N-*H*), $0.80 - 1.89$ (m, 10H, Cy-*H*), $2.51 - 2.70$ (m, 1H, CH), $7.2 - 7.5$ (m, 15H, Ph), 7.43 (dd, 1H, $^1J_{\text{P,H}} = 333.0$ Hz, $^3J_{\text{H,H}} = 4.0$ Hz, P-*H*).

$^{13}\text{C}\{^1\text{H}\}$ NMR (75.5 MHz, CDCl_3): δ = 25.1 (s_{br} , 2 CH_2), 25.3 (s , CH_2), 35.3 (d , $J_{\text{P,C}} = 4.5$ Hz, CH_2), 35.6 (d , $J_{\text{P,C}} = 3.6$ Hz, CH_2), 56.0 (d , $^2J_{\text{P,C}} = 4.9$ Hz, CH), 62.1 (d , $^1J_{\text{P,C}} = 20.0$ Hz, P-C), 127.2 (d , $J_{\text{P,C}} = 1.9$ Hz, CH_{Ar}), 128.3 (s , CH_{Ar}), 130.5 (d , $J_{\text{P,C}} = 6.8$ Hz, CH_{Ar}), 142.8 (s , *ipso-C*), 196.6 (d_{sat} , $^2J_{\text{P,C}} = 7.1$ Hz, $^1J_{\text{C,W}} = 126.7$ Hz, *cis-CO*), 198.7 (d , $^2J_{\text{P,C}} = 26.8$ Hz, *trans-CO*).

^{31}P NMR (121.5 MHz, CDCl_3): δ = 48.6 (dddm_{sat} , $^1J_{\text{P,H}} = 333.0$ Hz, $^2J_{\text{P,H}} = 7.2$ Hz, $^3J_{\text{P,H}} = 7.1$ Hz, $^1J_{\text{W,P}} = 260.4$ Hz).

MS (EI, 70 eV, ^{184}W , selected data): m/z (%) = 697.2 (1) $[\text{M}]^{+}$, 613.2 (1) $[\text{M} - 3 \text{CO}]^{+}$, 557.2 (20) $[\text{M} - 5 \text{CO}]^{+}$, 555.1 (2) $[\text{M} - 5 \text{CO} - \text{H}_2]^{+}$, 454.0 (50) $[\text{M} - \text{CPh}_3]^{+}$, 426.0 (20) $[\text{M} - \text{CPh}_3 - \text{CO}]^{+}$, 243.0 (100) $[\text{CPh}_3]^{+}$, 165.0 (50) $[\text{CPh}_3 - \text{C}_6\text{H}_6]^{+}$.

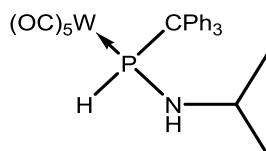
IR (ATR Diamond, $\tilde{\nu}$ [cm^{-1}], selected data): 3395 (w , $\nu(\text{NH})$), 2311 (w , $\nu(\text{PH})$), 2072 (s , $\nu(\text{CO})$), 1983 (s , $\nu(\text{CO})$), 1886 (vs , $\nu(\text{CO})$).

Elemental analysis:

calc.:	C	51.67	H	4.05	N	2.01
found:	C	51.50	H	4.35	N	2.06

Single crystal measurement: GSTR450, AKY-Cy // GXraymo_4395f

11.2.2.3 Pentacarbonyl[1-methylethylamino(triphenylmethyl)phosphane- κP]tungsten(0) [9.3b]



Purification: All volatiles were removed in *vacuo* (ca. 0.02 mbar) and the crude product was separated by extraction from the formed salt with 3 times 15 mL diethyl ether, followed by evaporation of the diethyl ether in *vacuo* (ca. 0.02 mbar) and low temperature column chromatography (Al_2O_3 , -20 °C, eluent: petroleum ether, petroleum ether/dichloromethane 10:1). The product was obtained as an oil from the second fraction after evaporation of all volatiles in *vacuo* (ca. 0.02 mbar). It was subsequently recrystallized by slow evaporation of a saturated diethyl ether solution at 4 °C to yield a yellow crystalline material.

Molecular formula: $\text{C}_{27}\text{H}_{24}\text{NO}_5\text{PW}$

Molecular weight: 657.297 g/mol

Melting point: 111 °C

Yield: 116.8 mg (0.180 mmol, 71 %)

^1H NMR (300.1 MHz, CDCl_3): δ = 0.89 (d, 3H, $^3J_{\text{H,H}} = 6.3$ Hz, CH_3), 0.99 (d, 3H, $^3J_{\text{H,H}} = 6.3$ Hz, CH_3), 1.40 (m, 1H, N-H), 3.04 (dsept, 1H, $^3J_{\text{P,H}} = 9.9$ Hz, $^3J_{\text{H,H}} = 6.3$ Hz, CH), 7.37 (m, 15H, CPh_3), 7.41 (dd, 1H, $^1J_{\text{P,H}} = 332.6$ Hz, $^3J_{\text{H,H}} = 4.3$ Hz, P-H).

$^{13}\text{C}\{^1\text{H}\}$ NMR (75.5 MHz, CDCl_3): δ = 24.8 (d, $^3J_{\text{P,C}} = 4.9$ Hz, CH_3), 24.9 (d, $^3J_{\text{P,C}} = 4.0$ Hz, CH_3), 49.2 (d, $^2J_{\text{P,C}} = 5.0$ Hz, CH), 62.2 (d, $^1J_{\text{P,C}} = 19.7$ Hz, P-C), 127.2 (d, $J_{\text{P,C}} = 2.0$ Hz, CH_{Ar}), 128.3 (d, $J_{\text{P,C}} = 0.6$ Hz, CH_{Ar}), 130.5 (d, $J_{\text{P,C}} = 6.8$ Hz, CH_{Ar}), 142.0 (s, *ipso*-C), 196.5 (d_{sat}, $^2J_{\text{P,C}} = 6.9$ Hz, $^1J_{\text{C,W}} = 126.7$, *cis*-CO), 198.6 (d, $^2J_{\text{P,C}} = 26.8$ Hz, *trans*-CO).

^{31}P NMR (121.5 MHz, CDCl_3): δ = 49.4 (d_{sat}, $^1J_{\text{P,H}} = 332.6$ Hz, $^1J_{\text{W,P}} = 260.5$ Hz).

MS (EI, 70 eV, ^{184}W , selected data): m/z (%) = 657.1 (1) $[\text{M}]^+$, 573.1 (1) $[\text{M} - 3 \text{CO}]^+$, 413.1 (40) $[\text{M} - \text{CPh}_3]^+$, 243.0 (100) $[\text{CPh}_3]^+$, 165.0 (40) $[\text{CPh}_3 - \text{C}_6\text{H}_6]^+$.

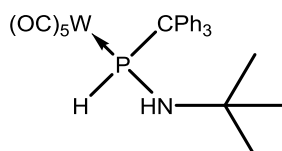
IR (ATR Diamond; $\tilde{\nu}[\text{cm}^{-1}]$, selected data): 3391 (w, $\nu(\text{NH})$), 2327 (w, $\nu(\text{PH})$), 2068 (s, $\nu(\text{CO})$), 1980 (s, $\nu(\text{CO})$), 1907 (vs, $\nu(\text{CO})$).

Elemental analysis:

calc.:	C	49.34	H	3.68	N	2.13
found:	C	50.85	H	4.71	N	1.92

Single crystal measurement: GSTR449, AKY-iPr // GXraymo_4396f

11.2.2.4 Pentacarbonyl[1,1-dimethylethylamino(triphenylmethyl)phosphane- κP]tungsten(0) [9.3c]



Purification: All volatiles were removed in *vacuo* (ca. 0.008 mbar). The crude mixture was dissolved in diethyl ether, filtered over Al_2O_3 ($\varnothing = 2$ cm, $h = 3$ cm) and the solvent was removed in *vacuo* (ca. 0.008 mbar). The product was obtained by recrystallization from *n*-pentane at -20 °C (overnight).

Molecular formula: $\text{C}_{28}\text{H}_{25}\text{NO}_5\text{PW}$

Molecular weight: 670.316 g/mol

Melting point: 135 °C

Yield: 562 mg (0.84 mmol, 84 %)

^1H NMR (300.1 MHz, CDCl_3): δ = 0.90 (d, 9H, $^4J_{\text{H,H}} = 0.68$ Hz, $\text{N-C}_4\text{H}_9$), 1.10 (dd, 1H, $^2J_{\text{P,H}} = 15.9$ Hz, $^3J_{\text{H,H}} = 10.2$ Hz, N-H), 7.11 – 7.46 (m, 15H, CPh_3), 7.54 (dd, 1H, $^1J_{\text{P,H}} = 342.3$ Hz, $^3J_{\text{H,H}} = 10.2$ Hz, P-H).

$^{13}\text{C}\{^1\text{H}\}$ NMR (75.5 MHz, CDCl_3): δ = 31.2 (d, $^3J_{\text{P,C}} = 3.1$ Hz, $^t\text{Bu-CH}_3$), 54.0 (d, $^2J_{\text{P,C}} = 11.5$ Hz, $^t\text{Bu-C}$), 63.5 (d, $^1J_{\text{P,C}} = 7.1$ Hz, P-C), 127.0 (d, $J_{\text{P,C}} = 2.0$ Hz, CH_{Ar}), 128.2 (s, CH_{Ar}), 130.9 (d, $J_{\text{P,C}} = 7.0$ Hz, CH_{Ar}), 142.6 (d, $^2J_{\text{P,C}} = 1.6$ Hz, *ipso-C*), 197.0 (d_{sat}, $^2J_{\text{P,C}} = 7.1$ Hz, $^1J_{\text{C,W}} = 126.7$ Hz, *cis-CO*), 199.1 (d, $^2J_{\text{P,C}} = 27.8$ Hz, *trans-CO*).

^{31}P NMR (121.5 MHz, CDCl_3): δ = 37.3 (dd_{sat}, $^1J_{\text{P,W}} = 263.7$ Hz, $^1J_{\text{P,H}} = 342.3$ Hz, $^2J_{\text{P,H}} = 15.9$ Hz).

MS (EI, 70 eV, ^{184}W , selected data): m/z (%) = 671.0 (0.02) $[\text{M}]^{++}$, 614.0 (0.01) $[\text{M} - \text{C}_4\text{H}_9]^+$, 427.9 (0.03) $[\text{M} - \text{CPh}_3]^+$, 400.0 (0.02) $[\text{M} - \text{CPh}_3 - \text{CO}]^+$, 243.3 (100) $[\text{CPh}_3]^+$, 165.1 (40) $[\text{CPh}_3 - \text{C}_6\text{H}_6]^+$.

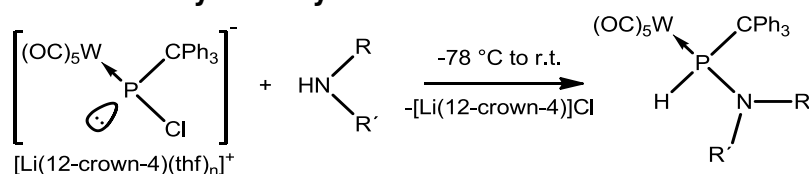
IR (ATR Diamond; $\tilde{\nu}[\text{cm}^{-1}]$, selected data): 3396 (m, $\nu(\text{NH})$), 2369 (w, $\nu(\text{PH})$), 2069 (s, $\nu(\text{CO})$), 1939 (m, $\nu(\text{CO})$), 1898 (vs, $\nu(\text{CO})$).

Elemental analysis:

calc.:	C	50.17	H	3.76	N	2.09
found:	C	50.75	H	4.28	N	1.97

Single crystal measurement: GSTR332, 3182f

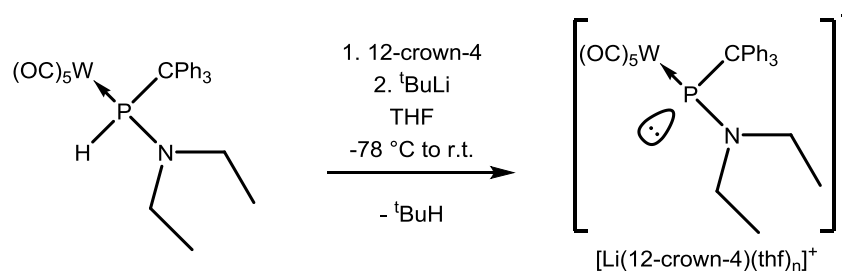
11.2.3 Attempted reactions of Li/Cl phosphinidenoid complex **2.3** with diisopropylamine and dicyclohexylamine



Synthesis and analysis: A solution of Li/Cl phosphinidenoid complex **2.3** was prepared as described in chapter 11.2.1, starting from 33.5 mg (0.05 mmol) of $[(\text{OC})_5\text{W}\{\text{PCl}_2(\text{CPh}_3)\}]$ (**1.3**). The solution was subsequently cooled back to -78 °C and either 0.015 mL (0.1 mmol, 2 eq.) of diisopropylamine (**5b**) or 0.01 mL (0.05 mmol, 1 eq.) of dicyclohexylamine (**5c**) was added. The solution was allowed slowly warming up to 0 °C before removing the cooling bath.

^{31}P NMR measurements of the reaction mixtures were performed. The spectra showed the presence of the Li/Cl phosphinidenoid complex **2.3** as main component of the mixtures and some unspecific decomposition products.

11.2.4 Synthesis of lithium(1,4,7,10-tetraoxacyclododecane) pentacarbonyl[diethylamino(triphenylmethyl)phosphanido- κP]tungsten(0) [7.3]

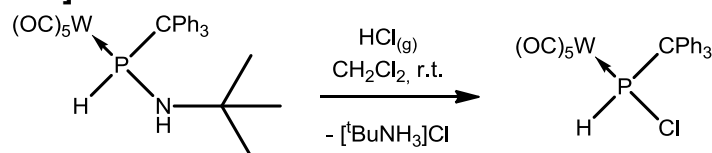


Synthesis and analysis: In a 10 mL Schlenk tube, 38.3 mg (0.057 mmol) of aminophosphane complex **6.3a** and 18 μL (0.11 mmol, 1.9 eq.) of 12-crown-4 were dissolved in 1.2 mL of THF. The solution was cooled to $-78\text{ }^\circ C$ and subsequently 0.035 mL (0.059 mmol, 1.04 eq.) of *tert*-butyllithium (1.7 M solution in *n*-pentane) was added dropwise. The solution was allowed slow warming up to ambient temperature and subsequently analysed by ^{31}P NMR.

^{31}P NMR (121.5 MHz, THF): $\delta = 160.3$ (s_{sat} , $^1J_{W,P} = 102.6$ Hz).

A ^{31}P NMR measurement of the solution after one day revealed reprotonation of the complex as well as small amounts of decomposition to unidentified products.

11.2.5 Synthesis of pentacarbonyl[chloro(triphenylmethyl)phosphane- κP]tungsten(0) [10.3]



Synthesis: In a 20 mL Schlenk tube, 200 mg (0.3 mmol) of aminophosphane complex **9.3c** were dissolved in 10 mL of CH_2Cl_2 . $HCl_{(g)}$ (prepared by dropping concentrated hydrochloric acid on anhydrous $CaCl_2$) was bubbled through the stirred solution for 30 minutes at ambient temperature. Stirring was continued for 2 h and precipitation of a white solid was observed over time.

Purification: All volatiles were removed in *vacuo* (ca. 0.02 mbar) and the product was extracted from the formed ammonium salt with 25 mL of diethyl ether. The crude product, obtained after evaporation of all volatiles in *vacuo* (ca. 0.02 mbar), was washed two times with diethyl ether at $-90\text{ }^\circ C$ (one time with 3 mL and one time with 2 mL) to yield the product as white solid, after drying in *vacuo* (ca. 0.02 mbar).

Molecular formula:	C ₂₄ H ₁₆ ClO ₅ PW
Molecular weight:	634.648 g/mol
Melting point:	163 °C (dec.)
Yield:	100 mg (0.158 mmol, 53 %)

¹H NMR (500.1 MHz, CDCl₃): δ = 7.28 – 7.46 (m, 15H, CPh₃), 7.94 (d, 1H, ¹J_{P,H} = 343.6 Hz, PH).

¹³C{¹H} NMR (125.8 MHz, CDCl₃): δ = 64.3 (d, ¹J_{P,C} = 6.9 Hz, P-C), 128.2 (s, *para*-CH_{Ar}), 128.8 (s, CH_{Ar}), 130.4 (d, ³J_{P,C} = 6.1 Hz, CH_{Ar}), 141.5 (s_{br}, *ipso*-C), 195.6 (d_{sat}, ²J_{P,C} = 6.5 Hz, ¹J_{P,W} = 127.1 Hz, *cis*-CO), 198.3 (d_{sat}, ²J_{P,C} = 35.7 Hz, ¹J_{P,W} = 144.5 Hz, *trans*-CO).

³¹P NMR (202.5 MHz, CDCl₃): δ = 71.2 (d_{sat}, ¹J_{P,W} = 263.7 Hz, ¹J_{P,H} = 342.3 Hz).

LIFDI-MS (¹⁸⁴W, selected data): m/z (%) = 634.1 (100) [M]⁺⁺, 243.2 (80) [CPh₃]⁺.

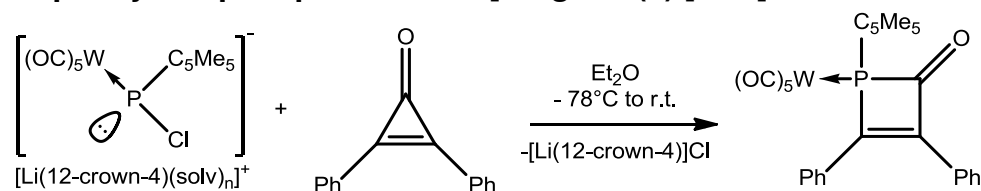
IR (ATR Diamond; $\tilde{\nu}$ [cm⁻¹], selected data): 2351 (w, ν (PH)), 2078 (s, ν (CO)), 1998 (m, ν (CO)), 1925 (vs, ν (CO)).

Elemental analysis:

calc.:	C	45.42	H	2.54
found:	C	45.32	H	2.57

Single crystal measurement: GSTR534, AKY-602 // GXray4926

11.2.6 Synthesis of pentacarbonyl[1-(1,2,3,4,5-pentamethylcyclopenta-2,4-dien-1-yl)-3,4-diphenyl-1*H*-phosphet-2-on- κ P]tungsten(0) [14.2]



Synthesis: A solution of Li/Cl phosphinidenoid complex **2.2** was prepared like described in chapter 11.2.1, starting from 168.3 mg (0.3 mmol) of [(OC)₅W{P(Cl₂(C₅Me₅))}] (**1.2**), but using only 0.8 equivalents of 12-crown-4 (40 μL, 0.25 mmol), and 61.8 mg (0.3 mmol, 1.0 eq.) of diphenylcyclopropenone (**12**) were added subsequently as solid. After the addition a rapid formation of a white precipitate and a change of the colour to yellow-orange was observed. The solution was allowed warming up to 0 °C, the cooling bath was removed at this point and stirring was continued for 1 h.

Purification: All volatiles were removed in *vacuo* (ca. 0.02 mbar). The product was purified by extraction from the formed salt with *n*-pentane (5 times 10 mL) and subsequent recrystallization by slow evaporation of a saturated *n*-pentane solution at ambient temperature. The product was obtained as orange, crystalline solid after drying in *vacuo* (ca. 0.02 mbar).

Molecular formula:	C ₃₀ H ₂₅ O ₆ PW
Molecular weight:	696.330 g/mol
Melting point:	126 °C
Yield:	103 mg (0.148 mmol, 49 %)

¹H NMR (300.1 MHz, CDCl₃): δ = 1.34 (s, 3H, C₅Me₅), 1.44 (d, 3H, J_{P,H} = 13.6 Hz, C₅Me₅), 1.75 (s, 3H, C₅Me₅), 1.76 (s, 3H, C₅Me₅), 2.02 (s, 3H, C₅Me₅), 7.30 – 7.70 (m, 10H, Ph).

¹³C{¹H} NMR (75.5 MHz, CDCl₃): δ = 11.5 (d, J_{P,C} = 1.5 Hz, C₅Me₃), 11.5 (d, J_{P,C} = 1.5 Hz, C₅Me₃), 11.8 (s, C₅Me₃), 12.1 (d, J_{P,C} = 1.6 Hz, C₅Me₃), 17.5 (d, J_{P,C} = 2.9 Hz, C₅Me₃), 62.4 (d, ¹J_{P,C} = 9.9 Hz, C₅Me₅), 128.4 (s, CH_{Ar}), 128.5 (s, CH_{Ar}), 128.9 (d, J_{P,C} = 14.9, C=C), 128.9 (s, 4 times CH_{Ar}), 129.2 (s, 2 times CH_{Ar}), 130.2 (s, CH_{Ar}), 131.0 (d, J_{P,C} = 0.8 Hz, CH_{Ar}), 133.9 (d, J_{P,C} = 9.8 Hz, C=C), 136.0 (d, J_{P,C} = 3.6 Hz, *ipso*-C), 136.4 (d, J_{P,C} = 0.6 Hz, *ipso*-C), 141.4 (d, J_{P,C} = 5.8 Hz, C=C), 142.7 (d, J_{P,C} = 7.1 Hz, C=C), 151.6 (d, ¹J_{P,C} = 46.2 Hz, P-C=C), 172.0 (d, ²J_{P,C} = 23.6 Hz, P-C=C), 193.1 (d, ¹J_{P,C} = 26.5 Hz, C=O), 195.6 (dq_{sat}, ¹J_{W,C} = 125.1 Hz, ²J_{P,C} = 6.1 Hz, *cis*-CO), 198.2 (d_{sat}, ¹J_{W,P} = 144.7 Hz, ²J_{P,C} = 26.0 Hz, *trans*-CO).

³¹P{¹H} NMR (121.5 MHz, CDCl₃): δ = 111.0 (s_{sat}, ¹J_{W,P} = 233.5 Hz).

MS (EI, 70 eV, ¹⁸⁴W, selected data): m/z (%) = 696.1 (1) [M]⁺⁺, 668.1 (50) [M - CO]⁺, 640.1 (5) [M - 2 CO]⁺, 612.1 (10) [M - 3 CO]⁺, 584.1 (10) [M - 4 CO]⁺, 556.1 (1) [M - 5 CO]⁺, 561.0 (30) [M - C₅Me₅]⁺, 533.0 (10) [M - C₅Me₅ - CO]⁺, 505.0 (45) [M - C₅Me₅ - 2 CO]⁺, 477.0 (50) [M - C₅Me₅ - 3 CO]⁺, 449.0 (100) [M - C₅Me₅ - 4 CO]⁺, 421.0 (15) [M - C₅Me₅ - 5 CO]⁺, 393.0 (50) [M - C₅Me₅ - 6 CO]⁺, 209.0 (25) [M - C₅Me₅ - CO - W(CO)₅]⁺, 178.0 (60) [PhCCPh]⁺, 135.1 (60) [C₅Me₅]⁺, 119.1 (40) [C₅Me₅ - CH₄]⁺, 105.0 (15) [C₅Me₅ - C₂H₆]⁺.

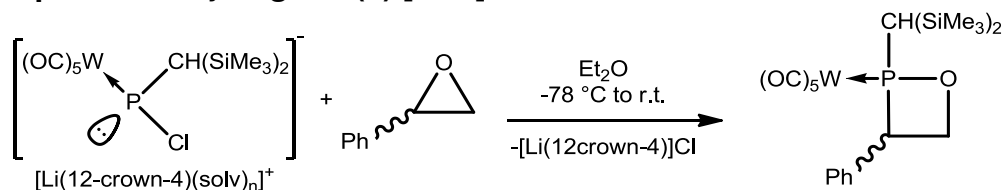
IR (ATR Diamond; $\tilde{\nu}$ [cm⁻¹], selected data): 2071 (m, ν (CO)), 1991 (w, ν (CO)), 1913 (vs, ν (CO)), 1729 (m, ν (CO)).

Elemental analysis:

calc.:	C	51.75	H	3.62
found:	C	52.00	H	3.67

Single crystal measurement: GSTR466, AKY-536 // GXraycu_4526f

11.2.7 Synthesis of pentacarbonyl{2-[bis(trimethylsilyl)methyl]-3-phenyl-1,2-oxaphosphetane- κ P}tungsten(0) [16.1]



Synthesis: A solution of Li/Cl phosphinidenoid complex **2.1** was prepared like described from 292.5 mg (0.5 mmol) of $[(OC)_5W\{P(CH(SiMe_3)_2)Cl_2\}]$ (**1.1**) and 0.06 mL (0.52 mmol, 1.04 eq.) of styrene oxide (**15**) was added subsequently. The solution was allowed warming up to ambient temperature and during the warming up period formation of a white precipitate was observed.

Purification: All volatiles were removed in *vacuo* (ca. 0.02 mbar). The product was separated from the formed salt by extraction with 3 times 15 mL of *n*-pentane, followed by low temperature column chromatography (SiO_2 , $-20\text{ }^\circ\text{C}$, eluents: petroleum ether, petroleum ether/diethyl ether 10:0,1) and obtained as white solid from the second fraction after removing of all volatiles in *vacuo* (ca. 0.02 mbar). The product was recrystallized by slow evaporation of a saturated *n*-pentane solution at $4\text{ }^\circ\text{C}$ to yield colorless crystals. It was obtained as mixture of different isomers and all data are given for the mixture.

Molecular formula:	$C_{20}H_{27}O_6PSi_2W$
Molecular weight:	634.410 g/mol
Melting point:	$181\text{ }^\circ\text{C}$ (dec.)
Yield:	128.0 mg (0.20 mmol, 40 %)

Isomeric ratio: 40 : 4 : 53 : 3

Isomer 1:

$^1\text{H NMR}$ (300.1 MHz, $CDCl_3$): $\delta = 0.29$ (s, 9H, $Si(CH_3)_3$), 0.40 (s, 9H, $Si(CH_3)_3$), 2.25 (d, 1H, $^2J_{P,H} = 6.4$ Hz, P-CH), 4.93 – 5.10 (m, 1H, CH), 5.02 – 5.15 (m, 2H, CH_2), 7.30 – 7.56 (m, 5H, Ph).

$^{13}\text{C}\{^1\text{H}\}$ NMR (75.5 MHz, $CDCl_3$): $\delta = 2.3$ (s, $Si(CH_3)_3$), 2.4 (s, $Si(CH_3)_3$), 41.0 (d, $^1J_{P,C} = 16.6$ Hz, CH), 52.1 (d, $^1J_{P,C} = 21.3$ Hz, CH), 74.9 (d, $^2J_{P,C} = 15.9$ Hz, O- CH_2), 128.1 (d, $^5J_{P,C} = 3.7$ Hz, *para*- CH_{Ar}), 128.9 (d, $J_{P,C} = 3.0$ Hz, CH_{Ar}), 129.1 (d, $J_{P,C} = 5.4$ Hz, CH_{Ar}), 136.0 (s_{br}, *ipso*-C), 196.6 (d_{sat}, $^1J_{W,C} = 126.1$ Hz, $^2J_{P,C} = 7.7$ Hz, *cis*-CO), 200.1 (d, $^2J_{P,C} = 25.0$, *trans*-CO).

$^{31}\text{P}\{^1\text{H}\}$ NMR (121.5 MHz, $CDCl_3$): $\delta = 220.2$ (s_{sat}, $^1J_{W,P} = 275.4$ Hz).

Isomer 2:

$^1\text{H NMR}$ (300.1 MHz, $CDCl_3$): $\delta = -0.20$ (s, 9H, $Si(CH_3)_3$), 1.70 (d, 1H, $^2J_{P,H} = 4.0$ Hz, P-CH), 3.89 (ddd, $^3J_{H,H} = 9.9$ Hz, $^2J_{H,H} = 8.7$ Hz, $^3J_{P,H} = 0.7$ Hz, CH_2), 4.54 (ddd, 1H, $^3J_{P,H} = 19.0$ Hz, $^2J_{H,H} = 8.7$ Hz, $^3J_{H,H} = 5.9$ Hz, CH_2), 5.39 (dd, 1H, $^3J_{H,H} = 9.9$ Hz, $^3J_{H,H} = 5.9$, CH), 7.30 – 7.55 (m, 5H, Ph).

$^{13}\text{C}\{^1\text{H}\}$ NMR (75.5 MHz, CDCl_3): $\delta = 2.1$ (d, $^3J_{\text{P,C}} = 4.2$ Hz, $\text{Si}(\text{CH}_3)_3$), 40.5 (s_{br} , CH), 58.7 (d, $^1J_{\text{P,C}} = 19.8$ Hz, CH), 70.4 (s_{br} , O- CH_2), 124.7 (s_{br} , *para*- CH_{Ar}), 126.1 (s, CH_{Ar}), 128.8 (s, CH_{Ar}), 135.4 (s_{br} , *ipso*-C), 196.6 (d, $^2J_{\text{P,C}} = 9.1$ Hz, *cis*-CO), 201.1 (d, $^2J_{\text{P,C}} = 26.8$, *trans*-CO).

$^{31}\text{P}\{^1\text{H}\}$ NMR (121.5 MHz, CDCl_3): $\delta = 210.7$ (s_{br}).

Isomer 3:

^1H NMR (300.1 MHz, CDCl_3): $\delta = 0.29$ (s, 9H, $\text{Si}(\text{CH}_3)_3$), 0.35 (s, 9H, $\text{Si}(\text{CH}_3)_3$), 2.59 (d, 1H, $^2J_{\text{P,H}} = 19.4$ Hz, P-CH), 4.86 (ddd, 1H, $^3J_{\text{H,H}} = 8.0$ Hz, $^2J_{\text{H,H}} = 7.0$, $^3J_{\text{P,H}} = 5.9$, CH_2), 5.05 (dd, 1H, $^3J_{\text{H,H}} = 8.4$ Hz, $^2J_{\text{H,H}} = 7.0$ Hz, CH_2), 5.26 (ddd, 1H, $^2J_{\text{P,H}} = 12.7$ Hz, $^3J_{\text{H,H}} = 8.4$ Hz, $^3J_{\text{H,H}} = 8.0$ Hz, CH), 7.30 – 7.55 (m, 5H, Ph).

$^{13}\text{C}\{^1\text{H}\}$ NMR (75.5 MHz, CDCl_3): $\delta = 2.5$ (d, $^3J_{\text{P,C}} = 2.5$ Hz, $\text{Si}(\text{CH}_3)_3$), 2.8 (d, $^3J_{\text{P,C}} = 2.6$ Hz, $\text{Si}(\text{CH}_3)_3$), 28.5 (d, $^1J_{\text{P,C}} = 34.0$ Hz, CH), 58.6 (d, $^1J_{\text{P,C}} = 22.5$ Hz, CH), 74.0 (d, $^2J_{\text{P,C}} = 16.0$ Hz, O- CH_2), 127.8 (d, $^5J_{\text{P,C}} = 3.0$ Hz, *para*- CH_{Ar}), 128.9 (d, $J_{\text{P,C}} = 4.1$ Hz, CH_{Ar}), 129.0 (d, $J_{\text{P,C}} = 3.0$ Hz, CH_{Ar}), 135.9 (d, $^2J_{\text{P,C}} = 10.2$ Hz, *ipso*-C), 197.2 (d_{sat} , $^1J_{\text{W,C}} = 126.0$ Hz, $^2J_{\text{P,C}} = 7.8$ Hz, *cis*-CO), 199.1 (d, $^2J_{\text{P,C}} = 26.8$, *trans*-CO).

$^{31}\text{P}\{^1\text{H}\}$ NMR (121.5 MHz, CDCl_3): $\delta = 195.1$ (s_{sat} , $^1J_{\text{W,P}} = 273.1$ Hz).

Isomer 4:

^1H NMR (300.1 MHz, CDCl_3): $\delta = 0.09$ (s, 9H, $\text{Si}(\text{CH}_3)_3$), 0.40 (s, 9H, $\text{Si}(\text{CH}_3)_3$), 2.29 (d, 1H, $^2J_{\text{P,H}} = 19.5$ Hz, P-CH), 3.42 – 3.53 (m, 1H, CH_2), 3.70 – 4.00 (m, 1H, CH_2), 6.00 – 6.20 (m, 1H, CH), 7.30 – 7.55 (m, 5H, Ph).

$^{13}\text{C}\{^1\text{H}\}$ NMR (75.5 MHz, CDCl_3): Due to the isomers low percentage of the mixture only very few resonance signals could be observed in the $^{13}\text{C}\{^1\text{H}\}$ NMR: $\delta = 2.4$ (d, $^3J_{\text{P,C}} = 4.3$ Hz, $\text{Si}(\text{CH}_3)_3$), 128.1 (s, *para*- CH_{Ar}), 128.5 (s, CH_{Ar}), 128.8 (s, CH_{Ar}), 196.9 (d, $^2J_{\text{P,C}} = 7.7$ Hz, *cis*-CO).

$^{31}\text{P}\{^1\text{H}\}$ NMR (121.5 MHz, CDCl_3): $\delta = 179.7$ (s_{sat} , $^1J_{\text{W,P}} = 281.1$ Hz).

MS (EI, 70 eV, ^{184}W , selected data): m/z (%) = 650.1 (5) $[\text{M} + \text{O}]^+$, 634.1 (1) $[\text{M}]^{++}$, 619.1 (5) $[\text{M} - \text{O}]^+$, 530.0 (90) $[\text{M} - \text{styrene}]^+$, 501.9 (30) $[\text{M} - \text{styrene} - \text{CO}]^+$, 474.0 (30) $[\text{M} - \text{styrene} - 2 \text{CO}]^+$, 446.0 (50) $[\text{M} - \text{styrene} - 3 \text{CO}]^+$, 418.0 (60) $[\text{M} - \text{styrene} - 4 \text{CO}]^+$, 389.9 (80) $[\text{M} - \text{styrene} - 5 \text{CO}]^+$, 104.0 (30) $[\text{styrene}]^+$, 73.1 (100) $[\text{SiMe}_3]^+$.

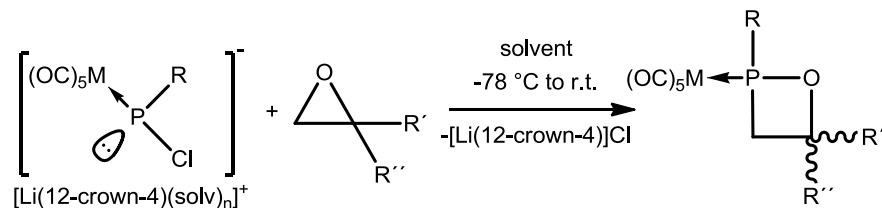
IR (ATR Diamond; $\tilde{\nu}[\text{cm}^{-1}]$, selected data): 2071 (s, $\nu(\text{CO})$), 1986 (m, $\nu(\text{CO})$), 1895 (vs, $\nu(\text{CO})$).

Elemental analysis:

calc.:	C	37.86	H	4.29
found:	C	38.10	H	4.41

Single crystal measurement: AKY-295 GSTR314, 2987f

11.2.8 Syntheses of 4-substituted 1,2-oxaphosphetane complexes:

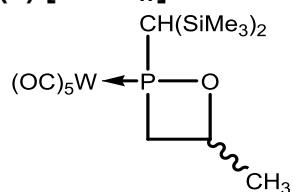


Solutions of the Li/Cl phosphinidenoid complexes **2.1-2.3** were prepared starting from complexes **1.1-1.3** as described in chapter 11.2.1. The corresponding epoxide was added via syringe and the solution was allowed slowly warming up. During the warming up period formation of a white precipitate was observed. The cooling bath was removed after reaching 0 °C and the solution was stirred for further 30 min.

Table 11.2: Used amounts of dichloro(organo)phosphane complexes and epoxides for the syntheses of 1,2-oxaphosphetane complexes.

	M	R	R'	R''	m (1) [mg]	n (1) [mmol]	epoxide	V (epoxide) [mL]	n (epoxide) [mmol]
21.1a_w	W	CH(SiMe ₃) ₂	H	CH ₃	292.5	0.5	20a	0.04	0.57
21.1a_{Mo}	Mo	CH(SiMe ₃) ₂	H	CH ₃	497.3	1.0	20a	0.15	2.14
21.1a_{Cr}	Cr	CH(SiMe ₃) ₂	H	CH ₃	453.3	1.0	20a	0.15	2.14
21.1b	W	CH(SiMe ₃) ₂	H	Et	292.5	0.5	20b	0.1	1.15
21.1c	W	CH(SiMe ₃) ₂	H	ⁱ Pr	292.5	0.5	20c	0.1	0.95
21.1d	W	CH(SiMe ₃) ₂	H	^t Bu	58.5	0.1	20d	0.012	0.1
21.1e	W	CH(SiMe ₃) ₂	H	CH ₂ Cl	292.5	0.5	20e	0.04	0.51
21.1f	W	CH(SiMe ₃) ₂	H	C ₂ H ₃ O	292.5	0.5	20f	0.045	0.5
21.1g	W	CH(SiMe ₃) ₂	H	CF ₃	585.0	1.0	20g	0.095	1.1
25.1a	W	CH(SiMe ₃) ₂	CH ₃	CH ₃	585.0	1.0	24a	0.15	1.68
25.1b	W	CH(SiMe ₃) ₂	CF ₃	CF ₃	585.0	1.0	24b	0.13	1.1
21.2a	W	C ₅ Me ₅	H	CH ₃	56.1	0.1	20a	0.01	0.14
21.2e	W	C ₅ Me ₅	H	CH ₂ Cl	56.1	0.1	20e	0.01	0.13
21.1g	W	C ₅ Me ₅	H	CF ₃	561.0	1.0	20g	0.095	1.1
25.2b	W	C ₅ Me ₅	CF ₃	CF ₃	561.0	1.0	24b	0.13	1.1
21.3a	W	CPh ₃	H	CH ₃	334.5	0.5	20a	0.1	1.4
21.3d	W	CPh ₃	H	^t Bu	66.9	0.1	20d	0.013	0.11
21.3g	W	CPh ₃	H	CF ₃	669.0	1.0	20g	0.13	1.1
25.3b	W	CPh ₃	CF ₃	CF ₃	501.8	0.75	24b	0.081	0.75

11.2.8.1 Pentacarbonyl{4-methyl-2-[bis(trimethylsilyl)methyl]-1,2-oxaphosphetane- κ P}tungsten(0) [21.1aw]



Purification: All volatiles were removed in *vacuo* (ca. 0.02 mbar). The product was separated from the formed salt by extraction with 3 times 15 mL *n*-pentane followed by low temperature column chromatography (SiO₂, -20 °C, eluent: petroleum ether, petroleum ether/diethyl ether 10:0,1). The crude product was obtained as a solid from the second fraction after removal of all volatiles in *vacuo* (ca 0.02 mbar). It was recrystallized by slow evaporation of a saturated *n*-pentane solution at 4 °C to yield colourless crystals and the product was obtained as mixture of different isomers. All data are given for the mixture.

<u>Molecular formula:</u>	C ₁₅ H ₂₅ O ₆ PSi ₂ W
<u>Molecular weight:</u>	572.340 g/mol
<u>Melting point:</u>	97 - 99 °C
<u>Yield:</u>	165 mg (0.29 mmol, 58 %)

Isomeric ratio: 30 : 4 : 19 : 47

Isomer 1:

¹H NMR (300.1 MHz, CDCl₃): δ = 0.27 (s, 9H, Si(CH₃)₃), 0.31 (s, 9H, Si(CH₃)₃), 1.64 (d, 3H, ⁴J_{P,H} = 6.2 Hz, CH₃), 1.99 (d, 1H, ²J_{P,H} = 6.2 Hz, P-CH), 3.04 (dd, 1H, ²J_{P,H} = 13.9 Hz, J_{H,H} = 6.20 Hz, CH₂), 3.49 – 3.67 (m, 1H, CH₂), 5.19 – 5.40 (m, 1H, CH).

¹³C{¹H} NMR (75.5 MHz, CDCl₃): δ = 2.0 (d, ²J_{P,C} = 3.6 Hz, Si(CH₃)₃), 25.3 (d, ³J_{P,C} = 5.0 Hz, CH₃), 38.1 (d, ¹J_{P,C} = 12.9 Hz, P-CH), 40.5 (d, ¹J_{P,C} = 29.3 Hz, P-CH₂), 78.9 (d, ²J_{P,C} = 13.1 Hz, O-CH), 197.3 (d, ²J_{P,C} = 7.7 Hz, *cis*-CO), 199.1 (d, ²J_{P,C} = 23.1 Hz, *trans*-CO).

³¹P{¹H} NMR (121.5 MHz, CDCl₃): δ = 176.4 (s_{sat}, ¹J_{W,P} = 273.4 Hz).

Isomer 2:

No resonance signals except in the ³¹P NMR and the ¹H NMR signal of the CH(SiMe₃)₂ group could be observed due to the isomers low percentage of the mixture.

¹H NMR (300.1 MHz, CDCl₃): δ = 2.46 ppm (²J_{P,H} ~ 19 Hz).

³¹P{¹H} NMR (121.5 MHz, CDCl₃): δ = 169.2 (s_{br}).

Isomer 3:

$^1\text{H NMR (300.1 MHz, CDCl}_3\text{)}$: $\delta = 0.27$ (s, 9H, Si(CH₃)₃), 0.31 (s, 9H, Si(CH₃)₃), 1.51 (s, 3H, CH₃), 2.24 (d, 1H, $^2J_{\text{P,H}} = 19.5$ Hz, P-CH), 2.77-2.94 (m, 1H, CH₂), 3.45 – 3.59 (m, 1H, CH₂), 5.05 – 5.21 (m, 1H, CH).

$^{13}\text{C}\{^1\text{H}\} \text{NMR (75.5 MHz, CDCl}_3\text{)}$: $\delta = 1.9$ (d, $^2J_{\text{P,C}} = 3.8$ Hz, Si(CH₃)₃), 27.5 (s_{br}, CH₃), 37.6 (d, $^1J = 10.6$ Hz, P-CH), 48.7 (d, $^1J_{\text{P,C}} = 28.3$ Hz, P-CH₂), 76.8 (d, $^2J_{\text{P,C}} = 13.3$ Hz, O-CH), 198.0 (d, $^2J_{\text{P,C}} = 8.1$ Hz, *cis*-CO), the resonance signal for the *trans*-CO could not be observed due to its low intensity.

$^{31}\text{P}\{^1\text{H}\} \text{NMR (121.5 MHz, CDCl}_3\text{)}$: $\delta = 164.5$ (s_{sat}, $^1J_{\text{W,P}} = 267.8$ Hz).

Isomer 4:

$^1\text{H NMR (300.1 MHz, CDCl}_3\text{)}$: $\delta = 0.27$ (s, 9H, Si(CH₃)₃), 0.31 (s, 9H, Si(CH₃)₃), 1.50 (d, 3H, $^4J_{\text{P,H}} = 6.3$ Hz, CH₃), 1.93 (d, 1H, $^2J_{\text{P,H}} = 6.0$ Hz, P-CH), 3.20 (dd, 1H, $^2J_{\text{P,H}} = 12.6$ Hz, $J_{\text{H,H}} = 6.1$ Hz, CH₂), 3.25 – 3.42 (m, 1H, CH₂), 5.05 – 5.21 (m, 1H, CH).

$^{13}\text{C}\{^1\text{H}\} \text{NMR (75.5 MHz, CDCl}_3\text{)}$: $\delta = 2.4$ (d, $^2J_{\text{P,C}} = 1.6$ Hz, Si(CH₃)₃), 2.7 (d, $^2J_{\text{P,C}} = 2.0$ Hz, Si(CH₃)₃), 25.3 (d, $^3J_{\text{P,C}} = 5.8$ Hz, CH₃), 38.4 (d, $^1J_{\text{P,C}} = 12.4$ Hz, P-CH), 44.9 (d, $^1J_{\text{P,C}} = 25.1$ Hz, P-CH₂), 75.8 (d, $^2J_{\text{P,C}} = 14.0$ Hz, O-CH), 197.1 (d_{sat}, $^1J_{\text{W,C}} = 124.2$ Hz, $^2J_{\text{P,C}} = 7.7$ Hz, *cis*-CO), 200.1 (d, $^2J_{\text{P,C}} = 25.0$, *trans*-CO).

$^{31}\text{P}\{^1\text{H}\} \text{NMR (121.5 MHz, CDCl}_3\text{)}$: $\delta = 164.4$ (s_{sat}, $^1J_{\text{W,P}} = 268.7$ Hz).

MS (EI, 70 eV, ^{184}W , selected data): *m/z* (%) = 572.0 (40) [M]⁺⁺, 544.0 (1) [M-CO]⁺, 530.0 (5) [M - C₃H₆]⁺, 516.0 (2) [M - 2 CO]⁺, 502.0 (5) [M - C₃H₆ - CO]⁺, 488.1 (10) [M - 3 CO]⁺, 474.0 (20) [M - C₃H₆ - 2 CO]⁺, 460.1 (2) [M - 4 CO]⁺, 446.0 (30) [M - C₃H₆ - 3 CO]⁺, 432.1 (10) [M - 5 CO]⁺, 418.0 (50) [M - C₃H₆ - 4 CO]⁺, 390.0 (5) [M - C₃H₆ - 5 CO]⁺, 73.1 (50) [SiMe₃]⁺.

IR (ATR Diamond; $\tilde{\nu}$ [cm⁻¹], selected data): 2069 (s, $\nu(\text{CO})$), 1987 (w, $\nu(\text{CO})$), 1899 (vs, $\nu(\text{CO})$).

Elemental analysis:

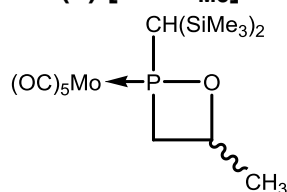
calc.:	C	31.48	H	4.40
found:	C	31.46	H	4.56

Single crystal measurement: AKY-301 GSTR321, 3087

11.2.8.2 Synthesis of pentacarbonyl{4-methyl-2-[bis(trimethylsilyl)methyl]-1,2-oxaphosphetane- κ P}tungsten(0) [21.1a_w] using R(+)-propylene oxide

The synthesis was performed analogue to the one using the racemic mixture of the epoxide starting from 58.5 mg (0.1 mmol) of complex **1.1**. The reaction mixture was analysed by $^{31}\text{P}\{^1\text{H}\}$ NMR after reaching ambient temperature. The ^{31}P NMR spectrum shows no significant difference to the one obtained for a reaction mixture using the racemic mixture of propylene oxide.

11.2.8.3 Pentacarbonyl{4-methyl-2-[bis(trimethylsilyl)methyl]-1,2-oxaphosphetane- κ P}molybdenum(0) [21.1a_{Mo}]



Purification: All volatiles were removed in *vacuo* (ca. 0.02 mbar) and the product was separated from the formed salt by extraction with 3 times 8 mL diethyl ether. The crude product was obtained as an oil after removal of all volatiles in *vacuo* (ca. 0.02 mbar). The product was then precipitated from *n*-pentane at -100 °C and subsequently recrystallized by slow evaporation of a saturated *n*-pentane solution at 4 °C to yield colourless crystals. The product was obtained as mixture of different isomers and all data are given for the mixture.

Molecular formula:	C ₁₅ H ₂₅ O ₆ PSi ₂ Mo
Molecular weight:	484.86 g/mol
Melting point:	80-81 °C
Yield:	132 mg (0.27 mmol, 27 %)

Isomeric ratio: 30 : 6 : 46 : 18

Isomer 1:

^1H NMR (300.1 MHz, CDCl₃): δ = 0.26 (s, 9H, Si(CH₃)₃), 0.30 (s, 9H, Si(CH₃)₃), 1.63 (d, 3H, $^4J_{\text{P,H}} = 5.9$ Hz, CH₃), 1.78 (d, 1H, $^2J_{\text{P,H}} = 3.80$ Hz, P-CH), 2.79 – 2.95 (m, 1H, CH₂), 3.25 – 3.49 (m, 1H, CH₂), 5.02 – 5.26 (m, 1H, CH).

$^{13}\text{C}\{^1\text{H}\}$ NMR (75.5 MHz, CDCl₃): δ = 2.0 – 3.0 (m, Si(CH₃)₃), 25.7 (d, $^3J_{\text{P,C}} = 4.2$ Hz, CH₃), 38.2 (d, $^1J_{\text{P,C}} = 18.0$ Hz, P-CH), 40.5 (d, $^1J_{\text{P,C}} = 26.6$ Hz, P-CH₂), 79.6 (d, $^2J_{\text{P,C}} = 13.3$ Hz, O-CH), 205.7 (d, $^2J_{\text{P,C}} = 10.0$ Hz, *cis*-CO), 210.6 (d_{br}, $^2J_{\text{P,C}} = \text{ca. } 27$ Hz, *trans*-CO).

$^{31}\text{P}\{^1\text{H}\}$ NMR (121.5 MHz, CDCl₃): δ = 209.8 (s).

Isomer 2:

No resonance signals except in the ^{31}P NMR could be observed due to the isomers low percentage of the mixture.

$^{31}\text{P}\{^1\text{H}\}$ NMR (121.5 MHz, 25 °C, CDCl_3 , in ppm): $\delta = 201.0$ (s).

Isomer 3:

^1H NMR (300.1 MHz, CDCl_3): $\delta = 0.26$ (s, 9H, $\text{Si}(\text{CH}_3)_3$), 0.30 (s, 9H, $\text{Si}(\text{CH}_3)_3$), 1.48 (d, 3H, $^4J_{\text{P,H}} = 5.8$ Hz, CH_3), 1.72 (d, 1H, $^2J_{\text{P,H}} = 3.3$ Hz, P-CH), 2.96 – 3.22 (m, 2H, CH_2), 5.02 – 5.26 (m, 1H, CH).

$^{13}\text{C}\{^1\text{H}\}$ NMR (75.5 MHz, CDCl_3): $\delta = 2.0 - 3.0$ (m, $\text{Si}(\text{CH}_3)_3$), 25.5 (d, $^3J_{\text{P,C}} = 4.5$ Hz, CH_3), 38.6 (d, $^1J_{\text{P,C}} = 18.4$ Hz, P-CH), 44.5 (d, $^1J_{\text{P,C}} = 21.0$ Hz, P- CH_2), 76.0 (d, $^2J_{\text{P,C}} = 12.6$ Hz, O-CH), 205.7 (d, $^2J_{\text{P,C}} = 10.0$ Hz, *cis*-CO), 210.6 (d_{br}, $^2J_{\text{P,C}} = \text{ca. } 27$ Hz, *trans*-CO).

$^{31}\text{P}\{^1\text{H}\}$ NMR (121.5 MHz, CDCl_3): $\delta = 196.2$ (s).

Isomer 4:

^1H NMR (300.1 MHz, CDCl_3): $\delta = 0.26$ (s, 9H, $\text{Si}(\text{CH}_3)_3$), 0.30 (s, 9H, $\text{Si}(\text{CH}_3)_3$), 1.53 (d, 3H, $^4J_{\text{P,H}} = 6.7$ Hz, CH_3), 1.96 (d, 1H, $^2J_{\text{P,H}} = 18.1$ Hz, P-CH), 2.52 – 2.70 (m, 1H, CH_2), 3.25 – 3.49 (m, 1H, CH_2), 5.02 – 5.26 (m, 1H, CH).

$^{13}\text{C}\{^1\text{H}\}$ NMR (75.5 MHz, CDCl_3): $\delta = 2.0 - 3.0$ (m, $\text{Si}(\text{CH}_3)_3$), 27.6 (s_{br}, CH_3), 40.5 (overlapping with the signal of a CH_2), 48.3 (d, $^1J_{\text{P,C}} = 22.6$ Hz, P- CH_2), 77.3 (d, $^2J_{\text{P,C}} = 13.0$ Hz, CH), 205.7 (d, $^2J_{\text{P,C}} = 10.0$ Hz, *cis*-CO), 210.6 (d_{br}, $^2J_{\text{P,C}} = \text{ca } 27$ Hz, *trans*-CO).

$^{31}\text{P}\{^1\text{H}\}$ NMR (121.5 MHz, CDCl_3): $\delta = 195.7$ (s).

MS (EI, 70 eV, ^{98}Mo , selected data): m/z (%) = 486.0 (40) $[\text{M}]^+$, 458.0 (5) $[\text{M}-\text{CO}]^+$, 430.0 (5) $[\text{M}-2\text{CO}]^+$, 416.0 (40) $[\text{M}-\text{CO}-\text{C}_3\text{H}_6]^+$, 402.0 (30) $[\text{M}-3\text{CO}]^+$, 388.0 (60) $[\text{M}-2\text{CO}-\text{C}_3\text{H}_6]^+$, 374.0 (10) $[\text{M}-4\text{CO}]^+$, 360.0 (30) $[\text{M}-3\text{CO}-\text{C}_3\text{H}_6]^+$, 344.0 (40) $[\text{M}-5\text{CO}]^+$, 332.0 (50) $[\text{M}-4\text{CO}-\text{C}_3\text{H}_6]^+$, 304.0 (90) $[\text{M}-\text{C}_3\text{H}_6-5\text{CO}]^+$, 73.1 (50) $[\text{SiMe}_3]^+$.

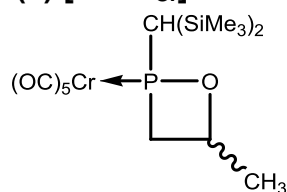
IR (ATR Diamond; $\tilde{\nu}[\text{cm}^{-1}]$, selected data): 2070 (s, $\nu(\text{CO})$), 1993 (w, $\nu(\text{CO})$), 1993 (m, $\nu(\text{CO})$), 1911 (ν_s , $\nu(\text{CO})$).

Elemental analysis:

calc.:	C	37.19	H	5.20
found:	C	37.08	H	5.32

Single crystal measurement: GSTR370, 3621.

11.2.8.4 Pentacarbonyl{4-methyl-2-[bis(trimethylsilyl)methyl]-1,2-oxaphosphetane- κ P}chromium(0) [21.1a_{Cr}]



Purification: All volatiles were removed in *vacuo* (ca. 0.02 mbar) and the product was separated from the formed salt by extraction with three times 8 mL of diethyl ether. The crude product was obtained as green oil after removal of all volatiles in *vacuo* (ca. 0.02 mbar). The product was precipitated from *n*-pentane at -100 °C, the supernatant was filtered off and the product subsequently recrystallized by slow evaporation of a saturated *n*-pentane solution at 4 °C, yielding slightly green coloured crystals. The product was obtained as mixture of different isomers and all data are given for the mixture.

Molecular formula:	C ₁₅ H ₂₅ O ₆ PSi ₂ Cr
Molecular weight:	440.496 g/mol
Melting point:	76 - 77 °C
Yield:	50 mg (0.11 mmol, 11 %)

Isomeric ratio: 23 : 3 : 14 : 60

Isomer 1:

¹H NMR (300.1 MHz, CDCl₃): δ = 0.26 (s, 9H, Si(CH₃)₃), 0.31 (s, 9H, Si(CH₃)₃), 1.63 (d, 3H, ⁴J_{P,H} = 6.0 Hz, CH₃), 1.88 (d, 1H, ²J_{P,H} = 6.80 Hz, P-CH), 2.92 – 3.04 (m, 1H, CH₂), 3.36 – 3.50 (m, 1H, CH₂), 5.10 – 5.30 (m, 1H, CH).

¹³C{¹H} NMR (75.5 MHz, CDCl₃): δ = 2.1 (d, ²J_{P,C} = 3.9 Hz, Si(CH₃)₃), 2.6 (d, ²J_{P,C} = 1.9 Hz, Si(CH₃)₃), 25.1 (d, ³J_{P,C} = 4.8 Hz, CH₃), 38.2 (d, ¹J_{P,C} = 17.5 Hz, P-CH), 40.4 (d, ¹J_{P,C} = 25.5 Hz, CH₂), 79.4 (d, ²J_{P,C} = 12.6 Hz, O-CH), 216.4 (d, J_{P,C} = 15.2 Hz, *cis*-CO), 221.4 (d, J_{P,C} = 6.8 Hz, *trans*-CO).

³¹P{¹H} NMR (121.5 MHz, CDCl₃): δ = 233.1 (s).

Isomer 2:

No resonance signals except in the ³¹P NMR and the ¹H NMR signal of the CH(SiMe₃)₂ group could be observed due to the isomers low percentage of the mixture.

¹H NMR (300.1 MHz, CDCl₃): δ = 2.30 (²J_{P,H} = 20.3 Hz).

³¹P{¹H} NMR (121.5 MHz, CDCl₃): δ = 226.7 (s).

Isomer 3:

^1H NMR (300.1 MHz, CDCl_3): δ = 0.26 (s, 9H, $\text{Si}(\text{CH}_3)_3$), 0.31 (s, 9H, $\text{Si}(\text{CH}_3)_3$), 1.52 (d, 3H, $^4J_{\text{P,H}} = 6.4$ Hz, CH_3), 2.09 (d, 1H, $^2J_{\text{P,H}} = 20.0$ Hz, P-CH), 2.59 – 2.73 (m, 1H, CH_2), 3.36 – 3.50 (m, 1H, CH_2), 5.10 – 5.30 (m, 1H, CH).

$^{13}\text{C}\{^1\text{H}\}$ NMR (75.5 MHz, CDCl_3): δ = 22.3 (d, $^2J_{\text{P,C}} = 3.9$ Hz, $\text{Si}(\text{CH}_3)_3$), 2.6 (d, $^2J_{\text{P,C}} = 3.2$ Hz, $\text{Si}(\text{CH}_3)_3$), 27.5 (s_{br}, CH_3), 42.2 (d, $^1J_{\text{P,C}} = 34.3$ Hz, P-CH), 47.9 (d, $^2J_{\text{P,C}} = 23.9$ Hz, P- CH_2), 77.3 (d, $^2J_{\text{P,C}} = 13.0$ Hz, O-CH), 216.4 (d, $^2J_{\text{P,C}} = 14.5$ Hz, *cis*-CO), the resonance signal for the *trans*-CO could not be observed due to its low intensity.

$^{31}\text{P}\{^1\text{H}\}$ NMR (121.5 MHz, CDCl_3): δ = 222.6 (s).

Isomer 4:

^1H NMR (300.1 MHz, CDCl_3): δ = 0.26 (s, 9H, $\text{Si}(\text{CH}_3)_3$), 0.31 (s, 9H, $\text{Si}(\text{CH}_3)_3$), 1.49 (d, 3H, $J_{\text{P,H}} = 6.4$ Hz, CH_3), 1.84 (d, 1H, $^2J_{\text{P,H}} = 6.1$ Hz, P-CH), 3.10 – 3.29 (m, 2H, CH_2), 5.05 – 5.21 (m, 1H, CH).

$^{13}\text{C}\{^1\text{H}\}$ NMR (75.5 MHz, CDCl_3): δ = 2.2 (d, $^2J_{\text{P,C}} = 3.6$ Hz, $\text{Si}(\text{CH}_3)_3$), 2.9 (d, $^2J_{\text{P,C}} = 2.3$ Hz, $\text{Si}(\text{CH}_3)_3$), 25.4 (d, $^3J_{\text{P,C}} = 5.5$ Hz, CH_3), 38.8 (d, $^1J_{\text{P,C}} = 17.1$ Hz, P-CH), 44.3 (d, $^1J_{\text{P,C}} = 21.3$ Hz, P- CH_2), 76.2 (d, $^2J_{\text{P,C}} = 12.9$ Hz, O-CH), 216.5 (d, $^2J_{\text{P,C}} = 14.9$ Hz, *cis*-CO), 221.2 (d, $^2J_{\text{P,C}} = 7.1$, *trans*-CO).

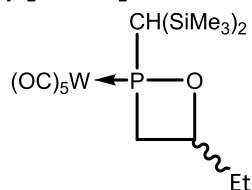
$^{31}\text{P}\{^1\text{H}\}$ NMR (121.5 MHz, CDCl_3): δ = 221.0 (s)

MS (EI, 70 eV, ^{52}Cr , selected data): m/z (%) = 440.1 (15) $[\text{M}]^{++}$, 370.0 (5) $[\text{M} - \text{CO} - \text{C}_3\text{H}_6]^+$, 328.1 (20) $[\text{M} - 4 \text{CO}]^+$, 314.0 (5) $[\text{M} - 3 \text{CO} - \text{C}_3\text{H}_6]^+$, 300.1 (100) $[\text{M} - 5 \text{CO}]^+$, 286.0 (15) $[\text{M} - 4 \text{CO} - \text{C}_3\text{H}_6]^+$, 258.1 (20) $[\text{M} - 5 \text{CO} - \text{C}_3\text{H}_6]^+$, 73.1 (10) $[\text{SiMe}_3]^+$.

IR (ATR Diamond; $\tilde{\nu}[\text{cm}^{-1}]$, selected data): 2061 (s, $\nu(\text{CO})$), 1986 (w, $\nu(\text{CO})$), 1973 (w, $\nu(\text{CO})$), 1944 (m, $\nu(\text{CO})$), 1910 (vs, $\nu(\text{CO})$).

Single crystal measurement: GSTR369, 3648.

11.2.8.5 Pentacarbonyl{4-ethyl-2-[bis(trimethylsilyl)methyl]-1,2-oxaphosphetane- κ P}tungsten(0) [21.1b]



Purification: All volatiles were removed in *vacuo* (ca. 0.02 mbar) and the product was separated from the formed salt by extraction with 4 times 20 mL of *n*-pentane. The *n*-pentane was removed in *vacuo* (ca. 0.02 mbar) followed by dissolving in 2 mL *n*-Pentane, precipitation at - 80 °C and filtering off the supernatant solvent. This procedure was repeated two times and the product was obtained as white powder as a mixture of different isomers. All data are given for the mixture.

<u>Molecular formula:</u>	C ₁₆ H ₂₇ O ₆ PSi ₂ W
<u>Molecular weight:</u>	586.367 g/mol
<u>Melting point:</u>	85 °C
<u>Yield:</u>	92 mg (0.157 mmol, 31 %)

Isomeric ratio: 29 : 4 : 23 : 44

Isomer 1:

¹H NMR (500.2 MHz, CDCl₃): δ = 0.27 (s, 9H, Si(CH₃)₃), 0.31 (s, 9H, Si(CH₃)₃), 0.86 – 0.96 (m, 3H, CH₃), 1.62 – 1.77 (m, 2H, CH₂), 1.99 (d, 1H, ²J_{P,H} = 6.9 Hz, P-CH), 2.96 – 3.05 (m, 1H, P-CH₂), 3.45 – 3.56 (m, 1H, P-CH₂), 4.86 – 4.97 (m, 1H, CH).

¹³C{¹H} NMR (125.8 MHz, CDCl₃): δ = 2.1 (d, ²J_{P,C} = 3.1 Hz, Si(CH₃)₃), 2.5 (s, Si(CH₃)₃), 9.0 (s, CH₃), 32.0 (d, ³J_{P,C} = 3.7 Hz, CH₂), 38.3 (d, ¹J_{P,C} = 13.0 Hz, P-CH), 39.0 (d, ¹J_{P,C} = 28.9 Hz, P-CH₂), 83.7 (d, ²J_{P,C} = 13.0 Hz, O-CH), 197.4 (d_{sat}, ²J_{P,C} = 7.7 Hz, ¹J_{W,C} = 125.6 Hz, *cis*-CO), 200.7 (d, ²J_{P,C} = 25.8 Hz, *trans*-CO).

²⁹Si{¹H} NMR (99.4 MHz, CDCl₃): δ = -1.85 (d, ²J_{P,Si} = 3.1 Hz, Si(CH₃)₃), 0.44 (d, ²J_{P,Si} = 6.9 Hz, Si(CH₃)₃).

³¹P{¹H} NMR (202.5 MHz, CDCl₃): δ = 177.1 (s_{sat}, ¹J_{W,P} = 274.8 Hz).

Isomer 2:

No resonance signals except in the ³¹P NMR could be observed due to the isomers low percentage of the mixture.

³¹P{¹H} NMR (202.5 MHz, CDCl₃): δ = 169.8 (s_{br}, ¹J_{W,P} = ca. 271 Hz).

Isomer 3:

^1H NMR (500.2 MHz, CDCl_3): δ = 0.27 (s, 9H, $\text{Si}(\text{CH}_3)_3$), 0.31 (s, 9H, $\text{Si}(\text{CH}_3)_3$), 0.86 – 0.96 (m, 3H, CH_3), 2.00 – 2.11 (m, 2H, CH_2), 2.21 (d, 1H, $^2J_{\text{P,H}} = 19.5$ Hz, P-CH), 2.78 – 2.89 (m, 1H, P- CH_2), 3.37 – 3.45 (m, 1H, P- CH_2), 4.86 – 4.97 (m, 1H, CH).

$^{13}\text{C}\{^1\text{H}\}$ NMR (125.8 MHz, CDCl_3): δ = 2.2 (s, $\text{Si}(\text{CH}_3)_3$), 2.5 (s, $\text{Si}(\text{CH}_3)_3$), 8.5 (s, CH_3), 34.1 (s, CH_2), 40.1 (d, $^1J_{\text{P,C}} = 28.3$ Hz, P-CH), 46.8 (d, $^1J_{\text{P,C}} = 26.9$ Hz, P- CH_2), 81.3 (d, $^2J_{\text{P,C}} = 13.2$ Hz, O-CH), 197.2 (d_{sat}, $^2J_{\text{P,C}} = 7.6$ Hz, $^1J_{\text{W,C}} = 125.1$ Hz, *cis*-CO), 199.4 (d, $^2J_{\text{P,C}} = 24.8$ Hz, *trans*-CO).

$^{29}\text{Si}\{^1\text{H}\}$ NMR (99.4 MHz, CDCl_3): δ = - 2.76 (d, $^2J_{\text{P,Si}} = 7.4$ Hz, $\text{Si}(\text{CH}_3)_3$), 0.62 (s, $\text{Si}(\text{CH}_3)_3$).

$^{31}\text{P}\{^1\text{H}\}$ NMR (202.5 MHz, CDCl_3): δ = 165.1 (s_{sat}, $^1J_{\text{W,P}} = 268.4$ Hz).

Isomer 4:

^1H NMR (500.2 MHz, CDCl_3): δ = 0.26 (s, 9H, $\text{Si}(\text{CH}_3)_3$), 0.30 (s, 9H, $\text{Si}(\text{CH}_3)_3$), 0.86 – 0.96 (m, 3H, CH_3), 1.80 – 1.96 (m, 2H, CH_2), 1.93 (d, 1H, $^2J_{\text{P,H}} = 6.0$ Hz, P-CH), 3.12 – 3.20 (m, 1H, P- CH_2), 3.21 – 3.33 (m, 1H, P- CH_2), 4.76 – 4.86 (m, 1H, CH).

$^{13}\text{C}\{^1\text{H}\}$ NMR (125.8 MHz, CDCl_3): δ = 2.2 (s, $\text{Si}(\text{CH}_3)_3$), 2.8 (d, $^2J_{\text{P,C}} = 1.7$ Hz, $\text{Si}(\text{CH}_3)_3$), 8.7 (s, CH_3), 32.5 (d, $^3J_{\text{P,C}} = 5.6$ Hz, CH_2), 38.7 (d, $^1J_{\text{P,C}} = 12.6$ Hz, P-CH), 43.5 (d, $^1J_{\text{P,C}} = 24.7$ Hz, P- CH_2), 80.6 (d, $^2J_{\text{P,C}} = 12.8$ Hz, O-CH), 197.3 (d_{sat}, $^2J_{\text{P,C}} = 7.7$ Hz, $^1J_{\text{W,C}} = 126.3$ Hz, *cis*-CO), 200.4 (d, $^2J_{\text{P,C}} = 25.1$ Hz, *trans*-CO).

$^{29}\text{Si}\{^1\text{H}\}$ NMR (99.4 MHz, CDCl_3): δ = -1.37 (d, $^2J_{\text{P,Si}} = 4.3$ Hz, $\text{Si}(\text{CH}_3)_3$), 0.25 (d, $^2J_{\text{P,Si}} = 6.9$ Hz, $\text{Si}(\text{CH}_3)_3$).

$^{31}\text{P}\{^1\text{H}\}$ NMR (202.5 MHz, CDCl_3): δ = 165.0 (s_{sat}, $^1J_{\text{W,P}} = 268.8$ Hz).

MS (EI, 70 eV, ^{184}W , selected data): m/z (%) = 586.0 (35) $[\text{M}]^{++}$, 529.9 (5) $[\text{M} - \text{C}_4\text{H}_8]^+$, 502.0 (35) $[\text{M} - \text{C}_4\text{H}_8 - \text{CO}]^+$, 474.0 (25) $[\text{M} - \text{C}_4\text{H}_8 - 2 \text{CO}]^+$, 446.0 (45) $[\text{M} - \text{C}_4\text{H}_8 - 3 \text{CO}]^+$, 418.0 (55) $[\text{M} - \text{C}_4\text{H}_8 - 4 \text{CO}]^+$, 390.0 (100) $[\text{M} - \text{C}_4\text{H}_8 - 5 \text{CO}]^+$, 73.0 (70) $[\text{SiMe}_3]^+$.

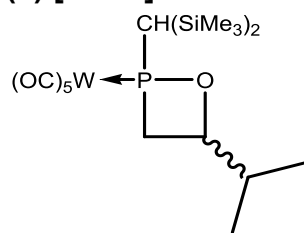
IR (ATR Diamond; $\tilde{\nu}[\text{cm}^{-1}]$, selected data): 2072 (s, $\nu(\text{CO})$), 1986 (w, $\nu(\text{CO})$), 1902 (vs, $\nu(\text{CO})$).

Elemental analysis:

calc.:	C	32.77	H	4.64
found:	C	32.44	H	4.72

Single crystal measurement: GSTR519, AKY-574 // GXray4852f

11.2.8.6 Pentacarbonyl{4-(1-methylethyl)-2-[bis(trimethylsilyl)methyl]-1,2-oxaphosphetane- κ P}tungsten(0) [21.1c]



Purification: All volatiles were removed in *vacuo* (ca. 0.02 mbar) and the product was purified by low temperature column chromatography ($\varnothing = 2$ cm, $h = 5$ cm, SiO_2 , -20 °C, eluent: petroleum ether, petroleum ether/diethyl ether 10:1). The first fraction using only petroleum ether 40/60 was collected until the first yellow colour faded and contained most of the side products; the product was obtained in the second fraction using a mixture of petroleum ether 40/60 and diethyl ether in the ratio 10:1. After removing of all volatiles in *vacuo* (ca. 0.02 mbar) the crude product was recrystallized by slow evaporation of a saturated *n*-pentane solution at 4 °C to yield colorless crystals. The product was obtained as mixture of different isomers and all data are given for the mixture.

Molecular formula:	$\text{C}_{17}\text{H}_{29}\text{O}_6\text{PSi}_2\text{W}$
Molecular weight:	600.393 g/mol
Melting point:	$82 - 83$ °C
Yield:	60 mg (0.20 mmol, 20 %)

Isomeric ratio: 29 : 5 : 24 : 42

Isomer 1:

^1H NMR (500.2 MHz, CDCl_3): $\delta = 0.27$ (s, 9H, $\text{Si}(\text{CH}_3)_3$), 0.30 (s, 9H, $\text{Si}(\text{CH}_3)_3$), 0.80 (d, 3H, $^5J_{\text{P,H}} = 6.7$ Hz, CH_3), $0.94 - 0.99$ (m, 3H, CH_3), 1.97 (d, 1H, $^2J_{\text{P,H}} = 6.1$ Hz, P-CH), $2.11 - 2.20$ (m, 1H, $\text{CH}(\text{CH}_3)_2$), $3.01 - 3.09$ (m, 1H, P- CH_2), $3.39 - 3.50$ (m, 1H, P- CH_2), $4.47 - 4.55$ (m, 1H, CH).

$^{13}\text{C}\{^1\text{H}\}$ NMR (125.8 MHz, CDCl_3): $\delta = 2.2$ (d, $^2J_{\text{P,C}} = 3.5$ Hz, $\text{Si}(\text{CH}_3)_3$), 2.6 (s, $\text{Si}(\text{CH}_3)_3$), 16.6 (s, CH_3), 17.9 (s, CH_3), 36.5 (d, $^3J_{\text{P,C}} = 3.5$ Hz, $\text{CH}(\text{CH}_3)_2$), 37.9 (d, $^1J_{\text{P,C}} = 32.4$ Hz, P- CH_2), 38.2 (d, $^1J_{\text{P,C}} = 18.1$ Hz, P-CH), 87.5 (d, $^2J_{\text{P,C}} = 12.8$ Hz, O-CH), 197.4 (d_{sat} , $^2J_{\text{P,C}} = 7.6$ Hz, $^1J_{\text{W,C}} = 125.7$ Hz, *cis*-CO), 200.7 (d, $^2J_{\text{P,C}} = 26.0$ Hz, *trans*-CO).

$^{29}\text{Si}\{^1\text{H}\}$ NMR (99.4 MHz, CDCl_3): $\delta = -1.80$ (d, $^2J_{\text{P,Si}} = 3.5$ Hz, $\text{Si}(\text{CH}_3)_3$), 0.44 (d, $^2J_{\text{P,Si}} = 7.1$ Hz, $\text{Si}(\text{CH}_3)_3$).

$^{31}\text{P}\{^1\text{H}\}$ NMR (202.5 MHz, CDCl_3): $\delta = 174.7$ (s_{sat} , $^1J_{\text{W,P}} = 274.8$ Hz).

Isomer 2:

No resonance signals except in the ^{31}P NMR could be observed due to the isomers low percentage of the mixture.

$^{31}\text{P}\{^1\text{H}\}$ NMR (202.5 MHz, CDCl_3): $\delta = 167.1$ (s_{br} , $^1J_{\text{W,P}} = \text{ca. } 274$ Hz).

Isomer 3:

^1H NMR (500.2 MHz, CDCl_3): $\delta = 0.25$ (s, 9H, $\text{Si}(\text{CH}_3)_3$), 0.31 (s, 9H, $\text{Si}(\text{CH}_3)_3$), 0.86 (d, 3H, $^5J_{\text{P,H}} = 6.8$ Hz, CH_3), 0.94 – 0.99 (m, 3H, CH_3), 2.20 (d, 1H, $^2J_{\text{P,H}} = 19.3$ Hz, P-CH), 1.94 – 2.02 (m, 1H, $\text{CH}(\text{CH}_3)_2$), 2.81 – 2.91 (m, 1H, P- CH_2), 3.28 – 3.37 (m, 1H, P- CH_2), 4.55 – 4.62 (m, 1H, CH).

$^{13}\text{C}\{^1\text{H}\}$ NMR (125.8 MHz, CDCl_3): $\delta = 2.3$ (d, $^2J_{\text{P,C}} = 3.5$ Hz, $\text{Si}(\text{CH}_3)_3$), 2.5 (d, $^2J_{\text{P,C}} = 2.2$ Hz, $\text{Si}(\text{CH}_3)_3$), 16.2 (s, CH_3), 17.5 (s, CH_3), 38.0 (s, $\text{CH}(\text{CH}_3)_2$), 39.6 (d, $^1J_{\text{P,C}} = 27.9$ Hz, P-CH), 45.5 (d, $^1J_{\text{P,C}} = 26.7$ Hz, P- CH_2), 84.6 (d, $^2J_{\text{P,C}} = 13.0$ Hz, O-CH), 197.2 (d_{sat} , $^2J_{\text{P,C}} = 7.2$ Hz, $^1J_{\text{W,C}} = 126.5$ Hz, *cis*-CO), 199.3 (d, $^2J_{\text{P,C}} = 24.5$ Hz, *trans*-CO).

$^{29}\text{Si}\{^1\text{H}\}$ NMR (99.4 MHz, CDCl_3): $\delta = -2.77$ (d, $^2J_{\text{P,Si}} = 7.6$ Hz, $\text{Si}(\text{CH}_3)_3$), 0.64 (s, $\text{Si}(\text{CH}_3)_3$).

$^{31}\text{P}\{^1\text{H}\}$ NMR (202.5 MHz, CDCl_3): $\delta = 162.6$ (s_{sat} , $^1J_{\text{W,P}} = 268.6$ Hz).

Isomer 4:

^1H NMR (500.2 MHz, CDCl_3): $\delta = 0.25$ (s, 9H, $\text{Si}(\text{CH}_3)_3$), 0.30 (s, 9H, $\text{Si}(\text{CH}_3)_3$), 0.84 (d, 3H, $^5J_{\text{P,H}} = 6.6$ Hz, CH_3), 0.94 – 0.99 (m, 3H, CH_3), 1.92 (d, 1H, $^2J_{\text{P,H}} = 6.1$ Hz, P-CH), 1.87 – 1.95 (m, 1H, $\text{CH}(\text{CH}_3)_2$), 3.09 – 3.18 (m, 1H, P- CH_2), 3.19 – 3.28 (m, 1H, P- CH_2), 4.31 – 4.43 (m, 1H, CH).

$^{13}\text{C}\{^1\text{H}\}$ NMR (125.8 MHz, CDCl_3): $\delta = 2.2$ (d, $^2J_{\text{P,C}} = 3.7$ Hz, $\text{Si}(\text{CH}_3)_3$), 2.8 (d, $^2J_{\text{P,C}} = 1.8$ Hz, $\text{Si}(\text{CH}_3)_3$), 16.1 (s, CH_3), 17.9 (s, CH_3), 37.2 (d, $^3J_{\text{P,C}} = 5.4$ Hz, $\text{CH}(\text{CH}_3)_2$), 38.6 (d, $^1J_{\text{P,C}} = 12.6$ Hz, P-CH), 42.8 (d, $^1J_{\text{P,C}} = 24.5$ Hz, P- CH_2), 84.3 (d, $^2J_{\text{P,C}} = 12.5$ Hz, O-CH), 197.4 (d_{sat} , $^2J_{\text{P,C}} = 7.4$ Hz, $^1J_{\text{W,C}} = 125.9$ Hz, *cis*-CO), 200.4 (d, $^2J_{\text{P,C}} = 25.1$ Hz, *trans*-CO).

$^{29}\text{Si}\{^1\text{H}\}$ NMR (99.4 MHz, CDCl_3): $\delta = -1.40$ (d, $^2J_{\text{P,Si}} = 4.2$ Hz, $\text{Si}(\text{CH}_3)_3$), 0.32 (d, $^2J_{\text{P,Si}} = 6.9$ Hz, $\text{Si}(\text{CH}_3)_3$).

$^{31}\text{P}\{^1\text{H}\}$ NMR (202.5 MHz, CDCl_3): $\delta = 161.7$ (s_{sat} , $^1J_{\text{W,P}} = 268.7$ Hz).

MS (EI, 70 eV, ^{184}W , selected data): m/z (%) = 600.1 (40) $[\text{M}]^+$, 530.0 (5) $[\text{M} - \text{C}_5\text{H}_{10}]^+$, 502.0 (20) $[\text{M} - \text{C}_5\text{H}_{10} - \text{CO}]^+$, 474.0 (20) $[\text{M} - \text{C}_5\text{H}_{10} - 2 \text{CO}]^+$, 460.1 (25) $[\text{M} - 5 \text{CO}]^+$, 446.0 (35) $[\text{M} - \text{C}_5\text{H}_{10} - 3 \text{CO}]^+$, 418.0 (55) $[\text{M} - \text{C}_5\text{H}_{10} - 4 \text{CO}]^+$, 390.0 (100) $[\text{M} - \text{C}_5\text{H}_{10} - 5 \text{CO}]^+$, 73.0 (50) $[\text{SiMe}_3]^+$.

IR (ATR Diamond; $\tilde{\nu}[\text{cm}^{-1}]$, selected data): 2068 (s, $\nu(\text{CO})$), 1979 (w, $\nu(\text{CO})$), 1895 (vs, $\nu(\text{CO})$).

Elemental analysis:

calc.:	C	34.01	H	4.87
found:	C	33.84	H	5.06

Single crystal measurement: GSTR518, AKY-575 // GXray4851f

11.2.8.7 Attempted synthesis of pentacarbonyl{4-(1,1-dimethylethyl)-2-[bis(trimethylsilyl)methyl]-1,2-oxaphosphetane- κP }tungsten(0) [21.1d]

The reaction was performed as described in chapter 11.2.8. The reaction mixture was submitted for $^{31}\text{P}\{^1\text{H}\}$ NMR measurement after reaching ambient temperature. The NMR spectrum showed the formation of diphosphen-complexes as main products (80.5 %) as well as small amounts of isomeric 1,2-oxaphosphetane complexes (9.5 %) and around 10% of unidentified compounds.

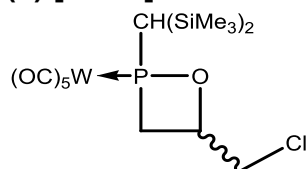
Isomeric ratio: 35 : 21 : 43

Isomer 1: $^{31}\text{P}\{^1\text{H}\}$ NMR (121.5 MHz, Et_2O): $\delta = 172.2$ (s)

Isomer 2: $^{31}\text{P}\{^1\text{H}\}$ NMR (121.5 MHz, Et_2O): $\delta = 166.5$ (s)

Isomer 3: $^{31}\text{P}\{^1\text{H}\}$ NMR (121.5 MHz, Et_2O): $\delta = 159.8$ (s)

11.2.8.8 Pentacarbonyl{4-(chloromethyl)-2-[bis(trimethylsilyl)methyl]-1,2-oxaphosphetane- κP }tungsten(0) [21.1e]



Purification: All volatiles were removed in *vacuo* (ca. 0.02 mbar) and the product was separated from the formed salt by extraction with three times 15 mL of *n*-pentane followed by low temperature column chromatography (SiO_2 , -20 °C, eluent: petroleum ether, petroleum ether/diethyl ether 10:0.1). It was obtained as solid from the second fraction after removing of all volatiles in *vacuo* (ca. 0.02 mbar). The crude product was crystallized by slow evaporation of a saturated *n*-pentane solution at 4 °C to yield colourless crystals. The product was obtained as mixtures of different isomers and all data are given for the mixture.

Molecular formula: $\text{C}_{15}\text{H}_{24}\text{ClO}_6\text{PSi}_2\text{W}$

Molecular weight: 606.785 g/mol

Melting point: 128 °C (dec.)

Yield: 186 mg (0.31 mmol, 61 %)

Isomeric ratio: 44 : 7 : 19 : 30

Isomer 1:

^1H NMR (300.1 MHz, CDCl_3): $\delta = 0.29$ (s, 9H, $\text{Si}(\text{CH}_3)_3$), 0.32 (s, 9H, $\text{Si}(\text{CH}_3)_3$), 2.04 (d, 1H, $^2J_{\text{P,H}} = 6.3$ Hz, P-CH), 3.06 – 3.18 (m, 1H, CH_2), 3.40 – 3.59 (m, 1H, CH_2), 3.68 – 3.82 (m, 2H, CH_2), 5.03 – 5.16 (m, 1H, CH).

$^{13}\text{C}\{^1\text{H}\}$ NMR (75.5 MHz, CDCl_3): $\delta = 2.0$ (d, $^2J_{\text{P,C}} = 4.3$ Hz, $\text{Si}(\text{CH}_3)_3$), 2.4 (d, $^2J_{\text{P,C}} = 1.5$ Hz, $\text{Si}(\text{CH}_3)_3$), 37.4 (d, $^1J_{\text{P,C}} = 28.6$ Hz, P- CH_2), 38.6 (d, $^1J_{\text{P,C}} = 12.9$ Hz, P-CH), 47.0 (d, $^3J_{\text{P,C}} = 4.9$ Hz, CH_2), 79.5 (d, $^2J_{\text{P,C}} = 12.8$ Hz, O-CH), 196.8 (d_{sat}, $^1J_{\text{W,C}} = 124.1$ Hz, $^2J_{\text{P,C}} = 7.5$ Hz, *cis*-CO), 198.8 (d, $^2J_{\text{P,C}} = 25.5$, *trans*-CO).

$^{29}\text{Si}\{^1\text{H}\}$ NMR (59.6 MHz, CDCl_3): $\delta = -3.33$ (d, $^2J_{\text{P,Si}} = 7.7$ Hz, $\text{Si}(\text{CH}_3)_3$), 0.00 (s, $\text{Si}(\text{CH}_3)_3$).

$^{31}\text{P}\{^1\text{H}\}$ NMR (121.5 MHz, CDCl_3): $\delta = 182.4$ (s_{sat}, $^1J_{\text{W,P}} = 278.6$ Hz).

Isomer 2:

No resonance signals except in the ^{31}P NMR could be observed due to the isomers low percentage of the mixture.

$^{31}\text{P}\{^1\text{H}\}$ NMR (121.5 MHz, CDCl_3): $\delta = 174.8$ (s_{sat}, $^1J_{\text{W,P}} = 281.0$ Hz).

Isomer 3:

^1H NMR (300.1 MHz, CDCl_3): $\delta = 0.28$ (s, 9H, $\text{Si}(\text{CH}_3)_3$), 0.31 (s, 9H, $\text{Si}(\text{CH}_3)_3$), 1.98 (d, 1H, $^2J_{\text{P,H}} = 5.9$ Hz, P-CH), 3.25 – 3.48 (m, 2H, CH_2), 3.62 – 3.72 (m, 2H, CH_2), 4.94 – 5.05 (m, 1H, CH).

$^{13}\text{C}\{^1\text{H}\}$ NMR (75.5 MHz, CDCl_3): $\delta = 2.0$ (d, $^2J_{\text{P,C}} = 3.6$ Hz, $\text{Si}(\text{CH}_3)_3$), 2.8 (d, $^2J_{\text{P,C}} = 2.3$ Hz, $\text{Si}(\text{CH}_3)_3$), 38.9 (d, $^1J_{\text{P,C}} = 13.3$ Hz, P-CH), 41.8 (d, $^1J_{\text{P,C}} = 25.3$ Hz, P- CH_2), 46.8 (d, $^3J_{\text{P,C}} = 6.0$ Hz, CH_2), 76.4 (d, $^2J_{\text{P,C}} = 12.6$ Hz, O-CH), 196.9 (d, $^2J_{\text{P,C}} = 7.8$ Hz, *cis*-CO), 199.6 (d, $^2J_{\text{P,C}} = 26.0$, *trans*-CO).

$^{29}\text{Si}\{^1\text{H}\}$ NMR (59.6 MHz, CDCl_3): $\delta = -2.50$ (d, $^2J_{\text{P,Si}} = 3.4$ Hz, $\text{Si}(\text{CH}_3)_3$), -0.15 (s, $\text{Si}(\text{CH}_3)_3$).

$^{31}\text{P}\{^1\text{H}\}$ NMR (121.5 MHz, CDCl_3): $\delta = 171.0$ (s_{sat}, $^1J_{\text{W,P}} = 274.4$ Hz).

Isomer 4:

^1H NMR (300.1 MHz, CDCl_3): $\delta = 0.27$ (s, 9H, $\text{Si}(\text{CH}_3)_3$), 0.31 (s, 9H, $\text{Si}(\text{CH}_3)_3$), 2.71 (d, 1H, $^2J_{\text{P,H}} = 19.9$ Hz, P-CH), 3.20 – 3.50 (m, 4H, CH_2), 5.20 – 5.31 (m, 1H, CH).

$^{13}\text{C}\{^1\text{H}\}$ NMR (75.5 MHz, CDCl_3): $\delta = 2.1$ (d, $^2J_{\text{P,C}} = 3.0$ Hz, $\text{Si}(\text{CH}_3)_3$), 2.2 (d, $^2J_{\text{P,C}} = 3.3$ Hz, $\text{Si}(\text{CH}_3)_3$), 37.9 (d, $^1J_{\text{P,C}} = 29.2$ Hz, P-CH), 43.8 (d, $^1J_{\text{P,C}} = 27.3$ Hz, P- CH_2), 48.8 (d, $^3J_{\text{P,C}} = 2.2$ Hz, CH_2), 76.5 (d, $^2J_{\text{P,C}} = 13.2$ Hz, O-CH), 196.9 (d, $^2J_{\text{P,C}} = 7.9$ Hz, *cis*-CO), 199.8 (d, $^2J_{\text{P,C}} = 28.1$, *trans*-CO).

$^{29}\text{Si}\{^1\text{H}\}$ NMR (59.6 MHz, CDCl_3): $\delta = -1.92$ (d, $^2J_{\text{P,Si}} = 4.6$ Hz, $\text{Si}(\text{CH}_3)_3$), -0.27 (s, $\text{Si}(\text{CH}_3)_3$).

$^{31}\text{P}\{^1\text{H}\}$ NMR (121.5 MHz, CDCl_3): $\delta = 170.1$ (s_{sat}, $^1J_{\text{W,P}} = 271.3$ Hz).

MS (EI, 70 eV, ^{184}W , selected data): m/z (%) = 605.9 (40) $[\text{M}]^{++}$, 578.0 (5) $[\text{M} - \text{CO}]^+$, 550.0 (1) $[\text{M} - 2 \text{CO}]^+$, 522.0 (5) $[\text{M} - 3 \text{CO}]^+$, 502.0 (15) $[\text{M} - \text{C}_2\text{H}_3\text{Cl} - \text{CO}]^+$, 494.0 (5) $[\text{M} - 4 \text{CO}]^+$, 474.0 (20) $[\text{M} - \text{C}_2\text{H}_3\text{Cl} - 2 \text{CO}]^+$, 466.0 (50) $[\text{M} - 5 \text{CO}]^+$, 446.0 (30) $[\text{M} - \text{C}_2\text{H}_3\text{Cl} - 3 \text{CO}]^+$, 418.0 (35) $[\text{M} - \text{C}_2\text{H}_3\text{Cl} - 4 \text{CO}]^+$, 390.0 (50) $[\text{M} - \text{C}_2\text{H}_3\text{Cl} - 5 \text{CO}]^+$, 73.1 (100) $[\text{SiMe}_3]^+$.

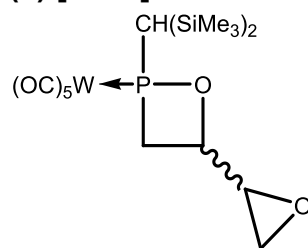
IR (ATR Diamond; $\tilde{\nu}[\text{cm}^{-1}]$, selected data): 2075 (m, $\nu(\text{CO})$), 1988 (w, $\nu(\text{CO})$), 1904 (vs, $\nu(\text{CO})$).

Elemental analysis:

calc.:	C	29.69	H	3.99
found:	C	30.53	H	4.74

Single crystal measurement: AKY-306 GSTR324, 3114

11.2.8.9 Pentacarbonyl{4-epoxy-2-[bis(trimethylsilyl)methyl]-1,2-oxaphosphetane- κP }tungsten(0) [21.1f]



Purification: All volatiles were removed *in vacuo* (ca. 0.02 mbar). The product was separated from the formed salt by extraction with 5 times 5 mL of *n*-pentane and obtained, after removal of all volatiles *in vacuo* (ca. 0.02 mbar), as a yellow oil. The oil was solidified by precipitation from *n*-pentane (1 mL) at $-100\text{ }^\circ\text{C}$ and filtering off the supernatant solution. This step was repeated three times. The product was obtained as a mixture of different isomers and all data are given for the mixture.

Molecular formula:	$\text{C}_{16}\text{H}_{25}\text{O}_7\text{PSi}_2\text{W}$
Molecular weight:	600.353 g/mol
Melting point:	$84\text{ }^\circ\text{C}$
Yield:	147 mg (0.245 mmol, 49 %)

Isomeric ratio: 39 : 7 : 44 : 10

Isomer 1:

^1H NMR (300.1 MHz, CDCl_3): δ = 0.28 (s, 9H, $\text{Si}(\text{CH}_3)_3$), 0.30 (s, 9H, $\text{Si}(\text{CH}_3)_3$), 2.01 (d, 1H, $^2J_{\text{P,H}} = 5.8$ Hz, P-CH), 2.76 - 2.93 (m, 2H, CH_2), 3.23 - 3.41 (m, 2H, CH_2), 3.42 - 3.62 (m, 1H, CH), 4.84 - 4.94 (m, 1H, P-O-CH).

$^{13}\text{C}\{^1\text{H}\}$ NMR (75.5 MHz, CDCl_3): δ = 2.2 (d, $^2J_{\text{P,C}} = 4.0$ Hz, $\text{Si}(\text{CH}_3)_3$), 2.54 (d, $^2J_{\text{P,C}} = 2.0$ Hz, $\text{Si}(\text{CH}_3)_3$), 35.8 (d, $^1J_{\text{P,C}} = 28.9$ Hz, P- CH_2), 39.1 (d, $^1J_{\text{P,C}} = 12.9$ Hz, P-CH), 44.8 (s, CH_2), 54.3 (s, CH), 80.3 (d,

$^2J_{P,C} = 12.8$ Hz, O-CH), 197.0 (d_{sat}, $^1J_{W,C} = 126.1$ Hz, $^2J_{P,C} = 7.9$ Hz, *cis*-CO), 200.3 (d, $^2J_{P,C} = 27.5$ Hz, *trans*-CO).

$^{31}P\{^1H\}$ NMR (121.5 MHz, CDCl₃): $\delta = 184.9$ (s_{sat}, $^1J_{W,P} = 280.7$ Hz).

Isomer 2:

$^{31}P\{^1H\}$ NMR (121.5 MHz, CDCl₃): $\delta = 177.7$ (s_{br}).

No resonance signals except in the ^{31}P NMR could be observed due to the isomers low percentage of the mixture.

Isomer 3:

1H NMR (300.1 MHz, CDCl₃): $\delta = 0.25$ (s, 9H, Si(CH₃)₃), 0.28 (s, 9H, Si(CH₃)₃), 2.84 (d, 1H, $^2J_{P,H} = 19.0$ Hz, P-CH), 2.69 - 2.98 (m, 2H, CH₂), 3.14 - 3.35 (m, 2H, CH₂), 3.39 - 3.51 (m, 1H, CH), 5.12 - 5.21 (m, 1H, P-O-CH).

$^{13}C\{^1H\}$ NMR (75.5 MHz, CDCl₃): $\delta = 2.2$ (d, $^2J_{P,C} = 4.0$ Hz, Si(CH₃)₃), 2.34 (d, $^2J_{P,C} = 3.3$ Hz, Si(CH₃)₃), 36.5 (d, $^1J_{P,C} = 27.5$ Hz, P-CH), 43.6 (d, $^1J_{P,C} = 28.1$ Hz, P-CH₂), 44.8 (s, CH₂), 54.3 (d, $^3J_{P,C} = 3.8$ Hz, CH), 75.1 (d, $^2J_{P,C} = 13.1$ Hz, O-CH), 197.0 (d_{sat}, $^1J_{W,C} = 125.6$ Hz, $^2J_{P,C} = 7.7$ Hz, *cis*-CO), 199.2 (d, $^2J_{P,C} = 25.0$ Hz, *trans*-CO).

$^{31}P\{^1H\}$ NMR (121.5 MHz, CDCl₃): $\delta = 174.7$ (s_{sat}, $^1J_{W,P} = 269.6$ Hz).

Isomer 4:

1H NMR (300.1 MHz, CDCl₃): $\delta = 0.29$ (s, 9H, Si(CH₃)₃), 0.32 (s, 9H, Si(CH₃)₃), 1.93 (d, 1H, $^2J_{P,H} = 5.2$ Hz, P-CH), 2.61 - 3.76 (m, 5H, CH₂ + CH₂ + CH), 4.68 - 4.77 (m, 1H, P-O-CH).

$^{13}C\{^1H\}$ NMR (75.5 MHz, CDCl₃): Due to the isomers low percentage of the mixture only very few resonance signals could be observed in the $^{13}C\{^1H\}$ NMR: $\delta = 2.8$ (d, $^2J_{P,C} = 2.4$ Hz, Si(CH₃)₃), 39.2 (d, $^1J_{P,C} = 12.8$ Hz, P-CH), 40.1 (d, $^1J_{P,C} = 25.5$ Hz, P-CH₂), 44.4 (s, CH₂), 54.1 (d, $^3J_{P,C} = 8.0$ Hz, CH).

$^{31}P\{^1H\}$ NMR (121.5 MHz, CDCl₃): $\delta = 173.3$ (s_{sat}, $^1J_{W,P} = 272.5$ Hz).

MS (EI, 70 eV, ^{184}W , selected data): m/z (%) = 600.0 (30) [M]⁺⁺, 584.0 (5) [M - O]⁺, 572.0 (10) [M - CO]⁺, 516.0 (5) [M - 3 CO]⁺, 488.0 (10) [M - 4 CO]⁺, 460.0 (25) [M - 5 CO]⁺, 388.0 (85) [M - C₃H₄O₂]⁺, 73.1 (50) [SiMe₃]⁺.

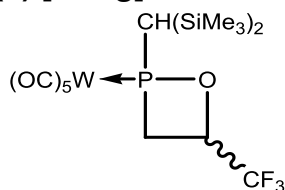
IR (ATR Diamond; $\tilde{\nu}$ [cm⁻¹], selected data): 2072 (s, ν (CO)), 1984 (w, ν (CO)), 1906 (vs, ν (CO)).

Elemental analysis:

calc.:	C	32.01	H	4.20
found:	C	31.82	H	4.40

Single crystal measurement: GSTR382, AKY-425 // GXraycollect

11.2.8.10 Pentacarbonyl{4-(trifluoromethyl)-2-[bis(trimethylsilyl)methyl]-1,2-oxaphosphetane- κ P}tungsten(0) [21.1g]



Purification: All volatiles were removed in *vacuo* (ca. 0.02 mbar). The crude product was extracted from the formed salt with diethyl ether (two times 5 mL) and the solvent was removed in *vacuo* (ca. 0.02 mbar). The product was obtained via precipitation from *n*-pentane and filtering off the solvent at -100 °C, which was repeated three times. It was obtained as mixture of different isomers and all data are given for the mixture.

<u>Molecular formula:</u>	C ₁₅ H ₂₂ F ₃ O ₆ PSi ₂ W
<u>Molecular weight:</u>	626.312 g/mol
<u>Melting point:</u>	86 - 87 °C
<u>Yield:</u>	218 mg (0.35 mmol, 35 %)

Isomeric ratio: 49 : 14 :31 :6 (before purification)

85 : 12 :3 :<1 (after purification)

Isomer 1:

¹H NMR (300.1 MHz, CDCl₃): δ = 0.31 (s, 9H, Si(CH₃)₃), 0.34 (s, 9H, Si(CH₃)₃), 2.11 (d, 1H, ²J_{P,H} = 5.6 Hz, P-CH), 3.40 – 3.60 (m, 2H, CH₂), 5.00 – 5.20 (m, 1H, CH).

¹³C{¹H} NMR (75.5 MHz, CDCl₃): δ = 2.0 (d, ²J_{P,C} = 3.9 Hz, Si(CH₃)₃), 2.4 (d, ²J_{P,C} = 2.6 Hz, Si(CH₃)₃), 32.5 (d, ¹J_{P,C} = 29.7 Hz, CH₂), 39.7 (d, ¹J_{P,C} = 12.3 Hz, CH), 75.9 (qd, ²J_{F,C} = 37.2 Hz, ²J_{P,C} = 13.1 Hz, O-CH), 123.6 (qd, ¹J_{F,C} = 280.0 Hz, ³J_{P,C} = 5.8 Hz, CF₃), 196.1 (d_{sat}, ¹J_{W,C} = 125.8, ²J_{P,C} = 7.8 Hz, *cis*-CO), 199.5 (d, ²J_{P,C} = 29.1 Hz, *trans*-CO).

¹⁹F{¹H} NMR (59.6 MHz, CDCl₃): δ = -80.6 (⁴J_{P,F} = 0.84 Hz, CF₃).

²⁹Si{¹H} NMR (59.6 MHz, CDCl₃): δ = -1.97 (²J_{P,Si} = 3.9 Hz, Si(CH₃)₃), 0.61 (²J_{P,Si} = 6.9 Hz, Si(CH₃)₃).

³¹P{¹H} NMR (121.5 MHz, CDCl₃): δ = 194.9 (s_{sat}, ¹J_{W,P} = 288.1 Hz).

No resonance signals except in the ³¹P NMR could be observed for the other isomers.

Isomer 2:

³¹P{¹H} NMR (121.5 MHz, CDCl₃): δ = 186.9 (s_{sat}, ¹J_{W,P} = 286.3 Hz).

Isomer 3:

$^{31}\text{P}\{^1\text{H}\}$ NMR (121.5 MHz, CDCl_3): $\delta = 183.3$ (s_{sat} , $^1J_{\text{W,P}} = 277.3$ Hz).

Isomer 4:

$^{31}\text{P}\{^1\text{H}\}$ NMR (121.5 MHz, CDCl_3): $\delta = 182.8$ (s_{sat} , $^1J_{\text{W,P}} = 284.5$ Hz).

MS (EI, 70 eV, ^{184}W , selected data): m/z (%) = 625.9 (60) $[\text{M}]^{++}$, 570.0 (5) $[\text{M} - 2 \text{CO}]^+$, 542.0 (60) $[\text{M} - 3 \text{CO}]^+$, 502.0 (5) $[\text{M} - \text{CO} - \text{C}_3\text{H}_3\text{F}_3]^+$, 486.0 (10) $[\text{M} - 5 \text{CO}]^+$, 473.9 (10) $[\text{M} - 2 \text{CO} - \text{C}_3\text{H}_3\text{F}_3]^+$, 445.9 (15) $[\text{M} - 3 \text{CO} - \text{C}_3\text{H}_3\text{F}_3]^+$, 418.0 (25) $[\text{M} - 4 \text{CO} - \text{C}_3\text{H}_3\text{F}_3]^+$, 390.0 (85) $[\text{M} - 5 \text{CO} - \text{C}_3\text{H}_3\text{F}_3]^+$, 73.1 (100) $[\text{SiMe}_3]^+$.

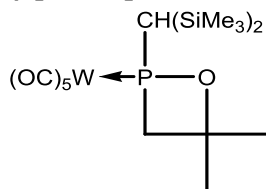
IR (ATR Diamond; $\tilde{\nu}[\text{cm}^{-1}]$, selected data): 2074 (s, $\nu(\text{CO})$), 1992 (w, $\nu(\text{CO})$), 1909 (vs, $\nu(\text{CO})$).

Elemental analysis:

calc.:	C	28.77	H	3.54
found:	C	29.07	H	3.89

Single crystal measurement: GSTR344, 3313

11.2.8.11 Pentacarbonyl{4,4-dimethyl-2-[bis(trimethylsilyl)methyl]-1,2-oxaphosphetane- κP }tungsten(0) [25.1a]



Purification: The crude product was purified by column chromatography ($\varnothing = 2$ cm, $h = 6$ cm, petroleum ether, -20 °C, SiO_2) after removing of all volatiles in *vacuo* (ca. 0.02 mbar).

The product was obtained from the second fraction using petroleum ether to remove all acyclic side products with the first fraction and then a mixture of petroleum ether and diethyl ether (50 : 1). All volatiles were removed in *vacuo* (ca. 0.02 mbar) and the product washed six times with 2 mL of *n*-pentane at -100 °C. The product was obtained as white powder, containing a mixture of two isomers, after drying in *vacuo* (ca. 0.02 mbar). All data are given for the mixture.

Molecular formula: $\text{C}_{16}\text{H}_{27}\text{O}_6\text{PSi}_2\text{W}$

Molecular weight: 568.366 g/mol

Melting point: 84 °C

Yield: 200 mg (0.35 mmol, 35 %).

Isomeric ratio: 36 : 64

Isomer 1:

^1H NMR (300.1 MHz, C_6D_6): δ = 0.09 (s, 9H, $\text{Si}(\text{CH}_3)_3$), 0.28 (s, 9H, $\text{Si}(\text{CH}_3)_3$), 1.08 (s, 3H, CH_3), 1.47 (s, 3H, CH_3), 1.87 (d, 1H, $^2J_{\text{P,H}} = 4.6$ Hz, P-CH), 2.80 (d, 1H, $^2J_{\text{H,H}} = 13.7$ Hz, CH_2), 3.12 (dd, 1H, $^2J_{\text{H,H}} = 13.7$ Hz, $^2J_{\text{P,H}} = 12.6$ Hz, CH_2).

$^{13}\text{C}\{^1\text{H}\}$ NMR (75.5 MHz, C_6D_6): δ = 2.5 (d, $^3J_{\text{P,C}} = 3.1$ Hz, $\text{Si}(\text{CH}_3)_3$), 2.9 (d, $^3J_{\text{P,C}} = 2.7$ Hz, $\text{Si}(\text{CH}_3)_3$), 31.0 (d, $^3J_{\text{P,C}} = 1.6$ Hz, CH_3), 33.1 (d, $^3J_{\text{P,C}} = 1.7$ Hz, CH_3), 39.7 (d, $^1J_{\text{P,C}} = 12.0$ Hz, P-CH), 46.8 (d, $^1J_{\text{P,C}} = 24.7$ Hz, CH_2), 85.6 (d, $^2J_{\text{P,C}} = 12.5$ Hz, O-C(CH_3) $_2$), 198.1 (d_{sat}, $^1J_{\text{W,C}} = 125.8$ Hz, $^2J_{\text{P,C}} = 7.7$ Hz, *cis*-CO), 200.4 (d, $^2J_{\text{P,C}} = 25.2$ Hz, *trans*-CO).

$^{29}\text{Si}\{^1\text{H}\}$ NMR (59.6 MHz, C_6D_6): δ = -1.56 (d, $^2J_{\text{P,Si}} = 7.2$ Hz, $\text{Si}(\text{CH}_3)_3$), -0.59 (d, $^2J_{\text{P,Si}} = 6.2$ Hz, $\text{Si}(\text{CH}_3)_3$).

^{31}P NMR (121.5 MHz, C_6D_6): δ = 156.9 (dd_{sat}, $^1J_{\text{W,P}} = 275.2$ Hz, $^2J_{\text{P,H}} = 12.6$ Hz, $^2J_{\text{P,H}} = 4.2$ Hz).

Isomer 2:

^1H NMR (300.1 MHz, C_6D_6): δ = 0.15 (s, 9H, $\text{Si}(\text{CH}_3)_3$), 0.32 (s, 9H, $\text{Si}(\text{CH}_3)_3$), 1.14 (s, 3H, CH_3), 1.37 (s, 3H, CH_3), 2.20 (d, 1H, $^2J_{\text{P,H}} = 18.9$ Hz, P-CH), 2.49 (dd, 1H, $^2J_{\text{H,H}} = 13.4$ Hz, $^2J_{\text{P,H}} = 11.3$ Hz, CH_2), 2.95 (d, 1H, $^2J_{\text{H,H}} = 13.4$ Hz, CH_2).

$^{13}\text{C}\{^1\text{H}\}$ NMR (75.5 MHz, C_6D_6): δ = 2.2 (d, $^3J_{\text{P,C}} = 3.9$ Hz, $\text{Si}(\text{CH}_3)_3$), 2.6 (d, $^3J_{\text{P,C}} = 3.1$ Hz, $\text{Si}(\text{CH}_3)_3$), 32.0 (d, $^3J_{\text{P,C}} = 3.9$ Hz, CH_3), 34.1 (s, CH_3), 38.6 (d, $^1J_{\text{P,C}} = 26.8$ Hz, P-CH), 51.5 (d, $^1J_{\text{P,C}} = 26.9$ Hz, CH_2), 85.5 (d, $^2J_{\text{P,C}} = 12.6$ Hz, O-C(CH_3) $_2$), 197.8 (d_{sat}, $^1J_{\text{W,C}} = 125.3$ Hz, $^2J_{\text{P,C}} = 7.7$ Hz, *cis*-CO), 199.2 (d, $^2J_{\text{P,C}} = 24.8$ Hz, *trans*-CO).

$^{29}\text{Si}\{^1\text{H}\}$ NMR (59.6 MHz, C_6D_6): δ = -2.83 (d, $^2J_{\text{P,Si}} = 8.0$ Hz, $\text{Si}(\text{CH}_3)_3$), -0.01 (d, $^2J_{\text{P,Si}} = 1.5$ Hz, $\text{Si}(\text{CH}_3)_3$).

^{31}P NMR (121.5 MHz, C_6D_6): δ = 150.7 (dd_{sat}, $^1J_{\text{W,P}} = 274.0$ Hz, $^2J_{\text{P,H}} = 18.9$ Hz, $^2J_{\text{P,H}} = 11.3$ Hz).

MS (EI, 70 eV, ^{184}W , selected data): m/z (%) = 586.1 (30) $[\text{M}]^{++}$, 530.1 (10) $[\text{M} - 2\text{CO}]^+$, 502.1 (20) $[\text{M} - 3\text{CO}]^+$, 474.0 (15) $[\text{M} - 4\text{CO}]^+$, 446.0 (35) $[\text{M} - 5\text{CO}]^+$, 418.0 (50) $[\text{M} - 4\text{CO} - \text{C}_4\text{H}_8]^+$, 390.0 (100) $[\text{M} - 5\text{CO} - \text{C}_4\text{H}_8]^+$, 73.1 (70) $[\text{SiMe}_3]^+$.

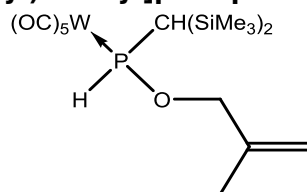
IR (ATR Diamond; $\tilde{\nu}[\text{cm}^{-1}]$, selected data): 2071 (s, $\nu(\text{CO})$), 1998 (w, $\nu(\text{CO})$), 1905 (vs, $\nu(\text{CO})$).

Elemental analysis:

calc.:	C	32.77	H	4.64
found:	C	32.64	H	4.84

Single crystal measurement: GSTR390, AKY-469-F2 // GXray3852f

11.2.8.12 Pentacarbonyl{[(2-methyl-2-propenyl)oxy][bis(trimethylsilyl)methyl]phosphane- κ P}tungsten(0) [4.1d]



Purification: The crude product was separated from the reaction mixture of the synthesis of **25.1a** by column chromatography ($\varnothing = 2$ cm, $h = 6$ cm, petroleum ether, -20 °C, SiO_2) after initial removal of all volatiles in *vacuo* (ca. 0.02 mbar). The first yellow fraction using pure petroleum ether was collected. After evaporation of all volatiles in *vacuo* (ca. 0.02 mbar) the product was washed at -100 °C three times with 2 mL of *n*-pentane to yield the product as yellow powder.

<u>Molecular formula:</u>	$\text{C}_{16}\text{H}_{27}\text{O}_6\text{PSi}_2\text{W}$
<u>Molecular weight:</u>	586.366 g/mol
<u>Melting point:</u>	44 °C
<u>Yield:</u>	85 mg (0.14 mmol, 14 %)

^1H NMR (300.1 MHz, C_6D_6): $\delta = 0.01$ (s, 9H, $\text{Si}(\text{CH}_3)_3$), 0.24 (s, 9H, $\text{Si}(\text{CH}_3)_3$), 0.87 (s_{br}, 1H, P-CH), 1.57 (s_{br}, 3H, CH_3), 4.00 (dd, 1H, $^3J_{\text{P,H}} = 8.4$ Hz, $^2J_{\text{H,H}} = 11.4$ Hz, O- CH_2), 3.67 (dd, 1H, $^3J_{\text{P,H}} = 9.0$ Hz, $^2J_{\text{H,H}} = 11.4$ Hz, O- CH_2), 4.76 (s_{br}, 1H, CH_2), 4.93 (s_{br}, 1H, CH_2), 7.69 (dd, 1H, $^1J_{\text{P,H}} = 322.4$ Hz, $^3J_{\text{H,H}} = 1.1$ Hz, P-H).

$^{13}\text{C}\{^1\text{H}\}$ NMR (75.5 MHz, C_6D_6): $\delta = 0.2$ (d, $^3J_{\text{P,C}} = 2.5$ Hz, $\text{Si}(\text{CH}_3)_3$), 2.1 (d, $^3J_{\text{P,C}} = 2.9$ Hz, $\text{Si}(\text{CH}_3)_3$), 19.5 (s, CH_3), 23.7 (d, $^1J_{\text{P,C}} = 13.3$ Hz, CH), 73.7 (d, $^2J_{\text{P,C}} = 3.6$ Hz, CH_2), 114.4 (s, CH_2), 140.6 (d, $^3J_{\text{P,C}} = 8.4$ Hz, $\text{C}=\text{CH}_2$), 197.2 (d_{sat}, $^1J_{\text{W,C}} = 125.4$ Hz, $^2J_{\text{P,C}} = 7.4$ Hz, *cis*-CO), 199.4 (d, $^2J_{\text{P,C}} = 24.6$ Hz, *trans*-CO).

$^{29}\text{Si}\{^1\text{H}\}$ NMR (59.6 MHz, C_6D_6): $\delta = 0.05$ (d, $^2J_{\text{P,Si}} = 5.7$ Hz, $\text{Si}(\text{CH}_3)_3$), 1.72 (d, $^2J_{\text{P,Si}} = 9.0$ Hz, $\text{Si}(\text{CH}_3)_3$).

^{31}P NMR (121.5 MHz, C_6D_6): $\delta = 103.6$ (ddd_{sat}, $^1J_{\text{W,P}} = 268.1$ Hz, $^1J_{\text{P,H}} = 322.3$ Hz, $^3J_{\text{P,H}} = 9.0$ Hz, $^3J_{\text{P,H}} = 8.4$ Hz).

MS (EI, 70 eV, ^{184}W , selected data): m/z (%) = 586.1 (55) $[\text{M}]^{++}$, 558.1 (5) $[\text{M} - \text{CO}]^+$, 530.1 (20) $[\text{M} - 2\text{CO}]^+$, 500.1 (85) $[\text{M} - 2\text{CO} - \text{C}_2\text{H}_6]^+$, 474.0 (15) $[\text{M} - 4\text{CO}]^+$, 444.1 (65) $[\text{M} - 4\text{CO} - \text{C}_2\text{H}_6]^+$, 73.1 (100) $[\text{SiMe}_3]^+$.

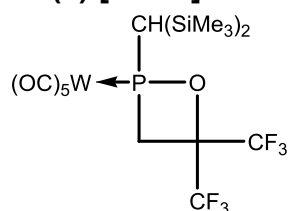
IR (ATR Diamond; $\tilde{\nu}[\text{cm}^{-1}]$, selected data): 2276 (w, $\nu(\text{PH})$), 2070 (s, $\nu(\text{CO})$), 1982 (m, $\nu(\text{CO})$), 1907 (vs, $\nu(\text{CO})$).

Elemental analysis:

calc.:	C	32.77	H	4.64
found:	C	32.87	H	4.70

Single crystal measurement: GSTR388, AKY-469-F1 // GXray3851f

11.2.8.13 Pentacarbonyl{4,4-bis(trifluoromethyl)-2-[bis(trimethylsilyl)methyl]-1,2-oxaphosphetane- κP }tungsten(0) [25.1b]



Purification: All volatiles were removed in *vacuo* (ca. 0.02 mbar). The crude product was extracted with diethyl ether (two times 15 mL) and the solvent was removed in *vacuo* (ca. 0.02 mbar). The product was obtained via precipitation from *n*-pentane at -100 °C and removing the supernatant solution by filtration, which was repeated three times. The product was obtained as mixture of two isomers (ratio (isomer 1 : isomer 2) 96:4) and all data are given for the mixture.

Thermal isomerization: 50 mg of the 96:4 mixture of **25.1¹** and **25.1²** were dissolved in 0.5 mL of toluene-*d*₈ and heated in a closed NMR tube with Young valve to 85 °C for 3 days. The ratio between the two isomers changed slowly to finally yield a mixture of 7:93 (**25.1¹**:**25.1²**) together with some unidentified impurities.

Molecular formula:	C ₁₆ H ₂₁ F ₆ O ₆ PSi ₂ W
Molecular weight:	694.310 g/mol
Melting point:	83 °C
Yield:	257 mg (0.37 mmol, 37 %)

Isomer 1:

¹H NMR (300.1 MHz, CDCl₃): δ = 0.30 (s, 9H, Si(CH₃)₃), 0.34 (s, 9H, Si(CH₃)₃), 2.25 (d, 1H, ²J_{P,H} = 4.0 Hz, CH), 3.57 (d, 1H, ²J_{H,H} = 15.0 Hz, CH₂), 3.85 (dd, 1H, ²J_{H,H} = 15.0 Hz, ²J_{P,H} = 11.3 Hz, CH₂).

¹³C{¹H} NMR (75.5 MHz, CDCl₃): δ = 2.6 (d, ³J_{P,C} = 3.2 Hz, Si(CH₃)₃), 2.9 (d, ³J_{P,C} = 1.9 Hz, Si(CH₃)₃), 35.0 (d, ¹J_{P,C} = 26.5 Hz, P-CH₂), 43.3 (d, ¹J_{P,C} = 12.9 Hz, P-CH), 79.0 – 82.0 (m, O-C(CF₃)₂), 121.7 (q, ¹J_{F,C} = 284.5 Hz, CF₃), 122.1 (qd, ¹J_{F,C} = 285.5 Hz, ³J_{P,C} = 4.5 Hz, CF₃), 196.2 (dq_{sat}, ¹J_{W,C} = 126.1 Hz, ²J_{P,C} = 7.8 Hz, ⁶J_{F,C} = 1.5 Hz, *cis*-CO), 199.0 (d, ²J_{P,C} = 31.0 Hz, *trans*-CO).

$^{19}\text{F}\{^1\text{H}\}$ NMR (282.4 MHz, CDCl_3): $\delta = -77.8$ (qd, $^4J_{\text{F,F}} = 9.9$ Hz, $^4J_{\text{P,F}} = 1.9$ Hz, CF_3), -76.3 (qd, $^4J_{\text{F,F}} = 9.9$ Hz, $^4J_{\text{P,F}} = 3.4$ Hz, CF_3).

$^{29}\text{Si}\{^1\text{H}\}$ NMR (59.6 MHz, CDCl_3): $\delta = -0.07$ (d, $^2J_{\text{P,Si}} = 7.6$ Hz, $\text{Si}(\text{CH}_3)_3$), 2.81 (d, $^2J_{\text{P,Si}} = 6.8$ Hz, $\text{Si}(\text{CH}_3)_3$).

$^{31}\text{P}\{^1\text{H}\}$ NMR (121.5 MHz, CDCl_3): $\delta = 198.2$ (s_{sat} , $^1J_{\text{W,P}} = 297.6$ Hz).

Isomer 2:

^1H NMR (300.1 MHz, toluene- d_8): $\delta = 0.05$ (s, 9H, $\text{Si}(\text{CH}_3)_3$), 0.22 (s, 9H, $\text{Si}(\text{CH}_3)_3$), 2.70 (d, 1H, $^2J_{\text{P,H}} = 19.5$ Hz, P-CH), 2.85 (dd, 1H, $^2J_{\text{H,H}} = 15.2$ Hz, $^2J_{\text{P,H}} = 10.5$ Hz, P- CH_2), 3.11 (d, 1H, $^2J_{\text{H,H}} = 15.2$ Hz, P- CH_2).

$^{13}\text{C}\{^1\text{H}\}$ NMR (75.5 MHz, toluene- d_8): $\delta = 1.9$ (d, $^3J_{\text{P,C}} = 4.2$ Hz, $\text{Si}(\text{CH}_3)_3$), 2.3 (d, $^3J_{\text{P,C}} = 3.6$ Hz, $\text{Si}(\text{CH}_3)_3$), 38.4 (d, $^1J_{\text{P,C}} = 27.5$ Hz, P-CH), 40.0 (d, $^1J_{\text{P,C}} = 28.1$ Hz, P- CH_2), $80 - 83$ (m, $\text{C}(\text{CF}_3)_2$), 122.0 (q, $^1J_{\text{F,C}} = 284.8$ Hz, CF_3), 122.6 (q, $^1J_{\text{F,C}} = 289.0$ Hz, CF_3), 196.1 (dq $_{\text{sat}}$, $^1J_{\text{W,C}} = 125.7$ Hz, $^2J_{\text{P,C}} = 7.5$ Hz, $^6J_{\text{F,C}} = 0.4$ Hz, *cis*-CO), 197.5 (d, $^2J_{\text{P,C}} = 29.4$ Hz, *trans*-CO).

$^{19}\text{F}\{^1\text{H}\}$ NMR (282.4 MHz, toluene- d_8): $\delta = -77.4$ (q, $^4J_{\text{F,F}} = 10.1$ Hz, CF_3), -76.6 (qd, $^4J_{\text{F,F}} = 10.1$ Hz, $^4J_{\text{P,F}} = 2.1$ Hz, CF_3).

$^{29}\text{Si}\{^1\text{H}\}$ NMR (59.6 MHz, toluene- d_8): $\delta = -1.60$ (d, $^2J_{\text{P,Si}} = 9.1$ Hz, $\text{Si}(\text{CH}_3)_3$), 1.46 (s, $\text{Si}(\text{CH}_3)_3$).

$^{31}\text{P}\{^1\text{H}\}$ NMR (121.5 MHz, toluene- d_8): $\delta = 191.5$ (s_{sat} , $^1J_{\text{W,P}} = 295.0$ Hz).

MS (EI, 70 eV, ^{184}W , selected data): m/z (%) = 694.0 (50) $[\text{M}]^+$, 638.0 (20) $[\text{M} - 2 \text{CO}]^+$, 610.0 (100) $[\text{M} - 3 \text{CO}]^+$, 554.0 (15) $[\text{M} - 5 \text{CO}]^+$, 474.0 (5) $[\text{M} - 1 \text{CO} - \text{C}_4\text{H}_2\text{F}_6]^+$, 446.0 (5) $[\text{M} - 2 \text{CO} - \text{C}_4\text{H}_2\text{F}_6]^+$, 446.0 (10) $[\text{M} - 3 \text{CO} - \text{C}_4\text{H}_2\text{F}_6]^+$, 418.0 (10) $[\text{M} - 4 \text{CO} - \text{C}_4\text{H}_2\text{F}_6]^+$, 390.0 (30) $[\text{M} - 5 \text{CO} - \text{C}_4\text{H}_2\text{F}_6]^+$, 73.1 (100) $[\text{SiMe}_3]^+$.

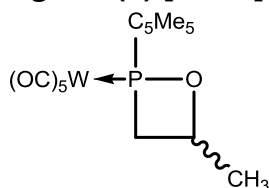
IR (ATR Diamond; $\tilde{\nu}[\text{cm}^{-1}]$, selected data): 2077 (s, $\nu(\text{CO})$), 1996 (w, $\nu(\text{CO})$), 1910 (vs, $\nu(\text{CO})$).

Elemental analysis:

calc.:	C	27.68	H	3.05
found:	C	27.69	H	3.28

Single crystal measurement: GSTR378, 3684f

11.2.8.14 Pentacarbonyl[4-methyl-2-(1,2,3,4,5-pentamethylcyclopenta-2,4-dien-1-yl)-1,2-oxaphosphetane- κP]tungsten(0) [21.2a]



Analysis: After reaching ambient temperature the reaction mixture was analysed by $^{31}\text{P}\{^1\text{H}\}$ NMR. The spectrum showed two isomeric 1,2-oxaphosphetane complexes.

Isomeric ratio: 53 : 47

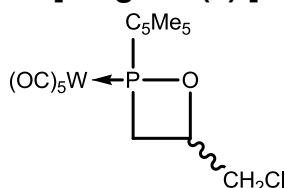
Isomer 1:

$^{31}\text{P}\{^1\text{H}\}$ NMR (121.5 MHz, Et_2O): $\delta = 184.8$ (s_{sat} , $^1J_{\text{W,P}} = 279.5$ Hz).

Isomer 2:

$^{31}\text{P}\{^1\text{H}\}$ NMR (121.5 MHz, Et_2O): $\delta = 174.0$ (s_{sat} , $^1J_{\text{W,P}} = 273.6$ Hz).

11.2.8.15 Pentacarbonyl[4-chloromethyl-2-(1,2,3,4,5-pentamethylcyclopenta-2,4-dien-1-yl)-1,2-oxaphosphetane- κP]tungsten(0) [21.2e]



Analysis: After reaching ambient temperature the reaction mixture was analysed by $^{31}\text{P}\{^1\text{H}\}$ NMR. The spectrum showed two isomeric 1,2-oxaphosphetane complexes.

Isomeric ratio: 53 : 47

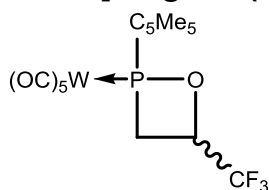
Isomer 1:

$^{31}\text{P}\{^1\text{H}\}$ NMR (121.5 MHz, Et_2O): $\delta = 189.6$ (s_{sat} , $^1J_{\text{W,P}} = 283.6$ Hz).

Isomer 2:

$^{31}\text{P}\{^1\text{H}\}$ NMR (121.5 MHz, Et_2O): $\delta = 178.4$ (s_{sat} , $^1J_{\text{W,P}} = 280.0$ Hz).

11.2.8.16 Pentacarbonyl[4-(trifluoromethyl)-2-(1,2,3,4,5-pentamethylcyclopenta-2,4-dien-1-yl)-1,2-oxaphosphetane-κP]tungsten(0) [21.2g]



Purification: All volatiles were removed in *vacuo* (ca. 0.02 mbar). The crude product was extracted from the formed salt with three times 20 mL of diethyl ether and the solvent was removed in *vacuo* (ca. 0.02 mbar). The product was purified via precipitation from 2 mL of *n*-pentane at -100 °C and filtering off the supernatant solution, which was repeated three times. A mixture of two isomers was obtained and all data are given for the mixture.

<u>Molecular formula:</u>	C ₁₈ H ₁₈ F ₃ O ₆ PW
<u>Molecular weight:</u>	602.145 g/mol
<u>Melting point:</u>	93 °C
<u>Yield:</u>	214 mg (0.36 mmol, 36 %)

Isomeric ratio: 73 : 27

Isomer 1:

¹H NMR (300.1 MHz, C₆D₆): δ = 1.73 (d, 3H, *J*_{P,H} = 11.0 Hz, C₅Me₅), 1.79 (s, 3H, C₅Me₅), 1.80 - 1.85 (m, 6H, C₅Me₅), 1.96 (s, 3H, C₅Me₅), 3.51 (dd, 1H, ²*J*_{H,H} = 14.5 Hz, ³*J*_{H,H} = 7.0 Hz, P-CH₂), 3.56 (ddd, 1H, ²*J*_{P,H} = 8.5 Hz, ²*J*_{H,H} = 14.5 Hz, ³*J*_{H,H} = 8.5 Hz, P-CH₂), 5.20 - 5.32 (m, 1H, O-CH).

¹³C{¹H} NMR (75.5 MHz, C₆D₆): δ = 11.7 - 11.9 (m, 3 times C₅Me₅), 11.96 (d, *J*_{P,C} = 2 Hz, C₅Me₅), 14.18 (d, *J*_{P,C} = 5.2 Hz, C₅Me₅), 30.4 (dq, ¹*J*_{P,C} = 24.1 Hz, ³*J*_{F,C} = 1 Hz, P-CH₂), 65.7 (d, *J*_{P,C} = 1.6 Hz, C₅Me₅), 78.6 (qd, ²*J*_{F,C} = 37.0 Hz, ²*J*_{P,C} = 11.9 Hz, O-CH), 123.2 (qd, ¹*J*_{F,C} = 279.8 Hz, ³*J*_{P,C} = 5.0 Hz, CF₃), 132.5 (d, *J*_{P,C} = 7.8 Hz, C=C), 138.8 (d, *J*_{P,C} = 2.2 Hz, C=C), 142.2 (d, *J*_{P,C} = 6.2 Hz, C=C), 144.1 (d, *J*_{P,C} = 7.2 Hz, C=C), 195.0 (d_{sat}, ¹*J*_{W,C} = 125.7 Hz, ²*J*_{P,C} = 7.6 Hz, *cis*-CO), 198.2 (d, ²*J*_{P,C} = 30.9 Hz, *trans*-CO).

¹⁹F{¹H} NMR (282.4 MHz, C₆D₆): δ = -81.3 (s, CF₃).

³¹P{¹H} NMR (121.5 MHz, C₆D₆): δ = 200.8 (s_{sat}, ¹*J*_{W,P} = 292.3 Hz).

Isomer 2:

¹H NMR (300.1 MHz, C₆D₆): δ = 1.61 (d, 3H, *J*_{P,H} = 12.1 Hz, C₅Me₅), 1.73 (s, 3H, C₅Me₅), 1.80 - 1.85 (m, 6H, 2 times C₅Me₅), 1.92 (s, 3H, C₅Me₅), 3.09 (ddd, 1H, ²*J*_{P,H} = 3.1 Hz, ²*J*_{H,H} = 13.3 Hz, ³*J*_{H,H} = 7.1 Hz, P-CH₂), 3.90 (ddd, 1H, ²*J*_{P,H} = 11.8 Hz, ²*J*_{H,H} = 13.3 Hz, ³*J*_{H,H} = 8.8 Hz, P-CH₂), 5.28 - 5.42 (m, 1H, O-CH).

$^{13}\text{C}\{^1\text{H}\}$ NMR (75.5 MHz, C_6D_6): $\delta = 11.3$ (d, $J_{\text{P,C}} = 2.8$ Hz, C_5Me_5), 11.7 (d, $J_{\text{P,C}} = 1.5$ Hz, C_5Me_5) 11.7 - 11.9 (m, 2 times C_5Me_5), 13.8 (dq, $J_{\text{P,C}} = 5.2$ Hz, $J_{\text{F,C}} = 2.6$ Hz, C_5Me_5), 32.8 (dq, $^1J_{\text{P,C}} = 20.3$ Hz, $^3J_{\text{F,C}} = 1.1$ Hz, P- CH_2), 65.5 (d, $J_{\text{P,C}} = 4.7$ Hz, C_5Me_5), 75.0 (qd, $^2J_{\text{F,C}} = 37.8$ Hz, $^2J_{\text{P,C}} = 12.0$ Hz, O-CH), 123.1 (qd, $^1J_{\text{F,C}} = 279.9$ Hz, $^3J_{\text{P,C}} = 6.4$ Hz, CF_3), 132.3 (d, $J_{\text{P,C}} = 8.0$ Hz, C=C), 138.5 (d, $J_{\text{P,C}} = 2.5$ Hz, C=C), 142.7 (d, $J_{\text{P,C}} = 6.4$ Hz, C=C), 144.8 (d, $J_{\text{P,C}} = 7.5$ Hz, C=C), 195.5 (d_{sat} , $^1J_{\text{W,C}} = 125.3$ Hz, $^2J_{\text{P,C}} = 7.5$ Hz, *cis*-CO), 197.9 (d, $^2J_{\text{P,C}} = 30.0$ Hz, *trans*-CO).

$^{19}\text{F}\{^1\text{H}\}$ NMR (282.4 MHz, C_6D_6): $\delta = -79.5$ (s, CF_3).

$^{31}\text{P}\{^1\text{H}\}$ NMR (121.5 MHz, C_6D_6): $\delta = 186.1$ (s_{sat} $^1J_{\text{W,P}} = 284.0$ Hz).

MS (EI, 70 eV, ^{184}W , selected data): m/z (%) = 601.9 (50) $[\text{M}]^{++}$, 517.9 (15) $[\text{M} - 3\text{CO}]^+$, 466.8 (50) $[\text{M} - \text{C}_5\text{Me}_5]^+$, 438.8 (100) $[\text{M} - \text{C}_5\text{Me}_5 - \text{CO}]^+$, 410.8 (20) $[\text{M} - \text{C}_5\text{Me}_5 - 2\text{CO}]^+$, 135.1 (15) $[\text{C}_5\text{Me}_5]^+$.

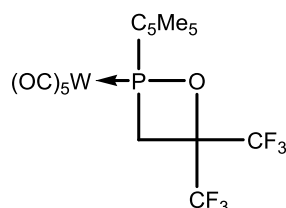
IR (ATR Diamond; $\tilde{\nu}[\text{cm}^{-1}]$, selected data): 2074 (s, $\nu(\text{CO})$), 2000 (w, $\nu(\text{CO})$), 1902 (vs, $\nu(\text{CO})$).

Elemental analysis:

calc.:	C	35.90	H	3.01
found:	C	35.78	H	3.28

Single crystal measurement: GSTR406, AKY-490 // GXray3961g

11.2.8.17 Pentacarbonyl[4,4-bis(trifluoromethyl)-2-(1,2,3,4,5-pentamethylcyclopenta-2,4-dien-1-yl)-1,2-oxaphosphetane- κP]tungsten(0) [25.2b]



Purification: All volatiles were removed in *vacuo* (ca. 0.02 mbar). The crude mixture was extracted from the formed salt with diethyl ether and the solvent was removed in *vacuo* (ca. 0.02 mbar). The pure product was obtained via precipitation from *n*-pentane at -100 °C and filtering off the supernatant solution, which was repeated three times.

Molecular formula: $\text{C}_{19}\text{H}_{17}\text{F}_6\text{O}_6\text{PW}$

Molecular weight: 670.139 g/mol

Melting point: 90 °C

Yield: 303 mg (0.45 mmol, 45 %)

$^1\text{H NMR}$ (300.1 MHz, CDCl_3): $\delta = 1.58$ (qd, 3H, $J_{\text{P,H}} = 11.5$ Hz, $J = 2.2$ Hz, C_5Me_5), 1.76 (s, 3H, C_5Me_5), 1.80 (d, 3H, $J_{\text{P,H}} = 2.8$ Hz, C_5Me_5), 1.82 (dd, 3H, $J_{\text{P,H}} = 1.98$ Hz, $J_{\text{H,H}} = 1.0$ Hz, C_5Me_5), 1.96 (s, 3H, C_5Me_5), 3.47 (dd, 1H, $^2J_{\text{H,H}} = 15.0$ Hz, $^2J_{\text{P,H}} = 2.2$ Hz, CH_2), 4.04 (dd, 1H, $^2J_{\text{H,H}} = 15.0$ Hz, $^2J_{\text{P,H}} = 10.7$ Hz, CH_2).

$^{13}\text{C}\{^1\text{H}\}$ NMR (75.5 MHz, CDCl_3): $\delta = 11.8$ (d, $J_{\text{P,C}} = 2.7$ Hz, C_5Me_5), 12.0 (s, C_5Me_5), 12.0 (d, $J_{\text{P,C}} = 2.1$ Hz, C_5Me_5), 12.0 (d, $J_{\text{P,C}} = 1.8$ Hz, C_5Me_5), 16.3 (dq, $J_{\text{P,C}} = 6.1$ Hz, $J_{\text{F,C}} = 6.1$ Hz, C_5Me_5), 32.0 (d, $^1J_{\text{P,C}} = 21.8$ Hz, P- CH_2), 66.8 (d, $^1J_{\text{P,C}} = 6.0$ Hz, P-C), 82.5 - 85.0 (m, $\text{C}(\text{CF}_3)_2$), 121.7 (q, $^1J_{\text{F,C}} = 284.9$ Hz, CF_3), 122.4 (qd, $^1J_{\text{F,C}} = 287.3$ Hz, $^3J_{\text{P,C}} = 2.7$ Hz, CF_3), 134.4 (d, $J_{\text{P,C}} = 10.1$ Hz, C=C), 139.7 (d, $J_{\text{P,C}} = 4.5$ Hz, C=C), 143.1 (d, $J_{\text{P,C}} = 6.9$ Hz, C=C), 144.0 (d, $J_{\text{P,C}} = 8.0$ Hz, C=C), 196.6 (dq_{sat}, $^1J_{\text{W,C}} = 126.0$ Hz, $^2J_{\text{P,C}} = 7.8$ Hz, $^6J_{\text{F,C}} = 2.6$ Hz *cis*-CO), 197.2 (d, $^2J_{\text{P,C}} = 33.1$ Hz, *trans*-CO).

$^{19}\text{F}\{^1\text{H}\}$ NMR (282.4 MHz, CDCl_3): $\delta = -74.6$ (qd, $^4J_{\text{F,F}} = 11.4$ Hz, $^4J_{\text{P,F}} = 3.8$ Hz, CF_3), -73.5 (qd, $^4J_{\text{F,F}} = 11.4$ Hz, $^4J_{\text{P,F}} = 0.4$ Hz, CF_3).

$^{31}\text{P}\{^1\text{H}\}$ NMR (121.5 MHz, CDCl_3): $\delta = 199.0$ (s_{sat}, $^1J_{\text{W,P}} = 295.1$ Hz).

MS (EI, 70 eV, ^{184}W , selected data): m/z (%) = 670.1 (40) $[\text{M}]^{++}$, 586.0 (300) $[\text{M} - 3 \text{CO}]^+$, 535.0 (40) $[\text{M} - \text{C}_5\text{Me}_5]^+$, 507.0 (70) $[\text{M} - \text{C}_5\text{Me}_5 - \text{CO}]^+$, 479.0 (20) $[\text{M} - \text{C}_5\text{Me}_5 - 2 \text{CO}]^+$, 464.0 (60) $[\text{M} - 5 \text{CO} - \text{C}_3\text{F}_6\text{O}]^+$, 135.1 (100) $[\text{C}_5\text{Me}_5]^+$.

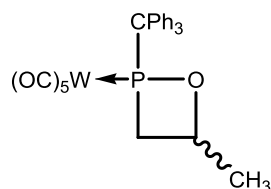
IR (ATR Diamond; $\tilde{\nu}[\text{cm}^{-1}]$, selected data): 2077 (s, $\nu(\text{CO})$), 1991 (w, $\nu(\text{CO})$), 1917 (vs, $\nu(\text{CO})$).

Elemental analysis:

calc.:	C	34.05	H	2.56
found:	C	34.25	H	2.84

Single crystal measurement: GSTR380, 3707f

11.2.8.18 Pentacarbonyl[4-methyl-2-(triphenylmethyl)-1,2-oxaphosphetane- κP]tungsten(0) [21.3a]



Purification: All volatiles were removed in *vacuo* (ca. 0.02 mbar) and the product was extracted from the formed salt with four times 20 mL of diethyl ether. Subsequent removal of the solvent in *vacuo* (ca. 0.02 mbar) and washing of the product with three times 3 mL of *n*-pentane at 0 °C yielded the product as slightly yellow powder. A mixture of two isomers was obtained and all data are given for the mixture.

<u>Molecular formula:</u>	C ₂₇ H ₂₁ O ₆ PW
<u>Molecular weight:</u>	656.058 g/mol
<u>Melting point:</u>	151 °C
<u>Yield:</u>	150 mg (0.23 mmol, 46 %)

Isomeric ratio: 47 : 53

Isomer 1:

¹H NMR (300.1 MHz, CDCl₃): δ = 1.62 (d, 3H, ³J_{H,H} = 6.4 Hz, CH₃), 3.08 (ddd, 1H, ³J_{P,H} = 2.1 Hz, ²J_{H,H} = 13.6 Hz, ³J_{H,H} = 6.3 Hz, CH₂), 3.36 (ddd, 1H, ³J_{P,H} = 11.0 Hz, ²J_{H,H} = 13.6 Hz, ³J_{H,H} = 8.6 Hz, CH₂), 4.86 - 4.82 (dm, 1H, ⁴J_{P,H} = 2.2 Hz, CH), 7.18 - 7.58 (m, 15H, CPh₃).

¹³C{¹H} NMR (75.5 MHz, CDCl₃): δ = 24.7 (d, ³J_{P,C} = 4.2 Hz, CH₃), 40.4 (d, ¹J_{P,C} = 25.5 Hz, P-CH₂), 67.3 (d, ¹J_{P,C} = 3.1 Hz, CPh₃), 81.5 (d, ²J_{P,C} = 12.6 Hz, O-CH), 127.8 (s_{br}, *para*-CH_{Ar}), 128.6 (s, CH_{Ar}), 131.4 (d, J_{P,C} = 7.1 Hz, CH_{Ar}), 140 - 142 (s_{br}, *ipso*-C), 196.5 (d_{sat}, ¹J_{W,C} = 126.4 Hz, ²J_{P,C} = 7.8 Hz, *cis*-CO), 199.1 (d, ²J_{P,C} = 31.0 Hz, *trans*-CO).

³¹P{¹H} NMR (121.5 MHz, CDCl₃): δ = 180.2 (s_{sat}, ¹J_{W,P} = 283.1 Hz).

Isomer 2:

¹H NMR (300.1 MHz, CDCl₃): δ = 1.16 (d, 3H, ³J_{H,H} = 6.2 Hz, CH₃), 3.10 - 3.16 (m, 2H, CH₂), 5.26 - 5.41 (dm, 1H, ⁴J_{P,H} = 1.8 Hz, CH), 7.18 - 7.58 (m, 15H, CPh₃).

¹³C{¹H} NMR (75.5 MHz, CDCl₃): δ = 23.4 (d, ³J_{P,C} = 4.0 Hz, CH₃), 42.6 (d, ¹J_{P,C} = 22.5 Hz, P-CH₂), 68.0 (d, ¹J_{P,C} = 4.4 Hz, CPh₃), 77.8 (d, ²J_{P,C} = 12.6 Hz, O-CH), 127.6 (s_{br}, *para*-CH_{Ar}), 128.6 (s, CH_{Ar}), 131.0 (d, J_{P,C} = 7.0 Hz, CH_{Ar}), 140 - 142 (s_{br}, *ipso*-C), 196.4 (d_{sat}, ¹J_{W,C} = 126.6 Hz, ²J_{P,C} = 7.3 Hz, *cis*-CO), 199.3 (d, ²J_{P,C} = 31.3 Hz, *trans*-CO).

³¹P{¹H} NMR (121.5 MHz, CDCl₃): δ = 161.0 (s_{sat}, ¹J_{W,P} = 278.3 Hz).

MS (EI, 70 eV, ¹⁸⁴W, selected data): m/z (%) = 656.0 (0.2) [M]⁺⁺, 572.0 (0.1) [M - 3 CO]⁺, 529.9 (5) [M - 3 CO - C₃H₆]⁺, 474.0 (5) [M - 5 CO - C₃H₆]⁺, 412.9 (10) [M - CPh₃]⁺, 370.8 (25) [M - CPh₃ - C₃H₆]⁺, 342.8 (10) [M - CO - CPh₃ - C₃H₆]⁺, 314.8 (5) [M - 2 CO - CPh₃ - C₃H₆]⁺, 243.0 (100) [CPh₃]⁺, 165.0 (60) [CPh₃ - C₆H₆]⁺.

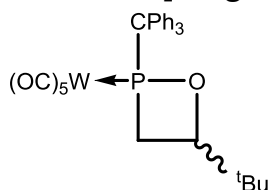
IR (ATR Diamond; ν[cm⁻¹], selected data): 2072 (s, ν(CO)), 1995 (w, ν(CO)), 1904 (vs, ν(CO)).

Elemental analysis:

calc.:	C	49.41	H	3.23
found:	C	49.90	H	3.55

Single crystal measurement: GSTR399, AKY-484 // GXray3939f

11.2.8.19 Attempted synthesis of pentacarbonyl[4-(1,1-dimethylethyl)-2-(triphenylmethyl)-1,2-oxaphosphetane- κ P]tungsten(0) [21.3d]



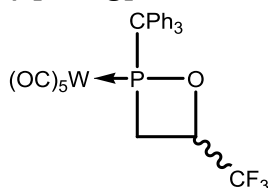
The synthesis of the complex was attempted as described in the general procedure. The reaction mixture was submitted for $^{31}\text{P}\{^1\text{H}\}$ NMR measurement. The NMR spectrum revealed full conversion to **21.3d** after 24 h as a mixture of two isomers.

Isomeric ratio: 52 : 48

Isomer 1: $^{31}\text{P}\{^1\text{H}\}$ NMR (121.5 MHz, Et_2O): $\delta = 181.0$ (s_{sat} , $^1J_{\text{W,P}} = 285.2$ Hz).

Isomer 2: $^{31}\text{P}\{^1\text{H}\}$ NMR (121.5 MHz, Et_2O): $\delta = 155.2$ (s_{sat} , $^1J_{\text{W,P}} = 279.9$ Hz).

11.2.8.20 Pentacarbonyl[4-(trifluoromethyl)-2-(triphenylmethyl)-1,2-oxaphosphetane- κ P]tungsten(0) [21.3g]



Purification: After the reaction was completed (checked by ^{31}P NMR spectroscopy), all volatiles were removed in *vacuo* (ca. 0.02 mbar). The crude product was extracted from the formed salt with 4 times 20 mL of diethyl ether and the solvent was removed in *vacuo* (ca. 0.02 mbar). The pure product was obtained by washing with *n*-pentane at 0° (two times 4 mL and two times 2 mL) and filtering off the supernatant solution, which was repeated three times. A mixture of two isomers was obtained and all data are given for the mixture.

Molecular formula:	$\text{C}_{27}\text{H}_{18}\text{F}_3\text{O}_6\text{PW}$
Molecular weight:	710.237 g/mol
Melting point:	169 $^\circ\text{C}$
Yield:	224 mg (0.32 mmol, 32 %)

Isomeric ratio: 42: 58

Isomer 1:

^1H NMR (300.1 MHz, CDCl_3): $\delta = 3.23 - 3.36$ (m, 1H, CH_2), 3.43 - 3.53 (m, 1 H, CH_2), 4.50 - 4.65 (m, 1H, CH), 7.10 - 7.70 (m, 15H, CPh_3).

$^{13}\text{C}\{^1\text{H}\}$ NMR (75.5 MHz, CDCl_3): $\delta = 33.3$ (d, $^1J_{\text{P,C}} = 27.2$ Hz, P- CH_2), 67.9 (d, $^1J_{\text{P,C}} = 1.8$ Hz, CPh_3), 77.7 (qd, $^2J_{\text{F,C}} = 37.5$ Hz, $^2J_{\text{P,C}} = 12.1$ Hz, O-CH), 123.2 (qd, $^1J_{\text{F,C}} = 279.8$ Hz, $^3J_{\text{P,C}} = 5.1$ Hz, CF_3), 128.0 - 128.2 (m, *para*- CH_{Ar}), 128.9 (s, CH_{Ar}), 131.0 (d, $J_{\text{P,C}} = 6.8$ Hz, CH_{Ar}), 140.7 (s_{br} , *ipso*-C), 195.3 (d_{sat} , $^1J_{\text{W,C}} = 126.3$ Hz, $^2J_{\text{P,C}} = 7.4$ Hz, *cis*-CO), 198.3 (d, $^2J_{\text{P,C}} = 34.3$ Hz, *trans*-CO).

$^{19}\text{F}\{^1\text{H}\}$ NMR (282.4 MHz, CDCl_3): $\delta = -79.7$ (d, $^4J_{\text{P,F}} = 0.7$ Hz, CF_3).

$^{31}\text{P}\{^1\text{H}\}$ NMR (121.5 MHz, CDCl_3): $\delta = 194.3$ (s_{sat} , $^1J_{\text{W,P}} = 295.3$ Hz).

Isomer 2:

^1H NMR (300.1 MHz, CDCl_3): $\delta = 2.98 - 3.07$ (m, 1H, CH_2), 3.65 - 3.80 (m, 1H, CH_2), 5.15 - 5.29 (m, 1H, CH), 7.18 - 7.58 (m, 15H, CPh_3).

$^{13}\text{C}\{^1\text{H}\}$ NMR (75.5 MHz, CDCl_3): $\delta = 36.1$ (d, $^1J_{\text{P,C}} = 24.2$ Hz, P- CH_2), 69.4 (d, $^1J_{\text{P,C}} = 5.5$ Hz, CPh_3), 73.3 (qd, $^2J_{\text{F,C}} = 38.8$ Hz, $^2J_{\text{P,C}} = 11.6$ Hz, O-CH), 122.1 (qd, $^1J_{\text{F,C}} = 280.8$ Hz, $^3J_{\text{P,C}} = 8.5$ Hz, CF_3), 128.0 - 128.2 (m, *para*- CH_{Ar}), 128.9 (s, CH_{Ar}), 131.2 (d, $J_{\text{P,C}} = 7.3$ Hz, CH_{Ar}), 139.3 (s_{br} , *ipso*-C), 195.5 (d_{sat} , $^1J_{\text{W,C}} = 126.5$ Hz, $^2J_{\text{P,C}} = 7.1$ Hz, *cis*-CO), 197.9 (d, $^2J_{\text{P,C}} = 33.3$ Hz, *trans*-CO).

$^{19}\text{F}\{^1\text{H}\}$ NMR (282.4 MHz, CDCl_3): $\delta = -77.3$ (d, $^4J_{\text{P,F}} = 0.9$ Hz, CF_3).

$^{31}\text{P}\{^1\text{H}\}$ NMR (121.5 MHz, CDCl_3): $\delta = 167.5$ (s_{sat} , $^1J_{\text{W,P}} = 287.1$ Hz).

MS (EI, 70 eV, ^{184}W , selected data): m/z (%) = 710.2 (0.02) $[\text{M}]^{++}$, 628.0 (0.02) $[\text{M} - 3 \text{CO}]^+$, 530.0 (0.01) $[\text{M} - 3 \text{CO} - \text{C}_3\text{H}_3\text{F}_3]^+$, 474.0 (0.3) $[\text{M} - 4 \text{CO} - \text{C}_3\text{H}_3\text{F}_3]^+$, 438.9 (0.5) $[\text{M} - \text{CPh}_3 - \text{CO}]^+$, 243.1 (100) $[\text{CPh}_3]^+$.

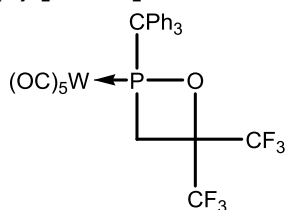
IR (ATR Diamond; $\tilde{\nu}[\text{cm}^{-1}]$, selected data): 2075 (s, $\nu(\text{CO})$), 1995 (w, $\nu(\text{CO})$), 1909 (vs, $\nu(\text{CO})$).

Elemental analysis:

calc.:	C	45.66	H	2.55
found:	C	46.01	H	3.07

Single crystal measurement: GSTR398, AKY-487 // GXray3940f

11.2.8.21 Pentacarbonyl[4,4-bis(trifluoromethyl)-2-(triphenylmethyl)-1,2-oxaphosphetane-κP]tungsten(0) [25.3b]



Purification: After the reaction solution reached $-10\text{ }^{\circ}\text{C}$ (ca. 105 min.), the solvent was removed in *vacuo* (ca. 0.02 mbar). The crude product was extracted with diethyl ether (three times 20 mL) and the extract, after evaporation of all volatiles in *vacuo* (ca. 0.02 mbar), subjected to column chromatography (Al_2O_3 , $\varnothing = 2\text{ cm}$, $h = 7\text{ cm}$, petroleum ether 40/60, $-20\text{ }^{\circ}\text{C}$). After 60 mL of petroleum ether were added a fraction using petroleum ether/toluene (5:1, 120 mL) and one fraction using petroleum ether/toluene (5:2, 135 mL) were collected. After combining, the solvent of the petroleum ether/toluene fractions was removed in *vacuo* (ca. 0.02 mbar) to yield the product as colourless foam that was washed once with 4 mL of petroleum ether at $-25\text{ }^{\circ}\text{C}$. Final drying at ca. 0.02 mbar yielded the product as white powder.

<u>Molecular formula:</u>	$\text{C}_{28}\text{H}_{17}\text{F}_6\text{O}_6\text{PW}$
<u>Molecular weight:</u>	778.235 g/mol
<u>Melting point:</u>	$147\text{ }^{\circ}\text{C}$
<u>Yield:</u>	188 mg (0.24 mmol, 32 %)

^1H NMR (500.17 MHz, CDCl_3): $\delta = 3.62$ (dd, 1H, $^2J_{\text{H,H}} = 15.2\text{ Hz}$, $^2J_{\text{P,H}} = 3.4\text{ Hz}$, CH_2), 4.26 (dd, 1H, $^2J_{\text{H,H}} = 15.2\text{ Hz}$, $^2J_{\text{P,H}} = 11.3\text{ Hz}$, CH_2), $7.30 - 7.56$ (m, 15H, CPh_3).

$^{13}\text{C}\{^1\text{H}\}$ NMR (125.78 MHz, CDCl_3): $\delta = 36.3$ (d, $^1J_{\text{P,C}} = 24.4\text{ Hz}$, P- CH_2), 70.6 (d, $^1J_{\text{P,C}} = 6.4\text{ Hz}$, CPh_3), $81.6 - 83.3$ (m, $\text{C}(\text{CF}_3)_2$), 120.4 (q, $^1J_{\text{F,C}} = 287.2\text{ Hz}$, CF_3), 122.3 (q, $^1J_{\text{P,C}} = 287.2\text{ Hz}$, CF_3), 128.2 (s, *para*- CH_{Ar}), 128.9 (s, CH_{Ar}), 131.8 (d, $J_{\text{P,C}} = 7.06\text{ Hz}$, CH_{Ar}), 139.4 (s_{br}, *ipso*-C), 195.3 (d_{sat,br}, $^2J_{\text{P,C}} = 4.6\text{ Hz}$, $^1J_{\text{W,C}} = 127.0\text{ Hz}$, *cis*-CO), 197.8 (d_{sat}, $^2J_{\text{P,C}} = 36.9\text{ Hz}$, $^1J_{\text{W,C}} = 136.7\text{ Hz}$, *trans*-CO).

$^{19}\text{F}\{^1\text{H}\}$ NMR (282.4 MHz, CDCl_3): $\delta = -72.6$ (qd, $^4J_{\text{P,F}} = 3.6\text{ Hz}$, $^4J_{\text{F,F}} = 10.7\text{ Hz}$, CF_3), -74.3 (q, $^4J_{\text{F,F}} = 10.7\text{ Hz}$, CF_3).

$^{31}\text{P}\{^1\text{H}\}$ NMR (202.5 MHz, CDCl_3): $\delta = 190.7$ (s_{sat}, $^1J_{\text{W,P}} = 299.0\text{ Hz}$).

LIFDI-MS: m/z (%) = 778.0 (100) $[\text{M}]^+$, 243.1 (15) $[\text{CPh}_3]^+$.

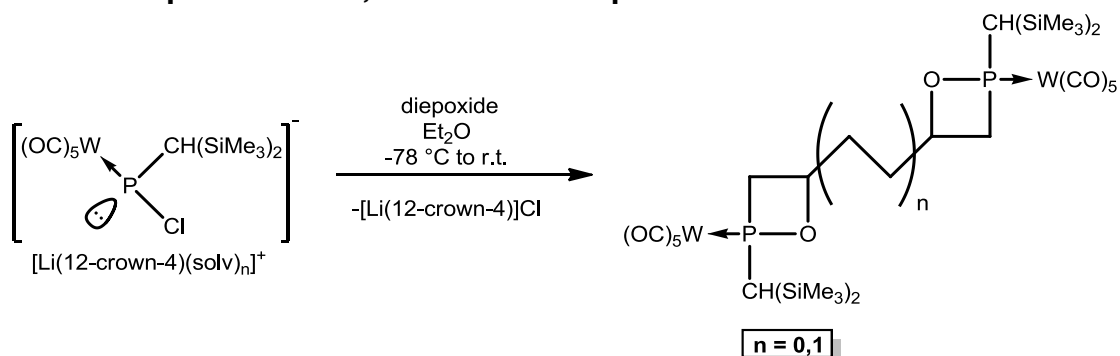
IR (ATR Diamond; $\tilde{\nu}[\text{cm}^{-1}]$, selected data): 2076 (s, $\nu(\text{CO})$), 1996 (m, $\nu(\text{CO})$), 1951 (w, $\nu(\text{CO})$), 1922 (vs, $\nu(\text{CO})$).

Elemental analysis:

calc.:	C	43.21	H	2.20
found:	C	43.23	H	2.46

Single crystal measurement: GSTR494, PB-13 // GXraymo_4641f

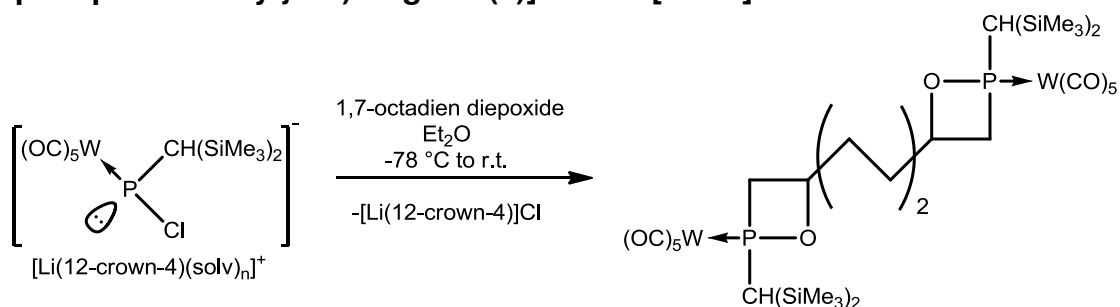
11.2.9 Attempted reactions of Li/Cl phosphinidenoid complex 2.1 with 1,3-butadiene diepoxide and 1,5-hexadiene diepoxide



Synthesis: A solution of Li/Cl phosphinidenoid complex **2.1** was prepared as described, starting from 117 mg (0.2 mmol) of $[(OC)_5W\{P(CH(SiMe_3)_2)Cl_2\}]$ (**1.1**) and either 9 μ L (0.1 mmol, 0.5 eq.) of 1,3-butadiene diepoxide (**20f**, $n = 0$) or 11 μ L (0.1 mmol, 0.5 eq.) of 1,5-hexadiene diepoxide (**28a**, $n = 1$) was added. The solution was allowed warming up to ambient temperature and during the warming up period formation of a white precipitate was observed.

Both reaction mixtures were subsequently analysed by $^{31}P\{^1H\}$ NMR measurement.

11.2.10 Synthesis of 1,4-bis[(pentacarbonyl{2-[bis(trimethylsilyl)methyl]-1,2-oxaphosphetane-4-yl}- κP)tungsten(0)]butane [**29.1c**]



Synthesis: A solution of Li/Cl phosphinidenoid complex **2.1** was prepared as described, starting from 585 mg (1.0 mmol) of $[(OC)_5W\{P(CH(SiMe_3)_2)Cl_2\}]$ (**1.1**) and 71 μ L (0.50 mmol, 0.5 eq.) of 1,7-octadiene diepoxide (**28b**) was added. The solution was allowed warming up to ambient temperature and during the warming up period formation of a white precipitate was observed.

Purification: All volatiles were removed in *vacuo* (ca 0.02 mbar). The product was purified by extraction with *n*-pentane (3 times 20 mL) and subsequent recrystallization from a saturated *n*-pentane solution at 4 °C. Complex **29.1c** was obtained as colorless crystals after drying in *vacuo* (ca. 0.02 mbar) and as a mixture of isomers. All data are given for the isomeric mixture.

Molecular formula: $C_{32}H_{52}O_{12}P_2Si_4W_2$

Molecular weight: 1170.724 g/mol

Yield: 180 mg (0.154 mmol, 31 %)

$^{31}P\{^1H\}$ NMR (121.5 MHz, $CDCl_3$): Three sets of signals between 165 - 168 ppm, 171 - 172 ppm and 177 - 180 ppm were observed. No further NMR distinguishing was possible due to the high amount of signals present.

MS (EI, 70 eV, ^{184}W , selected data): m/z (%) = 1170.1 (30) $[M]^{+}$, 1086.0 (5) $[M - 3 CO]^{+}$, 974.1 (5) $[M - 7 CO]^{+}$, 945.9 (5) $[M - 8 CO]^{+}$, 890.1 (20) $[M - 10 CO]^{+}$, 640.2 (40) $[M - (OC)_5WP(O)(CH(SiMe_3)_2)]^{+}$, 530.0 (20) $[(OC)_5WP(O)(CH(SiMe_3)_2)]^{+}$, 502.1 (40) $[(OC)_5WP(O)(CH(SiMe_3)_2) - CO]^{+}$, 474.0 (30) $[(OC)_5WP(O)(CH(SiMe_3)_2) - 2 CO]^{+}$, 446.0 (40) $[(OC)_5WP(O)(CH(SiMe_3)_2) - 3 CO]^{+}$, 418.0 (40) $[(OC)_5WP(O)(CH(SiMe_3)_2) - 4 CO]^{+}$, 390.0 (80) $[(OC)_5WP(O)(CH(SiMe_3)_2) - 5 CO]^{+}$, 73.1 (100) $[Me_3Si]^{+}$.

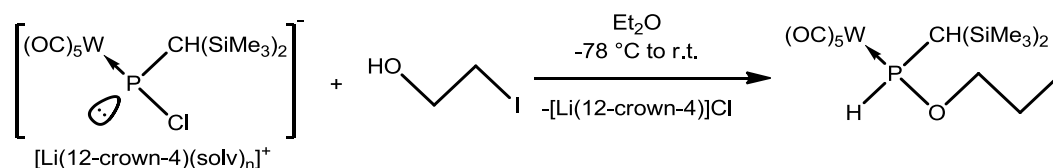
IR (ATR Diamond; $\tilde{\nu}[cm^{-1}]$, selected data): 2069 (s, $\nu(CO)$), 1978 (w, $\nu(CO)$), 1895 (vs, $\nu(CO)$).

Elemental analysis:

calc.:	C	32.83	H	4.48
found:	C	33.08	H	4.56

Single crystal measurement: GSTR348, 3322f

11.2.11 Synthesis of pentacarbonyl{(2-iodoethoxy)[bis(trimethylsilyl)methyl]phosphane- κ P}tungsten(0) [33.1_W]



Synthesis: A solution of Li/Cl phosphinidenoid complex **2.1** was prepared as described, starting from 585 mg (1.0 mmol) of [(OC)₅W{P(CH(SiMe₃)₂)Cl₂}] (**1.1**) and 0.08 mL (1.03 mmol, 1.03 eq.) of 2-iodoethanol (**35a**) was added. The solution was allowed warming up to ambient temperature and during the warming up period formation of a white precipitate was observed.

Purification: After the reaction was completed (checked by ³¹P NMR), all volatiles were removed in *vacuo* (ca. 0.02 mbar). The product was extracted from the formed salt with three times 20 mL of *n*-pentane and the solvent was removed in *vacuo* (ca. 0.02 mbar) to yield **33.1_W** as yellow oil.

Molecular formula: C₁₄H₂₄IO₆PSi₂W

Molecular weight: 686.226 g/mol

Yield: 624 mg (0.91 mmol, 91 %)

¹H NMR (300.1 MHz, CDCl₃): δ = 0.22 (s, 9H, Si(CH₃)₃), 0.30 (s, 9H, Si(CH₃)₃), 0.95 (s, 1H, P-CH), 3.30 (dd, 2H, ³J_{H,H} = 6.0 Hz, ³J_{H,H} = 6.0 Hz, CH₂-I), 3.73 - 3.91 (m, 1H, P-OCH₂), 4.00 - 4.18 (m, 1H, P-O-CH₂), 7.96 (dd, 1H, ¹J_{P,H} = 321.4 Hz, ³J_{H,H} = 1.2 Hz, P-H).

¹³C{¹H} NMR (75.5 MHz, CDCl₃): δ = 0.4 (d, ³J_{P,C} = 2.3 Hz, Si(CH₃)₃), 1.3 (d, ³J_{P,C} = 9.1 Hz, CH₂-I), 2.4 (d, ³J_{P,C} = 3.2 Hz, Si(CH₃)₃), 23.7 (d, ¹J_{P,C} = 13.6 Hz, P-CH), 70.0 (d, ²J_{P,C} = 2.6 Hz, P-OCH₂), 196.6 (d_{sat}, ¹J_{W,C} = 125.1 Hz, ²J_{P,C} = 7.4 Hz, *cis*-CO), 199.1 (d, ²J_{P,C} = 25.2 Hz, *trans*-CO).

²⁹Si{¹H} NMR (59.6 MHz, CDCl₃): δ = 0.89 (d, ²J_{P,Si} = 5.8 Hz, Si(CH₃)₃), 2.61 (d, ²J_{P,Si} = 9.2 Hz, Si(CH₃)₃).

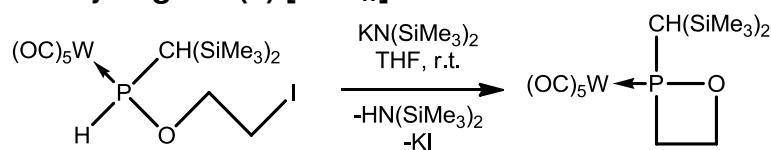
³¹P NMR (121.5 MHz, CDCl₃): δ = 106.7 (dm_{sat}, ¹J_{W,P} = 270.3 Hz, ¹J_{P,H} = 321.4 Hz).

MS (EI, 70 eV, ¹⁸⁴W, selected data): m/z (%) = 686.0 (15) [M]⁺, 657.9 (10) [M - CO]⁺, 602.0 (20) [M - 3 CO]⁺, 574.0 (30) [M - 4 CO]⁺, 546.0 (25) [M - 5 CO]⁺, 73.1 (100) [SiMe₃]⁺.

IR (ATR Diamond; $\tilde{\nu}$ [cm⁻¹], selected data): 2263 (w, ν (PH)), 2071 (s, ν (CO)), 1981 (w, ν (CO)), 1904 (vs, ν (CO)).

Single crystal measurement: GSTR383, AKY-424 // GXray3760f

11.2.12 Synthesis of pentacarbonyl{2-[bis(trimethylsilyl)methyl]-1,2-oxaphosphetane- κ P}tungsten(0) [34.1_w]



Synthesis: In a 50 mL Schlenk tube, 687.5 mg (1.26 mmol) of complex **33.1_w** were dissolved in 30 mL of THF. To it 315 mg (1.58 mmol, 1.25 eq.) of potassium hexamethyldisilazide in 3 mL of THF were added dropwise at room temperature. During addition a rapid formation of a precipitate and a change of the colour to yellow-brown was observed. The solution was kept on stirring for additional 60 minutes.

Purification: All volatiles were removed in *vacuo* (ca. 0.02 mbar). The product was purified by extraction from the formed salt with *n*-pentane (4 times 20 mL), followed by removal of all volatiles. Subsequent precipitation from 5 mL of *n*-pentane at -100 °C and filtering off the supernatant solution, which was repeated four times, yielded complex **34.1_w** as white powder, after drying in *vacuo* (ca. 0.02 mbar).

Molecular formula:	C ₁₄ H ₂₃ O ₆ PSi ₂ W
Molecular weight:	558.314 g/mol
Melting point:	77 °C
Yield:	457 mg (0.819 mmol, 65 %)

Measurement in C₆D₆:

¹H NMR (300.1 MHz, C₆D₆): δ = 0.08 (d, ⁴J_{P,H} = 0.4 Hz, 9H, Si(CH₃)₃), 0.16 (s, 9H, Si(CH₃)₃), 2.00 (d, 1H, ²J_{P,H} = 8.8 Hz, P-CH), 2.64 (ddd, 1H, ²J_{H,H} = 13.3 Hz, ³J_{H,H} = 8.2 Hz, ³J_{H,H} = 5.0 Hz, P-CH₂), 2.98 (dddd, 1H, ²J_{P,H} = 13.0 Hz, ²J_{H,H} = 13.3 Hz, ³J_{H,H} = 10.2 Hz, ³J_{H,H} = 8.2 Hz, P-CH₂), 4.04 (dddd, 1H, ³J_{P,H} = 10.5 Hz, ³J_{H,H} = 10.2 Hz, ²J_{H,H} = 7.5 Hz, ³J_{H,H} = 5.0 Hz, O-CH₂), 4.48 (dddd, 1H, ³J_{P,H} = 4.5 Hz, ³J_{H,H} = 8.2 Hz, ³J_{H,H} = 8.2 Hz, ²J_{H,H} = 7.5 Hz, O-CH₂).

¹³C{¹H} NMR (75.5 MHz, C₆D₆): δ = 1.7 (d, ³J_{P,C} = 4.2 Hz, Si(CH₃)₃), 2.1 (d, ³J_{P,C} = 2.6 Hz, Si(CH₃)₃), 35.4 (d_{br}, P-CH₂), 38.5 (d, ¹J_{P,C} = 14.6 Hz, P-CH), 68.9 (d, ²J_{P,C} = 15.2 Hz, O-CH₂), 197.5 (d_{sat}, ¹J_{W,C} = 125.8 Hz, ²J_{P,C} = 7.8 Hz, *cis*-CO), 200.7 (d, ²J_{P,C} = 25.2 Hz, *trans*-CO).

²⁹Si{¹H} NMR (59.6 MHz, C₆D₆): δ = -2.52 (s, Si(CH₃)₃), 0.05 (d, ²J_{P,Si} = 6.0 Hz, Si(CH₃)₃).

³¹P{¹H} NMR (121.5 MHz, C₆D₆): δ = 190.3 (s_{sat}, ¹J_{W,P} = 267.7 Hz).

Measurement in CDCl₃:

¹H NMR (300.1 MHz, CDCl₃): δ = 0.32 (d, ⁴J_{P,H} = 0.4 Hz, 9H, Si(CH₃)₃), 0.32 (s, 9H, Si(CH₃)₃), 2.10 (d, 1H, ²J_{P,H} = 8.7 Hz, P-CH), 3.21 (ddd, 1H, ²J_{H,H} = 13.2 Hz, ³J_{H,H} = 8.2 Hz, ³J_{H,H} = 5.0 Hz, P-CH₂), 3.60

(dddd, 1H, $^2J_{P,H} = 13.3$ Hz, $^2J_{H,H} = 13.2$ Hz, $^3J_{H,H} = 10.2$ Hz, $^3J_{H,H} = 8.0$ Hz, P-CH₂), 4.71 (dddd, 1H, $^3J_{P,H} = 10.3$ Hz, $^3J_{H,H} = 10.2$ Hz, $^2J_{H,H} = 7.4$ Hz, $^3J_{H,H} = 5.0$ Hz, O-CH₂), 5.00 (dddd, 1H, $^3J_{P,H} = 4.6$ Hz, $^3J_{H,H} = 8.2$ Hz, $^3J_{H,H} = 8.0$ Hz, $^2J_{H,H} = 7.4$ Hz, O-CH₂).

$^{13}\text{C}\{^1\text{H}\}$ NMR (125.8 MHz, CDCl₃): $\delta = 2.0$ (d, $^3J_{P,C} = 4.1$ Hz, Si(CH₃)₃), 2.3 (d, $^3J_{P,C} = 2.1$ Hz, Si(CH₃)₃), 35.4 (d_{br}, P-CH₂), 38.7 (d, $^1J_{P,C} = 14.2$ Hz, P-CH), 69.0 (d, $^2J_{P,C} = 15.3$ Hz, O-CH₂), 197.2 (d_{sat}, $^1J_{W,C} = 125.9$ Hz, $^2J_{P,C} = 7.9$ Hz, *cis*-CO), 200.6 (d_{sat}, $^1J_{W,C} = 137.7$ Hz, $^2J_{P,C} = 26.0$ Hz, *trans*-CO).

$^{31}\text{P}\{^1\text{H}\}$ NMR (121.5 MHz, CDCl₃): $\delta = 191.4$ (s_{sat}, $^1J_{W,P} = 268.5$ Hz).

MS (EI, 70 eV, ^{184}W , selected data): m/z (%) = 558.1 (50) [M]⁺, 502.1 (20) [M - 2 CO]⁺, 474.1 (30) [M - 3 CO]⁺, 446.0 (20) [M - 4 CO]⁺, 418.0 (40) [M - 5 CO]⁺, 390.0 (100) [M - 5 CO - C₂H₄]⁺, 73.1 (70) [SiMe₃]⁺.

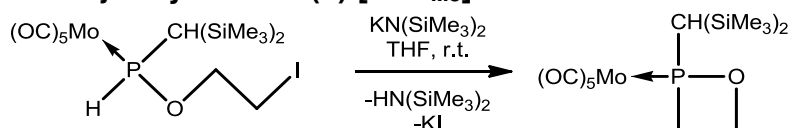
IR (ATR Diamond; $\tilde{\nu}$ [cm⁻¹], selected data): 2071 (s, $\nu(\text{CO})$), 1992 (w, $\nu(\text{CO})$), 1908 (vs, $\nu(\text{CO})$).

Elemental analysis:

calc.:	C	30.12	H	4.15
found:	C	30.23	H	4.30

Single crystal measurement: GSTR389, AKY-466 // GXray3853f

11.2.13 Synthesis of pentacarbonyl{2-[bis(trimethylsilyl)methyl]-1,2-oxaphosphetane- κ P}molybdenum(0) [34.1_{Mo}]



Synthesis: In a 50 mL Schlenk tube 522 mg (0.87 mmol) of complex **33.1_{Mo}** were dissolved in 10 mL of THF. To it 184 mg (0.92 mmol, 1.06 eq.) of potassium hexamethyldisilazide in 5 mL of THF were added dropwise at room temperature. The solution was kept on stirring for 30 minutes. During addition a rapid formation of a precipitate and a change of the colour to red-brown was observed.

Purification: All volatiles were removed in *vacuo* (ca. 0.02 mbar), yielding a red oil. This crude material was further purified by low temperature column chromatography ($\phi = 2$ cm, $h = 10$ cm, SiO₂, petroleum ether 40/60, -20 °C).

The product was obtained in the third, orange fraction using petroleum ether and diethyl ether (ratio PE/DE 50:2), after separation of the acyclic side products using pure petroleum ether (200 mL) and separating a yellow fraction using petroleum ether/diethyl ether mixture (50:2) (250 mL).

After evaporation of the solvent in *vacuo* (ca. 0.02 mbar) an orange oil was obtained. The final product was obtained by dissolving the oil in *n*-pentane and precipitation at -100 °C, followed by filtration and drying of the solid in *vacuo* (ca. 0.02 mbar).

<u>Molecular formula:</u>	C ₁₄ H ₂₃ MoO ₆ PSi ₂
<u>Molecular weight:</u>	470.433 g/mol
<u>Melting point:</u>	64 - 65 °C
<u>Yield:</u>	162 mg (0.34 mmol), 39 %

¹H NMR (500.1 MHz, CDCl₃): δ = 0.26 (s, 9H, Si(CH₃)₃), 0.31 (s, 9H, Si(CH₃)₃), 1.97 (d, 1H, ²J_{P,H} = 7.6 Hz, P-CH), 3.11 (ddd, 1H, ²J_{H,H} = 13.2 Hz, ³J_{H,H} = 8.2 Hz, ³J_{H,H} = 5.0 Hz, P-CH₂), 3.45 (dddd, 1H, ²J_{P,H} = 12.5 Hz, ²J_{H,H} = 13.2 Hz, ³J_{H,H} = 10.3 Hz, ³J_{H,H} = 8.5 Hz, P-CH₂), 4.73 (dddd, 1H, ³J_{P,H} = 9.8 Hz, ³J_{H,H} = 10.3 Hz, ²J_{H,H} = 7.5 Hz, ³J_{H,H} = 5.0 Hz, O-CH₂), 5.05 (dddd, 1H, ³J_{P,H} = 4.3 Hz, ³J_{H,H} = 8.5 Hz, ³J_{H,H} = 8.2 Hz, ²J_{H,H} = 7.5 Hz, O-CH₂).

¹³C{¹H} NMR (125.8 MHz, CDCl₃): δ = 2.0 (d, ³J_{P,C} = 4.2 Hz, Si(CH₃)₃), 2.3 (d, ³J_{P,C} = 2.2 Hz, Si(CH₃)₃), 35.1 (s_{br}, P-CH₂), 38.7 (d, ¹J_{P,C} = 19.8 Hz, P-CH), 69.3 (d, ²J_{P,C} = 14.2 Hz, O-CH₂), 205.5 (d_{sat}, ¹J_{Mo,C} = 68.2 Hz, ²J_{P,C} = 10.4 Hz, *cis*-CO), 210.8 (d, ²J_{P,C} = 27.5 Hz, *trans*-CO).

²⁹Si{¹H} NMR (99.4 MHz, CDCl₃): δ = -2.6 (s, Si(CH₃)₃), -0.26 (d, ²J_{P,Si} = 5.4 Hz, Si(CH₃)₃).

³¹P{¹H} NMR (202.5 MHz, CDCl₃): δ = 225.0 (s_{sat}, ¹J_{Mo,P} = 151.7 Hz).

MS (EI, 70 eV, ⁹⁸Mo, selected data): m/z (%) = 471.9 (35) [M]⁺, 443.9 (2) [M - CO]⁺, 415.9 (28) [M - 2 CO]⁺, 387.9 (91) [M - 3 CO]⁺, 359.9 (26) [M - 4 CO]⁺, 331.9 (65) [M - 5 CO]⁺, 301.9 (100) [M - 5 CO - C₂H₆]⁺, 271.9 (42) [M - 5 CO - 2 C₂H₆]⁺, 269.9 (56) [M - 5 CO - 2 C₂H₆ - H₂]⁺, 75.0 (16) [POC₂H₄]⁺, 73.0 (71) [SiMe₃]⁺.

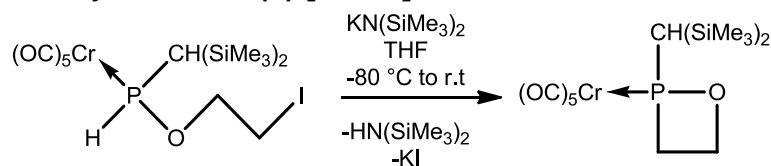
IR (ATR Diamond; ν̄[cm⁻¹], selected data): 1996 (s, ν(CO)), 1983 (s, ν(CO)), 1913 (vs, ν(CO)).

Elemental analysis:

calc.:	C	35.74	H	4.98
found:	C	35.73	H	5.04

Single crystal measurement: GSTR493, FG-oxa // GXray4661f

11.2.14 Synthesis of pentacarbonyl{2-[bis(trimethylsilyl)methyl]-1,2-oxaphosphetane- κ P}chromium(0) [34.1_{Cr}]



Synthesis: In a 100 mL Schlenk tube 1.108 g (2.0 mmol) of complex **33.1_{Cr}** were dissolved in 60 mL of THF. To it 439 mg (2.2 mmol, 1.1 eq.) of potassium hexamethyldisilazide were added as a solid at -80 °C. During addition a rapid formation of precipitate and a change of the colour to yellow-brown was observed. The solution was allowed to slowly warm up to ambient temperature overnight.

Purification: All volatiles were removed in *vacuo* (ca. 0.02 mbar). The crude material was subjected to low temperature column chromatography ($\varnothing = 3$ cm, $h = 5$ cm, SiO₂, PE, -20 °C). A first fraction using petroleum ether (200 mL) was discarded and a fraction using a mixture of petroleum ether and diethyl ether (40 : 1) was collected. All volatiles were removed from the second fraction in *vacuo* (ca. 0.02 mbar) and the formed solid was four times washed with 3 mL of *n*-pentane at -100 °C. Drying of the product in *vacuo* (ca. 0.02 mbar) yielded **34.1_{Cr}** as white solid.

Molecular formula:	C ₁₄ H ₂₃ CrO ₆ PSi ₂
Molecular weight:	426.470 g/mol
Melting point:	91 °C
Yield:	270 mg (0.63 mmol, 32 %)

¹H NMR (300.1 MHz, CDCl₃): $\delta = 0.26$ (s, 9H, Si(CH₃)₃), 0.32 (s, 9H, Si(CH₃)₃), 1.99 (d, 1H, ²J_{P,H} = 8.2 Hz, P-CH), 3.10 - 3.25 (m, 1H, P-CH₂), 3.35 - 3.57 (m, 1H, P-CH₂), 4.65 - 4.80 (m, 1H, O-CH₂), 4.96 - 5.11 (m, 1H, O-CH₂).

¹³C{¹H} NMR (75.5 MHz, CDCl₃): $\delta = 1.9$ (d, ³J_{P,C} = 4.0 Hz, Si(CH₃)₃), 2.3 (d, ³J_{P,C} = 1.9 Hz, Si(CH₃)₃), 34.6 (d_{br}, P-CH₂), 39.0 (d, ¹J_{P,C} = 18.6 Hz, P-CH), 69.3 (d, ²J_{P,C} = 14.6 Hz, O-CH₂), 216.2 (d, ²J_{P,C} = 15.2 Hz, *cis*-CO), 221.3 (d, ²J_{P,C} = 6.6 Hz, *trans*-CO).

³¹P{¹H} NMR (121.5 MHz, CDCl₃): $\delta = 250.2$ (s).

MS (EI, 70 eV, ⁵²Cr, selected data): m/z (%) = 426.0 (20) [M]⁺, 370.0 (10) [M - 2 CO]⁺, 342.0 (50) [M - 3 CO]⁺, 314.0 (35) [M - 4 CO]⁺, 286.0 (100) [M - 5 CO]⁺, 258.0 (80) [M - 5 CO - C₂H₄]⁺, 73.0 (25) [SiMe₃]⁺.

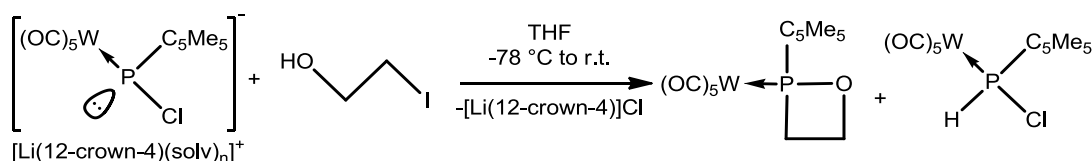
IR (ATR Diamond; $\tilde{\nu}$ [cm⁻¹], selected data): 2063 (s, ν (CO)), 1993 (w, ν (CO)), 1906 (vs, ν (CO)).

Elemental analysis:

calc.:	C	39.43	H	5.44
found:	C	39.21	H	5.51

Single crystal measurement: GSTR461, AKY-526 // GXraymo_4477f

11.2.15 Synthesis of pentacarbonyl[2-(1,2,3,4,5-pentamethylcyclopenta-2,4-dien-1-yl)-1,2-oxaphosphetane- κ P]tungsten(0) [34.2]



Synthesis: A solution of the Li/Cl phosphinidenoid complex **2.2** was prepared as described, starting from 841.5 mg (1.5 mmol) of dichlorophosphane complex $[(OC)_5W\{PCl_2(C_5Me_5)\}]$ (**2.2**), but using THF as solvent under otherwise similar conditions. 0.2 mL (2.58 mmol, 1.7 eq.) of 2-iodoethanol (**35a**) was added. The solution was allowed warming up to ambient temperature and during the warming up period formation of a white precipitate was observed.

Purification: After the reaction was completed (checked by ^{31}P NMR spectroscopy), a small amount of SiO_2 was added and all volatiles were removed in *vacuo* (ca. 0.02 mbar). The crude product was subjected to column chromatography ($\varnothing = 2$ cm, $h = 5$ cm, petroleum ether, -20 °C, SiO_2). The first fraction using pure petroleum ether contained acyclic side products. The second fraction using petroleum ether and diethyl ether (ratio 50:0.5) contained the product and **XXXVIII** as impurity. The solvent was removed in *vacuo* (ca. 0.02 mbar), the product was sublimed at 110 °C and $2.6 \cdot 10^{-2}$ mbar over one hour and obtained as slightly orange solid.

Molecular formula: $C_{17}H_{19}O_6PW$

Molecular weight: 534.143 g/mol

Melting point: 59-60 °C

Yield: 160 mg (0.30 mmol, 20 %)

1H NMR (400.1 MHz, $CDCl_3$): $\delta = 1.74$ (d, 3H, $J_{P,H} = 11.0$ Hz, C_5Me_5), 1.75 (s, 3H, C_5Me_5), 1.80 (dq, 3H, $J_{P,H} = 5.0$ Hz, $J_{H,H} = 1$ Hz, C_5Me_5), 1.82 (dq, 3H, $J_{P,H} = 4.3$ Hz, $J_{H,H} = 1.0$ Hz, C_5Me_5), 1.93 (s, 3H, C_5Me_5), 3.34 (dddd, 1H, $^2J_{P,H} = 0.4$ Hz, $^2J_{H,H} = 13.8$ Hz, $^3J_{H,H} = 9.2$ Hz, $^3J_{H,H} = 6.6$ Hz, P- CH_2), 3.63 (dddd, 1H, $^2J_{P,H} = 5.3$ Hz, $^2J_{H,H} = 13.8$ Hz, $^3J_{H,H} = 9.7$ Hz, $^3J_{H,H} = 6.5$ Hz, P- CH_2), 5.05 (dddd, 1H, $^3J_{P,H} = 2.2$ Hz, $^2J_{H,H} = 7.1$ Hz, $^3J_{H,H} = 9.7$ Hz, $^3J_{H,H} = 6.6$ Hz, O- CH_2), 5.16 (dddd, 1H, $^3J_{P,H} = 3.3$ Hz, $^2J_{H,H} = 7.1$ Hz, $^3J_{H,H} = 9.2$ Hz, $^3J_{H,H} = 6.5$ Hz, O- CH_2).

$^{13}\text{C}\{^1\text{H}\}$ NMR (100.7 MHz, CDCl_3): $\delta = 11.5$ (d, $J_{\text{P,C}} = 2.8$ Hz, C_5Me_5), 11.5 (d, $J_{\text{P,C}} = 1.5$ Hz, C_5Me_5), 11.7 (d, $J_{\text{P,C}} = 1.5$ Hz, C_5Me_5), 11.8 (d, $J_{\text{P,C}} = 2.0$ Hz, C_5Me_5), 13.2 (d, $J_{\text{P,C}} = 4.8$ Hz, C_5Me_5), 32.2 (d, $^1J_{\text{P,C}} = 23.5$ Hz, P- CH_2), 65.4 (d, $^1J_{\text{P,C}} = 2.9$ Hz, P- C_5Me_5), 73.1 (d, $^2J_{\text{P,C}} = 13.7$ Hz, O- CH_2), 132.7 (d, $J_{\text{P,C}} = 7.3$ Hz, C_5Me_5), 138.9 (d, $J_{\text{P,C}} = 1.7$ Hz, C_5Me_5), 141.4 (d, $J_{\text{P,C}} = 5.9$ Hz, C_5Me_5), 143.4 (d, $J_{\text{P,C}} = 7.0$ Hz, C_5Me_5), 196.1 (d_{sat}, $^1J_{\text{W,C}} = 125.6$ Hz, $^2J_{\text{P,C}} = 7.8$ Hz, *cis*-CO), 199.4 (d_{sat}, $^1J_{\text{W,C}} = 139.2$ Hz, $^2J_{\text{P,C}} = 28.0$ Hz, *trans*-CO).

$^{31}\text{P}\{^1\text{H}\}$ NMR (162.0 MHz, CDCl_3): $\delta = 204.8$ (s_{sat}, $^1J_{\text{W,P}} = 275.5$ Hz).

MS (EI, 70 eV, ^{184}W , selected data): m/z (%) = 534.0 (40) $[\text{M}]^{++}$, 450.0 (5) $[\text{M} - 3 \text{CO}]^+$, 398.8 (65) $[\text{M} - \text{C}_5\text{Me}_5]^+$, 370.8 (100) $[\text{M} - \text{C}_5\text{Me}_5 - \text{CO}]^+$, 342.8 (30) $[\text{M} - \text{C}_5\text{Me}_5 - 2 \text{CO}]^+$, 314.8 (20) $[\text{M} - \text{C}_5\text{Me}_5 - 3 \text{CO}]^+$, 286.8 (20) $[\text{M} - \text{C}_5\text{Me}_5 - 4 \text{CO}]^+$, 258.9 (10) $[\text{M} - \text{C}_5\text{Me}_5 - 5 \text{CO}]^+$, 135.1 (70) $[\text{C}_5\text{Me}_5]^+$, 119.0 (50) $[\text{C}_5\text{Me}_5 - \text{CH}_4]^+$, 105.0 (40) $[\text{C}_5\text{Me}_5 - \text{C}_2\text{H}_6]^+$, 91.0 (20) $[\text{C}_5\text{Me}_5 - \text{C}_3\text{H}_8]^+$.

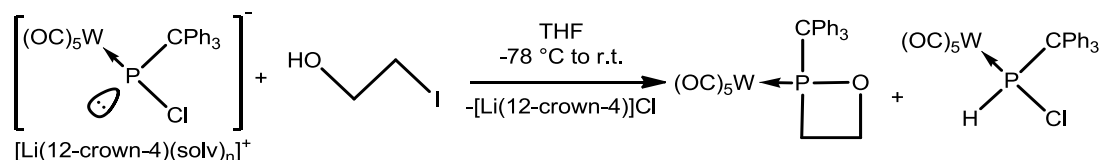
HR-MS: calculated for $\text{C}_{17}\text{H}_{19}\text{O}_6\text{PW}$: 532.0402 found: 532.0404 (standard deviation: 0.35 ppm).

IR (ATR Diamond; $\tilde{\nu}[\text{cm}^{-1}]$, selection): 2069 (s, $\nu(\text{CO})$), 1977 (w, $\nu(\text{CO})$), 1896 (vs, $\nu(\text{CO})$).

Elemental analysis:

calc.:	C	38.23	H	3.59
found:	C	38.68	H	3.74

11.2.16 Attempted synthesis of pentacarbonyl[2-(triphenylmethyl)-1,2-oxaphosphetane- κP]tungsten(0) [34.3]

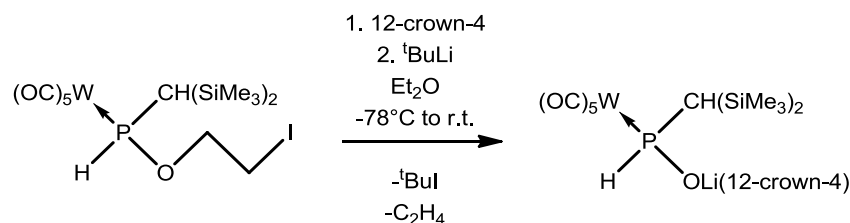


Synthesis: A solution of the Li/Cl phosphinidenoid complex **2.3** was prepared as described, starting from 334.5 mg (0.5 mmol) of dichlorophosphane complex $[(\text{OC})_5\text{W}\{\text{PCl}_2(\text{CPh}_3)\}]$ (**2.3**). 39 μL (0.50 mmol, 1 eq.) of 2-iodoethanol (**35a**) was added. The solution was allowed warming up to ambient temperature and during the warming up period formation of a white precipitate was observed. The $^{31}\text{P}\{^1\text{H}\}$ spectrum showed the resonance signals for 1,2-oxaphosphetane complex **34.3** and the chloro(organo)phosphane complex **10.3** as main products.

34.3:

$^{31}\text{P}\{^1\text{H}\}$ NMR (121.5 MHz, THF): $\delta = 193.4$ (s_{sat}, $^1J_{\text{W,P}} = 277.8$ Hz).

11.2.17 Synthesis of lithium(1,4,7,10-tetraoxacyclododecane) pentacarbonyl{[bis(trimethylsilyl)methyl]phosphanoxido- κ P}tungsten(0) [36.1]



Synthesis: In a 100 mL Schlenk tube, 643.2 mg (0.924 mmol) of complex **33.1_W** were dissolved in 30 mL of diethyl ether. To it 148 μL (0.925 mmol, 1 eq.) of 12-crown-4 was added at ambient temperature and the mixture was cooled to -78°C . Then 0.55 mL (0.93 mmol, 1.7 M in *n*-pentane, 1.0 eq.) of ^tBuLi was added upon which a change to a light yellow colour and the formation of a yellow precipitate was observed. The reaction mixture was kept on stirring while slowly warming up to ambient temperature.

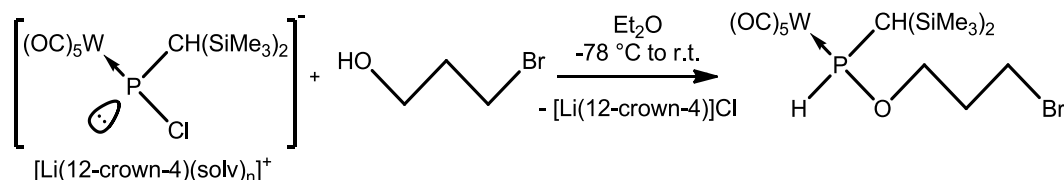
Purification: After the reaction was completed (checked by ³¹P NMR), all volatiles were removed in *vacuo* (ca. 0.02 mbar). The crude product was purified by washing it three times with 5 mL of *n*-pentane and drying it in *vacuo* (ca. 0.02 mbar), yielding a slightly yellow solid.

Molecular formula:	$\text{C}_{20}\text{H}_{36}\text{LiO}_{10}\text{PSi}_2\text{W}$
Molecular weight:	714.420 g/mol
Yield:	547 mg (0.77 mmol, 83 %)

All data are in good accordance to previously reported values.^[132]

³¹P{¹H} NMR (121.5 MHz, THF-*d*₈): $\delta = 46.0$ (S_{sat} , $^1J_{\text{W,P}} = 244.1$ Hz, $^1J_{\text{P,H}} = 302.6$ Hz).

11.2.18 Synthesis of {(4-bromopropoxy)[bis(trimethylsilyl)methyl]phosphane- κ P}pentacarbonyltungsten(0) [39.1]



Synthesis: A solution of Li/Cl phosphinidenoid complex **2.1** was prepared as described, starting from 877.5 mg (1.5 mmol) of $[(\text{OC})_5\text{W}\{\text{P}(\text{CH}(\text{SiMe}_3)_2)\text{Cl}_2\}]$ (**1.1**) and 0.14 mL (1.6 mmol, 1.06 eq.) of 3-bromopropane-1-ol (**38**) was added. The solution was allowed warming up to ambient temperature overnight and during warming up formation of a white precipitate was observed.

Purification: After the reaction was completed (checked by ^{31}P NMR), all volatiles were removed in *vacuo* (ca. 0.02 mbar). The crude mixture was extracted from the formed salt with *n*-pentane (3 times 40 mL) and the solvent was removed in *vacuo* (ca. 0.02 mbar). The crude product was subsequently placed in a sublimation flask and heated for 1.5 h (130 °C, $2 \cdot 10^{-2}$ mbar) to remove all volatile material and complexes with a lower molecular weight. The product was obtained as yellow-brownish oil.

Molecular formula: $\text{C}_{15}\text{H}_{26}\text{O}_6\text{BrPSi}_2\text{W}$

Molecular weight: 653.252 g/mol

Yield: 604 mg (0.930 mmol, 62 %)

^1H NMR (500.2 MHz, CDCl_3): δ = 0.21 (s, 9H, $\text{Si}(\text{CH}_3)_3$), 0.27 (s, 9H, $\text{Si}(\text{CH}_3)_3$), 0.93 (s, 1H, P-CH), 2.12 - 2.56 (m, 2H, CH_2), 3.46 - 3.51 (m, 2H, CH_2), 3.66 - 3.74 (m, 1H, CH_2), 3.87 - 3.96 (m, 1H, CH_2), 7.87 (dd, 1H, $^1J_{\text{P,H}} = 321.5$ Hz, $^3J_{\text{P,H}} = 0.8$ Hz, P-H).

$^{13}\text{C}\{^1\text{H}\}$ NMR (125.8 MHz, CDCl_3): δ = 0.3 (d, $^3J_{\text{P,C}} = 2.2$ Hz, $\text{Si}(\text{CH}_3)_3$), 2.2 (d, $^3J_{\text{P,C}} = 3.3$ Hz, $\text{Si}(\text{CH}_3)_3$), 23.5 (d, $^1J_{\text{P,C}} = 13.1$ Hz, P-CH), 29.4 (s, CH_2), 33.3 (d, $^1J_{\text{P,C}} = 8.7$ Hz, CH_2), 67.1 (d, $^2J_{\text{P,C}} = 3.5$ Hz, O- CH_2), 196.7 (d_{sat}, $^1J_{\text{W,C}} = 125.6$ Hz, $^2J_{\text{P,C}} = 7.4$ Hz, *cis*-CO), 199.3 (d_{sat}, $^1J_{\text{W,C}} = 140.3$ Hz, $^2J_{\text{P,C}} = 25.1$ Hz, *trans*-CO).

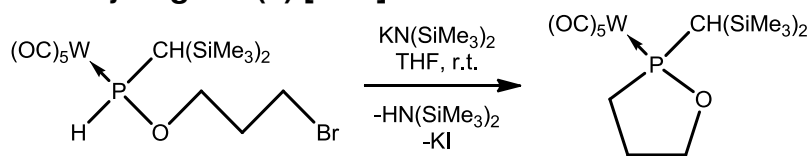
$^{29}\text{Si}\{^1\text{H}\}$ NMR (99.4 MHz, CDCl_3): δ = 1.12 (d, $^2J_{\text{P,Si}} = 5.5$ Hz, $\text{Si}(\text{CH}_3)_3$), 2.97 (d, $^2J_{\text{P,Si}} = 9.1$ Hz, $\text{Si}(\text{CH}_3)_3$).

^{31}P NMR (202.5 MHz, CDCl_3): δ = 104.7 (d_{sat}, $^1J_{\text{W,P}} = 268.1$ Hz, $^1J_{\text{P,H}} = 321.5$ Hz).

pos. ESI-MS: calculated for $(\text{C}_{15}\text{H}_{26}\text{O}_6\text{BrPSi}_2\text{W})^+$: 651.970; found: 651.946 [M]⁺.

IR (ATR Diamond; $\tilde{\nu}[\text{cm}^{-1}]$, selected data): 2262 (w, $\nu(\text{PH})$), 2071 (s, $\nu(\text{CO})$), 1981 (w, $\nu(\text{CO})$), 1906 (vs, $\nu(\text{CO})$).

11.2.19 Synthesis of pentacarbonyl{2-[bis(trimethylsilyl)methyl]-1,2-oxaphospholane-κP}tungsten(0) [19.1]



Synthesis: In a 50 mL Schlenk tube, 514 mg (0.787 mmol) of complex **39.1** were dissolved in 25 mL of THF. To it 164 mg (0.82 mmol, 1.04 eq.) of potassium hexamethyldisilazide, dissolved in 10 mL of THF, were added dropwise at ambient temperature. During the addition a rapid formation of precipitate and a change of the color to yellow-orange was observed. The solution was kept on stirring for 1 h.

Purification: All volatiles were removed in *vacuo* (ca. 0.02 mbar). The product was purified by extraction from the formed salt with *n*-pentane (4 times 20 mL), subsequent precipitation from *n*-pentane at -100 °C and filtering off the supernatant solution. This was repeated four times (once 5 mL and three times 2 mL) to yield the product as white powder after drying in *vacuo* (ca. 0.02 mbar).

Molecular formula:	C ₁₅ H ₂₅ O ₆ PSi ₂ W
Molecular weight:	572.340 g/mol
Melting point:	85 °C
Yield:	102.5 mg (0.180 mmol, 23 %)

Isomeric ratio: 99.5 : 0.5

Isomer 1:

¹H NMR (500.1 MHz, CDCl₃): δ = 0.24 (s, 9H, Si(CH₃)₃), 0.28 (s, 9H, Si(CH₃)₃), 1.64 (d, 1H, ²J_{P,H} = 12.8 Hz, P-CH), 2.05 - 2.25 (m, 2H, CH₂), 2.50 - 2.64 (m, 2H, CH₂), 4.01 - 4.10 (m, 1H, CH₂), 4.11 - 4.20 (m, 1H, CH₂).

¹³C{¹H} NMR (125.8 MHz, CDCl₃): δ = 2.6 (d, ³J_{P,C} = 3.3 Hz, Si(CH₃)₃), 2.8 (d, ³J_{P,C} = 2.2 Hz, Si(CH₃)₃), 25.3 (s, CH₂), 31.7 (s_{br}, P-CH), 37.2 (s_{br}, CH₂), 70.9 (d, ²J_{P,C} = 5.7 Hz, O-CH₂), 197.6 (d_{sat}, ¹J_{W,C} = 126.2 Hz, ²J_{P,C} = 8.2 Hz, *cis*-CO), 200.3 (d, ²J_{P,C} = 24.8 Hz, *trans*-CO).

³¹P{¹H} NMR (202.5 MHz, CDCl₃): δ = 139.5 (s_{br}, full-width at half-intensity (FWHI, *h*_{1/2}) = 760 Hz).

³¹P{¹H} NMR (202.5 MHz, CDCl₃, 60 °C): δ = 138.4 (¹J_{W,P} = 275.5 Hz).

Isomer 2:

No resonance signals except in the ³¹P NMR could be observed due to the isomers low percentage of the mixture.

³¹P{¹H} NMR (202.5 MHz, CDCl₃): δ = 125.2 (s_{sat}, ¹J_{W,P} = 267.1 Hz).

pos. ESI-MS: calculated for $(C_{15}H_{25}O_6PSi_2W)^+$: 572.04, found: 572.03 $[M]^+$, 287.11 $[M - W(CO)_5 + Na + O]^+$, 265.13 $[M - W(CO)_5 + H + O]^+$, 249.14 $[M - W(CO)_5 + H]^+$.

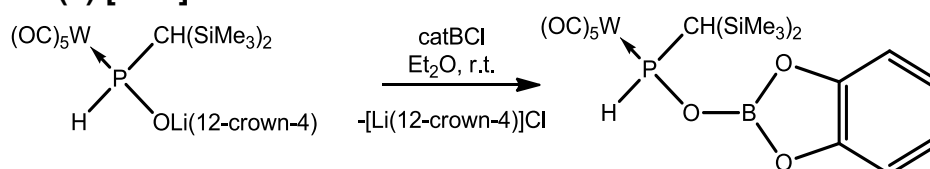
IR (ATR Diamond; $\tilde{\nu}[\text{cm}^{-1}]$, selected data): 2066 (s, $\nu(\text{CO})$), 1981 (w, $\nu(\text{CO})$), 1898 (vs, $\nu(\text{CO})$).

Elemental analysis:

calc.:	C	31.48	H	4.40
found:	C	31.41	H	4.34

Single crystal measurement: GSTR485, AKY-554 // GXraymo_4626f

11.2.20 Synthesis of pentacarbonyl{catecholboranoxo[bis(trimethylsilyl)methyl]phosphane- κP }tungsten(0) [41.1]



Synthesis: In a 10 mL Schlenk tube, 357.2 mg (0.5 mmol) of phosphinito complex **36.1** were dissolved in 2 mL of diethyl ether and a solution of 77.18 mg (0.5 mmol, 1.0 eq.) catechol(chloro)borane in 2 mL of diethyl ether was added dropwise.

Purification: After the reaction was completed (checked by ^{31}P NMR) all volatiles were removed in *vacuo* (ca. 0.02 mbar). The crude mixture was extracted from the formed salt with four times 1 mL of *n*-pentane and the solvent was removed in *vacuo* (ca. 0.02 mbar) to yield the product as white powder.

Molecular formula: $C_{18}H_{24}BO_8PSi_2W$

Molecular weight: 650.174 g/mol

Yield: 255 mg (0.39 mmol, 78 %)

^1H NMR (300.1 MHz, C_6D_6): $\delta = -0.03$ (d, 9H, $^4J_{\text{P,H}} = 0.4$ Hz, Si(CH₃)₃), 0.28 (s, 9H, Si(CH₃)₃), 0.98 (dd, 1H, $^2J_{\text{P,H}} = 3.2$ Hz, $^3J_{\text{H,H}} = 2.3$ Hz, P-CH), 6.66 - 6.72 (m, 2H, CH_{Ar}), 6.87 - 6.94 (m, 2H, CH_{Ar}), 8.46 (dd, 1H, $^1J_{\text{P,H}} = 341.8$ Hz, $^3J_{\text{H,H}} = 2.3$ Hz, P-H).

$^{11}\text{B}\{^1\text{H}\}$ NMR (96.3 MHz, C_6D_6): $\delta = 21.7$ (s).

$^{13}\text{C}\{^1\text{H}\}$ NMR (75.5 MHz, C_6D_6): $\delta = 0.0$ (d, $^3J_{\text{P,C}} = 2.9$ Hz, Si(CH₃)₃), 2.2 (d, $^3J_{\text{P,C}} = 3.2$ Hz, Si(CH₃)₃), 25.2 (d, $^1J_{\text{P,C}} = 11.0$ Hz, P-CH), 112.7 (s, CH_{Ar}), 123.3 (s, CH_{Ar}), 148.0 (s, O-C), 196.6 (d_{sat}, $^1J_{\text{W,C}} = 126.1$ Hz, $^2J_{\text{P,C}} = 7.4$ Hz, *cis*-CO), 199.2 (d, $^2J_{\text{P,C}} = 27.8$ Hz, *trans*-CO).

$^{29}\text{Si}\{^1\text{H}\}$ NMR (59.6 MHz, C_6D_6): $\delta = 1.0$ (d, $^2J_{\text{P,Si}} = 6.1$ Hz), 1.9 (d, $^2J_{\text{P,Si}} = 8.7$ Hz).

^{31}P NMR (121.5 MHz, C_6D_6): $\delta = 97.7$ (d_{sat} , $^1J_{\text{W,P}} = 277.1$ Hz, $^1J_{\text{P,H}} = 331.6$ Hz).

MS (EI, 70 eV, ^{184}W , selected data): m/z (%) = 650.0 (15) $[\text{M}]^+$, 622.0 (5) $[\text{M} - 1 \text{ CO}]^+$, 594.0 (55) $[\text{M} - 2 \text{ CO}]^+$, 73.1 (100) $[\text{SiMe}_3]^+$.

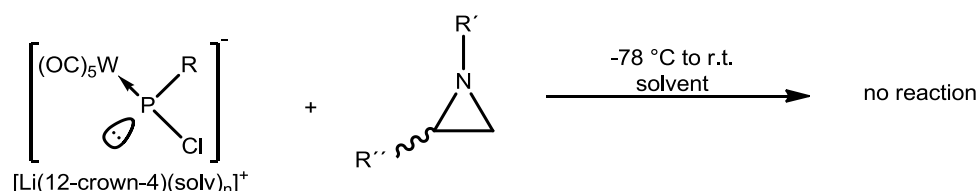
IR (ATR Diamond; $\tilde{\nu}[\text{cm}^{-1}]$, selected data): 2300 (w, $\nu(\text{PH})$), 2075 (m, $\nu(\text{CO})$), 1986 (w, $\nu(\text{CO})$), 1944 (w, $\nu(\text{CO})$) 1912 (vs, $\nu(\text{CO})$).

Elemental analysis:

calc.:	C	33.25	H	3.72
found:	C	33.49	H	3.97

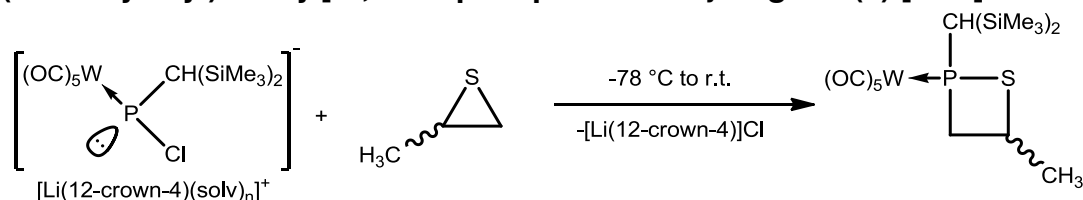
Single crystal measurement: GSTR385, AKY-458 // GXray3821

11.2.21 Attempted reactions of Li/Cl phosphinidenoid complexes 2.1 and 2.3 with aziridines 42a or 42b



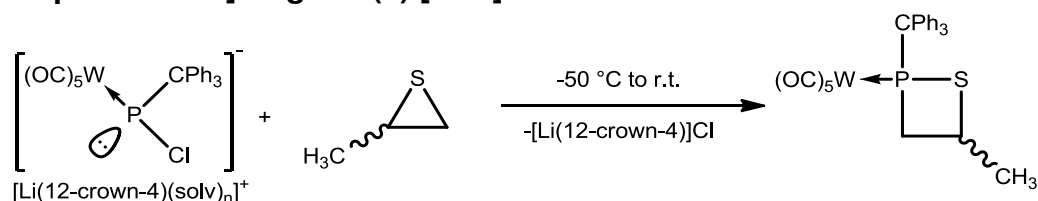
A solution of the Li/Cl phosphinidenoid complexes **2.1** or **2.3** was prepared starting from complexes **1.1** or **1.3**, respectively, as described in chapter 11.2.1. The corresponding aziridine (**42a** ($\text{R}' = \text{}^i\text{Pr}$, $\text{R}'' = \text{Ph}$) or **42b** ($\text{R}' = \text{PhCH}_2$, $\text{R}'' = \text{CF}_3$)) was added in a two times excess via syringe and the solution was allowed slowly warming up to ambient temperature. The reaction mixtures were analyzed by $^{31}\text{P}\{^1\text{H}\}$ NMR spectroscopy. No reaction was observed between the Li/Cl phosphinidenoid complexes and the used aziridines.

11.2.22 Attempted synthesis of pentacarbonyl{4-methyl-2-bis(trimethylsilyl)methyl}-1,2-thiaphosphetane- κP }tungsten(0) [46.1]



A solution of Li/Cl phosphinidenoid complex **2.1** was prepared as described, starting from 58.5 mg (0.1 mmol) of **1.1**, and 8 μL (0.102 mmol, 1.02 equivalents) of propylene sulfide (**45**) was added dropwise. The solution was allowed slowly warming up to ambient temperature and subsequently analysed by $^{31}\text{P}\{^1\text{H}\}$ NMR measurement. The NMR showed several resonance signals that could not be assigned to any desired or known product.

11.2.23 Synthesis of pentacarbonyl[4-methyl-2-(triphenylmethyl)-1,2-thiaphosphetane- κ P]tungsten(0) [46.3]



Synthesis: A solution of Li/Cl phosphinidene complex **2.3** was prepared as described, starting from 1.004 g (1.5 mmol) of $[(OC)_5W\{PCl_2(CPh_3)\}]$ (**1.3**) and 0.2 mL (2.55 mmol, 1.7 equivalents) of propylene sulfide (**45**) was added dropwise. The solution was kept on stirring for 12 h, while being allowed slowly warming up to ambient temperature.

Purification: All volatiles were removed in *vacuo* (ca. 0.02 mbar). The product was purified by dissolving in diethyl ether and filtration over Al_2O_3 ($\varnothing = 2$ cm, $h = 5$ cm). After removing of all volatiles in *vacuo* (ca. 0.02 mbar) the product was washed with three times 5 mL of petroleum ether 40/60 at -50 °C. Drying of the solid in *vacuo* (ca. 0.02 mbar) yielded the product as white solid.

Molecular formula:	$C_{27}H_{21}O_5PSW$
Molecular weight:	672.331 g/mol
Melting point:	138 °C
Yield:	390 mg (0.58 mmol, 39 %)

Isomeric ratio: 44 : 56

Isomer 1:

1H NMR (400.1 MHz, $CDCl_3$): $\delta = 1.43$ (d, 3H, $^3J_{H,H} = 6.6$ Hz, CH_3), 3.15 - 3.25 (m, 1H, CH_2), 3.15 - 3.25 (m, 1H, CH_2), 3.39 - 3.50 (m, 1H, S-CH), 7.3 - 7.45 (m, 15H, CPh_3).

$^{13}C\{^1H\}$ NMR (100.7 MHz, $CDCl_3$): $\delta = 25.7$ (s_{br} , CH_3), 39.1 (d, $^2J_{P,C} = 5.2$ Hz, S-CH), 42.1 (d, $^1J_{P,C} = 29.7$ Hz, P- CH_2), 65.3 (d, $^1J_{P,C} = 8.6$ Hz, CPh_3), 127.8 (s_{br} , *para*- CH_{Ar}), 128.4 (s_{br} , CH_{Ar}), 130.8 (s_{br} , CH_{Ar}), 142.3 (s, *ipso*-C), 197.5 (dq_{sat} , $^1J_{W,C} = 127.6$ Hz, $^2J_{P,C} = 6.5$ Hz, *cis*-CO), 200.0 (d, $^2J_{P,C} = 31.5$ Hz, *trans*-CO).

$^{31}P\{^1H\}$ NMR (162.0 MHz, $CDCl_3$): $\delta = 50.5$ (s_{sat} , $^1J_{W,P} = 254.6$ Hz).

Isomer 2:

1H NMR (400.1 MHz, $CDCl_3$): $\delta = 1.05$ (d, 3H, $J_{H,H} = 6.6$ Hz, CH_3), 2.80 - 2.90 (m, 1H, P- CH_2), 3.10 - 3.15 (m, 1H, P- CH_2), 4.15 - 4.28 (m, 1H, S-CH), 7.3 - 7.45 (m, 15H, CPh_3).

$^{13}C\{^1H\}$ NMR (100.7 MHz, $CDCl_3$): $\delta = 25.7$ (s_{br} , CH_3), 35.6 (d, $^2J_{P,C} = 4.5$ Hz, S-CH), 42.6 (d, $^1J_{P,C} = 24.6$ Hz, P- CH_2), 66.3 (d, $^1J_{P,C} = 9.3$ Hz, CPh_3), 128.0 (s_{br} , *para*- CH_{Ar}), 128.4 (s_{br} , CH_{Ar}), 131.1 (d, $J_{P,C}$

= 7.7 Hz, CH_{Ar}), 141.6 (d, $^2J_{\text{P,C}} = 2.7$ Hz, *ipso-C*), 197.2 (dq_{sat} , $^1J_{\text{W,C}} = 127.4$ Hz, $^2J_{\text{P,C}} = 6.5$ Hz, *cis-CO*), 199.5 (d, $^2J_{\text{P,C}} = 31.7$ Hz, *trans-CO*).

$^{31}\text{P}\{^1\text{H}\}$ NMR (162.0 MHz, CDCl_3): $\delta = 65.3$ (s_{sat} , $^1J_{\text{W,P}} = 256.7$ Hz).

MS (EI, 70 eV, ^{184}W , selected data): m/z (%) = 672.1 (2) $[\text{M}]^{++}$, 546.0 (8) $[\text{M} - 3 \text{CO} - \text{C}_3\text{H}_6]^+$, 490.0 (65) $[\text{M} - 5 \text{CO} - \text{C}_3\text{H}_6]^+$, 243.1 (100) $[\text{CPh}_3]^+$, 165.0 (30) $[\text{CPh}_3 - \text{C}_6\text{H}_6]^+$.

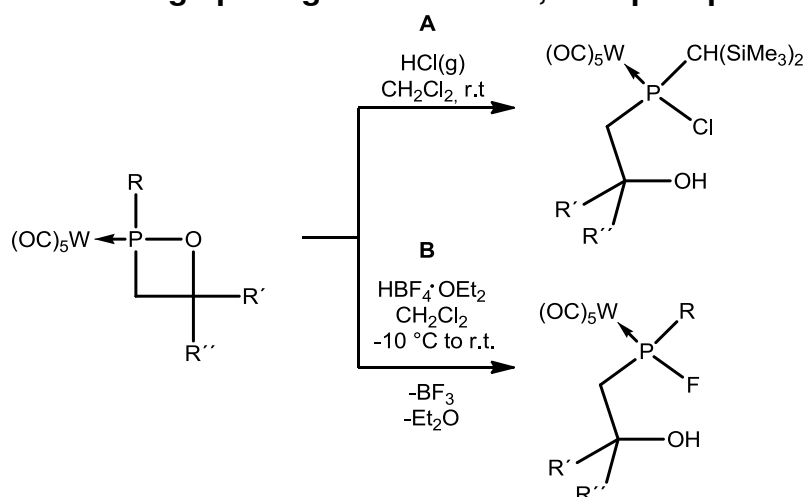
IR (ATR Diamond; $\tilde{\nu}[\text{cm}^{-1}]$, selected data): 2070 (s, $\nu(\text{CO})$), 1984 (w, $\nu(\text{CO})$), 1910 (vs, $\nu(\text{CO})$).

Elemental analysis:

calc.:	C	48.23	H	3.15	S	4.77
found:	C	48.54	H	3.20	S	4.79

Single crystal measurement: GSTR523, AKY-583 // GXray4889af

11.2.24 Acid induced ring opening reactions of 1,2-oxaphosphetane complexes



A: Ring opening reactions using $\text{HCl}_{(\text{g})}$

Syntheses: In a 10 mL Schlenk tube the 1,2-oxaphosphetane complex was dissolved in CH_2Cl_2 . A stream of $\text{HCl}_{(\text{g})}$ (prepared by dropping concentrated hydrochloric acid on anhydrous CaCl_2) and argon was bubbled through the solution for t^1 minutes. The solution was subsequently stirred for additional t^2 hours (see table 11.3 for details).

Table 11.3: Reaction conditions for the syntheses of **47.1a-c**.

	R	R'	R''	1,2-oxaphosphetane complex / m [mg] (n [mmol])	V (CH_2Cl_2) [mL]	t^1 [min]	t^2 [h]
47.1a	$\text{CH}(\text{SiMe}_3)_2$	H	H	34.1_W / 250 (0.45)	4	30	1
47.1b	$\text{CH}(\text{SiMe}_3)_2$	H	CH_3	21.1a_W / 300 (0.54)	5	60	2
47.1c	$\text{CH}(\text{SiMe}_3)_2$	H	CF_3	21.1g / 200 (0.32)	5	180	12

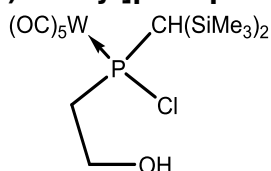
B: Ring opening reactions using HBF₄·OEt₂

Syntheses: In a 10 mL Schlenk tube the 1,2-oxaphosphetane complex was dissolved in CH₂Cl₂. The mixture was cooled to -10 °C and HBF₄·OEt₂ was added via syringe. The mixture was stirred and allowed slowly warming to ambient temperature (see table 11.4 for details).

Table 11.4: Reaction conditions for the syntheses of **48.1a,b** and **48.2b**.

	R	R'	R''	1,2-oxaphosphetane complex / m [mg] (n [mmol])	HBF ₄ ·OEt ₂ V in μL (n [mmol])	V (CH ₂ Cl ₂) [mL]
48.1a	CH(SiMe ₃) ₂	H	CF ₃	21.1g / 200 (0.32)	44 (0.32)	5
48.1b	CH(SiMe ₃) ₂	CF ₃	CF ₃	25.1b / 137 (0.20)	27 (0.20)	5
48.2b	C ₅ Me ₅	CF ₃	CF ₃	25.2b / 142 (0.21)	29 (0.21)	5

11.2.24.1 Pentacarbonyl{chloro(2-hydroxyethyl)[bis(trimethylsilyl)methyl]phosphane-κP}tungsten(0) [47.1a]



Purification: The colour of the solution changed to slightly blue during the reaction before all volatiles were removed in *vacuo* (ca. 0.02 mbar). The residue was extracted with *n*-pentane (two times 5 mL) to yield a clear yellow solution. The product was then crystallized by slow evaporation of this solution at 4 °C.

Molecular formula:	C ₁₄ H ₂₄ ClO ₆ PSi ₂ W
Molecular weight:	594.775 g/mol
Melting point:	84 °C
Yield:	189.6 mg (0.319 mmol, 71 %)

¹H NMR (300.1 MHz, CDCl₃): δ = 0.36 (s, 9H, Si(CH₃)₃), 0.38 (s, 9H, Si(CH₃)₃), 1.92 (d, 1H, ²J_{P,H} = 11.2 Hz, P-CH), 1.90 - 2.20 (s_{br}, 1H, OH), 2.62 (dddd, 1H, ²J_{H,H} = 14.0 Hz, ²J_{P,H} = 9.3 Hz, ³J_{H,H} = 7.1 Hz, ³J_{H,H} = 7.1 Hz, P-CH₂), 2.92 (dddd, 1H, ²J_{H,H} = 14.0 Hz, ²J_{P,H} = 12.7 Hz, ³J_{H,H} = 7.1 Hz, ³J_{H,H} = 7.1 Hz, P-CH₂), 4.17 (ddd, 2H, ³J_{P,H} = 10.1 Hz, ³J_{H,H} = 7.1 Hz, ³J_{H,H} = 7.1 Hz, O-CH₂).

¹³C{¹H} NMR (75.5 MHz, CDCl₃): δ = 3.2 (d, ³J_{P,C} = 3.8 Hz, Si(CH₃)₃), 4.0 (d, ³J_{P,C} = 2.5 Hz, Si(CH₃)₃), 32.0 (d, ¹J_{P,C} = 13.1 Hz, P-CH), 42.6 (d, ¹J_{P,C} = 14.4 Hz, P-CH₂), 59.8 (d, ²J_{P,C} = 6.5 Hz, CH₂), 197.2 (d_{sat}, ¹J_{W,C} = 127.0 Hz, ²J_{P,C} = 7.1 Hz, *cis*-CO), 199.3 (d_{sat}, ¹J_{W,C} = 141.4 Hz, ²J_{P,C} = 30.0 Hz, *trans*-CO).

²⁹Si{¹H} NMR (59.6 MHz, CDCl₃): δ = -0.12 (s, Si(CH₃)₃), 3.10 (d, ²J_{P,Si} = 6.7 Hz, Si(CH₃)₃).

³¹P{¹H} NMR (121.5 MHz, CDCl₃): δ = 111.5 (s_{sat}, ¹J_{W,P} = 272.9 Hz).

MS (EI, 70 eV, ^{184}W , selected data): m/z (%) = 594.0 (1) $[\text{M}]^+$, 566.0 (6) $[\text{M} - \text{CO}]^+$, 585.1 (5) $[\text{M} - \text{HCl}]^+$, 510.0 (30) $[\text{M} - 3 \text{CO}]^+$, 235.1 (50) $[\text{M} - \text{W}(\text{CO})_5 - \text{Cl}]^+$, 73.1 (100) $[\text{SiMe}_3]^+$.

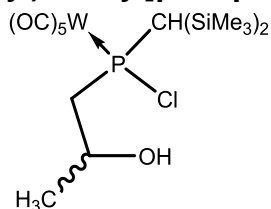
IR (ATR Diamond; $\tilde{\nu}[\text{cm}^{-1}]$, selected data): 3298 (s, $\nu(\text{OH})$), 2072 (m, $\nu(\text{CO})$), 1995 (w, $\nu(\text{CO})$), 1901 (vs, $\nu(\text{CO})$).

Elemental analysis:

calc.:	C	28.27	H	4.07
found:	C	28.49	H	4.26

Single crystal measurement: GSTR488, AKY-546 // GXraymo_4589f

11.2.24.2 Pentacarbonyl{chloro(2-hydroxypropyl)[bis(trimethylsilyl)methyl]phosphane- κP }tungsten(0) [47.1b]



Purification: All volatiles were removed in *vacuo* (ca. 0.02 mbar). The crude, oily product was dissolved in *n*-pentane and the product was obtained in form of big crystal needles after slow evaporation of the solvent at 4 °C.

Molecular formula:	$\text{C}_{15}\text{H}_{26}\text{ClO}_6\text{PSi}_2\text{W}$
Molecular weight:	608.801 g/mol
Melting point:	91-92 °C
Yield:	319 mg (0.524 mmol, 100 %)

Isomeric ratio: 25 : 75

Isomer 1:

^1H NMR (300.1 MHz, CDCl_3): δ = 0.36 (s, 18H, $\text{Si}(\text{CH}_3)_3$), 1.43 (dd, 3H, $^4J_{\text{P,H}} = 1.5$ Hz, $^3J_{\text{H,H}} = 6.3$ Hz, CH_3), 1.88 (s_{br} , 1H, OH), 2.19 (d, 1H, $^2J_{\text{P,H}} = 12.8$ Hz, P-CH), 2.48 (ddd, 1H, $^2J_{\text{P,H}} = 12.6$ Hz, $^3J_{\text{H,H}} = 14.5$ Hz, $^2J_{\text{H,H}} = 8.1$ Hz, P-CH_2), 2.83 (ddd, 1H, $^2J_{\text{P,H}} = 7.9$ Hz, $^3J_{\text{H,H}} = 15.0$ Hz, $^2J_{\text{H,H}} = 8.1$ Hz, P-CH_2), 4.37 - 4.57 (m, 1H, O-CH).

$^{13}\text{C}\{^1\text{H}\}$ NMR (75.5 MHz, CDCl_3): δ = 3.2 (d, $^2J_{\text{P,C}} = 3.6$ Hz, $\text{Si}(\text{CH}_3)_3$), 3.8 (d, $^2J_{\text{P,C}} = 2.9$ Hz, $\text{Si}(\text{CH}_3)_3$), 25.9 (d, $^3J_{\text{P,C}} = 12.6$ Hz, CH_3), 31.2 (d, $^1J_{\text{P,C}} = 16.8$ Hz, P-CH), 49.7 (d, $^1J_{\text{P,C}} = 13.9$ Hz, P-CH_2), 66.1 (s, O-CH), 197.0 (d_{sat} , $^2J_{\text{P,C}} = 7.1$ Hz, $^1J_{\text{W,C}} = 126.7$ Hz, *cis*-CO), 198.8 (d, $^2J_{\text{P,C}} = 30.4$ Hz, *trans*-CO).

$^{29}\text{Si}\{^1\text{H}\}$ NMR (59.6 MHz, CDCl_3): δ = 0.45 (s, $\text{Si}(\text{CH}_3)_3$), 2.74 (d, $^2J_{\text{P,Si}} = 2.86$ Hz, $\text{Si}(\text{CH}_3)_3$).

$^{31}\text{P}\{^1\text{H}\}$ NMR (121.5 MHz, CDCl_3): δ = 119.8 (s_{br} , $^1J_{\text{W,P}} = 276.0$ Hz).

Isomer 2:

^1H NMR (300.1 MHz, CDCl_3): δ = 0.35 (s, 9H, $\text{Si}(\text{CH}_3)_3$), 0.38 (s, 9H, $\text{Si}(\text{CH}_3)_3$), 1.40 (dd, 3H, $^4J_{\text{P,H}} = 1.4$ Hz, $^3J_{\text{H,H}} = 6.2$ Hz, CH_3), 1.88 (s_{br}, 1H, OH), 1.90 (d, 1H, $^2J_{\text{P,H}} = 10.2$ Hz, P-CH), 2.42 (ddd, 1H, $^2J_{\text{P,H}} = 8.5$ Hz, $^3J_{\text{H,H}} = 14.9$ Hz, $^2J_{\text{H,H}} = 2.0$ Hz, P- CH_2), 2.70 (ddd, 1H, $^2J_{\text{P,H}} = 14.2$ Hz, $^3J_{\text{H,H}} = 14.4$ Hz, $^2J_{\text{H,H}} = 2.0$ Hz, P- CH_2), 4.37 - 4.57 (m, 1H, O-CH).

$^{13}\text{C}\{^1\text{H}\}$ NMR (75.5 MHz, CDCl_3): δ = 3.1 (d, $^2J_{\text{P,C}} = 3.6$ Hz, $\text{Si}(\text{CH}_3)_3$), 3.8 (d, $^2J_{\text{P,C}} = 2.6$ Hz, $\text{Si}(\text{CH}_3)_3$), 26.7 (d, $^3J_{\text{P,C}} = 9.7$ Hz, CH_3), 32.3 (d, $^1J_{\text{P,C}} = 12.6$ Hz, P-CH), 48.0 (d, $^1J_{\text{P,C}} = 13.9$ Hz, P- CH_2), 64.8 (s, O-CH), 197.5 (d_{sat}, $^1J_{\text{W,C}} = 127.4$ Hz, $^2J_{\text{P,C}} = 7.4$ Hz, *cis*-CO), 199.7 (d, $^2J_{\text{P,C}} = 31.4$, *trans*-CO).

$^{29}\text{Si}\{^1\text{H}\}$ NMR (59.6 MHz, CDCl_3): δ = -0.50 (s, $\text{Si}(\text{CH}_3)_3$), 3.07 (d, $^2J_{\text{P,Si}} = 7.3$ Hz, $\text{Si}(\text{CH}_3)_3$).

$^{31}\text{P}\{^1\text{H}\}$ NMR (121.5 MHz, CDCl_3): δ = 115.1 (s_{sat}, $^1J_{\text{W,P}} = 274.2$ Hz).

MS (EI, 70 eV, ^{184}W , selected data): m/z (%) = 608.1 (1) $[\text{M}]^+$, 580.0 (10) $[\text{M} - \text{CO}]^+$, 524.0 (60) $[\text{M} - 3 \text{CO}]^+$, 488.0 (2) $[\text{M} - 3 \text{CO} - \text{HCl}]^+$, 466.0 (5) $[\text{M} - 3 \text{CO} - \text{HCl} - \text{C}_3\text{H}_6]^+$, 390.0 (15) $[\text{M} - 4 \text{CO} - \text{HCl} - \text{C}_3\text{H}_6]^+$, 249.1 (25) $[\text{M} - \text{W}(\text{CO})_5 - \text{Cl}]^+$, 207.0 (30) $[\text{HP}(\text{O})\text{CH}(\text{SiMe}_3)_2]^+$, 147.0 (45) $[\text{C}_3\text{H}_6\text{OPSi}_2]^+$, 73.0 (100) $[\text{SiMe}_3]^+$.

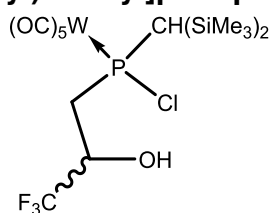
IR (ATR Diamond; $\tilde{\nu}[\text{cm}^{-1}]$, selected data): 2074 (m, $\nu(\text{CO})$), 1987 (w, $\nu(\text{CO})$), 1933 (vs, $\nu(\text{CO})$).

Elemental analysis:

calc.:	C	29.59	H	4.30
found:	C	29.63	H	4.57

Single crystal measurement: GSTR337, 3181

11.2.24.3 Pentacarbonyl{chloro(3,3,3-trifluoro-2-hydroxypropyl)[bis(trimethylsilyl)methyl]phosphane- κP }tungsten(0) [47.1c]



Purification: All volatiles were removed in *vacuo* (ca. 0.02 mbar) and the product was recrystallized by slow evaporation of a concentrated *n*-pentane solution at 4°C.

Molecular formula: $\text{C}_{15}\text{H}_{23}\text{ClF}_3\text{O}_6\text{PSi}_2\text{W}$

Molecular weight: 662.772 g/mol

Melting point: 106 °C

Yield: 70 mg (0.106 mmol, 33 %)

Isomeric ratio: 12 : 88

Isomer 1:

^1H NMR (500.2 MHz, CDCl_3): δ = 0.37 (s, 9H, $\text{Si}(\text{CH}_3)_3$), 0.38 (s, 9H, $\text{Si}(\text{CH}_3)_3$), 2.30 (d, 1H, $^2J_{\text{P,H}} = 13.7$ Hz, P-CH), 2.50 - 2.68 (s, 1H, OH), 2.64 (ddd, 1H, $^2J_{\text{H,H}} = 15.4$ Hz, $^2J_{\text{P,H}} = 2.1$ z, $^3J_{\text{H,H}} = 0.9$ Hz, P- CH_2), 2.88 (ddd, 1H, $^2J_{\text{H,H}} = 15.4$ Hz, $^3J_{\text{H,H}} = 9.9$ Hz, $^2J_{\text{P,H}} = 3.8$ z, P- CH_2), 4.57 - 4.68 (m, 1H, O-CH).

$^{13}\text{C}\{^1\text{H}\}$ NMR (125.8 MHz, CDCl_3): δ = 3.4 (d, $^3J_{\text{P,C}} = 3.8$ Hz, $\text{Si}(\text{CH}_3)_3$), 3.7 (d, $^3J_{\text{P,C}} = 3.0$ Hz, $\text{Si}(\text{CH}_3)_3$), 31.2 (d, $^1J_{\text{P,C}} = 19.6$ Hz, P-CH), 41.8 (d, $^1J_{\text{P,C}} = 16.0$ Hz, P- CH_2), 69.5 (q, $^2J_{\text{F,C}} = 32.6$ Hz, O-CH), 124.4 (qd, $^1J_{\text{F,C}} = 282.2$ Hz, $^4J_{\text{P,C}} = 15.4$ Hz, CF_3), 196.7 (d_{sat} , $^1J_{\text{W,C}} = 126.7$ Hz, $^2J_{\text{P,C}} = 7.1$ Hz, *cis*-CO), 198.2 (d, $^2J_{\text{P,C}} = 31.3$ Hz, *trans*-CO).

$^{19}\text{F}\{^1\text{H}\}$ NMR (282.4 MHz, CDCl_3): δ = -80.7 (s, CF_3).

$^{29}\text{Si}\{^1\text{H}\}$ NMR (99.4 MHz, CDCl_3): δ = -0.43 (d, $^2J_{\text{P,Si}} = 1.3$ Hz, $\text{Si}(\text{CH}_3)_3$), 3.58 (d, $^2J_{\text{P,Si}} = 8.3$ Hz, $\text{Si}(\text{CH}_3)_3$).

$^{31}\text{P}\{^1\text{H}\}$ NMR (202.5 MHz, CDCl_3): δ = 113.4 (s_{br} , FWHI, $h_{1/2} = 26$ Hz).

Isomer 2:

^1H NMR (500.2 MHz, CDCl_3): δ = 0.36 (s, 9H, $\text{Si}(\text{CH}_3)_3$), 0.39 (s, 9H, $\text{Si}(\text{CH}_3)_3$), 1.91 (d, 1H, $^2J_{\text{P,H}} = 9.0$ Hz, P-CH), 2.50 - 2.68 (s, 1H, OH), 2.57 (ddd, 1H, $^2J_{\text{H,H}} = 14.3$ Hz, $^2J_{\text{P,H}} = 12.9$ Hz, $^3J_{\text{H,H}} = 10.1$ Hz, P- CH_2), 2.93 (ddd, 1H, $^2J_{\text{P,H}} = 14.5$ z, $^2J_{\text{H,H}} = 14.3$ Hz, $^3J_{\text{H,H}} = 1.1$ Hz, P- CH_2), 4.53 - 4.63 (m, 1H, O-CH).

$^{13}\text{C}\{^1\text{H}\}$ NMR (125.8 MHz, CDCl_3): δ = 3.2 (d, $^3J_{\text{P,C}} = 3.8$ Hz, $\text{Si}(\text{CH}_3)_3$), 3.9 (d, $^3J_{\text{P,C}} = 2.2$ Hz, $\text{Si}(\text{CH}_3)_3$), 33.1 (d, $^1J_{\text{P,C}} = 11.2$ Hz, P-CH), 38.5 (d, $^1J_{\text{P,C}} = 15.3$ Hz, P- CH_2), 67.9 (q, $^2J_{\text{F,C}} = 32.4$ Hz, O-CH), 124.7 (qd, $^1J_{\text{F,C}} = 282.3$ Hz, $^4J_{\text{P,C}} = 14.3$ Hz, CF_3), 197.4 (d_{sat} , $^1J_{\text{W,C}} = 127.8$ Hz, $^2J_{\text{P,C}} = 7.4$ Hz, *cis*-CO), 199.4 (d_{sat} , $^1J_{\text{W,C}} = 142.0$ Hz, $^2J_{\text{P,C}} = 32.7$ Hz, *trans*-CO).

$^{19}\text{F}\{^1\text{H}\}$ NMR (282.4 MHz, CDCl_3): δ = -81.1 (s, CF_3).

$^{29}\text{Si}\{^1\text{H}\}$ NMR (99.4 MHz, CDCl_3): δ = -0.43 (d, $^2J_{\text{P,Si}} = 1.3$ Hz, $\text{Si}(\text{CH}_3)_3$), 3.58 (d, $^2J_{\text{P,Si}} = 8.3$ Hz, $\text{Si}(\text{CH}_3)_3$).

$^{31}\text{P}\{^1\text{H}\}$ NMR (202.5 MHz, CDCl_3): δ = 110.6 (s_{sat} , $^1J_{\text{W,P}} = 281.3$ Hz).

MS (EI, 70 eV, ^{184}W , selected data): m/z (%) = 662.0 (35) $[\text{M}]^{++}$, 634.0 (30) $[\text{M} - \text{CO}]^+$, 606.0 (5) $[\text{M} - 2\text{CO}]^+$, 578.0 (30) $[\text{M} - 3\text{CO}]^+$, 542.0 (5) $[\text{M} - 3\text{CO} - \text{HCl}]^+$, 73.0 (100) $[\text{SiMe}_3]^+$.

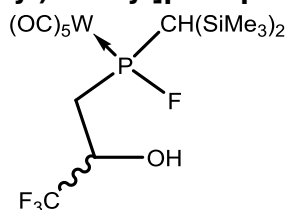
IR (ATR Diamond; $\tilde{\nu}[\text{cm}^{-1}]$, selected data): 3598 (m, $\nu(\text{OH})$), 2074 (m, $\nu(\text{CO})$), 1984 (w, $\nu(\text{CO})$), 1906 (vs, $\nu(\text{CO})$).

Elemental analysis:

calc.:	C	27.18	H	3.50
found:	C	27.36	H	3.69

Single crystal measurement: GSTR419, AKY-505 // GXray4067f

11.2.24.4 Pentacarbonyl{fluoro(3,3,3-trifluoro-2-hydroxypropyl)[bis(trimethylsilyl)methyl]phosphane- κ P}tungsten(0) [48.1a]



Purification: All volatiles were removed in *vacuo* (ca. 0.02 mbar) and the product was recrystallized by slow evaporation of a concentrated *n*-pentane solution at 4°C.

Molecular formula:	C ₁₅ H ₂₃ F ₄ O ₆ PSi ₂ W
Molecular weight:	646.318 g/mol
Melting point:	99 °C
Yield:	81 mg (0.126 mmol, 39 %)

Isomeric ratio: 26 : 74

Isomer 1:

¹H NMR (500.2 MHz, CDCl₃): δ = 0.28 (s, 9H, Si(CH₃)₃), 0.28 (s, 9H, Si(CH₃)₃), 2.11 (d, 1H, ²J_{P,H} = 12.2 Hz, P-CH), 2.44 (s, 1H, OH), 2.70 - 2.81 (m, 1H, P-CH₂), 2.75 (dddd, 1H, ²J_{P,H} = 13.5 Hz, J = 15.1 Hz, J = 10.5 Hz, J = 6.0 Hz, P-CH₂), 4.54 - 4.65 (m, 1H, O-CH).

¹³C{¹H} NMR (125.8 MHz, CDCl₃): δ = 2.4 (d, ³J_{P,C} = 2.7 Hz, Si(CH₃)₃), 2.8 (dd, J = 2.7 Hz, J = 1.9 Hz, Si(CH₃)₃), 34.1 (d, ¹J_{P,C} = 13.3 Hz, P-CH), 38.2 (dd, J = 19.5 Hz, J = 15.0 Hz, P-CH₂), 69.3 (q, ²J_{F,C} = 32.7 Hz, O-CH), 124.4 (qd, ¹J_{C,F} = 282.0 Hz, J = 17.7 Hz, CF₃), 196.0 (dd_{sat}, ¹J_{W,C} = 125.7 Hz, ²J_{P,C} = 7.9 Hz, ³J_{F,C} = 2.9 Hz, *cis*-CO), 198.3 (d_{sat}, ¹J_{W,C} = 137.2 Hz, ²J_{P,C} = 29.4 Hz, *trans*-CO).

¹⁹F{¹H} NMR (282.4 MHz, CDCl₃): δ = -111.0 (d, 1F, ¹J_{P,F} = 823.0 Hz, P-F), -80.7 (s, 3F, CF₃).

²⁹Si{¹H} NMR (99.4 MHz, CDCl₃): δ = -3.3 (d, J = 4.4 Hz, Si(CH₃)₃), 1.90 (dd, J = 14.2, J = 7.0, Si(CH₃)₃).

³¹P{¹H} NMR (202.5 MHz, CDCl₃): δ = 194.0 (d_{sat,br} full-width at half-intensity (FWHI, *h*_{1/2}) = 60 Hz, ¹J_{P,F} = 823.0 Hz, ¹J_{W,P} = ca. 290 Hz).

Isomer 2:

^1H NMR (500.1 MHz, CDCl_3): δ = 0.31 (s, 9H, $\text{Si}(\text{CH}_3)_3$), 0.32 (s, 9H, $\text{Si}(\text{CH}_3)_3$), 2.06 (d, 1H, $^2J_{\text{P,H}} = 11.0$ Hz, P-CH), 2.54 (s, 1H, OH), 2.70 - 2.81 (m, 1H, P- CH_2), 2.88 (ddd, 1H, $^2J_{\text{P,H}} = 15.0$ Hz, $J = 15.0$ Hz, $J = 2.7$ Hz, P- CH_2), 4.34 - 4.48 (m, 1H, O-CH).

$^{13}\text{C}\{^1\text{H}\}$ NMR (125.8 MHz, CDCl_3): δ = 2.5 (d, $^3J_{\text{P,C}} = 3.2$ Hz, $\text{Si}(\text{CH}_3)_3$), 2.7 (dd, $J = 3.0$ Hz, $J = 1.7$ Hz, $\text{Si}(\text{CH}_3)_3$), 34.9 (d, $^1J_{\text{P,C}} = 13.9$ Hz, P-CH), 37.0 (dd, $J = 20.7$ Hz, $J = 15.8$ Hz, P- CH_2), 66.8 (qd, $^2J_{\text{F,C}} = 32.8$ Hz, $J = 2.2$ Hz, O-CH), 124.6 (qd, $^1J_{\text{C,F}} = 282.2$ Hz, $J = 12.8$ Hz, CF_3), 196.7 (dd_{sat}, $^1J_{\text{W,C}} = 126.4$ Hz, $^2J_{\text{P,C}} = 8.1$ Hz, $^3J_{\text{F,C}} = 2.8$ Hz, *cis*-CO), 199.1 (d_{sat}, $^1J_{\text{W,C}} = 138.1$ Hz, $^2J_{\text{P,C}} = 29.2$ Hz, *trans*-CO).

$^{19}\text{F}\{^1\text{H}\}$ NMR (282.4 MHz, CDCl_3): δ = -81.2 (s, 3F, CF_3), -115.9 (d, 1F, $^1J_{\text{P,F}} = 821.8$ Hz, P-F).

$^{29}\text{Si}\{^1\text{H}\}$ NMR (99.4 MHz, CDCl_3): δ = -3.3 (d, $J = 4.4$ Hz, $\text{Si}(\text{CH}_3)_3$), 1.90 (dd, $J = 14.2$, $J = 7.0$, $\text{Si}(\text{CH}_3)_3$).

$^{31}\text{P}\{^1\text{H}\}$ NMR (202.5 MHz, CDCl_3): δ = 185.6 (d_{sat}, $^1J_{\text{P,F}} = 821.8$ Hz, $^1J_{\text{W,P}} = 294.0$ Hz).

MS (EI, 70 eV, ^{184}W , selected data): m/z (%) = 654.9 (30) $[\text{M}]^+$, 617.9 (60) $[\text{M} - \text{CO}]^+$, 589.9 (100) $[\text{M} - 2 \text{CO}]^+$, 561.9 (40) $[\text{M} - 3 \text{CO}]^+$, 543.9 (75) $[\text{M} - 4 \text{CO}]^+$, 73.1 (85) $[\text{SiMe}_3]^+$.

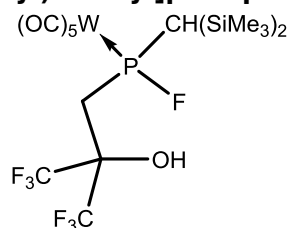
IR (ATR Diamond; $\tilde{\nu}[\text{cm}^{-1}]$, selected data): 3607 (m, $\nu(\text{OH})$), 2075 (m, $\nu(\text{CO})$), 1985 (w, $\nu(\text{CO})$), 1904 (vs, $\nu(\text{CO})$).

Elemental analysis:

calc.:	C	27.87	H	3.59
found:	C	27.87	H	3.71

Single crystal measurement: GSTR418, AKY-506 // GXray4066

11.2.24.5 Pentacarbonyl{[3,3,3-trifluoro-2-(trifluoromethyl)-2-hydroxypropyl][bis(trimethylsilyl)methyl]phosphane- κ P}tungsten(0) [48.1b]



Purification: The mixture turned slightly blue during the reaction. All volatiles were removed in *vacuo* (ca. 0.02 mbar) and the product was recrystallized by slow evaporation of a concentrated *n*-pentane solution at 4°C to yield colourless crystals.

Molecular formula:	C ₁₆ H ₂₂ F ₇ O ₆ PSi ₂ W
Molecular weight:	714.316 g/mol
Melting point:	110 °C
Yield:	98 mg (0.137 mmol, 70 %)

¹H NMR (300.1 MHz, CDCl₃): δ = 0.30 (d, 9H, ⁴J_{P,H} = 1.5 Hz, Si(CH₃)₃), 0.33 (s, 9H, Si(CH₃)₃), 2.08 (d_{br}, 1H, ²J_{P,H} = 5.7 Hz, P-CH), 2.41 - 2.67 (m, 1H, P-CH₂), 3.03 - 3.26 (m, 1H, P-CH₂), 3.41 (s, 1H, OH).

¹³C{¹H} NMR (75.5 MHz, CDCl₃): δ = 2.5 (d, ³J_{P,C} = 2.9 Hz, Si(CH₃)₃), 2.65 - 2.79 (m, Si(CH₃)₃), 34.8 - 35.8 (m, CH₂), 36.0 - 36.9 (m, P-CH), C(CF₃)₂ not observed due to low intensity, 122.5 (q, ¹J_{C,F} = 286.3 Hz, CF₃), 123.0 (qd, ¹J_{C,F} = 287.5 Hz, ¹J_{P,C} = 6.8 Hz, CF₃), 196.4 (dd_{sat}, ¹J_{W,C} = 125.5 Hz, ²J_{P,C} = 8.1 Hz, ³J_{F,C} = 2.9 Hz, *cis*-CO), 198.7 (dm, ²J_{P,C} = 31.6 Hz, *trans*-CO).

¹⁹F{¹H} NMR (282.4 MHz, CDCl₃): δ = -110.5 (dq, 1F, ¹J_{P,F} = 851.8 Hz, ⁵J_{F,F} = 17.4 Hz, P-F), -79.2 - -79.5 (m, 3F, CF₃), -76.6 - -77.0 (m, 3F, CF₃).

³¹P{¹H} NMR (121.5 MHz, CDCl₃): δ = 180.4 (d_{sat}, ¹J_{P,F} = 852.4 Hz, ¹J_{W,P} = 302.1 Hz).

MS (EI, 70 eV, ¹⁸⁴W, selected data): m/z (%) = 714.0 (25) [M]⁺, 686.0 (30) [M - CO]⁺, 658.0 (60) [M - 2 CO]⁺, 610.0 (100) [M - 3 CO - HF]⁺, 554.0 (20) [M - 5 CO - HF]⁺, 73.1 (70) [SiMe₃]⁺.

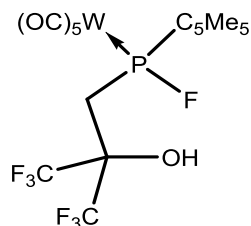
IR (ATR Diamond; $\tilde{\nu}$ [cm⁻¹], selected data): 3533 (m, ν (OH)), 2077 (m, ν (CO)), 1990 (w, ν (CO)), 1908 (vs, ν (CO)).

Elemental analysis:

calc.:	C	26.90	H	3.10
found:	C	27.02	H	3.17

Single crystal measurement: GSTR413, AKY-499A // GXray4033f

11.2.24.6 Pentacarbonyl{fluoro[3,3,3-trifluoro-2-(trifluoromethyl)-2-hydroxypropyl](1,2,3,4,5-pentamethylcyclopenta-2,4-dien-1-yl)phosphane- κP }tungsten(0) [48.2b]



Purification: The mixture turned yellow during the reaction. All volatiles were removed in *vacuo* (ca 0.02 mbar) to yield the product as slightly yellow solid.

Molecular formula: $C_{19}H_{18}F_7O_6PW$

Molecular weight: 690.145 g/mol

Yield: 146.3 mg (0.212 mmol, 100 %)

1H NMR (300.1 MHz, $CDCl_3$): δ = 1.46 (d, 3H, $J_{P,H}$ = 14.3 Hz, C_5Me_5), 1.84 (s, 6H, C_5Me_5), 1.85 (s, 3H, C_5Me_5), 1.93 (s, 3H, C_5Me_5), 2.30 - 2.58 (m, 1H, P- CH_2), 2.90 - 3.35 (m, 1H, P- CH_2), 3.54 (s, 1H, OH).

$^{13}C\{^1H\}$ NMR (75.5 MHz, $CDCl_3$): δ = 11.6 (s, C_5Me_5), 11.8 (s, C_5Me_5), 12.4 (d, J = 2.8 Hz, C_5Me_5), 12.5 (dd, J = 3.9 Hz, J = 1.3 Hz, C_5Me_5), 15.4 (s_{br}, C_5Me_5), 33.8 (s_{br}, P- CH_2), 64.8 (dd, J = 10.5 Hz, J = 8.7 Hz, P- C_5Me_5), 76.0 - 78.0 (m, $C(CF_3)_2$), 122.6 (qd, $^1J_{F,C}$ = 287.4 Hz, $^4J_{P,C}$ = 1.9 Hz, CF_3), 123.0 (qd, $^1J_{F,C}$ = 287.3 Hz, $^4J_{P,C}$ = 5.2 Hz, CF_3), 142.5 (s_{br}, C=C), 144.5 (s_{br}, C=C), 195.6 (d_{sat}, $^1J_{W,C}$ = 126.2 Hz, $^2J_{P,C}$ = 6.9 Hz, *cis*-CO), 197.5 (d, $^2J_{P,C}$ = 33.0 Hz, *trans*-CO).

$^{19}F\{^1H\}$ NMR (282.4 MHz, $CDCl_3$): δ = -144.1 (d, 1F, $^1J_{P,F}$ = 830 Hz, P-F), -78.5 (s, 3F, CF_3), -77.5 (s, 3F, CF_3).

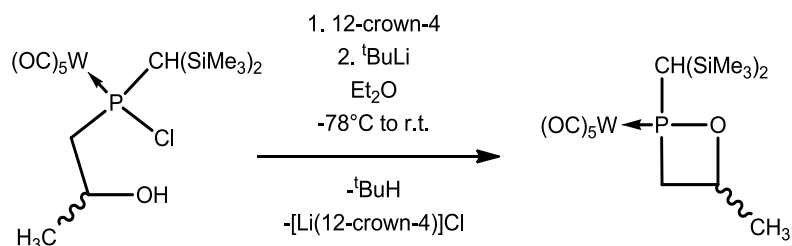
$^{31}P\{^1H\}$ NMR (121.5 MHz, $CDCl_3$): δ = 190.3 (d_{br}, $^1J_{P,F}$ = 830 Hz, full-width at half-intensity (FWHI, $h_{1/2}$) = 440 Hz).

MS (EI, 70 eV, ^{184}W , selected data): m/z (%) = 690.1 (10) $[M]^{+}$, 634.0 (5) $[M - 2 CO]^{+}$, 606.1 (40) $[M - 3 CO]^{+}$, 554.9 (15) $[M - C_5Me_5]^{+}$, 526.9 (40) $[M - C_5Me_5 - CO]^{+}$, 498.9 (40) $[M - C_5Me_5 - 2 CO]^{+}$, 470.9 (10) $[M - C_5Me_5 - 3 CO]^{+}$, 135.1 (100) $[C_5Me_5]^{+}$.

IR (ATR Diamond; $\tilde{\nu}$ [cm^{-1}], selected data): 3557 (m, $\nu(OH)$), 2078 (m, $\nu(CO)$), 1990 (w, $\nu(CO)$), 1917 (vs, $\nu(CO)$).

Single crystal measurement: GSTR392, AKY-476 // GXray3908f

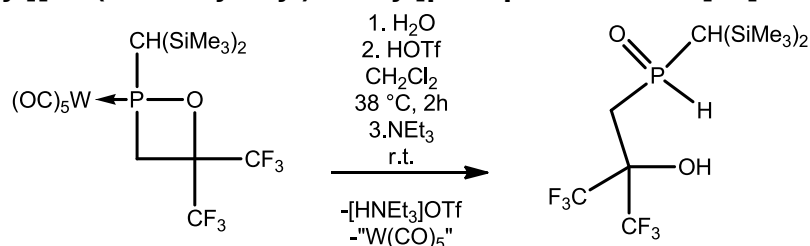
11.2.25 Synthesis of 1,2-oxaphosphetane complex (21.1a_W) from pentacarbonyl{chloro(2-hydroxypropyl)[bis(trimethylsilyl)methyl]phosphane-κP}tungsten(0) (47.1b)



Synthesis: In a 10 mL Schlenk tube, 22.7 mg (0.038 mmol) of chlorophosphane complex **47.1b** were dissolved in 1 mL of diethyl ether and 6 μ L (0.033 mmol) of 12-crown-4 were added. The solution was cooled to -78 °C and 0.025 mL (0.042 mmol, 1.1 eq., 1.7 M in *n*-pentane) of *tert*-butyllithium was added. The solution was allowed slowly warming up to ambient temperature. Formation of a white salt was observed and the reaction mixture subsequently analysed by $^{31}\text{P}\{^1\text{H}\}$ NMR.

The $^{31}\text{P}\{^1\text{H}\}$ NMR spectrum showed the selective conversion to **21.1a_W**¹⁻⁴. A mixture of the isomers that were described before was observed (ratio: 10:0:60:30).

11.2.26 Synthesis of [3,3,3-trifluoro-2-(trifluoromethyl)-2-hydroxypropyl][bis(trimethylsilyl)methyl]phosphane-oxide [52]



Synthesis: In a 50 mL Schlenk tube, 300 mg (0.432 mmol) of 1,2-oxaphosphetane complex **25.1b** were dissolved in 20 mL of CH_2Cl_2 and 10 μ L of H_2O (0.556 mmol, 1.29 eq.) were added. The mixture was treated with 0.1 mL of TfOH (1.130 mmol, 2.6 eq.) and heated to 38 °C for 2 h. After cooling to ambient temperature 0.4 mL of Net_3 (2.867 mmol, 6.6 eq.) were added, which led to a colour change of the solution to brown.

Purification: The solution was acidified with conc. HCl and the yellow organic phase separated from the violet inorganic phase. All volatiles were evaporated from the organic phase in *vacuo* (ca. 0.02 mbar) and the product was subsequently extracted with five times 10 mL of *n*-pentane. All volatiles were removed in *vacuo* (ca. 0.02 mbar) and the product purified by subliming off the remaining $\text{W}(\text{CO})_6$ at 55 °C/ $1.4 \cdot 10^{-2}$ mbar for 6 h. The progress was checked by IR spectroscopy and stopped after vanishing of all signals for the CO-vibration.

<u>Molecular formula:</u>	C ₁₁ H ₂₃ F ₆ O ₂ PSi ₂
<u>Molecular weight:</u>	388.434 g/mol
<u>Melting point:</u>	134 °C
<u>Yield:</u>	76.7 mg (0.197 mmol, 46 %)

¹H NMR (500.2 MHz, CDCl₃): δ = 0.27 (s, 9H, Si(CH₃)₃), 0.30 (s, 9H, Si(CH₃)₃), 0.7 (d, 1H, ²J_{P,H} = 18.2 Hz, P-CH), 2.12 (dd, 1H, ²J_{H,H} = 15.9 Hz, ²J_{P,H} = 5.0 Hz, P-CH₂), 2.52 (ddd, 1H, ²J_{H,H} = 15.9 Hz, ³J_{H,H} = 7.1 Hz, ²J_{F,H} = 17.3 Hz, P-CH₂), 7.50 (d, 1H, ¹J_{P,H} = 485.6 Hz, P-H), 7.53 (s_{br}, 1H, OH).

¹³C{¹H} NMR (125.8 MHz, CDCl₃): δ = 1.2 (d_{sat}, ³J_{P,C} = 4.0 Hz, ¹J_{Si,C} = 53.2 Hz, Si(CH₃)₃), 2.0 (d_{sat}, ³J_{P,C} = 3.2 Hz, ¹J_{Si,C} = 53.4 Hz, Si(CH₃)₃), 20.0 (d_{sat}, ¹J_{P,C} = 41.8 Hz, ¹J_{Si,C} = 32.0 Hz, P-CH), 27.9 (d, ¹J_{P,C} = 60.0 Hz, P-CH₂), 75.6 - 77.3 (dm, ²J_{P,C} = 5.7 Hz, C(CF₃)₂), 122.4 (qd, ¹J_{F,C} = 285.6 Hz, ³J_{P,C} = 12.2 Hz, CF₃), 123.5 (q, ¹J_{F,C} = 288.1 Hz, CF₃).

¹⁹F{¹H} NMR (469.7 MHz, CDCl₃): δ = -79.9 (q, ⁴J_{F,F} = 10.0 Hz, CF₃), -76.4 (qd, ⁴J_{F,F} = 10.0 Hz, ⁴J_{P,F} = 8.6 Hz, CF₃).

²⁹Si{¹H} NMR (99.4 MHz, CDCl₃): δ = 1.46 (d, ²J_{P,Si} = 4.0 Hz, Si(CH₃)₃), 1.58 (d, ²J_{P,Si} = 6.8 Hz, Si(CH₃)₃).

³¹P NMR (202.5 MHz, CDCl₃): δ = 34.3 (d, ¹J_{P,H} = 485.6 Hz).

MS (EI, 70 eV, ¹⁸⁴W, selected data): m/z (%) = 388.1 (10) [M]⁺, 373.1 (100) [M - CH₃]⁺, 319.1 (45) [M - CF₃]⁺, 73.1 (50) [SiMe₃]⁺.

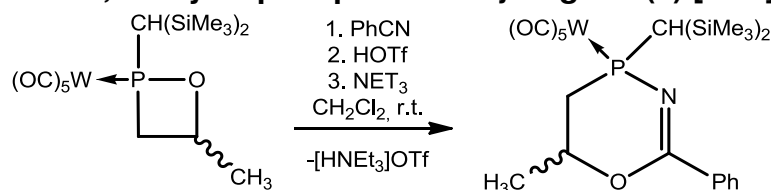
HR-MS: calculated for C₁₁H₂₃F₆O₂PSi₂: 388.0878, found: 388.0876 (+/- 0.47 ppm)

IR (ATR Diamond; $\tilde{\nu}$ [cm⁻¹], selected data): 2961 (m, ν(OH)), 2366 (w, ν(PH)).

Elemental analysis:

calc.:	C	34.01	H	5.97
found:	C	34.34	H	6.07

11.2.27 Synthesis of pentacarbonyl{6-methyl-4-[bis(trimethylsilyl)methyl]-2-phenyl-1-oxa-3-aza-5,6-dihydrophosphinine- κP }tungsten(0) [54.1]



Synthesis: In a 50 mL Schlenk tube, 572 mg (1.0 mmol) of the 1,2-oxaphosphetane complex **21.1a_w** were dissolved in 20 mL of CH₂Cl₂. Then 0.11 mL (1.1 mmol, 1.1 eq.) of PhCN and, subsequently, 0.13 mL (1.5 mmol, 1.5 eq.) of HOTf was added. The mixture was stirred for 30 minutes at ambient temperature, cooled to 0 °C and 0.21 mL (1.5 mmol, 1.5 eq.) of triethylamine was added.

Purification: After 20 min of stirring the solvent was removed in *vacuo* (ca. 0.02 mbar). The residue was purified by column chromatography (SiO₂, -20 °C, eluent: petroleum ether, petroleum ether/diethyl ether 10 : 0.1). The product was obtained as a yellow solid after evaporation of the second yellow fraction in *vacuo* (ca. 0.02 mbar) and recrystallization by slow evaporation of a saturated diethyl ether solution at 4 °C.

Molecular formula:	C ₂₂ H ₃₀ NO ₆ PSi ₂ W
Molecular weight:	675.461 g/mol
Melting point:	143 - 144 °C
Yield:	375.6 mg (0.560 mmol, 56 %)

¹H NMR (300.1 MHz, CDCl₃): δ = 0.20 (s, 9H, Si(CH₃)₃), 0.34 (s, 9H, Si(CH₃)₃), 1.50 (d_{sat}, 1H, ²J_{P,H} = 12.2 Hz, ²J_{Si,H} = 9.4 Hz, P-CH), 1.63 (dd, 3H, ⁴J_{P,H} = 2.0 Hz, ³J_{H,H} = 6.2 Hz, CH₃), 2.28 (ddd, 1H, ²J_{P,H} = 12.0 Hz, ²J_{H,H} = 13.6 Hz, ³J_{H,H} = 12.1 Hz, P-CH₂), 2.50 (dd, 1H, ²J_{H,H} = 13.6 Hz, ³J_{H,H} = 2.2 Hz, P-CH₂), 4.84 (dddq, 1H, ³J_{P,H} = 12.0 Hz, ³J_{H,H} = 12.1 Hz, ³J_{H,H} = 6.2 Hz, ³J_{H,H} = 2.2 Hz, O-CH), 7.36 - 7.52 (m, 3H, Ph), 7.95 - 8.01 (m, 2H, Ph).

¹³C{¹H} NMR (75.5 MHz, CDCl₃): δ = 2.8 (d, ²J_{P,C} = 6.5 Hz, Si(CH₃)₃), 2.9 (d, ²J_{P,C} = 4.5 Hz, Si(CH₃)₃), 23.5 (d, ³J_{P,C} = 10.0 Hz, CH₃), 24.9 (d, ¹J_{P,C} = 10.7 Hz, P-CH), 33.3 (d, ¹J_{P,C} = 19.4 Hz, P-CH₂), 71.1 (s, O-CH), 128.1 (s, CH_{Ar}), 128.3 (d, J_{P,C} = 1.0 Hz, CH_{Ar}), 131.5 (s, CH_{Ar}), 133.3 (d, ³J_{P,C} = 10.0 Hz, ipso-C), 157.0 (d, ²J_{P,C} = 12.9 Hz, C=N), 197.9 (d_{sat}, ¹J_{W,C} = 126.4 Hz, ²J_{P,C} = 7.8 Hz, *cis*-CO), 200.5 (d, ²J_{P,C} = 22.6, *trans*-CO).

²⁹Si{¹H} NMR (59.6 MHz, CDCl₃): δ = -2.50 (s, Si(CH₃)₃), -0.08 (d, ²J_{P,Si} = 9.4 Hz, Si(CH₃)₃).

³¹P NMR (121.5 MHz, CDCl₃): δ = 40.0 (ddd_{sat}, ¹J_{W,P} = 258.8 Hz, ²J_{P,H} = 12 Hz, ²J_{P,H} = 12 Hz, ³J_{P,H} = 12 Hz).

MS (EI, 70 eV, ^{184}W , selected data): m/z (%) = 675.0 (40) $[\text{M}]^{++}$, 647.1 (60) $[\text{M} - \text{CO}]^+$, 619.1 (40) $[\text{M} - 2 \text{CO}]^+$, 591.1 (40) $[\text{M} - 3 \text{CO}]^+$, 577.0 (10) $[\text{M} - \text{C}_3\text{H}_6 - 2 \text{CO}]^+$, 549.0 (10) $[\text{M} - \text{C}_3\text{H}_6 - 3 \text{CO}]^+$, 535.1 (20) $[\text{M} - 5 \text{CO}]^+$, 493.0 (90) $[\text{M} - \text{C}_3\text{H}_6 - 5 \text{CO}]^+$, 488.0 (20) $[\text{M} - \text{PhCN} - 3 \text{CO}]^+$, 432.0 (10) $[\text{M} - \text{PhCN} - 5 \text{CO}]^+$, 73.1 (100) $[\text{SiMe}_3]^+$.

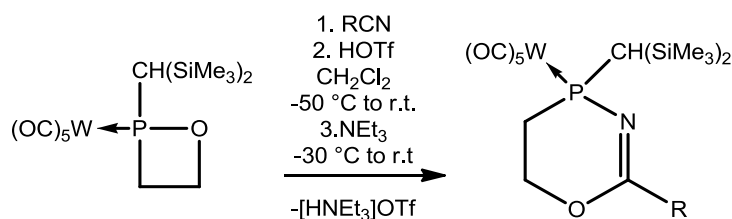
IR (ATR Diamond; $\tilde{\nu}[\text{cm}^{-1}]$, selected data): 2067 (m, $\nu(\text{CO})$), 1974 (w, $\nu(\text{CO})$), 1898 (s, $\nu(\text{CO})$), 1618 (m, $\nu(\text{C}=\text{N})$).

Elemental analysis:

calc.:	C	39.12	H	4.48	N	2.07
found:	C	39.08	H	4.60	N	2.13

Single crystal measurement: GSTR345, 3334

11.2.28 Optimized synthetic protocol for the acid induced ring expansion with nitriles:

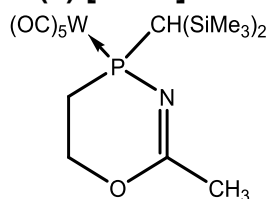


Synthesis: In a 20 mL Schlenk tube, 1,2-oxaphosphetane complex **34.1_w** was dissolved in 10 mL of CH_2Cl_2 and an excess of the corresponding nitrile was added. The mixture was cooled to $-50\text{ }^\circ\text{C}$ and TfOH was added dropwise. The solution was allowed warming up to $-30\text{ }^\circ\text{C}$, then the cooling bath was removed and stirring was continued for further 30 minutes at ambient temperature. The solution was again cooled to $-30\text{ }^\circ\text{C}$ and triethylamine was added. The reaction mixture was allowed to slowly warm up to ambient temperature overnight.

Table 11.5: Used amounts of 1,2-oxaphosphetane complex **34.1_w** and reagents for the acid induced ring expansion reaction with nitriles.

	R	m (34.1_w) [mg]	n (34.1_w) [mmol]	V (RCN) [mL]	V (HOTf) [mL]	V (NEt_3) [mL]
55.1a	CH_3	140	0.25	0.5	0.1	0.5
55.1b	Ph	140	0.25	0.5	0.1	0.5
55.1c	^tBu	167.5	0.3	0.25	0.1	0.25

11.2.28.1 Pentacarbonyl{2-methyl-4-[bis(trimethylsilyl)methyl]-1-oxa-3-aza-5,6-dihydrophosphinine- κP }tungsten(0) [55.1a]



Purification: All volatiles were removed in *vacuo* (ca. 0.02 mbar). The crude material was purified by filtration over SiO₂ (\varnothing = 2 cm, h = 3 cm) using a mixture of petroleum ether 40/60 and diethyl ether in a ratio of 10 : 1. The product was obtained as white powder after removing of all volatiles in *vacuo* (ca. 0.02 mbar).

Molecular formula:	C ₁₆ H ₂₄ NO ₆ PSi ₂ W
Molecular weight:	599.366 g/mol
Melting point:	153 °C
Yield:	149 mg (0.248 mmol, 99 %)

¹H NMR (500.2 MHz, CDCl₃): δ = 0.24 (s, 9H, Si(CH₃)₃), 0.30 (s, 9H, Si(CH₃)₃), 1.36 (d, 1H, ²J_{P,H} = 12.1 Hz, P-CH), 2.01 (d, 3H, ⁴J_{P,H} = 1.25 Hz, CH₃), 2.26 - 2.33 (m, 1H, P-CH₂), 2.40 - 2.52 (m, 1H, P-CH₂), 4.42 - 4.61 (m, 2H, O-CH₂).

¹³C{¹H} NMR (125.8 MHz, CDCl₃): δ = 2.9 (d, ³J_{P,C} = 3.7 Hz, Si(CH₃)₃), 3.1 (d, ³J_{P,C} = 1.7 Hz, Si(CH₃)₃), 23.5 (d, ³J_{P,C} = 8.8 Hz, CH₃), 25.3 (d, ¹J_{P,C} = 11.3 Hz, P-CH), 26.2 (d, ¹J_{P,C} = 19.6 Hz, P-CH₂), 63.7 (d, ²J_{P,C} = 1.7 Hz, O-CH₂), 160.0 (d, ²J_{P,C} = 13.7 Hz, C=N), 198.0 (d_{sat}, ¹J_{W,C} = 126.5 Hz, ²J_{P,C} = 7.6 Hz, *cis*-CO), 200.6 (d_{sat}, ¹J_{W,C} = 143.0 Hz, ²J_{P,C} = 22.9 Hz, *trans*-CO).

²⁹Si{¹H} NMR (99.4 MHz, CDCl₃): δ = -1.94 (s, Si(CH₃)₃), 0.59 (d, ²J_{P,Si} = 9.3 Hz, Si(CH₃)₃).

³¹P{¹H} NMR (202.5 MHz, CDCl₃): δ = 34.1 (s_{sat}, ¹J_{W,P} = 259.2 Hz).

MS (EI, 70 eV, ¹⁸⁴W, selected data): m/z (%) = 599.0 (30) [M]⁺, 570.9 (60) [M - CO]⁺, 558.0 (5) [M - CH₃CN]⁺, 543.0 (75) [M - 2 CO]⁺, 515.0 (60) [M - 3 CO]⁺, 502.0 (10) [M - CH₃CN - 2 CO]⁺, 486.9 (15) [M - 4 CO]⁺, 474.0 (10) [M - CH₃CN - 3 CO]⁺, 459.0 (50) [M - 5 CO]⁺, 446.0 (5) [M - CH₃CN - 4 CO]⁺, 418.0 (55) [M - CH₃CN - 5 CO]⁺, 390.0 (100) [M - CH₃CN - 5 CO - C₂H₄]⁺, 73.1 (50) [SiMe₃]⁺.

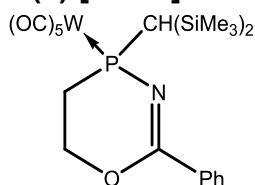
IR (ATR Diamond; $\tilde{\nu}$ [cm⁻¹], selected data): 2068 (s, ν (CO)), 1987 (w, ν (CO)), 1975 (w, ν (CO)), 1934 (w, ν (CO)), 1894 (vs, ν (CO)), 1642 (m, ν (C=N)).

Elemental analysis:

calc.:	C	32.06	H	4.37	N	2.34
found:	C	31.98	H	4.36	N	2.35

Single crystal measurement: GSTR510, AKY-569 // GXray4796

11.2.28.2 Pentacarbonyl{4-[bis(trimethylsilyl)methyl]-2-phenyl-1-oxa-3-aza-5,6-dihydrophosphinine- κ P}tungsten(0) [55.1b]



Purification: All volatiles were removed in *vacuo* (ca. 0.02 mbar). The crude material was purified by filtration over SiO₂ (\varnothing = 2 cm, h = 3 cm) using a mixture of petroleum ether 40/60 and diethyl ether in a ratio of 10 : 1. The product was obtained as yellow foam after removing of all volatiles in *vacuo* (ca. 0.02 mbar). It could be recrystallized by slow evaporation of a saturated diethyl ether solution at 4 °C to solidify it.

Molecular formula:	C ₂₁ H ₂₈ NO ₆ PSi ₂ W
Molecular weight:	661.435 g/mol
Melting point:	154 °C
Yield:	165 mg (0,248 mmol, 99 %)

¹H NMR (500.2 MHz, CDCl₃): δ = 0.22 (s, 9H, Si(CH₃)₃), 0.34 (s, 9H, Si(CH₃)₃), 1.51 (d, 1H, ²J_{P,H} = 12.0 Hz, P-CH), 2.41 - 2.47 (m, 1H, P-CH₂), 2.60 - 2.71 (m, 1H, P-CH₂), 4.69 - 4.84 (m, 2H, O-CH₂), 7.37 - 7.43 (m, 2H, CH_{Ar}), 7.45 - 7.50 (m, 1H, *para*-CH_{Ar}), 7.92 - 7.96 (m, 2H, CH_{Ar}).

¹³C{¹H} NMR (125.8 MHz, CDCl₃): δ = 2.9 (d, ³J_{P,C} = 3.8 Hz, Si(CH₃)₃), 3.1 (d, ³J_{P,C} = 1.7 Hz, Si(CH₃)₃), 25.2 (d, ¹J_{P,C} = 10.2 Hz, P-CH), 26.8 (d, ²J_{P,C} = 19.6 Hz, P-CH₂), 64.3 (d, ¹J_{P,C} = 1.8 Hz, O-CH₂), 128.3 (s, *ortho*-CH_{Ar} + *meta*-CH_{Ar}), 131.7 (s, *para*-CH_{Ar}), 133.5 (d, ³J_{P,C} = 9.6 Hz, *ipso*-C), 156.9 (d, ²J_{P,C} = 12.6 Hz, C=N), 198.0 (d_{sat}, ¹J_{W,C} = 126.5 Hz, ²J_{P,C} = 7.5 Hz, *cis*-CO), 200.6 (d_{sat}, ¹J_{W,C} = 143.0 Hz, ²J_{P,C} = 22.9 Hz, *trans*-CO).

²⁹Si{¹H} NMR (99.4 MHz, CDCl₃): δ = -1.74 (s, Si(CH₃)₃), 0.59 (d, ²J_{P,Si} = 9.1 Hz, Si(CH₃)₃).

³¹P{¹H} NMR (202.5 MHz, CDCl₃): δ = 36.1 (s_{sat}, ¹J_{W,P} = 259.6 Hz).

MS (EI, 70 eV, ^{184}W , selected data): m/z (%) = 661.1 (25) $[\text{M}]^{++}$, 633.1 (80) $[\text{M} - \text{CO}]^+$, 605.1 (70) $[\text{M} - 2 \text{CO}]^+$, 577.1 (80) $[\text{M} - 3 \text{CO}]^+$, 549.1 (5) $[\text{M} - 4 \text{CO}]^+$, 521.1 (70) $[\text{M} - 5 \text{CO}]^+$, 493.1 (100) $[\text{M} - 5 \text{CO} - \text{C}_2\text{H}_4]^+$, 390.0 (70) $[\text{M} - 5 \text{CO} - \text{PhCN} - \text{C}_2\text{H}_4]^+$, 73.1 (70) $[\text{SiMe}_3]^+$.

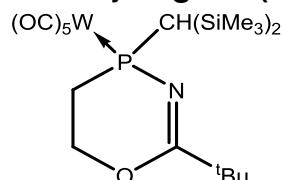
IR (ATR Diamond; $\tilde{\nu}[\text{cm}^{-1}]$, selected data): 2067 (s, $\nu(\text{CO})$), 1974 (w, $\nu(\text{CO})$), 1900 (vs, $\nu(\text{CO})$), 1626 (m, $\nu(\text{C}=\text{N})$).

Elemental analysis:

calc.:	C	38.13	H	4.27	N	2.12
found:	C	38.32	H	4.32	N	2.17

Single crystal measurement: GSTR509, AKY-570 // GXray4797

11.2.28.3 Pentacarbonyl{2-(1,1-dimethylethyl)-4-[bis(trimethylsilyl)methyl]-1-oxa-3-aza-5,6-dihydrophosphinine- κ P}tungsten(0) [55.1c]



Purification: All volatiles were removed in *vacuo* (ca. 0.02 mbar). The product was purified by filtration over SiO_2 ($\varnothing = 2$ cm, $h = 3$ cm) using diethyl ether. The crude yellow product, obtained as an oil in almost quantitative yield (99%) after removal of all volatiles in *vacuo* (ca. 0.02 mbar), was then recrystallized by slow evaporation of a saturated diethyl ether solution at 4 °C.

Molecular formula:	$\text{C}_{19}\text{H}_{32}\text{NO}_6\text{PSi}_2\text{W}$
Molecular weight:	641.445 g/mol
Melting point:	138 - 139 °C
Yield:	82 mg (0.13 mmol, 43 %)

^1H NMR (500.2 MHz, CDCl_3): $\delta = 0.27$ (s, 9H, $\text{Si}(\text{CH}_3)_3$), 0.31 (s, 9H, $\text{Si}(\text{CH}_3)_3$), 1.16 (s, 9H, $\text{C}(\text{CH}_3)_3$), 1.40 (d, 1H, $^2J_{\text{P,H}} = 12.1$ Hz, P-CH), 2.26 - 2.33 (m, 1H, P- CH_2), 2.40 - 2.52 (m, 1H, P- CH_2), 4.48 - 4.67 (m, 2H, O- CH_2).

$^{13}\text{C}\{^1\text{H}\}$ NMR (125.8 MHz, CDCl_3): $\delta = 3.0$ (d, $^3J_{\text{P,C}} = 3.5$ Hz, $\text{Si}(\text{CH}_3)_3$), 3.4 (d, $^3J_{\text{P,C}} = 1.6$ Hz, $\text{Si}(\text{CH}_3)_3$), 25.0 (d, $^1J_{\text{P,C}} = 10.1$ Hz, P-CH), 26.3 (d, $^1J_{\text{P,C}} = 20.2$ Hz, P- CH_2), 28.1 (s, $\text{C}(\text{CH}_3)_3$), 40.1 (d, $^2J_{\text{P,C}} = 7.6$ Hz, $\text{C}(\text{CH}_3)_3$), 64.3 (d, $^2J_{\text{P,C}} = 1.6$ Hz, P- CH_2), 168.8 (d, $^2J_{\text{P,C}} = 14.7$ Hz, C=N), 198.1 (d_{sat}, $^1J_{\text{W,C}} = 126.7$ Hz, $^2J_{\text{P,C}} = 7.6$ Hz, *cis*-CO), 200.6 (d_{sat}, $^1J_{\text{W,C}} = 142.8$ Hz, $^2J_{\text{P,C}} = 22.9$ Hz, *trans*-CO).

$^{29}\text{Si}\{^1\text{H}\}$ NMR (99.4 MHz, CDCl_3): $\delta = -1.84$ (s, $\text{Si}(\text{CH}_3)_3$), 0.75 (d, $^2J_{\text{P,Si}} = 9.3$ Hz, $\text{Si}(\text{CH}_3)_3$).

$^{31}\text{P}\{^1\text{H}\}$ NMR (202.5 MHz, CDCl_3): $\delta = 34.2$ (s_{sat}, $^1J_{\text{W,P}} = 260.9$ Hz).

MS (EI, 70 eV, ^{184}W , selected data): m/z (%) = 641.2 (40) $[\text{M}]^{++}$, 613.2 (20) $[\text{M} - \text{CO}]^+$, 585.2 (10) $[\text{M} - 2 \text{CO}]^+$, 557.2 (75) $[\text{M} - 3 \text{CO}]^+$, 501.1 (55) $[\text{M} - 5 \text{CO}]^+$, 473.1 (100) $[\text{M} - 4 \text{CO} - \text{C}_4\text{H}_8]^+$, 260.0 (20) $[\text{M} - \text{W}(\text{CO})_5 - \text{C}_4\text{H}_8]^+$, 73.1 (50) $[\text{SiMe}_3]^+$.

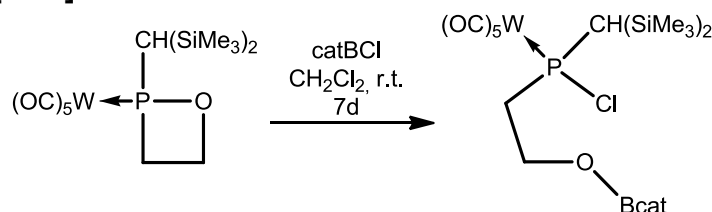
IR (ATR Diamond; $\tilde{\nu}[\text{cm}^{-1}]$, selected data): 2067 (s, $\nu(\text{CO})$), 1987 (w, $\nu(\text{CO})$), 1978 (w, $\nu(\text{CO})$), 1928 (s, $\nu(\text{CO})$), 1895 (vs, $\nu(\text{CO})$), 1631 (m, $\nu(\text{C}=\text{N})$).

Elemental analysis:

calc.:	C	35.58	H	5.03	N	2.18
found:	C	35.61	H	5.17	N	2.12

Single crystal measurement: GSTR529, AKY-599 // GXraymo_4925f

11.2.29 Synthesis of pentacarbonyl{[2-(catecholboranoxo)ethyl]chloro[bis(trimethylsilyl)methyl]phosphane- κP }tungsten(0) [56.1]



Synthesis: In a 10 mL Schlenk tube, 111.7 mg (0.2 mmol) of 1,2-oxaphosphetane complex **34.1_w** were dissolved in 3 mL of CH_2Cl_2 . To it 30.9 mg (0.2 mmol, 1 eq.) of catechol(chloro)borane were added at room temperature and the solution was kept on stirring for 7 days. During this time a colour change to slightly yellow brown was observed.

Purification: After the reaction was completed (checked by $^{31}\text{P}\{^1\text{H}\}$ NMR) all volatiles were removed in *vacuo* (ca. 0.02 mbar) and the product was obtained as a yellow oil.

Molecular formula: $\text{C}_{20}\text{H}_{27}\text{BO}_8\text{PSi}_2\text{W}$

Molecular weight: 712.672 g/mol

Yield: 142.5 mg (0.2 mmol, 100 %)

^1H NMR (300.1 MHz, CDCl_3): δ = 0.39 (s, 9H, $\text{Si}(\text{CH}_3)_3$), 0.40 (s, 9H, $\text{Si}(\text{CH}_3)_3$), 1.96 (d, 1H, $^2J_{\text{P,H}}$ = 11.0 Hz, P-CH), 2.73 - 2.88 (m, 1H, P- CH_2), 2.98 - 3.16 (m, 1H, P- CH_2), 4.56 - 4.75 (m, 2H, O- CH_2), 6.98 - 7.17 (m, 4H, Ph).

$^{11}\text{B}\{^1\text{H}\}$ NMR (96.3 MHz, CDCl_3): δ = 23.3 (s).

$^{13}\text{C}\{^1\text{H}\}$ NMR (75.5 MHz, CDCl_3): δ = 3.2 (d, $^3J_{\text{P,C}}$ = 3.8 Hz, $\text{Si}(\text{CH}_3)_3$), 3.9 (d, $^3J_{\text{P,C}}$ = 2.6 Hz, $\text{Si}(\text{CH}_3)_3$), 32.1 (d, $^1J_{\text{P,C}}$ = 13.1 Hz, P-CH), 41.5 (d, $^1J_{\text{P,C}}$ = 14.2 Hz, P- CH_2), 63.1 (d, $^2J_{\text{P,C}}$ = 7.7 Hz, O- CH_2), 112.3

(s, CH_{Ar}), 122.6 (s, CH_{Ar}), 148.0 (s, O-C), 197.0 (d_{sat}, ¹J_{W,C} = 126.9 Hz, ²J_{P,C} = 7.2 Hz, *cis*-CO), 199.1 (d, ²J_{P,C} = 30.8 Hz, *trans*-CO).

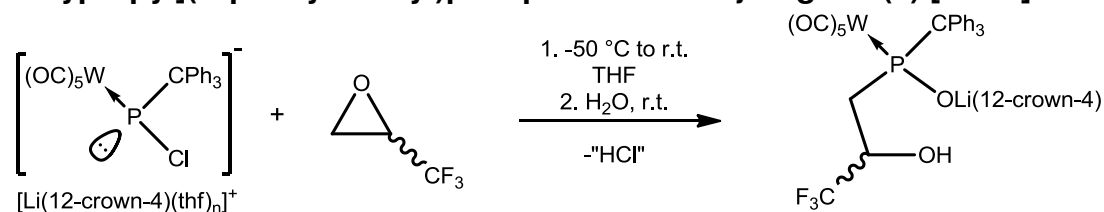
²⁹Si{¹H} NMR (59.6 MHz, CDCl₃): δ = 0.06 (s), 3.18 (d, ²J_{P,Si} = 6.3 Hz).

³¹P{¹H} NMR (121.5 MHz, CDCl₃): δ = 108.9 (s_{sat}, ¹J_{W,P} = 274.3 Hz).

MS (EI, 70 eV, ¹⁸⁴W, selected data): m/z (%) = 712.0 (40) [M]⁺⁺, 684.0 (50) [M - CO]⁺, 628.0 (45) [M - 3 CO]⁺, 572.0 (5) [M - 5 CO]⁺, 325.1 (80) [M - W(CO)₅ - Cl - C₂H₄]⁺, 254.1 (100) [catBOBcat]⁺, 73.1 (70) [SiMe₃]⁺.

IR (ATR Diamond; $\tilde{\nu}$ [cm⁻¹], selected data): 2074 (s, ν (CO)), 1987 (w, ν (CO)), 1911 (vs, ν (CO)).

11.2.30 Synthesis of lithium(1,4,7,10-tetraoxacyclododecane) pentacarbonyl{[3,3,3-trifluoro-2-hydroxypropyl](triphenylmethyl)phosphanoxido- κ P}tungsten(0) [57.3a]



Synthesis: A solution of Li/Cl phosphinidene complex **2.3** was prepared as described, starting from 133.8 mg (0.2 mmol) of [(OC)₅W{PCl₂(CPh₃)}] (**1.3**). 16 μ L of 1,1,1-trifluoro-2,3-propylene oxide (0.2 mmol, 1.0 eq.) were added and the solution allowed slow warming up to ambient temperature overnight. Subsequently 10 μ L of H₂O (0.556 mmol, 2.8 eq) were added and the reaction mixture was stirred for one more hour.

Purification: All volatiles were removed in *vacuo* (ca. 0.02 mbar). The crude product was purified by washing with *n*-pentane (once with 3 mL and once with 2 mL). The product was obtained as slightly yellow powder after drying in *vacuo* (ca. 0.02 mbar).

Molecular formula:	C ₃₅ H ₃₅ F ₃ LiO ₁₁ PW
Molecular weight:	910.396 g/mol
Melting point:	185 °C (dec.)
Yield:	145.5 mg (0.156 mmol, 79.9 %)

Isomeric ratio: 47:53

Isomer 1:

^1H NMR (300.1 MHz, THF- d_8): δ = 1.44 - 1.54 (m, 1H, CH_2), 2.37 – 2.57 (m, 1H, P- CH_2), 3.63 (s, 16H, 12-crown-4), 4.67 – 4.84 (m, 1H, O- CH), 6.15 (s, 1H, OH), 7.03 - 7.85 (m, 15H, CPh_3).

^7Li NMR (116.6 MHz, THF- d_8): δ = -0.18 (s, Li(12-crown-4)).

$^{13}\text{C}\{^1\text{H}\}$ NMR (75.5 MHz, THF- d_8): δ = 38.9 (d, $^1J_{\text{P,C}}$ = 10.7 Hz, P- CH_2), 70.2 (q, $2J_{\text{F,C}}$ = 31.5 Hz, O- CH), 68.6 (s, 12-crown-4), 71.4 (s, CPh_3), 126.3 (s, *para*- CH_{Ar}), 126.7 (d, $^5J_{\text{P,C}}$ = 1.6 Hz, *para*- CH_{Ar}), 127.3 (d, $^5J_{\text{P,C}}$ = 1.9 Hz, *para*- CH_{Ar}), 127.7 – 128.6 (m, CH_{Ar}), 131.3 – 128.8 (m, CH_{Ar}), 144.5 (d, $^2J_{\text{P,C}}$ = 4.8 Hz, *ipso*-C), 145.9 (d, $^2J_{\text{P,C}}$ = 4.2 Hz, *ipso*-C), 149.2 (d, $^2J_{\text{P,C}}$ = 6.1 Hz, *ipso*-C), 200.4 (d, $^2J_{\text{P,C}}$ = 8.4 Hz, *cis*-CO), 202.3 (d, $^2J_{\text{P,C}}$ = 22.3 Hz, *trans*-CO).

The signal for the CF_3 -carbon could not be detected due to a low signal to noise ratio.

$^{19}\text{F}\{^1\text{H}\}$ NMR (282.4 MHz, THF- d_8): δ = -80.8 (s, CF_3).

$^{31}\text{P}\{^1\text{H}\}$ NMR (121.5 MHz, THF- d_8): δ = 116.7 (s_{sat} , $^1J_{\text{W,P}}$ = 283.7.0 Hz).

Isomer 2:

^1H NMR (300.1 MHz, THF- d_8): δ = 2.25 – 2.51 (m, 2H, P- CH_2), 3.63 (s, 16H, 12-crown-4), 3.80 – 3.90 (m, 1H, O- CH), 5.13 (d, 1H, $J_{\text{P,H}}$ = 3.7 Hz, OH), 7.03 - 7.85 (m, 15H, CPh_3).

^7Li NMR (116.6 MHz, THF- d_8): δ = -0.18 (s, Li(12-crown-4)).

$^{13}\text{C}\{^1\text{H}\}$ NMR (75.5 MHz, THF- d_8): δ = 42.5 (d, $^1J_{\text{P,C}}$ = 7.1 Hz, P- CH_2), 70.2 (q, $2J_{\text{F,C}}$ = 31.5 Hz, O- CH), 68.6 (s, 12-crown-4), 71.5 (s, CPh_3), 126.3 (s, *para*- CH_{Ar}), 126.6 (s, *para*- CH_{Ar}), 127.0 (s, *para*- CH_{Ar}), 127.7 – 128.6 (m, CH_{Ar}), 131.3 – 128.8 (m, CH_{Ar}), 145.2 (d, $^2J_{\text{P,C}}$ = 9.1 Hz, *ipso*-C), 146.5 (d, $^2J_{\text{P,C}}$ = 4.2 Hz, *ipso*-C), 148.4 (d, $^2J_{\text{P,C}}$ = 3.2 Hz, *ipso*-C), 200.8 (d, $^2J_{\text{P,C}}$ = 8.7 Hz, *cis*-CO), 203.3 (d, $^2J_{\text{P,C}}$ = 22.3 Hz, *trans*-CO).

The signal for the CF_3 -carbon could not be detected due to a low signal to noise ratio.

$^{19}\text{F}\{^1\text{H}\}$ NMR (282.4 MHz, THF- d_8): δ = -81.3 (s, CF_3).

$^{31}\text{P}\{^1\text{H}\}$ NMR (121.5 MHz, THF- d_8): δ = 109.2 (s_{sat} , $^1J_{\text{W,P}}$ = 284.9 Hz).

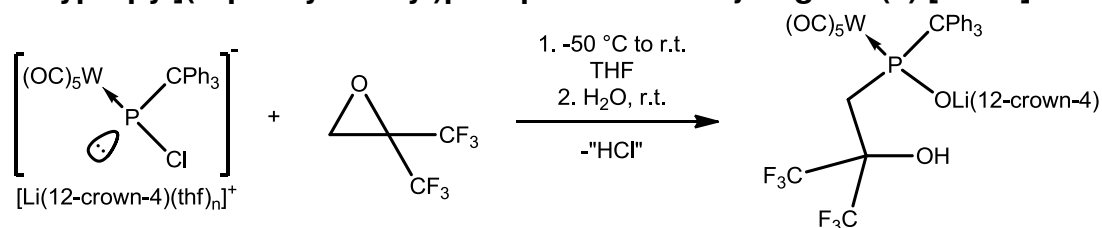
pos. ESI-MS: calculated for $(\text{Li}(12\text{-crown-4})^+)$: 183.121, found: 183.121.

neg. ESI-MS: calculated for $(\text{C}_{27}\text{H}_{19}\text{F}_3\text{O}_7\text{PW})^+$: 727.03, found: 727.1.

IR (ATR Diamond; $\tilde{\nu}$ [cm^{-1}], selected data): 2061 (m, $\nu(\text{CO})$), 1973 (w, $\nu(\text{CO})$), 1905 (vs, $\nu(\text{CO})$).

Single crystal measurement: GSTR505, PB-12 // GXraycu_4642g

11.2.31 Synthesis of lithium(1,4,7,10-tetraoxacyclododecane) pentacarbonyl{[3,3,3-trifluoro-2-(trifluoromethyl)-2-hydroxypropyl](triphenylmethyl)phosphanoxido- κP }tungsten(0) [57.3b]



Synthesis: A solution of Li/Cl phosphinidene complex **2.3** was prepared as described, starting from 334.5 mg (0.5 mmol) of $[(OC)_5W\{PCl_2(CPh_3)\}]$ (**1.3**). 0.1 mL of hexafluoroisobutene oxide (0.85 mmol, 1.7 eq.) were added and the solution allowed slow warming up to ambient temperature overnight. Subsequently 10 μ L of H_2O (0.556 mmol, 1.1 eq) were added and the reaction mixture was stirred for one more hour.

Purification: All volatiles were removed in *vacuo* (ca. 0.02 mbar). The crude product was purified by washing with a mixture of *n*-pentane and diethyl ether (10:1, 2 times 3 mL) and once with 3 mL of *n*-pentane. The product was obtained as white powder after drying in *vacuo* (ca. 0.02 mbar).

Molecular formula:	$C_{36}H_{34}F_6LiO_{11}PW$
Molecular weight:	978.394 g/mol
Melting point:	140 °C (dec.)
Yield:	323 mg (0.33 mmol, 66 %)

1H NMR (300.1 MHz, THF- d_8): δ = 1.82 (dd, 1H, $^2J_{H,H} = 16.0$ Hz, $^2J_{P,H} = 7.5$ Hz, CH_2), 2.89 (dd, 1H, $^2J_{H,H} = 16.0$ Hz, $^2J_{P,H} = 9.7$ Hz, P- CH_2), 3.64 (s, 16H, 12-crown-4), 7.04 - 7.74 (m, 15H, CPh_3), 9.41 (s_{br}, 1H, OH).

7Li NMR (116.6 MHz, THF- d_8): δ = 0.00 (s, Li(12-crown-4)).

$^{13}C\{^1H\}$ NMR (75.5 MHz, THF- d_8): δ = 31.6 (s, P- CH_2), 68.8 (s, 12-crown-4), 70.4 (s, CPh_3), 77.0 - 81.0 (m, $C(CF_3)_2$), 124.8 (q, $^1J_{F,C} = 293.0$ Hz, CF_3), 124.8 (q, $^1J_{F,C} = 310.8$ Hz, CF_3), 126.5 (s, *para*- CH_{Ar}), 126.8 (d, $^5J_{P,C} = 2.4$ Hz, *para*- CH_{Ar}), 127.5 (d, $^5J_{P,C} = 2.1$ Hz, *para*- CH_{Ar}), 128.2 (s, CH_{Ar}), 128.5 (s, CH_{Ar}), 128.6 (s, CH_{Ar}), 131.9 (d, $^2J_{P,C} = 6.0$ Hz, CH_{Ar}), 132.6 (d, $J_{P,C} = 1.2$ Hz, CH_{Ar}), 132.7 (d, $J_{P,C} = 7.2$ Hz, CH_{Ar}), 144.4 (d, $^2J_{P,C} = 5.9$ Hz, *ipso*-C), 145.5 (d, $^2J_{P,C} = 4.2$ Hz, *ipso*-C), 148.4 (d, $^2J_{P,C} = 7.5$ Hz, *ipso*-C), 200.3 (dq_{sat}, $^1J_{W,C} = 125.5$ Hz, $^2J_{P,C} = 8.2$ Hz, $^6J_{F,C} = 1.7$ Hz, *cis*-CO), 202.3 (d, $^2J_{P,C} = 25.6$ Hz, *trans*-CO).

$^{19}F\{^1H\}$ NMR (282.4 MHz, THF- d_8): δ = -79.6 (q, $^4J_{F,F} = 11.0$ Hz, CF_3), -76.7 (q, $^4J_{F,F} = 11.0$ Hz, CF_3).

$^{31}P\{^1H\}$ NMR (121.5 MHz, THF- d_8): δ = 123.8 (s_{sat}, $^1J_{W,P} = 295.0$ Hz).

pos. ESI-MS: calculated for $(C_{36}H_{34}F_6LiO_{11}PW)^+$: 978.14, found: 1611.1 $[Li_3(C_{28}H_{18}F_6O_7PW)_2]^+$, 985.1 $[Li_2(12\text{-crown-4})(C_{28}H_{18}F_6O_7PW)]^+$, 809.0 $[Li_2(C_{28}H_{18}F_6O_7PW)]^+$, 375.2 $[Na(12\text{-crown-4})_2]^+$.

IR (ATR Diamond; $\tilde{\nu}[\text{cm}^{-1}]$, selected data): 2063 (s, $\nu(\text{CO})$), 1971 (w, $\nu(\text{CO})$), 1923 (w, $\nu(\text{CO})$), 1911 (s, $\nu(\text{CO})$), 1890 (vs, $\nu(\text{CO})$).

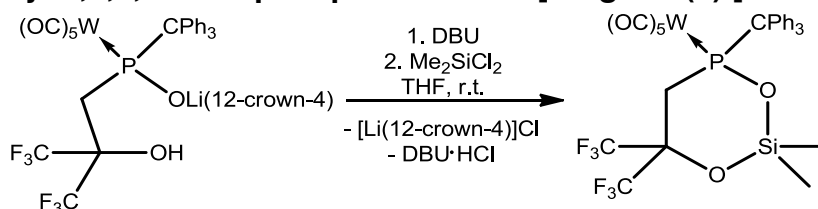
Elemental analysis:

calculated for: $C_{36}H_{34}F_6LiO_{11}PW + 2 H_2O$

calc.:	C	42.62	H	3.78
found:	C	42.55	H	3.89

Single crystal measurement: GSTR410, AKY-488-2 // GXray4012f

11.2.32 Synthesis of pentacarbonyl[6,6-bis(trifluoromethyl)-2,2-dimethyl-4-triphenylmethyl-1,3,4,2-dioxaphosphasilinan- κP]tungsten(0) [60.3a]



Synthesis: In a 20 mL Schlenk tube 250 mg (0.26 mmol) of phosphinito complex **57.3b** were suspended in 10 mL of THF, then 59.4 mg DBU (0.38 mmol, 1.46 eq.), dissolved in 1 mL of THF, were added while stirring. The mixture was stirred for additional ten minutes and 42.3 mg (0.33 mmol 1.27 eq.) Me_2SiCl_2 , dissolved in 2 mL of THF, were added slowly.

Purification: The solvent was removed in *vacuo* (ca. 0.02 mbar) after 24 h to give a greenish brown solid. The crude material was filtered over SiO_2 ($\varnothing = 1$ cm, $h = 3$ cm, Et_2O , r.t.) using 60 mL of Et_2O . The solvent was then removed in *vacuo* (ca. 0.02 mbar) and the crude product recrystallized from 2 mL of diethyl ether at 4 °C to yield a white solid.

Molecular formula: $C_{30}H_{23}F_6O_7PSiW$

Molecular weight: 852.389 g/mol

Melting point: 178 °C

Yield: 120 mg (0.14 mmol, 54 %).

1H NMR (500.2 MHz, $CDCl_3$): $\delta = -0.16$ (s, 3H, $Si(CH_3)_2$), 0.53 (s, 3H, $Si(CH_3)_2$), 2.55 (dd, 1H, $^2J_{H,H} = 16.0$ Hz, $^2J_{P,H} = 9.7$ Hz, P- CH_2), 3.40 (dd, 1H, $^2J_{H,H} = 16.0$ Hz, $^2J_{P,H} = 12.5$ Hz, P- CH_2), 7.27 - 7.48 (m, 15H, CPh_3).

$^{13}\text{C}\{^1\text{H}\}$ NMR (125.8 MHz, CDCl_3): $\delta = 0.4$ (q, $^5J_{\text{F,C}} = 3.4$ Hz, $\text{Si}(\text{CH}_3)_2$), 0.8 (s, $\text{Si}(\text{CH}_3)_2$), 29.4 (d, $^1J_{\text{P,C}} = 2.0$ Hz, P- CH_2), 70.8 (d, $^1J_{\text{P,C}} = 10.4$ Hz, CPh_3), $77.0 - 78.2$ (m, $\text{C}(\text{CF}_3)_2$), 122.7 (q, $^1J_{\text{F,C}} = 287.1$ Hz, CF_3 (only one set of signals was observed for both in the ^{13}C NMR)), 127.9 (s, 2 times *para*- CH_{Ar}), 128.2 (s, CH_{Ar}), 128.3 (s, CH_{Ar}), 128.4 (s, *para*- CH_{Ar}), 128.7 (s, CH_{Ar}), 131.6 (d, $J_{\text{P,C}} = 1.3$ Hz, CH_{Ar}), 131.8 (d, $^3J_{\text{P,C}} = 9.5$ Hz, CH_{Ar}), 132.0 ppm (d, $^3J_{\text{P,C}} = 7.9$ Hz, CH_{Ar}), 139.6 (d, $^2J_{\text{P,C}} = 6.3$ Hz, *ipso*-C), 140.0 (d, $^2J_{\text{P,C}} = 7.1$ Hz, *ipso*-C), 142.8 (d, $^2J_{\text{P,C}} = 7.1$ Hz, *ipso*-C), 197.4 (dq_{sat}, $^6J_{\text{F,C}} = 1.9$ Hz, $^2J_{\text{P,C}} = 7.0$ Hz, $^1J_{\text{W,C}} = 127.6$ Hz, *cis*-CO), 198.2 (d_{sat}, $^1J_{\text{W,C}} = 136.4$ Hz, $^2J_{\text{P,C}} = 33.4$ Hz, *trans*-CO).

$^{19}\text{F}\{^1\text{H}\}$ NMR (282.4 MHz, CDCl_3): $\delta = -76.9$ (q, $^4J_{\text{F,F}} = 11.5$ Hz, CF_3), -76.0 (q, $^4J_{\text{F,F}} = 11.5$ Hz, CF_3).

$^{29}\text{Si}\{^1\text{H}\}$ NMR (99.4 MHz, CDCl_3): $\delta = 3.0$ (d, $^2J_{\text{P,Si}} = 9.6$ Hz, $\text{Si}(\text{CH}_3)_2$).

$^{31}\text{P}\{^1\text{H}\}$ NMR (202.5 MHz, CDCl_3): $\delta = 125.6$ (s_{sat}, $^1J_{\text{W,P}} = 300.9$ Hz).

MS (EI, 70 eV, ^{184}W , selected data): m/z (%) = 768.0 (15) $[\text{M} - 3 \text{CO}]^+$, 608.9 (45) $[\text{M} - \text{CPh}_3]^+$, 580.9 (70) $[\text{M} - \text{CPh}_3 - \text{CO}]^+$, 552.9 (20) $[\text{M} - \text{CPh}_3 - 2 \text{CO}]^+$, 243.1 (100) $[\text{CPh}_3]^+$, 165.1 (25) $[\text{CPh}_3 - \text{C}_6\text{H}_6]^+$.

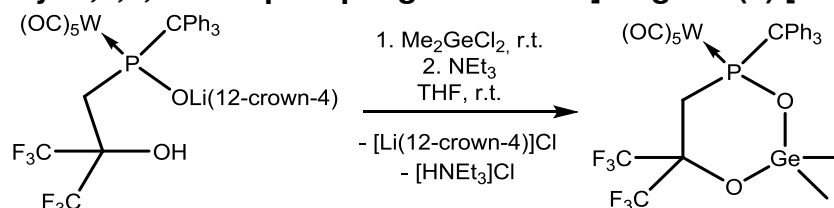
IR (ATR Diamond; $\tilde{\nu}[\text{cm}^{-1}]$, selected data): 2074 (s, $\nu(\text{CO})$), 1995 (m, $\nu(\text{CO})$), 1916 (vs, $\nu(\text{CO})$).

Elemental analysis:

calc.:	C	42.27	H	2.27
found:	C	42.35	H	2.79

Single crystal measurement: GSTR504, PB-35 // GXray4737

11.2.33 Synthesis of pentacarbonyl[6,6-bis(trifluoromethyl)-2,2-dimethyl-4-triphenylmethyl-1,3,4,2-dioxaphosphagerminan- κP]tungsten(0) [60.3b]



Synthesis: In a 20 mL Schlenk tube 250 mg (0.26 mmol) of phosphinito complex **57.3b** were suspended in 10 mL of THF, then 44 mg of Me_2GeCl_2 (0.26 mmol, 1.0 eq.), dissolved in 1 mL of THF, were added while stirring. The mixture was stirred for additional 2.5 h and 0.12 mL of NEt_3 (0.91 mmol, 3.5 eq.) were added dropwise.

Purification: The solvent was removed at elevated temperature in *vacuo* (ca. 0.02 mbar, 45 °C) after stirring for additional 80 minutes at ambient temperature. The brownish material was filtered over SiO_2 ($\varnothing = 2$ cm, $h = 2$ cm, Et_2O , r.t.). The crude product was obtained as white, sticky solid after removing all volatiles in *vacuo* (ca. 0.02 mbar) and subsequently washed two times with 5 mL of petroleum ether (40/60) at ambient temperature. The product was dried in *vacuo* (ca. 0.02 mbar, 45 °C) for 5 h to yield a white solid.

<u>Molecular formula:</u>	C ₃₀ H ₂₃ F ₆ GeO ₇ PW
<u>Molecular weight:</u>	896.943 g/mol
<u>Melting point:</u>	173 °C
<u>Yield:</u>	60 mg (0.065 mmol, 25 %)

¹H NMR (500.2 MHz, CDCl₃): δ = 0.44 (q, 3H, ⁶J_{F,H} = 1.7 Hz, Ge(CH₃)₂), 1.04 (s, 3H, Ge(CH₃)₂), 2.41 (dd, 1H, ²J_{H,H} = 16.0 Hz, ²J_{P,H} = 8.3 Hz, P-CH₂), 3.28 (dd, 1H, ²J_{H,H} = 16.0 Hz, ²J_{P,H} = 12.3 Hz, P-CH₂), 7.27-7.52 (m, 15H, CPh₃).

¹³C{¹H} NMR (125.8 MHz, CDCl₃): δ = 4.8 (q, ⁵J_{F,C} = 4.6 Hz, Ge(CH₃)₂), 4.9 (s, Ge(CH₃)₂), 30.4 (s, P-CH₂), 71.0 (d, ¹J_{P,C} = 10.2 Hz, CPh₃), 77.7 - 79.0 (m, C(CF₃)₂), 123.0 (q, ¹J_{F,C} = 285.3 Hz, CF₃), 123.3 (q, ¹J_{F,C} = 289.1 Hz, CF₃), 127.6 (d, ⁵J_{P,C} = 1.6 Hz, *para*-CH_{Ar}), 127.7 (d, ⁵J_{P,C} = 1.6 Hz, *para*-CH_{Ar}), 128.0 (d, ¹J_{P,C} = 1.1 Hz, CH_{Ar}), 128.2 (d, ¹J_{P,C} = 1.9 Hz, CH_{Ar}), 128.2 (s, *para*-CH_{Ar}), 128.7 (s, CH_{Ar}), 131.6 (d, ¹J_{P,C} = 2.5 Hz, CH_{Ar}), 131.8 (d, ³J_{P,C} = 8.7 Hz, CH_{Ar}), 132.1 ppm (d, ³J_{P,C} = 7.9 Hz, CH_{Ar}), 140.2 (d, ²J_{P,C} = 6.5 Hz, *ipso*-C), 140.3 (d, ²J_{P,C} = 6.0 Hz, *ipso*-C), 143.5 (d, ²J_{P,C} = 7.1 Hz, *ipso*-C), 197.7 (dq_{sat}, ²J_{P,C} = 7.4 Hz, ⁶J_{F,C} = 1.9 Hz, ¹J_{W,C} = 126.8 Hz, *cis*-CO), 198.8 (d, ²J_{P,C} = 32.3 Hz, *trans*-CO).

¹⁹F{¹H} NMR (282.4 MHz, CDCl₃): δ = -78.7 (q, ⁴J_{F,F} = 11.3 Hz, CF₃), -78.2 (q, ⁴J_{F,F} = 11.3 Hz, CF₃).

³¹P{¹H} NMR (202.5 MHz, CDCl₃): δ = 126.2 (s_{sat}, ¹J_{W,P} = 299.0 Hz).

LIFDI-MS: m/z (%) = 896 (25) [M]⁺, 243.1 (100) [CPh₃]⁺.

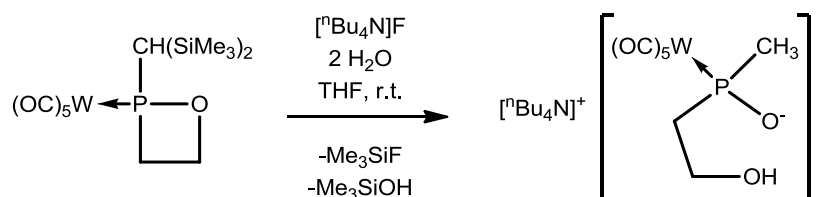
IR (ATR Diamond; $\tilde{\nu}$ [cm⁻¹], selected data): 2073 (s, ν (CO)), 1994 (m, ν (CO)), 1944 (w, ν (CO)), 1916 (vs, ν (CO)).

Elemental analysis:

calc.:	C	40.17	H	2.58
found:	C	39.63	H	2.86

Single crystal measurement: GSTR507, PB-47 // GXray4813

11.2.34 Synthesis of tetrabutylammonium pentacarbonyl[(2-hydroxyethyl)methylphosphanoxido-κP]tungsten(0) [61]



Synthesis: In a 10 mL Schlenk tube were dissolved 279.2 mg (0.5 mmol) of 1,2-oxaphosphetane complex **34.1_W** in 5 mL of THF and 0.5 mL of an ⁿBu₄NF solution (0.5 mmol, 1 M in THF, 1.0 eq.) were added. The mixture was stirred overnight at ambient temperature and a change of the colour to yellow was observed.

Purification: All volatiles were removed in *vacuo* (ca. 0.02 mbar) and the product was dried for 8 h at the same pressure. The product was obtained as yellow oil, which crystallized over time to yield a yellow solid.

Molecular formula: C₂₄H₄₄NO₇PW

Molecular weight: 673.422 g/mol

Yield: 336.7 mg (0.5 mmol, 100 %)

¹H NMR (300.1 MHz, THF-d₈): δ = 1.00 (d, 12H, ³J_{H,H} = 7.3 Hz, CH₂-CH₃), 1.34 - 1.49 (m, 8H, CH₂-CH₃), 1.62 - 1.76 (m, 8H, CH₂-CH₂-CH₂), 1.62 - 1.76 (m, 1H, CH₂), 1.68 (d, 3H, ²J_{P,H} = 6.5 Hz, P-CH₃), 2.10 - 2.25 (m, 2H, P-CH₂), 3.31 - 3.41 (m, 8H, N-CH₂), 3.86 - 4.18 (m, 2H, O-CH₂), 6.43 (s_{br}, 1H, OH).

¹³C{¹H} NMR (75.5 MHz, THF-d₈): δ = 13.9 (s, CH₃), 20.4 (s, CH₂), 24.5 (s, CH₂), 29.9 (d, ¹J_{P,C} = 17.8 Hz, P-CH₃), 44.7 (d, ¹J_{P,C} = 23.3 Hz, P-CH₂), 59.0 (s, CH₂), 61.4 (d, ²J_{P,C} = 4.9 Hz, O-CH₂), 201.9 (d_{sat}, ¹J_{W,C} = 125.6 Hz, ²J_{P,C} = 9.5 Hz, *cis*-CO), 205.5 (d, ²J_{P,C} = 10.7 Hz, *trans*-CO).

³¹P{¹H} NMR (121.5 MHz, THF-d₈): δ = 67.2 (s_{sat}, ¹J_{W,P} = 233.9 Hz).

pos. ESI-MS: calculated for (ⁿBu₄N)⁺: 242.285, found: 242.284 (ⁿBu₄N)⁺.

neg. ESI-MS: calculated for (C₈H₈O₇PW)⁻: 430.952, found: 430.952 [M]⁻, 402.957 [M - CO]⁻, 374.962 [M - 2 CO]⁻, 346.965 [M - 3 CO]⁻.

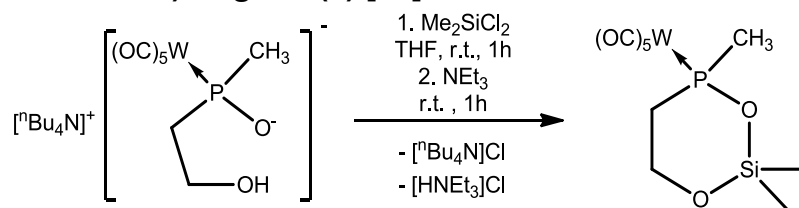
IR (ATR Diamond; ν̄[cm⁻¹], selected data): 3203 (w, ν(OH)), 2051 (m, ν(CO)), 1955 (w, ν(CO)), 1898 (s, ν(CO)), 1865 (vs, ν(CO)).

Elemental analysis:

calc.:	C	42.80	H	6.59	N	2.08
found:	C	42.28	H	6.52	N	2.06

Single crystal measurement: GSTR545, AKY-610 // GXrayneu

11.2.35 Synthesis of pentacarbonyl(2,2-dimethyl-4-methyl-1,3,4,2-dioxaphosphasilinan-κP)tungsten(0) [66]



Synthesis: In a 10 mL Schlenk tube, 54 mg (0.08 mmol) of phosphinito complex **61** were dissolved in 3 mL of THF, then 0.02 mL of Me_2SiCl_2 (0.16 mmol, 2 eq.) were added while stirring. The mixture was stirred for an additional hour at ambient temperature, then 0.05 mL of Net_3 (0.36 mmol, 4.5 eq.) were added slowly. Formation of a white solid was observed and the solution was kept stirring for an additional hour.

Purification: All volatiles were removed in *vacuo* (ca. 0.02 mbar) and the crude material was filtered over SiO_2 ($\varnothing = 1$ cm, $h = 2$ cm, Et_2O , r.t.) using 50 mL of diethyl ether. The solvent was then removed in *vacuo* (ca. 0.02 mbar) to yield the product as white, oily material.

Molecular formula:	$\text{C}_{10}\text{H}_{13}\text{O}_7\text{PSiW}$
Molecular weight:	488.105 g/mol
Yield:	33.1 mg (0.068 mmol, 85 %)

^1H NMR (300.1 MHz, C_6D_6): $\delta = -0.11$ (s_{sat} , 3H, $^2J_{\text{Si,H}} = 6.8$ Hz, $\text{Si}(\text{CH}_3)_2$), 0.10 (s_{sat} , 3H, $^2J_{\text{Si,H}} = 7.2$ Hz, $\text{Si}(\text{CH}_3)_2$), 1.13 (dddd, 1H, $^2J_{\text{H,H}} = 15.4$ Hz, $^3J_{\text{H,H}} = 4.7$ Hz, $^3J_{\text{H,H}} = 2.9$ Hz, $^2J_{\text{P,H}} = 2.5$ Hz, P- CH_2), 2.15 (dddd, 1H, $^2J_{\text{H,H}} = 15.4$ Hz, $^3J_{\text{H,H}} = 9.3$ Hz, $^3J_{\text{H,H}} = 4.6$ Hz, $^2J_{\text{P,H}} = 1.3$ Hz, P- CH_2), 3.63 (dddd, 1H, $^3J_{\text{P,H}} = 14.2$ Hz, $^2J_{\text{H,H}} = 12.0$ Hz, $^3J_{\text{H,H}} = 9.3$ Hz, $^3J_{\text{H,H}} = 2.9$ Hz, O- CH_2), 3.71 (dddd, 1H, $^3J_{\text{P,H}} = 12.7$ Hz, $^2J_{\text{H,H}} = 12.0$ Hz, $^3J_{\text{H,H}} = 4.7$ Hz, $^3J_{\text{H,H}} = 4.6$ Hz, O- CH_2).

$^{13}\text{C}\{^1\text{H}\}$ NMR (75.5 MHz, C_6D_6): $\delta = -0.6$ (d, $^3J_{\text{P,C}} = 0.6$ Hz, $\text{Si}(\text{CH}_3)_2$), -0.3 (s, $\text{Si}(\text{CH}_3)_2$), 25.5 (d, $^1J_{\text{P,C}} = 23.3$ Hz, P- CH_3), 39.3 (d, $^1J_{\text{P,C}} = 23.3$ Hz, P- CH_2), 58.7 (d, $^2J_{\text{P,C}} = 6.1$ Hz, O- CH_2), 197.0 (d_{sat} , $^2J_{\text{P,C}} = 8.4$ Hz, $^1J_{\text{W,C}} = 125.1$ Hz, *cis*-CO), 200.2 (d_{sat} , $^1J_{\text{W,C}} = 139.7$ Hz, $^2J_{\text{P,C}} = 24.2$ Hz, *trans*-CO).

$^{29}\text{Si}\{^1\text{H}\}$ NMR (59.6 MHz, C_6D_6): $\delta = -0.3$ (d, $^2J_{\text{P,Si}} = 12.1$ Hz, $\text{Si}(\text{CH}_3)_2$).

$^{31}\text{P}\{^1\text{H}\}$ NMR (121.5 MHz, C_6D_6): $\delta = 105.2$ (s_{sat} , $^1J_{\text{W,P}} = 279.6$ Hz).

MS (EI, 70 eV, ^{184}W , selection): m/z (%) = 505.9 (5) $[\text{M} + \text{H}_2\text{O}]^{++}$, 487.9 (30) $[\text{M}]^{++}$, 451.9 (20) $[\text{M} + \text{H}_2\text{O} - 2 \text{CO}]^+$, 431.9 (25) $[\text{M} - 2 \text{CO}]^+$, 404.0 (10) $[\text{M} - 3 \text{CO}]^+$, 375.9 (100) $[\text{M} - 4 \text{CO}]^+$, 348.0 (60) $[\text{M} - 5 \text{CO}]^+$.

IR (ATR Diamond; $\tilde{\nu}[\text{cm}^{-1}]$, selection): 2072 (s, $\nu(\text{CO})$), 1981(m, $\nu(\text{CO})$), 1901 (vs, $\nu(\text{CO})$).

Literature

- [1] a) D. Cordell, S. White, *Sustainability* **2011**, *3*, 2027; b) J. D. Edixhoven, J. Gupta, H. H. G. Savenije, *Earth Syst. Dynam.* **2014**, *5*, 491.
- [2] B. E. Rittmann, B. Mayer, P. Westerhoff, M. Edwards, *Chemosphere* **2011**, *84*, 846.
- [3] C. Elschenbroich, *Organometallchemie*, Vieweg+Teubner Verlag / GWV Fachverlage GmbH Wiesbaden, Wiesbaden, **2008**.
- [4] S. Bourbigot, S. Duquesne, *J. Mat. Chem.* **2007**, 2283.
- [5] S. Bourbigot, G. Fontaine, *Polym. Chem.* **2010**, 1413.
- [6] N. Gilbert, *Nature* **2009**, *461*, 716.
- [7] A. F. Holleman, E. Wiberg, N. Wiberg, *Lehrbuch der Anorganischen Chemie*, de Gruyter, Berlin, **2007**.
- [8] L. D. Quin, *A Guide to Organophosphorus Chemistry*, Wiley-Interscience, New York, **2000**.
- [9] N. G. Connelly, *Nomenclature of inorganic chemistry*, Royal Society of Chemistry, Cambridge, **2005**.
- [10] R. Streubel, A. W. Kyri, L. Duan, G. Schnakenburg, *Dalton Trans.* **2014**, *43*, 2088.
- [11] K. B. Dillon, J. F. Nixon, F. Mathey, *Phosphorus: The carbon copy*, John Wiley, New York, Chichester, **1998**.
- [12] D. Bourissou, O. Guerret, F. P. Gabbaï, G. Bertrand, *Chem. Rev.* **2000**, *100*, 39.
- [13] R. Brückner, *Reaktionsmechanismen. Organische Reaktionen Stereochemie Moderne Synthesemethoden*, Springer-Verlag, Berlin Heidelberg, **2009**.
- [14] G. Herzberg, *Proc. Roy. Soc.* **1961**, *262*, 291.
- [15] A. J. Arduengo, R. L. Harlow, M. Kline, *J. Am. Chem. Soc.* **1991**, *113*, 361.
- [16] a) G. R. Gillette, A. Baceiredo, G. Bertrand, *Angew. Chem. Int. Ed. Engl.* **1990**, *29*, 1429; b) A. Igau, A. Baceiredo, G. Trinquier, G. Bertrand, *Angew. Chem. Int. Ed. Engl.* **1989**, *28*, 621; c) G. Bertrand, *Heteroat. Chem.* **1991**, 29.
- [17] V. Lavallo, Y. Canac, C. Prasang, B. Donnadiou, G. Bertrand, *Angew. Chem. Int. Ed.* **2005**, *44*, 5705.
- [18] E. O. Fischer, A. Maasböl, *Angew. Chem. Int. Ed. Engl.* **1964**, *3*, 580.
- [19] R. R. Schrock, *J. Am. Chem. Soc.* **1974**, *96*, 6796.
- [20] J. Santamaría, E. Aguilar, *Org. Chem. Front.* **2016**, *3*, 1561.
- [21] G. Köbrich, A. Akhtar, F. Ansari, W. E. Breckoff, H. Büttner, W. Drischel, R. H. Fischer, K. Flory, H. Fröhlich, W. Goyert et al., *Angew. Chem. Int. Ed. Engl.* **1967**, *6*, 41.
- [22] R. H. V. Nishimura, V. E. Murie, R. A. Soldi, J. L. C. Lopes, G. C. Clososki, *J. Braz. Chem. Soc.* **2015**, 2175.
- [23] H. E. Simmons, R. D. Smith, *J. Am. Chem. Soc.* **1959**, *81*, 4256.
- [24] A. Müller, M. Marsch, K. Harms, J. C. W. Lohrenz, G. Boche, *Angew. Chem. Int. Ed. Engl.* **1996**, *35*, 1518.
- [25] G. Köbricht, *Angew. Chem. Int. Ed. Engl.* **1972**, *11*, 473.
- [26] G. Molev, D. Bravo-Zhivotovskii, M. Karni, B. Tumanskii, M. Botoshansky, Y. Apeloig, *J. Am. Chem. Soc.* **2006**, *128*, 2784.
- [27] Y. Suzuki, T. Sasamori, J.-D. Guo, S. Nagase, N. Tokitoh, *Chem. Eur. J.* **2016**, *22*, 13784.
- [28] M. Yoshifuji, I. Shima, N. Inamoto, K. Hirotsu, T. Higuchi, *J. Am. Chem. Soc.* **1981**, *103*, 4587.
- [29] M. Yoshifuji, T. Sato, N. Inamoto, *Chem. Lett.* **1988**, 1735.
- [30] H. Lang, G. Mohr, Scheidsteger, G. Huttner, *Chem. Ber.* **1985**, 574.
- [31] A. Özbolat, G. von Frantzius, J. M. Pérez, M. Nieger, R. Streubel, *Angew. Chem.* **2007**, *46*, 9327.
- [32] M. Bode, J. Daniels, R. Streubel, *Organometallics* **2009**, *28*, 4636.
- [33] V. Nesterov, G. Schnakenburg, A. Espinosa, R. Streubel, *Inorg. Chem.* **2012**, *51*, 12343.
- [34] M. Klein, *PhD Thesis*, University of Bonn, **2015**.
- [35] V. Nesterov. private communication, **2017**.
- [36] R. Streubel, A. Ozbolat-Schon, G. von Frantzius, H. Lee, G. Schnakenburg, D. Gudat, *Inorg. Chem.* **2013**, *52*, 3313.
- [37] V. Nesterov, T. Heurich, R. Streubel, *Pure Appl. Chem.* **2012**, *85*.
- [38] C. Schulten, G. von Frantzius, G. Schnakenburg, A. Espinosa, R. Streubel, *Chem. Sci.* **2012**, *3*, 3526.
- [39] C. Albrecht, M. Bode, J. M. Perez, J. Daniels, G. Schnakenburg, R. Streubel, *Dalton Trans.* **2011**, *40*, 2654.

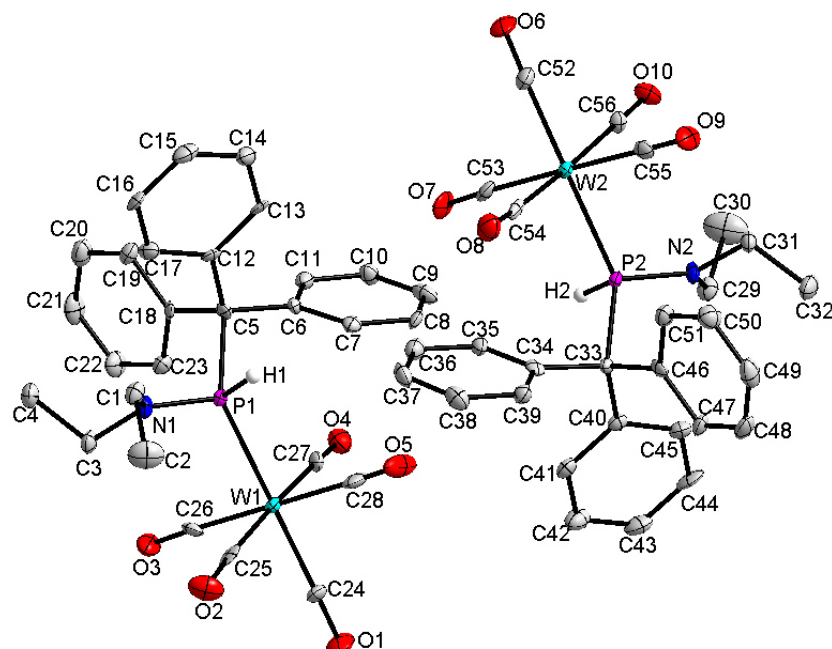
- [40] C. M. Garcia, A. E. Ferao, G. Schnakenburg, R. Streubel, *Dalton Trans.* **2016**, 45, 2378.
- [41] J. Faßbender, *planned PhD Thesis*, University of Bonn.
- [42] S. Fankel, H. Helten, G. von Frantzius, G. Schnakenburg, J. Daniels, V. Chu, C. Muller, R. Streubel, *Dalton Trans.* **2010**, 39, 3472.
- [43] A. Ozbolat-Schon, M. Bode, G. Schnakenburg, A. Anoop, M. van Gastel, F. Neese, R. Streubel, *Angew. Chem. Int. Ed.* **2010**, 49, 6894.
- [44] P. Junker, V. Nesterov, R. Streubel, *unpublished results*.
- [45] A. K. Bhattacharya, G. Thyagarajan, *Chem. Rev.* **1981**, 81, 415.
- [46] K. Diemert, A. Hinz, W. Kuchen, D. Lorenzen, *J. Organomet. Chem.* **1990**, 393, 379.
- [47] A. Marinetti, F. Mathey, *Organometallics* **1982**, 1, 1488.
- [48] G. Huttner, H.-D. Müller, *Angew. Chem.* **1975**, 87, 596.
- [49] G. Märkl, P. Kreitmeier, *Angew. Chem. Int. Ed. Engl.* **1988**, 27, 1360.
- [50] a) V. Plack, J. Münchenberg, H. Thönnessen, P. G. Jones, R. Schmutzler, *Eur. J. Inorg. Chem.* **1998**, 1998, 865; b) V. Plack, J. R. Goerlich, A. Fischer, R. Schmutzler, *Z. Anorg. Allg. Chem.* **1999**, 625, 1979.
- [51] A. H. Cowley, J. E. Kilduff, N. C. Norman, M. Pakulski, *J. Chem. Soc., Dalton Trans.* **1986**, 1801.
- [52] A. H. Cowley, J. E. Kilduff, N. C. Norman, J. L. Atwood, M. Pakulski, W. E. Hunter, *J. Am. Chem. Soc.* **1983**, 105, 4845.
- [53] M. Müller, H. Vahrenkamp, *Chem. Ber.* **1983**, 116, 2322.
- [54] F. Mathey, S. Holand, *Organometallics* **1988**, 7, 1796.
- [55] M. L. G. Borst, R. E. Bulo, C. W. Winkel, D. J. Gibney, A. W. Ehlers, M. Schakel, M. Lutz, A. L. Spek, K. Lammertsma, *J. Am. Chem. Soc.* **2005**, 127, 5800.
- [56] L. Duan, G. Schnakenburg, J. Daniels, R. Streubel, *Eur. J. Inorg. Chem.* **2012**, 2012, 3490.
- [57] L. Duan, G. Schnakenburg, J. Daniels, R. Streubel, *Eur. J. Inorg. Chem.* **2012**, 2012, 2314.
- [58] J. B. M. Wit, G. B. de Jong, M. Schakel, M. Lutz, A. W. Ehlers, J. C. Slootweg, K. Lammertsma, *Organometallics* **2016**, 35, 1170.
- [59] T. Ye, M. A. McKervey, *Chem. Rev.* **1994**, 1091.
- [60] Z. Hou, J. Wang, P. He, J. Wang, B. Qin, X. Liu, L. Lin, X. Feng, *Angew. Chem. Int. Ed.* **2010**, 49, 4763.
- [61] C. Murcia García, *PhD Thesis*, University of Bonn, **2016**.
- [62] R. Streubel, A. Schmer, A. W. Kyri, G. Schnakenburg, *Organometallics* **2017**.
- [63] P. K. Majhi, A. W. Kyri, A. Schmer, G. Schnakenburg, R. Streubel, *Chem. Eur. J.* **2016**, 22, 15413.
- [64] R. Streubel, U. Rohde, J. Jeske, F. Ruthe, P. G. Jones, *Eur. J. Inorg. Chem.* **1988**.
- [65] H. Nozaki, H. Takaya, S. Moriuti, R. Noyori, *Tetrahedron* **1968**, 24, 3655.
- [66] K. Okuma, Y. Tanaka, S. Kaji, H. Ohta, *J. Org. Chem.* **1983**, 5133.
- [67] E. J. Corey, M. Chaykovsky, *J. Am. Chem. Soc.* **1962**, 84, 867.
- [68] E. D. Butova, A. V. Barabash, A. A. Petrova, C. M. Kleiner, P. R. Schreiner, A. A. Fokin, *J. Org. Chem.* **2010**, 75, 6229.
- [69] R. A. Hunter, R. J. Whitby, M. E. Light, M. B. Hursthouse, *Tetrahedron Lett.* **2004**, 45, 7633.
- [70] K. Matsumoto, Y. Aoki, K. Oshima, K. Utimoto, N. A. Rahman, *Tetrahedron* **1993**, 49, 8487.
- [71] P. Ongoka, B. Mauzé, L. Miginiac, *J. Organomet. Chem.* **1985**, 139.
- [72] A. Marinetti, F. Mathey, *Organometallics* **1987**, 6, 2189.
- [73] T. L. Breen, D. W. Stephan, *J. Am. Chem. Soc.* **1995**, 11914.
- [74] J. M. Pérez, M. Klein, A. W. Kyri, G. Schnakenburg, R. Streubel, *Organometallics* **2011**, 30, 5636.
- [75] A. Marinetti, J. Fischer, F. Mathey, *J. Am. Chem. Soc.* **1985**, 5002.
- [76] N. H. Tran Huy, B. Donnadiou, G. Bertrand, F. Mathey, *Organometallics* **2010**, 29, 1302.
- [77] R. Streubel, H. Wilkens, U. Rohde, A. Ostrowski, J. Jeske, F. Ruthe, P. G. Jones, *Eur. J. Inorg. Chem.* **1999**, 1567.
- [78] A. Marinetti, F. Mathey, *Organometallics* **1988**, 7, 633.
- [79] P. Junker, *MSc thesis*, University of Bonn, **2016**.
- [80] A. K. Yudin, *Aziridines and Epoxides in Organic Synthesis*, Wiley-VCH, Weinheim, **2006**.
- [81] R. Klein, F. R. Wurm, *Macromol. Rapid Commun.* **2015**, 36, 1147.
- [82] S. Bauer, A. Marinetti, L. Ricard, F. Mathey, *Angew. Chem. Int. Ed. Engl.* **1990**, 29, 1166.
- [83] a) van der Knaap, T. A., T. C. Klebach, R. Lourens, M. Vos, F. Bickelhaupt, *J. Am. Chem. Soc.* **1983**, 4026; b) R. Appel, F. Knoch, H. Kunze, *Angew. Chem. Int. Ed. Engl.* **1984**, 23, 157.

- [84] O. J. Scherer, M. Regitz, *Multiple bonds and low coordination in phosphorus chemistry*, Georg Thieme Verlag, Stuttgart, **1990**.
- [85] A. Espinosa, R. Streubel, *Eur. J. Inorg. Chem.* **2017**.
- [86] G.-V. Rösenthaller, K. Sauerbrey, R. Schmutzler, *Chem. Ber.* **1978**, *111*, 3105.
- [87] M. Schnebel, I. Weidner, R. Wartchow, H. Butenschön, *Eur. J. Org. Chem.* **2003**, *2003*, 4363.
- [88] M. T. Boisdon, J. Barrans, *J. Chem. Soc., Chem. Commun.* **1988**, 615.
- [89] a) H. Quast, M. Heuschmann, *Angew. Chem. Int. Ed. Engl.* **1978**, *17*, 867; b) H. Quast, M. Heuschmann, *Liebigs Ann. Chem.* **1981**, *1981*, 977.
- [90] C. Müller, R. Bartsch, A. Fischer, P. G. Jones, R. Schmutzler, *Chem. Ber.* **1995**, *128*, 499.
- [91] G. Wittig, G. Geissler, *Liebigs Ann.* **1953**, *580*, 44.
- [92] G. Wittig, U. Schöllkopf, *Chem. Ber.* **1954**, *87*, 1318.
- [93] O. I. Kolodiazny, *Phosphorus Ylides*, Wiley-VCH Verlag GmbH, Weinheim, Germany, **1999**.
- [94] B. E. Maryanoff, A. B. Reitz, *Chem. Rev.* **1989**, *89*, 863.
- [95] T. Kawashima, K. Kato, R. Okazaki, *Angew. Chem. Int. Ed. Engl.* **1993**, *32*, 869.
- [96] M. Hamaguchi, Y. Iyama, E. Mochizuki, T. Oshima, *Tetrahedron Lett.* **2005**, *46*, 8949.
- [97] Mazhar-ul-Haque, C. N. Caughlan, F. Ramirez, J. F. Pilot, C. P. Smith, *J. Am. Chem. Soc.* **1971**, *93*, 5229.
- [98] G. Wittig, W. Haag, *Chem. Ber.* **1955**, *88*, 1654.
- [99] U. Dieckbreder, E. Lork, G.-V. Rösenthaller, A. A. Kolomeitsev, *Heteroat. Chem.* **1996**, *7*, 281.
- [100] B. Kaboudin, H. Haghghat, T. Yokomatsu, *Synthesis* **2011**, *2011*, 3185.
- [101] H. J. Bestmann, C. Riemer, R. Dötzer, *Chem. Ber.* **1992**, *125*, 225.
- [102] I. Wurtenberger, B. Angermaier, B. Kircher, R. Gust, *J. Med. Chem.* **2013**, *56*, 7951.
- [103] L. D. Quin, J. C. Kivalus, K. A. Mesch, *J. Org. Chem.* **1983**, *48*, 4466.
- [104] M. Grayson, C. E. Farley, *Chem. Commun.* **1967**, 830.
- [105] a) C. H. Schuster, B. Li, J. P. Morken, *Angew. Chem. Int. Ed.* **2011**, *50*, 7906; b) J. Heinicke, I. Kovacs, L. Nyulaszi, *Chem. Ber.* **1991**, *124*, 493.
- [106] R. Streubel, A. Kusenberg, J. Jeske, P. G. Jones, *Angew. Chem. Int. Ed. Engl.* **1994**, *33*, 2427.
- [107] J. Marinas Pérez, H. Helten, B. Donnadiou, C. A. Reed, R. Streubel, *Angew. Chem. Int. Ed.* **2010**, *49*, 2615.
- [108] J. M. Perez, H. Helten, G. Schnakenburg, R. Streubel, *Chem. Asian J.* **2011**, *6*, 1539.
- [109] C. Albrecht, L. Shi, J. M. Perez, M. van Gastel, S. Schwieger, F. Neese, R. Streubel, *Chem. Eur. J.* **2012**, *18*, 9780.
- [110] P. Malik, A. Espinosa Ferao, G. Schnakenburg, R. Streubel, *Angew. Chem. Int. Ed.* **2016**, *55*, 12693.
- [111] F. Mathey, D. Thavard, *J. Organomet. Chem.* **1976**, *117*, 377.
- [112] F. Mercier, F. Mathey, J. Angenault, J.-C. Couturier, Y. Mary, *J. Organomet. Chem.* **1982**, *231*, 237.
- [113] M. Bode. private communication.
- [114] J. M. Pérez, *PhD Thesis*, University of Bonn, **2010**.
- [115] R. Streubel, A. Ostrowski, H. Wilkens, F. Ruthe, J. Jeske, P. G. Jones, *Angew. Chem. Int. Ed. Engl.* **1997**, *36*, 378.
- [116] A. Ostrowski, *PhD Thesis*, Techn. Univ. Braunschweig, Braunschweig, **1997**.
- [117] D. Sainz, G. Muller, *J. Organomet. Chem.* **1995**, 103.
- [118] R. Streubel, S. Priemer, F. Ruthe, P. G. Jones, *Eur. J. Inorg. Chem.* **2000**, 1253.
- [119] N. Dufour, A.-M. Caminade, M. Basso-Bert, A. Igau, J.-P. Majoral, *Organometallics* **1992**, 1131.
- [120] H. Lang, O. Orama, G. Huttner, *J. Organomet. Chem.* **1985**, 293.
- [121] F. Mercier, F. Mathey, C. Afiong-Akpan, J. F. Nixon, *J. Organomet. Chem.* **1988**, *348*, 361.
- [122] K. Issleib, H.-R. Roloff, *Chem. Ber.* **1965**, 2091.
- [123] J. K. Crandall, M. Appar, *Org. React.* **2005**, 345.
- [124] J. Herzberger, K. Niederer, H. Pohlit, J. Seiwert, M. Worm, F. R. Wurm, H. Frey, *Chem. Rev.* **2016**, *116*, 2170.
- [125] M. Bode, *PhD Thesis*, University of Bonn, **2009**.
- [126] A. Özbolat-Schön, *PhD Thesis*, University of Bonn, **2011**.
- [127] F. Gingl, W. Hiller, J. Strähle, H. Borgholte, K. Dehnjcke, *Z. Anorg. Allg. Chem.* **1991**, *606*, 91.
- [128] a) F. A. Cotton, *Inorg. Chem.* **1964**, *3*, 702; b) L. E. Orgel, *Inorg. Chem.* **1962**, *1*, 25; c) F. A. Cotton, C. S. Kraihanzel, *J. Am. Chem. Soc.* **1962**, *84*, 4432.

- [129] O. J. Scherer, J. Braun, P. Walther, C. Heckmann, G. Wolmershäuser, *Angew. Chem. Int. Ed. Engl.* **1991**, *30*, 852.
- [130] L. Abdrakhmanova, A. Espinosa, R. Streubel, *Dalton Trans.* **2013**, *42*, 10510.
- [131] E. Lindner, A. Brösamle, *Chem. Ber.* **1984**, 2730.
- [132] L. Duan, G. Schnakenburg, R. Streubel, *Organometallics* **2011**, *30*, 3246.
- [133] L. Abdrakhmanova, G. Schnakenburg, A. Espinosa, R. Streubel, *Eur. J. Inorg. Chem.* **2014**, *2014*, 1727.
- [134] J. Y. Salaün, R. Rumin, F. Setifi, S. Triki, P. A. Jaffrès, *Organometallics* **2009**, *28*, 216.
- [135] T. Szymańska-Buzar, T. Głowiak, I. Czełusniak, *Polyhedron* **2002**, *21*, 1817.
- [136] A. W. Kyri, R. Kunzmann, G. Schnakenburg, Z.-W. Qu, S. Grimme, R. Streubel, *Chem. Commun.* **2016**, *52*, 13361.
- [137] H. Nakazawa, W. E. Buhro, G. Bertrand, J. A. Gladysz, *Inorg. Chem.* **1984**, *23*, 3431.
- [138] K. Afarinkia, J. I. G. Cadogan, C. W. Rees, *J. Chem. Soc., Chem. Commun.* **1992**, 285.
- [139] S. Goumri, Y. Leriche, H. Gornitzka, A. Barcelredo, G. Bertrand, *Eur. J. Inorg. Chem.* **1998**, 1539.
- [140] R. A. Watile, D. B. Bagal, Y. P. Patil, B. M. Bhanage, *Tetrahedron Lett.* **2011**, *52*, 6383.
- [141] A. V. Shcherbatiuk, O. S. Shyshlyk, D. V. Yarmoliuk, O. V. Shishkin, S. V. Shishkina, V. S. Starova, O. A. Zaporozhets, S. Zozulya, R. Moriev, O. Kravchuk et al., *Tetrahedron* **2013**, *69*, 3796.
- [142] H. W. Roesky, U. Otten, *J. Fluor. Chem.* **1990**, 433.
- [143] M. R. Foreman, A. M. Slawin, J. D. Woollins, *Phosphorus, Sulfur Silicon Relat. Elem.* **1997**, *124*, 469.
- [144] S. Wilker, S. Laurent, C. Sarter, C. Puke, G. Erker, *J. Am. Chem. Soc.* **1995**, 7293.
- [145] C. Puke, G. Erker, N. C. Aust, E.-U. Würthwein, R. Fröhlich, *J. Am. Chem. Soc.* **1998**, *120*, 4863.
- [146] R. D. Schuetz, R. L. Jacobs, *J. Org. Chem.* **1961**, *26*, 3467.
- [147] W. Davies, W. E. Savige, *J. Chem. Soc.* **1950**, 317.
- [148] a) R. Li, X. Tong, X. Li, C. Hu, *Pure Appl. Chem.* **2011**, *84*; b) A. Baba, H. Kashiwagi, H. Matsuda, *Tetrahedron Lett.* **1985**, 1323.
- [149] J. Marinas Perez, C. Albrecht, H. Helten, G. Schnakenburg, R. Streubel, *Chem. Commun.* **2010**, *46*, 7244.
- [150] M. Klein, C. Albrecht, G. Schnakenburg, R. Streubel, *Organometallics* **2013**, *32*, 4938.
- [151] C. A. Stewart, C. A. VanderWerf, *J. Am. Chem. Soc.* **1954**, *76*, 1259.
- [152] M. Segi, M. Takebe, S. Masuda, T. Nakajima, S. Suga, *Bull. Chem. Soc. Jpn.* **1982**, 167.
- [153] D. Starr, R. M. Hixon, *Org. Synth.* **1937**, *17*, 84.
- [154] C. Murcia-García, A. Bauzá, A. Frontera, R. Streubel, *CrystEngComm* **2015**, *17*, 6736.
- [155] T. Eicher, S. Hauptmann, *Chemie der Heterocyclen. Struktur, Reaktionen und Synthesen.*, Thieme, Stuttgart, **1994**.
- [156] H. Nöth, H. Reith, V. Thorn, *Z. Anorg. Allg. Chem.* **1979**, *458*, 219.
- [157] C. Xi, Y. Liu, C. Lai, L. Zhou, *Inorg. Chem. Commun.* **2004**, *7*, 1202.
- [158] H. Helten, J. M. Pérez, J. Daniels, R. Streubel, *Organometallics* **2009**, *28*, 1221.
- [159] B. L. Booth, K. O. Jibodu, M. F. J. R. P. Proença, *J. Chem. Soc., Perkin Trans. 1* **1983**, 1067.
- [160] J. Dale, S. B. Fredriksen, *Acta Chem. Scand.* **1991**, 82.
- [161] A. Espinosa, E. de las Heras, R. Streubel, *Inorg. Chem.* **2014**, *53*, 6132.
- [162] O. P. Singh, A. Chaturvedi, D. B. Saxena, R. K. Mehrotra, G. Srivastava, *Monatsh. Chem.* **1994**, *125*, 607.
- [163] M. Schlosser, K. F. Christmann, *Justus Liebigs Ann. Chem.* **1967**, *708*, 1.
- [164] E. Vedejs, *Phosphorus, Sulfur Silicon Relat. Elem.* **2014**, *190*, 612.
- [165] M. Bassetti, G. Gerichelli, B. Floris, *Tetrahedron* **1988**, 2997.
- [166] V. Nesterov, S. Schwieger, G. Schnakenburg, S. Grimme, R. Streubel, *Organometallics* **2012**, *31*, 3457.
- [167] H. Yue, Y. Zhao, X. Ma, J. Gong, *Chem. Soc. Rev.* **2012**, *41*, 4218.
- [168] S. A. Park, C. H. Lim, K.-H. Chung, *Bull. Korean Chem. Soc.* **2007**, *28*, 1834.
- [169] M. Schröder, *PhD Thesis*, Kaiserslautern, **1999**.
- [170] E. Nifant'ev, M. Koroteev, G. Kaziev, I. Zakharova, K. Lyssenko, L. Kuleshova, M. Antipin, *Tetrahedron Lett.* **2003**, *44*, 6327.
- [171] H. Schmidbaur, *J. Am. Chem. Soc.* **1963**, *85*, 2336.

- [172] R. Harris, B. Kimber, *J. Magn. Reson.* **1975**, *17*, 174.
- [173] W. Armarego, D. D. Perrin, *Purification of Laboratory chemicals*, Butterworth-Heinemann, Oxford, **1995**.
- [174] G. R. Fulmer, A. J. M. Miller, N. H. Sherden, H. E. Gottlieb, A. Nudelman, B. M. Stoltz, J. E. Bercaw, K. I. Goldberg, *Organometallics* **2010**, *29*, 2176.
- [175] G. M. Sheldrick, *Acta Crystallogr., Sect. A* **1990**, 467.
- [176] G. M. Sheldrick, *SHELXL-97*, Universität Göttingen, Göttingen.
- [177] G. M. Sheldrick, *Acta Cryst.* **2015**, *C71*, 3.
- [178] O. V. Dolomanov, L. J. Bourhis, R. J. Gildea, J. A. K. Howard, H. Puschmann, *J. Appl. Cryst.* **2009**, *42*.
- [179] U. Koelle, *J. Organomet. Chem.* **1977**, 53.
- [180] a) M. J. S. Gynane, A. Hudson, M. F. Lappert, Power, P. P., Goldwhite, H., *J. Chem. Soc., Dalton Trans.* **1980**, 2428; b) R. R. Ford, R. H. Neilson, *Polyhedron* **1986**, *5*, 643.
- [181] V. Plack, J. R. Goerlich, A. Fischer, H. Thönnessen, P. G. Jones, R. Schmutzler, *Z. Anorg. Allg. Chem.* **1995**, 1080.
- [182] P. Jutzi, H. Saleske, D. Nadler, *J. Organomet. Chem.* **1976**, C8-C10.
- [183] R. Kunzmann, *planned PhD Thesis*, University of Bonn.

12 X-ray crystallographic data

12.1 Pentacarbonyl[diethylamino(triphenylmethyl)phosphane- κP]tungsten(0) [6.3a]**Table 1:** Crystal data and structure refinement for **6.3a**.

Identification code	GSTR317, AKY-280 // GXraytwin5-merg
Crystal Habitus	pale yellow plate
Device Type	Bruker X8-KappaApexII
Empirical formula	C ₂₈ H ₂₆ NO ₅ PW
Moiety formula	C ₂₈ H ₂₆ N O ₅ P W
Formula weight	671.32
Temperature/K	100(2)
Crystal system	triclinic
Space group	P $\bar{1}$
a/Å	10.7367(7)
b/Å	15.6770(10)
c/Å	17.4538(10)
α /°	104.204(3)
β /°	98.484(3)
γ /°	104.184(3)
Volume/Å ³	2692.9(3)
Z	4
$\rho_{\text{calc}}/\text{cm}^3$	1.656
μ/mm^{-1}	4.386
F(000)	1320.0
Crystal size/mm ³	0.35 × 0.20 × 0.10
Absorption correction	empirical
Tmin; Tmax	0.3090; 0.6681
Radiation	MoK α (λ = 0.71073)
2 θ range for data collection/°	2.46 to 50.5°

Completeness to theta	0.950
Index ranges	-12 ≤ h ≤ 0, -18 ≤ k ≤ 18, -20 ≤ l ≤ 20
Reflections collected	11119
Independent reflections	11139 [R _{int} = 0.0700]
Data/restraints/parameters	11139/102/660
Goodness-of-fit on F ²	1.046
Final R indexes [I ≥ 2σ (I)]	R ₁ = 0.0419, wR ₂ = 0.0975
Final R indexes [all data]	R ₁ = 0.0538, wR ₂ = 0.1052
Largest diff. peak/hole / e Å ⁻³	2.07/-1.62

Table 2: Bond lengths for **6.3a**.

Atom	Atom	Length/Å	Atom	Atom	Length/Å
C1	N1	1.467(9)	C31	N2	1.482(8)
C1	C2	1.517(10)	C31	C32	1.505(10)
C3	N1	1.477(8)	C33	C34	1.539(9)
C3	C4	1.525(10)	C33	C46	1.540(9)
C5	C6	1.524(9)	C33	C40	1.551(9)
C5	C18	1.543(9)	C33	P2	1.954(6)
C5	C12	1.555(9)	C34	C39	1.382(10)
C5	P1	1.957(7)	C34	C35	1.411(10)
C6	C7	1.399(9)	C35	C36	1.382(10)
C6	C11	1.399(10)	C36	C37	1.396(10)
C7	C8	1.386(10)	C37	C38	1.376(11)
C8	C9	1.388(10)	C38	C39	1.394(10)
C9	C10	1.387(10)	C40	C41	1.390(9)
C10	C11	1.394(10)	C40	C45	1.402(10)
C12	C13	1.383(9)	C41	C42	1.392(10)
C12	C17	1.387(10)	C42	C43	1.382(11)
C13	C14	1.400(10)	C43	C44	1.395(11)
C14	C15	1.385(11)	C44	C45	1.383(10)
C15	C16	1.384(10)	C46	C51	1.398(10)
C16	C17	1.393(10)	C46	C47	1.398(9)
C18	C23	1.400(9)	C47	C48	1.385(10)
C18	C19	1.401(9)	C48	C49	1.399(11)
C19	C20	1.393(10)	C49	C50	1.379(11)
C20	C21	1.392(11)	C50	C51	1.391(10)
C21	C22	1.386(11)	C52	O6	1.137(9)
C22	C23	1.377(10)	C52	W2	2.024(8)
C24	O1	1.137(8)	C53	O7	1.132(8)
C24	W1	2.017(7)	C53	W2	2.065(8)
C25	O2	1.144(9)	C54	O8	1.145(9)
C25	W1	2.046(8)	C54	W2	2.044(8)
C26	O3	1.154(8)	C55	O9	1.144(8)
C26	W1	2.033(7)	C55	W2	2.048(8)
C27	O4	1.148(8)	C56	O10	1.146(8)
C27	W1	2.038(7)	C56	W2	2.039(7)
C28	O5	1.142(9)	N1	P1	1.673(6)
C28	W1	2.047(8)	N2	P2	1.678(6)
C29	N2	1.465(9)	P1	W1	2.5540(18)
C29	C30	1.507(10)	P2	W2	2.5509(17)

Table 3: Bond angles for **6.3a**.

Atom	Atom	Atom	Angle/°	Atom	Atom	Atom	Angle/°
N1	C1	C2	113.1(6)	C42	C43	C44	118.7(7)
N1	C3	C4	113.4(6)	C45	C44	C43	120.8(8)
C6	C5	C18	111.0(5)	C44	C45	C40	120.7(7)
C6	C5	C12	112.0(5)	C51	C46	C47	117.4(6)
C18	C5	C12	111.5(6)	C51	C46	C33	120.0(6)
C6	C5	P1	106.2(4)	C47	C46	C33	122.3(6)
C18	C5	P1	108.5(4)	C48	C47	C46	120.7(7)
C12	C5	P1	107.3(4)	C47	C48	C49	120.6(7)
C7	C6	C11	117.1(6)	C50	C49	C48	119.6(7)
C7	C6	C5	121.4(6)	C49	C50	C51	119.3(7)
C11	C6	C5	121.5(6)	C50	C51	C46	122.3(7)
C8	C7	C6	121.8(7)	O6	C52	W2	177.3(7)
C7	C8	C9	120.1(7)	O7	C53	W2	177.7(6)
C10	C9	C8	119.6(7)	O8	C54	W2	175.6(6)
C9	C10	C11	119.8(7)	O9	C55	W2	178.6(7)
C10	C11	C6	121.6(7)	O10	C56	W2	177.9(6)
C13	C12	C17	118.8(6)	C1	N1	C3	116.0(6)
C13	C12	C5	121.0(6)	C1	N1	P1	122.0(5)
C17	C12	C5	120.1(6)	C3	N1	P1	121.0(5)
C12	C13	C14	119.7(7)	C29	N2	C31	115.8(6)
C15	C14	C13	121.4(7)	C29	N2	P2	124.2(5)
C16	C15	C14	118.6(7)	C31	N2	P2	119.6(5)
C15	C16	C17	120.1(7)	N1	P1	C5	109.7(3)
C12	C17	C16	121.3(7)	N1	P1	W1	115.9(2)
C23	C18	C19	117.1(6)	C5	P1	W1	123.1(2)
C23	C18	C5	120.7(6)	N2	P2	C33	110.3(3)
C19	C18	C5	121.9(6)	N2	P2	W2	115.6(2)
C20	C19	C18	121.0(7)	C33	P2	W2	123.1(2)
C21	C20	C19	120.5(7)	C24	W1	C26	89.2(3)
C22	C21	C20	118.9(7)	C24	W1	C27	89.2(3)
C23	C22	C21	120.5(7)	C26	W1	C27	88.0(3)
C22	C23	C18	121.9(7)	C24	W1	C25	87.1(3)
O1	C24	W1	178.9(7)	C26	W1	C25	89.6(3)
O2	C25	W1	175.4(6)	C27	W1	C25	175.6(3)
O3	C26	W1	177.3(6)	C24	W1	C28	90.6(3)
O4	C27	W1	175.4(6)	C26	W1	C28	178.9(3)
O5	C28	W1	177.8(7)	C27	W1	C28	91.0(3)
N2	C29	C30	113.8(6)	C25	W1	C28	91.5(3)
N2	C31	C32	113.6(6)	C24	W1	P1	173.1(2)
C34	C33	C46	110.3(5)	C26	W1	P1	94.9(2)
C34	C33	C40	111.3(5)	C27	W1	P1	96.5(2)
C46	C33	C40	111.9(5)	C25	W1	P1	87.31(19)
C34	C33	P2	106.8(4)	C28	W1	P1	85.5(2)
C46	C33	P2	108.6(4)	C52	W2	C56	86.9(3)
C40	C33	P2	107.8(4)	C52	W2	C54	88.9(3)
C39	C34	C35	118.5(7)	C56	W2	C54	174.1(3)
C39	C34	C33	121.4(6)	C52	W2	C55	90.0(3)
C35	C34	C33	120.0(6)	C56	W2	C55	88.4(3)
C36	C35	C34	120.2(7)	C54	W2	C55	87.4(3)
C35	C36	C37	120.8(7)	C52	W2	C53	90.7(3)
C38	C37	C36	118.8(7)	C56	W2	C53	92.3(3)

C37	C38	C39	121.0(7)	C54	W2	C53	91.9(3)
C34	C39	C38	120.6(7)	C55	W2	C53	179.0(3)
C41	C40	C45	118.0(6)	C52	W2	P2	172.0(2)
C41	C40	C33	121.8(6)	C56	W2	P2	86.7(2)
C45	C40	C33	120.1(6)	C54	W2	P2	97.76(19)
C40	C41	C42	121.0(7)	C55	W2	P2	94.7(2)
C43	C42	C41	120.7(7)	C53	W2	P2	84.7(2)

Table 4: Torsion angles for **6.3a**.

A	B	C	D	Angle/°	A	B	C	D	Angle/°
C18	C5	C6	C7	-161.7(6)	C32	C31	N2	P2	123.4(6)
C12	C5	C6	C7	72.9(8)	C1	N1	P1	C5	-98.7(5)
P1	C5	C6	C7	-43.9(7)	C3	N1	P1	C5	93.4(5)
C18	C5	C6	C11	20.4(8)	C1	N1	P1	W1	116.4(5)
C12	C5	C6	C11	-105.0(7)	C3	N1	P1	W1	-51.6(5)
P1	C5	C6	C11	138.2(5)	C6	C5	P1	N1	178.5(4)
C11	C6	C7	C8	-1.2(10)	C18	C5	P1	N1	-62.1(5)
C5	C6	C7	C8	-179.2(6)	C12	C5	P1	N1	58.5(5)
C6	C7	C8	C9	1.1(10)	C6	C5	P1	W1	-39.6(5)
C7	C8	C9	C10	-0.2(10)	C18	C5	P1	W1	79.9(5)
C8	C9	C10	C11	-0.6(10)	C12	C5	P1	W1	-159.5(3)
C9	C10	C11	C6	0.5(10)	C29	N2	P2	C33	96.4(6)
C7	C6	C11	C10	0.4(10)	C31	N2	P2	C33	-91.0(5)
C5	C6	C11	C10	178.4(6)	C29	N2	P2	W2	-118.3(5)
C6	C5	C12	C13	1.7(9)	C31	N2	P2	W2	54.3(5)
C18	C5	C12	C13	-123.4(6)	C34	C33	P2	N2	-179.3(4)
P1	C5	C12	C13	117.9(6)	C46	C33	P2	N2	61.8(5)
C6	C5	C12	C17	178.4(6)	C40	C33	P2	N2	-59.6(5)
C18	C5	C12	C17	53.3(8)	C34	C33	P2	W2	38.5(5)
P1	C5	C12	C17	-65.4(7)	C46	C33	P2	W2	-80.4(5)
C17	C12	C13	C14	1.1(10)	C40	C33	P2	W2	158.2(4)
C5	C12	C13	C14	177.8(6)	O1	C24	W1	C26	-65(35)
C12	C13	C14	C15	1.6(11)	O1	C24	W1	C27	-152(35)
C13	C14	C15	C16	-2.9(11)	O1	C24	W1	C25	25(35)
C14	C15	C16	C17	1.6(11)	O1	C24	W1	C28	117(35)
C13	C12	C17	C16	-2.3(10)	O1	C24	W1	P1	62(35)
C5	C12	C17	C16	-179.1(6)	O3	C26	W1	C24	-11(13)
C15	C16	C17	C12	1.0(11)	O3	C26	W1	C27	78(13)
C6	C5	C18	C23	68.6(8)	O3	C26	W1	C25	-98(13)
C12	C5	C18	C23	-165.7(6)	O3	C26	W1	C28	67(21)
P1	C5	C18	C23	-47.8(7)	O3	C26	W1	P1	174(100)
C6	C5	C18	C19	-105.9(7)	O4	C27	W1	C24	34(8)
C12	C5	C18	C19	19.8(9)	O4	C27	W1	C26	-55(8)
P1	C5	C18	C19	137.7(6)	O4	C27	W1	C25	1(10)
C23	C18	C19	C20	2.7(10)	O4	C27	W1	C28	125(8)
C5	C18	C19	C20	177.4(6)	O4	C27	W1	P1	-150(8)
C18	C19	C20	C21	-0.7(11)	O2	C25	W1	C24	-21(8)
C19	C20	C21	C22	-0.9(12)	O2	C25	W1	C26	69(8)
C20	C21	C22	C23	0.4(12)	O2	C25	W1	C27	13(11)
C21	C22	C23	C18	1.8(11)	O2	C25	W1	C28	-111(8)
C19	C18	C23	C22	-3.3(10)	O2	C25	W1	P1	164(8)

C5	C18	C23	C22	-178.1(6)	O5	C28	W1	C24	-151(18)
C46	C33	C34	C39	-22.3(8)	O5	C28	W1	C26	131(19)
C40	C33	C34	C39	102.5(7)	O5	C28	W1	C27	120(18)
P2	C33	C34	C39	-140.1(6)	O5	C28	W1	C25	-63(18)
C46	C33	C34	C35	161.3(6)	O5	C28	W1	P1	24(18)
C40	C33	C34	C35	-73.9(8)	N1	P1	W1	C24	-70.3(18)
P2	C33	C34	C35	43.5(7)	C5	P1	W1	C24	149.8(18)
C39	C34	C35	C36	2.2(10)	N1	P1	W1	C26	55.5(3)
C33	C34	C35	C36	178.6(6)	C5	P1	W1	C26	-84.4(3)
C34	C35	C36	C37	-1.4(10)	N1	P1	W1	C27	144.0(3)
C35	C36	C37	C38	-0.6(11)	C5	P1	W1	C27	4.1(3)
C36	C37	C38	C39	1.8(11)	N1	P1	W1	C25	-33.9(3)
C35	C34	C39	C38	-1.0(10)	C5	P1	W1	C25	-173.7(3)
C33	C34	C39	C38	-177.4(6)	N1	P1	W1	C28	-125.6(3)
C37	C38	C39	C34	-1.0(11)	C5	P1	W1	C28	94.6(3)
C34	C33	C40	C41	-0.2(9)	O6	C52	W2	C56	8(15)
C46	C33	C40	C41	123.7(7)	O6	C52	W2	C54	-176(100)
P2	C33	C40	C41	-117.0(6)	O6	C52	W2	C55	97(15)
C34	C33	C40	C45	-178.9(6)	O6	C52	W2	C53	-84(15)
C46	C33	C40	C45	-54.9(8)	O6	C52	W2	P2	-29(16)
P2	C33	C40	C45	64.3(7)	O10	C56	W2	C52	48(17)
C45	C40	C41	C42	-0.6(10)	O10	C56	W2	C54	4(19)
C33	C40	C41	C42	-179.3(6)	O10	C56	W2	C55	-42(17)
C40	C41	C42	C43	-1.5(11)	O10	C56	W2	C53	139(17)
C41	C42	C43	C44	1.4(12)	O10	C56	W2	P2	-137(17)
C42	C43	C44	C45	0.8(11)	O8	C54	W2	C52	-35(8)
C43	C44	C45	C40	-3.0(11)	O8	C54	W2	C56	9(10)
C41	C40	C45	C44	2.8(10)	O8	C54	W2	C55	55(8)
C33	C40	C45	C44	-178.4(6)	O8	C54	W2	C53	-126(8)
C34	C33	C46	C51	-65.2(8)	O8	C54	W2	P2	149(8)
C40	C33	C46	C51	170.3(6)	O9	C55	W2	C52	50(26)
P2	C33	C46	C51	51.5(7)	O9	C55	W2	C56	137(26)
C34	C33	C46	C47	109.7(7)	O9	C55	W2	C54	-39(26)
C40	C33	C46	C47	-14.8(9)	O9	C55	W2	C53	-87(32)
P2	C33	C46	C47	-133.5(6)	O9	C55	W2	P2	-137(26)
C51	C46	C47	C48	-1.3(10)	O7	C53	W2	C52	-171(17)
C33	C46	C47	C48	-176.4(6)	O7	C53	W2	C56	102(17)
C46	C47	C48	C49	-0.4(11)	O7	C53	W2	C54	-82(17)
C47	C48	C49	C50	1.2(12)	O7	C53	W2	C55	-35(30)
C48	C49	C50	C51	-0.2(11)	O7	C53	W2	P2	15(17)
C49	C50	C51	C46	-1.6(11)	N2	P2	W2	C52	68.6(16)
C47	C46	C51	C50	2.3(10)	C33	P2	W2	C52	-151.0(15)
C33	C46	C51	C50	177.5(6)	N2	P2	W2	C56	30.9(3)
C2	C1	N1	C3	78.0(8)	C33	P2	W2	C56	171.3(3)
C2	C1	N1	P1	-90.5(7)	N2	P2	W2	C54	-145.3(3)
C4	C3	N1	C1	77.5(8)	C33	P2	W2	C54	-4.9(3)
C4	C3	N1	P1	-113.9(6)	N2	P2	W2	C55	-57.2(3)
C30	C29	N2	C31	-61.0(9)	C33	P2	W2	C55	83.2(3)
C30	C29	N2	P2	111.8(7)	N2	P2	W2	C53	123.5(3)
C32	C31	N2	C29	-63.5(8)	C33	P2	W2	C53	-96.1(3)

12.2 Pentacarbonyl[cyclohexylamino(triphenylmethyl)phosphane- κP]tungsten(0) [9.3a]

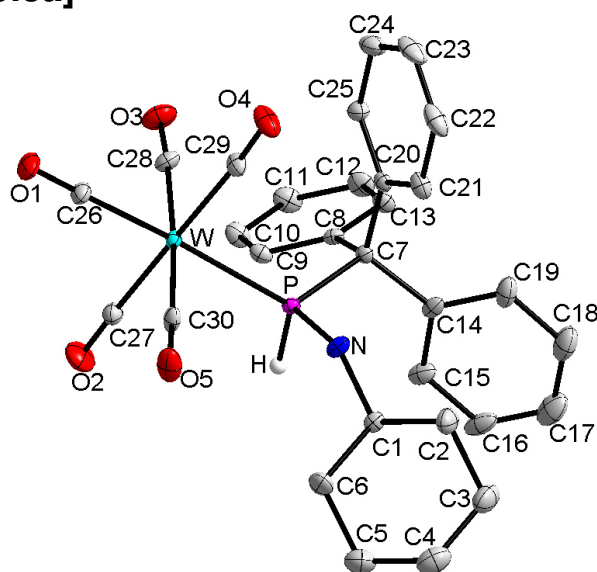


Table 1: Crystal data and structure refinement for **9.3a**.

Identification code	GSTR450, AKY-Cy // GXraymo_4395f
Crystal Habitus	clear colourless block
Device Type	Bruker D8-Venture
Empirical formula	C ₃₀ H ₂₈ NO ₅ PW
Moiety formula	C ₃₀ H ₂₈ N O ₅ P W
Formula weight	697.35
Temperature/K	100.0
Crystal system	monoclinic
Space group	P2 ₁ /c
a/Å	9.5897(3)
b/Å	27.4801(8)
c/Å	11.3823(3)
α/°	90
β/°	111.0141(9)
γ/°	90
Volume/Å ³	2800.04(14)
Z	4
ρ _{calc} /cm ³	1.654
μ/mm ⁻¹	4.222
F(000)	1376.0
Crystal size/mm ³	0.25 × 0.24 × 0.23
Absorption correction	empirical
Tmin; Tmax	0.4113; 0.7459
Radiation	MoKα (λ = 0.71073)
2θ range for data collection/°	4.786 to 55.996°
Completeness to theta	0.999
Index ranges	-12 ≤ h ≤ 12, -36 ≤ k ≤ 36, -15 ≤ l ≤ 14
Reflections collected	111139
Independent reflections	6760 [R _{int} = 0.0385, R _{sigma} = 0.0134]
Data/restraints/parameters	6760/145/346
Goodness-of-fit on F ²	1.085

Final R indexes [$I \geq 2\sigma(I)$]	$R_1 = 0.0184$, $wR_2 = 0.0403$
Final R indexes [all data]	$R_1 = 0.0205$, $wR_2 = 0.0410$
Largest diff. peak/hole / $e \text{ \AA}^{-3}$	1.05/-0.96

Table 2: Bond lengths for **9.3a**.

Atom	Atom	Length/Å	Atom	Atom	Length/Å
W	P	2.5210(5)	C7	C14	1.544(3)
W	C26	1.996(2)	C7	C20	1.537(3)
W	C27	2.035(2)	C8	C9	1.391(3)
W	C28	2.047(2)	C8	C13	1.403(3)
W	C29	2.061(2)	C9	C10	1.398(3)
W	C30	2.055(2)	C10	C11	1.387(3)
P	N	1.6652(18)	C11	C12	1.389(3)
P	C7	1.912(2)	C12	C13	1.388(3)
O1	C26	1.150(3)	C14	C15	1.406(3)
O2	C27	1.143(3)	C14	C19	1.394(3)
O3	C28	1.142(3)	C15	C16	1.389(3)
O4	C29	1.136(3)	C16	C17	1.383(4)
O5	C30	1.138(3)	C17	C18	1.377(4)
N	C1	1.470(3)	C18	C19	1.401(3)
C1	C2	1.518(3)	C20	C21	1.406(3)
C1	C6	1.523(3)	C20	C25	1.393(3)
C2	C3	1.529(3)	C21	C22	1.388(3)
C3	C4	1.508(4)	C22	C23	1.382(4)
C4	C5	1.527(4)	C23	C24	1.386(4)
C5	C6	1.536(3)	C24	C25	1.397(3)
C7	C8	1.540(3)			

Table 3: Bond angles for **9.3a**.

Atom	Atom	Atom	Angle/°	Atom	Atom	Atom	Angle/°
C26	W	P	174.72(7)	C20	C7	C8	112.09(16)
C26	W	C27	92.77(9)	C20	C7	C14	114.48(17)
C26	W	C28	88.48(9)	C9	C8	C7	124.93(18)
C26	W	C29	87.74(9)	C9	C8	C13	118.01(19)
C26	W	C30	88.64(9)	C13	C8	C7	117.05(18)
C27	W	P	87.49(6)	C8	C9	C10	120.9(2)
C27	W	C28	90.00(9)	C11	C10	C9	120.2(2)
C27	W	C29	179.47(9)	C10	C11	C12	119.5(2)
C27	W	C30	87.23(9)	C13	C12	C11	120.1(2)
C28	W	P	96.79(6)	C12	C13	C8	121.2(2)
C28	W	C29	90.15(9)	C15	C14	C7	118.05(19)
C28	W	C30	175.91(9)	C19	C14	C7	124.4(2)
C29	W	P	91.99(6)	C19	C14	C15	117.5(2)
C30	W	P	86.11(6)	C16	C15	C14	121.7(2)
C30	W	C29	92.65(9)	C17	C16	C15	119.8(3)
N	P	W	111.49(6)	C18	C17	C16	119.7(2)
N	P	C7	106.64(9)	C17	C18	C19	120.8(3)
C7	P	W	121.53(6)	C14	C19	C18	120.5(2)
C1	N	P	126.12(14)	C21	C20	C7	120.85(19)
N	C1	C2	110.37(17)	C25	C20	C7	121.32(19)

N	C1	C6	111.65(17)	C25	C20	C21	117.7(2)
C2	C1	C6	110.97(19)	C22	C21	C20	120.9(2)
C1	C2	C3	110.9(2)	C23	C22	C21	120.5(2)
C4	C3	C2	111.6(2)	C22	C23	C24	119.7(2)
C3	C4	C5	110.8(2)	C23	C24	C25	119.9(2)
C4	C5	C6	110.5(2)	C20	C25	C24	121.2(2)
C1	C6	C5	110.5(2)	O1	C26	W	178.3(2)
C8	C7	P	111.39(14)	O2	C27	W	178.3(2)
C8	C7	C14	105.69(16)	O3	C28	W	176.2(2)
C14	C7	P	108.96(13)	O4	C29	W	175.79(19)
C20	C7	P	104.33(13)	O5	C30	W	177.7(2)

Table 4: Torsion angles for **9.3a**.

A	B	C	D	Angle/°	A	B	C	D	Angle/°
W	P	N	C1	138.94(15)	C8	C7	C20	C25	12.3(3)
P	N	C1	C2	143.27(17)	C8	C9	C10	C11	0.8(3)
P	N	C1	C6	-92.8(2)	C9	C8	C13	C12	1.4(3)
P	C7	C8	C9	1.7(3)	C9	C10	C11	C12	0.7(4)
P	C7	C8	C13	-176.70(15)	C10	C11	C12	C13	-1.2(4)
P	C7	C14	C15	65.9(2)	C11	C12	C13	C8	0.1(3)
P	C7	C14	C19	-117.7(2)	C13	C8	C9	C10	-1.9(3)
P	C7	C20	C21	67.7(2)	C14	C7	C8	C9	119.9(2)
P	C7	C20	C25	-108.32(19)	C14	C7	C8	C13	-58.5(2)
N	C1	C2	C3	-179.61(19)	C14	C7	C20	C21	-51.3(3)
N	C1	C6	C5	179.57(19)	C14	C7	C20	C25	132.7(2)
C1	C2	C3	C4	-55.9(3)	C14	C15	C16	C17	-0.2(4)
C2	C1	C6	C5	-56.8(3)	C15	C14	C19	C18	-3.4(3)
C2	C3	C4	C5	56.1(3)	C15	C16	C17	C18	-2.0(4)
C3	C4	C5	C6	-56.5(3)	C16	C17	C18	C19	1.4(4)
C4	C5	C6	C1	56.8(3)	C17	C18	C19	C14	1.4(4)
C6	C1	C2	C3	56.1(3)	C19	C14	C15	C16	2.8(3)
C7	P	N	C1	-86.30(18)	C20	C7	C8	C9	-114.7(2)
C7	C8	C9	C10	179.7(2)	C20	C7	C8	C13	66.8(2)
C7	C8	C13	C12	180.0(2)	C20	C7	C14	C15	-177.74(18)
C7	C14	C15	C16	179.5(2)	C20	C7	C14	C19	-1.3(3)
C7	C14	C19	C18	-179.8(2)	C20	C21	C22	C23	1.6(3)
C7	C20	C21	C22	-179.0(2)	C21	C20	C25	C24	1.9(3)
C7	C20	C25	C24	178.1(2)	C21	C22	C23	C24	0.6(4)
C8	C7	C14	C15	-53.9(2)	C22	C23	C24	C25	-1.5(4)
C8	C7	C14	C19	122.5(2)	C23	C24	C25	C20	0.2(4)
C8	C7	C20	C21	-171.62(18)	C25	C20	C21	C22	-2.8(3)

12.3 Pentacarbonyl[1-methylethylamino(triphenylmethyl)phosphane- κ P]tungsten(0) [9.3b]

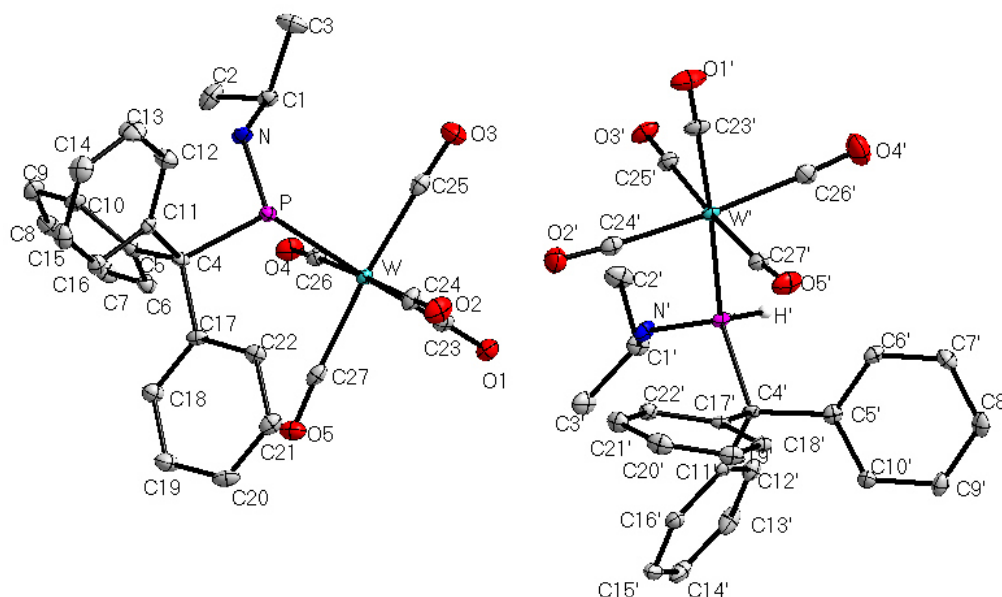


Table 1: Crystal data and structure refinement for **9.3b**.

Identification code	GSTR449, AKY-iPr // GXraymo_4396f
Crystal Habitus	clear colourless block
Device Type	Bruker D8-Venture
Empirical formula	$C_{27}H_{24}NO_5PW$
Moiety formula	$C_{27}H_{24}N O_5 P W$
Formula weight	657.29
Temperature/K	100.01
Crystal system	triclinic
Space group	$P\bar{1}$
a/Å	10.2830(5)
b/Å	12.3871(6)
c/Å	20.1318(9)
α /°	93.1130(15)
β /°	99.9351(15)
γ /°	90.4631(16)
Volume/Å ³	2521.7(2)
Z	4
$\rho_{\text{calc}}/\text{cm}^3$	1.731
μ/mm^{-1}	4.682
F(000)	1288.0
Crystal size/mm ³	0.24 × 0.22 × 0.18
Absorption correction	empirical
Tmin; Tmax	0.3187; 0.7459
Radiation	MoK α ($\lambda = 0.71073$)
2 θ range for data collection/°	4.824 to 55.998°
Completeness to theta	0.999
Index ranges	$-13 \leq h \leq 13, -16 \leq k \leq 16, -26 \leq l \leq 26$
Reflections collected	132861
Independent reflections	12179 [$R_{\text{int}} = 0.0688, R_{\text{sigma}} = 0.0300$]
Data/restraints/parameters	12179/0/642
Goodness-of-fit on F^2	1.070

Final R indexes [$I \geq 2\sigma(I)$]	$R_1 = 0.0258$, $wR_2 = 0.0630$
Final R indexes [all data]	$R_1 = 0.0320$, $wR_2 = 0.0671$
Largest diff. peak/hole / $e \text{ \AA}^{-3}$	2.07/-2.35

Table 2: Bond lengths for **9.3b**.

Atom	Atom	Length/Å	Atom	Atom	Length/Å
W	P	2.5361(8)	W'	P'	2.5344(8)
W	C23	1.996(3)	W'	C23'	2.009(3)
W	C24	2.054(3)	W'	C24'	2.049(3)
W	C25	2.035(3)	W'	C25'	2.042(3)
W	C26	2.042(3)	W'	C26'	2.037(3)
W	C27	2.063(3)	W'	C27'	2.069(3)
P	N	1.663(3)	P'	N'	1.674(3)
P	C4	1.924(3)	P'	C4'	1.927(3)
O1	C23	1.154(4)	O1'	C23'	1.147(4)
O2	C24	1.136(4)	O2'	C24'	1.142(4)
O3	C25	1.150(4)	O3'	C25'	1.137(4)
O4	C26	1.137(4)	O4'	C26'	1.140(4)
O5	C27	1.141(4)	O5'	C27'	1.135(4)
N	C1	1.474(4)	N'	C1'	1.483(4)
C1	C2	1.528(5)	C1'	C2'	1.526(4)
C1	C3	1.526(4)	C1'	C3'	1.521(5)
C4	C5	1.537(4)	C4'	C5'	1.537(4)
C4	C11	1.546(4)	C4'	C11'	1.546(4)
C4	C17	1.534(4)	C4'	C17'	1.536(4)
C5	C6	1.400(4)	C5'	C6'	1.396(4)
C5	C10	1.393(4)	C5'	C10'	1.396(4)
C6	C7	1.393(4)	C6'	C7'	1.391(4)
C7	C8	1.386(5)	C7'	C8'	1.391(5)
C8	C9	1.383(5)	C8'	C9'	1.387(5)
C9	C10	1.397(4)	C9'	C10'	1.397(4)
C11	C12	1.400(4)	C11'	C12'	1.401(4)
C11	C16	1.400(4)	C11'	C16'	1.393(4)
C12	C13	1.397(5)	C12'	C13'	1.389(5)
C13	C14	1.379(5)	C13'	C14'	1.384(5)
C14	C15	1.391(5)	C14'	C15'	1.390(5)
C15	C16	1.392(5)	C15'	C16'	1.397(4)
C17	C18	1.396(4)	C17'	C18'	1.396(4)
C17	C22	1.397(4)	C17'	C22'	1.399(4)
C18	C19	1.395(4)	C18'	C19'	1.395(4)
C19	C20	1.386(5)	C19'	C20'	1.383(5)
C20	C21	1.389(5)	C20'	C21'	1.393(5)
C21	C22	1.393(4)	C21'	C22'	1.390(4)

Table 3: Bond angles for **9.3b**.

Atom	Atom	Atom	Angle/°	Atom	Atom	Atom	Angle/°
C23	W	P	177.52(9)	C23'	W'	P'	176.43(9)
C23	W	C24	92.10(12)	C23'	W'	C24'	87.86(14)
C23	W	C25	88.48(13)	C23'	W'	C25'	91.16(13)
C23	W	C26	88.46(12)	C23'	W'	C26'	89.42(14)

C23	W	C27	86.17(12)	C23'	W'	C27'	87.49(13)
C24	W	P	87.65(9)	C24'	W'	P'	89.96(9)
C24	W	C27	91.35(12)	C24'	W'	C27'	93.13(13)
C25	W	P	89.04(9)	C25'	W'	P'	86.01(9)
C25	W	C24	88.60(13)	C25'	W'	C24'	90.07(13)
C25	W	C26	92.93(13)	C25'	W'	C27'	176.47(12)
C25	W	C27	174.65(12)	C26'	W'	P'	92.59(10)
C26	W	P	91.85(9)	C26'	W'	C24'	175.79(12)
C26	W	C24	178.38(12)	C26'	W'	C25'	86.76(13)
C26	W	C27	87.16(12)	C26'	W'	C27'	89.96(13)
C27	W	P	96.30(9)	C27'	W'	P'	95.46(9)
N	P	W	116.54(10)	N'	P'	W'	109.73(10)
N	P	C4	104.13(13)	N'	P'	C4'	107.54(13)
C4	P	W	122.83(9)	C4'	P'	W'	122.75(9)
C1	N	P	128.1(2)	C1'	N'	P'	125.7(2)
N	C1	C2	111.4(3)	N'	C1'	C2'	110.7(3)
N	C1	C3	109.4(3)	N'	C1'	C3'	110.7(3)
C3	C1	C2	111.7(3)	C3'	C1'	C2'	111.3(3)
C5	C4	P	104.41(19)	C5'	C4'	P'	109.63(19)
C5	C4	C11	111.0(2)	C5'	C4'	C11'	109.2(2)
C11	C4	P	112.04(19)	C11'	C4'	P'	108.16(19)
C17	C4	P	108.1(2)	C17'	C4'	P'	107.13(19)
C17	C4	C5	113.6(2)	C17'	C4'	C5'	111.0(2)
C17	C4	C11	107.8(2)	C17'	C4'	C11'	111.6(2)
C6	C5	C4	119.9(3)	C6'	C5'	C4'	122.5(3)
C10	C5	C4	121.7(3)	C6'	C5'	C10'	118.0(3)
C10	C5	C6	118.2(3)	C10'	C5'	C4'	119.3(3)
C7	C6	C5	120.8(3)	C7'	C6'	C5'	121.3(3)
C8	C7	C6	120.4(3)	C8'	C7'	C6'	120.1(3)
C9	C8	C7	119.3(3)	C9'	C8'	C7'	119.2(3)
C8	C9	C10	120.5(3)	C8'	C9'	C10'	120.6(3)
C5	C10	C9	120.8(3)	C5'	C10'	C9'	120.7(3)
C12	C11	C4	124.4(3)	C12'	C11'	C4'	119.3(3)
C12	C11	C16	117.3(3)	C16'	C11'	C4'	122.9(3)
C16	C11	C4	118.3(3)	C16'	C11'	C12'	117.7(3)
C13	C12	C11	121.1(3)	C13'	C12'	C11'	121.3(3)
C14	C13	C12	120.7(3)	C14'	C13'	C12'	120.4(3)
C13	C14	C15	119.2(3)	C13'	C14'	C15'	119.0(3)
C14	C15	C16	120.2(3)	C14'	C15'	C16'	120.6(3)
C15	C16	C11	121.5(3)	C11'	C16'	C15'	120.9(3)
C18	C17	C4	122.5(3)	C18'	C17'	C4'	122.0(3)
C18	C17	C22	118.0(3)	C18'	C17'	C22'	118.0(3)
C22	C17	C4	119.3(3)	C22'	C17'	C4'	120.0(3)
C19	C18	C17	120.9(3)	C19'	C18'	C17'	120.5(3)
C20	C19	C18	120.2(3)	C20'	C19'	C18'	120.9(3)
C19	C20	C21	119.8(3)	C19'	C20'	C21'	119.1(3)
C20	C21	C22	119.7(3)	C22'	C21'	C20'	120.1(3)
C21	C22	C17	121.4(3)	C21'	C22'	C17'	121.3(3)
O1	C23	W	177.6(3)	O1'	C23'	W'	178.0(3)
O2	C24	W	178.7(3)	O2'	C24'	W'	176.4(3)
O3	C25	W	177.6(3)	O3'	C25'	W'	179.5(3)
O4	C26	W	177.2(3)	O4'	C26'	W'	177.5(3)
O5	C27	W	174.3(3)	O5'	C27'	W'	174.8(3)

Table 4: Torsion angles for **9.3b**.

A	B	C	D	Angle/°	A	B	C	D	Angle/°
W	P	N	C1	1.7(3)	W'	P'	N'	C1'	134.0(2)
P	N	C1	C2	109.9(3)	P'	N'	C1'	C2'	-100.0(3)
P	N	C1	C3	-126.1(3)	P'	N'	C1'	C3'	136.1(3)
P	C4	C5	C6	67.9(3)	P'	C4'	C5'	C6'	31.7(3)
P	C4	C5	C10	-107.2(3)	P'	C4'	C5'	C10'	-152.7(2)
P	C4	C11	C12	18.4(4)	P'	C4'	C11'	C12'	67.5(3)
P	C4	C11	C16	-163.4(2)	P'	C4'	C11'	C16'	-115.5(3)
P	C4	C17	C18	-138.9(3)	P'	C4'	C17'	C18'	-130.3(3)
P	C4	C17	C22	46.4(3)	P'	C4'	C17'	C22'	50.9(3)
C4	P	N	C1	-136.9(3)	C4'	P'	N'	C1'	-90.3(3)
C4	C5	C6	C7	-175.6(3)	C4'	C5'	C6'	C7'	175.8(3)
C4	C5	C10	C9	176.4(3)	C4'	C5'	C10'	C9'	-175.8(3)
C4	C11	C12	C13	177.6(3)	C4'	C11'	C12'	C13'	178.6(3)
C4	C11	C16	C15	-177.7(3)	C4'	C11'	C16'	C15'	-177.8(3)
C4	C17	C18	C19	-175.5(3)	C4'	C17'	C18'	C19'	-178.5(3)
C4	C17	C22	C21	177.4(3)	C4'	C17'	C22'	C21'	179.1(3)
C5	C4	C11	C12	-97.9(3)	C5'	C4'	C11'	C12'	-51.7(3)
C5	C4	C11	C16	80.3(3)	C5'	C4'	C11'	C16'	125.3(3)
C5	C4	C17	C18	-23.5(4)	C5'	C4'	C17'	C18'	-10.7(4)
C5	C4	C17	C22	161.7(3)	C5'	C4'	C17'	C22'	170.5(3)
C5	C6	C7	C8	-0.8(5)	C5'	C6'	C7'	C8'	0.1(5)
C6	C5	C10	C9	1.1(5)	C6'	C5'	C10'	C9'	0.0(5)
C6	C7	C8	C9	1.1(5)	C6'	C7'	C8'	C9'	-0.5(5)
C7	C8	C9	C10	-0.2(5)	C7'	C8'	C9'	C10'	0.7(5)
C8	C9	C10	C5	-0.9(5)	C8'	C9'	C10'	C5'	-0.4(5)
C10	C5	C6	C7	-0.3(5)	C10'	C5'	C6'	C7'	0.2(5)
C11	C4	C5	C6	-171.2(3)	C11'	C4'	C5'	C6'	150.1(3)
C11	C4	C5	C10	13.7(4)	C11'	C4'	C5'	C10'	-34.4(4)
C11	C4	C17	C18	99.8(3)	C11'	C4'	C17'	C18'	111.4(3)
C11	C4	C17	C22	-74.9(3)	C11'	C4'	C17'	C22'	-67.3(3)
C11	C12	C13	C14	0.3(6)	C11'	C12'	C13'	C14'	-1.1(5)
C12	C11	C16	C15	0.6(5)	C12'	C11'	C16'	C15'	-0.8(4)
C12	C13	C14	C15	0.0(6)	C12'	C13'	C14'	C15'	0.1(5)
C13	C14	C15	C16	0.0(5)	C13'	C14'	C15'	C16'	0.6(5)
C14	C15	C16	C11	-0.3(5)	C14'	C15'	C16'	C11'	-0.2(5)
C16	C11	C12	C13	-0.6(5)	C16'	C11'	C12'	C13'	1.4(4)
C17	C4	C5	C6	-49.6(4)	C17'	C4'	C5'	C6'	-86.4(3)
C17	C4	C5	C10	135.3(3)	C17'	C4'	C5'	C10'	89.1(3)
C17	C4	C11	C12	137.1(3)	C17'	C4'	C11'	C12'	-174.9(3)
C17	C4	C11	C16	-44.7(3)	C17'	C4'	C11'	C16'	2.1(4)
C17	C18	C19	C20	-1.4(5)	C17'	C18'	C19'	C20'	-0.6(5)
C18	C17	C22	C21	2.4(4)	C18'	C17'	C22'	C21'	0.3(4)
C18	C19	C20	C21	1.8(5)	C18'	C19'	C20'	C21'	0.4(5)
C19	C20	C21	C22	-0.1(5)	C19'	C20'	C21'	C22'	0.1(5)
C20	C21	C22	C17	-2.0(5)	C20'	C21'	C22'	C17'	-0.5(5)
C22	C17	C18	C19	-0.7(5)	C22'	C17'	C18'	C19'	0.2(4)

12.4 Pentacarbonyl[1,1-dimethylethylamino(triphenylmethyl)phosphane- κ P]tungsten(0) [9.3c]

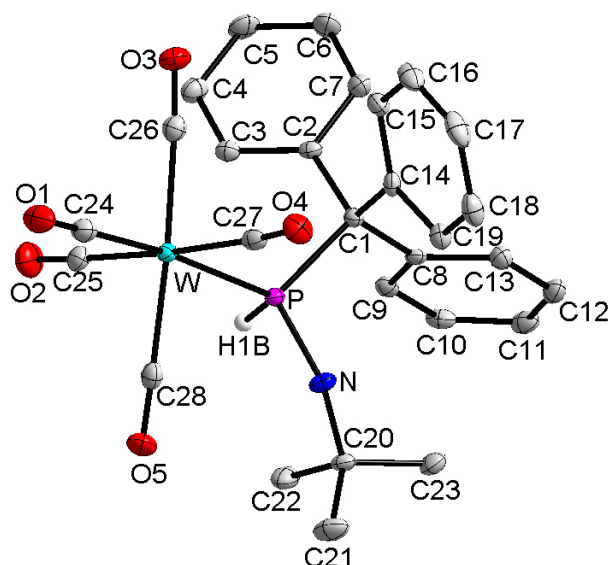


Table 1: Crystal data and structure refinement for **9.3c**.

Identification code	GSTR332, AKY-324 // GXray3182f
Crystal Habitus	pale yellow plate
Device Type	Bruker X8-KappaApexII
Empirical formula	C ₂₈ H ₂₆ NO ₅ PW
Moiety formula	C ₂₈ H ₂₆ N O ₅ P W
Formula weight	671.32
Temperature/K	100(2)
Crystal system	monoclinic
Space group	P2 ₁ /c
a/Å	9.5189(6)
b/Å	28.8723(17)
c/Å	10.3507(6)
α/°	90.00
β/°	110.8730(10)
γ/°	90.00
Volume/Å ³	2658.0(3)
Z	4
ρ _{calc} /cm ³	1.678
μ/mm ⁻¹	4.444
F(000)	1320.0
Crystal size/mm ³	0.11 × 0.10 × 0.04
Absorption correction	empirical
Tmin; Tmax	0.6406; 0.8423
Radiation	MoKα (λ = 0.71073)
2θ range for data collection/°	8.04 to 56°
Completeness to theta	0.990
Index ranges	-12 ≤ h ≤ 12, -38 ≤ k ≤ 36, -10 ≤ l ≤ 13
Reflections collected	17604
Independent reflections	6352 [R _{int} = 0.0257]
Data/restraints/parameters	6352/5/334

Goodness-of-fit on F^2	1.052
Final R indexes [$I \geq 2\sigma(I)$]	$R_1 = 0.0205$, $wR_2 = 0.0437$
Final R indexes [all data]	$R_1 = 0.0237$, $wR_2 = 0.0449$
Largest diff. peak/hole / $e \text{ \AA}^{-3}$	0.84/-0.56

Table 2: Bond lengths for **9.3c**.

Atom	Atom	Length/Å	Atom	Atom	Length/Å
C1	C14	1.529(3)	C16	C17	1.382(4)
C1	C8	1.541(3)	C17	C18	1.390(4)
C1	C2	1.543(3)	C18	C19	1.388(3)
C1	P	1.918(2)	C20	N	1.497(3)
C2	C3	1.392(3)	C20	C22	1.527(3)
C2	C7	1.400(3)	C20	C23	1.531(3)
C3	C4	1.395(3)	C20	C21	1.531(3)
C4	C5	1.386(3)	C24	O1	1.152(3)
C5	C6	1.391(4)	C24	W	2.003(2)
C6	C7	1.384(3)	C25	O2	1.138(3)
C8	C13	1.398(3)	C25	W	2.046(3)
C8	C9	1.403(3)	C26	O3	1.139(3)
C9	C10	1.389(3)	C26	W	2.054(3)
C10	C11	1.390(3)	C27	O4	1.134(3)
C11	C12	1.387(4)	C27	W	2.057(2)
C12	C13	1.393(3)	C28	O5	1.144(3)
C14	C15	1.395(3)	C28	W	2.046(3)
C14	C19	1.414(3)	N	P	1.670(2)
C15	C16	1.391(3)	P	W	2.5324(6)

Table 3: Bond angles for **9.3c**.

Atom	Atom	Atom	Angle/°	Atom	Atom	Atom	Angle/°
C14	C1	C8	114.15(18)	N	C20	C22	110.63(19)
C14	C1	C2	112.58(19)	N	C20	C23	111.83(19)
C8	C1	C2	104.77(17)	C22	C20	C23	110.0(2)
C14	C1	P	103.76(14)	N	C20	C21	105.83(19)
C8	C1	P	111.30(15)	C22	C20	C21	109.1(2)
C2	C1	P	110.43(14)	C23	C20	C21	109.3(2)
C3	C2	C7	117.4(2)	O1	C24	W	176.4(2)
C3	C2	C1	124.7(2)	O2	C25	W	178.2(2)
C7	C2	C1	117.7(2)	O3	C26	W	176.3(2)
C2	C3	C4	121.3(2)	O4	C27	W	174.2(2)
C5	C4	C3	120.2(2)	O5	C28	W	178.6(2)
C4	C5	C6	119.5(2)	C20	N	P	133.43(16)
C7	C6	C5	119.9(2)	N	P	C1	110.24(10)
C6	C7	C2	121.8(2)	N	P	W	110.99(7)
C13	C8	C9	117.9(2)	C1	P	W	119.08(7)
C13	C8	C1	123.5(2)	C24	W	C25	92.57(10)
C9	C8	C1	118.4(2)	C24	W	C28	87.87(10)
C10	C9	C8	121.2(2)	C25	W	C28	90.12(10)
C9	C10	C11	120.3(2)	C24	W	C26	89.30(10)
C12	C11	C10	118.9(2)	C25	W	C26	87.82(10)
C11	C12	C13	121.1(2)	C28	W	C26	176.42(9)

C12	C13	C8	120.5(2)	C24	W	C27	86.02(10)
C15	C14	C19	116.8(2)	C25	W	C27	176.56(9)
C15	C14	C1	123.3(2)	C28	W	C27	92.96(10)
C19	C14	C1	119.7(2)	C26	W	C27	89.03(10)
C16	C15	C14	121.8(2)	C24	W	P	173.38(7)
C17	C16	C15	120.4(2)	C25	W	P	90.04(7)
C16	C17	C18	119.3(2)	C28	W	P	86.04(7)
C19	C18	C17	120.3(2)	C26	W	P	96.88(7)
C18	C19	C14	121.3(2)	C27	W	P	91.70(7)

Table 4: Torsion angles for **9.3c**.

A	B	C	D	Angle/°	A	B	C	D	Angle/°
C14	C1	C2	C3	-121.8(2)	C21	C20	N	P	-142.1(2)
C8	C1	C2	C3	113.6(2)	C20	N	P	C1	-93.5(2)
P	C1	C2	C3	-6.3(3)	C20	N	P	W	132.4(2)
C14	C1	C2	C7	63.3(3)	C14	C1	P	N	-75.64(16)
C8	C1	C2	C7	-61.3(3)	C8	C1	P	N	47.56(18)
P	C1	C2	C7	178.73(17)	C2	C1	P	N	163.49(15)
C7	C2	C3	C4	-0.9(3)	C14	C1	P	W	54.29(16)
C1	C2	C3	C4	-175.8(2)	C8	C1	P	W	177.49(12)
C2	C3	C4	C5	0.0(4)	C2	C1	P	W	-66.58(16)
C3	C4	C5	C6	0.9(4)	O1	C24	W	C25	161(4)
C4	C5	C6	C7	-0.9(4)	O1	C24	W	C28	71(4)
C5	C6	C7	C2	0.0(4)	O1	C24	W	C26	-111(4)
C3	C2	C7	C6	0.9(4)	O1	C24	W	C27	-22(4)
C1	C2	C7	C6	176.2(2)	O1	C24	W	P	48(4)
C14	C1	C8	C13	-3.6(3)	O2	C25	W	C24	93(7)
C2	C1	C8	C13	120.0(2)	O2	C25	W	C28	-179(100)
P	C1	C8	C13	-120.7(2)	O2	C25	W	C26	3(7)
C14	C1	C8	C9	-177.7(2)	O2	C25	W	C27	27(8)
C2	C1	C8	C9	-54.1(2)	O2	C25	W	P	-93(7)
P	C1	C8	C9	65.2(2)	O5	C28	W	C24	63(10)
C13	C8	C9	C10	2.1(3)	O5	C28	W	C25	-29(10)
C1	C8	C9	C10	176.5(2)	O5	C28	W	C26	25(11)
C8	C9	C10	C11	0.2(4)	O5	C28	W	C27	149(10)
C9	C10	C11	C12	-1.7(4)	O5	C28	W	P	-119(10)
C10	C11	C12	C13	0.9(4)	O3	C26	W	C24	-12(3)
C11	C12	C13	C8	1.4(4)	O3	C26	W	C25	81(3)
C9	C8	C13	C12	-2.9(3)	O3	C26	W	C28	26(4)
C1	C8	C13	C12	-177.0(2)	O3	C26	W	C27	-98(3)
C8	C1	C14	C15	128.7(2)	O3	C26	W	P	171(3)
C2	C1	C14	C15	9.4(3)	O4	C27	W	C24	-18(2)
P	C1	C14	C15	-110.0(2)	O4	C27	W	C25	48(3)
C8	C1	C14	C19	-54.7(3)	O4	C27	W	C28	-106(2)
C2	C1	C14	C19	-174.00(19)	O4	C27	W	C26	71(2)
P	C1	C14	C19	66.6(2)	O4	C27	W	P	168(2)
C19	C14	C15	C16	0.2(3)	N	P	W	C24	-9.1(6)
C1	C14	C15	C16	176.9(2)	C1	P	W	C24	-138.7(6)
C14	C15	C16	C17	-0.7(4)	N	P	W	C25	-122.37(10)
C15	C16	C17	C18	1.0(4)	C1	P	W	C25	108.04(11)
C16	C17	C18	C19	-0.8(4)	N	P	W	C28	-32.25(10)

Index ranges	-12 ≤ h ≤ 12, -13 ≤ k ≤ 13, -15 ≤ l ≤ 15
Reflections collected	23636
Independent reflections	5598 [R _{int} = 0.0554, R _{sigma} = 0.0337]
Data/restraints/parameters	5598/0/292
Goodness-of-fit on F ²	1.052
Final R indexes [I ≥ 2σ(I)]	R ₁ = 0.0322, wR ₂ = 0.0842
Final R indexes [all data]	R ₁ = 0.0343, wR ₂ = 0.0862
Largest diff. peak/hole / e Å ⁻³	2.66/-2.40

Table 2: Bond lengths for 10.3.

Atom	Atom	Length/Å	Atom	Atom	Length/Å
W	P	2.4868(9)	O1	C20	1.142(5)
W	C23	2.035(4)	C8	C13	1.401(4)
W	C24	2.048(4)	C8	C9	1.397(5)
W	C22	2.062(4)	C14	C19	1.396(5)
W	C21	2.043(4)	C14	C15	1.403(5)
W	C20	2.012(4)	C2	C7	1.401(5)
P	Cl	2.0596(11)	C24	O5	1.134(5)
P	C1	1.917(3)	C22	O3	1.129(5)
O4	C23	1.150(5)	C7	C6	1.394(5)
O2	C21	1.145(6)	C13	C12	1.397(5)
C11	C12	1.388(5)	C9	C10	1.386(5)
C11	C10	1.388(5)	C19	C18	1.396(5)
C1	C8	1.546(4)	C15	C16	1.392(5)
C1	C14	1.531(5)	C4	C5	1.377(6)
C1	C2	1.539(4)	C6	C5	1.391(6)
C3	C2	1.386(5)	C18	C17	1.380(6)
C3	C4	1.402(5)	C16	C17	1.391(6)

Table 3: Bond angles for 10.3.

Atom	Atom	Atom	Angle/°	Atom	Atom	Atom	Angle/°
C23	W	P	89.72(11)	C13	C8	C1	120.8(3)
C23	W	C24	89.98(15)	C9	C8	C1	121.0(3)
C23	W	C22	91.05(16)	C9	C8	C13	118.1(3)
C23	W	C21	178.59(12)	C19	C14	C1	122.5(3)
C24	W	P	85.28(11)	C19	C14	C15	117.9(3)
C24	W	C22	178.24(13)	C15	C14	C1	119.6(3)
C22	W	P	96.14(11)	C3	C2	C1	122.1(3)
C21	W	P	89.06(12)	C3	C2	C7	118.4(3)
C21	W	C24	89.22(16)	C7	C2	C1	119.4(3)
C21	W	C22	89.77(17)	O5	C24	W	178.5(4)
C20	W	P	174.11(11)	O3	C22	W	176.7(4)
C20	W	C23	89.34(16)	O2	C21	W	178.8(4)
C20	W	C24	88.91(16)	C6	C7	C2	120.8(4)
C20	W	C22	89.69(16)	C12	C13	C8	121.0(3)
C20	W	C21	91.80(17)	C11	C12	C13	119.8(3)
Cl	P	W	107.55(5)	C10	C9	C8	120.8(3)
C1	P	W	128.54(10)	C9	C10	C11	120.6(3)
C1	P	Cl	104.19(10)	C14	C19	C18	120.6(4)
O4	C23	W	179.3(4)	C16	C15	C14	121.1(3)

C10	C11	C12	119.6(3)	C5	C4	C3	120.3(4)
C8	C1	P	105.6(2)	C5	C6	C7	119.9(4)
C14	C1	P	107.1(2)	C4	C5	C6	119.9(4)
C14	C1	C8	111.7(3)	O1	C20	W	178.5(4)
C14	C1	C2	112.7(3)	C17	C18	C19	120.9(4)
C2	C1	P	109.5(2)	C17	C16	C15	120.2(4)
C2	C1	C8	110.1(3)	C18	C17	C16	119.3(4)
C2	C3	C4	120.7(4)				

Table 4: Torsion angles for **10.3**.

A	B	C	D	Angle/°	A	B	C	D	Angle/°
P	C1	C8	C13	47.1(4)	C14	C1	C2	C3	-9.1(4)
P	C1	C8	C9	-136.3(3)	C14	C1	C2	C7	174.1(3)
P	C1	C14	C19	-126.3(3)	C14	C19	C18	C17	0.4(6)
P	C1	C14	C15	54.1(4)	C14	C15	C16	C17	-0.5(6)
P	C1	C2	C3	-128.1(3)	C2	C1	C8	C13	165.1(3)
P	C1	C2	C7	55.1(4)	C2	C1	C8	C9	-18.2(4)
C1	C8	C13	C12	178.1(3)	C2	C1	C14	C19	113.3(4)
C1	C8	C9	C10	-176.8(3)	C2	C1	C14	C15	-66.2(4)
C1	C14	C19	C18	179.5(3)	C2	C3	C4	C5	0.2(6)
C1	C14	C15	C16	-179.5(3)	C2	C7	C6	C5	-0.5(6)
C1	C2	C7	C6	178.1(3)	C7	C6	C5	C4	-0.4(6)
C3	C2	C7	C6	1.2(5)	C13	C8	C9	C10	-0.1(5)
C3	C4	C5	C6	0.5(6)	C12	C11	C10	C9	1.0(5)
C8	C1	C14	C19	-11.2(4)	C9	C8	C13	C12	1.4(5)
C8	C1	C14	C15	169.3(3)	C10	C11	C12	C13	0.3(5)
C8	C1	C2	C3	116.2(4)	C19	C14	C15	C16	1.0(5)
C8	C1	C2	C7	-60.5(4)	C19	C18	C17	C16	0.1(6)
C8	C13	C12	C11	-1.5(6)	C15	C14	C19	C18	-1.0(5)
C8	C9	C10	C11	-1.1(5)	C15	C16	C17	C18	-0.1(7)
C14	C1	C8	C13	-68.9(4)	C4	C3	C2	C1	-177.8(3)
C14	C1	C8	C9	107.7(3)	C4	C3	C2	C7	-1.0(5)

12.6 Pentacarbonyl[1-(1,2,3,4,5-pentamethylcyclopenta-2,4-dien-1-yl)-3,4-diphenyl-1*H*-phosphet-2-on- κ P]tungsten(0) [14.2]

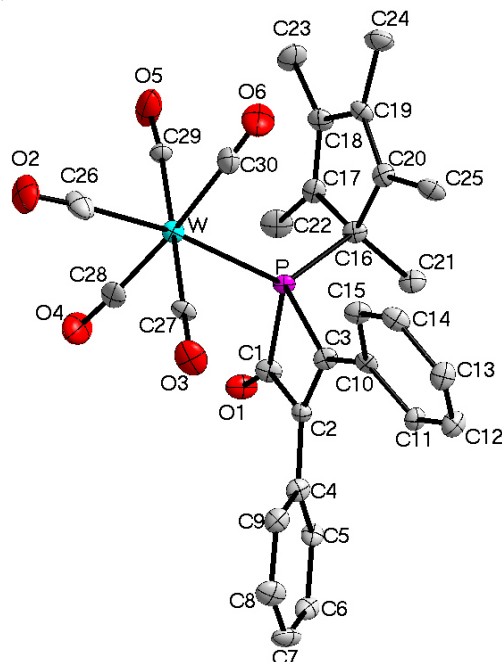


Table 1: Crystal data and structure refinement for **14.2**.

Identification code	GSTR466, AKY-536 // GXraycu_4526f
Crystal Habitus	clear yellow plate
Device Type	Bruker X8-KappaApexII
Empirical formula	C ₃₀ H ₂₅ O ₆ PW
Moiety formula	C ₃₀ H ₂₅ O ₆ P W
Formula weight	696.32
Temperature/K	122.99
Crystal system	triclinic
Space group	P $\bar{1}$
a/Å	8.8513(3)
b/Å	10.7052(4)
c/Å	14.8284(6)
α /°	92.8570(16)
β /°	99.0783(15)
γ /°	91.9166(15)
Volume/Å ³	1384.52(9)
Z	2
$\rho_{\text{calc}}/\text{cm}^3$	1.670
μ/mm^{-1}	8.626
F(000)	684.0
Crystal size/mm ³	0.3 × 0.2 × 0.05
Absorption correction	empirical
Tmin; Tmax	0.2129; 0.7536
Radiation	CuK α (λ = 1.54178)
2 θ range for data collection/°	6.046 to 135.482°
Completeness to theta	0.999
Index ranges	-10 ≤ h ≤ 9, -12 ≤ k ≤ 12, -17 ≤ l ≤ 17
Reflections collected	33677
Independent reflections	5024 [R _{int} = 0.0730, R _{sigma} = 0.0417]
Data/restraints/parameters	5024/54/348

Goodness-of-fit on F^2	1.067
Final R indexes [$I > 2\sigma(I)$]	$R_1 = 0.0671$, $wR_2 = 0.1829$
Final R indexes [all data]	$R_1 = 0.0685$, $wR_2 = 0.1853$
Largest diff. peak/hole / $e \text{ \AA}^{-3}$	5.06/-4.00

Table 2: Bond lengths for 14.2.

Atom	Atom	Length/Å	Atom	Atom	Length/Å
W	P	2.5004(17)	C5	C6	1.390(10)
W	C26	2.011(9)	C6	C7	1.392(11)
W	C27	2.010(7)	C7	C8	1.392(11)
W	C28	2.041(10)	C8	C9	1.378(10)
W	C29	2.020(8)	C10	C11	1.408(9)
W	C30	2.051(9)	C10	C15	1.386(10)
P	C1	1.905(7)	C11	C12	1.382(10)
P	C3	1.857(6)	C12	C13	1.369(11)
P	C16	1.877(7)	C13	C14	1.391(10)
O1	C1	1.201(8)	C14	C15	1.407(10)
O2	C26	1.146(10)	C16	C17	1.517(9)
O3	C27	1.160(10)	C16	C20	1.513(9)
O4	C28	1.149(12)	C16	C21	1.535(9)
O5	C29	1.154(11)	C17	C18	1.371(10)
O6	C30	1.146(12)	C17	C22	1.478(10)
C1	C2	1.480(9)	C18	C19	1.466(10)
C2	C3	1.362(9)	C18	C23	1.492(10)
C2	C4	1.468(9)	C19	C20	1.343(10)
C3	C10	1.465(9)	C19	C24	1.506(10)
C4	C5	1.397(9)	C20	C25	1.506(10)
C4	C9	1.399(9)			

Table 3: Bond angles for 14.2.

Atom	Atom	Atom	Angle/°	Atom	Atom	Atom	Angle/°
C26	W	P	171.0(2)	C6	C7	C8	120.0(6)
C26	W	C28	85.5(3)	C9	C8	C7	120.0(7)
C26	W	C29	90.6(3)	C8	C9	C4	120.8(7)
C26	W	C30	92.1(3)	C11	C10	C3	119.6(6)
C27	W	P	83.6(2)	C15	C10	C3	121.5(6)
C27	W	C26	88.9(3)	C15	C10	C11	118.9(6)
C27	W	C28	91.6(3)	C12	C11	C10	120.4(7)
C27	W	C29	179.0(2)	C13	C12	C11	120.5(7)
C27	W	C30	92.9(3)	C12	C13	C14	120.5(7)
C28	W	P	89.7(2)	C13	C14	C15	119.4(7)
C28	W	C30	174.9(3)	C10	C15	C14	120.4(7)
C29	W	P	96.8(2)	C17	C16	P	104.2(4)
C29	W	C28	87.5(3)	C17	C16	C21	113.8(6)
C29	W	C30	88.0(3)	C20	C16	P	108.8(4)
C30	W	P	93.3(2)	C20	C16	C17	104.4(5)
C1	P	W	113.9(2)	C20	C16	C21	113.8(6)
C3	P	W	116.6(2)	C21	C16	P	111.2(4)
C3	P	C1	70.9(3)	C18	C17	C16	107.5(6)
C3	P	C16	109.8(3)	C18	C17	C22	127.9(6)

C16	P	W	124.8(2)	C22	C17	C16	124.6(6)
C16	P	C1	108.1(3)	C17	C18	C19	109.3(6)
O1	C1	P	135.6(5)	C17	C18	C23	128.4(7)
O1	C1	C2	133.3(6)	C19	C18	C23	122.4(7)
C2	C1	P	91.1(4)	C18	C19	C24	123.7(6)
C3	C2	C1	100.3(6)	C20	C19	C18	110.8(6)
C3	C2	C4	133.3(6)	C20	C19	C24	125.5(7)
C4	C2	C1	126.0(6)	C19	C20	C16	108.0(6)
C2	C3	P	97.0(4)	C19	C20	C25	127.6(7)
C2	C3	C10	129.3(6)	C25	C20	C16	124.4(6)
C10	C3	P	133.5(5)	O2	C26	W	176.1(7)
C5	C4	C2	120.3(6)	O3	C27	W	177.4(7)
C5	C4	C9	118.9(6)	O4	C28	W	176.8(8)
C9	C4	C2	120.7(6)	O5	C29	W	174.7(7)
C6	C5	C4	120.4(6)	O6	C30	W	178.7(8)
C5	C6	C7	119.9(7)				

Table 4: Torsion angles for **14.2**.

A	B	C	D	Angle/°	A	B	C	D	Angle/°
W	P	C3	C2	102.3(4)	C4	C2	C3	C10	9.9(12)
W	P	C3	C10	-73.3(7)	C4	C5	C6	C7	0.9(10)
W	P	C16	C17	-52.3(5)	C5	C4	C9	C8	0.6(10)
W	P	C16	C20	58.6(5)	C5	C6	C7	C8	0.0(11)
W	P	C16	C21	-175.3(4)	C6	C7	C8	C9	-0.7(11)
P	C1	C2	C3	-6.6(5)	C7	C8	C9	C4	0.4(11)
P	C1	C2	C4	167.0(6)	C9	C4	C5	C6	-1.2(10)
P	C3	C10	C11	-153.9(5)	C10	C11	C12	C13	2.7(11)
P	C3	C10	C15	26.8(10)	C11	C10	C15	C14	-1.5(10)
P	C16	C17	C18	115.0(5)	C11	C12	C13	C14	-3.4(12)
P	C16	C17	C22	-66.4(7)	C12	C13	C14	C15	1.6(11)
P	C16	C20	C19	-110.4(5)	C13	C14	C15	C10	0.9(11)
P	C16	C20	C25	72.9(7)	C15	C10	C11	C12	-0.2(10)
O1	C1	C2	C3	175.4(8)	C16	P	C3	C2	-108.5(5)
O1	C1	C2	C4	-11.0(12)	C16	P	C3	C10	75.9(7)
C1	P	C3	C2	-5.5(4)	C16	C17	C18	C19	-1.9(8)
C1	P	C3	C10	178.9(7)	C16	C17	C18	C23	177.9(7)
C1	P	C16	C17	85.8(5)	C17	C16	C20	C19	0.4(7)
C1	P	C16	C20	-163.2(4)	C17	C16	C20	C25	-176.3(6)
C1	P	C16	C21	-37.1(5)	C17	C18	C19	C20	2.2(8)
C1	C2	C3	P	6.8(5)	C17	C18	C19	C24	179.9(6)
C1	C2	C3	C10	-177.3(7)	C18	C19	C20	C16	-1.5(8)
C1	C2	C4	C5	47.7(10)	C18	C19	C20	C25	175.0(7)
C1	C2	C4	C9	-129.0(7)	C20	C16	C17	C18	1.0(7)
C2	C3	C10	C11	31.7(10)	C20	C16	C17	C22	179.5(6)
C2	C3	C10	C15	-147.6(7)	C21	C16	C17	C18	-123.7(6)
C2	C4	C5	C6	-178.0(6)	C21	C16	C17	C22	54.8(9)
C2	C4	C9	C8	177.4(6)	C21	C16	C20	C19	125.0(6)
C3	P	C16	C17	161.5(4)	C21	C16	C20	C25	-51.6(9)
C3	P	C16	C20	-87.6(5)	C22	C17	C18	C19	179.7(7)
C3	P	C16	C21	38.5(5)	C22	C17	C18	C23	-0.5(13)
C3	C2	C4	C5	-141.0(8)	C23	C18	C19	C20	-177.6(7)

C3	C2	C4	C9	42.2(11)	C23	C18	C19	C24	0.0(11)
C3	C10	C11	C12	-179.5(7)	C24	C19	C20	C16	-179.1(6)
C3	C10	C15	C14	177.7(6)	C24	C19	C20	C25	-2.6(11)
C4	C2	C3	P	-166.0(7)					

12.7 Pentacarbonyl{2-[bis(trimethylsilyl)methyl]-3-phenyl-1,2-oxaphosphetane- κ P}tungsten(0) [16.1]

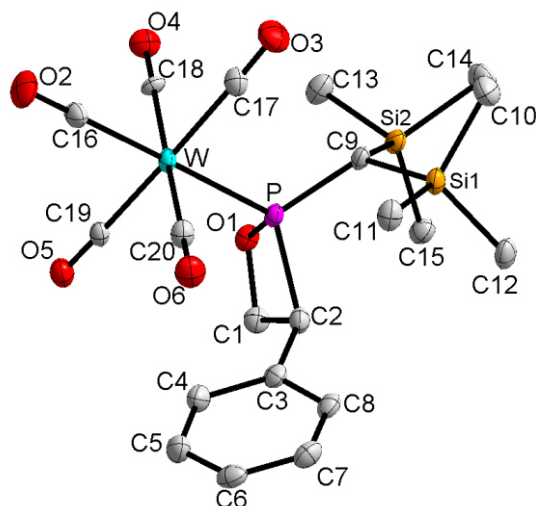


Table 1: Crystal data and structure refinement for **16.1**.

Identification code	GSTR314, AKY-276 // GXray2987f
Crystal Habitus	colourless plate
Device Type	Bruker X8-KappaApexII
Empirical formula	C ₂₀ H ₂₇ O ₆ PSi ₂ W
Moiety formula	C ₂₀ H ₂₇ O ₆ P Si ₂ W
Formula weight	634.42
Temperature/K	100(2)
Crystal system	triclinic
Space group	P $\bar{1}$
a/Å	9.1581(9)
b/Å	11.1649(9)
c/Å	13.6235(13)
α /°	67.265(4)
β /°	79.233(2)
γ /°	75.176(2)
Volume/Å ³	1235.9(2)
Z	2
ρ_{calc} /cm ³	1.705
μ /mm ⁻¹	4.866
F(000)	624.0
Crystal size/mm ³	0.40 × 0.18 × 0.10
Absorption correction	empirical
Tmin; Tmax	0.2463; 0.6418
Radiation	MoK α (λ = 0.71073)
2 θ range for data collection/°	5.32 to 50.5°

Completeness to theta	0.957
Index ranges	-10 ≤ h ≤ 10, -13 ≤ k ≤ 11, -16 ≤ l ≤ 16
Reflections collected	7378
Independent reflections	4271 [R _{int} = 0.0290]
Data/restraints/parameters	4271/0/277
Goodness-of-fit on F ²	1.065
Final R indexes [I ≥ 2σ (I)]	R ₁ = 0.0286, wR ₂ = 0.0740
Final R indexes [all data]	R ₁ = 0.0299, wR ₂ = 0.0749
Largest diff. peak/hole / e Å ⁻³	2.90/-1.70

Table 2: Bond lengths for **16.1**.

Atom	Atom	Length/Å	Atom	Atom	Length/Å
W	C16	2.020(5)	Si2	C13	1.867(5)
W	C18	2.034(4)	Si2	C9	1.912(5)
W	C17	2.037(5)	O1	C1	1.458(5)
W	C19	2.040(4)	O2	C16	1.145(6)
W	C20	2.070(5)	O3	C17	1.135(6)
W	P	2.4749(11)	O4	C18	1.141(6)
P	O1	1.677(3)	O5	C19	1.134(6)
P	C9	1.820(4)	O6	C20	1.132(6)
P	C2	1.894(5)	C1	C2	1.537(6)
P	C1	2.322(5)	C2	C3	1.501(6)
Si1	C10	1.866(5)	C3	C8	1.389(6)
Si1	C12	1.870(5)	C3	C4	1.414(6)
Si1	C11	1.879(5)	C4	C5	1.383(7)
Si1	C9	1.906(4)	C5	C6	1.382(7)
Si2	C15	1.857(5)	C6	C7	1.394(7)
Si2	C14	1.866(5)	C7	C8	1.389(7)

Table 3: Bond angles for **16.1**.

Atom	Atom	Atom	Angle/°	Atom	Atom	Atom	Angle/°
C16	W	C18	90.24(19)	C11	Si1	C9	110.86(19)
C16	W	C17	89.80(19)	C15	Si2	C14	106.9(2)
C18	W	C17	88.45(18)	C15	Si2	C13	111.0(2)
C16	W	C19	91.35(18)	C14	Si2	C13	107.7(2)
C18	W	C19	87.18(17)	C15	Si2	C9	113.1(2)
C17	W	C19	175.48(17)	C14	Si2	C9	109.6(2)
C16	W	C20	89.22(19)	C13	Si2	C9	108.4(2)
C18	W	C20	178.59(16)	C1	O1	P	95.3(3)
C17	W	C20	90.24(19)	O1	C1	C2	99.2(3)
C19	W	C20	94.15(18)	O1	C1	P	45.97(19)
C16	W	P	176.14(15)	C2	C1	P	54.3(2)
C18	W	P	86.91(12)	C3	C2	C1	118.6(4)
C17	W	P	92.73(13)	C3	C2	P	123.1(3)
C19	W	P	85.89(12)	C1	C2	P	84.5(3)
C20	W	P	93.68(13)	C8	C3	C4	117.9(4)

O1	P	C9	107.28(18)	C8	C3	C2	120.1(4)
O1	P	C2	79.20(18)	C4	C3	C2	122.0(4)
C9	P	C2	109.76(19)	C5	C4	C3	120.3(4)
O1	P	C1	38.70(16)	C6	C5	C4	121.2(4)
C9	P	C1	120.16(19)	C5	C6	C7	119.1(4)
C2	P	C1	41.23(18)	C8	C7	C6	120.0(4)
O1	P	W	111.47(11)	C3	C8	C7	121.4(4)
C9	P	W	116.91(15)	P	C9	Si1	114.1(2)
C2	P	W	124.78(14)	P	C9	Si2	114.8(2)
C1	P	W	121.41(12)	Si1	C9	Si2	117.0(2)
C10	Si1	C12	109.8(2)	O2	C16	W	179.3(5)
C10	Si1	C11	106.1(2)	O3	C17	W	177.6(4)
C12	Si1	C11	110.0(2)	O4	C18	W	179.1(4)
C10	Si1	C9	108.1(2)	O5	C19	W	176.9(4)
C12	Si1	C9	111.7(2)	O6	C20	W	177.0(5)

Table 4: Torsion angles for **16.1**.

A	B	C	D	Angle/°	A	B	C	D	Angle/°
C16	W	P	O1	-9.8(19)	C4	C3	C8	C7	-1.8(7)
C18	W	P	O1	-52.50(17)	C2	C3	C8	C7	177.1(4)
C17	W	P	O1	-140.79(18)	C6	C7	C8	C3	1.8(7)
C19	W	P	O1	34.89(17)	O1	P	C9	Si1	-139.7(2)
C20	W	P	O1	128.79(18)	C2	P	C9	Si1	-55.3(3)
C16	W	P	C9	114.1(19)	C1	P	C9	Si1	-99.6(3)
C18	W	P	C9	71.4(2)	W	P	C9	Si1	94.3(2)
C17	W	P	C9	-16.9(2)	O1	P	C9	Si2	-0.7(3)
C19	W	P	C9	158.8(2)	C2	P	C9	Si2	83.7(3)
C20	W	P	C9	-107.3(2)	C1	P	C9	Si2	39.4(3)
C16	W	P	C2	-101.4(19)	W	P	C9	Si2	-126.74(18)
C18	W	P	C2	-144.1(2)	C10	Si1	C9	P	-146.1(3)
C17	W	P	C2	127.6(2)	C12	Si1	C9	P	92.9(3)
C19	W	P	C2	-56.7(2)	C11	Si1	C9	P	-30.2(3)
C20	W	P	C2	37.2(2)	C10	Si1	C9	Si2	75.8(3)
C16	W	P	C1	-51.9(19)	C12	Si1	C9	Si2	-45.1(3)
C18	W	P	C1	-94.56(19)	C11	Si1	C9	Si2	-168.2(2)
C17	W	P	C1	177.1(2)	C15	Si2	C9	P	-62.4(3)
C19	W	P	C1	-7.18(18)	C14	Si2	C9	P	178.4(2)
C20	W	P	C1	86.72(19)	C13	Si2	C9	P	61.1(3)
C9	P	O1	C1	116.9(3)	C15	Si2	C9	Si1	75.3(3)
C2	P	O1	C1	9.4(3)	C14	Si2	C9	Si1	-43.9(3)
W	P	O1	C1	-113.9(2)	C13	Si2	C9	Si1	-161.2(3)
P	O1	C1	C2	-11.6(3)	C18	W	C16	O2	32(32)
C9	P	C1	O1	-79.9(3)	C17	W	C16	O2	121(32)
C2	P	C1	O1	-165.9(4)	C19	W	C16	O2	-55(32)
W	P	C1	O1	85.6(2)	C20	W	C16	O2	-149(32)
O1	P	C1	C2	165.9(4)	P	W	C16	O2	-10(33)
C9	P	C1	C2	86.0(3)	C16	W	C17	O3	-86(10)

W	P	C1	C2	-108.5(2)	C18	W	C17	O3	4(10)
O1	C1	C2	C3	135.2(4)	C19	W	C17	O3	18(12)
P	C1	C2	C3	124.9(4)	C20	W	C17	O3	-176(100)
O1	C1	C2	P	10.2(3)	P	W	C17	O3	91(10)
O1	P	C2	C3	-129.6(4)	C16	W	C18	O4	21(26)
C9	P	C2	C3	125.7(4)	C17	W	C18	O4	-69(26)
C1	P	C2	C3	-120.7(5)	C19	W	C18	O4	112(26)
W	P	C2	C3	-20.9(4)	C20	W	C18	O4	-47(29)
O1	P	C2	C1	-8.9(2)	P	W	C18	O4	-162(26)
C9	P	C2	C1	-113.6(3)	C16	W	C19	O5	102(7)
W	P	C2	C1	99.8(3)	C18	W	C19	O5	12(7)
C1	C2	C3	C8	148.0(4)	C17	W	C19	O5	-3(9)
P	C2	C3	C8	-109.0(4)	C20	W	C19	O5	-169(7)
C1	C2	C3	C4	-33.1(6)	P	W	C19	O5	-75(7)
P	C2	C3	C4	69.9(5)	C16	W	C20	O6	-43(7)
C8	C3	C4	C5	-0.1(7)	C18	W	C20	O6	25(12)
C2	C3	C4	C5	-178.9(5)	C17	W	C20	O6	47(7)
C3	C4	C5	C6	2.1(8)	C19	W	C20	O6	-135(7)
C4	C5	C6	C7	-2.2(8)	P	W	C20	O6	139(7)
C5	C6	C7	C8	0.3(7)					

12.8 Pentacarbonyl{4-methyl-2-[bis(trimethylsilyl)methyl]-1,2-oxaphosphetane- κ P}tungsten(0) [21.1a_W]

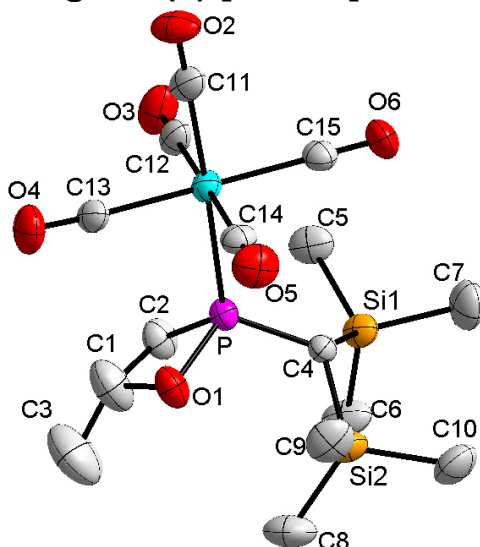


Table 1: Crystal data and structure refinement for **21.1a_W**.

Identification code	GSTR321, AKY-301 // GXray3087
Crystal Habitus	colourless plate
Device Type	Nonius KappaCCD
Empirical formula	C ₁₅ H ₂₅ O ₆ PSi ₂ W
Moiety formula	C ₁₅ H ₂₅ O ₆ P Si ₂ W
Formula weight	572.35
Temperature/K	123(2)
Crystal system	orthorhombic
Space group	P2 ₁ 2 ₁ 2 ₁

a/Å	10.5131(4)
b/Å	13.8027(5)
c/Å	15.4963(5)
α /°	90.00
β /°	90.00
γ /°	90.00
Volume/Å ³	2248.66(14)
Z	4
$\rho_{\text{calc}}/\text{cm}^3$	1.691
μ/mm^{-1}	5.339
F(000)	1120.0
Crystal size/mm ³	0.40 × 0.20 × 0.06
Absorption correction	Multi-Scan
Tmin; Tmax	0.2239; 0.7400
Radiation	MoK α (λ = 0.71073)
2 θ range for data collection/°	4.88 to 55.98°
Completeness to theta	0.995
Index ranges	-13 ≤ h ≤ 12, -17 ≤ k ≤ 18, -20 ≤ l ≤ 20
Reflections collected	18819
Independent reflections	5329 [R _{int} = 0.0632]
Data/restraints/parameters	5329/31/234
Goodness-of-fit on F ²	0.978
Final R indexes [$I \geq 2\sigma(I)$]	R ₁ = 0.0338, wR ₂ = 0.0619
Final R indexes [all data]	R ₁ = 0.0474, wR ₂ = 0.0654
Largest diff. peak/hole / e Å ⁻³	1.35/-1.87
Flack parameter	0.467(8)

Table 2: Bond lengths for 21.1aw.

Atom	Atom	Length/Å	Atom	Atom	Length/Å
C1	C3	1.375(9)	C10	Si2	1.878(7)
C1	O1	1.463(8)	C11	O2	1.144(6)
C1	C2	1.545(9)	C11	W	2.018(6)
C1	P	2.298(7)	C12	O3	1.135(7)
C2	P	1.827(5)	C12	W	2.047(6)
C4	P	1.800(5)	C13	O4	1.134(7)
C4	Si2	1.905(5)	C13	W	2.036(6)
C4	Si1	1.913(5)	C14	O5	1.134(7)
C5	Si1	1.859(6)	C14	W	2.034(6)
C6	Si1	1.863(6)	C15	O6	1.129(7)
C7	Si1	1.877(6)	C15	W	2.044(6)
C8	Si2	1.865(6)	O1	P	1.672(4)
C9	Si2	1.873(7)	P	W	2.4846(14)

Table 3: Bond angles for 21.1aw.

Atom	Atom	Atom	Angle/°	Atom	Atom	Atom	Angle/°
C3	C1	O1	117.7(7)	C5	Si1	C7	106.2(3)
C3	C1	C2	122.3(7)	C6	Si1	C7	110.1(3)
O1	C1	C2	96.5(5)	C5	Si1	C4	111.1(2)
C3	C1	P	150.8(7)	C6	Si1	C4	112.1(2)
O1	C1	P	46.6(2)	C7	Si1	C4	108.3(3)

C2	C1	P	52.4(3)	C8	Si2	C9	108.8(3)
C1	C2	P	85.5(4)	C8	Si2	C10	110.1(3)
P	C4	Si2	115.9(3)	C9	Si2	C10	107.8(3)
P	C4	Si1	113.9(3)	C8	Si2	C4	114.0(3)
Si2	C4	Si1	116.5(3)	C9	Si2	C4	108.3(3)
O2	C11	W	178.2(4)	C10	Si2	C4	107.5(3)
O3	C12	W	179.1(6)	C11	W	C14	91.2(2)
O4	C13	W	176.9(5)	C11	W	C13	88.8(2)
O5	C14	W	177.2(5)	C14	W	C13	89.2(2)
O6	C15	W	178.6(6)	C11	W	C15	91.4(2)
C1	O1	P	94.0(3)	C14	W	C15	91.5(3)
O1	P	C4	108.4(2)	C13	W	C15	179.3(3)
O1	P	C2	79.7(2)	C11	W	C12	91.5(2)
C4	P	C2	111.5(3)	C14	W	C12	177.3(3)
O1	P	C1	39.4(2)	C13	W	C12	91.0(2)
C4	P	C1	125.6(3)	C15	W	C12	88.3(2)
C2	P	C1	42.1(3)	C11	W	P	177.48(16)
O1	P	W	113.73(16)	C14	W	P	88.23(17)
C4	P	W	118.00(17)	C13	W	P	88.79(18)
C2	P	W	118.9(2)	C15	W	P	91.04(17)
C1	P	W	115.9(2)	C12	W	P	89.10(18)
C5	Si1	C6	109.1(3)				

Table 4: Torsion angles for **21.1aw**.

A	B	C	D	Angle^o	A	B	C	D	Angle^o
C3	C1	C2	P	-144.7(8)	O2	C11	W	C12	138(19)
O1	C1	C2	P	-15.9(5)	O2	C11	W	P	34(23)
C3	C1	O1	P	149.3(7)	O5	C14	W	C11	5(11)
C2	C1	O1	P	17.4(5)	O5	C14	W	C13	-84(11)
C1	O1	P	C4	-124.2(5)	O5	C14	W	C15	96(11)
C1	O1	P	C2	-14.8(5)	O5	C14	W	C12	-178(100)
C1	O1	P	W	102.4(4)	O5	C14	W	P	-173(11)
Si2	C4	P	O1	-10.1(4)	O4	C13	W	C11	34(11)
Si1	C4	P	O1	129.1(3)	O4	C13	W	C14	125(11)
Si2	C4	P	C2	-96.0(3)	O4	C13	W	C15	-70(26)
Si1	C4	P	C2	43.2(3)	O4	C13	W	C12	-58(11)
Si2	C4	P	C1	-50.3(4)	O4	C13	W	P	-147(11)
Si1	C4	P	C1	88.9(3)	O6	C15	W	C11	-124(21)
Si2	C4	P	W	121.0(2)	O6	C15	W	C14	145(21)
Si1	C4	P	W	-99.8(3)	O6	C15	W	C13	-19(36)
C1	C2	P	O1	14.0(4)	O6	C15	W	C12	-32(21)
C1	C2	P	C4	119.8(4)	O6	C15	W	P	57(21)
C1	C2	P	W	-97.6(4)	O3	C12	W	C11	14(38)
C3	C1	P	O1	-67.6(12)	O3	C12	W	C14	-164(35)
C2	C1	P	O1	-158.0(7)	O3	C12	W	C13	103(38)
C3	C1	P	C4	7.3(14)	O3	C12	W	C15	-78(38)
O1	C1	P	C4	74.9(5)	O3	C12	W	P	-169(100)
C2	C1	P	C4	-83.1(5)	O1	P	W	C11	-21(4)
C3	C1	P	C2	90.4(14)	C4	P	W	C11	-150(4)
O1	C1	P	C2	158.0(7)	C2	P	W	C11	70(4)
C3	C1	P	W	-164.2(12)	C1	P	W	C11	22(4)

O1	C1	P	W	-96.6(4)	O1	P	W	C14	55.2(2)
C2	C1	P	W	105.4(4)	C4	P	W	C14	-73.4(3)
P	C4	Si1	C5	26.9(4)	C2	P	W	C14	146.4(3)
Si2	C4	Si1	C5	165.9(3)	C1	P	W	C14	98.8(3)
P	C4	Si1	C6	-95.4(3)	O1	P	W	C13	-34.0(2)
Si2	C4	Si1	C6	43.6(4)	C4	P	W	C13	-162.6(2)
P	C4	Si1	C7	143.1(3)	C2	P	W	C13	57.1(3)
Si2	C4	Si1	C7	-77.9(4)	C1	P	W	C13	9.5(3)
P	C4	Si2	C8	63.6(4)	O1	P	W	C15	146.7(2)
Si1	C4	Si2	C8	-74.6(4)	C4	P	W	C15	18.1(2)
P	C4	Si2	C9	-57.7(4)	C2	P	W	C15	-122.2(3)
Si1	C4	Si2	C9	164.1(3)	C1	P	W	C15	-169.8(3)
P	C4	Si2	C10	-174.0(3)	O1	P	W	C12	-125.0(2)
Si1	C4	Si2	C10	47.8(4)	C4	P	W	C12	106.4(2)
O2	C11	W	C14	-42(19)	C2	P	W	C12	-33.8(3)
O2	C11	W	C13	47(19)	C1	P	W	C12	-81.5(3)
O2	C11	W	C15	-134(19)					

12.9 Pentacarbonyl{4-methyl-2-[bis(trimethylsilyl)methyl]-1,2-oxaphosphetane- κP }molybdenum(0) [21.1a_{Mo}]

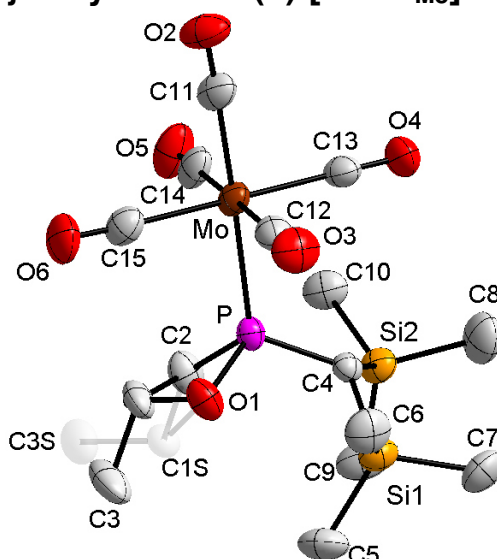


Table 1: Crystal data and structure refinement for **21.1a_{Mo}**.

Identification code	GSTR370, 3621
Empirical formula	C ₁₅ H ₂₅ MoO ₆ PSi ₂
Formula weight	484.44
Temperature/K	123.15
Crystal system	orthorhombic
Space group	P2 ₁ 2 ₁ 2 ₁
a/Å	10.5587(3)
b/Å	13.8356(5)
c/Å	15.4608(4)
α/°	90
β/°	90
γ/°	90
Volume/Å ³	2258.61(12)
Z	4

$\rho_{\text{calc}}/\text{cm}^3$	1.425
μ/mm^{-1}	0.782
F(000)	992.0
Crystal size/ mm^3	0.24 × 0.16 × 0.08
Radiation	MoK α ($\lambda = 0.71073$)
2 θ range for data collection/ $^\circ$	5.27 to 55.998
Index ranges	-13 ≤ h ≤ 13, -18 ≤ k ≤ 18, -20 ≤ l ≤ 20
Reflections collected	31032
Independent reflections	5424 [$R_{\text{int}} = 0.0529$, $R_{\text{sigma}} = 0.0457$]
Data/restraints/parameters	5424/18/257
Goodness-of-fit on F^2	0.983
Final R indexes [$I \geq 2\sigma(I)$]	$R_1 = 0.0274$, $wR_2 = 0.0498$
Final R indexes [all data]	$R_1 = 0.0412$, $wR_2 = 0.0527$
Largest diff. peak/hole / $e \text{ \AA}^{-3}$	0.40/-0.70
Flack parameter	0.51(3)

Table 2: Bond lengths for **21.1a_{Mo}**.

Atom	Atom	Length/ \AA	Atom	Atom	Length/ \AA
Mo	P	2.4883(8)	Si2	C8	1.873(4)
Mo	C11	2.014(4)	Si2	C9	1.864(3)
Mo	C12	2.045(4)	Si2	C10	1.863(3)
Mo	C13	2.042(4)	O1	C1	1.467(7)
Mo	C14	2.046(4)	O1	C1S	1.621(11)
Mo	C15	2.042(4)	O2	C11	1.149(4)
P	O1	1.673(2)	O3	C12	1.137(4)
P	C2	1.817(3)	O4	C13	1.137(4)
P	C4	1.806(3)	O5	C14	1.145(4)
P	C1	2.265(6)	O6	C15	1.145(4)
Si1	C4	1.907(3)	C2	C1	1.580(8)
Si1	C5	1.857(4)	C2	C1S	1.544(11)
Si1	C6	1.864(4)	C1	C3	1.512(14)
Si1	C7	1.875(4)	C1S	C3S	1.49(2)
Si2	C4	1.908(3)			

Table 3: Bond angles for **21.1a_{Mo}**.

Atom	Atom	Atom	Angle/ $^\circ$	Atom	Atom	Atom	Angle/ $^\circ$
C11	Mo	P	177.66(9)	C6	Si1	C7	107.30(19)
C11	Mo	C12	90.32(14)	C7	Si1	C4	107.56(15)
C11	Mo	C13	91.48(14)	C8	Si2	C4	107.77(17)
C11	Mo	C14	91.07(15)	C9	Si2	C4	111.82(14)
C11	Mo	C15	88.68(15)	C9	Si2	C8	110.4(2)
C12	Mo	P	88.66(10)	C10	Si2	C4	111.12(14)
C12	Mo	C14	178.60(16)	C10	Si2	C8	106.35(18)
C13	Mo	P	90.65(10)	C10	Si2	C9	109.24(17)
C13	Mo	C12	91.54(15)	C1	O1	P	92.1(3)
C13	Mo	C14	88.43(13)	C1S	O1	P	94.9(4)
C14	Mo	P	89.94(11)	C1	C2	P	83.3(3)
C15	Mo	P	89.20(11)	C1S	C2	P	92.2(4)
C15	Mo	C12	89.35(14)	P	C4	Si1	115.85(15)

C15	Mo	C13	179.09(16)	P	C4	Si2	114.15(15)
C15	Mo	C14	90.68(15)	Si1	C4	Si2	116.67(15)
O1	P	Mo	114.07(10)	O2	C11	Mo	177.9(3)
O1	P	C2	80.03(14)	O3	C12	Mo	178.5(3)
O1	P	C4	107.99(13)	O4	C13	Mo	178.9(4)
O1	P	C1	40.3(2)	O5	C14	Mo	179.0(3)
C2	P	Mo	119.89(13)	O6	C15	Mo	177.8(3)
C2	P	C1	43.9(2)	O1	C1	P	47.58(19)
C4	P	Mo	117.95(10)	O1	C1	C2	94.9(4)
C4	P	C2	110.41(16)	O1	C1	C3	107.4(9)
C4	P	C1	129.7(3)	C2	C1	P	52.8(2)
C1	P	Mo	111.8(3)	C3	C1	P	139.7(10)
C5	Si1	C4	114.56(17)	C3	C1	C2	114.0(8)
C5	Si1	C6	109.1(2)	C2	C1S	O1	90.4(6)
C5	Si1	C7	109.6(2)	C3S	C1S	O1	106.7(12)
C6	Si1	C4	108.41(16)	C3S	C1S	C2	111.8(12)

Table 4: Torsion angles for **21.1a_{Mo}**.

A	B	C	D	Angle/°	A	B	C	D	Angle/°
Mo	P	O1	C1	95.9(4)	C2	P	C4	Si1	-96.27(19)
Mo	P	O1	C1S	129.5(5)	C2	P	C4	Si2	43.5(2)
Mo	P	C2	C1	-91.2(4)	C4	P	O1	C1	-130.9(4)
Mo	P	C2	C1S	-123.7(6)	C4	P	O1	C1S	-97.3(6)
Mo	P	C4	Si1	120.65(13)	C4	P	C2	C1	126.6(4)
Mo	P	C4	Si2	-99.55(14)	C4	P	C2	C1S	94.0(6)
P	O1	C1	C2	25.8(5)	C1	P	O1	C1S	33.6(4)
P	O1	C1	C3	142.9(7)	C1	P	C2	C1S	-32.6(4)
P	O1	C1S	C2	-12.9(6)	C1	P	C4	Si1	-50.0(3)
P	O1	C1S	C3S	-125.8(10)	C1	P	C4	Si2	89.8(3)
P	C2	C1	O1	-23.8(4)	C1	O1	C1S	C2	73.4(8)
P	C2	C1	C3	-135.3(9)	C1	O1	C1S	C3S	-39.5(12)
P	C2	C1S	O1	11.8(6)	C1	C2	C1S	O1	-62.7(8)
P	C2	C1S	C3S	120.0(11)	C1	C2	C1S	C3S	45.5(11)
O1	P	C2	C1	21.0(4)	C1S	O1	C1	P	-95.8(8)
O1	P	C2	C1S	-11.6(6)	C1S	O1	C1	C2	-70.0(8)
O1	P	C4	Si1	-10.5(2)	C1S	O1	C1	C3	47.1(10)
O1	P	C4	Si2	129.31(15)	C1S	C2	C1	P	104.1(8)
C2	P	O1	C1	-22.5(5)	C1S	C2	C1	O1	80.4(9)
C2	P	O1	C1S	11.1(6)	C1S	C2	C1	C3	-31.1(10)

12.10 Pentacarbonyl{4-methyl-2-[bis(trimethylsilyl)methyl]-1,2-oxaphosphetane- κ P}chromium(0) [21.1a_{Cr}]

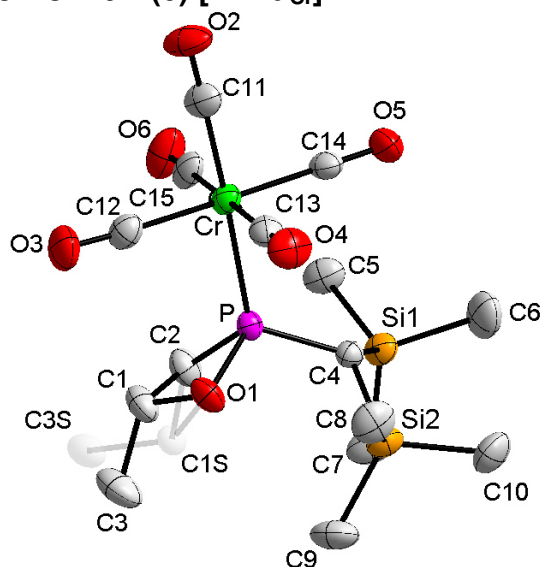


Table 1: Crystal data and structure refinement for **21.1a_{Cr}**.

Identification code	GSTR369, 3648
Empirical formula	C ₁₅ H ₂₅ CrO ₆ PSi ₂
Formula weight	440.50
Temperature/K	123.15
Crystal system	orthorhombic
Space group	P2 ₁ 2 ₁ 2 ₁
a/Å	10.4217(3)
b/Å	13.6908(7)
c/Å	15.3565(7)
α/°	90
β/°	90
γ/°	90
Volume/Å ³	2191.09(16)
Z	4
ρ _{calc} /cm ³	1.335
μ/mm ⁻¹	0.729
F(000)	920.0
Crystal size/mm ³	0.28 × 0.18 × 0.1
Radiation	MoKα (λ = 0.71073)
2θ range for data collection/°	4.724 to 55.982
Index ranges	-10 ≤ h ≤ 13, -13 ≤ k ≤ 18, -20 ≤ l ≤ 19
Reflections collected	15836
Independent reflections	5195 [R _{int} = 0.0517, R _{sigma} = 0.0596]
Data/restraints/parameters	5195/0/257
Goodness-of-fit on F ²	0.974
Final R indexes [I ≥ 2σ (I)]	R ₁ = 0.0319, wR ₂ = 0.0659
Final R indexes [all data]	R ₁ = 0.0430, wR ₂ = 0.0690
Largest diff. peak/hole / e Å ⁻³	0.23/-0.49
Flack parameter	0.52(2)

Table 2: Bond lengths for **21.1acr**.

Atom	Atom	Length/Å	Atom	Atom	Length/Å
Cr	P	2.3412(8)	Si2	C8	1.862(3)
Cr	C11	1.878(3)	Si2	C9	1.852(3)
Cr	C12	1.889(3)	Si2	C10	1.876(3)
Cr	C13	1.893(3)	O1	C1	1.459(5)
Cr	C14	1.894(3)	O1	C1S	1.632(15)
Cr	C15	1.896(3)	O2	C11	1.145(3)
P	O1	1.663(2)	O3	C12	1.147(4)
P	C2	1.830(3)	O4	C13	1.144(4)
P	C4	1.807(3)	O5	C14	1.141(4)
P	C1	2.287(4)	O6	C15	1.146(4)
Si1	C4	1.909(3)	C2	C1	1.575(6)
Si1	C5	1.852(3)	C2	C1S	1.538(13)
Si1	C6	1.869(3)	C1	C3	1.502(10)
Si1	C7	1.869(3)	C1S	C3S	1.50(3)
Si2	C4	1.911(3)			

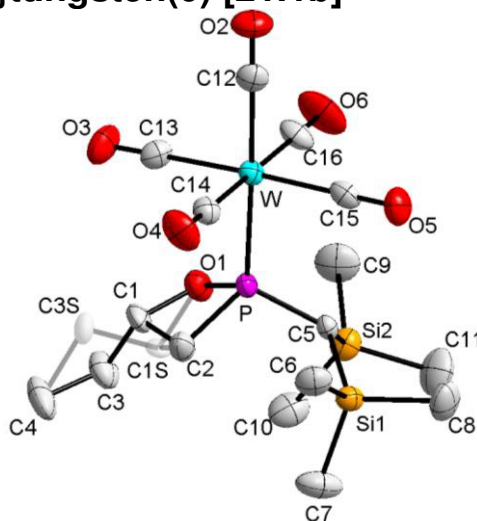
Table 3: Bond angles for **21.1acr**.

Atom	Atom	Atom	Angle/°	Atom	Atom	Atom	Angle/°
C11	Cr	P	176.98(9)	C7	Si1	C4	111.62(13)
C11	Cr	C12	88.27(13)	C7	Si1	C6	110.52(18)
C11	Cr	C13	90.59(13)	C8	Si2	C4	108.88(14)
C11	Cr	C14	91.30(13)	C8	Si2	C10	107.48(17)
C11	Cr	C15	91.35(14)	C9	Si2	C4	114.70(15)
C12	Cr	P	88.96(10)	C9	Si2	C8	108.90(17)
C12	Cr	C13	89.79(13)	C9	Si2	C10	109.61(17)
C12	Cr	C14	178.95(14)	C10	Si2	C4	107.03(14)
C12	Cr	C15	90.75(14)	C1	O1	P	94.0(2)
C13	Cr	P	88.20(9)	C1S	O1	P	94.5(5)
C13	Cr	C14	91.17(14)	C1	C2	P	84.1(2)
C13	Cr	C15	177.99(13)	C1S	C2	P	91.4(5)
C14	Cr	P	91.49(9)	P	C4	Si1	114.34(14)
C14	Cr	C15	88.30(13)	P	C4	Si2	115.72(14)
C15	Cr	P	89.88(10)	Si1	C4	Si2	116.28(12)
O1	P	Cr	114.06(7)	O2	C11	Cr	178.1(3)
O1	P	C2	79.90(13)	O3	C12	Cr	177.3(3)
O1	P	C4	107.73(12)	O4	C13	Cr	178.0(3)
O1	P	C1	39.51(15)	O5	C14	Cr	179.3(3)
C2	P	Cr	119.59(11)	O6	C15	Cr	179.4(3)
C2	P	C1	43.24(16)	O1	C1	P	46.49(14)
C4	P	Cr	118.22(9)	O1	C1	C2	95.4(3)
C4	P	C2	110.66(13)	O1	C1	C3	111.1(6)
C4	P	C1	127.1(2)	C2	C1	P	52.71(16)
C1	P	Cr	114.10(19)	C3	C1	P	141.3(7)
C5	Si1	C4	111.54(12)	C3	C1	C2	115.6(5)
C5	Si1	C6	105.88(16)	C2	C1S	O1	90.2(8)
C5	Si1	C7	109.23(15)	C3S	C1S	O1	105.2(15)
C6	Si1	C4	107.90(15)	C3S	C1S	C2	111.3(16)

Table 4: Torsion angles for **21.1acr.**

A	B	C	D	Angle/°	A	B	C	D	Angle/°
Cr	P	O1	C1	99.3(3)	C2	P	C4	Si1	43.45(19)
Cr	P	O1	C1S	132.0(7)	C2	P	C4	Si2	-95.78(17)
Cr	P	C2	C1	-94.7(3)	C4	P	O1	C1	-127.3(3)
Cr	P	C2	C1S	-126.9(8)	C4	P	O1	C1S	-94.6(7)
Cr	P	C4	Si1	-99.82(13)	C4	P	C2	C1	122.6(3)
Cr	P	C4	Si2	120.96(12)	C4	P	C2	C1S	90.5(8)
P	O1	C1	C2	21.6(3)	C1	P	O1	C1S	32.7(5)
P	O1	C1	C3	141.8(5)	C1	P	C2	C1S	-32.2(6)
P	O1	C1S	C2	-16.5(8)	C1	P	C4	Si1	89.7(2)
P	O1	C1S	C3S	-128.7(13)	C1	P	C4	Si2	-49.5(2)
P	C2	C1	O1	-19.6(3)	C1	O1	C1S	C2	74.0(10)
P	C2	C1	C3	-136.2(6)	C1	O1	C1S	C3S	-38.3(13)
P	C2	C1S	O1	14.9(7)	C1	C2	C1S	O1	-61.9(9)
P	C2	C1S	C3S	121.3(14)	C1	C2	C1S	C3S	44.6(14)
O1	P	C2	C1	17.3(3)	C1S	O1	C1	P	-92.1(9)
O1	P	C2	C1S	-14.8(8)	C1S	O1	C1	C2	-70.4(9)
O1	P	C4	Si1	129.08(14)	C1S	O1	C1	C3	49.8(10)
O1	P	C4	Si2	-10.14(17)	C1S	C2	C1	P	101.9(9)
C2	P	O1	C1	-18.7(3)	C1S	C2	C1	O1	82.3(10)
C2	P	O1	C1S	14.0(7)	C1S	C2	C1	C3	-34.3(10)

12.11 Pentacarbonyl{4-ethyl-2-[bis(trimethylsilyl)methyl]-1,2-oxaphosphetane- κP }tungsten(0) [21.1b]

**Table 1:** Crystal data and structure refinement for **21.1b.**

Identification code	GSTR519, AKY-574 // GXray4852f
Crystal Habitus	clear colourless plate
Device Type	Bruker X8-KappaApexII
Empirical formula	C ₁₆ H ₂₇ O ₆ Si ₂ PW
Moiety formula	C16 H27 O6 P Si2 W
Formula weight	586.37
Temperature/K	100
Crystal system	triclinic
Space group	P $\bar{1}$
a/Å	8.8913(4)

b/Å	10.6987(5)
c/Å	13.6623(7)
α /°	102.842(3)
β /°	94.549(3)
γ /°	113.104(3)
Volume/Å ³	1145.22(10)
Z	2
$\rho_{\text{calc}}/\text{cm}^3$	1.700
μ/mm^{-1}	5.244
F(000)	576.0
Crystal size/mm ³	0.18 × 0.16 × 0.04
Absorption correction	empirical
Tmin; Tmax	0.4450; 0.7459
Radiation	MoK α (λ = 0.71073)
2 θ range for data collection/°	6.226 to 55.998°
Completeness to theta	0.997
Index ranges	-11 ≤ h ≤ 11, -14 ≤ k ≤ 14, -18 ≤ l ≤ 18
Reflections collected	23442
Independent reflections	5524 [R _{int} = 0.0668, R _{sigma} = 0.0612]
Data/restraints/parameters	5524/0/260
Goodness-of-fit on F ²	1.039
Final R indexes [$\geq 2\sigma$ (I)]	R ₁ = 0.0346, wR ₂ = 0.0773
Final R indexes [all data]	R ₁ = 0.0478, wR ₂ = 0.0839
Largest diff. peak/hole / e Å ⁻³	1.60/-1.27

Table 2: Bond lengths for **21.1b**.

Atom	Atom	Length/Å	Atom	Atom	Length/Å
W	P	2.4789(12)	Si2	C10	1.864(6)
W	C12	2.031(5)	Si2	C11	1.863(6)
W	C13	2.044(5)	O1	C1	1.511(9)
W	C14	2.042(5)	O1	C1S	1.467(16)
W	C15	2.032(5)	O2	C12	1.133(6)
W	C16	2.035(6)	O3	C13	1.124(6)
P	O1	1.668(3)	O4	C14	1.128(6)
P	C2	1.800(5)	O5	C15	1.145(6)
P	C5	1.809(4)	O6	C16	1.137(7)
Si1	C5	1.914(4)	C1	C2	1.507(9)
Si1	C6	1.869(6)	C1	C3	1.499(13)
Si1	C7	1.869(5)	C1S	C2	1.658(18)
Si1	C8	1.863(6)	C1S	C3S	1.51(3)
Si2	C5	1.906(5)	C3	C4	1.494(11)
Si2	C9	1.867(6)	C3S	C4	1.632(19)

Table 3: Bond angles for **21.1b**.

Atom	Atom	Atom	Angle/°	Atom	Atom	Atom	Angle/°
C12	W	P	175.85(13)	C9	Si2	C5	109.9(3)
C12	W	C13	90.0(2)	C10	Si2	C5	114.4(3)
C12	W	C14	89.90(19)	C10	Si2	C9	108.1(3)
C12	W	C15	91.56(19)	C11	Si2	C5	108.5(3)
C12	W	C16	89.8(2)	C11	Si2	C9	106.2(3)

C13	W	P	86.80(14)	C11	Si2	C10	109.4(3)
C14	W	P	92.73(13)	C1	O1	P	92.0(4)
C14	W	C13	89.2(2)	C1S	O1	P	99.0(7)
C15	W	P	91.68(13)	C2	C1	O1	94.9(5)
C15	W	C13	177.89(18)	C3	C1	O1	110.5(8)
C15	W	C14	89.44(19)	C3	C1	C2	116.3(9)
C15	W	C16	90.3(2)	O1	C1S	C2	90.5(9)
C16	W	P	87.60(15)	O1	C1S	C3S	106.8(15)
C16	W	C13	91.1(2)	C3S	C1S	C2	108.5(16)
C16	W	C14	179.57(19)	C1	C2	P	87.2(4)
O1	P	W	114.11(13)	C1S	C2	P	87.2(6)
O1	P	C2	79.7(2)	C4	C3	C1	110.7(9)
O1	P	C5	108.6(2)	C1S	C3S	C4	105.1(15)
C2	P	W	119.5(2)	P	C5	Si1	113.3(2)
C2	P	C5	111.3(2)	P	C5	Si2	116.0(2)
C5	P	W	117.41(14)	Si2	C5	Si1	117.2(2)
C6	Si1	C5	111.4(2)	O2	C12	W	178.6(4)
C6	Si1	C7	109.0(3)	O3	C13	W	178.7(5)
C7	Si1	C5	112.3(2)	O4	C14	W	178.5(5)
C8	Si1	C5	108.1(2)	O5	C15	W	179.2(5)
C8	Si1	C6	106.7(3)	O6	C16	W	179.3(5)
C8	Si1	C7	109.2(3)				

Table 4: Torsion angles for **21.1b**.

A	B	C	D	Angle/°	A	B	C	D	Angle/°
W	P	O1	C1	-100.3(4)	O1	C1	C3	C4	-175.7(6)
W	P	O1	C1S	-132.5(9)	O1	C1S	C2	P	-14.4(9)
W	P	C2	C1	94.4(5)	O1	C1S	C3S	C4	-177.4(10)
W	P	C2	C1S	124.8(8)	C2	P	O1	C1	17.5(5)
W	P	C5	Si1	100.7(2)	C2	P	O1	C1S	-14.7(9)
W	P	C5	Si2	-119.48(19)	C2	P	C5	Si1	-42.1(3)
P	O1	C1	C2	-20.8(5)	C2	P	C5	Si2	97.6(3)
P	O1	C1	C3	-141.2(8)	C2	C1	C3	C4	77.6(12)
P	O1	C1S	C2	15.7(9)	C2	C1S	C3S	C4	-81.0(15)
P	O1	C1S	C3S	125.2(13)	C3	C1	C2	P	135.0(8)
O1	P	C2	C1	-17.6(5)	C3S	C1S	C2	P	-122.4(13)
O1	P	C2	C1S	12.8(8)	C5	P	O1	C1	126.7(5)
O1	P	C5	Si1	-128.0(2)	C5	P	O1	C1S	94.5(9)
O1	P	C5	Si2	11.8(3)	C5	P	C2	C1	-123.6(5)
O1	C1	C2	P	19.2(5)	C5	P	C2	C1S	-93.2(8)

12.12 Pentacarbonyl{4-(1-methylethyl)-2-[bis(trimethylsilyl)methyl]-1,2-oxaphosphetane- κ P}tungsten(0) [21.1c]

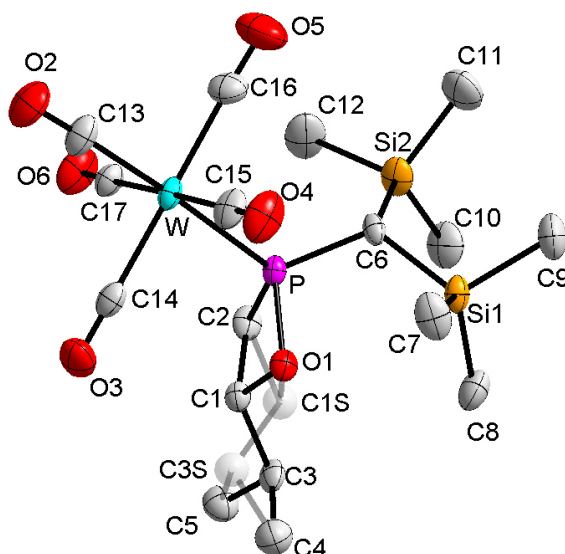


Table 1: Crystal data and structure refinement for **21.1c**.

Identification code	GSTR518, AKY-575 // GXray4851f
Crystal Habitus	clear colourless plank
Device Type	Bruker X8-KappaApexII
Empirical formula	C ₁₇ H ₂₉ O ₆ Si ₂ PW
Moiety formula	C ₁₇ H ₂₉ O ₆ P Si ₂ W
Formula weight	600.40
Temperature/K	100
Crystal system	orthorhombic
Space group	P2 ₁ 2 ₁ 2 ₁
a/Å	9.1548(5)
b/Å	14.3346(8)
c/Å	18.6104(9)
α/°	90
β/°	90
γ/°	90
Volume/Å ³	2442.3(2)
Z	4
ρ _{calc} /cm ³	1.633
μ/mm ⁻¹	4.920
F(000)	1184.0
Crystal size/mm ³	0.32 × 0.21 × 0.18
Absorption correction	empirical
Tmin; Tmax	0.4382; 0.7459
Radiation	MoKα (λ = 0.71073)
2θ range for data collection/°	7.158 to 55.988°
Completeness to theta	0.991
Index ranges	-12 ≤ h ≤ 10, -12 ≤ k ≤ 18, -18 ≤ l ≤ 24
Reflections collected	12514
Independent reflections	5861 [R _{int} = 0.0386, R _{sigma} = 0.0528]
Data/restraints/parameters	5861/48/270
Goodness-of-fit on F ²	1.015
Final R indexes [I ≥ 2σ (I)]	R ₁ = 0.0302, wR ₂ = 0.0602
Final R indexes [all data]	R ₁ = 0.0342, wR ₂ = 0.0615

Largest diff. peak/hole / e Å ⁻³	1.65/-0.57
Flack parameter	0.398(10)

Table 2: Bond lengths for **21.1c**.

Atom	Atom	Length/Å	Atom	Atom	Length/Å
W	P	2.4818(15)	Si2	C12	1.874(9)
W	C13	2.014(7)	O1	C1	1.475(9)
W	C14	2.054(8)	O1	C1S	1.59(4)
W	C15	2.053(8)	O2	C13	1.140(8)
W	C16	2.046(8)	O3	C14	1.130(9)
W	C17	2.041(6)	O4	C15	1.139(9)
P	O1	1.668(5)	O5	C16	1.127(9)
P	C2	1.846(6)	O6	C17	1.137(7)
P	C6	1.808(6)	C1	C2	1.536(11)
Si1	C6	1.907(6)	C1	C3	1.522(13)
Si1	C7	1.860(7)	C2	C1S	1.54(4)
Si1	C8	1.871(8)	C3	C4	1.522(13)
Si1	C9	1.863(8)	C3	C5	1.546(12)
Si2	C6	1.922(6)	C4	C3S	1.64(4)
Si2	C10	1.857(8)	C5	C3S	1.49(4)
Si2	C11	1.852(9)	C1S	C3S	1.39(6)

Table 3: Bond angles for **21.1c**.

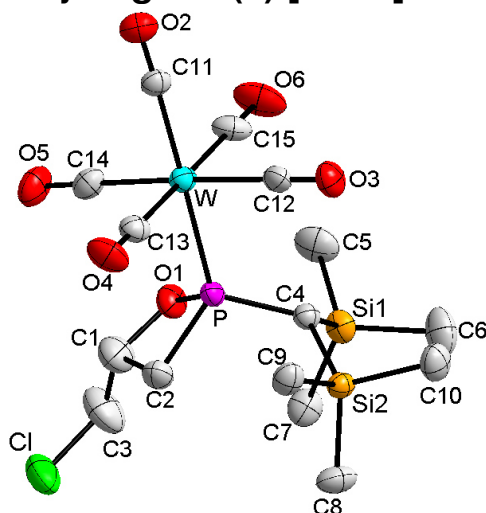
Atom	Atom	Atom	Angle/°	Atom	Atom	Atom	Angle/°
C13	W	P	177.1(3)	C11	Si2	C6	107.5(4)
C13	W	C14	89.4(3)	C11	Si2	C10	111.0(4)
C13	W	C15	90.7(3)	C11	Si2	C12	107.0(5)
C13	W	C16	91.2(3)	C12	Si2	C6	112.3(3)
C13	W	C17	89.2(3)	C1	O1	P	93.4(4)
C14	W	P	87.94(17)	C1S	O1	P	95.1(13)
C15	W	P	90.42(18)	O1	C1	C2	96.9(6)
C15	W	C14	90.0(3)	O1	C1	C3	111.3(7)
C16	W	P	91.4(2)	C3	C1	C2	118.0(7)
C16	W	C14	178.0(4)	C1	C2	P	84.8(4)
C16	W	C15	91.8(4)	C1S	C2	P	89.8(14)
C17	W	P	89.66(17)	C1	C3	C5	107.7(8)
C17	W	C14	88.9(3)	C4	C3	C1	110.5(7)
C17	W	C15	178.9(4)	C4	C3	C5	112.3(7)
C17	W	C16	89.3(4)	P	C6	Si1	116.0(4)
O1	P	W	114.59(15)	P	C6	Si2	114.0(3)
O1	P	C2	79.6(3)	Si1	C6	Si2	116.5(3)
O1	P	C6	107.0(3)	O2	C13	W	177.4(8)
C2	P	W	118.7(2)	O3	C14	W	179.5(7)
C6	P	W	118.6(2)	O4	C15	W	179.4(9)
C6	P	C2	111.5(3)	O5	C16	W	178.0(7)
C7	Si1	C6	108.8(3)	O6	C17	W	177.7(7)
C7	Si1	C8	109.2(4)	C2	C1S	O1	92(2)
C7	Si1	C9	106.8(4)	C3S	C1S	O1	110(3)
C8	Si1	C6	114.2(3)	C3S	C1S	C2	119(4)
C9	Si1	C6	109.4(4)	C5	C3S	C4	109(3)

C9	Si1	C8	108.1(4)	C1S	C3S	C4	108(3)
C10	Si2	C6	111.7(4)	C1S	C3S	C5	113(4)
C10	Si2	C12	107.3(4)				

Table 4: Torsion angles for **21.1c**.

A	B	C	D	Angle/°	A	B	C	D	Angle/°
W	P	O1	C1	100.7(4)	O1	C1	C3	C4	57.0(11)
W	P	O1	C1S	129.9(16)	O1	C1	C3	C5	180.0(6)
W	P	C2	C1	-96.9(4)	O1	C1S	C3S	C4	-64(4)
W	P	C2	C1S	-125.8(17)	O1	C1S	C3S	C5	176(2)
W	P	C6	Si1	121.5(3)	C2	P	O1	C1	-16.2(4)
W	P	C6	Si2	-99.1(3)	C2	P	O1	C1S	13.0(17)
P	O1	C1	C2	19.4(5)	C2	P	C6	Si1	-95.2(4)
P	O1	C1	C3	143.1(7)	C2	P	C6	Si2	44.2(4)
P	O1	C1S	C2	-15.4(19)	C2	C1	C3	C4	167.7(7)
P	O1	C1S	C3S	-137(3)	C2	C1	C3	C5	-69.4(10)
P	C2	C1S	O1	13.8(17)	C2	C1S	C3S	C4	-168(2)
P	C2	C1S	C3S	128(4)	C2	C1S	C3S	C5	72(5)
O1	P	C2	C1	15.6(4)	C3	C1	C2	P	-136.1(8)
O1	P	C2	C1S	-13.3(17)	O6	P	O1	C1	-125.7(4)
O1	P	C6	Si1	-9.9(4)	O6	P	O1	C1S	-96.5(17)
O1	P	C6	Si2	129.5(3)	O6	P	C2	C1	119.9(5)
O1	C1	C2	P	-17.5(5)	O6	P	C2	C1S	91.0(17)

12.13 Pentacarbonyl{4-(chloromethyl)-2-[bis(trimethylsilyl)methyl]-1,2-oxaphosphetane- κP }tungsten(0) [21.1e]

**Table 1:** Crystal data and structure refinement for **21.1e**.

Identification code	GSTR324, AKY-306 // GXray3114
Crystal Habitus	colourless plate
Device Type	Nonius KappaCCD
Empirical formula	C ₁₅ H ₂₄ ClO ₆ PSi ₂ W
Moiety formula	C ₁₅ H ₂₄ Cl O ₆ P Si ₂ W
Formula weight	606.79
Temperature/K	123(2)

Crystal system	triclinic
Space group	$P\bar{1}$
a/Å	8.7534(3)
b/Å	10.7464(4)
c/Å	13.5918(5)
α /°	102.8140(18)
β /°	93.438(2)
γ /°	113.6090(18)
Volume/Å ³	1126.40(7)
Z	2
$\rho_{\text{calc}}/\text{cm}^3$	1.789
μ/mm^{-1}	5.449
F(000)	592.0
Crystal size/mm ³	0.08 × 0.06 × 0.02
Absorption correction	empirical
Tmin; Tmax	0.6697; 0.8988
Radiation	MoK α (λ = 0.71073)
2 θ range for data collection/°	5.56 to 56°
Completeness to theta	0.998
Index ranges	-11 ≤ h ≤ 11, -14 ≤ k ≤ 14, -17 ≤ l ≤ 17
Reflections collected	37295
Independent reflections	5438 [R_{int} = 0.0757]
Data/restraints/parameters	5438/5/241
Goodness-of-fit on F^2	0.993
Final R indexes [$I \geq 2\sigma(I)$]	$R_1 = 0.0309$, $wR_2 = 0.0658$
Final R indexes [all data]	$R_1 = 0.0427$, $wR_2 = 0.0687$
Largest diff. peak/hole / e Å ⁻³	1.44/-1.49

Table 2: Bond lengths for **21.1e**.

Atom	Atom	Length/Å	Atom	Atom	Length/Å
C2	C1	1.527(7)	C10	Si2	1.858(4)
C2	P	1.835(4)	C11	O2	1.144(5)
C1	C3	1.474(7)	C11	W	2.027(4)
C1	O1	1.527(6)	C12	O3	1.145(5)
C1	P	2.320(5)	C12	W	2.036(4)
C3	Cl	1.753(6)	C13	O4	1.140(5)
C4	P	1.813(4)	C13	W	2.046(4)
C4	Si1	1.906(4)	C14	O5	1.156(5)
C4	Si2	1.922(4)	C14	W	2.031(5)
C5	Si1	1.867(5)	C15	O6	1.148(5)
C6	Si1	1.869(5)	C15	W	2.035(4)
C7	Si1	1.859(5)	O1	P	1.693(3)
C8	Si2	1.869(4)	P	W	2.4726(10)
C9	Si2	1.880(4)			

Table 3: Bond angles for **21.1e**.

Atom	Atom	Atom	Angle/°	Atom	Atom	Atom	Angle/°
C1	C2	P	86.8(3)	C7	Si1	C5	109.1(2)
C3	C1	C2	118.8(5)	C7	Si1	C6	109.1(2)
C3	C1	O1	107.9(4)	C5	Si1	C6	107.3(3)

C2	C1	O1	96.5(3)	C7	Si1	C4	113.87(19)
C3	C1	P	138.3(4)	C5	Si1	C4	109.4(2)
C2	C1	P	52.2(2)	C6	Si1	C4	107.8(2)
O1	C1	P	46.82(18)	C10	Si2	C8	109.4(2)
C1	C3	Cl	109.6(4)	C10	Si2	C9	106.7(2)
P	C4	Si1	116.6(2)	C8	Si2	C9	109.5(2)
P	C4	Si2	113.28(19)	C10	Si2	C4	108.00(19)
Si1	C4	Si2	117.1(2)	C8	Si2	C4	111.91(19)
O2	C11	W	177.2(4)	C9	Si2	C4	111.13(18)
O3	C12	W	179.6(4)	C11	W	C14	91.10(17)
O4	C13	W	178.2(4)	C11	W	C15	89.70(16)
O5	C14	W	179.5(4)	C14	W	C15	91.00(18)
O6	C15	W	179.6(5)	C11	W	C12	90.71(16)
C1	O1	P	92.0(3)	C14	W	C12	177.95(16)
O1	P	C4	108.25(17)	C15	W	C12	89.97(17)
O1	P	C2	80.35(18)	C11	W	C13	89.17(16)
C4	P	C2	111.42(19)	C14	W	C13	90.03(17)
O1	P	C1	41.14(17)	C15	W	C13	178.49(16)
C4	P	C1	125.9(2)	C12	W	C13	89.04(16)
C2	P	C1	41.1(2)	C11	W	P	175.57(11)
O1	P	W	112.31(11)	C14	W	P	85.77(13)
C4	P	W	117.65(13)	C15	W	P	87.22(12)
C2	P	W	120.31(16)	C12	W	P	92.48(12)
C1	P	W	115.86(15)	C13	W	P	93.96(12)

Table 4: Torsion angles for **21.1e**.

A	B	C	D	Angle/°	A	B	C	D	Angle/°
P	C2	C1	C3	130.7(5)	O2	C11	W	C15	74(7)
P	C2	C1	O1	16.1(3)	O2	C11	W	C12	164(7)
C2	C1	C3	Cl	69.8(6)	O2	C11	W	C13	-107(7)
O1	C1	C3	Cl	178.1(4)	O2	C11	W	P	28(8)
P	C1	C3	Cl	134.0(5)	O5	C14	W	C11	-92(43)
C3	C1	O1	P	-140.7(4)	O5	C14	W	C15	178(100)
C2	C1	O1	P	-17.5(3)	O5	C14	W	C12	60(44)
C1	O1	P	C4	124.1(3)	O5	C14	W	C13	-3(43)
C1	O1	P	C2	14.6(3)	O5	C14	W	P	91(43)
C1	O1	P	W	-104.3(2)	O6	C15	W	C11	119(85)
Si1	C4	P	O1	9.7(3)	O6	C15	W	C14	-150(85)
Si2	C4	P	O1	-130.63(19)	O6	C15	W	C12	28(85)
Si1	C4	P	C2	96.3(3)	O6	C15	W	C13	77(86)
Si2	C4	P	C2	-44.1(3)	O6	C15	W	P	-64(85)
Si1	C4	P	C1	52.0(3)	O3	C12	W	C11	154(65)
Si2	C4	P	C1	-88.4(3)	O3	C12	W	C14	2(68)
Si1	C4	P	W	-118.89(18)	O3	C12	W	C15	-116(65)
Si2	C4	P	W	100.76(18)	O3	C12	W	C13	65(65)
C1	C2	P	O1	-14.6(3)	O3	C12	W	P	-29(65)
C1	C2	P	C4	-120.6(3)	O4	C13	W	C11	-13(13)
C1	C2	P	W	95.6(3)	O4	C13	W	C14	-104(13)
C3	C1	P	O1	65.1(6)	O4	C13	W	C15	29(17)
C2	C1	P	O1	157.7(4)	O4	C13	W	C12	78(13)
C3	C1	P	C4	-10.9(7)	O4	C13	W	P	170(13)

C2	C1	P	C4	81.7(4)	O1	P	W	C11	-16.5(15)
O1	C1	P	C4	-76.0(3)	C4	P	W	C11	110.2(15)
C3	C1	P	C2	-92.6(7)	C2	P	W	C11	-108.2(15)
O1	C1	P	C2	-157.7(4)	C1	P	W	C11	-61.6(15)
C3	C1	P	W	160.1(6)	O1	P	W	C14	28.56(17)
C2	C1	P	W	-107.3(3)	C4	P	W	C14	155.22(18)
O1	C1	P	W	94.9(2)	C2	P	W	C14	-63.2(2)
P	C4	Si1	C7	-69.4(3)	C1	P	W	C14	-16.5(2)
Si2	C4	Si1	C7	69.4(3)	O1	P	W	C15	-62.65(18)
P	C4	Si1	C5	52.9(3)	C4	P	W	C15	64.01(19)
Si2	C4	Si1	C5	-168.2(2)	C2	P	W	C15	-154.4(2)
P	C4	Si1	C6	169.3(3)	C1	P	W	C15	-107.8(2)
Si2	C4	Si1	C6	-51.8(3)	O1	P	W	C12	-152.50(16)
P	C4	Si2	C10	-145.0(2)	C4	P	W	C12	-25.83(18)
Si1	C4	Si2	C10	74.8(3)	C2	P	W	C12	115.8(2)
P	C4	Si2	C8	94.4(3)	C1	P	W	C12	162.39(19)
Si1	C4	Si2	C8	-45.7(3)	O1	P	W	C13	118.29(17)
P	C4	Si2	C9	-28.3(3)	C4	P	W	C13	-115.04(18)
Si1	C4	Si2	C9	-168.4(2)	C2	P	W	C13	26.6(2)
O2	C11	W	C14	-17(7)	C1	P	W	C13	73.18(19)

12.14 Pentacarbonyl{4-epoxy-2-[bis(trimethylsilyl)methyl]-1,2-oxaphosphetane- κP }tungsten(0) [21.1f]

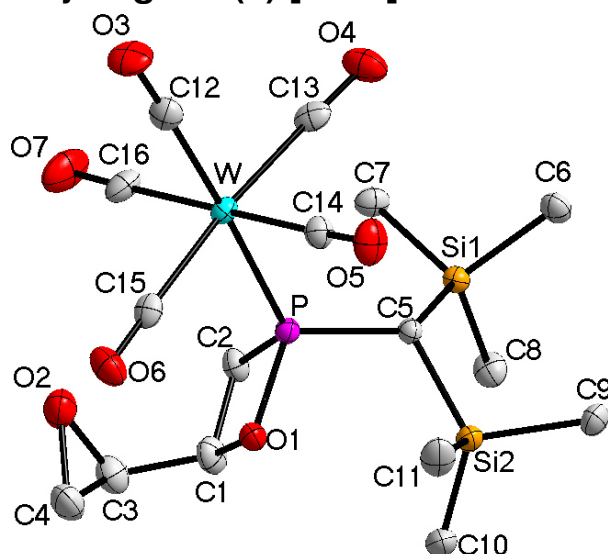


Table 1: Crystal data and structure refinement for **21.1f**.

Identification code	GSTR382, AKY-425 // GXraycollect
Device Type	Nonius KappaCCD
Empirical formula	C ₁₆ H ₂₅ O ₇ PSi ₂ W
Formula weight	600.36
Temperature/K	123.0
Crystal system	orthorhombic
Space group	P2 ₁ 2 ₁ 2 ₁
a/Å	9.3903(2)
b/Å	11.0600(2)
c/Å	21.8725(4)
α /°	90.00

$\beta/^\circ$	90.00
$\gamma/^\circ$	90.00
Volume/ \AA^3	2271.61(8)
Z	4
$\rho_{\text{calc}}/\text{cm}^3$	1.755
μ/mm^{-1}	5.293
F(000)	1176.0
Crystal size/ mm^3	0.28 × 0.22 × 0.12
Absorption correction	multi-scan
Tmin; Tmax	0.29346; 0.64943
Radiation	MoK α ($\lambda = 0.71073$)
2 θ range for data collection/ $^\circ$	5.7 to 55.98 $^\circ$
Completeness to theta	0.997
Index ranges	-10 ≤ h ≤ 12, -13 ≤ k ≤ 14, -28 ≤ l ≤ 28
Reflections collected	26317
Independent reflections	5435 [$R_{\text{int}} = 0.0630$, $R_{\text{sigma}} = 0.0391$]
Data/restraints/parameters	5435/0/250
Goodness-of-fit on F^2	1.053
Final R indexes [$I \geq 2\sigma(I)$]	$R_1 = 0.0226$, $wR_2 = 0.0494$
Final R indexes [all data]	$R_1 = 0.0245$, $wR_2 = 0.0499$
Largest diff. peak/hole / $e \text{\AA}^{-3}$	0.59/-1.32
Flack parameter	-0.005(6)

Table 2: Bond lengths for **21.1f**.

Atom	Atom	Length/ \AA	Atom	Atom	Length/ \AA
W	P	2.4914(10)	Si2	C9	1.861(4)
W	C12	2.009(4)	Si2	C10	1.865(4)
W	C13	2.045(4)	Si2	C11	1.875(4)
W	C14	2.041(4)	O1	C1	1.474(5)
W	C15	2.050(4)	O2	C3	1.451(5)
W	C16	2.054(4)	O2	C4	1.462(5)
P	O1	1.679(3)	O3	C12	1.145(5)
P	C2	1.841(4)	O5	C14	1.138(5)
P	C5	1.809(4)	O4	C13	1.136(5)
Si1	C5	1.916(4)	O6	C15	1.142(5)
Si1	C6	1.860(4)	O7	C16	1.130(5)
Si1	C7	1.877(4)	C2	C1	1.532(6)
Si1	C8	1.879(4)	C1	C3	1.487(6)
Si2	C5	1.915(4)	C3	C4	1.465(6)

Table 3: Bond angles for **21.1f**.

Atom	Atom	Atom	Angle/ $^\circ$	Atom	Atom	Atom	Angle/ $^\circ$
C12	W	P	176.64(13)	C8	Si1	C5	112.08(18)
C12	W	C13	90.28(17)	C9	Si2	C5	108.67(17)
C12	W	C14	90.05(17)	C9	Si2	C10	109.2(2)
C12	W	C15	92.05(16)	C9	Si2	C11	106.7(2)
C12	W	C16	86.91(17)	C10	Si2	C5	113.42(18)
C13	W	P	90.99(11)	C10	Si2	C11	109.7(2)
C13	W	C15	173.26(18)	C11	Si2	C5	108.91(18)
C13	W	C16	95.34(18)	C1	O1	P	95.4(2)

C14	W	P	93.13(12)	C3	O2	C4	60.4(3)
C14	W	C13	86.63(17)	C1	C2	P	87.2(3)
C14	W	C15	87.04(16)	O1	C1	C2	97.6(3)
C14	W	C16	176.39(17)	O1	C1	C3	113.1(4)
C15	W	P	87.04(11)	C3	C1	C2	114.7(4)
C15	W	C16	91.11(17)	O2	C3	C1	114.9(4)
C16	W	P	89.87(12)	O2	C3	C4	60.2(3)
O1	P	W	114.27(10)	C4	C3	C1	122.7(4)
O1	P	C2	79.79(16)	O2	C4	C3	59.4(3)
O1	P	C5	108.86(15)	P	C5	Si1	115.68(19)
C2	P	W	123.86(14)	P	C5	Si2	115.00(19)
C5	P	W	115.35(12)	Si2	C5	Si1	116.37(18)
C5	P	C2	109.03(18)	O3	C12	W	177.4(4)
C6	Si1	C5	106.87(17)	O4	C13	W	175.6(4)
C6	Si1	C7	106.68(18)	O5	C14	W	177.2(4)
C6	Si1	C8	110.73(19)	O6	C15	W	177.4(4)
C7	Si1	C5	112.43(17)	O7	C16	W	176.9(4)
C7	Si1	C8	107.94(19)				

Table 4: Torsion angles for **21.1f**.

A	B	C	D	Angle^o	A	B	C	D	Angle^o
W	P	O1	C1	121.2(2)	C11	Si2	C5	P	-56.6(3)
W	P	C2	C1	-111.0(2)	C11	Si2	C5	Si1	163.5(2)
W	P	C5	Si1	-102.11(18)	C12	W	P	O1	-79(2)
W	P	C5	Si2	117.73(16)	C12	W	P	C2	15(2)
P	W	C12	O3	1(10)	C12	W	P	C5	154(2)
P	W	C13	O4	-102(5)	C12	W	C13	O4	81(5)
P	W	C14	O5	-178(100)	C12	W	C14	O5	1(8)
P	W	C15	O6	109(8)	C12	W	C15	O6	-75(8)
P	W	C16	O7	168(8)	C12	W	C16	O7	-11(8)
P	O1	C1	C2	1.8(3)	C13	W	P	O1	168.86(16)
P	O1	C1	C3	-119.3(3)	C13	W	P	C2	-97.2(2)
P	C2	C1	O1	-1.6(3)	C13	W	P	C5	41.57(18)
P	C2	C1	C3	118.2(4)	C13	W	C12	O3	113(9)
O1	P	C2	C1	1.4(2)	C13	W	C14	O5	91(8)
O1	P	C5	Si1	127.92(19)	C13	W	C15	O6	35(9)
O1	P	C5	Si2	-12.2(2)	C13	W	C16	O7	-101(8)
O1	C1	C3	O2	49.9(5)	C14	W	P	O1	82.19(16)
O1	C1	C3	C4	-19.4(6)	C14	W	P	C2	176.1(2)
C2	P	O1	C1	-1.5(2)	C14	W	P	C5	-45.10(17)
C2	P	C5	Si1	42.5(3)	C14	W	C12	O3	-161(9)
C2	P	C5	Si2	-97.6(2)	C14	W	C13	O4	-9(5)
C2	C1	C3	O2	-60.8(5)	C14	W	C15	O6	15(8)
C2	C1	C3	C4	-130.1(4)	C14	W	C16	O7	22(10)
C1	C3	C4	O2	102.1(5)	C15	W	P	O1	-4.69(15)
C4	O2	C3	C1	-114.8(4)	C15	W	P	C2	89.23(19)
C5	P	O1	C1	-108.2(2)	C15	W	P	C5	-131.98(17)
C5	P	C2	C1	108.0(3)	C15	W	C12	O3	-74(9)
C6	Si1	C5	P	137.3(2)	C15	W	C13	O4	-29(6)
C6	Si1	C5	Si2	-83.1(2)	C15	W	C14	O5	-91(8)
C7	Si1	C5	P	20.6(3)	C15	W	C16	O7	81(8)

C7	Si1	C5	Si2	160.19(19)	C16	W	P	O1	-95.80(17)
C8	Si1	C5	P	-101.2(2)	C16	W	P	C2	-1.9(2)
C8	Si1	C5	Si2	38.4(3)	C16	W	P	C5	136.91(19)
C9	Si2	C5	P	-172.5(2)	C16	W	C12	O3	17(9)
C9	Si2	C5	Si1	47.7(3)	C16	W	C13	O4	168(5)
C10	Si2	C5	P	65.9(3)	C16	W	C14	O5	-32(10)
C10	Si2	C5	Si1	-74.0(2)	C16	W	C15	O6	-162(8)

12.15 Pentacarbonyl{4-(trifluoromethyl)-2-[bis(trimethylsilyl)methyl]-1,2-oxaphosphetane- κP }tungsten(0) [21.1g]

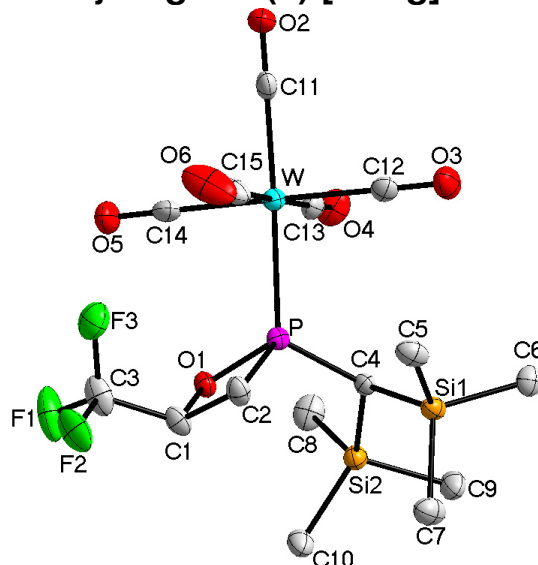


Table 1: Crystal data and structure refinement for **21.1g**.

Identification code	GSTR344, AKY-360 //GXRay3313
Crystal Habitus	colourless plate
Device Type	Nonius KappaCCD
Empirical formula	C ₁₅ H ₂₂ F ₃ O ₆ PSi ₂ W
Moiety formula	C15 H22 F3 O6 P Si2 W
Formula weight	626.33
Temperature/K	123(2)
Crystal system	orthorhombic
Space group	P2 ₁ 2 ₁ 2 ₁
a/Å	9.3854(3)
b/Å	11.0383(2)
c/Å	22.0540(6)
α/°	90.00
β/°	90.00
γ/°	90.00
Volume/Å ³	2284.77(10)
Z	4
ρ _{calc} /cm ³	1.821
μ/mm ⁻¹	5.281
F(000)	1216.0
Crystal size/mm ³	0.28 × 0.18 × 0.06
Absorption correction	Multi-Scan
Tmin; Tmax	0.3194; 0.7423
Radiation	MoKα (λ = 0.71073)

2 θ range for data collection/°	5.22 to 56°
Completeness to theta	0.993
Index ranges	-11 ≤ h ≤ 12, -11 ≤ k ≤ 14, -29 ≤ l ≤ 28
Reflections collected	23791
Independent reflections	5449 [R _{int} = 0.0529, R _{sigma} = 0.0529]
Data/restraints/parameters	5449/8/260
Goodness-of-fit on F ²	1.017
Final R indexes [I ≥ 2σ (I)]	R ₁ = 0.0280, wR ₂ = 0.0484
Final R indexes [all data]	R ₁ = 0.0340, wR ₂ = 0.0500
Largest diff. peak/hole / e Å ⁻³	1.40/-1.80
Flack parameter	0.646(6)

Table 2: Bond lengths for **21.1g**.

Atom	Atom	Length/Å	Atom	Atom	Length/Å
C1	O1	1.446(5)	C9	Si2	1.859(4)
C1	C3	1.499(6)	C10	Si2	1.863(4)
C1	C2	1.531(6)	C11	O2	1.150(5)
C1	P	2.336(4)	C11	W	2.017(4)
C2	P	1.858(4)	C12	O3	1.138(5)
C3	F2	1.332(5)	C12	W	2.047(4)
C3	F1	1.339(5)	C13	O4	1.148(5)
C3	F3	1.342(6)	C13	W	2.036(5)
C4	P	1.802(4)	C14	O5	1.145(5)
C4	Si2	1.911(4)	C14	W	2.046(5)
C4	Si1	1.919(4)	C15	O6	1.125(5)
C5	Si1	1.875(4)	C15	W	2.048(5)
C6	Si1	1.854(4)	O1	P	1.687(3)
C7	Si1	1.872(4)	P	W	2.4672(11)
C8	Si2	1.868(5)			

Table 3: Bond angles for **21.1g**.

Atom	Atom	Atom	Angle/°	Atom	Atom	Atom	Angle/°
O1	C1	C3	110.7(4)	C2	P	W	124.24(15)
O1	C1	C2	98.5(3)	C1	P	W	128.06(13)
C3	C1	C2	114.1(4)	C6	Si1	C7	111.1(2)
O1	C1	P	45.92(16)	C6	Si1	C5	107.6(2)
C3	C1	P	124.4(3)	C7	Si1	C5	107.0(2)
C2	C1	P	52.6(2)	C6	Si1	C4	106.98(19)
C1	C2	P	86.6(3)	C7	Si1	C4	111.86(19)
F2	C3	F1	107.1(4)	C5	Si1	C4	112.29(18)
F2	C3	F3	107.7(3)	C9	Si2	C10	110.1(2)
F1	C3	F3	107.3(4)	C9	Si2	C8	107.3(2)
F2	C3	C1	110.0(4)	C10	Si2	C8	109.3(2)
F1	C3	C1	111.5(4)	C9	Si2	C4	107.64(18)
F3	C3	C1	113.0(4)	C10	Si2	C4	113.16(19)
P	C4	Si2	115.9(2)	C8	Si2	C4	109.2(2)
P	C4	Si1	115.2(2)	C11	W	C13	90.98(17)
Si2	C4	Si1	116.6(2)	C11	W	C14	90.84(17)
O2	C11	W	178.5(4)	C13	W	C14	88.19(18)
O3	C12	W	176.7(4)	C11	W	C12	89.62(17)

O4	C13	W	177.4(4)	C13	W	C12	87.15(18)
O5	C14	W	177.4(4)	C14	W	C12	175.32(19)
O6	C15	W	178.7(5)	C11	W	C15	88.02(19)
C1	O1	P	96.1(2)	C13	W	C15	178.5(2)
O1	P	C4	108.24(16)	C14	W	C15	90.8(2)
O1	P	C2	78.83(17)	C12	W	C15	93.9(2)
C4	P	C2	108.5(2)	C11	W	P	177.25(12)
O1	P	C1	37.99(14)	C13	W	P	91.46(13)
C4	P	C1	114.83(18)	C14	W	P	87.98(12)
C2	P	C1	40.86(17)	C12	W	P	91.76(12)
O1	P	W	114.28(11)	C15	W	P	89.52(14)
C4	P	W	116.32(13)				

Table 4: Torsion angles for **21.1g**.

A	B	C	D	Angle/°	A	B	C	D	Angle/°
O1	C1	C2	P	1.4(3)	P	C4	Si2	C8	55.2(3)
C3	C1	C2	P	-115.8(4)	Si1	C4	Si2	C8	-164.2(2)
O1	C1	C3	F2	179.5(3)	O2	C11	W	C13	-178(100)
C2	C1	C3	F2	-70.5(5)	O2	C11	W	C14	94(15)
P	C1	C3	F2	-130.5(3)	O2	C11	W	C12	-90(15)
O1	C1	C3	F1	60.9(5)	O2	C11	W	C15	3(15)
C2	C1	C3	F1	170.8(4)	O2	C11	W	P	30(17)
P	C1	C3	F1	110.9(4)	O4	C13	W	C11	-25(8)
O1	C1	C3	F3	-60.2(5)	O4	C13	W	C14	66(8)
C2	C1	C3	F3	49.8(5)	O4	C13	W	C12	-115(8)
P	C1	C3	F3	-10.2(6)	O4	C13	W	C15	21(14)
C3	C1	O1	P	118.3(3)	O4	C13	W	P	154(8)
C2	C1	O1	P	-1.6(3)	O5	C14	W	C11	92(9)
C1	O1	P	C4	107.2(3)	O5	C14	W	C13	1(9)
C1	O1	P	C2	1.3(3)	O5	C14	W	C12	-4(10)
C1	O1	P	W	-121.4(2)	O5	C14	W	C15	-180(100)
Si2	C4	P	O1	10.3(3)	O5	C14	W	P	-90(9)
Si1	C4	P	O1	-130.9(2)	O3	C12	W	C11	-77(7)
Si2	C4	P	C2	94.2(3)	O3	C12	W	C13	14(7)
Si1	C4	P	C2	-46.9(3)	O3	C12	W	C14	19(9)
Si2	C4	P	C1	50.6(3)	O3	C12	W	C15	-165(7)
Si1	C4	P	C1	-90.5(2)	O3	C12	W	P	105(7)
Si2	C4	P	W	-119.99(18)	O6	C15	W	C11	38(19)
Si1	C4	P	W	98.9(2)	O6	C15	W	C13	-8(24)
C1	C2	P	O1	-1.2(2)	O6	C15	W	C14	-52(19)
C1	C2	P	C4	-106.9(3)	O6	C15	W	C12	128(19)
C1	C2	P	W	110.7(2)	O6	C15	W	P	-140(19)
C3	C1	P	O1	-86.2(4)	O1	P	W	C11	74(3)
C2	C1	P	O1	178.1(4)	C4	P	W	C11	-158(3)
O1	C1	P	C4	-88.2(3)	C2	P	W	C11	-19(3)
C3	C1	P	C4	-174.4(3)	C1	P	W	C11	33(3)
C2	C1	P	C4	89.9(3)	O1	P	W	C13	-78.33(16)
O1	C1	P	C2	-178.1(4)	C4	P	W	C13	48.98(19)
C3	C1	P	C2	95.7(4)	C2	P	W	C13	-171.2(2)
O1	C1	P	W	81.1(2)	C1	P	W	C13	-120.19(19)
C3	C1	P	W	-5.0(4)	O1	P	W	C14	9.80(17)

C2	C1	P	W	-100.8(3)	C4	P	W	C14	137.1(2)
P	C4	Si1	C6	-135.9(2)	C2	P	W	C14	-83.1(2)
Si2	C4	Si1	C6	83.3(2)	C1	P	W	C14	-32.1(2)
P	C4	Si1	C7	102.2(3)	O1	P	W	C12	-165.53(16)
Si2	C4	Si1	C7	-38.6(3)	C4	P	W	C12	-38.21(19)
P	C4	Si1	C5	-18.1(3)	C2	P	W	C12	101.6(2)
Si2	C4	Si1	C5	-158.9(2)	C1	P	W	C12	152.6(2)
P	C4	Si2	C9	171.4(2)	O1	P	W	C15	100.59(19)
Si1	C4	Si2	C9	-48.0(3)	C4	P	W	C15	-132.1(2)
P	C4	Si2	C10	-66.8(3)	C2	P	W	C15	7.7(2)
Si1	C4	Si2	C10	73.8(3)	C1	P	W	C15	58.7(2)

12.16 Pentacarbonyl{4,4-dimethyl-2-[bis(trimethylsilyl)methyl]-1,2-oxaphosphetane- κ P}tungsten(0) [25.1a]

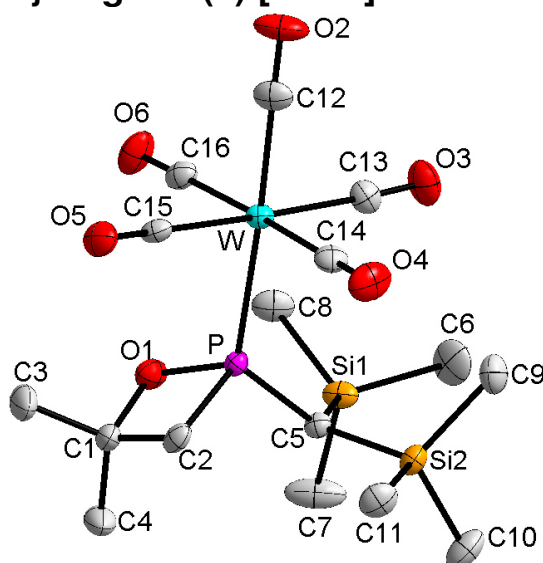


Table 1: Crystal data and structure refinement for **25.1a**.

Identification code	GSTR390, AKY-469-F2 // GXray3852f
Device Type	Bruker X8-KappaApexII
Empirical formula	C ₁₆ H ₂₇ O ₆ PSi ₂ W
Formula weight	586.37
Temperature/K	100
Crystal system	monoclinic
Space group	P2 ₁ /n
a/Å	10.3369(6)
b/Å	21.4329(12)
c/Å	10.6585(6)
α /°	90
β /°	98.7415(18)
γ /°	90
Volume/Å ³	2334.0(2)
Z	4
$\rho_{\text{calc}}/\text{cm}^3$	1.669
μ/mm^{-1}	5.146
F(000)	1152.0
Crystal size/mm ³	0.14 × 0.12 × 0.03
Absorption correction	empirical

Tmin; Tmax	0.5236; 0.7460
Radiation	MoK α (λ = 0.71073)
2 θ range for data collection/ $^{\circ}$	6.374 to 55.996 $^{\circ}$
Completeness to theta	0.993
Index ranges	-13 \leq h \leq 13, -28 \leq k \leq 28, -14 \leq l \leq 14
Reflections collected	20193
Independent reflections	5602 [R_{int} = 0.0343, R_{sigma} = 0.0333]
Data/restraints/parameters	5602/1/243
Goodness-of-fit on F^2	1.051
Final R indexes [$I \geq 2\sigma(I)$]	R_1 = 0.0244, wR_2 = 0.0423
Final R indexes [all data]	R_1 = 0.0318, wR_2 = 0.0439
Largest diff. peak/hole / e \AA^{-3}	0.60/-0.59

Table 2: Bond lengths for **25.1a**.

Atom	Atom	Length/ \AA	Atom	Atom	Length/ \AA
W1	P1	2.4879(7)	Si2	C5	1.902(3)
W1	C15	2.044(3)	Si2	C9	1.867(3)
W1	C13	2.045(3)	Si2	C11	1.866(3)
W1	C16	2.060(3)	Si2	C10	1.866(3)
W1	C14	2.025(3)	O5	C15	1.136(3)
W1	C12	2.017(3)	O1	C1	1.493(4)
P1	C5	1.809(3)	C2	C1	1.537(4)
P1	O1	1.664(2)	O2	C12	1.141(4)
P1	C2	1.804(3)	O4	C14	1.151(4)
Si1	C7	1.865(3)	C13	O3	1.133(4)
Si1	C5	1.917(3)	C1	C3	1.505(4)
Si1	C8	1.857(3)	C1	C4	1.520(4)
Si1	C6	1.865(4)	C16	O6	1.134(4)

Table 3: Bond angles for **25.1a**.

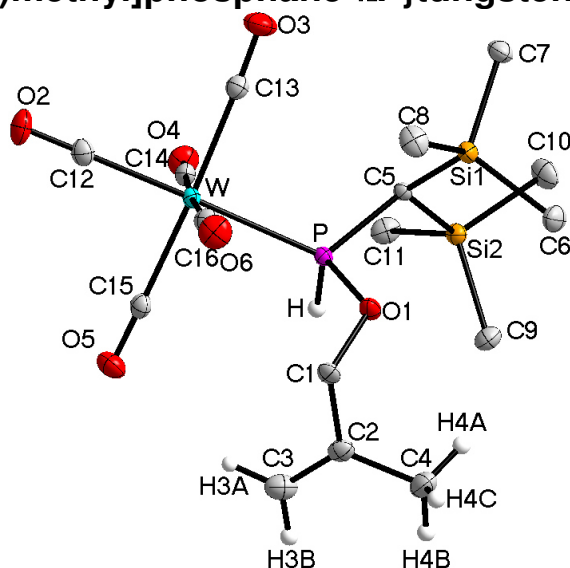
Atom	Atom	Atom	Angle/ $^{\circ}$	Atom	Atom	Atom	Angle/ $^{\circ}$
C15	W1	P1	88.90(8)	C8	Si1	C6	105.65(17)
C15	W1	C13	177.06(11)	C6	Si1	C5	114.90(15)
C15	W1	C16	89.88(12)	C9	Si2	C5	114.26(14)
C13	W1	P1	93.80(9)	C11	Si2	C5	110.38(14)
C13	W1	C16	91.42(12)	C11	Si2	C9	107.87(15)
C16	W1	P1	87.15(8)	C11	Si2	C10	108.31(16)
C14	W1	P1	92.06(8)	C10	Si2	C5	106.85(14)
C14	W1	C15	86.91(12)	C10	Si2	C9	109.03(17)
C14	W1	C13	91.82(12)	P1	C5	Si1	115.58(15)
C14	W1	C16	176.72(13)	P1	C5	Si2	117.59(14)
C12	W1	P1	177.19(10)	Si2	C5	Si1	116.27(15)
C12	W1	C15	89.76(12)	C1	O1	P1	94.79(16)
C12	W1	C13	87.59(13)	C1	C2	P1	87.85(19)
C12	W1	C16	90.38(12)	O5	C15	W1	177.8(3)
C12	W1	C14	90.33(12)	O3	C13	W1	177.1(3)
C5	P1	W1	123.37(10)	O1	C1	C2	96.2(2)
O1	P1	W1	114.34(8)	O1	C1	C3	109.0(3)
O1	P1	C5	104.47(12)	O1	C1	C4	108.1(3)
O1	P1	C2	81.08(12)	C3	C1	C2	114.7(3)

C2	P1	W1	119.24(10)	C3	C1	C4	112.7(3)
C2	P1	C5	105.79(13)	C4	C1	C2	114.5(3)
C7	Si1	C5	104.17(14)	O6	C16	W1	178.1(3)
C7	Si1	C6	109.15(19)	O4	C14	W1	177.4(3)
C8	Si1	C7	109.56(16)	O2	C12	W1	179.4(3)
C8	Si1	C5	113.35(14)				

Table 4: Torsion angles for **25.1a**.

A	B	C	D	Angle/°	A	B	C	D	Angle/°
W1	P1	C5	Si1	-76.74(16)	P1	C2	C1	C4	111.6(3)
W1	P1	C5	Si2	66.76(18)	C5	P1	O1	C1	102.66(17)
W1	P1	O1	C1	-119.60(14)	C5	P1	C2	C1	-101.20(18)
W1	P1	C2	C1	114.38(15)	O1	P1	C5	Si1	56.06(18)
P1	O1	C1	C2	1.71(19)	O1	P1	C5	Si2	-160.44(15)
P1	O1	C1	C3	120.5(2)	O1	P1	C2	C1	1.42(16)
P1	O1	C1	C4	-116.6(2)	C2	P1	C5	Si1	140.69(15)
P1	C2	C1	O1	-1.57(18)	C2	P1	C5	Si2	-75.81(19)
P1	C2	C1	C3	-115.9(3)	C2	P1	O1	C1	-1.46(17)

12.17 Pentacarbonyl{[(2-methyl-2-propenyl)oxy]-[bis(trimethylsilyl)methyl]phosphane- κP }tungsten(0) [4.1d]

**Table 1:** Crystal data and structure refinement for **4.1d**.

Identification code	GSTR388, AKY-469-F1 // GXray3851f
Device Type	Bruker X8-KappaApexII
Empirical formula	C ₁₆ H ₂₇ O ₆ PSi ₂ W
Formula weight	586.37
Temperature/K	100
Crystal system	monoclinic
Space group	P2 ₁ /c
a/Å	16.7313(8)
b/Å	9.3726(4)
c/Å	14.9852(7)
α /°	90

$\beta/^\circ$	103.5173(17)
$\gamma/^\circ$	90
Volume/ \AA^3	2284.82(18)
Z	4
$\rho_{\text{calc}}/\text{cm}^3$	1.705
μ/mm^{-1}	5.257
F(000)	1152.0
Crystal size/ mm^3	0.2 × 0.06 × 0.03
Absorption correction	empirical
Tmin; Tmax	0.4035; 0.7460
Radiation	MoK α ($\lambda = 0.71073$)
2 θ range for data collection/ $^\circ$	7.64 to 55.996 $^\circ$
Completeness to theta	0.993
Index ranges	-22 ≤ h ≤ 14, -12 ≤ k ≤ 12, -19 ≤ l ≤ 19
Reflections collected	20157
Independent reflections	5488 [$R_{\text{int}} = 0.0226$, $R_{\text{sigma}} = 0.0194$]
Data/restraints/parameters	5488/0/245
Goodness-of-fit on F^2	1.138
Final R indexes [$I \geq 2\sigma(I)$]	$R_1 = 0.0160$, $wR_2 = 0.0392$
Final R indexes [all data]	$R_1 = 0.0165$, $wR_2 = 0.0394$
Largest diff. peak/hole / $e \text{\AA}^{-3}$	1.00/-1.08

Table 2: Bond lengths for 4.1d.

Atom	Atom	Length/ \AA	Atom	Atom	Length/ \AA
W	P	2.4849(4)	Si2	C9	1.865(2)
W	C12	2.0155(19)	Si2	C10	1.870(2)
W	C13	2.037(2)	Si2	C11	1.865(2)
W	C14	2.031(2)	O1	C1	1.454(2)
W	C15	2.043(2)	O2	C12	1.139(2)
W	C16	2.055(2)	O3	C13	1.135(3)
P	O1	1.6242(13)	O4	C14	1.141(2)
P	C5	1.8087(18)	O5	C15	1.136(3)
Si1	C5	1.9063(18)	O6	C16	1.134(2)
Si1	C6	1.863(2)	C1	C2	1.495(3)
Si1	C7	1.864(2)	C2	C3	1.323(3)
Si1	C8	1.865(2)	C2	C4	1.502(3)
Si2	C5	1.8986(18)			

Table 3: Bond angles for 4.1d.

Atom	Atom	Atom	Angle/ $^\circ$	Atom	Atom	Atom	Angle/ $^\circ$
C12	W	P	177.67(6)	C7	Si1	C8	107.37(10)
C12	W	C13	88.57(8)	C8	Si1	C5	113.53(9)
C12	W	C14	92.52(7)	C9	Si2	C5	110.81(9)
C12	W	C15	89.20(8)	C9	Si2	C10	109.20(10)
C12	W	C16	90.69(8)	C9	Si2	C11	110.30(10)
C13	W	P	92.81(5)	C10	Si2	C5	112.11(9)
C13	W	C15	176.26(7)	C11	Si2	C5	107.26(8)
C13	W	C16	90.01(8)	C11	Si2	C10	107.08(10)
C14	W	P	85.65(5)	C1	O1	P	119.57(11)
C14	W	C13	88.00(8)	O1	C1	C2	111.54(15)

C14	W	C15	89.10(8)	C1	C2	C4	116.24(18)
C14	W	C16	176.18(7)	C3	C2	C1	120.49(18)
C15	W	P	89.32(5)	C3	C2	C4	123.2(2)
C15	W	C16	93.02(8)	P	C5	Si1	114.51(9)
C16	W	P	91.20(5)	P	C5	Si2	110.94(9)
O1	P	W	120.82(5)	Si2	C5	Si1	116.70(9)
O1	P	C5	99.94(7)	O2	C12	W	179.6(2)
C5	P	W	119.00(6)	O3	C13	W	177.33(17)
C6	Si1	C5	111.02(8)	O4	C14	W	178.56(17)
C6	Si1	C7	111.30(9)	O5	C15	W	177.55(18)
C6	Si1	C8	107.74(10)	O6	C16	W	178.43(18)
C7	Si1	C5	105.86(8)				

Table 4: Torsion angles for 4.1d.

A	B	C	D	Angle/°	A	B	C	D	Angle/°
W	P	O1	C1	49.91(15)	C5	P	O1	C1	-177.43(13)
W	P	C5	Si1	91.80(9)	C9	Si2	C5	P	-52.23(12)
W	P	C5	Si2	-133.52(6)	C9	Si2	C5	Si1	81.36(12)
P	O1	C1	C2	93.19(17)	C10	Si2	C5	P	-174.52(10)
O1	P	C5	Si1	-41.98(10)	C10	Si2	C5	Si1	-40.92(13)
O1	P	C5	Si2	92.70(9)	C11	Si2	C5	P	68.21(11)
O1	C1	C2	C3	-113.4(2)	C11	Si2	C5	Si1	-158.19(10)
O1	C1	C2	C4	68.8(2)					

**12.18 Pentacarbonyl{4,4-bis(trifluoromethyl)-2-[bis(trimethylsilyl)methyl]-1,2-oxaphosphetane- κP }tungsten(0)
[25.1b]**

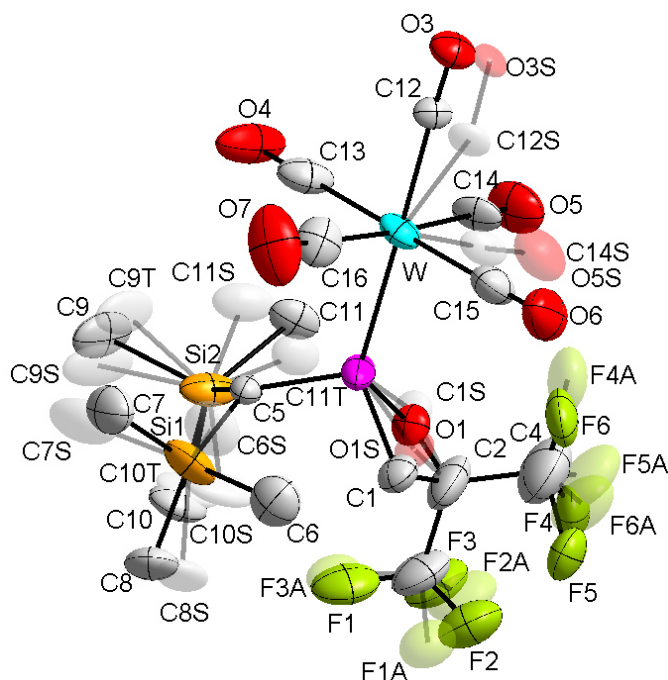


Table 1: Crystal data and structure refinement for **25.1b**.

Identification code	GSTR378, 3684f
Device Type	Bruker X8-KappaApexII
Empirical formula	C ₁₆ H ₂₁ F ₆ O ₆ PSi ₂ W
Formula weight	694.33
Temperature/K	100
Crystal system	triclinic
Space group	P $\bar{1}$
a/Å	8.9748(9)
b/Å	10.3623(9)
c/Å	15.4170(13)
α /°	70.869(5)
β /°	79.168(6)
γ /°	66.889(5)
Volume/Å ³	1243.0(2)
Z	2
$\rho_{\text{calc}}/\text{cm}^3$	1.855
μ/mm^{-1}	4.880
F(000)	672.0
Crystal size/mm ³	0.05 × 0.04 × 0.01
Absorption correction	empirical
Tmin; Tmax	0.5698; 0.7460
Radiation	MoK α (λ = 0.71073)
2 θ range for data collection/°	5.52 to 56°
Completeness to theta	0.984
Index ranges	-11 ≤ h ≤ 9, -13 ≤ k ≤ 13, -19 ≤ l ≤ 20
Reflections collected	12106
Independent reflections	5889 [R _{int} = 0.0426, R _{sigma} = 0.0712]
Data/restraints/parameters	5889/293/486
Goodness-of-fit on F ²	1.024
Final R indexes [$I \geq 2\sigma(I)$]	R ₁ = 0.0464, wR ₂ = 0.1034
Final R indexes [all data]	R ₁ = 0.0747, wR ₂ = 0.1170
Largest diff. peak/hole / e Å ⁻³	2.43/-2.73

Table 2: Bond lengths for **25.1b**.

Atom	Atom	Length/Å	Atom	Atom	Length/Å
W	P	2.4562(19)	Si2	C9T	1.8100(11)
W	C13	2.028(10)	Si2	C10T	1.8100(11)
W	C15	2.039(10)	Si2	C11T	1.8100(11)
W	C16	2.039(10)	F1	C3	1.22(2)
W	C14	2.081(12)	F6	C4	1.23(2)
W	C12	2.062(10)	F3	C3	1.403(18)
W	C12S	1.87(3)	F4	C4	1.34(4)
W	C14S	1.95(4)	F5	C4	1.76(3)
P	C2	2.317(9)	F2	C3	1.293(16)
P	C5	1.805(7)	O4	C13	1.149(11)
P	O1	1.568(12)	O6	C15	1.148(10)
P	C1	2.04(2)	O7	C16	1.139(11)
P	O1S	1.579(12)	C2	C3	1.568(15)
P	C1S	1.980(17)	C2	C4	1.531(18)
Si1	C5	1.898(7)	C2	O1	1.208(17)
Si1	C6	1.968(19)	C2	C1	1.79(2)

Si1	C7	1.750(17)	C2	O1S	1.241(16)
Si1	C8	1.886(19)	C2	C1S	1.72(2)
Si1	C6S	1.8103(11)	C3	F2A	1.20(2)
Si1	C7S	1.8104(11)	C3	F3A	1.384(10)
Si1	C8S	1.8098(11)	C3	F1A	1.51(3)
Si2	C5	1.915(7)	C4	F6A	1.151(19)
Si2	C9	1.90(4)	C4	F4A	1.49(2)
Si2	C10	1.97(3)	C4	F5A	1.36(3)
Si2	C11	2.07(3)	O3	C12	1.112(14)
Si2	C11S	1.8099(11)	O5	C14	1.092(16)
Si2	C9S	1.8101(11)	C12S	O3S	1.36(4)
Si2	C10S	1.8101(11)	C14S	O5S	1.30(5)

Table 3: Bond angles for **25.1b**.

Atom	Atom	Atom	Angle/°	Atom	Atom	Atom	Angle/°
C13	W	P	91.4(2)	C9T	Si2	C5	106.6(18)
C13	W	C15	177.7(4)	C9T	Si2	C9	15(2)
C13	W	C16	88.6(4)	C9T	Si2	C10	114(3)
C13	W	C14	87.7(6)	C9T	Si2	C11	95(2)
C13	W	C12	88.1(4)	C9T	Si2	C9S	31.5(18)
C15	W	P	89.6(2)	C9T	Si2	C10S	129.5(19)
C15	W	C16	89.3(4)	C9T	Si2	C10T	116(4)
C15	W	C14	94.3(6)	C9T	Si2	C11T	109(2)
C15	W	C12	90.8(4)	C10T	Si2	C5	119(3)
C16	W	P	90.5(3)	C10T	Si2	C9	102(4)
C16	W	C14	176.1(6)	C10T	Si2	C10	9(4)
C16	W	C12	88.5(4)	C10T	Si2	C11	111(3)
C14	W	P	91.1(4)	C10T	Si2	C10S	16(4)
C12	W	P	178.9(4)	C10T	Si2	C11T	98(3)
C12	W	C14	89.8(4)	C11T	Si2	C5	108.3(12)
C12S	W	P	159.5(16)	C11T	Si2	C9	119(2)
C12S	W	C13	102.6(12)	C11T	Si2	C10	106(2)
C12S	W	C15	76.9(12)	C11T	Si2	C11	15.1(13)
C12S	W	C16	104.5(13)	C11T	Si2	C10S	84.4(18)
C12S	W	C14	74.9(12)	C3	C2	P	125.3(7)
C12S	W	C12	21.5(13)	C3	C2	C1	102.4(11)
C12S	W	C14S	83.0(15)	C3	C2	C1S	107.3(10)
C14S	W	P	79.9(12)	C4	C2	P	120.8(9)
C14S	W	C13	100.3(12)	C4	C2	C3	113.8(9)
C14S	W	C15	81.9(12)	C4	C2	C1	113.9(12)
C14S	W	C16	166.9(14)	C4	C2	C1S	105.7(13)
C14S	W	C14	16.8(11)	O1	C2	P	38.7(7)
C14S	W	C12	101.2(11)	O1	C2	C3	114.5(11)
C2	P	W	126.2(3)	O1	C2	C4	114.3(14)
C5	P	W	116.1(2)	O1	C2	C1	95.9(10)
C5	P	C2	117.8(4)	O1	C2	O1S	78.6(9)
C5	P	C1	104.0(7)	O1	C2	C1S	17.8(8)
C5	P	C1S	106.4(6)	C1	C2	P	57.9(7)
O1	P	W	123.6(5)	O1S	C2	P	39.9(7)
O1	P	C2	28.8(6)	O1S	C2	C3	120.1(12)
O1	P	C5	111.4(5)	O1S	C2	C4	111.0(12)

O1	P	C1	76.5(7)	O1S	C2	C1	20.8(9)
O1	P	O1S	59.1(6)	O1S	C2	C1S	96.2(9)
O1	P	C1S	17.6(7)	C1S	C2	P	56.4(6)
C1	P	W	117.4(6)	C1S	C2	C1	113.7(9)
C1	P	C2	48.1(7)	F1	C3	F3	106.2(14)
O1S	P	W	117.0(4)	F1	C3	F2	116.1(17)
O1S	P	C2	30.3(6)	F1	C3	C2	111.8(13)
O1S	P	C5	117.7(5)	F1	C3	F3A	15(2)
O1S	P	C1	19.9(6)	F1	C3	F1A	83.1(15)
O1S	P	C1S	76.6(7)	F3	C3	C2	110.9(12)
C1S	P	W	116.1(6)	F3	C3	F1A	123.1(11)
C1S	P	C2	46.4(6)	F2	C3	F3	107.3(11)
C1S	P	C1	94.1(7)	F2	C3	C2	104.4(11)
C5	Si1	C6	106.5(6)	F2	C3	F3A	129.5(18)
C7	Si1	C5	112.0(7)	F2	C3	F1A	33.1(9)
C7	Si1	C6	108.1(10)	F2A	C3	F1	126(2)
C7	Si1	C8	112.6(11)	F2A	C3	F3	26.3(12)
C7	Si1	C6S	61.6(11)	F2A	C3	F2	82.2(14)
C7	Si1	C7S	35.0(10)	F2A	C3	C2	111.1(15)
C7	Si1	C8S	119.2(12)	F2A	C3	F3A	117.1(15)
C8	Si1	C5	113.5(9)	F2A	C3	F1A	104.7(15)
C8	Si1	C6	103.4(9)	F3A	C3	F3	94.2(16)
C6S	Si1	C5	109.2(7)	F3A	C3	C2	109.5(15)
C6S	Si1	C6	49.1(9)	F3A	C3	F1A	97.0(17)
C6S	Si1	C8	134.8(10)	F1A	C3	C2	116.9(11)
C6S	Si1	C7S	96.7(12)	F6	C4	F4	144(2)
C7S	Si1	C5	101.0(8)	F6	C4	F5	91.4(18)
C7S	Si1	C6	141.6(10)	F6	C4	C2	109.0(13)
C7S	Si1	C8	89.4(11)	F6	C4	F4A	44.0(12)
C8S	Si1	C5	123.0(10)	F6	C4	F5A	122(2)
C8S	Si1	C6	80.3(10)	F4	C4	F5	96.6(19)
C8S	Si1	C8	23.1(8)	F4	C4	C2	104.4(16)
C8S	Si1	C6S	115.7(12)	F4	C4	F4A	111(2)
C8S	Si1	C7S	106.5(12)	F4	C4	F5A	24.0(16)
C5	Si2	C10	113(2)	C2	C4	F5	97.3(13)
C5	Si2	C11	107.1(11)	F6A	C4	F6	72.4(17)
C9	Si2	C5	110.6(19)	F6A	C4	F4	102.3(19)
C9	Si2	C10	100(3)	F6A	C4	F5	25.2(11)
C9	Si2	C11	107(2)	F6A	C4	C2	118.7(19)
C10	Si2	C11	119(2)	F6A	C4	F4A	108.5(17)
C11S	Si2	C5	116.6(7)	F6A	C4	F5A	108.5(15)
C11S	Si2	C9	82.7(19)	F4A	C4	F5	132.3(15)
C11S	Si2	C10	126(2)	F4A	C4	C2	111.1(11)
C11S	Si2	C11	24.4(10)	F5A	C4	F5	112.4(14)
C11S	Si2	C9S	101.1(12)	F5A	C4	C2	118.0(18)
C11S	Si2	C10S	110.8(17)	F5A	C4	F4A	87.6(18)
C11S	Si2	C9T	71(2)	P	C5	Si1	118.8(4)
C11S	Si2	C10T	118(3)	P	C5	Si2	114.5(4)
C11S	Si2	C11T	37.8(13)	Si1	C5	Si2	117.6(3)
C9S	Si2	C5	101.4(9)	O4	C13	W	177.5(9)
C9S	Si2	C9	18.4(17)	O6	C15	W	178.8(9)
C9S	Si2	C10	90(3)	O7	C16	W	177.7(9)
C9S	Si2	C11	125.5(13)	O5	C14	W	177.0(12)

C9S	Si2	C10S	110.1(15)	O3	C12	W	177.6(10)
C9S	Si2	C10T	94(3)	O3S	C12S	W	158(3)
C9S	Si2	C11T	137.3(14)	O5S	C14S	W	177(3)
C10S	Si2	C5	115.2(15)	C2	O1	P	112.5(11)
C10S	Si2	C9	116.9(19)	C2	C1	P	74.0(9)
C10S	Si2	C10	23(2)	C2	O1S	P	109.9(11)
C10S	Si2	C11	98.4(17)	C2	C1S	P	77.2(8)

Table 4: Torsion angles for **25.1b**.

A	B	C	D	Angle/°	A	B	C	D	Angle/°
W	P	C2	C3	178.6(8)	C14	W	C12S	O3S	130(6)
W	P	C2	C4	-4.2(14)	C14	W	C14S	O5S	35(50)
W	P	C2	O1	-95.5(11)	C12	W	P	C2	-149(15)
W	P	C2	C1	96.3(9)	C12	W	P	C5	31(15)
W	P	C2	O1S	82.2(11)	C12	W	P	O1	175(100)
W	P	C2	C1S	-93.2(9)	C12	W	P	C1	-93(15)
W	P	C5	Si1	-109.0(3)	C12	W	P	O1S	-115(15)
W	P	C5	Si2	104.9(3)	C12	W	P	C1S	157(15)
W	P	O1	C2	105.1(11)	C12	W	C13	O4	-61(17)
W	P	C1	C2	-115.3(6)	C12	W	C15	O6	35(41)
W	P	O1S	C2	-116.1(9)	C12	W	C16	O7	1(21)
W	P	C1S	C2	116.2(6)	C12	W	C14	O5	-165(27)
P	W	C13	O4	118(17)	C12	W	C12S	O3S	-3(5)
P	W	C15	O6	-144(41)	C12	W	C14S	O5S	-13(53)
P	W	C16	O7	-178(100)	C12S	W	P	C2	10(2)
P	W	C14	O5	14(27)	C12S	W	P	C5	-170(2)
P	W	C12	O3	115(26)	C12S	W	P	O1	-25(2)
P	W	C12S	O3S	179(5)	C12S	W	P	C1	66(2)
P	W	C14S	O5S	167(53)	C12S	W	P	O1S	44(2)
P	C2	C3	F1	-12.6(19)	C12S	W	P	C1S	-44(2)
P	C2	C3	F3	105.8(13)	C12S	W	C13	O4	-77(17)
P	C2	C3	F2	-138.9(13)	C12S	W	C15	O6	52(41)
P	C2	C3	F2A	134.0(18)	C12S	W	C16	O7	16(21)
P	C2	C3	F3A	3(2)	C12S	W	C14	O5	179(100)
P	C2	C3	F1A	-105.9(16)	C12S	W	C12	O3	-45(23)
P	C2	C4	F6	31(2)	C12S	W	C14S	O5S	-24(53)
P	C2	C4	F4	-136.4(19)	C14S	W	P	C2	43.6(12)
P	C2	C4	F5	124.7(10)	C14S	W	P	C5	-136.1(12)
P	C2	C4	F6A	110.5(17)	C14S	W	P	O1	8.4(13)
P	C2	C4	F4A	-16(2)	C14S	W	P	C1	100.1(13)
P	C2	C4	F5A	-115.0(17)	C14S	W	P	O1S	77.7(13)
C2	P	C5	Si1	71.3(6)	C14S	W	P	C1S	-10.0(13)
C2	P	C5	Si2	-74.8(5)	C14S	W	C13	O4	-162(17)
C3	C2	C4	F6	-151.8(19)	C14S	W	C15	O6	136(41)
C3	C2	C4	F4	41(2)	C14S	W	C16	O7	140(21)
C3	C2	C4	F5	-57.8(15)	C14S	W	C14	O5	62(26)
C3	C2	C4	F6A	-72(2)	C14S	W	C12	O3	-78(24)
C3	C2	C4	F4A	161.3(14)	C14S	W	C12S	O3S	145(6)
C3	C2	C4	F5A	62(2)	O1	P	C2	C3	-85.9(14)
C3	C2	O1	P	116.6(11)	O1	P	C2	C4	91.3(17)
C3	C2	C1	P	-124.1(8)	O1	P	C2	C1	-168.2(15)

C3	C2	O1S	P	-110.3(11)	O1	P	C2	O1S	177.6(17)
C3	C2	C1S	P	121.3(8)	O1	P	C2	C1S	2.3(15)
C4	C2	C3	F1	170.1(17)	O1	P	C5	Si1	102.3(6)
C4	C2	C3	F3	-71.6(17)	O1	P	C5	Si2	-43.8(6)
C4	C2	C3	F2	43.7(18)	O1	P	C1	C2	5.8(7)
C4	C2	C3	F2A	-43(2)	O1	P	O1S	C2	-1.3(10)
C4	C2	C3	F3A	-174.3(19)	O1	P	C1S	C2	-4(2)
C4	C2	C3	F1A	76.7(19)	O1	C2	C3	F1	-56(2)
C4	C2	O1	P	-109.6(13)	O1	C2	C3	F3	62.5(16)
C4	C2	C1	P	112.6(11)	O1	C2	C3	F2	177.8(15)
C4	C2	O1S	P	113.4(12)	O1	C2	C3	F2A	91(2)
C4	C2	C1S	P	-116.9(10)	O1	C2	C3	F3A	-40(2)
C5	P	C2	C3	-1.7(12)	O1	C2	C3	F1A	-149.2(17)
C5	P	C2	C4	175.5(12)	O1	C2	C4	F6	74(2)
C5	P	C2	O1	84.2(12)	O1	C2	C4	F4	-93(2)
C5	P	C2	C1	-84.0(9)	O1	C2	C4	F5	168.1(12)
C5	P	C2	O1S	-98.2(11)	O1	C2	C4	F6A	153.9(17)
C5	P	C2	C1S	86.5(9)	O1	C2	C4	F4A	27(2)
C5	P	O1	C2	-109.0(11)	O1	C2	C4	F5A	-72(2)
C5	P	C1	C2	114.9(7)	O1	C2	C1	P	-7.4(9)
C5	P	O1S	C2	98.2(10)	O1	C2	O1S	P	1.5(11)
C5	P	C1S	C2	-113.0(7)	O1	C2	C1S	P	5(3)
C13	W	P	C2	143.8(5)	C1	P	C2	C3	82.3(14)
C13	W	P	C5	-35.8(4)	C1	P	C2	C4	-100.5(15)
C13	W	P	O1	108.6(7)	C1	P	C2	O1	168.2(15)
C13	W	P	C1	-159.7(7)	C1	P	C2	O1S	-14.1(14)
C13	W	P	O1S	177.9(6)	C1	P	C2	C1S	170.5(13)
C13	W	P	C1S	90.3(7)	C1	P	C5	Si1	21.6(7)
C13	W	C15	O6	-26(46)	C1	P	C5	Si2	-124.6(6)
C13	W	C16	O7	-87(21)	C1	P	O1	C2	-9.0(12)
C13	W	C14	O5	-77(27)	C1	P	O1S	C2	148(3)
C13	W	C12	O3	-178(100)	C1	P	C1S	C2	-7.1(10)
C13	W	C12S	O3S	46(6)	C1	C2	C3	F1	46.6(17)
C13	W	C14S	O5S	77(53)	C1	C2	C3	F3	165.0(13)
C15	W	P	C2	-38.2(5)	C1	C2	C3	F2	-79.7(15)
C15	W	P	C5	142.1(4)	C1	C2	C3	F2A	-166.7(18)
C15	W	P	O1	-73.4(7)	C1	C2	C3	F3A	62.3(18)
C15	W	P	C1	18.2(7)	C1	C2	C3	F1A	-46.7(17)
C15	W	P	O1S	-4.2(6)	C1	C2	C4	F6	-35(2)
C15	W	P	C1S	-91.8(7)	C1	C2	C4	F4	158(2)
C15	W	C13	O4	0(23)	C1	C2	C4	F5	59.2(14)
C15	W	C16	O7	92(21)	C1	C2	C4	F6A	45(2)
C15	W	C14	O5	104(27)	C1	C2	C4	F4A	-81.8(18)
C15	W	C12	O3	4(24)	C1	C2	C4	F5A	179.4(17)
C15	W	C12S	O3S	-132(6)	C1	C2	O1	P	10.0(13)
C15	W	C14S	O5S	-102(53)	C1	C2	O1S	P	-144(3)
C16	W	P	C2	-127.5(5)	C1	C2	C1S	P	8.8(12)
C16	W	P	C5	52.8(4)	O1S	P	C2	C3	96.4(15)
C16	W	P	O1	-162.7(6)	O1S	P	C2	C4	-86.4(15)
C16	W	P	C1	-71.1(7)	O1S	P	C2	O1	-177.6(17)
C16	W	P	O1S	-93.4(6)	O1S	P	C2	C1	14.1(14)
C16	W	P	C1S	178.9(7)	O1S	P	C2	C1S	-175.4(14)
C16	W	C13	O4	27(17)	O1S	P	C5	Si1	37.0(7)

C16	W	C15	O6	-53(41)	O1S	P	C5	Si2	-109.1(6)
C16	W	C14	O5	-100(26)	O1S	P	O1	C2	1.4(10)
C16	W	C12	O3	93(24)	O1S	P	C1	C2	-21(2)
C16	W	C12S	O3S	-46(6)	O1S	P	C1S	C2	2.4(7)
C16	W	C14S	O5S	-150(50)	O1S	C2	C3	F1	35(2)
C9	Si2	C5	P	-141.1(16)	O1S	C2	C3	F3	153.2(14)
C9	Si2	C5	Si1	72.3(16)	O1S	C2	C3	F2	-91.5(16)
C10	Si2	C5	P	108(3)	O1S	C2	C3	F2A	-178.5(19)
C10	Si2	C5	Si1	-39(3)	O1S	C2	C3	F3A	51(2)
C11	Si2	C5	P	-24.7(11)	O1S	C2	C3	F1A	-58.5(19)
C11	Si2	C5	Si1	-171.3(11)	O1S	C2	C4	F6	-13(2)
C11S	Si2	C5	P	-49.0(10)	O1S	C2	C4	F4	-180(2)
C11S	Si2	C5	Si1	164.4(10)	O1S	C2	C4	F5	81.5(14)
C9S	Si2	C5	P	-157.7(9)	O1S	C2	C4	F6A	67(2)
C9S	Si2	C5	Si1	55.7(9)	O1S	C2	C4	F4A	-60(2)
C10S	Si2	C5	P	83.5(14)	O1S	C2	C4	F5A	-158.3(17)
C10S	Si2	C5	Si1	-63.1(14)	O1S	C2	O1	P	-1.5(11)
C9T	Si2	C5	P	-125.7(17)	O1S	C2	C1	P	26(3)
C9T	Si2	C5	Si1	87.7(18)	O1S	C2	C1S	P	-3.0(9)
C10T	Si2	C5	P	102(3)	C1S	P	C2	C3	-88.2(13)
C10T	Si2	C5	Si1	-45(3)	C1S	P	C2	C4	89.0(15)
C11T	Si2	C5	P	-8.9(12)	C1S	P	C2	O1	-2.3(15)
C11T	Si2	C5	Si1	-155.5(12)	C1S	P	C2	C1	-170.5(13)
C6	Si1	C5	P	1.0(7)	C1S	P	C2	O1S	175.4(14)
C6	Si1	C5	Si2	146.1(7)	C1S	P	C5	Si1	120.2(7)
C7	Si1	C5	P	119.0(9)	C1S	P	C5	Si2	-26.0(7)
C7	Si1	C5	Si2	-95.8(9)	C1S	P	O1	C2	175(4)
C8	Si1	C5	P	-112.1(9)	C1S	P	C1	C2	6.9(9)
C8	Si1	C5	Si2	33.1(9)	C1S	P	O1S	C2	-3.4(11)
C6S	Si1	C5	P	52.7(9)	C1S	C2	C3	F1	-73.3(17)
C6S	Si1	C5	Si2	-162.2(9)	C1S	C2	C3	F3	45.0(14)
C7S	Si1	C5	P	153.8(10)	C1S	C2	C3	F2	160.3(14)
C7S	Si1	C5	Si2	-61.0(10)	C1S	C2	C3	F2A	73.3(19)
C8S	Si1	C5	P	-88.0(11)	C1S	C2	C3	F3A	-57.7(19)
C8S	Si1	C5	Si2	57.1(11)	C1S	C2	C3	F1A	-166.7(15)
C14	W	P	C2	56.1(7)	C1S	C2	C4	F6	91(2)
C14	W	P	C5	-123.6(6)	C1S	C2	C4	F4	-76(2)
C14	W	P	O1	20.9(8)	C1S	C2	C4	F5	-175.3(10)
C14	W	P	C1	112.5(8)	C1S	C2	C4	F6A	170.5(16)
C14	W	P	O1S	90.2(7)	C1S	C2	C4	F4A	43.7(18)
C14	W	P	C1S	2.5(8)	C1S	C2	C4	F5A	-55(2)
C14	W	C13	O4	-151(17)	C1S	C2	O1	P	-174(4)
C14	W	C15	O6	125(41)	C1S	C2	C1	P	-8.6(12)
C14	W	C16	O7	-64(23)	C1S	C2	O1S	P	3.9(12)
C14	W	C12	O3	-90(24)					

12.19 Pentacarbonyl[4-(trifluoromethyl)-2-(1,2,3,4,5-pentamethylcyclopenta-2,4-dien-1-yl)-1,2-oxaphosphetane- κP]tungsten(0) [21.2g]

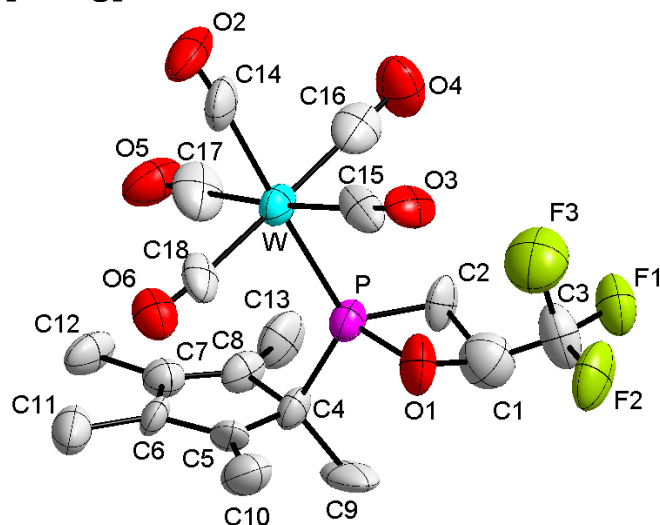


Table 1: Crystal data and structure refinement for **21.2g**.

Identification code	GSTR406, AKY-490 // GXray3961g
Device Type	Bruker X8-KappaApexII
Empirical formula	C ₁₈ H ₁₈ O ₆ F ₃ PW
Moiety formula	C ₁₈ H ₁₈ F ₃ O ₆ P W
Formula weight	602.14
Temperature/K	100
Crystal system	monoclinic
Space group	P2 ₁ /c
a/Å	9.86(2)
b/Å	14.30(3)
c/Å	16.92(3)
α/°	90
β/°	94.00(11)
γ/°	90
Volume/Å ³	2381(8)
Z	4
ρ _{calc} /cm ³	1.680
μ/mm ⁻¹	4.969
F(000)	1160.0
Crystal size/mm ³	0.1 × 0.1 × 0.06
Absorption correction	empirical
Tmin; Tmax	0.3735; 0.7459
Radiation	MoKα (λ = 0.71073)
2θ range for data collection/°	4.14 to 55.986°
Completeness to theta	0.993
Index ranges	-12 ≤ h ≤ 12, -13 ≤ k ≤ 18, -22 ≤ l ≤ 20
Reflections collected	29201
Independent reflections	5670 [R _{int} = 0.3262, R _{sigma} = 0.4193]
Data/restraints/parameters	5670/19/267
Goodness-of-fit on F ²	0.852
Final R indexes [I >= 2σ (I)]	R ₁ = 0.1136, wR ₂ = 0.2527
Final R indexes [all data]	R ₁ = 0.2554, wR ₂ = 0.3744
Largest diff. peak/hole / e Å ⁻³	2.79/-3.90

Table 2: Bond lengths for **21.2g**.

Atom	Atom	Length/Å	Atom	Atom	Length/Å
W	P	2.554(7)	O4	C16	1.20(4)
W	C14	2.17(3)	O5	C17	1.15(3)
W	C15	2.11(3)	O6	C18	1.24(3)
W	C16	2.17(4)	C1	C2	1.62(4)
W	C17	2.13(3)	C1	C3	1.43(4)
W	C18	2.16(3)	C4	C5	1.59(3)
P	O1	1.761(17)	C4	C8	1.61(3)
P	C2	1.95(2)	C4	C9	1.57(3)
P	C4	1.96(2)	C5	C6	1.42(3)
F1	C3	1.42(3)	C5	C10	1.52(3)
F2	C3	1.35(3)	C6	C7	1.53(3)
F3	C3	1.57(3)	C6	C11	1.59(3)
O1	C1	1.60(3)	C7	C8	1.42(3)
O2	C14	1.14(3)	C7	C12	1.60(3)
O3	C15	1.23(3)	C8	C13	1.56(4)

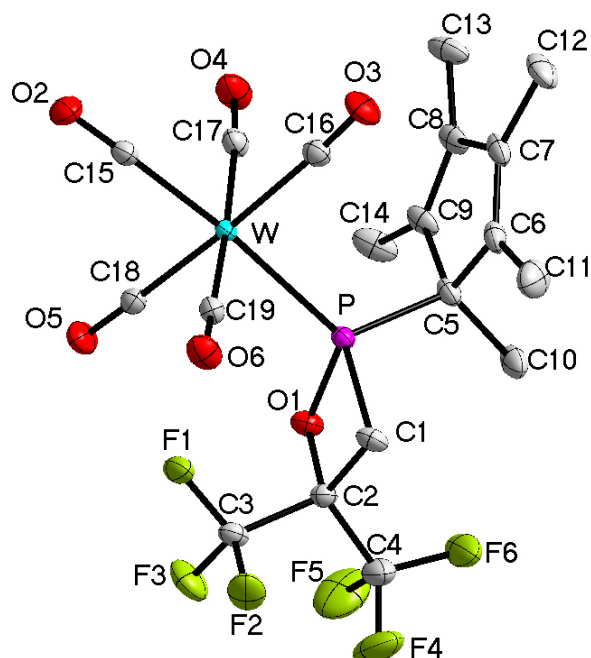
Table 3: Bond angles for **21.2g**.

Atom	Atom	Atom	Angle/°	Atom	Atom	Atom	Angle/°
C14	W	P	177.8(8)	F2	C3	F1	111(2)
C14	W	C16	89.1(11)	F2	C3	F3	100.1(19)
C15	W	P	86.7(6)	F2	C3	C1	121(3)
C15	W	C14	92.9(9)	C1	C3	F3	102(2)
C15	W	C16	86.8(10)	C5	C4	P	107.0(14)
C15	W	C17	174.8(11)	C5	C4	C8	102.6(17)
C15	W	C18	91.6(9)	C8	C4	P	105.7(14)
C16	W	P	88.7(7)	C9	C4	P	112.7(15)
C17	W	P	94.9(8)	C9	C4	C5	111.3(18)
C17	W	C14	85.2(10)	C9	C4	C8	116.7(19)
C17	W	C16	88.4(12)	C6	C5	C4	110.3(19)
C17	W	C18	93.2(11)	C6	C5	C10	125(2)
C18	W	P	93.0(6)	C10	C5	C4	124.8(19)
C18	W	C14	89.2(10)	C5	C6	C7	108.0(19)
C18	W	C16	177.5(8)	C5	C6	C11	131(2)
O1	P	W	115.1(7)	C7	C6	C11	121.2(18)
O1	P	C2	79.1(8)	C6	C7	C12	121(2)
O1	P	C4	103.9(9)	C8	C7	C6	111.4(18)
C2	P	W	119.6(8)	C8	C7	C12	128(2)
C2	P	C4	106.6(10)	C7	C8	C4	108(2)
C4	P	W	123.2(6)	C7	C8	C13	130.4(19)
C1	O1	P	96.0(15)	C13	C8	C4	122(2)
O1	C1	C2	95(2)	O2	C14	W	175(3)
C3	C1	O1	114(2)	O3	C15	W	176.5(19)
C3	C1	C2	119(3)	O4	C16	W	179(3)
C1	C2	P	88.4(17)	O5	C17	W	177(3)
F1	C3	F3	99(2)	O6	C18	W	174.1(18)
F1	C3	C1	118(2)				

Table 4: Torsion angles for **21.2g**.

A	B	C	D	Angle/°	A	B	C	D	Angle/°
W	P	O1	C1	-127.4(14)	C5	C4	C8	C7	1(2)
P	O1	C1	C2	11.5(17)	C5	C4	C8	C13	-176.7(19)
P	O1	C1	C3	136(2)	C5	C6	C7	C8	-2(2)
P	C4	C5	C6	108.7(17)	C5	C6	C7	C12	176.4(18)
P	C4	C5	C10	-68(2)	C6	C7	C8	C4	0(2)
P	C4	C8	C7	-110.8(17)	C6	C7	C8	C13	178(2)
P	C4	C8	C13	71(2)	C8	C4	C5	C6	-2(2)
O1	C1	C2	P	-10.3(15)	C8	C4	C5	C10	-179(2)
O1	C1	C3	F1	-158(2)	C9	C4	C5	C6	-128(2)
O1	C1	C3	F2	59(4)	C9	C4	C5	C10	55(3)
O1	C1	C3	F3	-51(3)	C9	C4	C8	C7	123(2)
C2	P	O1	C1	-9.6(15)	C9	C4	C8	C13	-55(3)
C2	C1	C3	F1	-47(4)	C10	C5	C6	C7	179.5(19)
C2	C1	C3	F2	169(2)	C10	C5	C6	C11	-3(4)
C2	C1	C3	F3	60(3)	C11	C6	C7	C8	-179.7(18)
C3	C1	C2	P	-132(3)	C11	C6	C7	C12	-2(3)
C4	P	O1	C1	95.0(16)	C12	C7	C8	C4	-177.7(19)
C4	C5	C6	C7	2(2)	C12	C7	C8	C13	0(4)
C4	C5	C6	C11	-179.9(19)					

12.20 Pentacarbonyl[4,4-bis(trifluoromethyl)-2-(1,2,3,4,5-pentamethylcyclopenta-2,4-dien-1-yl)-1,2-oxaphosphetane- κP]tungsten(0) [25.2b]

**Table 1:** Crystal data and structure refinement for **25.2b**.

Identification code	GSTR380, 3707f
Device Type	Bruker X8-KappaApexII
Empirical formula	C ₁₉ H ₁₇ F ₆ O ₆ PW
Formula weight	670.15

Temperature/K	100
Crystal system	monoclinic
Space group	P2 ₁ /c
a/Å	12.3230(7)
b/Å	14.0254(7)
c/Å	16.2599(7)
α/°	90.00
β/°	125.699(3)
γ/°	90.00
Volume/Å ³	2282.2(2)
Z	4
ρ _{calc} /cm ³	1.950
μ/mm ⁻¹	5.213
F(000)	1288.0
Crystal size/mm ³	0.2 × 0.13 × 0.05
Absorption correction	empirical
Tmin; Tmax	0.4590; 0.7460
Radiation	MoKα (λ = 0.71073)
2θ range for data collection/°	6.72 to 56°
Completeness to theta	0.997
Index ranges	-16 ≤ h ≤ 16, -18 ≤ k ≤ 18, -21 ≤ l ≤ 21
Reflections collected	48670
Independent reflections	5508 [R _{int} = 0.0264, R _{sigma} = 0.0144]
Data/restraints/parameters	5508/2/298
Goodness-of-fit on F ²	1.091
Final R indexes [I ≥ 2σ (I)]	R ₁ = 0.0171, wR ₂ = 0.0413
Final R indexes [all data]	R ₁ = 0.0191, wR ₂ = 0.0422
Largest diff. peak/hole / e Å ⁻³	1.59/-0.91

Table 2: Bond lengths for 25.2b.

Atom	Atom	Length/Å	Atom	Atom	Length/Å
W	P	2.4768(6)	O3	C16	1.136(3)
W	C15	2.012(2)	O4	C17	1.138(3)
W	C16	2.054(2)	O5	C18	1.136(3)
W	C17	2.057(3)	O6	C19	1.139(3)
W	C18	2.055(2)	C1	C2	1.518(3)
W	C19	2.047(2)	C2	C3	1.541(3)
P	O1	1.7272(17)	C2	C4	1.545(4)
P	C1	1.835(2)	C5	C6	1.524(3)
P	C2	2.349(2)	C5	C9	1.513(4)
P	C5	1.849(2)	C5	C10	1.538(3)
F1	C3	1.326(3)	O6	C7	1.346(4)
F2	C3	1.332(3)	O6	C11	1.502(4)
F3	C3	1.335(3)	C7	C8	1.473(4)
F4	C4	1.299(4)	C7	C12	1.509(3)
F5	C4	1.355(4)	C8	C9	1.351(3)
F6	C4	1.310(3)	C8	C13	1.499(4)
O1	C2	1.446(3)	C9	C14	1.497(3)
O2	C15	1.150(3)			

Table 3: Bond angles for **25.2b**.

Atom	Atom	Atom	Angle/°	Atom	Atom	Atom	Angle/°
C15	W	P	174.78(7)	C4	C2	P	132.87(17)
C15	W	C16	89.10(10)	F1	C3	F2	106.9(2)
C15	W	C17	88.30(10)	F1	C3	F3	107.5(2)
C15	W	C18	89.34(9)	F1	C3	C2	111.40(19)
C15	W	C19	87.81(10)	F2	C3	F3	107.4(2)
C16	W	P	93.95(7)	F2	C3	C2	111.4(2)
C16	W	C17	90.55(9)	F3	C3	C2	112.0(2)
C16	W	C18	176.86(9)	F4	C4	F5	105.4(3)
C17	W	P	95.90(7)	F4	C4	F6	107.6(3)
C18	W	P	87.81(7)	F4	C4	C2	113.1(3)
C18	W	C17	86.68(9)	F5	C4	C2	110.5(2)
C19	W	P	88.06(7)	F6	C4	F5	106.3(3)
C19	W	C16	87.94(9)	F6	C4	C2	113.4(2)
C19	W	C17	175.85(10)	C6	C5	P	106.48(16)
C19	W	C18	94.72(9)	C6	C5	C10	111.9(2)
O1	P	W	116.92(7)	C9	C5	P	107.60(17)
O1	P	C1	77.70(9)	C9	C5	C6	103.08(19)
O1	P	C2	37.83(8)	C9	C5	C10	110.4(2)
O1	P	C5	106.48(10)	C10	C5	P	116.43(17)
C1	P	W	121.01(8)	C7	C6	C5	108.6(2)
C1	P	C2	40.24(9)	C7	C6	C11	128.1(2)
C1	P	C5	107.91(12)	C11	C6	C5	123.2(2)
C2	P	W	124.19(6)	C6	C7	C8	109.9(2)
C5	P	W	119.11(8)	C6	C7	C12	128.2(3)
C5	P	C2	116.42(10)	C8	C7	C12	121.9(2)
C2	O1	P	95.08(13)	C7	C8	C13	122.9(2)
C2	C1	P	88.44(15)	C9	C8	C7	109.4(2)
O1	C2	P	47.08(9)	C9	C8	C13	127.7(2)
O1	C2	C1	97.88(17)	C8	C9	C5	109.0(2)
O1	C2	C3	110.49(19)	C8	C9	C14	129.3(2)
O1	C2	C4	109.8(2)	C14	C9	C5	121.6(2)
C1	C2	P	51.32(11)	O2	C15	W	178.4(2)
C1	C2	C3	112.1(2)	O3	C16	W	176.0(2)
C1	C2	C4	117.1(2)	O4	C17	W	174.7(2)
C3	C2	P	117.63(16)	O5	C18	W	177.4(2)
C3	C2	C4	108.86(19)	O6	C19	W	177.6(2)

Table 4: Torsion angles for **25.2b**.

A	B	C	D	Angle/°	A	B	C	D	Angle/°
W	P	O1	C2	-111.96(12)	C5	P	C1	C2	-110.00(15)
W	P	C1	C2	107.74(13)	C5	P	C2	O1	-82.91(16)
W	P	C2	O1	90.99(13)	C5	P	C2	C1	86.82(17)
W	P	C2	C1	-99.28(15)	C5	P	C2	C3	-175.94(17)
W	P	C2	C3	-2.0(2)	C5	P	C2	C4	-6.3(3)
W	P	C2	C4	167.6(2)	C5	C6	C7	C8	1.9(3)
W	P	C5	C6	61.37(18)	C5	C6	C7	C12	-176.3(2)
W	P	C5	C9	-48.60(17)	C6	C5	C9	C8	3.2(3)
W	P	C5	C10	-173.07(17)	C6	C5	C9	C14	179.8(2)
P	W	C15	O2	10(8)	C6	C7	C8	C9	0.2(3)

P	W	C16	O3	-164(3)	C6	C7	C8	C13	-178.4(2)
P	W	C17	O4	158(2)	C7	C8	C9	C5	-2.2(3)
P	W	C18	O5	-99(5)	C7	C8	C9	C14	-178.5(3)
P	W	C19	O6	135(5)	C9	C5	C6	C7	-3.1(3)
P	O1	C2	C1	-8.08(17)	C9	C5	C6	C11	-179.9(2)
P	O1	C2	C3	109.18(17)	C10	C5	C6	C7	115.6(2)
P	O1	C2	C4	-130.72(18)	C10	C5	C6	C11	-61.3(3)
P	C1	C2	O1	7.58(16)	C10	C5	C9	C8	-116.5(2)
P	C1	C2	C3	-108.39(18)	C10	C5	C9	C14	60.1(3)
P	C1	C2	C4	124.7(2)	C11	C6	C7	C8	178.6(3)
P	C2	C3	F1	-0.2(3)	C11	C6	C7	C12	0.3(4)
P	C2	C3	F2	-119.45(19)	C12	C7	C8	C9	178.6(2)
P	C2	C3	F3	120.24(19)	C12	C7	C8	C13	0.0(4)
P	C2	C4	F4	145.5(2)	C13	C8	C9	C5	176.3(2)
P	C2	C4	F5	-96.6(3)	C13	C8	C9	C14	0.1(5)
P	C2	C4	F6	22.6(4)	C15	W	P	O1	55.6(8)
P	C5	C6	C7	-116.2(2)	C15	W	P	C1	-35.9(8)
P	C5	C6	C11	67.0(3)	C15	W	P	C2	12.1(8)
P	C5	C9	C8	115.5(2)	C15	W	P	C5	-174.1(8)
P	C5	C9	C14	-67.9(3)	C15	W	C16	O3	11(3)
O1	P	C1	C2	-6.43(14)	C15	W	C17	O4	-19(2)
O1	P	C2	C1	169.7(2)	C15	W	C18	O5	85(5)
O1	P	C2	C3	-93.0(2)	C15	W	C19	O6	-48(5)
O1	P	C2	C4	76.6(3)	C16	W	P	O1	-178.80(10)
O1	P	C5	C6	-163.80(16)	C16	W	P	C1	89.70(11)
O1	P	C5	C9	86.23(16)	C16	W	P	C2	137.75(10)
O1	P	C5	C10	-38.2(2)	C16	W	P	C5	-48.50(11)
O1	C2	C3	F1	-51.5(3)	C16	W	C15	O2	-116(8)
O1	C2	C3	F2	-170.78(19)	C16	W	C17	O4	-108(2)
O1	C2	C3	F3	68.9(2)	C16	W	C18	O5	25(6)
O1	C2	C4	F4	-165.2(2)	C16	W	C19	O6	41(5)
O1	C2	C4	F5	-47.3(3)	C17	W	P	O1	-87.83(10)
O1	C2	C4	F6	71.9(3)	C17	W	P	C1	-179.34(11)
C1	P	O1	C2	6.77(14)	C17	W	P	C2	-131.28(10)
C1	P	C2	O1	-169.7(2)	C17	W	P	C5	42.47(11)
C1	P	C2	C3	97.2(2)	C17	W	C15	O2	153(8)
C1	P	C2	C4	-93.1(3)	C17	W	C16	O3	100(3)
C1	P	C5	C6	-81.73(18)	C17	W	C18	O5	-3(5)
C1	P	C5	C9	168.30(15)	C17	W	C19	O6	-28(6)
C1	P	C5	C10	43.8(2)	C18	W	P	O1	-1.39(10)
C1	C2	C3	F1	56.6(3)	C18	W	P	C1	-92.90(11)
C1	C2	C3	F2	-62.7(3)	C18	W	P	C2	-44.85(10)
C1	C2	C3	F3	177.0(2)	C18	W	P	C5	128.90(11)
C1	C2	C4	F4	84.4(3)	C18	W	C15	O2	67(8)
C1	C2	C4	F5	-157.7(2)	C18	W	C16	O3	71(4)
C1	C2	C4	F6	-38.5(4)	C18	W	C17	O4	70(2)
C2	P	C5	C6	-124.40(16)	C18	W	C19	O6	-138(5)
C2	P	C5	C9	125.63(15)	C19	W	P	O1	93.40(10)
C2	P	C5	C10	1.2(2)	C19	W	P	C1	1.90(11)
C3	C2	C4	F4	-44.1(3)	C19	W	P	C2	49.95(10)
C3	C2	C4	F5	73.7(3)	C19	W	P	C5	-136.30(11)
C3	C2	C4	F6	-167.0(3)	C19	W	C15	O2	-28(8)
C4	C2	C3	F1	-172.2(2)	C19	W	C16	O3	-77(3)

C4	C2	C3	F2	68.5(3)	C19	W	C17	O4	-40(3)
C4	C2	C3	F3	-51.8(3)	C19	W	C18	O5	173(5)
C5	P	O1	C2	112.07(15)					

12.21 Pentacarbonyl[4-methyl-2-(triphenylmethyl)-1,2-oxaphosphetane- κ P]tungsten(0) [21.3a]

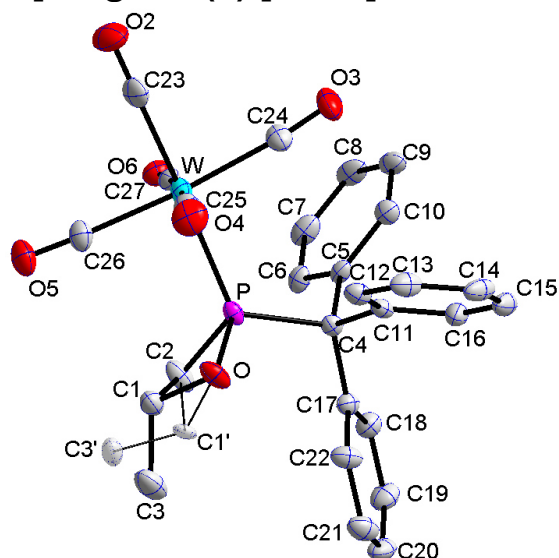


Table 1: Crystal data and structure refinement for **21.3a**.

Identification code	GSTR399, AKY-484 // GXray3939f
Device Type	Bruker X8-KappaApexII
Empirical formula	C ₂₇ H ₂₁ O ₆ PW
Moiety formula	C ₂₇ H ₂₁ O ₆ P W
Formula weight	656.26
Temperature/K	100
Crystal system	triclinic
Space group	P $\bar{1}$
a/Å	9.6166(9)
b/Å	10.6720(12)
c/Å	12.9879(12)
α /°	75.820(6)
β /°	83.265(5)
γ /°	73.806(6)
Volume/Å ³	1239.3(2)
Z	2
$\rho_{\text{calc}}/\text{cm}^3$	1.759
μ/mm^{-1}	4.765
F(000)	640.0
Crystal size/mm ³	0.12 × 0.09 × 0.06
Absorption correction	empirical
Tmin; Tmax	0.4935; 0.7459
Radiation	MoK α (λ = 0.71073)
2 θ range for data collection/°	5.466 to 56°
Completeness to theta	0.997
Index ranges	-12 ≤ h ≤ 12, -14 ≤ k ≤ 14, -17 ≤ l ≤ 17
Reflections collected	24114
Independent reflections	5969 [R _{int} = 0.0473, R _{sigma} = 0.0441]

Data/restraints/parameters	5969/0/337
Goodness-of-fit on F^2	1.102
Final R indexes [$I \geq 2\sigma(I)$]	$R_1 = 0.0327$, $wR_2 = 0.0761$
Final R indexes [all data]	$R_1 = 0.0424$, $wR_2 = 0.0810$
Largest diff. peak/hole / $e \text{ \AA}^{-3}$	2.09/-1.42

Table 2: Bond lengths for **21.3a**.

Atom	Atom	Length/Å	Atom	Atom	Length/Å
W	P	2.4926(12)	C4	C11	1.542(5)
W	C23	2.028(5)	C4	C17	1.535(6)
W	C24	2.064(5)	C5	C6	1.397(6)
W	C25	2.057(5)	C5	C10	1.397(6)
W	C26	2.038(5)	C6	C7	1.387(6)
W	C27	2.032(5)	C7	C8	1.372(7)
P	O1	1.656(3)	C8	C9	1.384(7)
P	C2	1.843(4)	C9	C10	1.383(6)
P	C4	1.905(4)	C11	C12	1.385(6)
O1	C1	1.515(8)	C11	C16	1.404(6)
O1	C1'	1.512(11)	C12	C13	1.391(6)
O2	C23	1.132(6)	C13	C14	1.371(7)
O3	C24	1.131(6)	C14	C15	1.383(7)
O4	C25	1.137(6)	C15	C16	1.387(6)
O5	C26	1.137(5)	C17	C18	1.393(6)
O6	C27	1.140(5)	C17	C22	1.397(6)
C1	C2	1.547(9)	C18	C19	1.387(6)
C1	C3	1.515(15)	C19	C20	1.391(7)
C1'	C2	1.611(12)	C20	C21	1.388(7)
C1'	C3'	1.51(2)	C21	C22	1.383(7)
C4	C5	1.539(5)			

Table 3: Bond angles for **21.3a**.

Atom	Atom	Atom	Angle/°	Atom	Atom	Atom	Angle/°
C23	W	P	176.50(14)	C11	C4	P	110.5(3)
C23	W	C24	86.04(19)	C17	C4	P	111.3(3)
C23	W	C25	92.3(2)	C17	C4	C5	114.0(3)
C23	W	C26	89.01(19)	C17	C4	C11	105.7(3)
C23	W	C27	88.79(19)	C6	C5	C4	120.1(4)
C24	W	P	95.65(14)	C6	C5	C10	117.4(4)
C25	W	P	90.80(14)	C10	C5	C4	122.4(4)
C25	W	C24	89.65(18)	C7	C6	C5	121.0(4)
C26	W	P	89.41(14)	C8	C7	C6	120.5(4)
C26	W	C24	174.59(19)	C7	C8	C9	119.8(4)
C26	W	C25	88.37(18)	C10	C9	C8	120.0(4)
C27	W	P	88.02(12)	C9	C10	C5	121.4(4)
C27	W	C24	94.50(18)	C12	C11	C4	124.3(4)
C27	W	C25	175.78(17)	C12	C11	C16	118.1(4)
C27	W	C26	87.57(18)	C16	C11	C4	117.4(4)
O1	P	W	115.21(13)	C11	C12	C13	120.9(4)
O1	P	C2	80.49(18)	C14	C13	C12	120.5(5)
O1	P	C4	106.90(18)	C13	C14	C15	119.7(4)

C2	P	W	117.62(17)	C14	C15	C16	120.2(5)
C2	P	C4	107.1(2)	C15	C16	C11	120.6(4)
C4	P	W	121.82(13)	C18	C17	C4	123.2(4)
C1	O1	P	91.8(3)	C18	C17	C22	117.3(4)
C1'	O1	P	97.5(4)	C22	C17	C4	119.3(4)
O1	C1	C2	95.4(5)	C19	C18	C17	121.1(4)
O1	C1	C3	107.8(8)	C18	C19	C20	120.9(4)
C3	C1	C2	114.1(9)	C21	C20	C19	118.4(4)
O1	C1'	C2	92.9(6)	C22	C21	C20	120.5(4)
C3'	C1'	O1	105.5(11)	C21	C22	C17	121.7(4)
C3'	C1'	C2	113.6(12)	O2	C23	W	177.1(5)
C1	C2	P	84.0(4)	O3	C24	W	174.0(4)
C1'	C2	P	87.0(4)	O4	C25	W	179.5(5)
C5	C4	P	102.6(3)	O5	C26	W	177.2(4)
C5	C4	C11	112.8(3)	O6	C27	W	175.1(4)

Table 4: Torsion angles for **21.3a**.

A	B	C	D	Angle/°	A	B	C	D	Angle/°
W	P	O1	C1	95.8(5)	C4	C5	C10	C9	-178.0(4)
W	P	O1	C1'	126.8(7)	C4	C11	C12	C13	174.9(4)
W	P	C2	C1	-93.6(5)	C4	C11	C16	C15	-175.9(4)
W	P	C2	C1'	-123.5(6)	C4	C17	C18	C19	177.9(4)
P	O1	C1	C2	24.2(6)	C4	C17	C22	C21	-177.8(4)
P	O1	C1	C3	141.7(8)	C5	C4	C11	C12	120.7(4)
P	O1	C1'	C2	-12.0(7)	C5	C4	C11	C16	-65.0(5)
P	O1	C1'	C3'	-127.5(9)	C5	C4	C17	C18	0.0(5)
P	C4	C5	C6	-60.8(4)	C5	C4	C17	C22	175.6(4)
P	C4	C5	C10	116.0(4)	C5	C6	C7	C8	-1.1(7)
P	C4	C11	C12	6.4(5)	C6	C5	C10	C9	-1.1(6)
P	C4	C11	C16	-179.3(3)	C6	C7	C8	C9	0.0(7)
P	C4	C17	C18	115.6(4)	C7	C8	C9	C10	0.5(7)
P	C4	C17	C22	-68.9(4)	C8	C9	C10	C5	0.1(7)
O1	P	C2	C1	20.0(5)	C10	C5	C6	C7	1.6(6)
O1	P	C2	C1'	-9.9(6)	C11	C4	C5	C6	-179.7(4)
O1	C1	C2	P	-21.7(5)	C11	C4	C5	C10	-3.0(5)
O1	C1	C2	C1'	72.7(10)	C11	C4	C17	C18	-124.4(4)
O1	C1'	C2	P	10.7(7)	C11	C4	C17	C22	51.1(5)
O1	C1'	C2	C1	-72.5(10)	C11	C12	C13	C14	-0.2(7)
C1	O1	C1'	C2	69.0(10)	C12	C11	C16	C15	-1.3(6)
C1	O1	C1'	C3'	-46.5(12)	C12	C13	C14	C15	0.4(7)
C1'	O1	C1	C2	-77.3(11)	C13	C14	C15	C16	-1.1(7)
C1'	O1	C1	C3	40.2(11)	C14	C15	C16	C11	1.5(7)
C2	P	O1	C1	-20.3(5)	C16	C11	C12	C13	0.6(6)
C2	P	O1	C1'	10.6(7)	C17	C4	C5	C6	59.7(5)
C3	C1	C2	P	-134.0(8)	C17	C4	C5	C10	-123.5(4)
C3	C1	C2	C1'	-39.6(11)	C17	C4	C11	C12	-114.1(4)
C3'	C1'	C2	P	119.0(11)	C17	C4	C11	C16	60.2(5)
C3'	C1'	C2	C1	35.9(12)	C17	C18	C19	C20	-1.1(7)
C4	P	O1	C1	-125.4(5)	C18	C17	C22	C21	-2.0(7)
C4	P	O1	C1'	-94.4(7)	C18	C19	C20	C21	-0.3(7)
C4	P	C2	C1	124.9(5)	C19	C20	C21	C22	0.6(7)

C4	P	C2	C1'	95.0(6)	C20	C21	C22	C17	0.6(7)
C4	C5	C6	C7	178.6(4)	C22	C17	C18	C19	2.2(6)

12.22 Pentacarbonyl[4-(trifluoromethyl)-2-(triphenylmethyl)-1,2-oxaphosphetane- κ P]tungsten(0) [21.3g]

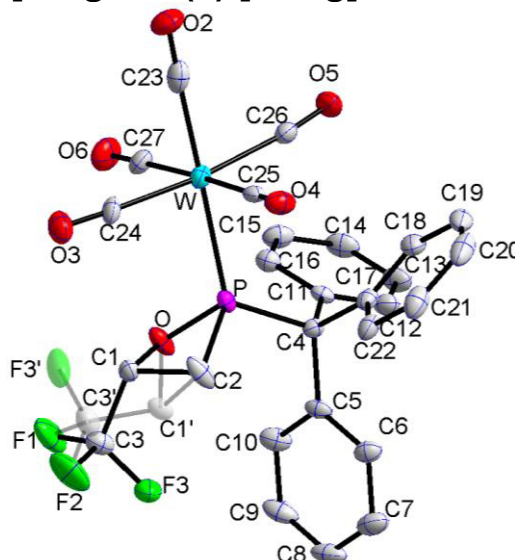


Table 1: Crystal data and structure refinement for **21.3g**.

Identification code	GSTR398, AKY-487 // GXray3940f
Device Type	Bruker X8-KappaApexII
Empirical formula	C ₂₇ H ₁₈ F ₃ O ₆ PW
Moiety formula	C ₂₇ H ₁₈ F ₃ O ₆ P W
Formula weight	710.23
Temperature/K	100
Crystal system	triclinic
Space group	P $\bar{1}$
a/Å	9.6002(10)
b/Å	10.5444(11)
c/Å	13.8429(14)
α /°	71.032(3)
β /°	76.087(3)
γ /°	75.469(4)
Volume/Å ³	1263.3(2)
Z	2
$\rho_{\text{calc}}/\text{cm}^3$	1.867
μ/mm^{-1}	4.699
F(000)	688.0
Crystal size/mm ³	0.11 × 0.09 × 0.04
Absorption correction	empirical
Tmin; Tmax	0.5035; 0.7460
Radiation	MoK α (λ = 0.71073)
2 θ range for data collection/°	4.158 to 51.996°
Completeness to theta	0.961
Index ranges	-7 ≤ h ≤ 11, -13 ≤ k ≤ 13, -17 ≤ l ≤ 17
Reflections collected	12605
Independent reflections	4756 [R _{int} = 0.0286, R _{sigma} = 0.0385]
Data/restraints/parameters	4756/13/371

Goodness-of-fit on F^2	1.056
Final R indexes [$I > 2\sigma(I)$]	$R_1 = 0.0237$, $wR_2 = 0.0481$
Final R indexes [all data]	$R_1 = 0.0298$, $wR_2 = 0.0511$
Largest diff. peak/hole / $e \text{ \AA}^{-3}$	1.17/-0.83

Table 2: Bond lengths for **21.3g**.

Atom	Atom	Length/Å	Atom	Atom	Length/Å
W	P	2.4695(9)	C3'	F3'	1.369(9)
W	C23	2.035(4)	C4	C5	1.542(4)
W	C24	2.018(4)	C4	C11	1.532(4)
W	C25	2.037(4)	C4	C17	1.547(5)
W	C26	2.063(4)	C5	C6	1.383(5)
W	C27	2.045(4)	C5	C10	1.396(5)
P	O1	1.681(2)	C6	C7	1.395(5)
P	C2	1.841(4)	C7	C8	1.374(6)
P	C4	1.885(4)	C8	C9	1.370(6)
O1	C1	1.457(6)	C9	C10	1.386(5)
O1	C1'	1.538(9)	C11	C12	1.388(5)
O2	C23	1.116(4)	C11	C16	1.388(5)
O3	C24	1.145(4)	C12	C13	1.373(5)
O4	C25	1.137(4)	C13	C14	1.384(6)
O5	C26	1.121(4)	C14	C15	1.371(6)
O6	C27	1.137(4)	C15	C16	1.383(5)
C1	C3	1.503(10)	C17	C18	1.379(5)
C1	C2	1.603(7)	C17	C22	1.394(5)
C3	F1	1.305(9)	C18	C19	1.392(5)
C3	F2	1.325(9)	C19	C20	1.372(6)
C3	F3	1.316(10)	C20	C21	1.359(6)
C1'	C3'	1.429(18)	C21	C22	1.381(5)
C1'	C2	1.556(9)			

Table 3: Bond angles for **21.3g**.

Atom	Atom	Atom	Angle/°	Atom	Atom	Atom	Angle/°
C23	W	P	176.36(10)	C1'	C2	P	88.4(3)
C23	W	C25	88.78(14)	C5	C4	P	112.6(2)
C23	W	C26	86.73(14)	C5	C4	C17	113.7(3)
C23	W	C27	91.15(14)	C11	C4	P	111.0(2)
C24	W	P	89.21(10)	C11	C4	C5	105.2(2)
C24	W	C23	88.42(15)	C11	C4	C17	112.9(3)
C24	W	C25	88.56(15)	C17	C4	P	101.7(2)
C24	W	C26	174.00(14)	C6	C5	C4	123.2(3)
C24	W	C27	87.56(15)	C6	C5	C10	118.2(3)
C25	W	P	88.40(9)	C10	C5	C4	118.3(3)
C25	W	C26	94.86(14)	C5	C6	C7	120.4(3)
C25	W	C27	176.11(15)	C8	C7	C6	120.6(4)
C26	W	P	95.80(9)	C9	C8	C7	119.5(3)
C27	W	P	91.51(10)	C8	C9	C10	120.6(4)
C27	W	C26	89.01(15)	C9	C10	C5	120.7(4)
O1	P	W	114.60(10)	C12	C11	C4	117.9(3)
O1	P	C2	79.20(14)	C12	C11	C16	118.3(3)

O1	P	C4	107.25(14)	C16	C11	C4	123.5(3)
C2	P	W	118.33(14)	C13	C12	C11	121.1(4)
C2	P	C4	106.88(18)	C12	C13	C14	119.7(4)
C4	P	W	122.23(10)	C15	C14	C13	120.0(3)
C1	O1	P	93.1(3)	C14	C15	C16	120.1(4)
C1'	O1	P	95.1(3)	C15	C16	C11	120.6(3)
O1	C1	C3	108.7(5)	C18	C17	C4	121.8(3)
O1	C1	C2	94.4(4)	C18	C17	C22	117.7(3)
C3	C1	C2	114.1(5)	C22	C17	C4	120.4(3)
F1	C3	C1	108.2(6)	C17	C18	C19	120.5(4)
F1	C3	F2	107.1(7)	C20	C19	C18	120.6(4)
F1	C3	F3	113.3(6)	C21	C20	C19	119.7(4)
F2	C3	C1	110.4(6)	C20	C21	C22	120.3(4)
F3	C3	C1	114.8(7)	C21	C22	C17	121.2(4)
F3	C3	F2	102.6(6)	O2	C23	W	178.0(4)
O1	C1'	C2	93.2(5)	O3	C24	W	177.9(3)
C3'	C1'	O1	106.8(9)	O4	C25	W	175.5(3)
C3'	C1'	C2	111.6(8)	O5	C26	W	174.3(3)
F3'	C3'	C1'	113.2(11)	O6	C27	W	178.3(4)
C1	C2	P	82.7(3)				

Table 4: Torsion angles for **21.3g**.

A	B	C	D	Angle/°	A	B	C	D	Angle/°
W	P	O1	C1	-92.6(3)	C2	C1	C3	F2	75.7(8)
W	P	O1	C1'	-130.9(4)	C2	C1	C3	F3	-39.6(8)
W	P	C2	C1	90.6(3)	C2	C1'	C3'	F3'	37.6(14)
W	P	C2	C1'	126.5(4)	C4	P	O1	C1	128.2(3)
W	P	C4	C5	176.72(17)	C4	P	O1	C1'	90.0(4)
W	P	C4	C11	-65.6(2)	C4	P	C2	C1	-126.5(3)
W	P	C4	C17	54.7(2)	C4	P	C2	C1'	-90.7(5)
P	O1	C1	C3	-144.3(5)	C4	C5	C6	C7	-175.9(3)
P	O1	C1	C2	-27.1(3)	C4	C5	C10	C9	176.7(3)
P	O1	C1'	C3'	130.6(7)	C4	C11	C12	C13	176.0(3)
P	O1	C1'	C2	16.9(5)	C4	C11	C16	C15	-174.7(3)
P	C4	C5	C6	-116.5(3)	C4	C17	C18	C19	180.0(3)
P	C4	C5	C10	69.2(4)	C4	C17	C22	C21	180.0(3)
P	C4	C11	C12	174.6(2)	C5	C4	C11	C12	-63.3(4)
P	C4	C11	C16	-11.9(4)	C5	C4	C11	C16	110.2(3)
P	C4	C17	C18	-113.1(3)	C5	C4	C17	C18	125.7(3)
P	C4	C17	C22	64.2(3)	C5	C4	C17	C22	-57.1(4)
O1	P	C2	C1	-21.6(3)	C5	C6	C7	C8	-0.1(6)
O1	P	C2	C1'	14.3(5)	C6	C5	C10	C9	2.1(5)
O1	P	C4	C5	-48.0(2)	C6	C7	C8	C9	1.4(6)
O1	P	C4	C11	69.7(2)	C7	C8	C9	C10	-0.8(6)
O1	P	C4	C17	-169.95(19)	C8	C9	C10	C5	-0.9(6)
O1	C1	C3	F1	-63.5(8)	C10	C5	C6	C7	-1.6(5)
O1	C1	C3	F2	179.6(5)	C11	C4	C5	C6	122.4(4)
O1	C1	C3	F3	64.2(8)	C11	C4	C5	C10	-51.8(4)
O1	C1	C2	P	24.7(3)	C11	C4	C17	C18	5.9(5)

O1	C1	C2	C1'	-72.5(6)	C11	C4	C17	C22	-176.8(3)
O1	C1'	C3'	F3'	-62.9(12)	C11	C12	C13	C14	-1.6(5)
O1	C1'	C2	P	-15.4(5)	C12	C11	C16	C15	-1.3(5)
O1	C1'	C2	C1	64.5(6)	C12	C13	C14	C15	-0.1(6)
C1	O1	C1'	C3'	42.1(8)	C13	C14	C15	C16	1.0(5)
C1	O1	C1'	C2	-71.6(6)	C14	C15	C16	C11	-0.3(5)
C3	C1	C2	P	137.5(5)	C16	C11	C12	C13	2.2(5)
C3	C1	C2	C1'	40.2(7)	C17	C4	C5	C6	-1.6(5)
C1'	O1	C1	C3	-50.0(7)	C17	C4	C5	C10	-175.8(3)
C1'	O1	C1	C2	67.2(7)	C17	C4	C11	C12	61.2(4)
C3'	C1'	C2	P	-124.9(8)	C17	C4	C11	C16	-125.3(3)
C3'	C1'	C2	C1	-45.0(9)	C17	C18	C19	C20	-1.1(6)
C2	P	O1	C1	23.7(3)	C18	C17	C22	C21	-2.7(5)
C2	P	O1	C1'	-14.5(5)	C18	C19	C20	C21	-0.6(6)
C2	P	C4	C5	35.7(3)	C19	C20	C21	C22	0.6(6)
C2	P	C4	C11	153.4(2)	C20	C21	C22	C17	1.1(6)
C2	P	C4	C17	-86.3(2)	C22	C17	C18	C19	2.7(5)
C2	C1	C3	F1	-167.3(5)					

12.23 Pentacarbonyl[4,4-bis(trifluoromethyl)-2-(triphenylmethyl)-1,2-oxaphosphetane- κP]tungsten(0) [25.3b]

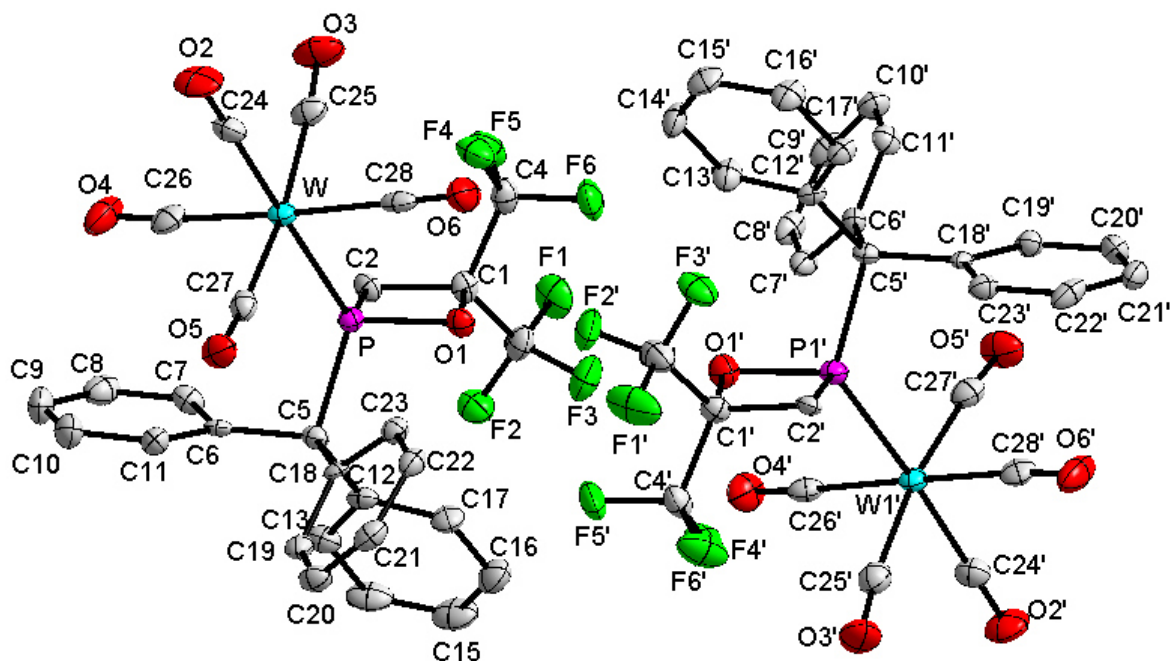


Table 1: Crystal data and structure refinement for **25.3b**.

Identification code	GSTR494, PB-13 // GXraymo_4641f
Crystal Habitus	clear colourless plate
Device Type	Bruker D8-Venture
Empirical formula	C ₂₈ H ₁₇ O ₆ F ₆ PW
Moiety formula	C ₂₈ H ₁₇ F ₆ O ₆ P W
Formula weight	778.23
Temperature/K	150.0
Crystal system	monoclinic
Space group	P2 ₁ /n
a/Å	14.5390(8)

b/Å	11.5901(6)
c/Å	32.8290(18)
α /°	90
β /°	100.6203(19)
γ /°	90
Volume/Å ³	5437.2(5)
Z	8
$\rho_{\text{calc}}/\text{cm}^3$	1.901
μ/mm^{-1}	4.391
F(000)	3008.0
Crystal size/mm ³	0.14 × 0.12 × 0.05
Absorption correction	empirical
Tmin; Tmax	0.4359; 0.7459
Radiation	MoK α (λ = 0.71073)
2 θ range for data collection/°	4.3 to 55.996°
Completeness to theta	1.000
Index ranges	-19 ≤ h ≤ 19, -15 ≤ k ≤ 15, -43 ≤ l ≤ 43
Reflections collected	106615
Independent reflections	13119 [R _{int} = 0.1371, R _{sigma} = 0.0792]
Data/restraints/parameters	13119/1/757
Goodness-of-fit on F ²	1.008
Final R indexes [$I \geq 2\sigma(I)$]	R ₁ = 0.0384, wR ₂ = 0.0603
Final R indexes [all data]	R ₁ = 0.0720, wR ₂ = 0.0665
Largest diff. peak/hole / e Å ⁻³	1.02/-1.08

Table 2: Bond lengths for **25.3b**.

Atom	Atom	Length/Å	Atom	Atom	Length/Å
W	P	2.5017(11)	W1'	P1'	2.4915(11)
W	C24	2.007(5)	W1'	C24'	2.015(5)
W	C25	2.034(4)	W1'	C25'	2.039(5)
W	C26	2.028(5)	W1'	C26'	2.048(5)
W	C27	2.049(4)	W1'	C27'	2.038(5)
W	C28	2.056(5)	W1'	C28'	2.043(5)
P	O1	1.706(3)	P1'	O1'	1.713(3)
P	C2	1.843(4)	P1'	C2'	1.800(4)
P	C5	1.914(4)	P1'	C5'	1.913(4)
F1	C3	1.342(5)	F1'	C3'	1.343(5)
F2	C3	1.324(5)	F2'	C3'	1.319(6)
F3	C3	1.331(5)	F3'	C3'	1.320(5)
F4	C4	1.335(5)	F4'	C4'	1.332(5)
F5	C4	1.326(5)	F5'	C4'	1.327(5)
F6	C4	1.334(5)	F6'	C4'	1.327(5)
O1	C1	1.433(4)	O1'	C1'	1.444(5)
O2	C24	1.140(5)	O2'	C24'	1.147(5)
O3	C25	1.138(5)	O3'	C25'	1.143(5)
O4	C26	1.147(5)	O4'	C26'	1.138(5)
O5	C27	1.145(5)	O5'	C27'	1.143(5)
O6	C28	1.140(5)	O6'	C28'	1.135(5)
C1	C2	1.541(5)	C1'	C2'	1.499(5)
C1	C3	1.545(6)	C1'	C3'	1.540(6)
C1	C4	1.545(6)	C1'	C4'	1.547(6)
C5	C6	1.543(6)	C5'	C6'	1.531(5)

C5	C12	1.546(5)	C5'	C12'	1.542(5)
C5	C18	1.546(5)	C5'	C18'	1.552(5)
C6	C7	1.410(5)	C6'	C7'	1.393(5)
C6	C11	1.409(5)	C6'	C11'	1.401(5)
C7	C8	1.377(6)	C7'	C8'	1.385(5)
C8	C9	1.386(6)	C8'	C9'	1.376(6)
C9	C10	1.382(6)	C9'	C10'	1.376(6)
C10	C11	1.380(6)	C10'	C11'	1.384(5)
C12	C13	1.391(5)	C12'	C13'	1.402(6)
C12	C17	1.386(6)	C12'	C17'	1.386(5)
C13	C14	1.389(6)	C13'	C14'	1.385(6)
C14	C15	1.380(7)	C14'	C15'	1.372(6)
C15	C16	1.373(6)	C15'	C16'	1.379(6)
C16	C17	1.398(6)	C16'	C17'	1.397(6)
C18	C19	1.398(5)	C18'	C19'	1.392(5)
C18	C23	1.383(5)	C18'	C23'	1.411(5)
C19	C20	1.374(5)	C19'	C20'	1.387(5)
C20	C21	1.378(6)	C20'	C21'	1.375(6)
C21	C22	1.383(5)	C21'	C22'	1.393(6)
C22	C23	1.383(5)	C22'	C23'	1.378(6)

Table 3: Bond angles for **25.3b**.

Atom	Atom	Atom	Angle/°	Atom	Atom	Atom	Angle/°
C24	W	P	179.05(13)	C24'	W1'	P1'	176.42(12)
C24	W	C25	86.92(17)	C24'	W1'	C25'	85.12(17)
C24	W	C26	88.44(18)	C24'	W1'	C26'	91.10(17)
C24	W	C27	85.20(16)	C24'	W1'	C27'	87.37(17)
C24	W	C28	90.39(17)	C24'	W1'	C28'	89.80(17)
C25	W	P	92.98(12)	C25'	W1'	P1'	91.59(13)
C25	W	C27	171.80(16)	C25'	W1'	C26'	92.53(17)
C25	W	C28	91.26(17)	C25'	W1'	C28'	85.35(18)
C26	W	P	92.50(12)	C26'	W1'	P1'	87.62(12)
C26	W	C25	85.60(18)	C27'	W1'	P1'	96.01(13)
C26	W	C27	91.93(17)	C27'	W1'	C25'	171.42(18)
C26	W	C28	176.70(17)	C27'	W1'	C26'	91.74(17)
C27	W	P	94.94(12)	C27'	W1'	C28'	90.50(17)
C27	W	C28	91.05(16)	C28'	W1'	P1'	91.35(12)
C28	W	P	88.67(12)	C28'	W1'	C26'	177.62(16)
O1	P	W	119.37(10)	O1'	P1'	W1'	120.44(11)
O1	P	C2	78.41(15)	O1'	P1'	C2'	77.60(16)
O1	P	C5	105.26(16)	O1'	P1'	C5'	104.85(16)
C2	P	W	118.95(14)	C2'	P1'	W1'	115.44(14)
C2	P	C5	110.55(18)	C2'	P1'	C5'	111.42(18)
C5	P	W	117.59(12)	C5'	P1'	W1'	119.57(12)
C1	O1	P	95.8(2)	C1'	O1'	P1'	95.0(2)
O1	C1	C2	98.0(3)	O1'	C1'	C2'	96.9(3)
O1	C1	C3	111.5(3)	O1'	C1'	C3'	113.0(3)
O1	C1	C4	109.6(3)	O1'	C1'	C4'	109.7(3)
C2	C1	C3	114.7(3)	C2'	C1'	C3'	113.2(4)
C2	C1	C4	114.3(3)	C2'	C1'	C4'	114.9(3)
C3	C1	C4	108.3(3)	C3'	C1'	C4'	108.7(3)

C1	C2	P	86.8(2)	C1'	C2'	P1'	89.6(2)
F1	C3	C1	111.6(4)	F1'	C3'	C1'	109.6(4)
F2	C3	F1	106.6(3)	F2'	C3'	F1'	108.1(4)
F2	C3	F3	108.0(4)	F2'	C3'	F3'	108.4(4)
F2	C3	C1	112.8(3)	F2'	C3'	C1'	111.3(4)
F3	C3	F1	106.7(3)	F3'	C3'	F1'	106.2(4)
F3	C3	C1	110.8(3)	F3'	C3'	C1'	113.0(4)
F4	C4	C1	110.9(3)	F4'	C4'	C1'	111.7(3)
F5	C4	F4	107.6(4)	F5'	C4'	F4'	106.3(3)
F5	C4	F6	108.3(3)	F5'	C4'	C1'	111.8(4)
F5	C4	C1	111.9(3)	F6'	C4'	F4'	107.5(4)
F6	C4	F4	106.3(3)	F6'	C4'	F5'	108.0(3)
F6	C4	C1	111.6(4)	F6'	C4'	C1'	111.3(3)
C6	C5	P	100.6(2)	C6'	C5'	P1'	108.3(3)
C6	C5	C12	114.5(3)	C6'	C5'	C12'	106.0(3)
C6	C5	C18	113.5(3)	C6'	C5'	C18'	113.8(3)
C12	C5	P	114.3(2)	C12'	C5'	P1'	114.2(2)
C18	C5	P	108.0(3)	C12'	C5'	C18'	114.1(3)
C18	C5	C12	106.1(3)	C18'	C5'	P1'	100.5(2)
C7	C6	C5	120.6(3)	C7'	C6'	C5'	124.2(3)
C11	C6	C5	122.8(4)	C7'	C6'	C11'	116.9(4)
C11	C6	C7	116.4(4)	C11'	C6'	C5'	118.5(3)
C8	C7	C6	121.8(4)	C8'	C7'	C6'	121.4(4)
C7	C8	C9	120.7(4)	C9'	C8'	C7'	120.4(4)
C10	C9	C8	118.6(4)	C8'	C9'	C10'	119.5(4)
C11	C10	C9	121.4(4)	C9'	C10'	C11'	120.3(4)
C10	C11	C6	121.0(4)	C10'	C11'	C6'	121.4(4)
C13	C12	C5	124.2(4)	C13'	C12'	C5'	117.9(3)
C17	C12	C5	118.5(4)	C17'	C12'	C5'	124.9(4)
C17	C12	C13	117.0(4)	C17'	C12'	C13'	117.0(4)
C14	C13	C12	121.3(4)	C14'	C13'	C12'	121.6(4)
C15	C14	C13	120.5(4)	C15'	C14'	C13'	120.5(4)
C16	C15	C14	119.4(4)	C14'	C15'	C16'	119.0(4)
C15	C16	C17	119.7(5)	C15'	C16'	C17'	120.8(4)
C12	C17	C16	122.0(4)	C12'	C17'	C16'	121.0(4)
C19	C18	C5	119.2(3)	C19'	C18'	C5'	122.5(3)
C23	C18	C5	123.2(3)	C19'	C18'	C23'	117.3(4)
C23	C18	C19	117.4(4)	C23'	C18'	C5'	120.1(3)
C20	C19	C18	121.1(4)	C20'	C19'	C18'	121.4(4)
C19	C20	C21	120.7(4)	C21'	C20'	C19'	120.7(4)
C20	C21	C22	118.9(4)	C20'	C21'	C22'	118.7(4)
C23	C22	C21	120.3(4)	C23'	C22'	C21'	121.0(4)
C22	C23	C18	121.3(4)	C22'	C23'	C18'	120.7(4)
O2	C24	W	179.3(4)	O2'	C24'	W1'	179.1(4)
O3	C25	W	175.3(4)	O3'	C25'	W1'	174.3(4)
O4	C26	W	174.9(4)	O4'	C26'	W1'	177.7(4)
O5	C27	W	174.1(4)	O5'	C27'	W1'	174.3(4)
O6	C28	W	179.9(5)	O6'	C28'	W1'	175.3(4)

Table 4: Torsion angles for **25.3b**.

A	B	C	D	Angle/°	A	B	C	D	Angle/°
W	P	O1	C1	-109.9(2)	W1'	P1'	O1'	C1'	105.3(2)
W	P	C2	C1	110.9(2)	W1'	P1'	C2'	C1'	-111.2(2)
P	O1	C1	C2	-8.2(3)	P1'	O1'	C1'	C2'	8.4(3)
P	O1	C1	C3	-128.9(3)	P1'	O1'	C1'	C3'	127.2(3)
P	O1	C1	C4	111.2(3)	P1'	O1'	C1'	C4'	-111.2(3)
P	C5	C6	C7	65.7(4)	P1'	C5'	C6'	C7'	17.4(5)
P	C5	C6	C11	-110.0(4)	P1'	C5'	C6'	C11'	-169.9(3)
P	C5	C12	C13	-112.4(4)	P1'	C5'	C12'	C13'	-73.3(4)
P	C5	C12	C17	72.7(4)	P1'	C5'	C12'	C17'	111.9(4)
P	C5	C18	C19	165.7(3)	P1'	C5'	C18'	C19'	111.4(4)
P	C5	C18	C23	-19.6(5)	P1'	C5'	C18'	C23'	-65.8(4)
O1	P	C2	C1	-6.4(2)	O1'	P1'	C2'	C1'	6.8(2)
O1	C1	C2	P	7.6(3)	O1'	C1'	C2'	P1'	-7.9(3)
O1	C1	C3	F1	-154.0(3)	O1'	C1'	C3'	F1'	163.0(3)
O1	C1	C3	F2	86.1(4)	O1'	C1'	C3'	F2'	43.4(5)
O1	C1	C3	F3	-35.2(5)	O1'	C1'	C3'	F3'	-78.8(5)
O1	C1	C4	F4	-40.0(5)	O1'	C1'	C4'	F4'	33.2(5)
O1	C1	C4	F5	-160.2(3)	O1'	C1'	C4'	F5'	-85.8(4)
O1	C1	C4	F6	78.3(4)	O1'	C1'	C4'	F6'	153.4(3)
C2	P	O1	C1	6.9(2)	C2'	P1'	O1'	C1'	-7.1(2)
C2	C1	C3	F1	95.7(4)	C2'	C1'	C3'	F1'	-88.2(4)
C2	C1	C3	F2	-24.2(5)	C2'	C1'	C3'	F2'	152.3(3)
C2	C1	C3	F3	-145.5(3)	C2'	C1'	C3'	F3'	30.1(5)
C2	C1	C4	F4	68.9(4)	C2'	C1'	C4'	F4'	-74.7(5)
C2	C1	C4	F5	-51.3(5)	C2'	C1'	C4'	F5'	166.4(3)
C2	C1	C4	F6	-172.8(3)	C2'	C1'	C4'	F6'	45.5(5)
C3	C1	C2	P	125.8(3)	C3'	C1'	C2'	P1'	-126.7(3)
C3	C1	C4	F4	-161.8(3)	C3'	C1'	C4'	F4'	157.3(4)
C3	C1	C4	F5	78.0(4)	C3'	C1'	C4'	F5'	38.4(5)
C3	C1	C4	F6	-43.5(4)	C3'	C1'	C4'	F6'	-82.5(5)
C4	C1	C2	P	-108.3(3)	C4'	C1'	C2'	P1'	107.6(3)
C4	C1	C3	F1	-33.3(5)	C4'	C1'	C3'	F1'	40.8(5)
C4	C1	C3	F2	-153.2(3)	C4'	C1'	C3'	F2'	-78.7(4)
C4	C1	C3	F3	85.5(4)	C4'	C1'	C3'	F3'	159.0(4)
C5	P	O1	C1	115.3(2)	C5'	P1'	O1'	C1'	-116.3(2)
C5	P	C2	C1	-108.6(2)	C5'	P1'	C2'	C1'	108.1(3)
C5	C6	C7	C8	-179.4(4)	C5'	C6'	C7'	C8'	175.9(4)
C5	C6	C11	C10	179.2(4)	C5'	C6'	C11'	C10'	-176.9(4)
C5	C12	C13	C14	-177.2(4)	C5'	C12'	C13'	C14'	-177.7(4)
C5	C12	C17	C16	177.7(4)	C5'	C12'	C17'	C16'	176.6(4)
C5	C18	C19	C20	-179.6(4)	C5'	C18'	C19'	C20'	179.8(4)
C5	C18	C23	C22	-179.3(4)	C5'	C18'	C23'	C22'	179.6(4)
C6	C5	C12	C13	2.9(5)	C6'	C5'	C12'	C13'	45.7(4)
C6	C5	C12	C17	-172.0(3)	C6'	C5'	C12'	C17'	-129.0(4)
C6	C5	C18	C19	55.0(5)	C6'	C5'	C18'	C19'	-4.1(5)
C6	C5	C18	C23	-130.2(4)	C6'	C5'	C18'	C23'	178.7(3)
C6	C7	C8	C9	2.1(7)	C6'	C7'	C8'	C9'	-0.2(6)
C7	C6	C11	C10	3.3(6)	C7'	C6'	C11'	C10'	-3.6(6)
C7	C8	C9	C10	-0.4(7)	C7'	C8'	C9'	C10'	-2.4(6)
C8	C9	C10	C11	0.3(7)	C8'	C9'	C10'	C11'	1.9(6)
C9	C10	C11	C6	-1.9(7)	C9'	C10'	C11'	C6'	1.2(6)

C11	C6	C7	C8	-3.5(6)	C11'	C6'	C7'	C8'	3.1(6)
C12	C5	C6	C7	-57.3(5)	C12'	C5'	C6'	C7'	-105.5(4)
C12	C5	C6	C11	127.0(4)	C12'	C5'	C6'	C11'	67.2(4)
C12	C5	C18	C19	-71.5(4)	C12'	C5'	C18'	C19'	-125.9(4)
C12	C5	C18	C23	103.3(4)	C12'	C5'	C18'	C23'	56.9(5)
C12	C13	C14	C15	0.5(6)	C12'	C13'	C14'	C15'	1.0(7)
C13	C12	C17	C16	2.5(6)	C13'	C12'	C17'	C16'	1.9(6)
C13	C14	C15	C16	1.3(7)	C13'	C14'	C15'	C16'	1.3(7)
C14	C15	C16	C17	-1.1(7)	C14'	C15'	C16'	C17'	-2.0(6)
C15	C16	C17	C12	-0.8(7)	C15'	C16'	C17'	C12'	0.3(6)
C17	C12	C13	C14	-2.3(6)	C17'	C12'	C13'	C14'	-2.6(6)
C18	C5	C6	C7	-179.3(3)	C18'	C5'	C6'	C7'	128.2(4)
C18	C5	C6	C11	5.1(5)	C18'	C5'	C6'	C11'	-59.1(5)
C18	C5	C12	C13	128.8(4)	C18'	C5'	C12'	C13'	171.8(3)
C18	C5	C12	C17	-46.1(4)	C18'	C5'	C12'	C17'	-2.9(5)
C18	C19	C20	C21	-1.7(6)	C18'	C19'	C20'	C21'	2.1(6)
C19	C18	C23	C22	-4.5(6)	C19'	C18'	C23'	C22'	2.3(6)
C19	C20	C21	C22	-3.0(6)	C19'	C20'	C21'	C22'	-0.6(6)
C20	C21	C22	C23	3.9(6)	C20'	C21'	C22'	C23'	-0.1(6)
C21	C22	C23	C18	-0.1(6)	C21'	C22'	C23'	C18'	-0.8(6)
C23	C18	C19	C20	5.4(6)	C23'	C18'	C19'	C20'	-2.9(6)

12.24 1,4-Bis[(pentacarbonyl{2-[bis(trimethylsilyl)methyl]-1,2-oxaphosphetane-4-yl}-κP)tungsten(0)]butane [29.1c]

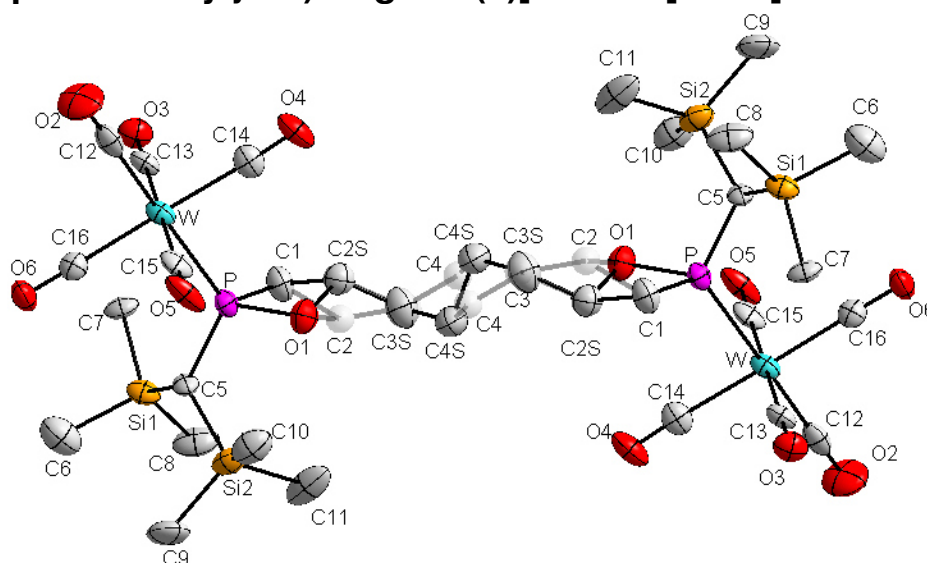


Table 1: Crystal data and structure refinement for **29.1c**.

Identification code	GSTR348, AKY-363 // GXray3322f
Crystal Habitus	colourless plate
Device Type	Bruker X8-KappaApexII
Empirical formula	C ₃₂ H ₅₂ O ₁₂ P ₂ Si ₄ W ₂
Moiety formula	C32 H52 O12 P2 Si4 W2
Formula weight	1170.74
Temperature/K	100(2)
Crystal system	monoclinic
Space group	P2 ₁ /c
a/Å	12.416(3)

b/Å	12.978(3)
c/Å	18.692(4)
α /°	90.00
β /°	129.782(11)
γ /°	90.00
Volume/Å ³	2314.6(10)
Z	2
$\rho_{\text{calc}}/\text{cm}^3$	1.680
μ/mm^{-1}	5.189
F(000)	1148.0
Crystal size/mm ³	0.12 × 0.05 × 0.03
Absorption correction	empirical
Tmin; Tmax	0.5748; 0.8599
Radiation	MoK α (λ = 0.71073)
2 θ range for data collection/°	6.48 to 50.5°
Completeness to theta	0.975
Index ranges	-12 ≤ h ≤ 14, -9 ≤ k ≤ 15, -22 ≤ l ≤ 15
Reflections collected	8151
Independent reflections	4088 [R_{int} = 0.0483]
Data/restraints/parameters	4088/67/264
Goodness-of-fit on F^2	1.039
Final R indexes [$I \geq 2\sigma(I)$]	$R_1 = 0.0554$, $wR_2 = 0.1339$
Final R indexes [all data]	$R_1 = 0.0843$, $wR_2 = 0.1500$
Largest diff. peak/hole / e Å ⁻³	2.38/-2.15

Table 2: Bond lengths for **29.1c**.

Atom	Atom	Length/Å	Atom	Atom	Length/Å
W	C12	2.017(15)	Si2	C11	1.890(15)
W	C15	2.025(14)	O1	C2S	1.47(2)
W	C13	2.034(12)	O1	C2	1.58(7)
W	C16	2.036(13)	O3	C13	1.155(14)
W	C14	2.046(13)	O4	C14	1.120(15)
W	P	2.480(3)	O5	C15	1.151(15)
P	O1	1.689(9)	O6	C16	1.160(14)
P	C5	1.809(12)	C1	C2	1.53(7)
P	C1	1.824(14)	C1	C2S	1.55(2)
P	C2S	2.312(18)	O2	C12	1.138(16)
Si1	C8	1.854(14)	C2	C3	1.37(13)
Si1	C6	1.857(17)	C3	C4	1.61(8)
Si1	C7	1.875(12)	C4	C4 ¹	1.56(17)
Si1	C5	1.948(12)	C2S	C3S	1.40(3)
Si2	C10	1.855(15)	C3S	C4S	1.51(3)
Si2	C9	1.861(16)	C4S	C4S ¹	1.50(4)
Si2	C5	1.870(13)			

Table 3: Bond angles for **29.1c**.

Atom	Atom	Atom	Angle/°	Atom	Atom	Atom	Angle/°
C12	W	C15	90.6(5)	C10	Si2	C5	109.7(6)
C12	W	C13	90.2(5)	C9	Si2	C5	107.5(7)
C15	W	C13	179.2(5)	C10	Si2	C11	108.7(8)

C12	W	C16	91.2(5)	C9	Si2	C11	109.3(8)
C15	W	C16	90.7(5)	C5	Si2	C11	113.7(6)
C13	W	C16	89.3(5)	C2S	O1	C2	33(3)
C12	W	C14	90.4(5)	C2S	O1	P	93.8(8)
C15	W	C14	89.9(5)	C2	O1	P	94(3)
C13	W	C14	90.1(5)	C2	C1	C2S	33(3)
C16	W	C14	178.3(5)	C2	C1	P	90(3)
C12	W	P	177.3(4)	C2S	C1	P	86.0(9)
C15	W	P	87.1(4)	P	C5	Si2	118.2(6)
C13	W	P	92.1(4)	P	C5	Si1	110.6(6)
C16	W	P	90.1(3)	Si2	C5	Si1	117.7(6)
C14	W	P	88.3(4)	O3	C13	W	178.3(11)
O1	P	C5	108.0(5)	O4	C14	W	177.0(12)
O1	P	C1	79.1(5)	O5	C15	W	179.3(13)
C5	P	C1	111.7(6)	O6	C16	W	178.4(11)
O1	P	C2S	39.4(5)	O2	C12	W	177.1(13)
C5	P	C2S	126.8(7)	C3	C2	C1	126(7)
C1	P	C2S	42.1(6)	C3	C2	O1	128(6)
O1	P	W	114.0(3)	C1	C2	O1	92(4)
C5	P	W	116.7(4)	C2	C3	C4	121(8)
C1	P	W	120.9(5)	C4 ¹	C4	C3	124(8)
C2S	P	W	115.8(5)	C3S	C2S	O1	112.0(18)
C8	Si1	C6	107.9(8)	C3S	C2S	C1	119.2(16)
C8	Si1	C7	110.4(6)	O1	C2S	C1	95.5(12)
C6	Si1	C7	103.8(7)	C3S	C2S	P	143.7(18)
C8	Si1	C5	112.4(7)	O1	C2S	P	46.8(6)
C6	Si1	C5	109.3(7)	C1	C2S	P	51.9(7)
C7	Si1	C5	112.4(5)	C2S	C3S	C4S	119.2(18)
C10	Si2	C9	107.8(8)	C4S ¹	C4S	C3S	113(2)

Table 4: Torsion angles for **29.1c**.

A	B	C	D	Angle/°	A	B	C	D	Angle/°
C12	W	P	O1	25(8)	C14	W	C13	O3	84(36)
C15	W	P	O1	54.1(5)	P	W	C13	O3	172(36)
C13	W	P	O1	-126.0(5)	C12	W	C14	O4	7(21)
C16	W	P	O1	144.7(5)	C15	W	C14	O4	98(21)
C14	W	P	O1	-36.0(5)	C13	W	C14	O4	-83(21)
C12	W	P	C5	-102(8)	C16	W	C14	O4	-151(19)
C15	W	P	C5	-73.0(6)	P	W	C14	O4	-175(21)
C13	W	P	C5	107.0(5)	C12	W	C15	O5	-82(100)
C16	W	P	C5	17.7(6)	C13	W	C15	O5	98(100)
C14	W	P	C5	-163.0(6)	C16	W	C15	O5	9(100)
C12	W	P	C1	117(8)	C14	W	C15	O5	-173(100)
C15	W	P	C1	145.5(6)	P	W	C15	O5	99(100)
C13	W	P	C1	-34.5(6)	C12	W	C16	O6	-95(41)
C16	W	P	C1	-123.8(6)	C15	W	C16	O6	174(100)
C14	W	P	C1	55.5(6)	C13	W	C16	O6	-5(41)
C12	W	P	C2S	69(8)	C14	W	C16	O6	63(50)
C15	W	P	C2S	97.7(6)	P	W	C16	O6	87(41)
C13	W	P	C2S	-82.3(6)	C15	W	C12	O2	6(25)
C16	W	P	C2S	-171.7(6)	C13	W	C12	O2	-174(25)

C14	W	P	C2S	7.7(6)	C16	W	C12	O2	-85(25)
C5	P	O1	C2S	-126.6(10)	C14	W	C12	O2	96(25)
C1	P	O1	C2S	-17.1(10)	P	W	C12	O2	35(31)
W	P	O1	C2S	102.0(9)	C2S	C1	C2	C3	77(9)
C5	P	O1	C2	-94(3)	P	C1	C2	C3	159(8)
C1	P	O1	C2	16(3)	C2S	C1	C2	O1	-65(4)
C2S	P	O1	C2	33(3)	P	C1	C2	O1	17(3)
W	P	O1	C2	135(3)	C2S	O1	C2	C3	-67(9)
O1	P	C1	C2	-16(3)	P	O1	C2	C3	-159(9)
C5	P	C1	C2	89(3)	C2S	O1	C2	C1	73(5)
C2S	P	C1	C2	-32(3)	P	O1	C2	C1	-18(4)
W	P	C1	C2	-128(3)	C1	C2	C3	C4	-115(10)
O1	P	C1	C2S	16.2(10)	O1	C2	C3	C4	14(15)
C5	P	C1	C2S	121.4(10)	C2	C3	C4	C4 ¹	-55(16)
W	P	C1	C2S	-95.3(10)	C2	O1	C2S	C3S	54(5)
O1	P	C5	Si2	-5.7(8)	P	O1	C2S	C3S	144.5(16)
C1	P	C5	Si2	-90.9(8)	C2	O1	C2S	C1	-71(5)
C2S	P	C5	Si2	-45.3(10)	P	O1	C2S	C1	19.9(11)
W	P	C5	Si2	124.2(6)	C2	O1	C2S	P	-91(5)
O1	P	C5	Si1	134.1(6)	C2	C1	C2S	C3S	-40(5)
C1	P	C5	Si1	48.9(8)	P	C1	C2S	C3S	-137(2)
C2S	P	C5	Si1	94.5(8)	C2	C1	C2S	O1	78(5)
W	P	C5	Si1	-96.0(6)	P	C1	C2S	O1	-18.4(10)
C10	Si2	C5	P	-52.5(9)	C2	C1	C2S	P	97(5)
C9	Si2	C5	P	-169.5(8)	O1	P	C2S	C3S	-66(2)
C11	Si2	C5	P	69.4(10)	C5	P	C2S	C3S	7(3)
C10	Si2	C5	Si1	170.5(8)	C1	P	C2S	C3S	89(3)
C9	Si2	C5	Si1	53.5(9)	W	P	C2S	C3S	-163(2)
C11	Si2	C5	Si1	-67.6(10)	C5	P	C2S	O1	72.5(10)
C8	Si1	C5	P	-99.9(8)	C1	P	C2S	O1	154.5(15)
C6	Si1	C5	P	140.3(8)	W	P	C2S	O1	-97.1(8)
C7	Si1	C5	P	25.5(8)	O1	P	C2S	C1	-154.5(15)
C8	Si1	C5	Si2	40.1(10)	C5	P	C2S	C1	-82.0(11)
C6	Si1	C5	Si2	-79.7(9)	W	P	C2S	C1	108.5(9)
C7	Si1	C5	Si2	165.5(7)	O1	C2S	C3S	C4S	52(3)
C12	W	C13	O3	-7(36)	C1	C2S	C3S	C4S	162.3(19)
C15	W	C13	O3	173(32)	P	C2S	C3S	C4S	98(3)
C16	W	C13	O3	-98(36)	C2S	C3S	C4S	C4S ¹	62(3)

12.25 Pentacarbonyl{(2-iodoethoxy)[bis(trimethylsilyl)methyl]phosphane- κP }tungsten(0) [33.1w]

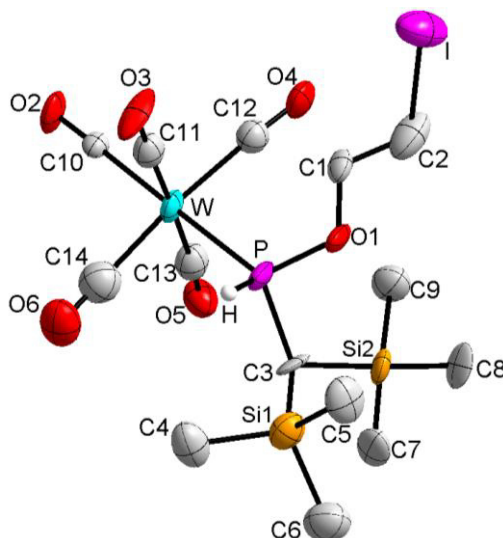


Table 1: Crystal data and structure refinement for **33.1w**.

Identification code	GSTR383, AKY-424 // GXray3760f
Device Type	Bruker APEX-II CCD
Empirical formula	C ₁₄ H ₂₄ IO ₆ PSi ₂ W
Formula weight	686.23
Temperature/K	100
Crystal system	triclinic
Space group	P $\bar{1}$
a/Å	9.179(3)
b/Å	10.433(4)
c/Å	14.066(5)
α /°	86.293(10)
β /°	81.810(10)
γ /°	65.584(9)
Volume/Å ³	1214.0(7)
Z	2
$\rho_{\text{calc}}/\text{cm}^3$	1.877
μ/mm^{-1}	6.216
F(000)	652.0
Crystal size/mm ³	0.11 × 0.1 × 0.03
Absorption correction	empirical
Tmin; Tmax	0.3610; 0.7459
Radiation	MoK α (λ = 0.71073)
2 θ range for data collection/°	2.92 to 50.5°
Completeness to theta	0.852
Index ranges	-10 ≤ h ≤ 10, -12 ≤ k ≤ 12, -16 ≤ l ≤ 16
Reflections collected	8231
Independent reflections	3734 [R _{int} = 0.0751, R _{sigma} = 0.1060]
Data/restraints/parameters	3734/51/235
Goodness-of-fit on F ²	1.231
Final R indexes [I ≥ 2 σ (I)]	R ₁ = 0.1405, wR ₂ = 0.3049
Final R indexes [all data]	R ₁ = 0.1918, wR ₂ = 0.3359
Largest diff. peak/hole / e Å ⁻³	5.69/-4.76

Table 2: Bond lengths for **33.1w**.

Atom	Atom	Length/Å	Atom	Atom	Length/Å
W	P	2.486(8)	Si2	C7	1.88(5)
W	C14	1.98(6)	Si1	C4	1.85(5)
W	C11	2.01(4)	Si1	C6	1.88(5)
W	C10	2.07(3)	Si1	C5	1.93(4)
W	C13	2.00(4)	Si1	C3	1.87(4)
W	C12	2.02(5)	O4	C12	1.20(5)
I	C2	2.16(5)	O2	C10	1.09(3)
P	O1	1.63(2)	O1	C1	1.46(4)
P	C3	1.79(3)	O5	C13	1.21(5)
Si2	C9	1.87(4)	O3	C11	1.21(4)
Si2	C8	1.81(4)	O6	C14	1.10(6)
Si2	C3	1.93(4)	C1	C2	1.44(6)

Table 3: Bond angles for **33.1w**.

Atom	Atom	Atom	Angle/°	Atom	Atom	Atom	Angle/°
C14	W	P	87.0(14)	C8	Si2	C3	110.6(16)
C14	W	C11	90.8(19)	C8	Si2	C7	115.4(18)
C14	W	C10	92.8(16)	C7	Si2	C3	106.8(17)
C14	W	C13	88.3(19)	C4	Si1	C6	108(3)
C14	W	C12	174.5(17)	C4	Si1	C5	112(2)
C11	W	P	86.6(10)	C4	Si1	C3	109.1(19)
C11	W	C10	90.0(13)	C6	Si1	C5	103(2)
C11	W	C12	92.6(16)	C3	Si1	C6	112(2)
C10	W	P	176.5(9)	C3	Si1	C5	112.0(19)
C13	W	P	94.8(11)	C1	O1	P	120.8(18)
C13	W	C11	178.3(16)	C2	C1	O1	105(3)
C13	W	C10	88.6(13)	O6	C14	W	174(5)
C13	W	C12	88.3(17)	C1	C2	I	109(3)
C12	W	P	88.9(10)	O3	C11	W	177(4)
C12	W	C10	91.5(14)	P	C3	Si2	116(2)
O1	P	W	120.0(10)	P	C3	Si1	111.8(19)
O1	P	C3	99.5(14)	Si1	C3	Si2	116.6(15)
C3	P	W	122.5(12)	O2	C10	W	175(3)
C9	Si2	C3	112.3(17)	O5	C13	W	176(4)
C9	Si2	C7	107(2)	O4	C12	W	171(3)
C8	Si2	C9	105(2)				

Table 4: Torsion angles for **33.1w**.

A	B	C	D	Angle/°	A	B	C	D	Angle/°
W	P	O1	C1	51(3)	C11	W	P	O1	-75.4(17)
W	P	C3	Si2	92.5(18)	C11	W	P	C3	158(2)
W	P	C3	Si1	-130.9(13)	C11	W	C14	O6	-23(42)
P	W	C14	O6	64(42)	C11	W	C10	O2	-29(33)

P	W	C11	O3	108(67)	C11	W	C13	O5	-56(87)
P	W	C10	O2	-25(47)	C11	W	C12	O4	-169(19)
P	W	C13	O5	90(46)	C3	P	O1	C1	-172(3)
P	W	C12	O4	105(19)	C10	W	P	O1	-80(17)
P	O1	C1	C2	-152(3)	C10	W	P	C3	154(16)
O1	P	C3	Si2	-43(2)	C10	W	C14	O6	-113(42)
O1	P	C3	Si1	94(2)	C10	W	C11	O3	-72(67)
O1	C1	C2	I	-179(2)	C10	W	C13	O5	-90(46)
C14	W	P	O1	-166.4(19)	C10	W	C12	O4	-79(19)
C14	W	P	C3	67(2)	C7	Si2	C3	P	-147(2)
C14	W	C11	O3	-165(67)	C7	Si2	C3	Si1	78(2)
C14	W	C10	O2	62(33)	C13	W	P	O1	105.5(18)
C14	W	C13	O5	3(46)	C13	W	P	C3	-21(2)
C14	W	C12	O4	63(30)	C13	W	C14	O6	159(42)
C9	Si2	C3	P	-30(3)	C13	W	C11	O3	-106(87)
C9	Si2	C3	Si1	-165(2)	C13	W	C10	O2	150(33)
C4	Si1	C3	P	64(3)	C13	W	C12	O4	10(19)
C4	Si1	C3	Si2	-159(2)	C12	W	P	O1	17.3(16)
C6	Si1	C3	P	-175(2)	C12	W	P	C3	-109(2)
C6	Si1	C3	Si2	-39(3)	C12	W	C14	O6	106(43)
C8	Si2	C3	P	86(2)	C12	W	C11	O3	19(67)
C8	Si2	C3	Si1	-48(3)	C12	W	C10	O2	-122(33)
C5	Si1	C3	P	-60(3)	C12	W	C13	O5	179(100)
C5	Si1	C3	Si2	76(2)					

12.26 Pentacarbonyl{2-[bis(trimethylsilyl)methyl]-1,2-oxaphosphetane- κP }tungsten(0) [34.1_w]

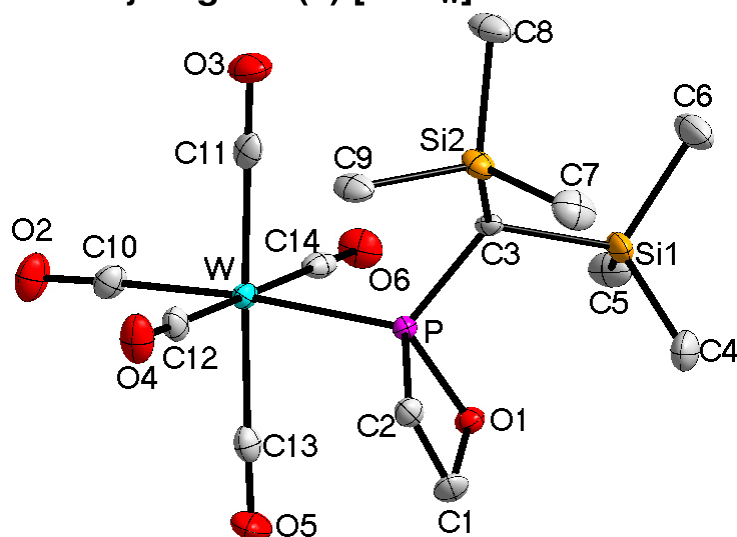


Table 1: Crystal data and structure refinement for 34.1_w.

Identification code	GSTR389, AKY-466 // GXray3853f
Device Type	Bruker X8-KappaApexII
Empirical formula	C ₁₄ H ₂₃ O ₆ PSi ₂ W
Formula weight	558.32
Temperature/K	100
Crystal system	orthorhombic
Space group	P2 ₁ 2 ₁ 2 ₁
a/Å	9.7786(5)

b/Å	9.9521(4)
c/Å	21.9977(10)
α /°	90
β /°	90
γ /°	90
Volume/Å ³	2140.76(17)
Z	4
$\rho_{\text{calc}}/\text{cm}^{-3}$	1.732
μ/mm^{-1}	5.606
F(000)	1088.0
Crystal size/mm ³	0.12 × 0.09 × 0.04
Absorption correction	empirical
Tmin; Tmax	0.5298; 0.7460
Radiation	MoK α (λ = 0.71073)
2 θ range for data collection/°	6.128 to 55.972°
Completeness to theta	0.994
Index ranges	-12 ≤ h ≤ 10, -11 ≤ k ≤ 13, -28 ≤ l ≤ 18
Reflections collected	15593
Independent reflections	5137 [R _{int} = 0.0371, R _{sigma} = 0.0490]
Data/restraints/parameters	5137/0/217
Goodness-of-fit on F ²	0.940
Final R indexes [$\geq 2\sigma$ (I)]	R ₁ = 0.0230, wR ₂ = 0.0392
Final R indexes [all data]	R ₁ = 0.0252, wR ₂ = 0.0398
Largest diff. peak/hole / e Å ⁻³	0.44/-0.38
Flack parameter	0.126(5)

Table 2: Bond lengths for **34.1w**.

Atom	Atom	Length/Å	Atom	Atom	Length/Å
W	P	2.4654(13)	Si1	C6	1.876(5)
W	C10	2.022(6)	Si2	C3	1.918(5)
W	C11	2.024(5)	Si2	C7	1.862(6)
W	C12	2.028(6)	Si2	C8	1.866(5)
W	C13	2.056(5)	Si2	C9	1.867(5)
W	C14	2.056(5)	O1	C1	1.462(6)
P	O1	1.672(3)	O2	C10	1.142(7)
P	C2	1.830(5)	O3	C11	1.150(5)
P	C3	1.810(4)	O4	C12	1.152(6)
Si1	C3	1.902(5)	O5	C13	1.138(5)
Si1	C4	1.857(6)	O6	C14	1.141(6)
Si1	C5	1.865(6)	C1	C2	1.531(6)

Table 3: Bond angles for **34.1w**.

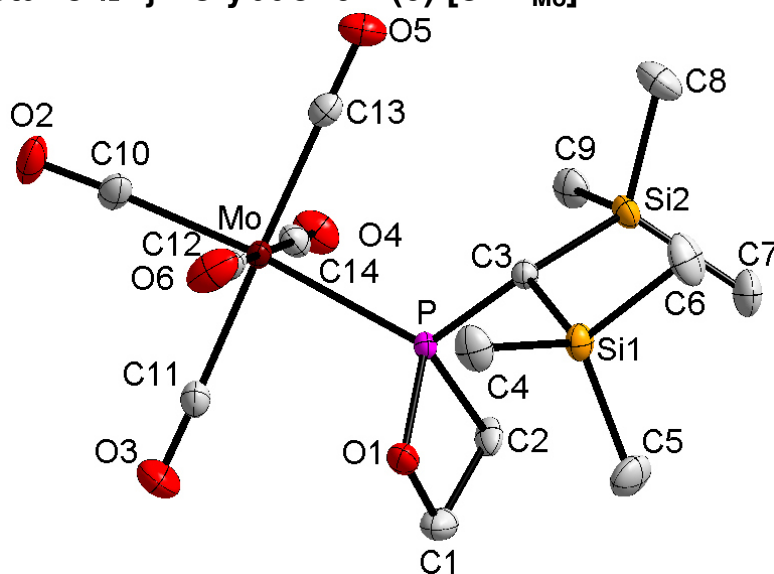
Atom	Atom	Atom	Angle/°	Atom	Atom	Atom	Angle/°
C10	W	P	174.96(14)	C4	Si1	C5	111.4(3)
C10	W	C11	91.9(2)	C4	Si1	C6	107.8(3)
C10	W	C12	88.6(2)	C5	Si1	C3	107.8(3)
C10	W	C13	90.21(19)	C5	Si1	C6	107.7(3)
C10	W	C14	93.2(2)	C6	Si1	C3	108.4(2)
C11	W	P	92.29(16)	C7	Si2	C3	112.6(3)
C11	W	C12	88.72(19)	C7	Si2	C8	110.5(3)
C11	W	C13	177.7(2)	C7	Si2	C9	107.6(3)

C11	W	C14	90.22(18)	C8	Si2	C3	106.8(2)
C12	W	P	88.66(16)	C8	Si2	C9	107.9(2)
C12	W	C13	92.2(2)	C9	Si2	C3	111.4(2)
C12	W	C14	177.9(2)	C1	O1	P	93.6(3)
C13	W	P	85.65(14)	O1	C1	C2	98.4(3)
C14	W	P	89.58(16)	C1	C2	P	85.4(3)
C14	W	C13	88.78(19)	P	C3	Si1	114.2(2)
O1	P	W	113.90(15)	P	C3	Si2	113.9(2)
O1	P	C2	80.5(2)	Si1	C3	Si2	116.8(3)
O1	P	C3	107.44(19)	O2	C10	W	176.9(5)
C2	P	W	119.28(18)	O3	C11	W	179.1(5)
C3	P	W	118.71(19)	O4	C12	W	178.8(4)
C3	P	C2	110.3(3)	O5	C13	W	178.6(5)
C4	Si1	C3	113.5(2)	O6	C14	W	179.8(5)

Table 4: Torsion angles for **34.1w**.

A	B	C	D	Angle/°	A	B	C	D	Angle/°
W	P	O1	C1	-107.7(3)	O1	P	C3	Si2	-133.9(3)
W	P	C2	C1	102.4(3)	O1	C1	C2	P	11.2(3)
W	P	C3	Si1	-127.1(2)	C2	P	O1	C1	10.3(3)
W	P	C3	Si2	95.1(3)	C2	P	C3	Si1	90.0(3)
P	O1	C1	C2	-12.3(4)	C2	P	C3	Si2	-47.8(4)
O1	P	C2	C1	-9.8(3)	C3	P	O1	C1	118.7(3)
O1	P	C3	Si1	3.9(4)	C3	P	C2	C1	-115.0(3)

12.27 Pentacarbonyl{2-[bis(trimethylsilyl)methyl]-1,2-oxaphosphetane- κ P}molybdenum(0) [**34.1_{Mo}**]

**Table 1:** Crystal data and structure refinement for **34.1_{Mo}**.

Identification code	GSTR493, FG-oxa // GXray4661f
Crystal Habitus	clear colourless block
Device Type	Bruker X8-KappaApexII
Empirical formula	C ₁₄ H ₂₃ O ₆ Si ₂ PMo
Moiety formula	C ₁₄ H ₂₃ Mo O ₆ P Si ₂
Formula weight	470.41
Temperature/K	100

Crystal system	orthorhombic
Space group	P2 ₁ 2 ₁ 2 ₁
a/Å	10.5481(4)
b/Å	13.2373(4)
c/Å	15.1957(5)
α/°	90
β/°	90
γ/°	90
Volume/Å ³	2121.75(12)
Z	4
ρ _{calc} /cm ³	1.473
μ/mm ⁻¹	0.830
F(000)	960.0
Crystal size/mm ³	0.5 × 0.4 × 0.3
Absorption correction	empirical
T _{min} ; T _{max}	0.6030; 0.7459
Radiation	MoKα (λ = 0.71073)
2θ range for data collection/°	4.08 to 55.998°
Completeness to theta	0.991
Index ranges	-8 ≤ h ≤ 13, -16 ≤ k ≤ 17, -10 ≤ l ≤ 20
Reflections collected	11052
Independent reflections	5081 [R _{int} = 0.0204, R _{sigma} = 0.0272]
Data/restraints/parameters	5081/0/224
Goodness-of-fit on F ²	1.019
Final R indexes [I >= 2σ (I)]	R ₁ = 0.0184, wR ₂ = 0.0416
Final R indexes [all data]	R ₁ = 0.0204, wR ₂ = 0.0424
Largest diff. peak/hole / e Å ⁻³	0.36/-0.57
Flack parameter	0.52(3)

Table 2: Bond lengths for **34.1Mo**.

Atom	Atom	Length/Å	Atom	Atom	Length/Å
Mo	P	2.4768(6)	Si1	C6	1.873(3)
Mo	C10	2.023(2)	Si2	C3	1.913(2)
Mo	C11	2.044(3)	Si2	C7	1.874(3)
Mo	C12	2.038(3)	Si2	C8	1.869(3)
Mo	C13	2.053(3)	Si2	C9	1.866(3)
Mo	C14	2.065(3)	O1	C1	1.462(3)
P	O1	1.6759(17)	O2	C10	1.141(3)
P	C2	1.833(2)	O3	C11	1.135(3)
P	C3	1.809(2)	O4	C14	1.137(3)
Si1	C3	1.908(2)	O5	C13	1.136(3)
Si1	C4	1.865(3)	O6	C12	1.137(3)
Si1	C5	1.858(3)	C1	C2	1.543(4)

Table 3: Bond angles for **34.1Mo**.

Atom	Atom	Atom	Angle/°	Atom	Atom	Atom	Angle/°
C10	Mo	P	172.41(7)	C4	Si1	C6	106.35(14)
C10	Mo	C11	88.69(10)	C5	Si1	C3	112.91(12)
C10	Mo	C12	88.26(10)	C5	Si1	C4	110.29(14)
C10	Mo	C13	92.01(10)	C5	Si1	C6	109.53(14)

C10	Mo	C14	93.34(10)	C6	Si1	C3	109.07(12)
C11	Mo	P	87.22(7)	C7	Si2	C3	112.92(11)
C11	Mo	C13	178.50(10)	C8	Si2	C3	106.80(11)
C11	Mo	C14	90.34(10)	C8	Si2	C7	110.25(13)
C12	Mo	P	85.43(7)	C9	Si2	C3	111.62(11)
C12	Mo	C11	91.16(10)	C9	Si2	C7	107.94(13)
C12	Mo	C13	90.18(10)	C9	Si2	C8	107.17(13)
C12	Mo	C14	177.83(10)	C1	O1	P	94.28(14)
C13	Mo	P	92.23(7)	O1	C1	C2	97.95(19)
C13	Mo	C14	88.30(9)	C1	C2	P	85.64(15)
C14	Mo	P	93.08(7)	P	C3	Si1	115.76(11)
O1	P	Mo	111.00(6)	P	C3	Si2	112.51(12)
O1	P	C2	80.40(11)	Si1	C3	Si2	115.84(11)
O1	P	C3	108.33(10)	O2	C10	Mo	175.6(2)
C2	P	Mo	123.09(8)	O3	C11	Mo	178.7(2)
C3	P	Mo	118.17(7)	O6	C12	Mo	178.8(2)
C3	P	C2	108.86(11)	O5	C13	Mo	179.5(2)
C4	Si1	C3	108.47(11)	O4	C14	Mo	178.6(2)

Table 4: Torsion angles for 34.1_{Mo}.

A	B	C	D	Angle/°	A	B	C	D	Angle/°
Mo	P	O1	C1	112.42(13)	O1	P	C3	Si2	137.28(11)
Mo	P	C2	C1	-99.91(15)	O1	C1	C2	P	-10.24(16)
Mo	P	C3	Si1	128.19(9)	C2	P	O1	C1	-9.47(15)
Mo	P	C3	Si2	-95.45(11)	C2	P	C3	Si1	-84.93(15)
P	O1	C1	C2	11.21(18)	C2	P	C3	Si2	51.44(15)
O1	P	C2	C1	8.96(14)	C3	P	O1	C1	-116.29(15)
O1	P	C3	Si1	0.91(15)	C3	P	C2	C1	115.18(15)

12.28 Pentacarbonyl{2-[bis(trimethylsilyl)methyl]-1,2-oxaphosphetane- κ P}chromium(0) [34.1_{Cr}]

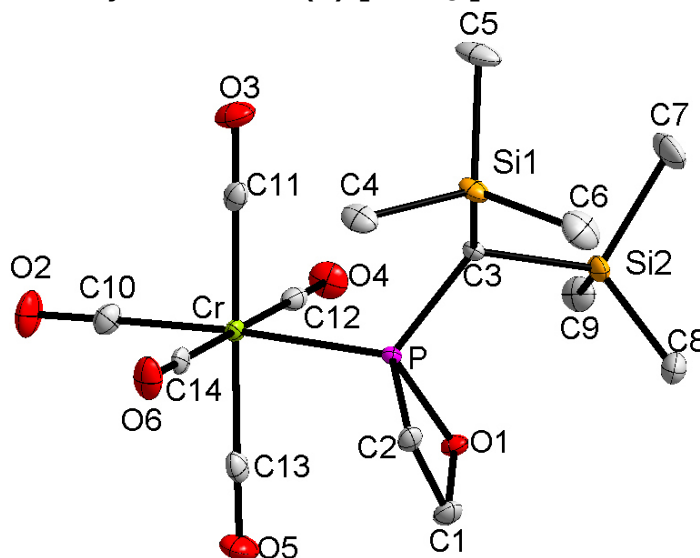


Table 1: Crystal data and structure refinement for **34.1cr**.

Identification code	GSTR461, AKY-526 // GXraymo_4477f
Crystal Habitus	clear colourless block
Device Type	Bruker D8-Venture
Empirical formula	C ₁₄ H ₂₃ O ₆ Si ₂ PCr
Moiety formula	C14 H23 Cr O6 P Si2
Formula weight	426.47
Temperature/K	100
Crystal system	orthorhombic
Space group	P2 ₁ 2 ₁ 2 ₁
a/Å	9.5614(5)
b/Å	9.8975(6)
c/Å	21.8528(13)
α/°	90
β/°	90
γ/°	90
Volume/Å ³	2068.0(2)
Z	4
ρ _{calc} /cm ³	1.370
μ/mm ⁻¹	0.770
F(000)	888.0
Crystal size/mm ³	0.26 × 0.24 × 0.24
Absorption correction	empirical
Tmin; Tmax	0.6116; 0.7459
Radiation	MoKα (λ = 0.71073)
2θ range for data collection/°	4.65 to 55.99°
Completeness to theta	0.998
Index ranges	-12 ≤ h ≤ 12, -13 ≤ k ≤ 12, -28 ≤ l ≤ 27
Reflections collected	19858
Independent reflections	4983 [R _{int} = 0.0468, R _{sigma} = 0.0481]
Data/restraints/parameters	4983/0/229
Goodness-of-fit on F ²	1.060
Final R indexes [I ≥ 2σ (I)]	R ₁ = 0.0333, wR ₂ = 0.0600
Final R indexes [all data]	R ₁ = 0.0405, wR ₂ = 0.0618
Largest diff. peak/hole / e Å ⁻³	0.31/-0.30
Flack parameter	0.005(10)

Table 2: Bond lengths for **34.1cr**.

Atom	Atom	Length/Å	Atom	Atom	Length/Å
Cr	P	2.3183(8)	Si1	C6	1.869(3)
Cr	C10	1.875(3)	Si2	C3	1.905(3)
Cr	C11	1.884(3)	Si2	C7	1.867(4)
Cr	C12	1.905(3)	Si2	C8	1.863(3)
Cr	C13	1.908(3)	Si2	C9	1.865(3)
Cr	C14	1.890(3)	O1	C1	1.470(4)
P	O1	1.669(2)	O2	C10	1.142(4)
P	C1	2.304(3)	O3	C11	1.144(4)
P	C2	1.838(3)	O4	C12	1.144(4)
P	C3	1.808(3)	O5	C13	1.138(4)
Si1	C3	1.915(3)	O6	C14	1.147(4)
Si1	C4	1.868(3)	C1	C2	1.529(4)
Si1	C5	1.862(3)			

Table 3: Bond angles for **34.1_{cr}**.

Atom	Atom	Atom	Angle/°	Atom	Atom	Atom	Angle/°
C10	Cr	P	176.34(10)	C4	Si1	C3	111.99(13)
C10	Cr	C11	91.16(13)	C4	Si1	C6	106.94(16)
C10	Cr	C12	92.30(13)	C5	Si1	C3	106.85(14)
C10	Cr	C13	89.75(12)	C5	Si1	C4	107.97(15)
C10	Cr	C14	89.42(12)	C5	Si1	C6	110.34(17)
C11	Cr	P	92.32(9)	C6	Si1	C3	112.68(14)
C11	Cr	C12	90.32(13)	C7	Si2	C3	108.62(14)
C11	Cr	C13	178.92(13)	C8	Si2	C3	113.30(14)
C11	Cr	C14	88.97(13)	C8	Si2	C7	108.10(16)
C12	Cr	P	88.82(9)	C8	Si2	C9	110.97(16)
C12	Cr	C13	89.06(13)	C9	Si2	C3	108.58(13)
C13	Cr	P	86.78(8)	C9	Si2	C7	107.06(16)
C14	Cr	P	89.51(8)	C1	O1	P	94.21(16)
C14	Cr	C12	178.15(13)	O1	C1	P	46.27(11)
C14	Cr	C13	91.63(13)	O1	C1	C2	97.8(2)
O1	P	Cr	114.00(8)	C2	C1	P	52.71(14)
O1	P	C1	39.52(10)	C1	C2	P	85.86(18)
O1	P	C2	80.11(11)	P	C3	Si1	114.23(14)
O1	P	C3	107.07(12)	P	C3	Si2	114.33(14)
C1	P	Cr	120.07(9)	Si2	C3	Si1	116.52(14)
C2	P	Cr	120.29(10)	O2	C10	Cr	178.3(3)
C2	P	C1	41.44(12)	O3	C11	Cr	179.0(3)
C3	P	Cr	118.66(9)	O4	C12	Cr	179.4(3)
C3	P	C1	120.74(12)	O5	C13	Cr	178.9(3)
C3	P	C2	109.79(13)	O6	C14	Cr	179.2(3)

Table 4: Torsion angles for **34.1_{cr}**.

A	B	C	D	Angle/°	A	B	C	D	Angle/°
Cr	P	O1	C1	-108.79(15)	O1	C1	C2	P	10.95(19)
Cr	P	C2	C1	102.42(16)	C1	P	C3	Si1	-92.43(17)
Cr	P	C3	Si1	95.96(13)	C1	P	C3	Si2	45.38(19)
Cr	P	C3	Si2	-126.23(11)	C2	P	O1	C1	10.08(17)
P	O1	C1	C2	-12.1(2)	C2	P	C3	Si1	-47.90(18)
O1	P	C2	C1	-9.69(17)	C2	P	C3	Si2	89.91(17)
O1	P	C3	Si1	-133.29(13)	C3	P	O1	C1	117.90(17)
O1	P	C3	Si2	4.52(17)	C3	P	C2	C1	-114.40(18)

12.29 Pentacarbonyl{2-[bis(trimethylsilyl)methyl]-1,2-oxaphospholane- κ P}tungsten(0) [19.1]

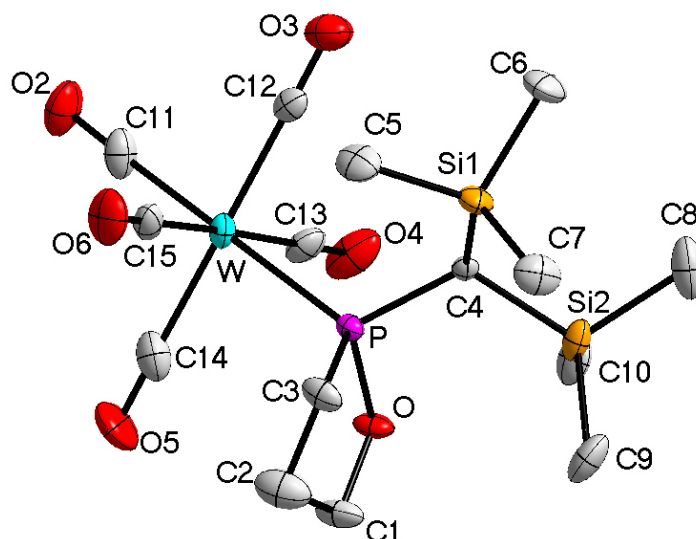


Table 1: Crystal data and structure refinement for **19.1**.

Identification code	GSTR485, AKY-554 // GXraymo_4626f
Crystal Habitus	clear light yellow plate
Device Type	Bruker D8-Venture
Empirical formula	C ₁₅ H ₂₅ O ₆ Si ₂ PW
Moiety formula	C ₁₅ H ₂₅ O ₆ P Si ₂ W
Formula weight	572.35
Temperature/K	123
Crystal system	orthorhombic
Space group	P2 ₁ 2 ₁ 2 ₁
a/Å	9.2343(4)
b/Å	10.3502(4)
c/Å	23.1652(11)
α/°	90
β/°	90
γ/°	90
Volume/Å ³	2214.06(17)
Z	4
ρ _{calc} /cm ³	1.717
μ/mm ⁻¹	5.422
F(000)	1120.0
Crystal size/mm ³	0.26 × 0.14 × 0.05
Absorption correction	empirical
Tmin; Tmax	0.4738; 0.7459
Radiation	MoKα (λ = 0.71073)
2θ range for data collection/°	5.278 to 55.994°
Completeness to theta	0.998
Index ranges	-9 ≤ h ≤ 12, -13 ≤ k ≤ 10, -30 ≤ l ≤ 24
Reflections collected	17907
Independent reflections	5344 [R _{int} = 0.0633, R _{sigma} = 0.0738]
Data/restraints/parameters	5344/18/233
Goodness-of-fit on F ²	0.999
Final R indexes [I ≥ 2σ (I)]	R ₁ = 0.0367, wR ₂ = 0.0549
Final R indexes [all data]	R ₁ = 0.0535, wR ₂ = 0.0584

Largest diff. peak/hole / e Å ⁻³	0.89/-1.02
Flack parameter	0.503(10)

Table 2: Bond lengths for 19.1.

Atom	Atom	Length/Å	Atom	Atom	Length/Å
W	P	2.4937(17)	Si2	C4	1.912(6)
W	C11	2.018(8)	Si2	C8	1.885(8)
W	C12	2.023(7)	Si2	C9	1.861(9)
W	C13	2.031(8)	Si2	C10	1.872(8)
W	C14	2.046(7)	O1	C1	1.449(8)
W	C15	2.046(8)	O2	C11	1.148(9)
P	O1	1.640(5)	O3	C12	1.152(7)
P	C3	1.835(7)	O4	C13	1.139(8)
P	C4	1.816(6)	O5	C14	1.138(8)
Si1	C4	1.910(7)	O6	C15	1.146(8)
Si1	C5	1.862(7)	C1	C2	1.499(11)
Si1	C6	1.872(7)	C2	C3	1.520(9)
Si1	C7	1.863(8)			

Table 3: Bond angles for 19.1.

Atom	Atom	Atom	Angle/°	Atom	Atom	Atom	Angle/°
C11	W	P	178.4(2)	C5	Si1	C7	106.4(5)
C11	W	C12	88.1(3)	C6	Si1	C4	107.7(3)
C11	W	C13	93.8(3)	C7	Si1	C4	111.4(3)
C11	W	C14	90.3(4)	C7	Si1	C6	110.6(4)
C11	W	C15	91.4(3)	C8	Si2	C4	109.5(3)
C12	W	P	92.4(2)	C9	Si2	C4	113.8(3)
C12	W	C13	88.9(3)	C9	Si2	C8	107.4(4)
C12	W	C14	177.3(3)	C9	Si2	C10	109.2(4)
C12	W	C15	90.8(3)	C10	Si2	C4	109.4(3)
C13	W	P	84.7(2)	C10	Si2	C8	107.2(4)
C13	W	C14	89.0(3)	C1	O1	P	114.3(4)
C13	W	C15	174.9(3)	O1	C1	C2	109.2(6)
C14	W	P	89.2(3)	C1	C2	C3	107.5(6)
C14	W	C15	91.4(4)	C2	C3	P	102.3(6)
C15	W	P	90.2(2)	P	C4	Si1	114.1(3)
O1	P	W	110.7(2)	P	C4	Si2	116.1(3)
O1	P	C3	93.4(3)	Si1	C4	Si2	115.5(3)
O1	P	C4	105.7(3)	O2	C11	W	178.7(9)
C3	P	W	119.8(3)	O3	C12	W	178.2(7)
C4	P	W	116.5(2)	O4	C13	W	178.9(7)
C4	P	C3	107.6(3)	O5	C14	W	178.7(8)
C5	Si1	C4	114.2(3)	O6	C15	W	178.8(7)
C5	Si1	C6	106.5(4)				

Table 4: Torsion angles for 19.1.

A	B	C	D	Angle/°	A	B	C	D	Angle/°
W	P	O1	C1	-108.3(5)	O1	C1	C2	C3	-28.7(10)

W	P	C3	C2	86.0(5)	C1	C2	C3	P	37.0(9)
W	P	C4	Si1	89.9(3)	C3	P	O1	C1	15.4(6)
W	P	C4	Si2	-131.9(3)	C3	P	C4	Si1	-47.9(4)
P	O1	C1	C2	5.3(9)	C3	P	C4	Si2	90.3(4)
O1	P	C3	C2	-30.2(6)	C4	P	O1	C1	124.7(5)
O1	P	C4	Si1	-146.8(3)	C4	P	C3	C2	-137.9(5)
O1	P	C4	Si2	-8.6(4)					

12.30

Pentacarbonyl{catecholboranoxo[bis(trimethylsilyl)methyl]phosphane- κP }tungsten(0) [41.1]

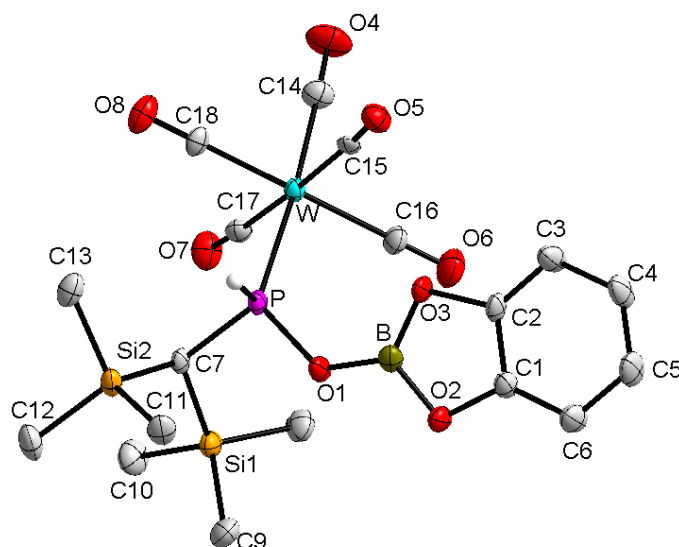


Table 1: Crystal data and structure refinement for **41.1**.

Identification code	GSTR385, AKY-458 // GXray3821
Device Type	Nonius KappaCCD
Empirical formula	C ₁₈ H ₂₄ BO ₈ PSi ₂ W
Formula weight	650.18
Temperature/K	123
Crystal system	triclinic
Space group	P $\bar{1}$
a/Å	8.7638(3)
b/Å	11.0103(4)
c/Å	14.5026(6)
α /°	108.2413(19)
β /°	105.4429(17)
γ /°	91.170(2)
Volume/Å ³	1272.82(8)
Z	2
$\rho_{\text{calc}}/\text{cm}^3$	1.696
μ/mm^{-1}	4.733
F(000)	636.0
Crystal size/mm ³	0.34 × 0.16 × 0.1
Absorption correction	multi-scan
Tmin; Tmax	0.3464; 0.6657
Radiation	MoK α (λ = 0.71073)
2 θ range for data collection/°	4.86 to 56°

Completeness to theta	0.999
Index ranges	-11 ≤ h ≤ 11, -14 ≤ k ≤ 14, -19 ≤ l ≤ 19
Reflections collected	14299
Independent reflections	5900 [R _{int} = 0.0610, R _{sigma} = 0.0576]
Data/restraints/parameters	5900/0/289
Goodness-of-fit on F ²	1.013
Final R indexes [I ≥ 2σ (I)]	R ₁ = 0.0329, wR ₂ = 0.0763
Final R indexes [all data]	R ₁ = 0.0371, wR ₂ = 0.0778
Largest diff. peak/hole / e Å ⁻³	2.37/-2.35

Table 2: Bond lengths for 41.1.

Atom	Atom	Length/Å	Atom	Atom	Length/Å
W	P	2.4695(9)	O1	B	1.353(5)
W	C14	2.024(4)	O2	C1	1.386(5)
W	C15	2.051(4)	O2	B	1.387(5)
W	C16	2.064(4)	O3	C2	1.400(4)
W	C17	2.045(4)	O3	B	1.376(6)
W	C18	2.037(4)	O4	C14	1.135(5)
P	O1	1.656(3)	O5	C15	1.135(5)
P	C7	1.798(4)	O6	C16	1.126(5)
Si1	C7	1.910(4)	O7	C17	1.139(5)
Si1	C8	1.865(4)	O8	C18	1.136(5)
Si1	C9	1.865(4)	C1	C2	1.379(6)
Si1	C10	1.875(4)	C1	C6	1.368(6)
Si2	C7	1.908(4)	C2	C3	1.358(6)
Si2	C11	1.872(4)	C3	C4	1.394(6)
Si2	C12	1.872(5)	C4	C5	1.378(7)
Si2	C13	1.867(4)	C5	C6	1.403(6)

Table 3: Bond angles for 41.1.

Atom	Atom	Atom	Angle/°	Atom	Atom	Atom	Angle/°
C14	W	P	175.90(12)	C13	Si2	C7	107.62(17)
C14	W	C15	90.30(16)	C13	Si2	C11	109.6(2)
C14	W	C16	92.05(17)	C13	Si2	C12	107.3(2)
C14	W	C17	88.42(16)	B	O1	P	127.2(3)
C14	W	C18	89.85(17)	C1	O2	B	104.1(3)
C15	W	P	90.15(9)	B	O3	C2	104.1(3)
C15	W	C16	89.73(17)	C2	C1	O2	109.7(3)
C16	W	P	92.03(11)	C6	C1	O2	128.7(4)
C17	W	P	90.99(10)	C6	C1	C2	121.6(4)
C17	W	C15	177.69(13)	C1	C2	O3	109.1(3)
C17	W	C16	92.23(17)	C3	C2	O3	127.8(4)
C18	W	P	86.09(11)	C3	C2	C1	123.1(4)
C18	W	C15	87.83(16)	C2	C3	C4	116.2(4)
C18	W	C16	176.92(14)	C5	C4	C3	121.4(4)
C18	W	C17	90.25(16)	C4	C5	C6	121.5(4)
O1	P	W	121.76(10)	C1	C6	C5	116.2(4)
O1	P	C7	100.11(16)	P	C7	Si1	114.44(18)
C7	P	W	119.14(12)	P	C7	Si2	111.2(2)
C8	Si1	C7	112.97(19)	Si2	C7	Si1	117.05(19)

C8	Si1	C10	107.8(2)	O4	C14	W	178.2(4)
C9	Si1	C7	111.69(19)	O5	C15	W	177.5(3)
C9	Si1	C8	107.4(2)	O6	C16	W	177.6(4)
C9	Si1	C10	110.5(2)	O7	C17	W	177.0(4)
C10	Si1	C7	106.42(19)	O8	C18	W	179.8(4)
C11	Si2	C7	110.21(17)	O1	B	O2	121.8(4)
C12	Si2	C7	110.8(2)	O1	B	O3	125.2(4)
C12	Si2	C11	111.2(2)	O3	B	O2	113.0(3)

Table 4: Torsion angles for 41.1.

A	B	C	D	Angle/°	A	B	C	D	Angle/°
W	P	O1	B	45.0(4)	C12	Si2	C7	Si1	-46.6(3)
W	P	C7	Si1	92.11(18)	C13	Si2	C7	P	62.3(2)
W	P	C7	Si2	-132.53(13)	C13	Si2	C7	Si1	-163.7(2)
P	W	C14	O4	-24(16)	C14	W	P	O1	-170.3(19)
P	W	C15	O5	-110(7)	C14	W	P	C7	64.2(19)
P	W	C16	O6	-55(9)	C14	W	C15	O5	66(7)
P	W	C17	O7	151(7)	C14	W	C16	O6	125(9)
P	W	C18	O8	101(100)	C14	W	C17	O7	-25(7)
P	O1	B	O2	-174.1(3)	C14	W	C18	O8	-79(100)
P	O1	B	O3	4.2(6)	C15	W	P	O1	-73.96(18)
O1	P	C7	Si1	-43.3(2)	C15	W	P	C7	160.49(18)
O1	P	C7	Si2	92.1(2)	C15	W	C14	O4	-120(14)
O2	C1	C2	O3	1.1(4)	C15	W	C16	O6	35(9)
O2	C1	C2	C3	-179.0(4)	C15	W	C17	O7	31(9)
O2	C1	C6	C5	178.2(4)	C15	W	C18	O8	11(100)
O3	C2	C3	C4	-179.3(4)	C16	W	P	O1	15.78(19)
C1	O2	B	O1	178.1(4)	C16	W	P	C7	-109.77(19)
C1	O2	B	O3	-0.4(4)	C16	W	C14	O4	150(14)
C1	C2	C3	C4	0.9(7)	C16	W	C15	O5	158(7)
C2	O3	B	O1	-177.3(4)	C16	W	C17	O7	-117(7)
C2	O3	B	O2	1.1(4)	C16	W	C18	O8	49(100)
C2	C1	C6	C5	0.0(7)	C17	W	P	O1	108.05(18)
C2	C3	C4	C5	-0.9(7)	C17	W	P	C7	-17.51(19)
C3	C4	C5	C6	0.4(8)	C17	W	C14	O4	58(14)
C4	C5	C6	C1	0.0(7)	C17	W	C15	O5	10(9)
C6	C1	C2	O3	179.7(4)	C17	W	C16	O6	-147(9)
C6	C1	C2	C3	-0.5(7)	C17	W	C18	O8	-168(100)
C7	P	O1	B	178.8(3)	C18	W	P	O1	-161.77(18)
C8	Si1	C7	P	-27.6(3)	C18	W	P	C7	72.68(19)
C8	Si1	C7	Si2	-160.2(2)	C18	W	C14	O4	-32(14)
C9	Si1	C7	P	93.6(2)	C18	W	C15	O5	-24(7)
C9	Si1	C7	Si2	-39.0(3)	C18	W	C16	O6	-3(11)
C10	Si1	C7	P	-145.7(2)	C18	W	C17	O7	65(7)
C10	Si1	C7	Si2	81.7(2)	B	O2	C1	C2	-0.4(4)
C11	Si2	C7	P	-57.2(3)	B	O2	C1	C6	-178.8(4)
C11	Si2	C7	Si1	76.9(3)	B	O3	C2	C1	-1.3(4)
C12	Si2	C7	P	179.3(2)	B	O3	C2	C3	178.8(4)

12.31 Pentacarbonyl[4-methyl-2-(triphenylmethyl)-1,2-thiaphosphetane- κP]tungsten(0) [46.3]

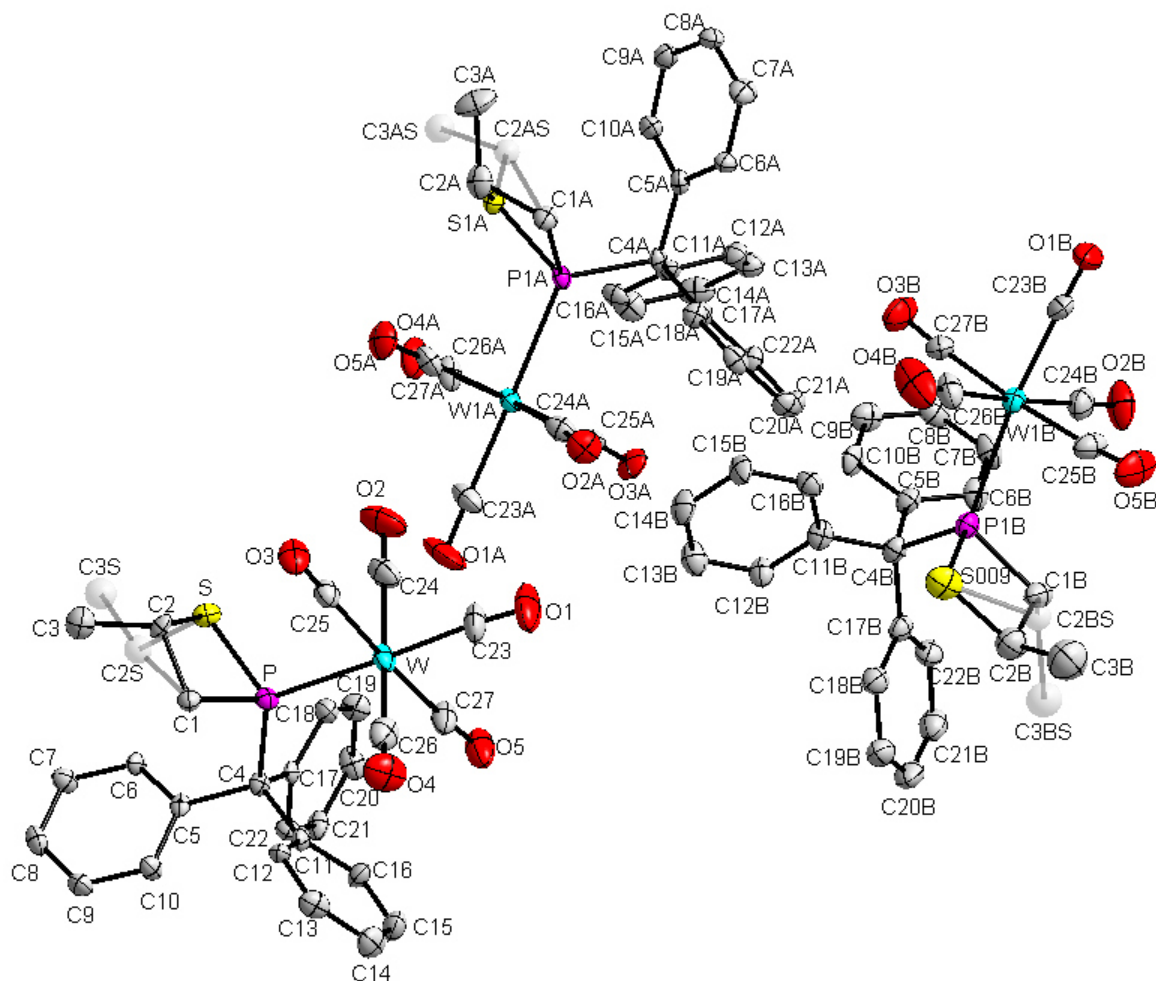


Table 1: Crystal data and structure refinement for **46.3**.

Identification code	GSTR523, AKY-583 // GXray4889af
Crystal Habitus	clear colourless plate
Device Type	Bruker X8-KappaApexII
Empirical formula	$C_{27}H_{21}O_5PSW$
Moiety formula	$C_{27}H_{21}O_5P S W$
Formula weight	672.32
Temperature/K	100
Crystal system	monoclinic
Space group	$P2_1/c$
a/Å	10.8752(8)
b/Å	44.889(3)
c/Å	16.0622(12)
α /°	90
β /°	90.964(3)
γ /°	90
Volume/Å ³	7840.0(10)
Z	12
ρ_{calc}/cm^3	1.709
μ/mm^{-1}	4.596
F(000)	3936.0

Crystal size/mm ³	0.08 × 0.04 × 0.01
Absorption correction	empirical
Tmin; Tmax	0.5126; 0.7459
Radiation	MoK α (λ = 0.71073)
2 θ range for data collection/°	3.854 to 56°
Completeness to theta	0.998
Index ranges	-14 ≤ h ≤ 14, -59 ≤ k ≤ 59, -21 ≤ l ≤ 14
Reflections collected	107550
Independent reflections	18901 [R _{int} = 0.1095, R _{sigma} = 0.0837]
Data/restraints/parameters	18901/54/1009
Goodness-of-fit on F ²	1.121
Final R indexes [$I \geq 2\sigma(I)$]	R ₁ = 0.0559, wR ₂ = 0.0983
Final R indexes [all data]	R ₁ = 0.0922, wR ₂ = 0.1168
Largest diff. peak/hole / e Å ⁻³	1.39/-2.57

Table 2: Bond lengths for **46.3**.

Atom	Atom	Length/Å	Atom	Atom	Length/Å
W	P	2.5158(18)	C4A	C11A	1.531(9)
W	C23	1.997(8)	C4A	C17A	1.553(9)
W	C24	2.031(9)	C5A	C6A	1.383(9)
W	C25	2.033(8)	C5A	C10A	1.401(9)
W	C26	2.031(9)	C6A	C7A	1.387(9)
W	C27	2.054(8)	C7A	C8A	1.388(10)
S	P	2.125(3)	C8A	C9A	1.380(10)
S	C2	1.876(10)	C9A	C10A	1.384(10)
S	C2S	1.82(3)	C11A	C12A	1.397(9)
P	C1	1.861(7)	C11A	C16A	1.391(9)
P	C4	1.922(7)	C12A	C13A	1.379(10)
O1	C23	1.144(9)	C13A	C14A	1.382(10)
O2	C24	1.148(10)	C14A	C15A	1.382(10)
O3	C25	1.137(9)	C15A	C16A	1.387(9)
O4	C26	1.147(10)	C17A	C18A	1.401(9)
O5	C27	1.135(9)	C17A	C22A	1.374(9)
C1	C2	1.529(12)	C18A	C19A	1.377(9)
C1	C2S	1.62(3)	C19A	C20A	1.389(10)
C2	C3	1.514(19)	C20A	C21A	1.363(10)
C2S	C3S	1.49(4)	C21A	C22A	1.389(10)
C4	C5	1.549(9)	W1B	P1B	2.539(2)
C4	C11	1.534(9)	W1B	C23B	2.006(8)
C4	C17	1.539(9)	W1B	C24B	2.031(9)
C5	C6	1.393(9)	W1B	C25B	2.023(8)
C5	C10	1.414(9)	W1B	C26B	2.045(9)
C6	C7	1.384(9)	W1B	C27B	2.049(8)
C7	C8	1.375(10)	S009	P1B	2.115(3)
C8	C9	1.383(10)	S009	C2B	1.832(16)
C9	C10	1.377(9)	S009	C2BS	1.92(2)
C11	C12	1.404(9)	P1B	C1B	1.872(8)
C11	C16	1.382(9)	P1B	C4B	1.936(7)
C12	C13	1.383(9)	O1B	C23B	1.136(9)
C13	C14	1.391(11)	O2B	C24B	1.148(9)
C14	C15	1.391(11)	O3B	C27B	1.143(9)
C15	C16	1.380(10)	O4B	C26B	1.136(10)

C17	C18	1.390(9)	O5B	C25B	1.124(9)
C17	C22	1.402(9)	C1B	C2B	1.612(17)
C18	C19	1.386(9)	C1B	C2BS	1.50(2)
C19	C20	1.367(10)	C2B	C3B	1.51(3)
C20	C21	1.390(10)	C2BS	C3BS	1.57(4)
C21	C22	1.382(9)	C4B	C5B	1.521(10)
W1A	P1A	2.5060(18)	C4B	C11B	1.550(10)
W1A	C23A	2.006(8)	C4B	C17B	1.537(10)
W1A	C24A	2.056(8)	C5B	C6B	1.392(10)
W1A	C25A	2.044(8)	C5B	C10B	1.414(9)
W1A	C26A	2.049(8)	C6B	C7B	1.372(10)
W1A	C27A	2.037(8)	C7B	C8B	1.390(11)
S1A	P1A	2.132(2)	C8B	C9B	1.381(11)
S1A	C2A	1.901(11)	C9B	C10B	1.386(10)
S1A	C2AS	1.83(2)	C11B	C12B	1.400(10)
P1A	C1A	1.856(7)	C11B	C16B	1.374(10)
P1A	C4A	1.920(7)	C12B	C13B	1.383(10)
O1A	C23A	1.132(9)	C13B	C14B	1.383(11)
O2A	C24A	1.133(8)	C14B	C15B	1.374(10)
O3A	C25A	1.132(9)	C15B	C16B	1.406(10)
O4A	C26A	1.131(9)	C17B	C18B	1.423(10)
O5A	C27A	1.139(9)	C17B	C22B	1.394(10)
C1A	C2A	1.509(13)	C18B	C19B	1.392(11)
C1A	C2AS	1.66(3)	C19B	C20B	1.371(12)
C2A	C3A	1.52(2)	C20B	C21B	1.385(12)
C2AS	C3AS	1.50(4)	C21B	C22B	1.381(11)
C4A	C5A	1.544(9)			

Table 3: Bond angles for 46.3.

Atom	Atom	Atom	Angle ^o	Atom	Atom	Atom	Angle ^o
C23	W	P	177.6(3)	C11A	C4A	P1A	112.1(4)
C23	W	C24	89.1(4)	C11A	C4A	C5A	107.1(5)
C23	W	C25	90.9(3)	C11A	C4A	C17A	111.5(5)
C23	W	C26	86.9(4)	C17A	C4A	P1A	103.9(4)
C23	W	C27	88.0(3)	C6A	C5A	C4A	124.5(6)
C24	W	P	90.4(3)	C6A	C5A	C10A	117.3(6)
C24	W	C25	84.4(3)	C10A	C5A	C4A	118.2(6)
C24	W	C26	172.1(3)	C5A	C6A	C7A	121.9(7)
C24	W	C27	92.2(4)	C6A	C7A	C8A	119.8(7)
C25	W	P	86.7(2)	C9A	C8A	C7A	119.5(7)
C25	W	C27	176.5(3)	C8A	C9A	C10A	120.2(7)
C26	W	P	93.3(2)	C9A	C10A	C5A	121.3(7)
C26	W	C25	88.9(3)	C12A	C11A	C4A	118.6(6)
C26	W	C27	94.4(4)	C16A	C11A	C4A	124.4(6)
C27	W	P	94.4(2)	C16A	C11A	C12A	116.9(6)
C2	S	P	78.7(3)	C13A	C12A	C11A	122.2(7)
C2S	S	P	82.2(8)	C12A	C13A	C14A	119.4(7)
S	P	W	113.59(9)	C13A	C14A	C15A	120.1(7)
C1	P	W	117.4(2)	C14A	C15A	C16A	119.8(7)
C1	P	S	80.8(2)	C15A	C16A	C11A	121.6(7)
C1	P	C4	105.7(3)	C18A	C17A	C4A	119.2(6)

C4	P	W	121.6(2)	C22A	C17A	C4A	123.8(6)
C4	P	S	110.5(2)	C22A	C17A	C18A	117.0(6)
C2	C1	P	96.8(5)	C19A	C18A	C17A	121.4(7)
C2S	C1	P	96.6(10)	C18A	C19A	C20A	120.2(7)
C1	C2	S	98.5(6)	C21A	C20A	C19A	119.0(7)
C3	C2	S	112.8(9)	C20A	C21A	C22A	120.6(7)
C3	C2	C1	113.8(10)	C17A	C22A	C21A	121.7(7)
C1	C2S	S	97.5(14)	O1A	C23A	W1A	177.8(8)
C3S	C2S	S	114(2)	O2A	C24A	W1A	175.2(7)
C3S	C2S	C1	114(2)	O3A	C25A	W1A	176.5(7)
C5	C4	P	110.7(4)	O4A	C26A	W1A	177.6(7)
C11	C4	P	103.1(4)	O5A	C27A	W1A	179.0(7)
C11	C4	C5	112.5(5)	C23B	W1B	P1B	172.3(2)
C11	C4	C17	112.5(5)	C23B	W1B	C24B	86.9(3)
C17	C4	P	110.4(4)	C23B	W1B	C25B	85.8(3)
C17	C4	C5	107.7(5)	C23B	W1B	C26B	89.7(3)
C6	C5	C4	120.0(6)	C23B	W1B	C27B	90.5(3)
C6	C5	C10	117.4(6)	C24B	W1B	P1B	93.2(2)
C10	C5	C4	122.6(6)	C24B	W1B	C26B	176.5(3)
C7	C6	C5	121.2(6)	C24B	W1B	C27B	90.2(3)
C8	C7	C6	120.6(7)	C25B	W1B	P1B	86.5(2)
C7	C8	C9	119.3(7)	C25B	W1B	C24B	89.2(3)
C10	C9	C8	120.8(7)	C25B	W1B	C26B	89.8(4)
C9	C10	C5	120.6(6)	C25B	W1B	C27B	176.4(3)
C12	C11	C4	119.2(6)	C26B	W1B	P1B	90.1(3)
C16	C11	C4	122.9(6)	C26B	W1B	C27B	90.5(3)
C16	C11	C12	117.9(6)	C27B	W1B	P1B	97.1(2)
C13	C12	C11	121.2(7)	C2B	S009	P1B	82.1(5)
C12	C13	C14	120.0(7)	C2BS	S009	P1B	77.0(6)
C13	C14	C15	118.9(7)	S009	P1B	W1B	114.19(10)
C16	C15	C14	120.7(8)	C1B	P1B	W1B	114.4(3)
C15	C16	C11	121.2(7)	C1B	P1B	S009	81.8(3)
C18	C17	C4	125.2(6)	C1B	P1B	C4B	106.7(3)
C18	C17	C22	117.8(6)	C4B	P1B	W1B	124.5(2)
C22	C17	C4	116.9(6)	C4B	P1B	S009	106.9(2)
C19	C18	C17	120.2(7)	C2B	C1B	P1B	96.3(7)
C20	C19	C18	121.8(7)	C2BS	C1B	P1B	95.9(9)
C19	C20	C21	119.0(7)	C1B	C2B	S009	98.7(9)
C22	C21	C20	119.9(7)	C3B	C2B	S009	110.6(13)
C21	C22	C17	121.4(7)	C3B	C2B	C1B	114.9(14)
O1	C23	W	175.2(9)	C1B	C2BS	S009	99.3(12)
O2	C24	W	175.1(8)	C1B	C2BS	C3BS	111.0(18)
O3	C25	W	178.4(7)	C3BS	C2BS	S009	112.5(17)
O4	C26	W	174.7(8)	C5B	C4B	P1B	105.3(5)
O5	C27	W	176.1(7)	C5B	C4B	C11B	110.6(6)
C23A	W1A	P1A	177.6(3)	C5B	C4B	C17B	112.5(6)
C23A	W1A	C24A	87.8(3)	C11B	C4B	P1B	109.5(5)
C23A	W1A	C25A	87.3(3)	C17B	C4B	P1B	109.5(5)
C23A	W1A	C26A	89.3(3)	C17B	C4B	C11B	109.4(6)
C23A	W1A	C27A	92.4(3)	C6B	C5B	C4B	121.3(7)
C24A	W1A	P1A	94.6(2)	C6B	C5B	C10B	117.2(7)
C25A	W1A	P1A	92.0(2)	C10B	C5B	C4B	121.5(7)
C25A	W1A	C24A	93.1(3)	C7B	C6B	C5B	122.6(7)

C25A	W1A	C26A	92.3(3)	C6B	C7B	C8B	119.7(8)
C26A	W1A	P1A	88.4(2)	C9B	C8B	C7B	119.3(8)
C26A	W1A	C24A	173.7(3)	C8B	C9B	C10B	121.2(8)
C27A	W1A	P1A	88.3(2)	C9B	C10B	C5B	120.1(7)
C27A	W1A	C24A	88.3(3)	C12B	C11B	C4B	118.9(6)
C27A	W1A	C25A	178.6(3)	C16B	C11B	C4B	122.3(7)
C27A	W1A	C26A	86.3(3)	C16B	C11B	C12B	118.7(7)
C2A	S1A	P1A	78.0(4)	C13B	C12B	C11B	120.0(7)
C2AS	S1A	P1A	83.7(8)	C12B	C13B	C14B	121.1(7)
S1A	P1A	W1A	113.52(9)	C15B	C14B	C13B	119.2(7)
C1A	P1A	W1A	118.0(2)	C14B	C15B	C16B	120.1(7)
C1A	P1A	S1A	80.6(2)	C11B	C16B	C15B	120.8(7)
C1A	P1A	C4A	106.0(3)	C18B	C17B	C4B	118.8(7)
C4A	P1A	W1A	122.1(2)	C22B	C17B	C4B	123.5(7)
C4A	P1A	S1A	108.9(2)	C22B	C17B	C18B	117.7(7)
C2A	C1A	P1A	97.7(6)	C19B	C18B	C17B	119.4(8)
C2AS	C1A	P1A	97.9(9)	C20B	C19B	C18B	121.5(8)
C1A	C2A	S1A	98.1(7)	C19B	C20B	C21B	119.5(8)
C1A	C2A	C3A	114.6(13)	C22B	C21B	C20B	120.2(8)
C3A	C2A	S1A	113.0(11)	C21B	C22B	C17B	121.6(8)
C1A	C2AS	S1A	95.7(12)	O1B	C23B	W1B	176.8(7)
C3AS	C2AS	S1A	115(2)	O2B	C24B	W1B	177.2(7)
C3AS	C2AS	C1A	111(2)	O5B	C25B	W1B	175.5(8)
C5A	C4A	P1A	110.7(4)	O4B	C26B	W1B	176.7(8)
C5A	C4A	C17A	111.6(5)	O3B	C27B	W1B	175.2(7)

Table 4: Torsion angles for **46.3**.

A	B	C	D	Angle/°	A	B	C	D	Angle/°
W	P	C1	C2	94.6(6)	C5A	C4A	C17A	C18A	65.7(8)
W	P	C1	C2S	124.5(13)	C5A	C4A	C17A	C22A	-111.9(7)
S	P	C1	C2	-17.3(6)	C5A	C6A	C7A	C8A	2.0(11)
S	P	C1	C2S	12.6(13)	C6A	C5A	C10A	C9A	-1.9(10)
P	S	C2	C1	-17.3(6)	C6A	C7A	C8A	C9A	-2.8(11)
P	S	C2	C3	-137.7(11)	C7A	C8A	C9A	C10A	1.2(11)
P	S	C2S	C1	12.8(13)	C8A	C9A	C10A	C5A	1.1(11)
P	S	C2S	C3S	133(3)	C10A	C5A	C6A	C7A	0.3(10)
P	C1	C2	S	19.6(6)	C11A	C4A	C5A	C6A	-130.2(7)
P	C1	C2	C3	139.3(9)	C11A	C4A	C5A	C10A	50.1(8)
P	C1	C2S	S	-14.7(15)	C11A	C4A	C17A	C18A	-174.6(6)
P	C1	C2S	C3S	-135(2)	C11A	C4A	C17A	C22A	7.8(9)
P	C4	C5	C6	69.5(7)	C11A	C12A	C13A	C14A	2.4(11)
P	C4	C5	C10	-113.6(6)	C12A	C11A	C16A	C15A	2.1(11)
P	C4	C11	C12	58.4(7)	C12A	C13A	C14A	C15A	-0.2(11)
P	C4	C11	C16	-121.2(6)	C13A	C14A	C15A	C16A	-1.0(12)
P	C4	C17	C18	5.0(8)	C14A	C15A	C16A	C11A	0.0(12)
P	C4	C17	C22	-178.0(5)	C16A	C11A	C12A	C13A	-3.3(10)
C4	P	C1	C2	-126.1(6)	C17A	C4A	C5A	C6A	-7.9(9)
C4	P	C1	C2S	-96.2(13)	C17A	C4A	C5A	C10A	172.4(6)
C4	C5	C6	C7	-178.2(6)	C17A	C4A	C11A	C12A	-68.8(8)
C4	C5	C10	C9	179.9(6)	C17A	C4A	C11A	C16A	111.9(7)
C4	C11	C12	C13	177.3(6)	C17A	C18A	C19A	C20A	-0.2(11)

C4	C11	C16	C15	-177.7(7)	C18A	C17A	C22A	C21A	-1.7(10)
C4	C17	C18	C19	177.5(6)	C18A	C19A	C20A	C21A	-0.6(11)
C4	C17	C22	C21	-177.1(6)	C19A	C20A	C21A	C22A	0.3(11)
C5	C4	C11	C12	-60.8(8)	C20A	C21A	C22A	C17A	0.9(11)
C5	C4	C11	C16	119.6(7)	C22A	C17A	C18A	C19A	1.3(10)
C5	C4	C17	C18	125.9(7)	W1B	P1B	C1B	C2B	120.8(7)
C5	C4	C17	C22	-57.0(7)	W1B	P1B	C1B	C2BS	93.8(11)
C5	C6	C7	C8	-2.7(11)	S009	P1B	C1B	C2B	7.9(7)
C6	C5	C10	C9	-3.2(10)	S009	P1B	C1B	C2BS	-19.1(11)
C6	C7	C8	C9	-1.2(11)	P1B	S009	C2B	C1B	8.1(8)
C7	C8	C9	C10	2.8(11)	P1B	S009	C2B	C3B	128.9(14)
C8	C9	C10	C5	-0.6(11)	P1B	C1B	C2B	S009	-9.1(9)
C10	C5	C6	C7	4.8(10)	P1B	C1B	C2B	C3B	-126.7(14)
C11	C4	C5	C6	-175.8(6)	P1B	C1B	C2BS	S009	21.2(11)
C11	C4	C5	C10	1.1(9)	P1B	C1B	C2BS	C3BS	139.8(17)
C11	C4	C17	C18	-109.6(7)	P1B	C4B	C5B	C6B	49.9(8)
C11	C4	C17	C22	67.5(7)	P1B	C4B	C5B	C10B	-130.3(6)
C11	C12	C13	C14	0.6(11)	P1B	C4B	C11B	C12B	-155.7(6)
C12	C11	C16	C15	2.7(11)	P1B	C4B	C11B	C16B	28.1(8)
C12	C13	C14	C15	2.2(12)	P1B	C4B	C17B	C18B	76.4(7)
C13	C14	C15	C16	-2.6(12)	P1B	C4B	C17B	C22B	-104.8(7)
C14	C15	C16	C11	0.1(12)	C4B	P1B	C1B	C2B	-97.4(8)
C16	C11	C12	C13	-3.0(10)	C4B	P1B	C1B	C2BS	-124.4(11)
C17	C4	C5	C6	-51.2(8)	C4B	C5B	C6B	C7B	179.1(7)
C17	C4	C5	C10	125.6(6)	C4B	C5B	C10B	C9B	-178.9(7)
C17	C4	C11	C12	177.4(6)	C4B	C11B	C12B	C13B	-177.7(7)
C17	C4	C11	C16	-2.3(9)	C4B	C11B	C16B	C15B	177.5(7)
C17	C18	C19	C20	-0.8(11)	C4B	C17B	C18B	C19B	-179.7(7)
C18	C17	C22	C21	0.2(10)	C4B	C17B	C22B	C21B	-179.7(7)
C18	C19	C20	C21	0.4(11)	C5B	C4B	C11B	C12B	88.8(8)
C19	C20	C21	C22	0.4(11)	C5B	C4B	C11B	C16B	-87.5(8)
C20	C21	C22	C17	-0.6(11)	C5B	C4B	C17B	C18B	-167.0(6)
C22	C17	C18	C19	0.5(10)	C5B	C4B	C17B	C22B	11.9(10)
W1A	P1A	C1A	C2A	-93.2(7)	C5B	C6B	C7B	C8B	0.5(12)
W1A	P1A	C1A	C2AS	-122.5(12)	C6B	C5B	C10B	C9B	0.9(11)
S1A	P1A	C1A	C2A	18.5(7)	C6B	C7B	C8B	C9B	-0.5(12)
S1A	P1A	C1A	C2AS	-10.7(12)	C7B	C8B	C9B	C10B	0.7(12)
P1A	S1A	C2AS	C1A	-10.8(12)	C8B	C9B	C10B	C5B	-1.0(12)
P1A	S1A	C2AS	C3AS	-128(3)	C10B	C5B	C6B	C7B	-0.7(11)
P1A	C1A	C2A	S1A	-20.8(8)	C11B	C4B	C5B	C6B	168.1(7)
P1A	C1A	C2A	C3A	-140.7(12)	C11B	C4B	C5B	C10B	-12.1(9)
P1A	C1A	C2AS	S1A	12.4(14)	C11B	C4B	C17B	C18B	-43.6(8)
P1A	C1A	C2AS	C3AS	133(2)	C11B	C4B	C17B	C22B	135.2(7)
P1A	C4A	C5A	C6A	107.4(7)	C11B	C12B	C13B	C14B	0.9(12)
P1A	C4A	C5A	C10A	-72.3(7)	C12B	C11B	C16B	C15B	1.2(11)
P1A	C4A	C11A	C12A	175.1(5)	C12B	C13B	C14B	C15B	-0.3(13)
P1A	C4A	C11A	C16A	-4.2(9)	C13B	C14B	C15B	C16B	0.2(12)
P1A	C4A	C17A	C18A	-53.6(7)	C14B	C15B	C16B	C11B	-0.7(12)
P1A	C4A	C17A	C22A	128.8(6)	C16B	C11B	C12B	C13B	-1.3(11)
C4A	P1A	C1A	C2A	125.6(8)	C17B	C4B	C5B	C6B	-69.2(9)
C4A	P1A	C1A	C2AS	96.3(12)	C17B	C4B	C5B	C10B	110.6(8)
C4A	C5A	C6A	C7A	-179.4(7)	C17B	C4B	C11B	C12B	-35.7(8)
C4A	C5A	C10A	C9A	177.8(6)	C17B	C4B	C11B	C16B	148.0(7)

C4A	C11A	C12A	C13A	177.3(6)	C17B	C18B	C19B	C20B	-1.0(12)
C4A	C11A	C16A	C15A	-178.6(7)	C18B	C17B	C22B	C21B	-0.8(11)
C4A	C17A	C18A	C19A	-176.4(6)	C18B	C19B	C20B	C21B	0.0(13)
C4A	C17A	C22A	C21A	175.9(6)	C19B	C20B	C21B	C22B	0.6(13)
C5A	C4A	C11A	C12A	53.5(8)	C20B	C21B	C22B	C17B	-0.2(12)
C5A	C4A	C11A	C16A	-125.8(7)	C22B	C17B	C18B	C19B	1.4(11)

12.32 Pentacarbonyl{chloro(2-hydroxyethyl)[bis(trimethylsilyl)methyl]phosphane- κ P}tungsten(0) [47.1a]

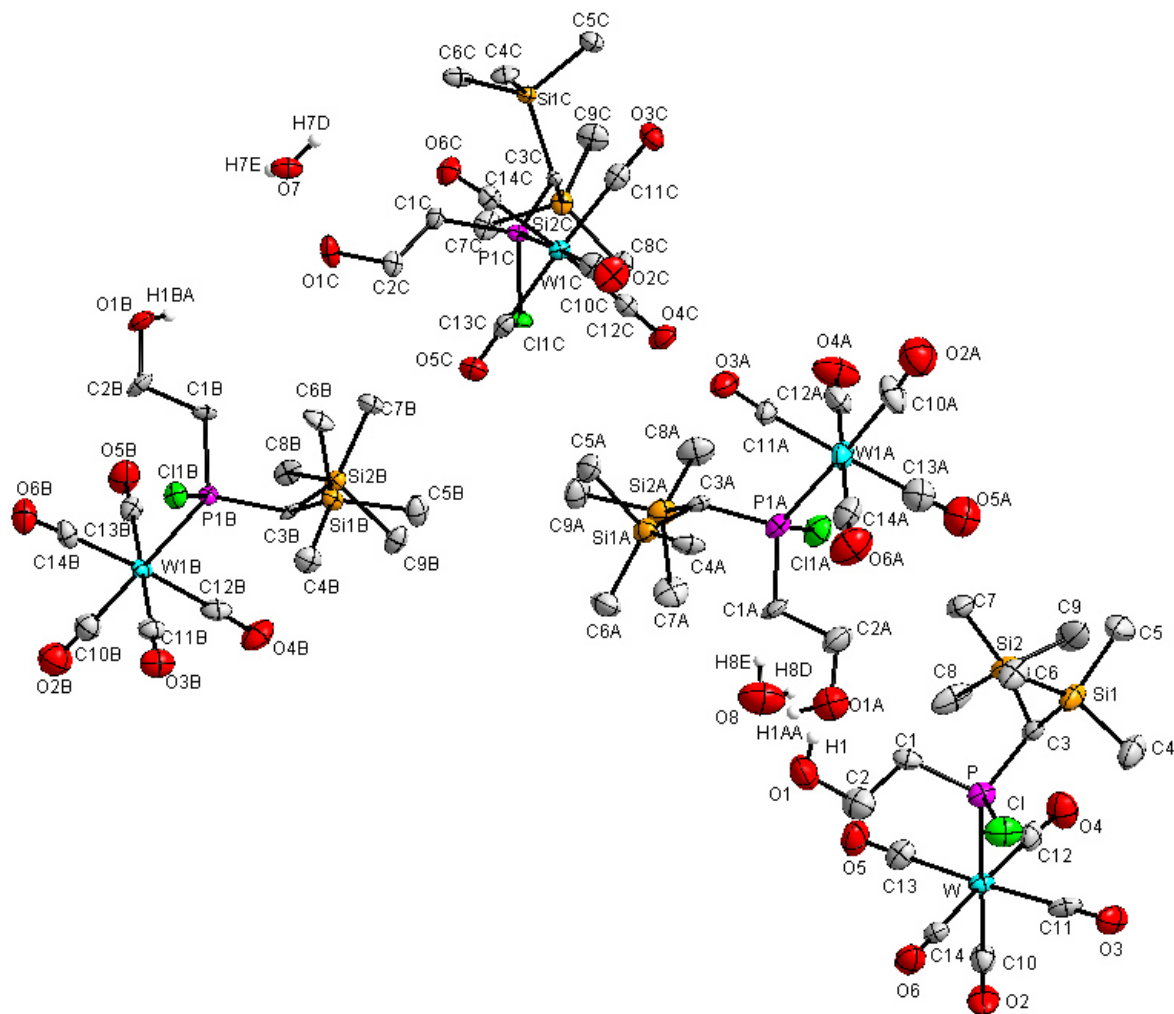


Table 1: Crystal data and structure refinement for **47.1a**.

Identification code	GSTR488, AKY-546 // GXraymo_4589f
Crystal Habitus	colourless plank
Device Type	Bruker D8-Venture
Empirical formula	C ₅₆ H ₉₈ Cl ₄ O ₂₅ P ₄ Si ₈ W ₄
Moiety formula	4(C ₁₄ H ₂₄ Cl O ₆ P Si ₂ W), H ₂ O
Formula weight	2397.14
Temperature/K	123
Crystal system	monoclinic
Space group	P2/c
a/Å	30.4139(18)
b/Å	9.3529(6)

c/Å	33.347(2)
α /°	90
β /°	103.110(2)
γ /°	90
Volume/Å ³	9238.5(10)
Z	4
$\rho_{\text{calc}}/\text{cm}^3$	1.723
μ/mm^{-1}	5.315
F(000)	4680.0
Crystal size/mm ³	0.13 × 0.05 × 0.04
Absorption correction	empirical
Tmin; Tmax	0.6755; 0.7459
Radiation	MoK α (λ = 0.71073)
2 θ range for data collection/°	4.314 to 56°
Completeness to theta	0.999
Index ranges	-40 ≤ h ≤ 40, -12 ≤ k ≤ 12, -42 ≤ l ≤ 44
Reflections collected	121518
Independent reflections	22312 [R _{int} = 0.1186, R _{sigma} = 0.0917]
Data/restraints/parameters	22312/36/921
Goodness-of-fit on F ²	1.052
Final R indexes [$I \geq 2\sigma(I)$]	R ₁ = 0.0701, wR ₂ = 0.1317
Final R indexes [all data]	R ₁ = 0.1227, wR ₂ = 0.1490
Largest diff. peak/hole / e Å ⁻³	4.66/-3.18

Table 2: Bond lengths for **47.1a**.

Atom	Atom	Length/Å	Atom	Atom	Length/Å
W	P	2.491(3)	W1B	P1B	2.501(2)
W	C10	2.020(12)	W1B	C10B	1.980(12)
W	C11	2.046(12)	W1B	C11B	2.057(11)
W	C12	2.019(13)	W1B	C12B	2.041(12)
W	C13	2.035(12)	W1B	C13B	2.025(11)
W	C14	2.021(12)	W1B	C14B	2.039(11)
Cl	P	2.082(4)	Cl1B	P1B	2.085(3)
P	C1	1.842(11)	P1B	C1B	1.816(9)
P	C3	1.803(11)	P1B	C3B	1.807(9)
Si1	C3	1.928(11)	Si1B	C3B	1.938(9)
Si1	C4	1.865(12)	Si1B	C4B	1.844(10)
Si1	C5	1.862(13)	Si1B	C5B	1.869(10)
Si1	C6	1.870(12)	Si1B	C6B	1.874(10)
Si2	C3	1.917(10)	Si2B	C3B	1.925(9)
Si2	C7	1.871(11)	Si2B	C7B	1.863(9)
Si2	C8	1.897(12)	Si2B	C8B	1.890(10)
Si2	C9	1.847(12)	Si2B	C9B	1.869(10)
O1	C2	1.427(15)	O1B	C2B	1.429(11)
O2	C10	1.132(13)	O2B	C10B	1.177(13)
O3	C11	1.130(13)	O3B	C11B	1.137(12)
O4	C12	1.156(14)	O4B	C12B	1.134(13)
O5	C13	1.139(13)	O5B	C13B	1.143(12)
O6	C14	1.164(13)	O6B	C14B	1.141(13)
C1	C2	1.484(16)	C1B	C2B	1.525(13)
W1A	P1A	2.494(3)	W1C	P1C	2.490(2)
W1A	C10A	1.995(13)	W1C	C10C	2.020(11)

W1A	C11A	2.024(11)	W1C	C11C	2.032(11)
W1A	C12A	2.050(15)	W1C	C12C	2.033(11)
W1A	C13A	2.030(14)	W1C	C13C	2.042(11)
W1A	C14A	2.007(14)	W1C	C14C	2.057(10)
Cl1A	P1A	2.101(4)	Cl1C	P1C	2.090(3)
P1A	C1A	1.823(10)	P1C	C1C	1.836(9)
P1A	C3A	1.801(10)	P1C	C3C	1.811(9)
Si1A	C3A	1.946(10)	Si1C	C3C	1.933(9)
Si1A	C4A	1.876(10)	Si1C	C4C	1.865(10)
Si1A	C5A	1.853(11)	Si1C	C5C	1.850(10)
Si1A	C6A	1.863(11)	Si1C	C6C	1.871(10)
Si2A	C3A	1.906(10)	Si2C	C3C	1.927(10)
Si2A	C7A	1.868(12)	Si2C	C7C	1.853(10)
Si2A	C8A	1.895(12)	Si2C	C8C	1.880(10)
Si2A	C9A	1.885(11)	Si2C	C9C	1.868(10)
O1A	C2A	1.425(14)	O1C	C2C	1.411(11)
O2A	C10A	1.161(15)	O2C	C10C	1.131(12)
O3A	C11A	1.147(12)	O3C	C11C	1.154(12)
O4A	C12A	1.118(15)	O4C	C12C	1.138(12)
O5A	C13A	1.160(15)	O5C	C13C	1.143(12)
O6A	C14A	1.159(15)	O6C	C14C	1.134(11)
C1A	C2A	1.524(14)	C1C	C2C	1.521(13)

Table 3: Bond angles for 47.1a.

Atom	Atom	Atom	Angle/°	Atom	Atom	Atom	Angle/°
C10	W	P	176.6(4)	C10B	W1B	P1B	178.2(3)
C10	W	C11	91.1(4)	C10B	W1B	C11B	91.7(4)
C10	W	C13	91.3(5)	C10B	W1B	C12B	89.1(4)
C10	W	C14	89.8(5)	C10B	W1B	C13B	88.1(4)
C11	W	P	86.7(3)	C10B	W1B	C14B	90.0(4)
C12	W	P	92.5(3)	C11B	W1B	P1B	87.2(3)
C12	W	C10	89.9(5)	C12B	W1B	P1B	92.2(3)
C12	W	C11	85.7(4)	C12B	W1B	C11B	87.8(4)
C12	W	C13	92.2(4)	C13B	W1B	P1B	93.0(3)
C12	W	C14	177.0(4)	C13B	W1B	C11B	179.4(4)
C13	W	P	91.1(3)	C13B	W1B	C12B	92.8(4)
C13	W	C11	176.8(4)	C13B	W1B	C14B	92.4(4)
C14	W	P	87.7(3)	C14B	W1B	P1B	88.6(3)
C14	W	C11	91.3(4)	C14B	W1B	C11B	87.0(4)
C14	W	C13	90.8(4)	C14B	W1B	C12B	174.7(4)
Cl	P	W	105.90(14)	Cl1B	P1B	W1B	106.99(12)
C1	P	W	118.8(4)	C1B	P1B	W1B	121.1(3)
C1	P	Cl	97.7(4)	C1B	P1B	Cl1B	97.6(3)
C3	P	W	120.8(4)	C3B	P1B	W1B	117.5(3)
C3	P	Cl	105.9(4)	C3B	P1B	Cl1B	107.4(3)
C3	P	C1	104.5(5)	C3B	P1B	C1B	103.9(4)
C4	Si1	C3	111.3(5)	C4B	Si1B	C3B	109.2(4)
C4	Si1	C6	113.3(6)	C4B	Si1B	C5B	105.6(5)
C5	Si1	C3	110.6(6)	C4B	Si1B	C6B	111.5(5)
C5	Si1	C4	102.5(6)	C5B	Si1B	C3B	109.7(4)
C5	Si1	C6	108.4(6)	C5B	Si1B	C6B	108.8(5)

C6	Si1	C3	110.4(5)	C6B	Si1B	C3B	111.9(4)
C7	Si2	C3	111.3(5)	C7B	Si2B	C3B	111.8(4)
C7	Si2	C8	105.7(5)	C7B	Si2B	C8B	106.6(5)
C8	Si2	C3	112.7(5)	C7B	Si2B	C9B	111.1(5)
C9	Si2	C3	108.7(5)	C8B	Si2B	C3B	114.1(4)
C9	Si2	C7	112.3(6)	C9B	Si2B	C3B	107.0(4)
C9	Si2	C8	106.0(7)	C9B	Si2B	C8B	106.1(5)
C2	C1	P	114.6(8)	C2B	C1B	P1B	115.6(7)
O1	C2	C1	111.4(10)	O1B	C2B	C1B	111.4(8)
P	C3	Si1	117.2(6)	P1B	C3B	Si1B	117.9(4)
P	C3	Si2	115.8(6)	P1B	C3B	Si2B	114.1(4)
Si2	C3	Si1	113.1(5)	Si2B	C3B	Si1B	113.4(5)
O2	C10	W	179.0(12)	O2B	C10B	W1B	176.3(10)
O3	C11	W	178.6(11)	O3B	C11B	W1B	179.6(11)
O4	C12	W	176.6(10)	O4B	C12B	W1B	177.1(10)
O5	C13	W	179.2(12)	O5B	C13B	W1B	177.3(9)
O6	C14	W	178.4(10)	O6B	C14B	W1B	177.9(10)
C10A	W1A	P1A	176.5(4)	C10C	W1C	P1C	178.5(3)
C10A	W1A	C11A	87.9(5)	C10C	W1C	C11C	90.1(4)
C10A	W1A	C12A	93.4(5)	C10C	W1C	C12C	89.8(4)
C10A	W1A	C13A	92.4(6)	C10C	W1C	C13C	90.9(4)
C10A	W1A	C14A	89.2(6)	C10C	W1C	C14C	90.3(4)
C11A	W1A	P1A	91.1(3)	C11C	W1C	P1C	91.3(3)
C11A	W1A	C12A	88.9(5)	C11C	W1C	C12C	89.2(4)
C11A	W1A	C13A	177.0(5)	C11C	W1C	C13C	177.1(4)
C12A	W1A	P1A	83.2(4)	C11C	W1C	C14C	93.7(4)
C13A	W1A	P1A	88.5(4)	C12C	W1C	P1C	89.5(3)
C13A	W1A	C12A	88.1(5)	C12C	W1C	C13C	88.1(4)
C14A	W1A	P1A	94.2(4)	C12C	W1C	C14C	177.1(4)
C14A	W1A	C11A	93.3(5)	C13C	W1C	P1C	87.7(3)
C14A	W1A	C12A	176.6(5)	C13C	W1C	C14C	89.0(4)
C14A	W1A	C13A	89.7(5)	C14C	W1C	P1C	90.2(3)
Cl1A	P1A	W1A	107.82(15)	Cl1C	P1C	W1C	106.11(11)
C1A	P1A	W1A	122.2(4)	C1C	P1C	W1C	118.9(3)
C1A	P1A	Cl1A	96.8(4)	C1C	P1C	Cl1C	97.6(3)
C3A	P1A	W1A	116.8(3)	C3C	P1C	W1C	120.5(3)
C3A	P1A	Cl1A	106.2(3)	C3C	P1C	Cl1C	106.6(3)
C3A	P1A	C1A	104.2(5)	C3C	P1C	C1C	104.0(4)
C4A	Si1A	C3A	113.4(5)	C4C	Si1C	C3C	114.5(4)
C5A	Si1A	C3A	107.3(5)	C4C	Si1C	C6C	106.8(5)
C5A	Si1A	C4A	107.9(5)	C5C	Si1C	C3C	108.8(4)
C5A	Si1A	C6A	110.8(6)	C5C	Si1C	C4C	103.9(5)
C6A	Si1A	C3A	110.8(5)	C5C	Si1C	C6C	111.4(5)
C6A	Si1A	C4A	106.7(5)	C6C	Si1C	C3C	111.2(4)
C7A	Si2A	C3A	111.7(5)	C7C	Si2C	C3C	112.0(4)
C7A	Si2A	C8A	112.0(6)	C7C	Si2C	C8C	111.2(5)
C7A	Si2A	C9A	109.0(6)	C7C	Si2C	C9C	107.3(5)
C8A	Si2A	C3A	108.8(5)	C8C	Si2C	C3C	110.4(4)
C9A	Si2A	C3A	109.9(5)	C9C	Si2C	C3C	110.8(4)
C9A	Si2A	C8A	105.1(6)	C9C	Si2C	C8C	104.9(5)
C2A	C1A	P1A	114.4(8)	C2C	C1C	P1C	115.0(6)
O1A	C2A	C1A	110.9(10)	O1C	C2C	C1C	110.8(8)
P1A	C3A	Si1A	112.4(5)	P1C	C3C	Si1C	113.6(5)

P1A	C3A	Si2A	119.9(5)	P1C	C3C	Si2C	117.5(5)
Si2A	C3A	Si1A	113.9(5)	Si2C	C3C	Si1C	113.5(4)
O2A	C10A	W1A	174.2(13)	O2C	C10C	W1C	179.9(14)
O3A	C11A	W1A	175.3(10)	O3C	C11C	W1C	177.2(9)
O4A	C12A	W1A	176.3(12)	O4C	C12C	W1C	178.7(9)
O5A	C13A	W1A	177.5(13)	O5C	C13C	W1C	178.2(9)
O6A	C14A	W1A	178.6(13)	O6C	C14C	W1C	176.8(9)

Table 4: Torsion angles for **47.1a**.

A	B	C	D	Angle/°	A	B	C	D	Angle/°
W	P	C1	C2	47.9(10)	W1B	P1B	C1B	C2B	48.9(8)
W	P	C3	Si1	-138.3(4)	W1B	P1B	C3B	Si1B	-139.1(4)
W	P	C3	Si2	84.0(6)	W1B	P1B	C3B	Si2B	84.2(5)
Cl	P	C1	C2	-65.1(9)	Cl1B	P1B	C1B	C2B	-66.2(7)
Cl	P	C3	Si1	-18.2(6)	Cl1B	P1B	C3B	Si1B	-18.5(5)
Cl	P	C3	Si2	-155.9(5)	Cl1B	P1B	C3B	Si2B	-155.3(3)
P	C1	C2	O1	176.2(9)	P1B	C1B	C2B	O1B	-174.9(7)
C1	P	C3	Si1	84.4(6)	C1B	P1B	C3B	Si1B	84.2(6)
C1	P	C3	Si2	-53.3(7)	C1B	P1B	C3B	Si2B	-52.6(6)
C3	P	C1	C2	-173.8(9)	C3B	P1B	C1B	C2B	-176.2(7)
W1A	P1A	C1A	C2A	-49.5(10)	W1C	P1C	C1C	C2C	-50.0(8)
W1A	P1A	C3A	Si1A	-84.8(5)	W1C	P1C	C3C	Si1C	-84.9(5)
W1A	P1A	C3A	Si2A	137.3(4)	W1C	P1C	C3C	Si2C	139.1(3)
Cl1A	P1A	C1A	C2A	66.6(9)	Cl1C	P1C	C1C	C2C	63.3(7)
Cl1A	P1A	C3A	Si1A	154.9(4)	Cl1C	P1C	C3C	Si1C	154.3(4)
Cl1A	P1A	C3A	Si2A	17.0(6)	Cl1C	P1C	C3C	Si2C	18.3(5)
P1A	C1A	C2A	O1A	176.6(9)	P1C	C1C	C2C	O1C	-175.4(6)
C1A	P1A	C3A	Si1A	53.3(6)	C1C	P1C	C3C	Si1C	51.7(6)
C1A	P1A	C3A	Si2A	-84.6(7)	C1C	P1C	C3C	Si2C	-84.3(6)
C3A	P1A	C1A	C2A	175.3(9)	C3C	P1C	C1C	C2C	172.6(7)

12.33 Pentacarbonyl{chloro(2-hydroxypropyl)[bis(trimethylsilyl)methyl]phosphane- κ P}tungsten(0) [47.1b]

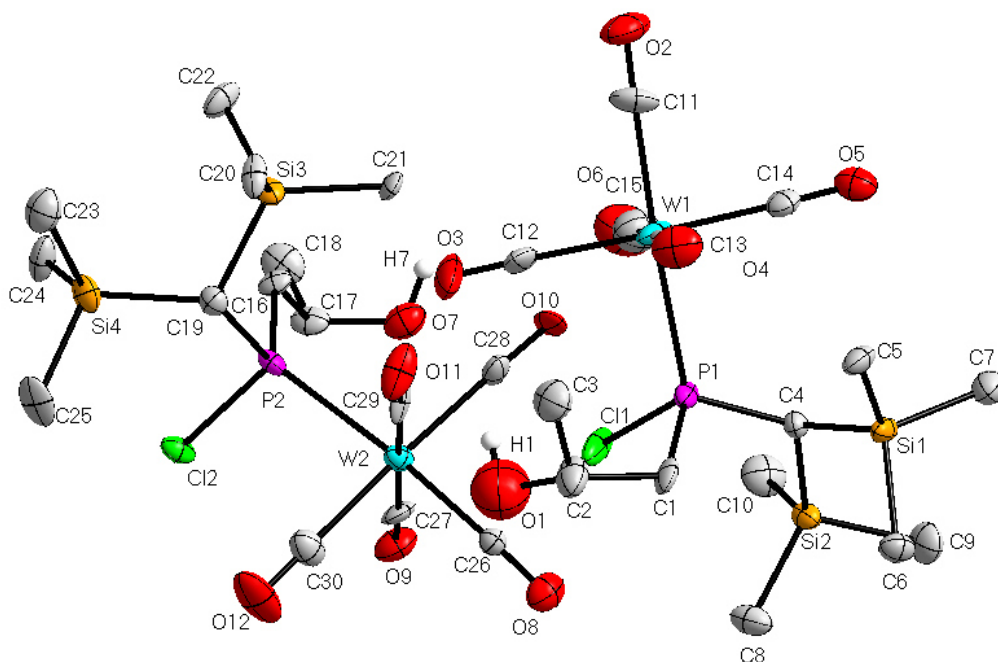


Table 1: Crystal data and structure refinement for **47.1b**.

Identification code	GSTR337, AKY-326 // GXray3181
Crystal Habitus	colourless block
Device Type	Nonius KappaCCD
Empirical formula	$C_{15}H_{26}ClO_6PSi_2W$
Moiety formula	$C_{15}H_{26}ClO_6P Si_2W$
Formula weight	608.81
Temperature/K	123(2)
Crystal system	monoclinic
Space group	$P2_1/n$
a/Å	22.215(2)
b/Å	9.2037(8)
c/Å	23.011(2)
α /°	90.00
β /°	97.555(4)
γ /°	90.00
Volume/Å ³	4664.0(7)
Z	8
$\rho_{\text{calc}}/\text{cm}^3$	1.734
μ/mm^{-1}	5.264
F(000)	2384.0
Crystal size/mm ³	0.32 × 0.26 × 0.22
Absorption correction	empirical
Tmin; Tmax	0.2836; 0.3905
Radiation	MoK α ($\lambda = 0.71073$)
2 θ range for data collection/°	2.4 to 50.5°
Completeness to theta	0.941
Index ranges	$-26 \leq h \leq 26, 0 \leq k \leq 10, 0 \leq l \leq 27$
Reflections collected	8532
Independent reflections	8538 [$R_{\text{int}} = 0.0000$]

Data/restraints/parameters	8538/126/486
Goodness-of-fit on F^2	1.177
Final R indexes [$I \geq 2\sigma(I)$]	$R_1 = 0.0850$, $wR_2 = 0.1843$
Final R indexes [all data]	$R_1 = 0.1039$, $wR_2 = 0.1930$
Largest diff. peak/hole / $e \text{ \AA}^{-3}$	3.07/-1.35

Table 2: Bond lengths for **47.1b**.

Atom	Atom	Length/Å	Atom	Atom	Length/Å
C1	C2	1.58(3)	C17	O7	1.44(2)
C1	P1	1.84(2)	C17	C18	1.52(3)
C2	C3	1.30(3)	C19	P2	1.796(19)
C2	O1	1.50(3)	C19	Si3	1.917(19)
C4	P1	1.818(18)	C19	Si4	1.930(19)
C4	Si2	1.919(18)	C20	Si3	1.868(19)
C4	Si1	1.924(18)	C21	Si3	1.863(18)
C5	Si1	1.89(2)	C22	Si3	1.88(2)
C6	Si1	1.895(19)	C23	Si4	1.88(2)
C7	Si1	1.87(2)	C24	Si4	1.87(2)
C8	Si2	1.84(2)	C25	Si4	1.86(2)
C9	Si2	1.89(2)	C26	O8	1.14(2)
C10	Si2	1.85(2)	C26	W2	2.002(19)
C11	O2	1.09(2)	C27	O9	1.16(2)
C11	W1	2.04(2)	C27	W2	2.02(2)
C12	O3	1.12(3)	C28	O10	1.12(2)
C12	W1	2.07(2)	C28	W2	2.07(2)
C13	O4	1.13(3)	C29	O11	1.14(2)
C13	W1	2.05(3)	C29	W2	2.018(19)
C14	O5	1.15(2)	C30	O12	1.14(3)
C14	W1	2.02(2)	C30	W2	2.03(2)
C15	O6	1.13(3)	P1	Cl1	2.098(7)
C15	W1	2.03(3)	P1	W1	2.503(5)
C16	C17	1.52(2)	P2	Cl2	2.117(6)
C16	P2	1.849(18)	P2	W2	2.504(5)

Table 3: Bond angles for **47.1b**.

Atom	Atom	Atom	Angle/°	Atom	Atom	Atom	Angle/°
C2	C1	P1	117.7(16)	C25	Si4	C19	110.2(10)
C3	C2	O1	103(2)	C24	Si4	C19	113.0(9)
C3	C2	C1	112(2)	C23	Si4	C19	111.5(9)
O1	C2	C1	111(2)	C4	P1	C1	103.5(9)
P1	C4	Si2	118.9(9)	C4	P1	Cl1	105.5(6)
P1	C4	Si1	113.4(10)	C1	P1	Cl1	98.3(7)
Si2	C4	Si1	114.2(9)	C4	P1	W1	116.8(6)
O2	C11	W1	178(2)	C1	P1	W1	122.2(6)
O3	C12	W1	178(2)	Cl1	P1	W1	108.0(2)
O4	C13	W1	178(2)	C19	P2	C16	102.0(8)
O5	C14	W1	178.1(18)	C19	P2	Cl2	105.9(6)
O6	C15	W1	178(3)	C16	P2	Cl2	96.5(6)
C17	C16	P2	114.5(13)	C19	P2	W2	117.8(6)
O7	C17	C18	108.8(17)	C16	P2	W2	125.5(6)

O7	C17	C16	107.0(16)	Cl2	P2	W2	105.9(2)
C18	C17	C16	111.4(16)	C14	W1	C15	89.2(10)
P2	C19	Si3	113.8(10)	C14	W1	C11	86.3(9)
P2	C19	Si4	120.2(10)	C15	W1	C11	93.6(10)
Si3	C19	Si4	113.6(10)	C14	W1	C13	93.0(8)
O8	C26	W2	177.2(17)	C15	W1	C13	177.2(9)
O9	C27	W2	178.1(18)	C11	W1	C13	88.2(8)
O10	C28	W2	177.3(18)	C14	W1	C12	177.6(8)
O11	C29	W2	177.8(19)	C15	W1	C12	89.0(11)
O12	C30	W2	177(2)	C11	W1	C12	92.2(9)
C7	Si1	C5	107.1(10)	C13	W1	C12	88.8(9)
C7	Si1	C6	111.4(10)	C14	W1	P1	90.9(6)
C5	Si1	C6	106.0(10)	C15	W1	P1	86.3(8)
C7	Si1	C4	107.0(10)	C11	W1	P1	177.2(7)
C5	Si1	C4	114.7(8)	C13	W1	P1	92.0(6)
C6	Si1	C4	110.6(8)	C12	W1	P1	90.6(6)
C8	Si2	C10	110.8(11)	C26	W2	C29	88.6(7)
C8	Si2	C9	107.2(10)	C26	W2	C27	91.6(8)
C10	Si2	C9	104.5(11)	C29	W2	C27	179.2(8)
C8	Si2	C4	113.1(9)	C26	W2	C30	87.9(8)
C10	Si2	C4	110.0(10)	C29	W2	C30	90.1(8)
C9	Si2	C4	110.8(9)	C27	W2	C30	90.6(9)
C21	Si3	C20	107.2(9)	C26	W2	C28	89.6(7)
C21	Si3	C22	104.5(10)	C29	W2	C28	89.4(8)
C20	Si3	C22	114.1(10)	C27	W2	C28	89.8(8)
C21	Si3	C19	115.4(9)	C30	W2	C28	177.4(8)
C20	Si3	C19	107.3(9)	C26	W2	P2	175.4(5)
C22	Si3	C19	108.5(9)	C29	W2	P2	91.9(5)
C25	Si4	C24	110.7(10)	C27	W2	P2	87.9(5)
C25	Si4	C23	104.9(11)	C30	W2	P2	87.6(6)
C24	Si4	C23	106.2(11)	C28	W2	P2	95.0(5)

Table 4: Torsion angles for **47.1b**.

A	B	C	D	Angle/°	A	B	C	D	Angle/°
P1	C1	C2	C3	-59(3)	O4	C13	W1	C11	-143(53)
P1	C1	C2	O1	55(2)	O4	C13	W1	C12	125(53)
P2	C16	C17	O7	-80.0(17)	O4	C13	W1	P1	35(53)
P2	C16	C17	C18	161.2(15)	O3	C12	W1	C14	99(72)
P1	C4	Si1	C7	-143.7(11)	O3	C12	W1	C15	55(76)
Si2	C4	Si1	C7	75.9(12)	O3	C12	W1	C11	149(76)
P1	C4	Si1	C5	-25.0(14)	O3	C12	W1	C13	-123(76)
Si2	C4	Si1	C5	-165.5(10)	O3	C12	W1	P1	-31(76)
P1	C4	Si1	C6	94.8(12)	C4	P1	W1	C14	-10.9(9)
Si2	C4	Si1	C6	-45.6(13)	C1	P1	W1	C14	118.1(9)
P1	C4	Si2	C8	-53.4(14)	Cl1	P1	W1	C14	-129.5(6)
Si1	C4	Si2	C8	84.7(12)	C4	P1	W1	C15	78.3(10)
P1	C4	Si2	C10	71.1(14)	C1	P1	W1	C15	-152.8(11)
Si1	C4	Si2	C10	-150.8(11)	Cl1	P1	W1	C15	-40.3(8)
P1	C4	Si2	C9	-173.8(11)	C4	P1	W1	C11	-10(13)
Si1	C4	Si2	C9	-35.7(14)	C1	P1	W1	C11	119(13)
P2	C19	Si3	C21	-23.3(14)	Cl1	P1	W1	C11	-128(13)

Si4	C19	Si3	C21	-165.7(10)	C4	P1	W1	C13	-103.9(9)
P2	C19	Si3	C20	-142.7(11)	C1	P1	W1	C13	25.0(10)
Si4	C19	Si3	C20	74.9(12)	Cl1	P1	W1	C13	137.5(6)
P2	C19	Si3	C22	93.5(12)	C4	P1	W1	C12	167.3(10)
Si4	C19	Si3	C22	-48.9(13)	C1	P1	W1	C12	-63.8(11)
P2	C19	Si4	C25	73.2(14)	Cl1	P1	W1	C12	48.7(8)
Si3	C19	Si4	C25	-146.9(11)	O8	C26	W2	C29	156(36)
P2	C19	Si4	C24	-51.2(15)	O8	C26	W2	C27	-25(36)
Si3	C19	Si4	C24	88.7(13)	O8	C26	W2	C30	66(36)
P2	C19	Si4	C23	-170.7(11)	O8	C26	W2	C28	-114(36)
Si3	C19	Si4	C23	-30.9(14)	O8	C26	W2	P2	60(40)
Si2	C4	P1	C1	85.4(12)	O11	C29	W2	C26	-83(46)
Si1	C4	P1	C1	-53.0(12)	O11	C29	W2	C27	171(68)
Si2	C4	P1	Cl1	-17.3(12)	O11	C29	W2	C30	4(46)
Si1	C4	P1	Cl1	-155.7(7)	O11	C29	W2	C28	-173(46)
Si2	C4	P1	W1	-137.2(8)	O11	C29	W2	P2	92(46)
Si1	C4	P1	W1	84.4(10)	O9	C27	W2	C26	137(56)
C2	C1	P1	C4	-173.6(15)	O9	C27	W2	C29	-117(73)
C2	C1	P1	Cl1	-65.4(15)	O9	C27	W2	C30	49(56)
C2	C1	P1	W1	51.9(17)	O9	C27	W2	C28	-133(56)
Si3	C19	P2	C16	-59.1(12)	O9	C27	W2	P2	-38(56)
Si4	C19	P2	C16	80.7(12)	O12	C30	W2	C26	71(42)
Si3	C19	P2	Cl2	-159.4(8)	O12	C30	W2	C29	-18(42)
Si4	C19	P2	Cl2	-19.7(12)	O12	C30	W2	C27	163(42)
Si3	C19	P2	W2	82.4(10)	O12	C30	W2	C28	63(52)
Si4	C19	P2	W2	-137.9(8)	O12	C30	W2	P2	-109(42)
C17	C16	P2	C19	-172.1(14)	O10	C28	W2	C26	-36(40)
C17	C16	P2	Cl2	-64.3(14)	O10	C28	W2	C29	52(40)
C17	C16	P2	W2	50.5(16)	O10	C28	W2	C27	-128(40)
O5	C14	W1	C15	43(51)	O10	C28	W2	C30	-28(53)
O5	C14	W1	C11	-51(51)	O10	C28	W2	P2	144(40)
O5	C14	W1	C13	-139(51)	C19	P2	W2	C26	84(7)
O5	C14	W1	C12	-1(65)	C16	P2	W2	C26	-144(7)
O5	C14	W1	P1	129(51)	Cl2	P2	W2	C26	-34(7)
O6	C15	W1	C14	-178(100)	C19	P2	W2	C29	-12.4(9)
O6	C15	W1	C11	-91(73)	C16	P2	W2	C29	119.2(9)
O6	C15	W1	C13	40(86)	Cl2	P2	W2	C29	-130.5(6)
O6	C15	W1	C12	1(73)	C19	P2	W2	C27	168.4(9)
O6	C15	W1	P1	92(73)	C16	P2	W2	C27	-60.0(9)
O2	C11	W1	C14	12(80)	Cl2	P2	W2	C27	50.3(6)
O2	C11	W1	C15	-77(80)	C19	P2	W2	C30	77.7(9)
O2	C11	W1	C13	105(80)	C16	P2	W2	C30	-150.8(10)
O2	C11	W1	C12	-166(100)	Cl2	P2	W2	C30	-40.5(7)
O2	C11	W1	P1	11(90)	C19	P2	W2	C28	-101.9(9)
O4	C13	W1	C14	-56(53)	C16	P2	W2	C28	29.6(9)
O4	C13	W1	C15	86(59)	Cl2	P2	W2	C28	139.9(6)

12.34 Pentacarbonyl{chloro(3,3,3-trifluoro-2-hydroxypropyl)[bis(trimethylsilyl)methyl]phosphane- κP }tungsten(0) [47.1c]

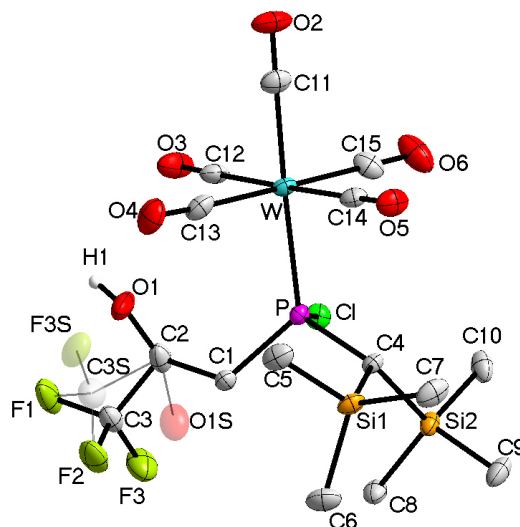


Table 1: Crystal data and structure refinement for **47.1c**.

Identification code	GSTR419, AKY-505 // GXray4067f
Device Type	Bruker X8-KappaApexII
Empirical formula	C ₁₅ H ₂₃ O ₆ F ₃ Si ₂ PClW
Moiety formula	C ₁₅ H ₂₃ Cl F ₃ O ₆ P Si ₂ W
Formula weight	662.78
Temperature/K	100
Crystal system	triclinic
Space group	P $\bar{1}$
a/Å	9.3179(3)
b/Å	11.0538(4)
c/Å	12.1332(4)
α /°	101.7900(15)
β /°	92.3518(16)
γ /°	96.5430(15)
Volume/Å ³	1212.70(7)
Z	2
$\rho_{\text{calc}}/\text{cm}^3$	1.815
μ/mm^{-1}	5.087
F(000)	644.0
Crystal size/mm ³	0.14 × 0.11 × 0.03
Absorption correction	empirical
Tmin; Tmax	0.5045; 0.7460
Radiation	MoK α (λ = 0.71073)
2 θ range for data collection/°	6.706 to 55.998°
Completeness to theta	0.995
Index ranges	-12 ≤ h ≤ 12, -14 ≤ k ≤ 14, -15 ≤ l ≤ 16
Reflections collected	34093
Independent reflections	5823 [R _{int} = 0.0248, R _{sigma} = 0.0178]
Data/restraints/parameters	5823/0/298
Goodness-of-fit on F ²	1.053
Final R indexes [$I \geq 2\sigma(I)$]	R ₁ = 0.0132, wR ₂ = 0.0309
Final R indexes [all data]	R ₁ = 0.0142, wR ₂ = 0.0312
Largest diff. peak/hole / e Å ⁻³	0.81/-0.42

Table 2: Bond lengths for **47.1c**.

Atom	Atom	Length/Å	Atom	Atom	Length/Å
W	P	2.4872(4)	F1	C3	1.344(2)
W	C11	2.0220(17)	F1	C3S	1.523(14)
W	C12	2.0444(18)	F2	C3	1.356(2)
W	C13	2.0304(19)	F2	C3S	1.231(14)
W	C14	2.0449(17)	F3	C3	1.340(3)
W	C15	2.0475(19)	F3S	C3S	1.312(17)
Cl	P	2.0969(5)	O1	C2	1.441(2)
P	C1	1.8463(16)	O1S	C2	1.717(9)
P	C4	1.8131(16)	O2	C11	1.137(2)
Si1	C4	1.9306(16)	O3	C12	1.138(2)
Si1	C5	1.8714(18)	O4	C13	1.145(2)
Si1	C6	1.8693(19)	O5	C14	1.140(2)
Si1	C7	1.8618(19)	O6	C15	1.140(2)
Si2	C4	1.9224(15)	C1	C2	1.517(2)
Si2	C8	1.8686(17)	C2	C3	1.490(3)
Si2	C9	1.8706(19)	C2	C3S	1.527(14)
Si2	C10	1.8710(19)			

Table 3: Bond angles for **47.1c**.

Atom	Atom	Atom	Angle/°	Atom	Atom	Atom	Angle/°
C11	W	P	176.88(5)	C9	Si2	C4	110.10(8)
C11	W	C12	89.82(7)	C9	Si2	C10	104.97(9)
C11	W	C13	89.74(7)	C10	Si2	C4	109.00(8)
C11	W	C14	88.95(7)	C2	C1	P	114.88(11)
C11	W	C15	90.08(8)	O1	C2	C1	106.57(14)
C12	W	P	89.65(5)	O1	C2	C3	108.41(16)
C12	W	C14	178.75(6)	C1	C2	O1S	93.0(3)
C12	W	C15	90.42(7)	C1	C2	C3S	112.5(6)
C13	W	P	93.32(5)	C3	C2	C1	112.61(15)
C13	W	C12	88.89(7)	C3S	C2	O1S	93.2(7)
C13	W	C14	90.86(7)	F1	C3	F2	105.64(17)
C13	W	C15	179.29(7)	F1	C3	C2	111.74(17)
C14	W	P	91.59(4)	F2	C3	C2	113.39(18)
C14	W	C15	89.82(7)	F3	C3	F1	109.27(18)
C15	W	P	86.85(5)	F3	C3	F2	106.55(18)
Cl	P	W	106.553(19)	F3	C3	C2	110.00(18)
C1	P	W	123.67(5)	F1	C3S	C2	100.6(9)
C1	P	Cl	96.28(5)	F2	C3S	F1	102.2(9)
C4	P	W	117.76(5)	F2	C3S	F3S	113.5(12)
C4	P	Cl	105.85(5)	F2	C3S	C2	118.8(11)
C4	P	C1	103.48(7)	F3S	C3S	F1	122.7(11)
C5	Si1	C4	114.29(7)	F3S	C3S	C2	99.5(9)
C6	Si1	C4	111.22(8)	P	C4	Si1	114.17(8)
C6	Si1	C5	106.76(9)	P	C4	Si2	118.29(8)
C7	Si1	C4	106.90(8)	Si2	C4	Si1	114.43(8)
C7	Si1	C5	105.51(9)	O2	C11	W	179.30(19)
C7	Si1	C6	112.11(9)	O3	C12	W	178.75(16)

C8	Si2	C4	112.50(7)	O4	C13	W	177.53(16)
C8	Si2	C9	108.50(8)	O5	C14	W	179.11(14)
C8	Si2	C10	111.50(8)	O6	C15	W	179.35(16)

Table 4: Torsion angles for **47.1c**.

A	B	C	D	Angle/°	A	B	C	D	Angle/°
W	P	C1	C2	53.00(14)	C1	C2	C3	F2	50.8(2)
W	P	C4	Si1	85.42(8)	C1	C2	C3	F3	-68.4(2)
W	P	C4	Si2	-135.44(7)	C1	C2	C3S	F1	-150.8(5)
Cl	P	C1	C2	-61.69(12)	C1	C2	C3S	F2	-40.4(13)
Cl	P	C4	Si1	-155.62(6)	C1	C2	C3S	F3S	83.1(9)
Cl	P	C4	Si2	-16.49(10)	C3	F1	C3S	F2	-64.5(8)
P	C1	C2	O1	-76.26(16)	C3	F1	C3S	F3S	167.0(18)
P	C1	C2	O1S	111.3(4)	C3	F1	C3S	C2	58.4(7)
P	C1	C2	C3	165.01(15)	C3	F2	C3S	F1	54.4(7)
P	C1	C2	C3S	-154.0(6)	C3	F2	C3S	F3S	-171.4(16)
O1	C2	C3	F1	52.4(2)	C3	F2	C3S	C2	-55.1(9)
O1	C2	C3	F2	-66.9(2)	C3	C2	C3S	F1	-52.5(6)
O1	C2	C3	F3	173.95(16)	C3	C2	C3S	F2	57.9(10)
O1	C2	C3S	F1	108.0(7)	C3	C2	C3S	F3S	-178.6(15)
O1	C2	C3S	F2	-141.6(12)	C3S	F1	C3	F2	56.2(8)
O1	C2	C3S	F3S	-18.1(7)	C3S	F1	C3	F3	170.5(9)
O1S	C2	C3	F1	-112.5(5)	C3S	F1	C3	C2	-67.5(9)
O1S	C2	C3	F2	128.3(5)	C3S	F2	C3	F1	-69.3(9)
O1S	C2	C3	F3	9.1(4)	C3S	F2	C3	F3	174.5(9)
O1S	C2	C3S	F1	-56.2(8)	C3S	F2	C3	C2	53.4(9)
O1S	C2	C3S	F2	54.2(12)	C3S	C2	C3	F1	72.0(9)
O1S	C2	C3S	F3S	177.7(9)	C3S	C2	C3	F2	-47.2(9)
C1	P	C4	Si1	-54.96(10)	C3S	C2	C3	F3	-166.4(9)
C1	P	C4	Si2	84.17(10)	C4	P	C1	C2	-169.68(12)
C1	C2	C3	F1	170.06(16)					

12.35 Pentacarbonyl{fluoro(3,3,3-trifluoro-2-hydroxypropyl) [bis(trimethylsilyl)methyl]phosphane- κP }tungsten(0) [48.1a]

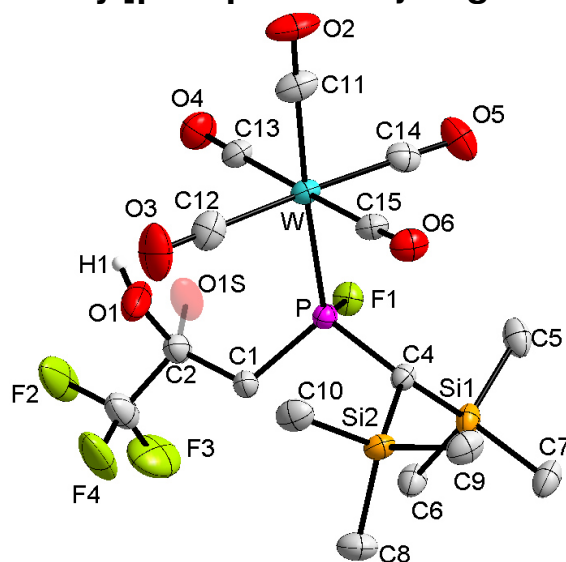


Table 1: Crystal data and structure refinement for **48.1a**.

Identification code	GSTR418, AKY-506 // GXray4066
Device Type	STOE IPDS 2T
Empirical formula	C ₁₅ H ₂₃ F ₄ O ₆ PSi ₂ W
Moiety formula	C15 H23 F4 O6 P Si2 W
Formula weight	646.33
Temperature/K	123(2)
Crystal system	triclinic
Space group	P $\bar{1}$
a/Å	9.2501(4)
b/Å	11.1432(4)
c/Å	11.8158(5)
α /°	100.802(3)
β /°	92.088(3)
γ /°	98.468(3)
Volume/Å ³	1180.73(8)
Z	2
ρ_{calc} /cm ³	1.818
μ /mm ⁻¹	5.119
F(000)	628.0
Crystal size/mm ³	0.24 × 0.15 × 0.03
Absorption correction	integration
Tmin; Tmax	0.4061; 0.8325
Radiation	MoK α (λ = 0.71073)
2 θ range for data collection/°	5.37 to 50.5°
Completeness to theta	0.900
Index ranges	-10 ≤ h ≤ 11, -13 ≤ k ≤ 13, -14 ≤ l ≤ 11
Reflections collected	8394
Independent reflections	4182 [R _{int} = 0.0367, R _{sigma} = 0.0355]
Data/restraints/parameters	4182/1/274
Goodness-of-fit on F ²	0.979
Final R indexes [$ I > 2\sigma(I)$]	R ₁ = 0.0229, wR ₂ = 0.0533
Final R indexes [all data]	R ₁ = 0.0265, wR ₂ = 0.0539
Largest diff. peak/hole / e Å ⁻³	0.98/-1.00

Table 2: Bond lengths for **48.1a**.

Atom	Atom	Length/Å	Atom	Atom	Length/Å
W	P	2.4682(9)	Si2	C9	1.867(4)
W	C11	2.029(4)	Si2	C10	1.873(4)
W	C12	2.041(5)	F2	C3	1.338(6)
W	C13	2.048(4)	F3	C3	1.325(7)
W	C14	2.045(4)	F4	C3	1.307(6)
W	C15	2.044(4)	O1	C2	1.343(6)
P	F1	1.614(2)	O1S	C2	1.319(7)
P	C1	1.835(4)	O2	C11	1.133(5)
P	C4	1.803(4)	O3	C12	1.125(6)
Si1	C4	1.919(4)	O4	C13	1.128(5)
Si1	C5	1.871(4)	O5	C14	1.140(5)
Si1	C6	1.866(4)	O6	C15	1.136(5)
Si1	C7	1.872(4)	C1	C2	1.502(5)
Si2	C4	1.923(4)	C2	C3	1.521(6)
Si2	C8	1.871(4)			

Table 3: Bond angles for **48.1a**.

Atom	Atom	Atom	Angle/°	Atom	Atom	Atom	Angle/°
C11	W	P	175.80(14)	C8	Si2	C4	111.48(19)
C11	W	C12	91.57(19)	C8	Si2	C10	107.3(2)
C11	W	C13	89.72(16)	C9	Si2	C4	106.97(18)
C11	W	C14	90.74(18)	C9	Si2	C8	111.5(2)
C11	W	C15	88.34(16)	C9	Si2	C10	106.0(2)
C12	W	P	92.63(13)	C10	Si2	C4	113.51(17)
C12	W	C13	89.13(17)	C2	C1	P	114.7(2)
C12	W	C14	177.66(17)	O1	C2	C1	113.0(4)
C12	W	C15	89.90(16)	O1	C2	C3	107.1(4)
C13	W	P	90.36(11)	O1S	C2	C1	121.0(6)
C14	W	P	85.05(11)	O1S	C2	C3	106.8(6)
C14	W	C13	91.19(16)	C1	C2	C3	111.0(3)
C15	W	P	91.64(10)	F2	C3	C2	110.8(4)
C15	W	C13	177.81(15)	F3	C3	F2	107.3(5)
C15	W	C14	89.86(16)	F3	C3	C2	112.7(4)
F1	P	W	108.53(9)	F4	C3	F2	106.6(4)
F1	P	C1	96.38(16)	F4	C3	F3	106.7(4)
F1	P	C4	102.92(15)	F4	C3	C2	112.3(4)
C1	P	W	123.32(13)	P	C4	Si1	115.5(2)
C4	P	W	117.44(12)	P	C4	Si2	116.04(19)
C4	P	C1	104.51(16)	Si1	C4	Si2	115.20(18)
C5	Si1	C4	108.81(17)	O2	C11	W	178.3(4)
C5	Si1	C7	106.3(2)	O3	C12	W	179.6(4)
C6	Si1	C4	112.41(17)	O4	C13	W	177.7(4)
C6	Si1	C5	110.3(2)	O5	C14	W	178.3(4)
C6	Si1	C7	109.14(19)	O6	C15	W	178.7(3)
C7	Si1	C4	109.70(19)				

Table 4: Torsion angles for **48.1a**.

A	B	C	D	Angle/°	A	B	C	D	Angle/°
W	P	C1	C2	51.3(4)	O1	C2	C3	F4	-66.5(6)
W	P	C4	Si1	-133.33(14)	O1S	C2	C3	F2	-49.7(8)
W	P	C4	Si2	87.39(19)	O1S	C2	C3	F3	70.5(7)
P	C1	C2	O1	-70.6(4)	O1S	C2	C3	F4	-168.9(7)
P	C1	C2	O1S	42.8(8)	C1	P	C4	Si1	86.0(2)
P	C1	C2	C3	169.1(3)	C1	P	C4	Si2	-53.3(2)
F1	P	C1	C2	-65.8(3)	C1	C2	C3	F2	176.5(4)
F1	P	C4	Si1	-14.2(2)	C1	C2	C3	F3	-63.3(5)
F1	P	C4	Si2	-153.50(18)	C1	C2	C3	F4	57.3(6)
O1	C2	C3	F2	52.7(6)	C4	P	C1	C2	-171.0(3)
O1	C2	C3	F3	172.9(4)					

12.36 Pentacarbonyl{[3,3,3-trifluoro-2-(trifluoromethyl)-2-hydroxypropyl][bis(trimethylsilyl)methyl]phosphane- κ P}tungsten(0) [48.1b]

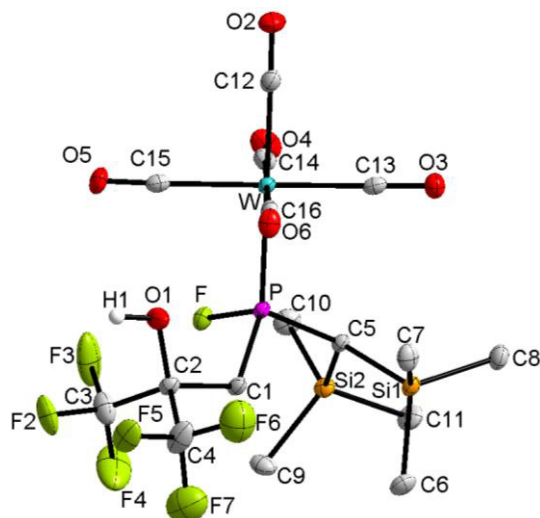


Table 1: Crystal data and structure refinement for **48.1b**.

Identification code	GSTR413, AKY-499A // GXray4033f
Device Type	Bruker X8-KappaApexII
Empirical formula	C ₁₆ H ₂₂ O ₆ F ₇ Si ₂ PW
Moiety formula	C ₁₆ H ₂₂ F ₇ O ₆ P Si ₂ W
Formula weight	714.33
Temperature/K	100
Crystal system	triclinic
Space group	P $\bar{1}$
a/Å	9.8833(5)
b/Å	11.1477(7)
c/Å	11.5906(6)
α /°	78.723(3)
β /°	87.936(3)
γ /°	87.386(3)
Volume/Å ³	1250.57(12)
Z	2
$\rho_{\text{calc}}/\text{cm}^3$	1.897
μ/mm^{-1}	4.859
F(000)	692.0
Crystal size/mm ³	0.12 × 0.1 × 0.04
Absorption correction	empirical
Tmin; Tmax	0.5721; 0.7460
Radiation	MoK α (λ = 0.71073)
2 θ range for data collection/°	4.128 to 55.996°
Completeness to theta	0.992
Index ranges	-12 ≤ h ≤ 13, -14 ≤ k ≤ 14, -15 ≤ l ≤ 15
Reflections collected	11761
Independent reflections	5964 [R _{int} = 0.0226, R _{sigma} = 0.0346]
Data/restraints/parameters	5964/61/305
Goodness-of-fit on F ²	1.056
Final R indexes [$ I \geq 2\sigma(I)$]	R ₁ = 0.0280, wR ₂ = 0.0664
Final R indexes [all data]	R ₁ = 0.0315, wR ₂ = 0.0681
Largest diff. peak/hole / e Å ⁻³	2.66/-1.85

Table 2: Bond lengths for **48.1b**.

Atom	Atom	Length/Å	Atom	Atom	Length/Å
W	P	2.4767(9)	Si2	C11	1.871(4)
W	C12	2.030(4)	F2	C3	1.334(5)
W	C13	2.045(4)	F3	C3	1.323(6)
W	C14	2.051(4)	F4	C3	1.310(6)
W	C15	2.068(4)	F5	C4	1.332(5)
W	C16	2.031(4)	F6	C4	1.311(6)
P	F1	1.600(2)	F7	C4	1.339(6)
P	C1	1.844(4)	O1	C2	1.391(5)
P	C5	1.812(4)	O2	C12	1.137(5)
Si1	C5	1.922(4)	O3	C13	1.136(5)
Si1	C6	1.870(4)	O4	C14	1.131(5)
Si1	C7	1.881(4)	O5	C15	1.132(5)
Si1	C8	1.864(4)	O6	C16	1.140(5)
Si2	C5	1.919(4)	C1	C2	1.536(5)
Si2	C9	1.869(4)	C2	C3	1.536(6)
Si2	C10	1.860(4)	C2	C4	1.550(5)

Table 3: Bond angles for **48.1b**.

Atom	Atom	Atom	Angle/°	Atom	Atom	Atom	Angle/°
C12	W	P	176.38(11)	C10	Si2	C9	109.5(2)
C12	W	C13	88.70(15)	C10	Si2	C11	105.9(2)
C12	W	C14	90.19(16)	C11	Si2	C5	110.16(18)
C12	W	C15	90.23(15)	C2	C1	P	121.3(3)
C12	W	C16	89.74(15)	O1	C2	C1	110.2(3)
C13	W	P	91.36(10)	O1	C2	C3	109.3(3)
C13	W	C14	89.51(15)	O1	C2	C4	107.9(3)
C13	W	C15	177.64(14)	C1	C2	C4	107.7(3)
C14	W	P	86.19(11)	C3	C2	C1	111.9(3)
C14	W	C15	92.60(16)	C3	C2	C4	109.8(3)
C15	W	P	89.84(11)	F2	C3	C2	111.7(3)
C16	W	P	93.88(10)	F3	C3	F2	106.0(4)
C16	W	C13	90.04(14)	F3	C3	C2	110.0(4)
C16	W	C14	179.54(16)	F4	C3	F2	108.4(4)
C16	W	C15	87.85(15)	F4	C3	F3	106.9(4)
F1	P	W	109.63(9)	F4	C3	C2	113.5(4)
F1	P	C1	98.49(15)	F5	C4	F7	107.3(4)
F1	P	C5	103.01(14)	F5	C4	C2	112.4(4)
C1	P	W	125.75(12)	F6	C4	F5	106.9(4)
C5	P	W	115.50(12)	F6	C4	F7	107.7(4)
C5	P	C1	101.20(16)	F6	C4	C2	111.0(4)
C6	Si1	C5	111.25(18)	F7	C4	C2	111.4(4)
C6	Si1	C7	106.92(19)	P	C5	Si1	117.30(18)
C7	Si1	C5	114.27(17)	P	C5	Si2	114.54(19)
C8	Si1	C5	106.99(17)	Si2	C5	Si1	115.90(18)
C8	Si1	C6	111.47(19)	O2	C12	W	179.2(4)
C8	Si1	C7	105.89(19)	O3	C13	W	179.0(3)
C9	Si2	C5	112.41(17)	O4	C14	W	177.7(3)

C9	Si2	C11	109.22(19)	O5	C15	W	176.8(3)
C10	Si2	C5	109.41(17)	O6	C16	W	178.3(3)

Table 4: Torsion angles for **48.1b**.

A	B	C	D	Angle/°	A	B	C	D	Angle/°
W	P	C1	C2	50.4(4)	C1	P	C5	Si1	-48.5(2)
W	P	C5	Si1	90.51(19)	C1	P	C5	Si2	92.4(2)
W	P	C5	Si2	-128.61(14)	C1	C2	C3	F2	173.3(3)
P	C1	C2	O1	-37.4(4)	C1	C2	C3	F3	-69.4(4)
P	C1	C2	C3	84.4(4)	C1	C2	C3	F4	50.4(5)
P	C1	C2	C4	-154.8(3)	C1	C2	C4	F5	174.1(4)
F1	P	C1	C2	-71.3(3)	C1	C2	C4	F6	54.5(5)
F1	P	C5	Si1	-150.01(18)	C1	C2	C4	F7	-65.4(5)
F1	P	C5	Si2	-9.1(2)	C3	C2	C4	F5	-63.7(5)
O1	C2	C3	F2	-64.4(5)	C3	C2	C4	F6	176.7(4)
O1	C2	C3	F3	52.9(4)	C3	C2	C4	F7	56.7(5)
O1	C2	C3	F4	172.7(4)	C4	C2	C3	F2	53.7(5)
O1	C2	C4	F5	55.2(5)	C4	C2	C3	F3	171.0(4)
O1	C2	C4	F6	-64.4(5)	C4	C2	C3	F4	-69.2(5)
O1	C2	C4	F7	175.7(4)	C5	P	C1	C2	-176.5(3)

12.37 Pentacarbonyl{fluoro[3,3,3-trifluoro-2-(trifluoromethyl)-2-hydroxypropyl](1,2,3,4,5-pentamethylcyclopenta-2,4-dien-1-yl)phosphane- κP }tungsten(0) [48.2b]

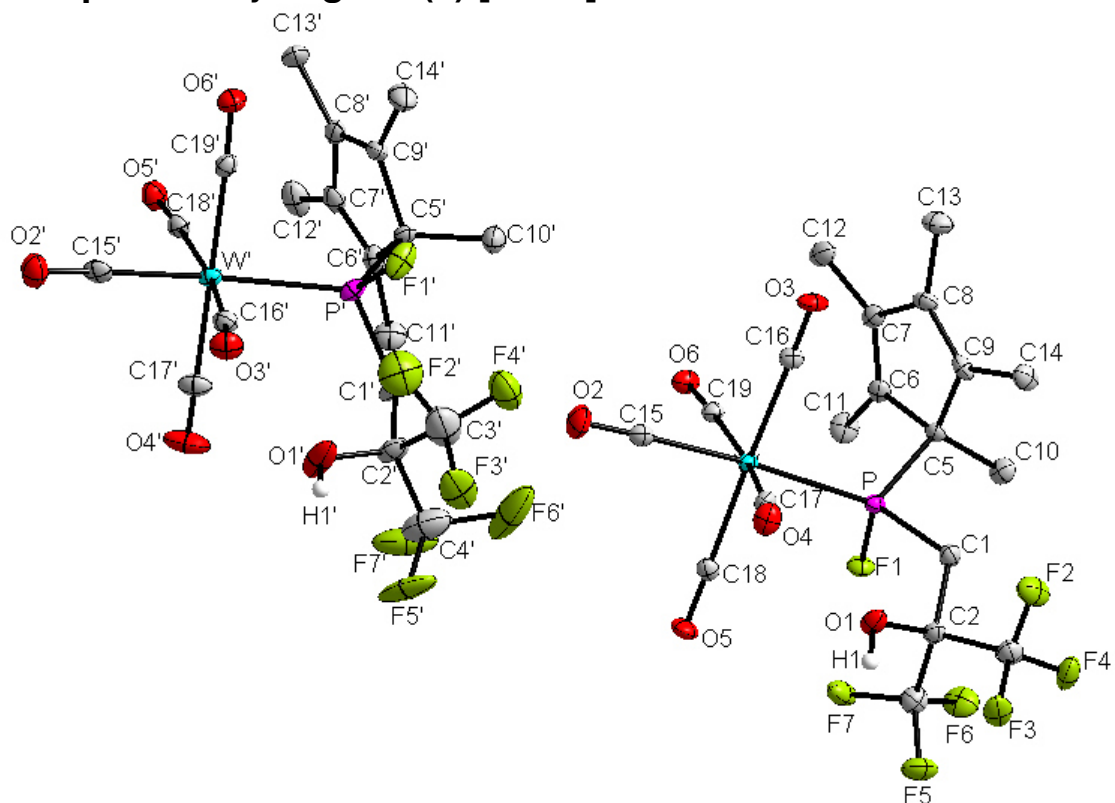


Table 1: Crystal data and structure refinement for **48.2b**.

Identification code	GSTR392, AKY-476 // GXray3908f
Device Type	Bruker X8-KappaApexII
Empirical formula	C ₁₉ H ₁₈ O ₆ F ₇ PW
Moiety formula	C ₁₉ H ₁₈ F ₇ O ₆ P W
Formula weight	690.15
Temperature/K	100
Crystal system	monoclinic
Space group	P2 ₁ /n
a/Å	9.2003(6)
b/Å	40.630(3)
c/Å	12.4604(8)
α/°	90
β/°	103.517(3)
γ/°	90
Volume/Å ³	4528.8(5)
Z	8
ρ _{calc} /cm ³	2.024
μ/mm ⁻¹	5.263
F(000)	2656.0
Crystal size/mm ³	0.12 × 0.11 × 0.05
Absorption correction	empirical
Tmin; Tmax	0.5182; 0.7460
Radiation	MoKα (λ = 0.71073)
2θ range for data collection/°	2.004 to 55.996°
Completeness to theta	0.992
Index ranges	-12 ≤ h ≤ 12, -53 ≤ k ≤ 53, -15 ≤ l ≤ 16
Reflections collected	83151
Independent reflections	10828 [R _{int} = 0.0401, R _{sigma} = 0.0293]
Data/restraints/parameters	10828/37/625
Goodness-of-fit on F ²	1.068
Final R indexes [I > 2σ (I)]	R ₁ = 0.0452, wR ₂ = 0.1007
Final R indexes [all data]	R ₁ = 0.0495, wR ₂ = 0.1027
Largest diff. peak/hole / e Å ⁻³	3.42/-5.62

Table 2: Bond lengths for **48.2b**.

Atom	Atom	Length/Å	Atom	Atom	Length/Å
W	P	2.5014(15)	W'	P'	2.4793(16)
W	C15	1.998(6)	W'	C15'	2.007(6)
W	C16	2.063(6)	W'	C16'	2.051(6)
W	C17	2.051(6)	W'	C17'	2.068(7)
W	C18	2.039(6)	W'	C18'	2.059(6)
W	C19	2.052(6)	W'	C19'	2.027(6)
P	F1	1.600(4)	P'	F1'	1.598(4)
P	C1	1.849(6)	P'	C1'	1.840(7)
P	C5	1.872(6)	P'	C5'	1.862(6)
F2	C3	1.335(8)	F2'	C3'	1.389(12)
F3	C3	1.338(7)	F3'	C3'	1.324(10)
F4	C3	1.328(8)	F4'	C3'	1.266(10)
F5	C4	1.337(8)	F5'	C4'	1.359(10)
F6	C4	1.340(8)	F6'	C4'	1.477(13)
F7	C4	1.332(7)	F7'	C4'	1.294(12)

O1	C2	1.394(7)	O1'	C2'	1.356(8)
O2	C15	1.153(8)	O2'	C15'	1.149(8)
O3	C16	1.128(7)	O3'	C16'	1.139(8)
O4	C17	1.140(8)	O4'	C17'	1.121(8)
O5	C18	1.134(7)	O5'	C18'	1.139(8)
O6	C19	1.140(7)	O6'	C19'	1.146(8)
C1	C2	1.543(8)	C1'	C2'	1.535(9)
C2	C3	1.557(8)	C2'	C3'	1.591(12)
C2	C4	1.538(9)	C2'	C4'	1.517(11)
C5	C6	1.528(8)	C5'	C6'	1.506(8)
C5	C9	1.526(8)	C5'	C9'	1.526(8)
C5	C10	1.537(8)	C5'	C10'	1.539(8)
C6	C7	1.340(8)	C6'	C7'	1.347(9)
C6	C11	1.502(8)	C6'	C11'	1.500(9)
C7	C8	1.474(8)	C7'	C8'	1.469(9)
C7	C12	1.500(9)	C7'	C12'	1.512(9)
C8	C9	1.343(9)	C8'	C9'	1.346(9)
C8	C13	1.489(8)	C8'	C13'	1.497(9)
C9	C14	1.504(8)	C9'	C14'	1.496(9)

Table 3: Bond angles for **48.2b**.

Atom	Atom	Atom	Angle ^o	Atom	Atom	Atom	Angle ^o
C15	W	P	173.57(17)	C15'	W'	P'	172.13(18)
C15	W	C16	91.2(2)	C15'	W'	C16'	83.7(2)
C15	W	C17	85.0(2)	C15'	W'	C17'	91.8(3)
C15	W	C18	89.1(2)	C15'	W'	C18'	87.4(2)
C15	W	C19	84.4(2)	C15'	W'	C19'	90.2(2)
C16	W	P	94.17(17)	C16'	W'	P'	88.39(18)
C17	W	P	99.01(17)	C16'	W'	C17'	93.7(3)
C17	W	C16	85.2(2)	C16'	W'	C18'	170.9(2)
C17	W	C19	169.0(2)	C17'	W'	P'	89.0(2)
C18	W	P	85.85(17)	C18'	W'	P'	100.46(16)
C18	W	C16	175.4(2)	C18'	W'	C17'	88.7(3)
C18	W	C17	90.3(2)	C19'	W'	P'	89.99(17)
C18	W	C19	92.5(2)	C19'	W'	C16'	93.3(2)
C19	W	P	91.79(16)	C19'	W'	C17'	172.8(2)
C19	W	C16	92.2(2)	C19'	W'	C18'	84.5(2)
F1	P	W	110.67(15)	F1'	P'	W'	111.65(16)
F1	P	C1	99.8(2)	F1'	P'	C1'	100.5(3)
F1	P	C5	98.5(2)	F1'	P'	C5'	99.0(3)
C1	P	W	122.1(2)	C1'	P'	W'	119.5(2)
C1	P	C5	101.0(3)	C1'	P'	C5'	100.8(3)
C5	P	W	120.52(19)	C5'	P'	W'	121.70(19)
C2	C1	P	123.1(4)	C2'	C1'	P'	122.7(5)
O1	C2	C1	109.1(5)	O1'	C2'	C1'	110.6(6)
O1	C2	C3	108.8(5)	O1'	C2'	C3'	104.0(6)
O1	C2	C4	109.5(5)	O1'	C2'	C4'	113.2(7)
C1	C2	C3	106.7(5)	C1'	C2'	C3'	112.1(6)
C4	C2	C1	112.8(5)	C4'	C2'	C1'	108.7(6)
C4	C2	C3	109.9(5)	C4'	C2'	C3'	108.2(7)
F2	C3	F3	106.8(5)	F2'	C3'	C2'	108.8(7)

F2	C3	C2	110.5(5)	F3'	C3'	F2'	109.5(8)
F3	C3	C2	111.0(5)	F3'	C3'	C2'	109.4(8)
F4	C3	F2	108.3(5)	F4'	C3'	F2'	104.8(8)
F4	C3	F3	108.0(5)	F4'	C3'	F3'	111.0(8)
F4	C3	C2	112.1(5)	F4'	C3'	C2'	113.3(8)
F5	C4	F6	107.6(5)	F5'	C4'	F6'	111.1(8)
F5	C4	C2	111.2(5)	F5'	C4'	C2'	112.5(7)
F6	C4	C2	112.4(5)	F6'	C4'	C2'	104.4(8)
F7	C4	F5	107.2(5)	F7'	C4'	F5'	105.8(9)
F7	C4	F6	107.6(5)	F7'	C4'	F6'	108.3(8)
F7	C4	C2	110.6(5)	F7'	C4'	C2'	114.8(8)
C6	C5	P	105.7(4)	C6'	C5'	P'	109.0(4)
C6	C5	C10	111.2(5)	C6'	C5'	C9'	103.3(5)
C9	C5	P	109.7(4)	C6'	C5'	C10'	113.8(5)
C9	C5	C6	102.8(5)	C9'	C5'	P'	105.9(4)
C9	C5	C10	113.1(5)	C9'	C5'	C10'	110.8(5)
C10	C5	P	113.5(4)	C10'	C5'	P'	113.3(4)
C7	C6	C5	108.6(5)	C7'	C6'	C5'	108.5(5)
C7	C6	C11	127.9(6)	C7'	C6'	C11'	126.0(6)
C11	C6	C5	123.3(5)	C11'	C6'	C5'	125.4(5)
C6	C7	C8	109.9(5)	C6'	C7'	C8'	110.3(6)
C6	C7	C12	127.7(6)	C6'	C7'	C12'	125.7(6)
C8	C7	C12	122.4(6)	C8'	C7'	C12'	124.0(6)
C7	C8	C13	123.0(6)	C7'	C8'	C13'	123.2(6)
C9	C8	C7	109.9(5)	C9'	C8'	C7'	109.1(5)
C9	C8	C13	127.0(6)	C9'	C8'	C13'	127.7(6)
C8	C9	C5	108.7(5)	C8'	C9'	C5'	108.7(5)
C8	C9	C14	127.3(6)	C8'	C9'	C14'	127.6(6)
C14	C9	C5	123.9(5)	C14'	C9'	C5'	123.3(6)
O2	C15	W	177.7(5)	O2'	C15'	W'	176.7(5)
O3	C16	W	175.5(5)	O3'	C16'	W'	173.9(6)
O4	C17	W	171.9(5)	O4'	C17'	W'	177.3(6)
O5	C18	W	177.9(5)	O5'	C18'	W'	173.0(5)
O6	C19	W	172.3(5)	O6'	C19'	W'	174.9(5)

Table 4: Torsion angles for **48.2b**.

A	B	C	D	Angle/°	A	B	C	D	Angle/°
W	P	C1	C2	56.7(6)	W'	P'	C1'	C2'	-63.9(7)
W	P	C5	C6	-46.4(4)	W'	P'	C5'	C6'	-62.9(4)
W	P	C5	C9	63.8(4)	W'	P'	C5'	C9'	47.7(4)
W	P	C5	C10	-168.6(3)	W'	P'	C5'	C10'	169.2(3)
P	C1	C2	O1	-57.8(7)	P'	C1'	C2'	O1'	50.3(9)
P	C1	C2	C3	-175.1(4)	P'	C1'	C2'	C3'	-65.3(8)
P	C1	C2	C4	64.1(7)	P'	C1'	C2'	C4'	175.1(7)
P	C5	C6	C7	111.9(5)	P'	C5'	C6'	C7'	111.2(5)
P	C5	C6	C11	-72.7(6)	P'	C5'	C6'	C11'	-72.6(7)
P	C5	C9	C8	-110.0(5)	P'	C5'	C9'	C8'	-112.8(5)
P	C5	C9	C14	73.9(6)	P'	C5'	C9'	C14'	73.9(6)
F1	P	C1	C2	-65.4(5)	F1'	P'	C1'	C2'	58.5(7)
F1	P	C5	C6	73.7(4)	F1'	P'	C5'	C6'	174.6(4)
F1	P	C5	C9	-176.1(4)	F1'	P'	C5'	C9'	-74.8(4)

F1	P	C5	C10	-48.4(4)	F1'	P'	C5'	C10'	46.8(5)
O1	C2	C3	F2	-66.8(6)	O1'	C2'	C3'	F2'	-41.0(8)
O1	C2	C3	F3	51.4(7)	O1'	C2'	C3'	F3'	78.5(8)
O1	C2	C3	F4	172.3(5)	O1'	C2'	C3'	F4'	-157.2(8)
O1	C2	C4	F5	-73.3(6)	O1'	C2'	C4'	F5'	-39.3(11)
O1	C2	C4	F6	166.0(5)	O1'	C2'	C4'	F6'	-159.8(6)
O1	C2	C4	F7	45.7(7)	O1'	C2'	C4'	F7'	81.8(10)
C1	P	C5	C6	175.5(4)	C1'	P'	C5'	C6'	72.0(5)
C1	P	C5	C9	-74.3(4)	C1'	P'	C5'	C9'	-177.4(4)
C1	P	C5	C10	53.4(5)	C1'	P'	C5'	C10'	-55.8(5)
C1	C2	C3	F2	50.7(7)	C1'	C2'	C3'	F2'	78.5(8)
C1	C2	C3	F3	168.9(5)	C1'	C2'	C3'	F3'	-162.0(7)
C1	C2	C3	F4	-70.2(6)	C1'	C2'	C3'	F4'	-37.7(10)
C1	C2	C4	F5	165.1(5)	C1'	C2'	C4'	F5'	-162.6(8)
C1	C2	C4	F6	44.4(7)	C1'	C2'	C4'	F6'	76.9(8)
C1	C2	C4	F7	-75.9(6)	C1'	C2'	C4'	F7'	-41.5(11)
C3	C2	C4	F5	46.2(7)	C3'	C2'	C4'	F5'	75.4(10)
C3	C2	C4	F6	-74.5(7)	C3'	C2'	C4'	F6'	-45.1(8)
C3	C2	C4	F7	165.2(5)	C3'	C2'	C4'	F7'	-163.5(8)
C4	C2	C3	F2	173.3(5)	C4'	C2'	C3'	F2'	-161.7(7)
C4	C2	C3	F3	-68.5(7)	C4'	C2'	C3'	F3'	-42.1(10)
C4	C2	C3	F4	52.4(7)	C4'	C2'	C3'	F4'	82.2(9)
C5	P	C1	C2	-166.1(5)	C5'	P'	C1'	C2'	159.9(6)
C5	C6	C7	C8	3.0(7)	C5'	C6'	C7'	C8'	0.0(7)
C5	C6	C7	C12	-177.3(6)	C5'	C6'	C7'	C12'	178.2(6)
C6	C5	C9	C8	2.1(6)	C6'	C5'	C9'	C8'	1.8(6)
C6	C5	C9	C14	-174.1(5)	C6'	C5'	C9'	C14'	-171.5(6)
C6	C7	C8	C9	-1.6(7)	C6'	C7'	C8'	C9'	1.2(7)
C6	C7	C8	C13	174.2(6)	C6'	C7'	C8'	C13'	-179.7(6)
C7	C8	C9	C5	-0.5(7)	C7'	C8'	C9'	C5'	-1.8(7)
C7	C8	C9	C14	175.5(6)	C7'	C8'	C9'	C14'	171.1(6)
C9	C5	C6	C7	-3.1(6)	C9'	C5'	C6'	C7'	-1.1(6)
C9	C5	C6	C11	172.2(5)	C9'	C5'	C6'	C11'	175.1(6)
C10	C5	C6	C7	-124.5(5)	C10'	C5'	C6'	C7'	-121.3(6)
C10	C5	C6	C11	50.9(7)	C10'	C5'	C6'	C11'	54.9(8)
C10	C5	C9	C8	122.2(5)	C10'	C5'	C9'	C8'	124.1(6)
C10	C5	C9	C14	-54.0(7)	C10'	C5'	C9'	C14'	-49.2(8)
C11	C6	C7	C8	-172.1(6)	C11'	C6'	C7'	C8'	-176.1(6)
C11	C6	C7	C12	7.7(10)	C11'	C6'	C7'	C12'	2.0(10)
C12	C7	C8	C9	178.6(5)	C12'	C7'	C8'	C9'	-177.0(6)
C12	C7	C8	C13	-5.6(9)	C12'	C7'	C8'	C13'	2.1(10)
C13	C8	C9	C5	-176.1(6)	C13'	C8'	C9'	C5'	179.1(6)
C13	C8	C9	C14	-0.1(10)	C13'	C8'	C9'	C14'	-8.0(11)

12.38 Pentacarbonyl{6-methyl-4-[bis(trimethylsilyl)methyl]-2-phenyl-1-oxa-3-aza-5,6-dihydrophosphine- κ -P}tungsten(0) [54.1]

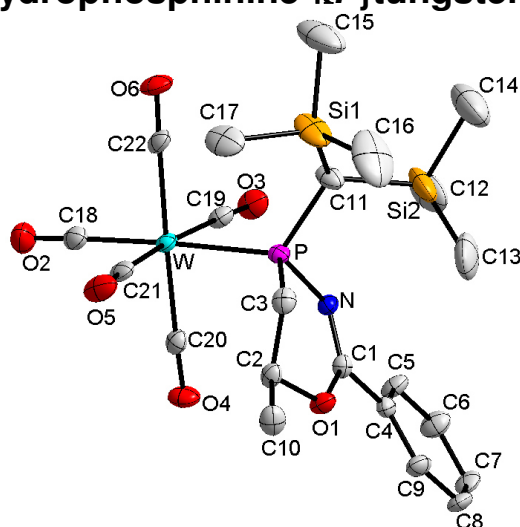


Table 1: Crystal data and structure refinement for **54.1**.

Identification code	GSTR345,AKY-343 // GXray3334
Crystal Habitus	colourless plate
Device Type	Nonius KappaCCD
Empirical formula	C ₂₂ H ₃₀ NO ₆ PSi ₂ W
Moiety formula	C ₂₂ H ₃₀ N O ₆ P Si ₂ W
Formula weight	675.47
Temperature/K	123(2)
Crystal system	monoclinic
Space group	P2 ₁ /c
a/Å	9.1834(2)
b/Å	22.5886(6)
c/Å	15.4583(4)
α /°	90.00
β /°	117.6820(10)
γ /°	90.00
Volume/Å ³	2839.64(12)
Z	4
$\rho_{\text{calc}}/\text{cm}^3$	1.580
μ/mm^{-1}	4.242
F(000)	1336.0
Crystal size/mm ³	0.42 × 0.36 × 0.12
Absorption correction	Multi-Scan
Tmin; Tmax	0.2688; 0.6300
Radiation	MoK α (λ = 0.71073)
2 θ range for data collection/°	4.84 to 52°
Completeness to theta	0.997
Index ranges	-11 ≤ h ≤ 11, -25 ≤ k ≤ 27, -12 ≤ l ≤ 19
Reflections collected	14906
Independent reflections	5564 [R _{int} = 0.0584]
Data/restraints/parameters	5564/17/305
Goodness-of-fit on F ²	1.037
Final R indexes [$I \geq 2\sigma(I)$]	R ₁ = 0.0295, wR ₂ = 0.0743
Final R indexes [all data]	R ₁ = 0.0354, wR ₂ = 0.0762
Largest diff. peak/hole / e Å ⁻³	1.81/-1.89

Table 2: Bond lengths for 54.1.

Atom	Atom	Length/Å	Atom	Atom	Length/Å
W	C18	2.014(4)	O1	C1	1.357(4)
W	C20	2.039(4)	O1	C2	1.458(4)
W	C21	2.041(4)	O2	C18	1.147(5)
W	C19	2.052(4)	O3	C19	1.137(5)
W	C22	2.052(4)	O4	C20	1.135(4)
W	P	2.4989(10)	O5	C21	1.134(5)
P	N	1.703(3)	O6	C22	1.139(5)
P	C11	1.821(4)	N	C1	1.271(4)
P	C3	1.828(4)	C1	C4	1.481(5)
Si1	C13	1.845(6)	C2	C3	1.517(5)
Si1	C12	1.858(6)	C2	C10	1.519(5)
Si1	C14	1.882(6)	C4	C9	1.394(5)
Si1	C11	1.906(4)	C4	C5	1.402(5)
Si2	C17	1.871(5)	C5	C6	1.390(5)
Si2	C16	1.873(7)	C6	C7	1.387(5)
Si2	C15	1.882(6)	C7	C8	1.364(6)
Si2	C11	1.915(4)	C8	C9	1.387(5)

Table 3: Bond angles for 54.1.

Atom	Atom	Atom	Angle/°	Atom	Atom	Atom	Angle/°
C18	W	C20	90.12(15)	C16	Si2	C15	112.2(3)
C18	W	C21	91.56(16)	C17	Si2	C11	114.9(2)
C20	W	C21	90.94(15)	C16	Si2	C11	111.5(3)
C18	W	C19	94.59(16)	C15	Si2	C11	106.8(2)
C20	W	C19	87.65(15)	C1	O1	C2	118.9(3)
C21	W	C19	173.69(15)	C1	N	P	123.7(3)
C18	W	C22	90.09(16)	N	C1	O1	128.6(3)
C20	W	C22	176.94(14)	N	C1	C4	120.4(3)
C21	W	C22	92.10(15)	O1	C1	C4	111.0(3)
C19	W	C22	89.30(15)	O1	C2	C3	111.6(3)
C18	W	P	177.45(11)	O1	C2	C10	105.7(3)
C20	W	P	87.35(11)	C3	C2	C10	113.5(3)
C21	W	P	88.15(12)	C2	C3	P	108.0(2)
C19	W	P	85.64(11)	C9	C4	C5	118.9(4)
C22	W	P	92.45(11)	C9	C4	C1	121.7(3)
N	P	C11	104.83(17)	C5	C4	C1	119.4(3)
N	P	C3	99.80(16)	C6	C5	C4	120.2(3)
C11	P	C3	105.63(18)	C7	C6	C5	119.9(4)
N	P	W	107.06(11)	C8	C7	C6	120.1(4)
C11	P	W	118.40(15)	C7	C8	C9	121.0(3)
C3	P	W	118.70(13)	C8	C9	C4	119.9(4)
C13	Si1	C12	111.5(3)	P	C11	Si1	115.2(2)
C13	Si1	C14	106.8(3)	P	C11	Si2	115.0(2)
C12	Si1	C14	105.7(3)	Si1	C11	Si2	115.7(2)
C13	Si1	C11	112.8(2)	O2	C18	W	177.3(3)
C12	Si1	C11	109.3(2)	O3	C19	W	177.6(3)
C14	Si1	C11	110.5(2)	O4	C20	W	177.9(4)

C17	Si2	C16	106.3(3)	O5	C21	W	176.6(4)
C17	Si2	C15	105.2(3)	O6	C22	W	178.1(3)

Table 4: Torsion angles for **54.1**.

A	B	C	D	Angle/°	A	B	C	D	Angle/°
C18	W	P	N	44(2)	C3	P	C11	Si1	91.7(2)
C20	W	P	N	36.85(14)	W	P	C11	Si1	-132.41(18)
C21	W	P	N	127.88(15)	N	P	C11	Si2	-151.6(2)
C19	W	P	N	-50.99(15)	C3	P	C11	Si2	-46.7(3)
C22	W	P	N	-140.10(15)	W	P	C11	Si2	89.2(2)
C18	W	P	C11	162(2)	C13	Si1	C11	P	-55.3(3)
C20	W	P	C11	154.90(17)	C12	Si1	C11	P	69.4(3)
C21	W	P	C11	-114.07(18)	C14	Si1	C11	P	-174.7(3)
C19	W	P	C11	67.06(18)	C13	Si1	C11	Si2	82.8(3)
C22	W	P	C11	-22.04(18)	C12	Si1	C11	Si2	-152.5(3)
C18	W	P	C3	-67(2)	C14	Si1	C11	Si2	-36.6(4)
C20	W	P	C3	-74.92(17)	C17	Si2	C11	P	-28.2(3)
C21	W	P	C3	16.10(18)	C16	Si2	C11	P	92.8(3)
C19	W	P	C3	-162.76(18)	C15	Si2	C11	P	-144.3(3)
C22	W	P	C3	108.13(17)	C17	Si2	C11	Si1	-166.4(2)
C11	P	N	C1	127.5(3)	C16	Si2	C11	Si1	-45.4(3)
C3	P	N	C1	18.3(3)	C15	Si2	C11	Si1	77.5(3)
W	P	N	C1	-106.0(3)	C20	W	C18	O2	47(8)
P	N	C1	O1	0.4(6)	C21	W	C18	O2	-44(8)
P	N	C1	C4	-178.9(3)	C19	W	C18	O2	135(8)
C2	O1	C1	N	9.7(5)	C22	W	C18	O2	-136(8)
C2	O1	C1	C4	-170.9(3)	P	W	C18	O2	40(10)
C1	O1	C2	C3	-44.1(4)	C18	W	C19	O3	-150(9)
C1	O1	C2	C10	-167.9(3)	C20	W	C19	O3	-60(9)
O1	C2	C3	P	62.0(3)	C21	W	C19	O3	17(10)
C10	C2	C3	P	-178.7(3)	C22	W	C19	O3	120(9)
N	P	C3	C2	-46.7(3)	P	W	C19	O3	27(9)
C11	P	C3	C2	-155.3(3)	C18	W	C20	O4	143(9)
W	P	C3	C2	69.0(3)	C21	W	C20	O4	-125(9)
N	C1	C4	C9	161.2(4)	C19	W	C20	O4	48(9)
O1	C1	C4	C9	-18.3(5)	C22	W	C20	O4	49(11)
N	C1	C4	C5	-19.7(5)	P	W	C20	O4	-37(9)
O1	C1	C4	C5	160.9(3)	C18	W	C21	O5	160(7)
C9	C4	C5	C6	-0.6(6)	C20	W	C21	O5	70(7)
C1	C4	C5	C6	-179.7(4)	C19	W	C21	O5	-7(7)
C4	C5	C6	C7	0.1(6)	C22	W	C21	O5	-110(7)
C5	C6	C7	C8	-0.5(6)	P	W	C21	O5	-17(7)
C6	C7	C8	C9	1.4(6)	C18	W	C22	O6	-107(11)
C7	C8	C9	C4	-1.9(6)	C20	W	C22	O6	-13(13)
C5	C4	C9	C8	1.4(6)	C21	W	C22	O6	161(11)
C1	C4	C9	C8	-179.4(3)	C19	W	C22	O6	-13(11)
N	P	C11	Si1	-13.2(3)	P	W	C22	O6	73(11)

12.39 Pentacarbonyl{2-methyl-4-[bis(trimethylsilyl)methyl]-1-oxa-3-aza-5,6-dihydrophosphinine- κ P}tungsten(0) [55.1a]

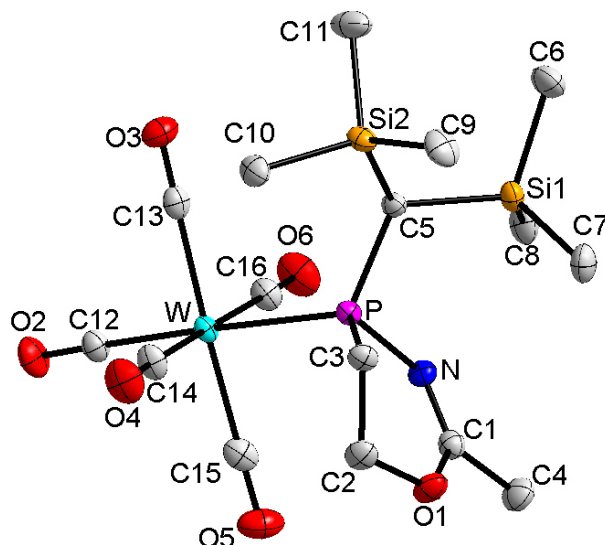


Table 1: Crystal data and structure refinement for **55.1a**.

Identification code	GSTR510, AKY-569 // GXray4796
Crystal Habitus	clear colourless plank
Device Type	Nonius KappaCCD
Empirical formula	C ₁₆ H ₂₆ NO ₆ PSi ₂ W
Moiety formula	C ₁₆ H ₂₆ N O ₆ P Si ₂ W
Formula weight	599.38
Temperature/K	123
Crystal system	orthorhombic
Space group	P2 ₁ 2 ₁ 2 ₁
a/Å	9.52110(10)
b/Å	10.1536(2)
c/Å	24.1643(5)
α/°	90
β/°	90
γ/°	90
Volume/Å ³	2336.05(7)
Z	4
ρ _{calc} /cm ³	1.704
μ/mm ⁻¹	5.145
F(000)	1176.0
Crystal size/mm ³	0.14 × 0.07 × 0.06
Absorption correction	multi-scan
Tmin; Tmax	0.6259; 0.7323
Radiation	MoKα (λ = 0.71073)
2θ range for data collection/°	5.866 to 55.996°
Completeness to theta	0.998
Index ranges	-11 ≤ h ≤ 12, -13 ≤ k ≤ 9, -29 ≤ l ≤ 31
Reflections collected	13893
Independent reflections	5546 [R _{int} = 0.0338, R _{sigma} = 0.0386]
Data/restraints/parameters	5546/0/252
Goodness-of-fit on F ²	1.030
Final R indexes [I ≥ 2σ (I)]	R ₁ = 0.0225, wR ₂ = 0.0456
Final R indexes [all data]	R ₁ = 0.0241, wR ₂ = 0.0462

Largest diff. peak/hole / e Å⁻³ 0.85/-0.56
 Flack parameter 0.469(7)

Table 2: Bond lengths for **55.1a**.

Atom	Atom	Length/Å	Atom	Atom	Length/Å
W	P	2.5089(12)	Si2	C9	1.859(6)
W	C12	2.018(5)	Si2	C10	1.887(5)
W	C13	2.042(5)	Si2	C11	1.861(6)
W	C14	2.030(5)	O1	C1	1.355(6)
W	C15	2.056(6)	O1	C2	1.449(6)
W	C16	2.066(5)	O2	C12	1.139(6)
P	N	1.700(4)	O3	C13	1.137(6)
P	C3	1.835(5)	O4	C14	1.137(6)
P	C5	1.820(5)	O5	C15	1.131(6)
Si1	C5	1.920(5)	O6	C16	1.121(6)
Si1	C6	1.872(5)	N	C1	1.268(6)
Si1	C7	1.866(5)	C1	C4	1.497(7)
Si1	C8	1.868(5)	C2	C3	1.520(7)
Si2	C5	1.907(5)			

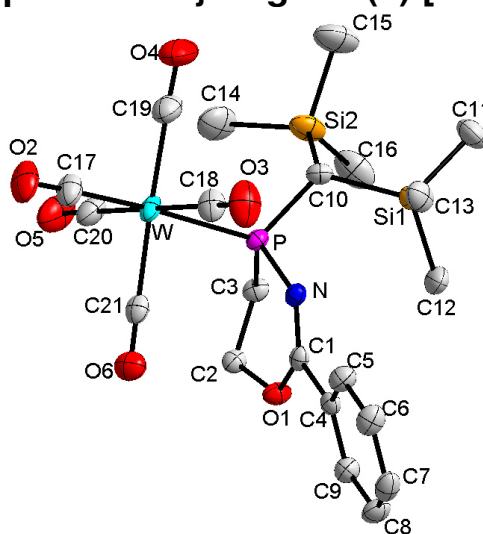
Table 3: Bond angles for **55.1a**.

Atom	Atom	Atom	Angle/°	Atom	Atom	Atom	Angle/°
C12	W	P	176.44(15)	C7	Si1	C8	111.7(3)
C12	W	C13	90.2(2)	C8	Si1	C5	110.4(2)
C12	W	C14	92.8(2)	C8	Si1	C6	105.3(3)
C12	W	C15	90.6(2)	C9	Si2	C5	112.2(3)
C12	W	C16	89.7(2)	C9	Si2	C10	106.7(3)
C13	W	P	92.27(13)	C9	Si2	C11	109.9(3)
C13	W	C15	177.2(2)	C10	Si2	C5	113.6(2)
C13	W	C16	88.6(2)	C11	Si2	C5	107.9(2)
C14	W	P	89.69(15)	C11	Si2	C10	106.3(3)
C14	W	C13	91.3(2)	C1	O1	C2	119.0(4)
C14	W	C15	91.3(2)	C1	N	P	124.5(3)
C14	W	C16	177.5(2)	O1	C1	C4	109.6(4)
C15	W	P	86.83(14)	N	C1	O1	128.3(4)
C15	W	C16	88.7(2)	N	C1	C4	122.2(5)
C16	W	P	87.76(15)	O1	C2	C3	112.8(4)
N	P	W	108.69(14)	C2	C3	P	107.3(4)
N	P	C3	98.8(2)	P	C5	Si1	115.2(3)
N	P	C5	105.3(2)	P	C5	Si2	114.7(2)
C3	P	W	119.12(17)	Si2	C5	Si1	115.9(3)
C5	P	W	116.73(16)	O2	C12	W	178.7(5)
C5	P	C3	105.9(2)	O3	C13	W	179.5(5)
C6	Si1	C5	109.5(2)	O4	C14	W	177.8(4)
C7	Si1	C5	112.0(2)	O5	C15	W	179.0(5)
C7	Si1	C6	107.8(3)	O6	C16	W	179.1(5)

Table 4: Torsion angles for **55.1a**.

A	B	C	D	Angle/°	A	B	C	D	Angle/°
W	P	N	C1	-104.8(4)	N	P	C5	Si2	-149.3(2)
W	P	C3	C2	69.1(4)	C1	O1	C2	C3	-40.8(6)
W	P	C5	Si1	-131.6(2)	C2	O1	C1	N	5.3(8)
W	P	C5	Si2	90.0(3)	C2	O1	C1	C4	-174.7(4)
P	N	C1	O1	1.7(7)	C3	P	N	C1	20.2(5)
P	N	C1	C4	-178.4(4)	C3	P	C5	Si1	93.2(3)
O1	C2	C3	P	61.8(5)	C3	P	C5	Si2	-45.2(3)
N	P	C3	C2	-48.2(4)	C5	P	N	C1	129.4(4)
N	P	C5	Si1	-10.9(3)	C5	P	C3	C2	-157.0(4)

12.40 Pentacarbonyl{4-[bis(trimethylsilyl)methyl]-2-phenyl-1-oxa-3-aza-5,6-dihydrophosphinine- κP }tungsten(0) [55.1b]

**Table 1:** Crystal data and structure refinement for **55.1b**.

Identification code	GSTR509, AKY-570 // GXray4797
Crystal Habitus	clear colourless plate
Device Type	Nonius KappaCCD
Empirical formula	C ₂₁ H ₂₈ NO ₆ PSi ₂ W
Moiety formula	C ₂₁ H ₂₈ N O ₆ P Si ₂ W
Formula weight	661.44
Temperature/K	123
Crystal system	monoclinic
Space group	P2 ₁ /a
a/Å	10.1827(3)
b/Å	15.4432(3)
c/Å	17.7407(4)
α /°	90
β /°	104.4804(11)
γ /°	90
Volume/Å ³	2701.16(11)
Z	4
$\rho_{\text{calc}}/\text{cm}^3$	1.626
μ/mm^{-1}	4.458
F(000)	1304.0
Crystal size/mm ³	0.15 × 0.14 × 0.05

Absorption correction	multi-scan
Tmin; Tmax	0.7175; 1.2457
Radiation	MoK α (λ = 0.71073)
2 θ range for data collection/ $^{\circ}$	4.976 to 56 $^{\circ}$
Completeness to theta	0.999
Index ranges	-13 \leq h \leq 12, -20 \leq k \leq 16, -23 \leq l \leq 23
Reflections collected	28202
Independent reflections	6519 [R _{int} = 0.0678, R _{sigma} = 0.0398]
Data/restraints/parameters	6519/54/295
Goodness-of-fit on F ²	1.023
Final R indexes [$ I > 2\sigma(I)$]	R ₁ = 0.0307, wR ₂ = 0.0714
Final R indexes [all data]	R ₁ = 0.0385, wR ₂ = 0.0754
Largest diff. peak/hole / e \AA^{-3}	1.92/-1.74

Table 2: Bond lengths for **55.1b**.

Atom	Atom	Length/ \AA	Atom	Atom	Length/ \AA
W	P	2.5171(8)	O1	C1	1.358(4)
W	C17	2.017(4)	O1	C2	1.443(4)
W	C18	2.058(4)	O2	C17	1.143(5)
W	C19	2.023(4)	O3	C18	1.131(5)
W	C20	2.036(4)	O4	C19	1.158(5)
W	C21	2.032(4)	O5	C20	1.138(5)
P	N	1.696(3)	O6	C21	1.145(4)
P	C3	1.833(3)	N	C1	1.272(4)
P	C10	1.827(3)	C1	C4	1.485(4)
Si1	C10	1.914(4)	C2	C3	1.520(5)
Si1	C11	1.872(4)	C4	C5	1.392(5)
Si1	C12	1.868(4)	C4	C9	1.394(5)
Si1	C13	1.860(4)	C5	C6	1.383(5)
Si2	C10	1.910(3)	C6	C7	1.392(5)
Si2	C14	1.880(5)	C7	C8	1.376(6)
Si2	C15	1.876(5)	C8	C9	1.393(5)
Si2	C16	1.864(5)			

Table 3: Bond angles for **55.1b**.

Atom	Atom	Atom	Angle/ $^{\circ}$	Atom	Atom	Atom	Angle/ $^{\circ}$
C17	W	P	172.64(13)	C15	Si2	C10	107.5(2)
C17	W	C18	89.85(16)	C15	Si2	C14	106.2(2)
C17	W	C19	92.35(18)	C16	Si2	C10	112.09(19)
C17	W	C20	90.85(17)	C16	Si2	C14	106.6(2)
C17	W	C21	89.69(16)	C16	Si2	C15	110.9(2)
C18	W	P	84.04(11)	C1	O1	C2	119.7(3)
C19	W	P	91.69(13)	C1	N	P	124.8(2)
C19	W	C18	89.52(18)	O1	C1	C4	111.3(3)
C19	W	C20	90.34(17)	N	C1	O1	127.6(3)
C19	W	C21	177.81(16)	N	C1	C4	121.1(3)
C20	W	P	95.27(12)	O1	C2	C3	113.7(3)
C20	W	C18	179.29(17)	C2	C3	P	108.6(2)
C21	W	P	86.20(10)	C5	C4	C1	119.1(3)
C21	W	C18	89.69(16)	C5	C4	C9	119.2(3)
C21	W	C20	90.43(15)	C9	C4	C1	121.7(3)

N	P	W	103.91(10)	C6	C5	C4	120.3(3)
N	P	C3	100.12(15)	C5	C6	C7	120.2(3)
N	P	C10	105.42(14)	C8	C7	C6	119.8(3)
C3	P	W	121.37(12)	C7	C8	C9	120.3(3)
C10	P	W	118.54(11)	C8	C9	C4	120.1(3)
C10	P	C3	104.79(16)	P	C10	Si1	114.97(17)
C11	Si1	C10	111.70(18)	P	C10	Si2	113.84(18)
C12	Si1	C10	113.08(17)	Si2	C10	Si1	115.48(18)
C12	Si1	C11	106.3(2)	O2	C17	W	177.2(4)
C13	Si1	C10	107.81(17)	O3	C18	W	179.6(4)
C13	Si1	C11	105.5(2)	O4	C19	W	178.3(4)
C13	Si1	C12	112.2(2)	O5	C20	W	178.2(4)
C14	Si2	C10	113.46(19)	O6	C21	W	179.6(4)

Table 4: Torsion angles for **55.1b**.

A	B	C	D	Angle/°	A	B	C	D	Angle/°
W	P	N	C1	106.2(3)	C1	C4	C5	C6	179.1(3)
W	P	C3	C2	-69.4(3)	C1	C4	C9	C8	-179.7(3)
W	P	C10	Si1	133.57(14)	C2	O1	C1	N	-11.9(5)
W	P	C10	Si2	-90.00(18)	C2	O1	C1	C4	168.4(3)
P	N	C1	O1	3.7(5)	C3	P	N	C1	-19.9(3)
P	N	C1	C4	-176.6(2)	C3	P	C10	Si1	-87.3(2)
O1	C1	C4	C5	-166.1(3)	C3	P	C10	Si2	49.2(2)
O1	C1	C4	C9	13.0(4)	C4	C5	C6	C7	0.2(6)
O1	C2	C3	P	-57.8(3)	C5	C4	C9	C8	-0.5(5)
N	P	C3	C2	43.9(3)	C5	C6	C7	C8	0.4(6)
N	P	C10	Si1	17.9(2)	C6	C7	C8	C9	-1.1(6)
N	P	C10	Si2	154.30(17)	C7	C8	C9	C4	1.1(5)
N	C1	C4	C5	14.1(5)	C9	C4	C5	C6	-0.1(5)
N	C1	C4	C9	-166.7(3)	C10	P	N	C1	-128.4(3)
C1	O1	C2	C3	42.1(4)	C10	P	C3	C2	152.9(2)

12.41 Pentacarbonyl{2-(1,1-dimethylethyl)-4-[bis(trimethylsilyl)methyl]-1-oxa-3-aza-5,6-dihydrophosphinine- κP }tungsten(0) [55.1c]

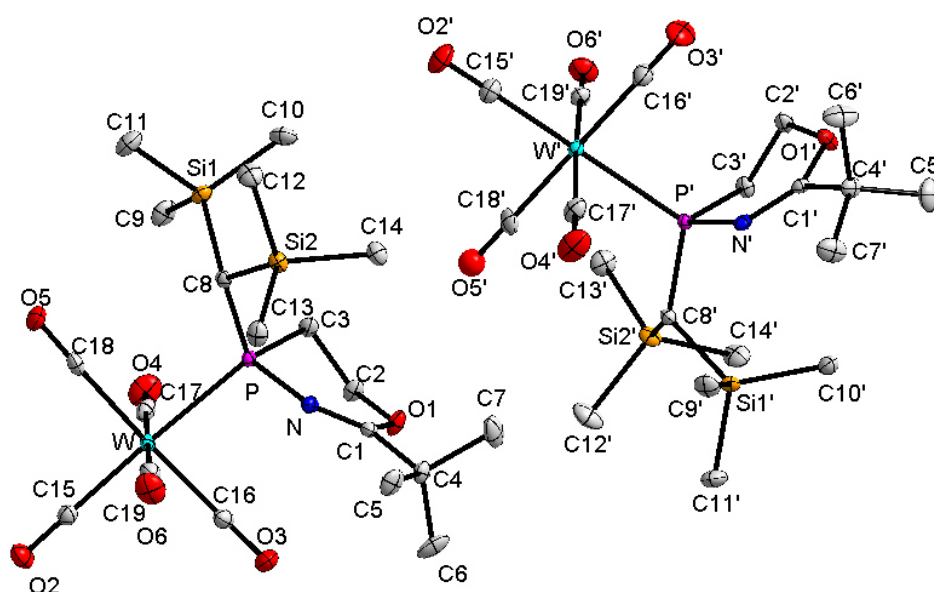


Table 1: Crystal data and structure refinement for **55.1c**.

Identification code	GSTR529, AKY-599 // GXraymo_4925f
Crystal Habitus	clear colourless plate
Device Type	Bruker D8-Venture
Empirical formula	C ₁₉ H ₃₂ NO ₆ Si ₂ PW
Moiety formula	C ₁₉ H ₃₂ N O ₆ P Si ₂ W
Formula weight	641.45
Temperature/K	100.0
Crystal system	triclinic
Space group	P $\bar{1}$
a/Å	12.6617(9)
b/Å	13.6989(10)
c/Å	16.0934(13)
α /°	72.085(3)
β /°	88.886(3)
γ /°	77.237(3)
Volume/Å ³	2586.9(3)
Z	4
ρ_{calc} /cm ³	1.647
μ /mm ⁻¹	4.652
F(000)	1272.0
Crystal size/mm ³	0.18 × 0.15 × 0.04
Absorption correction	empirical
Tmin; Tmax	0.4504; 0.7459
Radiation	MoK α (λ = 0.71073)
2 θ range for data collection/°	4.35 to 55.998°
Completeness to theta	0.999
Index ranges	-16 ≤ h ≤ 16, -18 ≤ k ≤ 18, -21 ≤ l ≤ 21
Reflections collected	114135
Independent reflections	12480 [R _{int} = 0.0815, R _{sigma} = 0.0395]
Data/restraints/parameters	12480/0/559

Goodness-of-fit on F^2	1.023
Final R indexes [$I > 2\sigma(I)$]	$R_1 = 0.0250$, $wR_2 = 0.0565$
Final R indexes [all data]	$R_1 = 0.0385$, $wR_2 = 0.0624$
Largest diff. peak/hole / $e \text{ \AA}^{-3}$	1.40/-1.64

Table 2: Bond lengths for **55.1c**.

Atom	Atom	Length/Å	Atom	Atom	Length/Å
W	P	2.5084(8)	W'	P'	2.5030(8)
W	C15	2.017(3)	W'	C15'	2.012(3)
W	C16	2.041(3)	W'	C16'	2.047(4)
W	C17	2.039(3)	W'	C17'	2.062(3)
W	C18	2.030(3)	W'	C18'	2.028(4)
W	C19	2.067(4)	W'	C19'	2.038(3)
P	N	1.702(3)	P'	N'	1.705(3)
P	C3	1.830(3)	P'	C3'	1.826(3)
P	C8	1.833(3)	P'	C8'	1.832(3)
Si1	C8	1.913(3)	Si1'	C8'	1.912(3)
Si1	C9	1.885(4)	Si1'	C9'	1.863(4)
Si1	C10	1.868(4)	Si1'	C10'	1.878(3)
Si1	C11	1.874(4)	Si1'	C11'	1.870(3)
Si2	C8	1.908(3)	Si2'	C8'	1.910(3)
Si2	C12	1.877(3)	Si2'	C12'	1.869(4)
Si2	C13	1.865(3)	Si2'	C13'	1.874(4)
Si2	C14	1.873(3)	Si2'	C14'	1.877(4)
O1	C1	1.358(4)	O1'	C1'	1.358(4)
O1	C2	1.443(4)	O1'	C2'	1.443(4)
O2	C15	1.141(4)	O2'	C15'	1.149(4)
O3	C16	1.145(4)	O3'	C16'	1.142(4)
O4	C17	1.146(4)	O4'	C17'	1.129(4)
O5	C18	1.145(4)	O5'	C18'	1.142(4)
O6	C19	1.131(4)	O6'	C19'	1.139(4)
N	C1	1.270(4)	N'	C1'	1.265(4)
C1	C4	1.526(4)	C1'	C4'	1.532(4)
C2	C3	1.518(4)	C2'	C3'	1.512(4)
C4	C5	1.521(5)	C4'	C5'	1.534(5)
C4	C6	1.530(5)	C4'	C6'	1.540(5)
C4	C7	1.535(5)	C4'	C7'	1.522(5)

Table 3: Bond angles for **55.1c**.

Atom	Atom	Atom	Angle/°	Atom	Atom	Atom	Angle/°
C15	W	P	174.14(10)	C15'	W'	P'	176.16(10)
C15	W	C16	91.33(13)	C15'	W'	C16'	89.88(14)
C15	W	C17	93.17(14)	C15'	W'	C17'	91.91(14)
C15	W	C18	91.02(13)	C15'	W'	C18'	90.14(14)
C15	W	C19	88.15(13)	C15'	W'	C19'	92.88(13)
C16	W	P	87.91(9)	C16'	W'	P'	88.37(10)
C16	W	C19	91.12(14)	C16'	W'	C17'	90.69(15)
C17	W	P	92.65(10)	C17'	W'	P'	84.69(10)
C17	W	C16	90.16(13)	C18'	W'	P'	91.60(10)
C17	W	C19	178.14(13)	C18'	W'	C16'	179.95(16)

C18	W	P	89.84(9)	C18'	W'	C17'	89.26(14)
C18	W	C16	177.52(12)	C18'	W'	C19'	87.75(14)
C18	W	C17	88.92(13)	C19'	W'	P'	90.61(9)
C18	W	C19	89.75(13)	C19'	W'	C16'	92.30(14)
C19	W	P	86.05(10)	C19'	W'	C17'	174.36(13)
N	P	W	108.06(9)	N'	P'	W'	109.37(9)
N	P	C3	99.46(14)	N'	P'	C3'	99.04(14)
N	P	C8	106.04(14)	N'	P'	C8'	105.42(13)
C3	P	W	119.05(11)	C3'	P'	W'	118.47(11)
C3	P	C8	106.92(14)	C3'	P'	C8'	106.43(14)
C8	P	W	115.43(10)	C8'	P'	W'	116.08(10)
C9	Si1	C8	114.34(15)	C9'	Si1'	C8'	108.77(15)
C10	Si1	C8	111.21(15)	C9'	Si1'	C10'	113.87(16)
C10	Si1	C9	107.58(17)	C9'	Si1'	C11'	104.54(17)
C10	Si1	C11	110.76(17)	C10'	Si1'	C8'	112.17(14)
C11	Si1	C8	108.13(15)	C11'	Si1'	C8'	111.52(16)
C11	Si1	C9	104.65(17)	C11'	Si1'	C10'	105.71(16)
C12	Si2	C8	111.23(15)	C12'	Si2'	C8'	107.92(15)
C13	Si2	C8	108.94(15)	C12'	Si2'	C13'	105.09(17)
C13	Si2	C12	104.71(16)	C12'	Si2'	C14'	110.85(17)
C13	Si2	C14	112.64(16)	C13'	Si2'	C8'	115.13(15)
C14	Si2	C8	112.45(15)	C13'	Si2'	C14'	107.04(17)
C14	Si2	C12	106.59(16)	C14'	Si2'	C8'	110.69(15)
C1	O1	C2	120.3(2)	C1'	O1'	C2'	119.0(2)
C1	N	P	124.2(2)	C1'	N'	P'	124.4(2)
O1	C1	C4	109.3(3)	O1'	C1'	C4'	109.3(3)
N	C1	O1	127.7(3)	N'	C1'	O1'	128.2(3)
N	C1	C4	123.0(3)	N'	C1'	C4'	122.5(3)
O1	C2	C3	113.7(3)	O1'	C2'	C3'	113.5(2)
C2	C3	P	108.0(2)	C2'	C3'	P'	107.8(2)
C1	C4	C6	108.5(3)	C1'	C4'	C5'	110.2(3)
C1	C4	C7	108.7(3)	C1'	C4'	C6'	107.3(3)
C5	C4	C1	110.5(3)	C5'	C4'	C6'	110.0(3)
C5	C4	C6	109.4(3)	C7'	C4'	C1'	110.8(3)
C5	C4	C7	110.1(3)	C7'	C4'	C5'	109.8(3)
C6	C4	C7	109.6(3)	C7'	C4'	C6'	108.7(3)
P	C8	Si1	115.14(16)	P'	C8'	Si1'	115.16(16)
P	C8	Si2	116.31(16)	P'	C8'	Si2'	115.20(16)
Si2	C8	Si1	114.71(15)	Si2'	C8'	Si1'	115.37(16)
O2	C15	W	178.6(3)	O2'	C15'	W'	178.9(3)
O3	C16	W	178.5(3)	O3'	C16'	W'	179.4(3)
O4	C17	W	178.7(3)	O4'	C17'	W'	177.5(3)
O5	C18	W	178.5(3)	O5'	C18'	W'	179.8(4)
O6	C19	W	179.2(3)	O6'	C19'	W'	177.1(3)

Table 4: Torsion angles for **55.1c**.

A	B	C	D	Angle/°	A	B	C	D	Angle/°
W	P	N	C1	102.5(3)	W'	P'	N'	C1'	-104.6(3)
W	P	C3	C2	-69.5(2)	W'	P'	C3'	C2'	70.8(2)
W	P	C8	Si1	-93.43(16)	W'	P'	C8'	Si1'	-131.57(13)
W	P	C8	Si2	128.22(13)	W'	P'	C8'	Si2'	90.34(16)

P	N	C1	O1	1.8(5)	P'	N'	C1'	O1'	0.8(5)
P	N	C1	C4	-178.4(2)	P'	N'	C1'	C4'	179.3(2)
O1	C1	C4	C5	-178.4(3)	O1'	C1'	C4'	C5'	-46.3(3)
O1	C1	C4	C6	-58.5(3)	O1'	C1'	C4'	C6'	73.4(3)
O1	C1	C4	C7	60.7(4)	O1'	C1'	C4'	C7'	-168.1(3)
O1	C2	C3	P	-58.4(3)	O1'	C2'	C3'	P'	60.8(3)
N	P	C3	C2	47.3(2)	N'	P'	C3'	C2'	-47.1(2)
N	P	C8	Si1	146.97(16)	N'	P'	C8'	Si1'	-10.4(2)
N	P	C8	Si2	8.6(2)	N'	P'	C8'	Si2'	-148.46(16)
N	C1	C4	C5	1.7(4)	N'	C1'	C4'	C5'	135.0(3)
N	C1	C4	C6	121.7(3)	N'	C1'	C4'	C6'	-105.3(4)
N	C1	C4	C7	-119.2(4)	N'	C1'	C4'	C7'	13.2(4)
C1	O1	C2	C3	37.9(4)	C1'	O1'	C2'	C3'	-40.4(4)
C2	O1	C1	N	-6.0(5)	C2'	O1'	C1'	N'	6.0(5)
C2	O1	C1	C4	174.1(3)	C2'	O1'	C1'	C4'	-172.6(3)
C3	P	N	C1	-22.4(3)	C3'	P'	N'	C1'	20.0(3)
C3	P	C8	Si1	41.5(2)	C3'	P'	C8'	Si1'	94.18(19)
C3	P	C8	Si2	-96.82(19)	C3'	P'	C8'	Si2'	-43.9(2)
C8	P	N	C1	-133.2(3)	C8'	P'	N'	C1'	129.9(3)
C8	P	C3	C2	157.4(2)	C8'	P'	C3'	C2'	-156.3(2)

12.42 Lithium(1,4,7,10-tetraoxacyclododecane) pentacarbonyl{[3,3,3-trifluoro-2-hydroxypropyl](triphenylmethyl)phosphanoxido- κ P}tungsten(0) [57.3a]

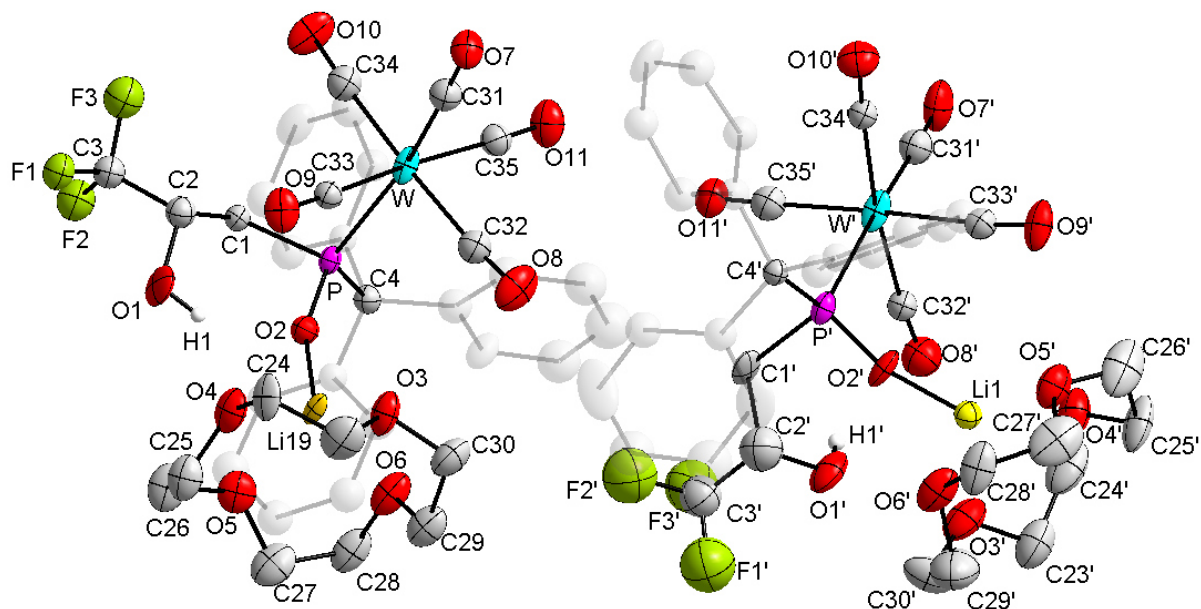


Table 1: Crystal data and structure refinement for **57.3a**.

Identification code	GSTR505, PB-12 // GXraycu_4642g
Crystal Habitus	clear colourless plank
Device Type	Bruker D8-Venture
Empirical formula	C ₃₅ H ₃₅ LiO ₁₁ F ₃ PW
Moiety formula	C ₃₅ H ₃₅ F ₃ Li O ₁₁ P W
Formula weight	910.39
Temperature/K	100

Crystal system	triclinic
Space group	$P\bar{1}$
a/Å	11.7656(6)
b/Å	17.3287(8)
c/Å	18.3627(8)
$\alpha/^\circ$	100.314(2)
$\beta/^\circ$	96.610(2)
$\gamma/^\circ$	92.386(3)
Volume/Å ³	3651.4(3)
Z	4
$\rho_{\text{calc}}/\text{cm}^3$	1.656
μ/mm^{-1}	6.923
F(000)	1808.0
Crystal size/mm ³	0.16 × 0.04 × 0.03
Absorption correction	empirical
Tmin; Tmax	0.2779; 0.7542
Radiation	CuK α ($\lambda = 1.54178$)
2 θ range for data collection/ $^\circ$	4.93 to 135.496 $^\circ$
Completeness to theta	0.985
Index ranges	-14 ≤ h ≤ 14, -20 ≤ k ≤ 20, -22 ≤ l ≤ 22
Reflections collected	62711
Independent reflections	13041 [R _{int} = 0.1191, R _{sigma} = 0.0826]
Data/restraints/parameters	13041/382/939
Goodness-of-fit on F ²	1.878
Final R indexes [$l \geq 2\sigma(l)$]	R ₁ = 0.1909, wR ₂ = 0.4301
Final R indexes [all data]	R ₁ = 0.2084, wR ₂ = 0.4480
Largest diff. peak/hole / e Å ⁻³	11.26/-12.98

Table 2: Bond lengths for 57.3a.

Atom	Atom	Length/Å	Atom	Atom	Length/Å
W	P	2.553(4)	W'	P'	2.569(4)
W	C31	1.94(2)	W'	C31'	1.92(2)
W	C32	2.01(2)	W'	C32'	2.051(17)
W	C33	1.993(17)	W'	C33'	2.04(2)
W	C34	2.00(2)	W'	C34'	2.037(17)
W	C35	2.051(19)	W'	C35'	2.07(2)
P	O2	1.547(13)	P'	O2'	1.556(12)
P	C1	1.856(16)	P'	C1'	1.88(2)
P	C4	1.965(18)	P'	C4'	1.943(17)
F1	C3	1.32(2)	F1'	C3'	1.26(3)
F2	C3	1.33(2)	F2'	C3'	1.40(4)
F3	C3	1.37(2)	F3'	C3'	1.29(3)
O1	C2	1.41(2)	O1'	C2'	1.43(3)
O2	Li19	1.84(3)	O2'	Li1	1.77(3)
O3	C23	1.40(3)	O3'	C23'	1.47(3)
O3	C30	1.42(3)	O3'	C30'	1.395(10)
O3	Li19	2.11(3)	O3'	Li1	2.06(3)
O4	C24	1.44(3)	O4'	C24'	1.394(10)
O4	C25	1.42(3)	O4'	C25'	1.41(3)
O4	Li19	2.13(3)	O4'	Li1	2.23(3)
O5	C26	1.43(3)	O5'	C26'	1.389(10)
O5	C27	1.43(3)	O5'	C27'	1.42(3)

O5	Li19	2.14(3)	O5'	Li1	2.15(3)
O6	C28	1.45(3)	O6'	C28'	1.43(3)
O6	C29	1.391(10)	O6'	C29'	1.46(3)
O6	Li19	2.08(3)	O6'	Li1	2.16(3)
O7	C31	1.23(2)	O7'	C31'	1.18(3)
O8	C32	1.14(3)	O8'	C32'	1.15(2)
O9	C33	1.17(2)	O9'	C33'	1.14(2)
O10	C34	1.19(3)	O10'	C34'	1.12(2)
O11	C35	1.14(2)	O11'	C35'	1.12(3)
C1	C2	1.50(2)	C1'	C2'	1.45(3)
C2	C3	1.48(3)	C2'	C3'	1.51(4)
C4	C5	1.53(2)	C4'	C5'	1.53(2)
C4	C11	1.54(3)	C4'	C11'	1.57(2)
C4	C17	1.55(3)	C4'	C17'	1.54(2)
C5	C6	1.33(3)	C5'	C6'	1.39(3)
C5	C10	1.40(3)	C5'	C10'	1.41(3)
C6	C7	1.42(3)	C6'	C7'	1.37(3)
C7	C8	1.44(3)	C7'	C8'	1.36(3)
C8	C9	1.37(3)	C8'	C9'	1.35(3)
C9	C10	1.44(3)	C9'	C10'	1.42(3)
C11	C12	1.39(3)	C11'	C12'	1.34(3)
C11	C16	1.39(3)	C11'	C16'	1.43(3)
C12	C13	1.33(3)	C12'	C13'	1.39(3)
C13	C14	1.41(3)	C13'	C14'	1.42(3)
C14	C15	1.39(3)	C14'	C15'	1.37(3)
C15	C16	1.38(3)	C15'	C16'	1.45(3)
C17	C18	1.40(3)	C17'	C18'	1.36(3)
C17	C22	1.42(3)	C17'	C22'	1.41(4)
C18	C19	1.42(4)	C18'	C19'	1.39(4)
C19	C20	1.29(4)	C19'	C20'	1.32(5)
C20	C21	1.38(4)	C20'	C21'	1.37(4)
C21	C22	1.35(4)	C21'	C22'	1.40(4)
C23	C24	1.51(3)	C23'	C24'	1.55(4)
C25	C26	1.54(3)	C25'	C26'	1.58(3)
C27	C28	1.50(4)	C27'	C28'	1.48(4)
C29	C30	1.57(3)	C29'	C30'	1.50(4)

Table 3: Bond angles for **57.3a**.

Atom	Atom	Atom	Angle/°	Atom	Atom	Atom	Angle/°
C31	W	P	167.9(6)	C31'	W'	P'	174.1(6)
C31	W	C32	89.0(8)	C31'	W'	C32'	89.9(8)
C31	W	C33	87.0(8)	C31'	W'	C33'	92.4(9)
C31	W	C34	91.5(9)	C31'	W'	C34'	87.2(8)
C31	W	C35	89.8(8)	C31'	W'	C35'	89.8(9)
C32	W	P	93.4(6)	C32'	W'	P'	84.3(5)
C32	W	C35	85.4(8)	C32'	W'	C35'	91.9(8)
C33	W	P	81.3(5)	C33'	W'	P'	88.6(5)
C33	W	C32	88.2(8)	C33'	W'	C32'	86.4(7)
C33	W	C34	96.1(8)	C33'	W'	C35'	177.3(8)
C33	W	C35	172.9(8)	C34'	W'	P'	98.7(5)
C34	W	P	87.0(6)	C34'	W'	C32'	173.6(7)

C34	W	C32	175.6(8)	C34'	W'	C33'	88.0(7)
C34	W	C35	90.3(8)	C34'	W'	C35'	93.7(8)
C35	W	P	102.2(5)	C35'	W'	P'	89.1(6)
O2	P	W	111.3(5)	O2'	P'	W'	113.1(5)
O2	P	C1	102.3(7)	O2'	P'	C1'	103.6(8)
O2	P	C4	107.1(7)	O2'	P'	C4'	106.0(7)
C1	P	W	110.6(5)	C1'	P'	W'	110.5(7)
C1	P	C4	100.9(8)	C1'	P'	C4'	102.5(8)
C4	P	W	122.4(5)	C4'	P'	W'	119.5(5)
P	O2	Li19	156.7(12)	P'	O2'	Li1	164.6(13)
C23	O3	C30	115.3(19)	C23'	O3'	Li1	116.3(17)
C23	O3	Li19	110.5(16)	C30'	O3'	C23'	115(2)
C30	O3	Li19	108.8(16)	C30'	O3'	Li1	111.7(16)
C24	O4	Li19	108.9(13)	C24'	O4'	C25'	113.3(19)
C25	O4	C24	113.5(17)	C24'	O4'	Li1	107.0(17)
C25	O4	Li19	112.9(15)	C25'	O4'	Li1	109.9(16)
C26	O5	Li19	109.4(15)	C26'	O5'	C27'	117(2)
C27	O5	C26	117.8(18)	C26'	O5'	Li1	112.0(15)
C27	O5	Li19	110.0(16)	C27'	O5'	Li1	111.2(17)
C28	O6	Li19	110.0(15)	C28'	O6'	C29'	111(2)
C29	O6	C28	112.1(17)	C28'	O6'	Li1	109.9(16)
C29	O6	Li19	110.9(14)	C29'	O6'	Li1	110.2(19)
C2	C1	P	113.8(13)	C2'	C1'	P'	112.7(16)
O1	C2	C1	110.2(14)	O1'	C2'	C1'	114(2)
O1	C2	C3	106.5(15)	O1'	C2'	C3'	102(2)
C3	C2	C1	115.8(17)	C1'	C2'	C3'	113(2)
F1	C3	F2	108.7(15)	F1'	C3'	F2'	103(2)
F1	C3	F3	106.6(15)	F1'	C3'	F3'	115(3)
F1	C3	C2	114.1(17)	F1'	C3'	C2'	109(3)
F2	C3	F3	104.6(16)	F2'	C3'	C2'	109(2)
F2	C3	C2	112.3(16)	F3'	C3'	F2'	103(2)
F3	C3	C2	110.0(15)	F3'	C3'	C2'	117(2)
C5	C4	P	112.6(12)	C5'	C4'	P'	109.5(11)
C5	C4	C11	110.2(14)	C5'	C4'	C11'	107.0(13)
C5	C4	C17	110.4(14)	C5'	C4'	C17'	109.4(14)
C11	C4	P	104.4(11)	C11'	C4'	P'	110.1(12)
C11	C4	C17	113.0(14)	C17'	C4'	P'	108.5(11)
C17	C4	P	106.1(13)	C17'	C4'	C11'	112.3(14)
C6	C5	C4	124.4(16)	C6'	C5'	C4'	124.2(17)
C6	C5	C10	119.8(17)	C6'	C5'	C10'	117.4(17)
C10	C5	C4	115.5(15)	C10'	C5'	C4'	118.5(15)
C5	C6	C7	123.3(18)	C7'	C6'	C5'	122.7(19)
C6	C7	C8	117.8(19)	C8'	C7'	C6'	119.9(19)
C9	C8	C7	119(2)	C9'	C8'	C7'	120(2)
C8	C9	C10	121(2)	C8'	C9'	C10'	121(2)
C5	C10	C9	119.0(18)	C5'	C10'	C9'	118.2(18)
C12	C11	C4	123.2(16)	C12'	C11'	C4'	123.0(18)
C12	C11	C16	115.5(18)	C12'	C11'	C16'	121.5(19)
C16	C11	C4	121.3(16)	C16'	C11'	C4'	115.1(16)
C13	C12	C11	124(2)	C11'	C12'	C13'	121(2)
C12	C13	C14	121(2)	C12'	C13'	C14'	121(2)
C15	C14	C13	117(2)	C15'	C14'	C13'	116.8(19)
C16	C15	C14	120(2)	C14'	C15'	C16'	124(2)

C15	C16	C11	122(2)	C11'	C16'	C15'	115.0(18)
C18	C17	C4	124(2)	C18'	C17'	C4'	126.9(18)
C18	C17	C22	120(2)	C18'	C17'	C22'	118.2(19)
C22	C17	C4	116.8(17)	C22'	C17'	C4'	114.9(18)
C17	C18	C19	119(2)	C17'	C18'	C19'	123(2)
C20	C19	C18	120(3)	C20'	C19'	C18'	118(3)
C19	C20	C21	123(3)	C19'	C20'	C21'	122(3)
C22	C21	C20	121(3)	C20'	C21'	C22'	120(3)
C21	C22	C17	118(2)	C21'	C22'	C17'	118(2)
O3	C23	C24	107.8(19)	O3'	C23'	C24'	103(2)
O4	C24	C23	109.3(18)	O4'	C24'	C23'	112(2)
O4	C25	C26	103.0(19)	O4'	C25'	C26'	103.6(18)
O5	C26	C25	109.7(18)	O5'	C26'	C25'	110.0(19)
O5	C27	C28	106(2)	O5'	C27'	C28'	110(2)
O6	C28	C27	109.9(18)	O6'	C28'	C27'	111.6(18)
O6	C29	C30	105.5(17)	O6'	C29'	C30'	103(2)
O3	C30	C29	108.9(19)	O3'	C30'	C29'	111(2)
O7	C31	W	176.9(16)	O7'	C31'	W'	177.9(19)
O8	C32	W	173.9(18)	O8'	C32'	W'	175.3(16)
O9	C33	W	178.2(16)	O9'	C33'	W'	174.9(17)
O10	C34	W	176.3(18)	O10'	C34'	W'	176.5(16)
O11	C35	W	176.0(17)	O11'	C35'	W'	178(2)
O2	Li19	O3	128.2(16)	O2'	Li1	O3'	104.3(15)
O2	Li19	O4	114.2(13)	O2'	Li1	O4'	122.0(16)
O2	Li19	O5	102.8(14)	O2'	Li1	O5'	132.9(16)
O2	Li19	O6	114.5(13)	O2'	Li1	O6'	107.6(14)
O3	Li19	O4	79.6(11)	O3'	Li1	O4'	78.1(11)
O3	Li19	O5	129.0(14)	O3'	Li1	O5'	122.4(15)
O4	Li19	O5	77.9(10)	O3'	Li1	O6'	78.4(11)
O6	Li19	O3	80.5(11)	O5'	Li1	O4'	76.8(11)
O6	Li19	O4	129.7(14)	O5'	Li1	O6'	78.7(12)
O6	Li19	O5	79.9(12)	O6'	Li1	O4'	128.8(15)

Table 4: Torsion angles for **57.3a**.

A	B	C	D	Angle/°	A	B	C	D	Angle/°
W	P	O2	Li19	-45(3)	W'	P'	O2'	Li1	44(5)
W	P	C1	C2	-73.1(12)	W'	P'	C1'	C2'	123.9(17)
P	O2	Li19	O3	32(4)	P'	O2'	Li1	O3'	-146(4)
P	O2	Li19	O4	128(2)	P'	O2'	Li1	O4'	-61(5)
P	O2	Li19	O5	-150(2)	P'	O2'	Li1	O5'	41(6)
P	O2	Li19	O6	-65(4)	P'	O2'	Li1	O6'	132(4)
P	C1	C2	O1	-64.9(17)	P'	C1'	C2'	O1'	-63(3)
P	C1	C2	C3	174.2(12)	P'	C1'	C2'	C3'	-178.1(19)
P	C4	C5	C6	33(2)	P'	C4'	C5'	C6'	33(2)
P	C4	C5	C10	-153.9(15)	P'	C4'	C5'	C10'	-146.6(14)
P	C4	C11	C12	-112.7(17)	P'	C4'	C11'	C12'	-133.8(17)
P	C4	C11	C16	65.3(18)	P'	C4'	C11'	C16'	53.3(18)
P	C4	C17	C18	-128.1(19)	P'	C4'	C17'	C18'	-113(2)
P	C4	C17	C22	55.8(19)	P'	C4'	C17'	C22'	65(2)
O1	C2	C3	F1	54(2)	O1'	C2'	C3'	F1'	73(3)
O1	C2	C3	F2	-70(2)	O1'	C2'	C3'	F2'	-176(2)

O1	C2	C3	F3	173.5(16)	O1'	C2'	C3'	F3'	-60(3)
O2	P	C1	C2	45.6(13)	O2'	P'	C1'	C2'	3(2)
O3	C23	C24	O4	55(3)	O3'	C23'	C24'	O4'	54(3)
O4	C25	C26	O5	57(2)	O4'	C25'	C26'	O5'	58(3)
O5	C27	C28	O6	54(2)	O5'	C27'	C28'	O6'	49(3)
O6	C29	C30	O3	56(2)	O6'	C29'	C30'	O3'	55(3)
C1	P	O2	Li19	-163(3)	C1'	P'	O2'	Li1	164(5)
C1	C2	C3	F1	176.7(14)	C1'	C2'	C3'	F1'	-165(2)
C1	C2	C3	F2	52(2)	C1'	C2'	C3'	F2'	-53(3)
C1	C2	C3	F3	-64(2)	C1'	C2'	C3'	F3'	62(3)
C4	P	O2	Li19	91(3)	C4'	P'	O2'	Li1	-89(5)
C4	P	C1	C2	156.0(12)	C4'	P'	C1'	C2'	-107.6(19)
C4	C5	C6	C7	176(2)	C4'	C5'	C6'	C7'	177.6(17)
C4	C5	C10	C9	-176.5(19)	C4'	C5'	C10'	C9'	-175.3(16)
C4	C11	C12	C13	177.6(19)	C4'	C11'	C12'	C13'	-172.9(18)
C4	C11	C16	C15	-177.8(18)	C4'	C11'	C16'	C15'	178.0(16)
C4	C17	C18	C19	-180(2)	C4'	C17'	C18'	C19'	179(2)
C4	C17	C22	C21	176(2)	C4'	C17'	C22'	C21'	-178(2)
C5	C4	C11	C12	8(2)	C5'	C4'	C11'	C12'	-15(2)
C5	C4	C11	C16	-173.5(16)	C5'	C4'	C11'	C16'	172.3(15)
C5	C4	C17	C18	110(2)	C5'	C4'	C17'	C18'	127(2)
C5	C4	C17	C22	-67(2)	C5'	C4'	C17'	C22'	-55(2)
C5	C6	C7	C8	-3(3)	C5'	C6'	C7'	C8'	-1(3)
C6	C5	C10	C9	-3(3)	C6'	C5'	C10'	C9'	5(3)
C6	C7	C8	C9	2(3)	C6'	C7'	C8'	C9'	2(3)
C7	C8	C9	C10	-2(3)	C7'	C8'	C9'	C10'	0(3)
C8	C9	C10	C5	2(3)	C8'	C9'	C10'	C5'	-4(3)
C10	C5	C6	C7	3(3)	C10'	C5'	C6'	C7'	-2(3)
C11	C4	C5	C6	-84(2)	C11'	C4'	C5'	C6'	-86(2)
C11	C4	C5	C10	90(2)	C11'	C4'	C5'	C10'	94.1(18)
C11	C4	C17	C18	-14(3)	C11'	C4'	C17'	C18'	9(3)
C11	C4	C17	C22	169.6(16)	C11'	C4'	C17'	C22'	-173.5(18)
C11	C12	C13	C14	1(3)	C11'	C12'	C13'	C14'	-4(3)
C12	C11	C16	C15	0(3)	C12'	C11'	C16'	C15'	5(3)
C12	C13	C14	C15	-2(3)	C12'	C13'	C14'	C15'	4(3)
C13	C14	C15	C16	1(3)	C13'	C14'	C15'	C16'	1(3)
C14	C15	C16	C11	-1(3)	C14'	C15'	C16'	C11'	-5(3)
C16	C11	C12	C13	-1(3)	C16'	C11'	C12'	C13'	0(3)
C17	C4	C5	C6	151(2)	C17'	C4'	C5'	C6'	152.1(17)
C17	C4	C5	C10	-36(2)	C17'	C4'	C5'	C10'	-28(2)
C17	C4	C11	C12	132.5(19)	C17'	C4'	C11'	C12'	105(2)
C17	C4	C11	C16	-50(2)	C17'	C4'	C11'	C16'	-68(2)
C17	C18	C19	C20	4(4)	C17'	C18'	C19'	C20'	0(4)
C18	C17	C22	C21	0(3)	C18'	C17'	C22'	C21'	0(4)
C18	C19	C20	C21	0(5)	C18'	C19'	C20'	C21'	-3(4)
C19	C20	C21	C22	-4(5)	C19'	C20'	C21'	C22'	4(5)
C20	C21	C22	C17	4(4)	C20'	C21'	C22'	C17'	-2(4)
C22	C17	C18	C19	-4(3)	C22'	C17'	C18'	C19'	1(3)
C23	O3	C30	C29	86(2)	C23'	O3'	C30'	C29'	93(3)
C24	O4	C25	C26	-168.9(16)	C24'	O4'	C25'	C26'	-166(2)
C25	O4	C24	C23	88(2)	C25'	O4'	C24'	C23'	76(3)
C26	O5	C27	C28	-168.5(18)	C26'	O5'	C27'	C28'	-166(2)
C27	O5	C26	C25	84(2)	C27'	O5'	C26'	C25'	90(3)

C28	O6	C29	C30	-167.8(17)	C28'	O6'	C29'	C30'	-163(2)
C29	O6	C28	C27	85(2)	C29'	O6'	C28'	C27'	86(3)
C30	O3	C23	C24	-167(2)	C30'	O3'	C23'	C24'	-170.7(19)
Li19	O3	C23	C24	-43(2)	Li1	O3'	C23'	C24'	-37(3)
Li19	O3	C30	C29	-38(2)	Li1	O3'	C30'	C29'	-43(3)
Li19	O4	C24	C23	-38(2)	Li1	O4'	C24'	C23'	-45(2)
Li19	O4	C25	C26	-44(2)	Li1	O4'	C25'	C26'	-47(2)
Li19	O5	C26	C25	-43(2)	Li1	O5'	C26'	C25'	-40(3)
Li19	O5	C27	C28	-42(2)	Li1	O5'	C27'	C28'	-36(2)
Li19	O6	C28	C27	-39(2)	Li1	O6'	C28'	C27'	-36(3)
Li19	O6	C29	C30	-45(2)	Li1	O6'	C29'	C30'	-41(3)

12.43 Lithium(1,4,7,10-tetraoxacyclododecane) pentacarbonyl{[3,3,3-trifluoro-2-(trifluoromethyl)-2-hydroxypropyl](triphenylmethyl)phosphanoxido- κ P}tungsten(0) [57.3b]

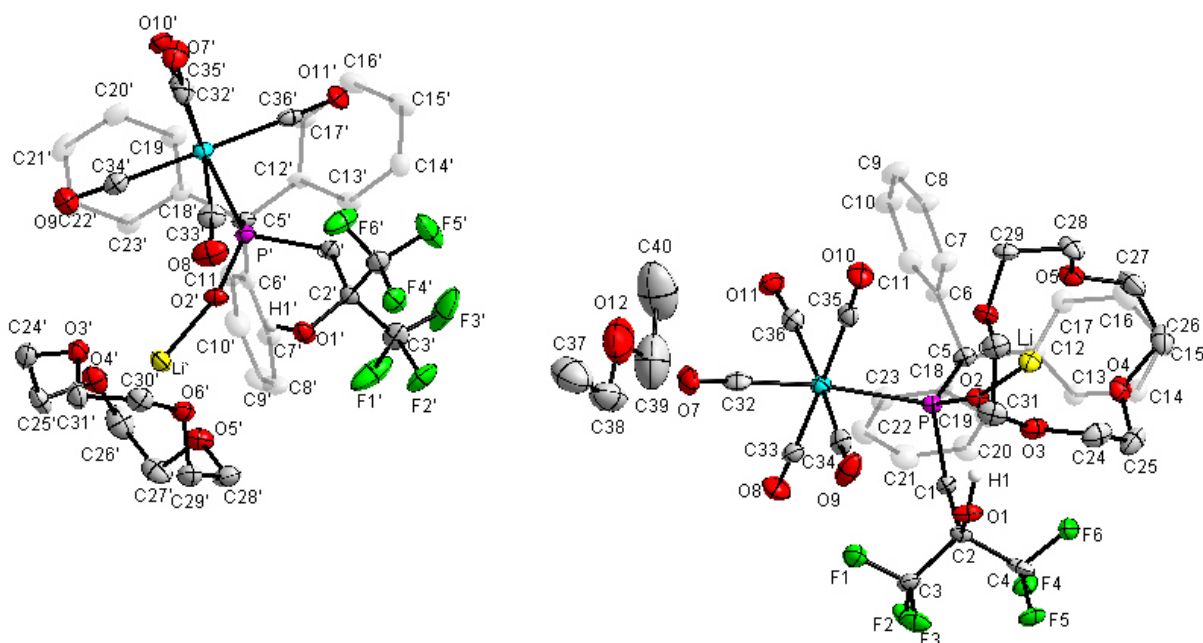


Table 1: Crystal data and structure refinement for **57.3b**.

Identification code	GSTR410, AKY-488-2 // GXray4012f
Device Type	Bruker X8-KappaApexII
Empirical formula	C ₇₆ H ₇₈ F ₁₂ Li ₂ O ₂₃ P ₂ W ₂
Moiety formula	2(C ₃₆ H ₃₄ F ₆ Li O ₁₁ P W), C ₄ H ₁₀ O
Formula weight	2030.90
Temperature/K	100
Crystal system	triclinic
Space group	P $\bar{1}$
a/Å	11.7408(5)
b/Å	18.5934(8)
c/Å	20.0735(8)
α /°	86.722(3)
β /°	74.872(2)
γ /°	73.209(3)
Volume/Å ³	4049.1(3)

Z	2
$\rho_{\text{calc}}/\text{cm}^3$	1.666
μ/mm^{-1}	2.979
F(000)	2020.0
Crystal size/ mm^3	0.1 × 0.08 × 0.04
Absorption correction	empirical
Tmin; Tmax	0.6293; 0.7459
Radiation	MoK α ($\lambda = 0.71073$)
2 θ range for data collection/ $^\circ$	4.936 to 56 $^\circ$
Completeness to theta	0.997
Index ranges	-15 ≤ h ≤ 15, -24 ≤ k ≤ 24, -26 ≤ l ≤ 26
Reflections collected	97310
Independent reflections	19472 [$R_{\text{int}} = 0.0787$, $R_{\text{sigma}} = 0.0923$]
Data/restraints/parameters	19472/27/1058
Goodness-of-fit on F^2	1.010
Final R indexes [$ I \geq 2\sigma(I)$]	$R_1 = 0.0516$, $wR_2 = 0.1223$
Final R indexes [all data]	$R_1 = 0.1086$, $wR_2 = 0.1496$
Largest diff. peak/hole / $e \text{ \AA}^{-3}$	4.51/-2.56

Table 2: Bond lengths for **57.3b**.

Atom	Atom	Length/Å	Atom	Atom	Length/Å
W	P	2.5759(16)	C14	C13	1.390(9)
W	C36	2.051(7)	C6	C11	1.390(8)
W	C33	2.042(7)	C6	C5	1.529(8)
W	C34	2.030(7)	C11	C10	1.387(9)
W	C32	1.982(7)	F5'	C4'	1.340(8)
W	C35	2.042(7)	C23	C22	1.373(9)
W'	P'	2.5633(15)	C11'	C10'	1.378(9)
W'	C35'	2.041(6)	C12	C5	1.538(9)
W'	C32'	1.992(7)	C12	C17	1.396(8)
W'	C33'	2.034(7)	C12	C13	1.392(9)
W'	C36'	2.034(7)	C17	C16	1.388(9)
W'	C34'	2.046(7)	C16'	C17'	1.375(9)
P'	O2'	1.542(4)	C16'	C15'	1.377(9)
P'	C1'	1.903(6)	C23'	C22'	1.382(9)
P'	C5'	1.948(6)	C20'	C19'	1.388(9)
P	C1	1.892(5)	C20'	C21'	1.390(10)
P	O2	1.542(4)	C7'	C8'	1.392(9)
P	C5	1.952(6)	C15	C16	1.364(10)
O10'	C35'	1.142(7)	C10	C9	1.373(10)
F5	C4	1.353(7)	C9'	C8'	1.362(10)
F2	C3	1.345(7)	C9'	C10'	1.384(10)
F4	C4	1.325(7)	C17'	C12'	1.415(8)
F2'	C3'	1.394(7)	C22	C21	1.375(9)
O11	C36	1.140(8)	C14'	C15'	1.393(9)
F1	C3	1.327(7)	C14'	C13'	1.393(8)
O1	C2	1.392(7)	C8	C9	1.385(10)
C1	C2	1.555(8)	C22'	C21'	1.380(9)
C18	C23	1.374(9)	O5	C28	1.436(7)
C18	C5	1.534(8)	O5	C27	1.443(8)
C18	C19	1.414(8)	O5	Li	2.087(11)
F3	C3	1.334(7)	O4	C26	1.432(8)

O1'	C2'	1.388(7)	O4	C25	1.436(8)
O2'	Li'	1.847(11)	O4	Li	2.076(12)
O8	C33	1.134(7)	O6	C29	1.436(7)
F6	C4	1.359(7)	O6	C30	1.433(7)
O2	Li	1.848(11)	O6	Li	2.164(11)
O10	C35	1.146(7)	O3	C31	1.452(7)
C1'	C2'	1.545(8)	O3	C24	1.432(8)
F4'	C4'	1.331(7)	O3	Li	2.078(11)
C2	C4	1.535(9)	C29	C28	1.507(9)
C2	C3	1.550(8)	C31	C30	1.496(8)
O7'	C32'	1.157(7)	C26	C27	1.498(10)
F6'	C4'	1.322(8)	C24	C25	1.511(9)
C2'	C3'	1.481(9)	C12'	C13'	1.385(8)
C2'	C4'	1.541(9)	O12	C38	1.478(11)
C5'	C6'	1.552(8)	O12	C39	1.422(8)
C5'	C18'	1.537(9)	C38	C37	1.541(13)
C5'	C12'	1.538(8)	Li'	O3'	2.125(12)
O9'	C34'	1.154(8)	Li'	O5'	2.115(11)
O11'	C36'	1.140(8)	Li'	O6'	2.082(11)
C6'	C11'	1.392(9)	Li'	O4'	2.130(12)
C6'	C7'	1.379(8)	C39	C40	1.710(17)
C33'	O8'	1.151(7)	O3'	C24'	1.437(8)
C18'	C23'	1.392(9)	O3'	C31'	1.442(8)
C18'	C19'	1.400(8)	O5'	C27'	1.420(8)
C20	C21	1.381(10)	O5'	C28'	1.425(8)
C20	C19	1.385(9)	O6'	C30'	1.428(8)
C3'	F1'	1.350(8)	O6'	C29'	1.441(7)
C3'	F3'	1.342(8)	O4'	C25'	1.429(8)
O9	C34	1.142(8)	O4'	C26'	1.423(8)
O7	C32	1.161(8)	C24'	C25'	1.499(9)
C7	C6	1.390(8)	C30'	C31'	1.481(9)
C7	C8	1.380(8)	C29'	C28'	1.497(9)
C14	C15	1.371(9)	C26'	C27'	1.512(10)

Table 3: Bond angles for **57.3b**.

Atom	Atom	Atom	Angle/°	Atom	Atom	Atom	Angle/°
C36	W	P	101.78(18)	C17	C12	C5	119.8(6)
C33	W	P	88.98(19)	C13	C12	C5	124.0(5)
C33	W	C36	89.9(2)	C13	C12	C17	115.9(6)
C34	W	P	86.04(18)	C18	C5	P	106.7(4)
C34	W	C36	170.3(2)	C18	C5	C12	111.0(5)
C34	W	C33	96.0(2)	C6	C5	P	105.8(4)
C34	W	C35	86.3(3)	C6	C5	C18	112.2(5)
C32	W	P	171.59(19)	C6	C5	C12	107.8(5)
C32	W	C36	86.5(3)	C12	C5	P	113.3(4)
C32	W	C33	89.7(3)	C16	C17	C12	121.8(6)
C32	W	C34	85.8(3)	C17'	C16'	C15'	120.7(6)
C32	W	C35	90.2(2)	C22'	C23'	C18'	121.6(6)
C35	W	P	91.45(18)	C19'	C20'	C21'	120.7(6)
C35	W	C36	87.8(2)	C6'	C7'	C8'	121.0(6)
C35	W	C33	177.7(2)	O9'	C34'	W'	178.3(6)

C35'	W'	P'	102.96(16)	C16	C15	C14	119.4(7)
C35'	W'	C34'	86.6(2)	C9	C10	C11	120.1(6)
C32'	W'	P'	168.8(2)	C8'	C9'	C10'	119.4(6)
C32'	W'	C35'	86.3(2)	C9'	C8'	C7'	120.7(7)
C32'	W'	C33'	88.0(3)	O10	C35	W	176.8(6)
C32'	W'	C36'	86.3(3)	C16'	C17'	C12'	121.5(6)
C32'	W'	C34'	95.0(3)	C23	C22	C21	121.2(7)
C33'	W'	P'	83.80(18)	C14	C13	C12	122.3(6)
C33'	W'	C35'	168.9(3)	C15'	C14'	C13'	120.6(6)
C33'	W'	C36'	97.5(3)	C22	C21	C20	117.9(6)
C33'	W'	C34'	84.4(3)	C20	C19	C18	120.1(6)
C36'	W'	P'	87.15(17)	C15	C16	C17	120.6(6)
C36'	W'	C35'	91.6(2)	C7	C8	C9	119.8(6)
C36'	W'	C34'	177.7(2)	C16'	C15'	C14'	118.9(6)
C34'	W'	P'	91.80(17)	C21'	C22'	C23'	120.6(7)
O2'	P'	W'	111.64(16)	C10	C9	C8	119.8(6)
O2'	P'	C1'	103.0(2)	C20'	C19'	C18'	120.7(6)
O2'	P'	C5'	108.6(2)	C22'	C21'	C20'	118.9(7)
C1'	P'	W'	114.14(19)	C11'	C10'	C9'	119.7(7)
C1'	P'	C5'	98.9(3)	F4'	C4'	C2'	113.2(5)
C5'	P'	W'	118.77(18)	F4'	C4'	F5'	106.8(5)
C1	P	W	113.44(19)	F6'	C4'	F4'	106.7(5)
C1	P	C5	100.3(2)	F6'	C4'	C2'	111.1(5)
O2	P	W	111.52(16)	F6'	C4'	F5'	106.2(5)
O2	P	C1	103.3(2)	F5'	C4'	C2'	112.5(5)
O2	P	C5	107.6(2)	C28	O5	C27	114.2(5)
C5	P	W	119.06(19)	C28	O5	Li	109.0(4)
O10'	C35'	W'	173.3(5)	C27	O5	Li	107.9(5)
C2	C1	P	116.7(4)	C26	O4	C25	114.6(5)
O11	C36	W	173.3(6)	C26	O4	Li	112.1(5)
C23	C18	C5	121.8(5)	C25	O4	Li	110.0(5)
C23	C18	C19	117.0(6)	C29	O6	Li	109.3(4)
C19	C18	C5	121.2(6)	C30	O6	C29	114.0(5)
P'	O2'	Li'	160.6(4)	C30	O6	Li	110.5(5)
P	O2	Li	160.4(4)	C31	O3	Li	109.9(4)
C2'	C1'	P'	117.4(4)	C24	O3	C31	114.7(5)
O1	C2	C1	116.8(4)	C24	O3	Li	107.8(5)
O1	C2	C4	107.1(5)	O6	C29	C28	109.6(5)
O1	C2	C3	105.3(5)	O5	C28	C29	105.5(5)
C4	C2	C1	109.1(5)	O3	C31	C30	110.4(5)
C4	C2	C3	108.2(5)	O4	C26	C27	106.8(6)
C3	C2	C1	110.0(5)	O6	C30	C31	106.8(5)
O1'	C2'	C1'	117.1(5)	O3	C24	C25	105.8(5)
O1'	C2'	C3'	106.6(5)	O4	C25	C24	108.9(5)
O1'	C2'	C4'	105.9(5)	O5	C27	C26	110.7(6)
C3'	C2'	C1'	106.2(5)	C17'	C12'	C5'	120.2(5)
C3'	C2'	C4'	108.5(5)	C13'	C12'	C5'	122.6(5)
C4'	C2'	C1'	112.1(5)	C13'	C12'	C17'	117.1(6)
O7'	C32'	W'	175.5(6)	C12'	C13'	C14'	121.1(6)
O8	C33	W	177.1(6)	C39	O12	C38	104.1(9)
C6'	C5'	P'	114.5(4)	O12	C38	C37	104.5(8)
C18'	C5'	P'	106.4(4)	O2'	Li'	O3'	118.7(6)
C18'	C5'	C6'	106.1(5)	O2'	Li'	O5'	110.4(6)

C18'	C5'	C12'	115.0(5)	O2'	Li'	O6'	104.0(5)
C12'	C5'	P'	106.4(4)	O2'	Li'	O4'	126.0(6)
C12'	C5'	C6'	108.7(5)	O3'	Li'	O4'	79.4(4)
F5	C4	F6	104.6(5)	O5'	Li'	O3'	130.1(5)
F5	C4	C2	113.1(5)	O5'	Li'	O4'	79.1(4)
F4	C4	F5	106.9(5)	O6'	Li'	O3'	80.2(4)
F4	C4	F6	106.4(5)	O6'	Li'	O5'	80.1(4)
F4	C4	C2	115.8(6)	O6'	Li'	O4'	129.8(5)
F6	C4	C2	109.2(5)	O2	Li	O5	127.5(6)
C11'	C6'	C5'	117.1(5)	O2	Li	O4	112.9(5)
C7'	C6'	C5'	125.3(6)	O2	Li	O6	115.1(6)
C7'	C6'	C11'	117.4(6)	O2	Li	O3	101.7(5)
O8'	C33'	W'	172.9(6)	O5	Li	O6	78.9(4)
C23'	C18'	C5'	118.2(5)	O4	Li	O5	80.8(4)
C23'	C18'	C19'	117.6(6)	O4	Li	O6	130.7(5)
C19'	C18'	C5'	124.0(6)	O4	Li	O3	80.8(4)
C21	C20	C19	121.6(6)	O3	Li	O5	130.7(6)
F2'	C3'	C2'	114.6(5)	O3	Li	O6	79.5(4)
F1'	C3'	F2'	102.4(5)	O12	C39	C40	94.7(9)
F1'	C3'	C2'	112.1(6)	C24'	O3'	Li'	110.0(5)
F3'	C3'	F2'	103.2(5)	C24'	O3'	C31'	113.8(5)
F3'	C3'	C2'	117.0(6)	C31'	O3'	Li'	109.5(5)
F3'	C3'	F1'	106.0(5)	C27'	O5'	Li'	111.8(5)
O9	C34	W	172.9(6)	C27'	O5'	C28'	114.8(5)
C8	C7	C6	121.5(6)	C28'	O5'	Li'	108.7(5)
C15	C14	C13	120.0(7)	C30'	O6'	Li'	109.6(5)
O7	C32	W	178.4(5)	C30'	O6'	C29'	114.6(5)
O11'	C36'	W'	178.6(5)	C29'	O6'	Li'	109.6(5)
F2	C3	C2	111.3(5)	C25'	O4'	Li'	107.9(5)
F1	C3	F2	107.1(5)	C26'	O4'	Li'	109.4(5)
F1	C3	F3	107.2(5)	C26'	O4'	C25'	114.0(5)
F1	C3	C2	111.4(5)	O3'	C24'	C25'	109.5(5)
F3	C3	F2	107.0(5)	O6'	C30'	C31'	110.7(5)
F3	C3	C2	112.6(5)	O6'	C29'	C28'	105.6(5)
C7	C6	C5	118.3(5)	O4'	C25'	C24'	106.8(5)
C11	C6	C7	117.6(5)	O3'	C31'	C30'	107.4(5)
C11	C6	C5	123.8(5)	O4'	C26'	C27'	110.5(6)
C10	C11	C6	121.2(6)	O5'	C27'	C26'	107.0(5)
C22	C23	C18	122.2(6)	O5'	C28'	C29'	110.5(6)
C10'	C11'	C6'	121.8(6)				

Table 4: Torsion angles for **57.3b**.

A	B	C	D	Angle/°	A	B	C	D	Angle/°
W	P	C1	C2	-84.3(4)	C23	C22	C21	C20	1.1(10)
W	P	O2	Li	-86.0(13)	C11'	C6'	C7'	C8'	0.7(9)
W'	P'	O2'	Li'	81.9(13)	C12	C17	C16	C15	1.5(10)
P'	O2'	Li'	O3'	-72.1(15)	C5	P	C1	C2	147.7(4)
P'	O2'	Li'	O5'	117.0(12)	C5	P	O2	Li	46.4(13)
P'	O2'	Li'	O6'	-158.4(10)	C5	C18	C23	C22	-175.2(6)
P'	O2'	Li'	O4'	25.9(18)	C5	C18	C19	C20	176.3(6)
P'	C1'	C2'	O1'	16.0(7)	C5	C6	C11	C10	-176.3(6)

P'	C1'	C2'	C3'	134.9(5)	C5	C12	C17	C16	-173.3(6)
P'	C1'	C2'	C4'	-106.7(5)	C5	C12	C13	C14	172.2(5)
P'	C5'	C6'	C11'	164.6(5)	C17	C12	C5	P	-155.3(4)
P'	C5'	C6'	C7'	-20.1(8)	C17	C12	C5	C18	84.7(6)
P'	C5'	C18'	C23'	-58.2(6)	C17	C12	C5	C6	-38.7(7)
P'	C5'	C18'	C19'	126.6(5)	C17	C12	C13	C14	-0.3(8)
P'	C5'	C12'	C17'	-64.9(6)	C16'	C17'	C12'	C5'	178.1(6)
P'	C5'	C12'	C13'	111.3(6)	C16'	C17'	C12'	C13'	1.7(9)
P	C1	C2	O1	-5.4(7)	C23'	C18'	C19'	C20'	1.4(9)
P	C1	C2	C4	-127.0(4)	C23'	C22'	C21'	C20'	0.0(10)
P	C1	C2	C3	114.5(5)	C7'	C6'	C11'	C10'	-0.4(10)
P	O2	Li	O5	-17.9(18)	C15	C14	C13	C12	0.1(9)
P	O2	Li	O4	-114.0(12)	C8'	C9'	C10'	C11'	2.7(11)
P	O2	Li	O6	77.4(14)	C17'	C16'	C15'	C14'	-1.1(10)
P	O2	Li	O3	161.1(10)	C17'	C12'	C13'	C14'	-1.4(9)
O1	C2	C4	F5	62.4(6)	C13	C14	C15	C16	1.0(10)
O1	C2	C4	F4	-173.7(4)	C13	C12	C5	P	32.4(7)
O1	C2	C4	F6	-53.7(6)	C13	C12	C5	C18	-87.6(7)
O1	C2	C3	F2	-167.4(5)	C13	C12	C5	C6	149.1(5)
O1	C2	C3	F1	73.2(6)	C13	C12	C17	C16	-0.5(9)
O1	C2	C3	F3	-47.2(6)	C21	C20	C19	C18	0.1(10)
C1	P	O2	Li	151.9(13)	C19	C18	C23	C22	2.2(9)
C1	C2	C4	F5	-170.3(5)	C19	C18	C5	P	-117.9(5)
C1	C2	C4	F4	-46.5(6)	C19	C18	C5	C6	126.7(6)
C1	C2	C4	F6	73.6(6)	C19	C18	C5	C12	6.0(7)
C1	C2	C3	F2	66.0(6)	C19	C20	C21	C22	-0.1(10)
C1	C2	C3	F1	-53.5(6)	C8	C7	C6	C11	3.3(10)
C1	C2	C3	F3	-173.9(5)	C8	C7	C6	C5	177.5(6)
C18	C23	C22	C21	-2.3(10)	C15'	C16'	C17'	C12'	-0.4(10)
O1'	C2'	C3'	F2'	-59.0(7)	C15'	C14'	C13'	C12'	0.0(10)
O1'	C2'	C3'	F1'	57.2(7)	C19'	C18'	C23'	C22'	-1.3(9)
O1'	C2'	C3'	F3'	179.9(5)	C19'	C20'	C21'	C22'	0.0(10)
O1'	C2'	C4'	F4'	49.9(7)	C21'	C20'	C19'	C18'	-0.8(10)
O1'	C2'	C4'	F6'	-70.1(6)	C10'	C9'	C8'	C7'	-2.4(11)
O1'	C2'	C4'	F5'	171.0(5)	C4'	C2'	C3'	F2'	54.7(7)
O2	P	C1	C2	36.6(5)	C4'	C2'	C3'	F1'	170.9(5)
C1'	P'	O2'	Li'	-155.2(13)	C4'	C2'	C3'	F3'	-66.4(7)
C1'	C2'	C3'	F2'	175.4(5)	O4	C26	C27	O5	51.9(7)
C1'	C2'	C3'	F1'	-68.4(6)	O6	C29	C28	O5	56.4(7)
C1'	C2'	C3'	F3'	54.3(7)	O3	C31	C30	O6	53.4(7)
C1'	C2'	C4'	F4'	178.8(5)	O3	C24	C25	O4	56.0(7)
C1'	C2'	C4'	F6'	58.7(7)	C29	O6	C30	C31	-161.6(5)
C1'	C2'	C4'	F5'	-60.1(7)	C28	O5	C27	C26	79.5(6)
C5'	P'	O2'	Li'	-51.0(13)	C31	O3	C24	C25	-171.8(5)
C5'	C6'	C11'	C10'	175.2(6)	C26	O4	C25	C24	92.9(7)
C5'	C6'	C7'	C8'	-174.5(6)	C30	O6	C29	C28	91.2(6)
C5'	C18'	C23'	C22'	-176.8(6)	C24	O3	C31	C30	79.4(7)
C5'	C18'	C19'	C20'	176.6(6)	C25	O4	C26	C27	-162.2(5)
C5'	C12'	C13'	C14'	-177.8(6)	C27	O5	C28	C29	-172.5(5)
C4	C2	C3	F2	-53.2(7)	C12'	C5'	C6'	C11'	-76.6(7)
C4	C2	C3	F1	-172.6(5)	C12'	C5'	C6'	C7'	98.7(7)
C4	C2	C3	F3	67.0(6)	C12'	C5'	C18'	C23'	-175.7(5)
C6'	C5'	C18'	C23'	64.1(7)	C12'	C5'	C18'	C19'	9.1(8)

C6'	C5'	C18'	C19'	-111.0(6)	C13'	C14'	C15'	C16'	1.3(10)
C6'	C5'	C12'	C17'	171.3(5)	C38	O12	C39	C40	179.2(8)
C6'	C5'	C12'	C13'	-12.5(8)	Li'	O3'	C24'	C25'	34.9(6)
C6'	C11'	C10'	C9'	-1.3(11)	Li'	O3'	C31'	C30'	39.4(7)
C6'	C7'	C8'	C9'	0.7(10)	Li'	O5'	C27'	C26'	39.5(7)
C18'	C5'	C6'	C11'	47.6(7)	Li'	O5'	C28'	C29'	37.5(7)
C18'	C5'	C6'	C7'	-137.1(6)	Li'	O6'	C30'	C31'	40.3(7)
C18'	C5'	C12'	C17'	52.6(8)	Li'	O6'	C29'	C28'	45.9(7)
C18'	C5'	C12'	C13'	-131.2(6)	Li'	O4'	C25'	C24'	48.8(7)
C18'	C23'	C22'	C21'	0.6(10)	Li'	O4'	C26'	C27'	39.3(7)
C3'	C2'	C4'	F4'	-64.2(7)	Li	O5	C28	C29	-51.8(6)
C3'	C2'	C4'	F6'	175.7(5)	Li	O5	C27	C26	-41.9(7)
C3'	C2'	C4'	F5'	56.9(7)	Li	O4	C26	C27	-35.9(7)
C7	C6	C11	C10	-2.4(10)	Li	O4	C25	C24	-34.5(7)
C7	C6	C5	P	54.2(6)	Li	O6	C29	C28	-33.0(7)
C7	C6	C5	C18	170.1(5)	Li	O6	C30	C31	-38.1(7)
C7	C6	C5	C12	-67.3(7)	Li	O3	C31	C30	-42.1(7)
C7	C8	C9	C10	1.0(11)	Li	O3	C24	C25	-49.1(6)
C14	C15	C16	C17	-1.8(10)	C39	O12	C38	C37	-179.9(9)
C3	C2	C4	F5	-50.7(7)	O3'	C24'	C25'	O4'	-56.5(7)
C3	C2	C4	F4	73.2(6)	O6'	C30'	C31'	O3'	-53.6(7)
C3	C2	C4	F6	-166.8(5)	O6'	C29'	C28'	O5'	-55.9(7)
C6	C7	C8	C9	-2.6(11)	O4'	C26'	C27'	O5'	-52.7(7)
C6	C11	C10	C9	0.9(10)	C24'	O3'	C31'	C30'	163.0(5)
C11	C6	C5	P	-132.0(5)	C30'	O6'	C29'	C28'	169.5(5)
C11	C6	C5	C18	-16.0(8)	C29'	O6'	C30'	C31'	-83.3(7)
C11	C6	C5	C12	106.5(7)	C25'	O4'	C26'	C27'	-81.6(7)
C11	C10	C9	C8	-0.1(11)	C31'	O3'	C24'	C25'	-88.4(6)
C23	C18	C5	P	59.3(6)	C26'	O4'	C25'	C24'	170.6(5)
C23	C18	C5	C6	-56.0(7)	C27'	O5'	C28'	C29'	-88.6(7)
C23	C18	C5	C12	-176.8(5)	C28'	O5'	C27'	C26'	164.0(5)
C23	C18	C19	C20	-1.1(9)					

12.44 Pentacarbonyl[6,6-bis(trifluoromethyl)-2,2-dimethyl-4-triphenylmethyl-1,3,4,2-dioxaphosasilinan- κ P]tungsten(0) [60.3a]

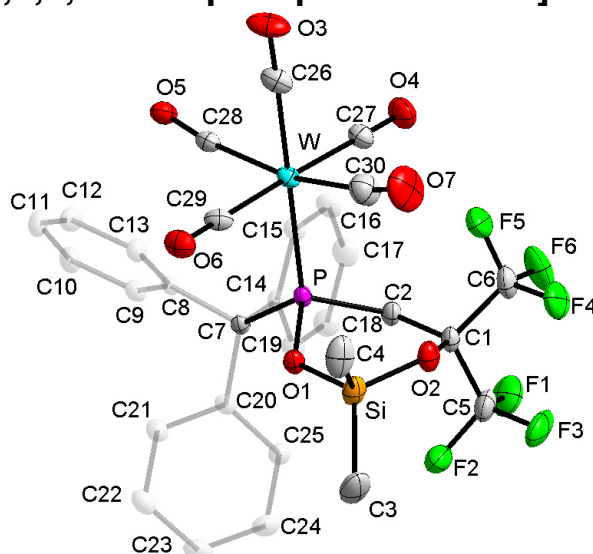


Table 1: Crystal data and structure refinement for **60.3a**.

Identification code	GSTR504, PB-35 // GXray4737
Crystal Habitus	clear colourless plate
Device Type	Nonius KappaCCD
Empirical formula	C ₃₀ H ₂₃ F ₆ O ₇ PSiW
Moiety formula	C30 H23 F6 O7 P Si W
Formula weight	852.39
Temperature/K	123
Crystal system	triclinic
Space group	P $\bar{1}$
a/Å	8.9870(3)
b/Å	13.1455(3)
c/Å	13.3173(2)
α /°	87.0836(15)
β /°	82.7857(15)
γ /°	89.8868(13)
Volume/Å ³	1558.80(7)
Z	2
$\rho_{\text{calc}}/\text{cm}^3$	1.816
μ/mm^{-1}	3.877
F(000)	832.0
Crystal size/mm ³	0.22 × 0.14 × 0.1
Absorption correction	multi-scan
Tmin; Tmax	0.5781; 1.071
Radiation	MoK α (λ = 0.71073)
2 θ range for data collection/°	5.182 to 55.998°
Completeness to theta	0.998
Index ranges	-11 ≤ h ≤ 11, -17 ≤ k ≤ 17, -17 ≤ l ≤ 17
Reflections collected	20755
Independent reflections	7500 [R _{int} = 0.0446, R _{sigma} = 0.0371]
Data/restraints/parameters	7500/0/417
Goodness-of-fit on F ²	1.025
Final R indexes [$I \geq 2\sigma(I)$]	R ₁ = 0.0249, wR ₂ = 0.0582
Final R indexes [all data]	R ₁ = 0.0277, wR ₂ = 0.0598
Largest diff. peak/hole / e Å ⁻³	1.14/-1.74

Table 2: Bond lengths for **60.3a**.

Atom	Atom	Length/Å	Atom	Atom	Length/Å
W	P	2.5376(7)	C1	C2	1.563(4)
W	C26	2.007(3)	C1	C5	1.545(4)
W	C27	2.040(3)	C1	C6	1.544(4)
W	C28	2.044(3)	C7	C8	1.538(3)
W	C29	2.044(3)	C7	C14	1.535(3)
W	C30	2.030(3)	C7	C20	1.549(3)
P	O1	1.623(2)	C8	C9	1.397(4)
P	C2	1.869(3)	C8	C13	1.392(4)
P	C7	1.957(3)	C9	C10	1.391(4)
Si	O1	1.662(2)	C10	C11	1.391(4)
Si	O2	1.665(2)	C11	C12	1.381(4)
Si	C3	1.844(4)	C12	C13	1.397(4)
Si	C4	1.834(4)	C14	C15	1.403(4)
F1	C5	1.327(4)	C14	C19	1.397(4)

F2	C5	1.347(4)	C15	C16	1.387(4)
F3	C5	1.326(4)	C16	C17	1.392(4)
F4	C6	1.326(4)	C17	C18	1.390(4)
F5	C6	1.318(4)	C18	C19	1.392(4)
F6	C6	1.339(4)	C20	C21	1.398(4)
O2	C1	1.410(3)	C20	C25	1.391(4)
O3	C26	1.139(4)	C21	C22	1.393(4)
O4	C27	1.144(4)	C22	C23	1.387(4)
O5	C28	1.144(3)	C23	C24	1.374(4)
O6	C29	1.143(4)	C24	C25	1.391(4)
O7	C30	1.145(4)			

Table 3: Bond angles for **60.3a**.

Atom	Atom	Atom	Angle/°	Atom	Atom	Atom	Angle/°
C26	W	P	177.30(8)	F4	C6	F6	107.2(3)
C26	W	C27	88.72(12)	F4	C6	C1	112.7(3)
C26	W	C28	80.73(11)	F5	C6	F4	107.6(3)
C26	W	C29	92.21(11)	F5	C6	F6	107.3(3)
C26	W	C30	85.42(13)	F5	C6	C1	111.2(2)
C27	W	P	89.56(8)	F6	C6	C1	110.6(3)
C27	W	C28	91.29(11)	C8	C7	P	107.55(16)
C27	W	C29	177.99(11)	C8	C7	C20	108.3(2)
C28	W	P	97.23(7)	C14	C7	P	105.68(16)
C29	W	P	89.58(7)	C14	C7	C8	111.0(2)
C29	W	C28	90.62(11)	C14	C7	C20	112.1(2)
C30	W	P	96.66(10)	C20	C7	P	112.17(16)
C30	W	C27	89.89(14)	C9	C8	C7	119.2(2)
C30	W	C28	166.07(12)	C13	C8	C7	122.3(2)
C30	W	C29	88.41(13)	C13	C8	C9	118.3(2)
O1	P	W	113.69(7)	C10	C9	C8	121.2(3)
O1	P	C2	101.81(11)	C9	C10	C11	119.8(3)
O1	P	C7	101.67(10)	C12	C11	C10	119.6(3)
C2	P	W	114.98(9)	C11	C12	C13	120.6(3)
C2	P	C7	101.91(11)	C8	C13	C12	120.5(3)
C7	P	W	120.28(7)	C15	C14	C7	119.7(2)
O1	Si	O2	103.66(11)	C19	C14	C7	122.8(2)
O1	Si	C3	109.34(15)	C19	C14	C15	117.5(2)
O1	Si	C4	112.58(13)	C16	C15	C14	121.4(2)
O2	Si	C3	112.45(15)	C15	C16	C17	120.5(3)
O2	Si	C4	107.57(15)	C18	C17	C16	118.7(3)
C4	Si	C3	111.05(19)	C17	C18	C19	120.8(3)
P	O1	Si	126.51(12)	C18	C19	C14	121.0(2)
C1	O2	Si	131.04(18)	C21	C20	C7	120.9(2)
O2	C1	C2	115.7(2)	C25	C20	C7	122.0(2)
O2	C1	C5	107.1(2)	C25	C20	C21	117.0(2)
O2	C1	C6	105.0(2)	C22	C21	C20	121.5(2)
C5	C1	C2	109.3(2)	C23	C22	C21	120.2(3)
C6	C1	C2	110.8(2)	C24	C23	C22	119.1(3)
C6	C1	C5	108.8(2)	C23	C24	C25	120.6(3)
C1	C2	P	117.63(19)	C24	C25	C20	121.7(3)
F1	C5	F2	106.6(3)	O3	C26	W	177.0(3)

F1	C5	C1	112.2(3)	O4	C27	W	178.6(3)
F2	C5	C1	110.1(2)	O5	C28	W	170.2(2)
F3	C5	F1	108.0(3)	O6	C29	W	179.3(3)
F3	C5	F2	106.4(3)	O7	C30	W	171.6(3)
F3	C5	C1	113.2(3)				

Table 4: Torsion angles for **60.3a**.

A	B	C	D	Angle/°	A	B	C	D	Angle/°
W	P	O1	Si	-77.94(15)	C6	C1	C5	F3	54.7(4)
W	P	C2	C1	82.4(2)	C7	P	O1	Si	151.31(14)
P	C7	C8	C9	-53.4(3)	C7	P	C2	C1	-145.8(2)
P	C7	C8	C13	132.6(2)	C7	C8	C9	C10	-176.4(2)
P	C7	C14	C15	-57.2(3)	C7	C8	C13	C12	176.0(2)
P	C7	C14	C19	123.5(2)	C7	C14	C15	C16	179.3(2)
P	C7	C20	C21	133.9(2)	C7	C14	C19	C18	-179.8(2)
P	C7	C20	C25	-50.2(3)	C7	C20	C21	C22	177.7(2)
Si	O2	C1	C2	33.4(3)	C7	C20	C25	C24	-177.8(3)
Si	O2	C1	C5	-88.7(3)	C8	C7	C14	C15	59.1(3)
Si	O2	C1	C6	155.8(2)	C8	C7	C14	C19	-120.1(3)
O1	P	C2	C1	-41.0(2)	C8	C7	C20	C21	15.3(3)
O1	Si	O2	C1	-30.4(3)	C8	C7	C20	C25	-168.7(2)
O2	Si	O1	P	-18.16(18)	C8	C9	C10	C11	0.6(4)
O2	C1	C2	P	8.2(3)	C9	C8	C13	C12	1.9(4)
O2	C1	C5	F1	179.3(2)	C9	C10	C11	C12	1.2(4)
O2	C1	C5	F2	60.7(3)	C10	C11	C12	C13	-1.4(4)
O2	C1	C5	F3	-58.2(3)	C11	C12	C13	C8	-0.2(4)
O2	C1	C6	F4	51.4(3)	C13	C8	C9	C10	-2.1(4)
O2	C1	C6	F5	-69.6(3)	C14	C7	C8	C9	-168.6(2)
O2	C1	C6	F6	171.4(2)	C14	C7	C8	C13	17.4(3)
C2	P	O1	Si	46.32(17)	C14	C7	C20	C21	-107.4(3)
C2	C1	C5	F1	53.3(3)	C14	C7	C20	C25	68.5(3)
C2	C1	C5	F2	-65.2(3)	C14	C15	C16	C17	1.0(4)
C2	C1	C5	F3	175.8(3)	C15	C14	C19	C18	1.0(4)
C2	C1	C6	F4	176.9(2)	C15	C16	C17	C18	-0.1(4)
C2	C1	C6	F5	56.0(3)	C16	C17	C18	C19	-0.4(4)
C2	C1	C6	F6	-63.1(3)	C17	C18	C19	C14	-0.1(4)
C3	Si	O1	P	-138.28(18)	C19	C14	C15	C16	-1.4(4)
C3	Si	O2	C1	87.6(3)	C20	C7	C8	C9	68.0(3)
C4	Si	O1	P	97.8(2)	C20	C7	C8	C13	-106.0(3)
C4	Si	O2	C1	-149.9(2)	C20	C7	C14	C15	-179.7(2)
C5	C1	C2	P	129.1(2)	C20	C7	C14	C19	1.1(3)
C5	C1	C6	F4	-62.9(3)	C20	C21	C22	C23	-0.1(4)
C5	C1	C6	F5	176.1(3)	C21	C20	C25	C24	-1.7(4)
C5	C1	C6	F6	57.0(3)	C21	C22	C23	C24	-1.2(5)
C6	C1	C2	P	-111.1(2)	C22	C23	C24	C25	1.0(5)
C6	C1	C5	F1	-67.8(3)	C23	C24	C25	C20	0.5(5)
C6	C1	C5	F2	173.7(3)	C25	C20	C21	C22	1.6(4)

12.45 Pentacarbonyl[6,6-bis(trifluoromethyl)-2,2-dimethyl-4-triphenylmethyl-1,3,4,2-dioxaphosphagerminan- κ P]tungsten(0) [60.3b]

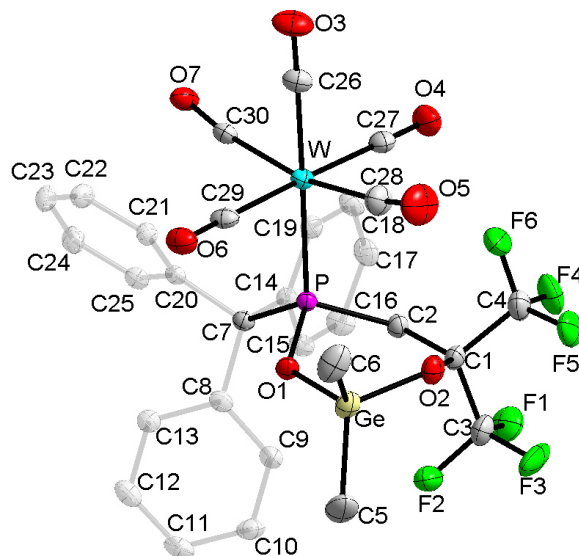


Table 1: Crystal data and structure refinement for **60.3b**.

Identification code	GSTR507, PB-47 // GXray4813
Crystal Habitus	clear colourless plate
Device Type	Nonius KappaCCD
Empirical formula	C ₃₀ H ₂₃ F ₆ GeO ₇ PW
Moiety formula	C ₃₀ H ₂₃ F ₆ Ge O ₇ P W
Formula weight	896.89
Temperature/K	123(2)
Crystal system	triclinic
Space group	P $\bar{1}$
a/Å	9.0079(2)
b/Å	13.1369(3)
c/Å	13.2698(2)
α /°	92.8970(10)
β /°	97.6730(10)
γ /°	90.1710(10)
Volume/Å ³	1554.17(5)
Z	2
$\rho_{\text{calc}}/\text{cm}^3$	1.917
μ/mm^{-1}	4.798
F(000)	868.0
Crystal size/mm ³	0.3 × 0.22 × 0.04
Absorption correction	multi-scan
Tmin; Tmax	0.3452; 0.7795
Radiation	MoK α (λ = 0.71073)
2 θ range for data collection/°	5.852 to 55.996°
Completeness to theta	0.999
Index ranges	-11 ≤ h ≤ 11, -17 ≤ k ≤ 17, -17 ≤ l ≤ 17
Reflections collected	36507
Independent reflections	7498 [R _{int} = 0.0689, R _{sigma} = 0.0401]
Data/restraints/parameters	7498/0/417
Goodness-of-fit on F ²	1.059
Final R indexes [I ≥ 2 σ (I)]	R ₁ = 0.0263, wR ₂ = 0.0611

Final R indexes [all data]
Largest diff. peak/hole / e Å⁻³

R₁ = 0.0304, wR₂ = 0.0628
1.24/-1.62

Table 2: Bond lengths for **60.3b**.

Atom	Atom	Length/Å	Atom	Atom	Length/Å
W	P	2.5439(7)	C1	C2	1.561(4)
W	C26	1.998(3)	C1	C3	1.549(4)
W	C27	2.040(3)	C1	C4	1.541(4)
W	C28	2.032(3)	C7	C8	1.547(4)
W	C29	2.037(3)	C7	C14	1.542(4)
W	C30	2.048(3)	C7	C20	1.532(4)
Ge	O1	1.803(2)	C8	C9	1.394(4)
Ge	O2	1.804(2)	C8	C13	1.401(4)
Ge	C5	1.926(4)	C9	C10	1.387(4)
Ge	C6	1.911(4)	C10	C11	1.377(5)
P	O1	1.613(2)	C11	C12	1.379(5)
P	C2	1.875(3)	C12	C13	1.397(4)
P	C7	1.959(3)	C14	C15	1.398(4)
F1	C3	1.333(4)	C14	C19	1.398(4)
F2	C3	1.346(4)	C15	C16	1.392(4)
F3	C3	1.326(4)	C16	C17	1.379(4)
F4	C4	1.342(4)	C17	C18	1.386(4)
F5	C4	1.323(4)	C18	C19	1.386(4)
F6	C4	1.327(4)	C20	C21	1.393(4)
O2	C1	1.401(4)	C20	C25	1.403(4)
O3	C26	1.146(4)	C21	C22	1.396(4)
O4	C27	1.140(4)	C22	C23	1.384(5)
O5	C28	1.141(4)	C23	C24	1.387(5)
O6	C29	1.148(4)	C24	C25	1.386(4)
O7	C30	1.139(4)			

Table 3: Bond angles for **60.3b**.

Atom	Atom	Atom	Angle/°	Atom	Atom	Atom	Angle/°
C26	W	P	177.27(9)	F4	C4	C1	111.1(3)
C26	W	C27	88.69(12)	F5	C4	F4	107.2(3)
C26	W	C28	85.72(14)	F5	C4	F6	107.6(3)
C26	W	C29	92.35(12)	F5	C4	C1	113.1(3)
C26	W	C30	80.43(12)	F6	C4	F4	107.0(3)
C27	W	P	90.12(8)	F6	C4	C1	110.6(3)
C27	W	C30	91.00(12)	C8	C7	P	111.48(19)
C28	W	P	96.72(10)	C14	C7	P	105.75(18)
C28	W	C27	88.84(14)	C14	C7	C8	112.2(2)
C28	W	C29	90.00(14)	C20	C7	P	107.91(18)
C28	W	C30	166.15(13)	C20	C7	C8	108.4(2)
C29	W	P	88.89(8)	C20	C7	C14	111.0(2)
C29	W	C27	178.38(12)	C9	C8	C7	122.3(3)
C29	W	C30	90.40(12)	C9	C8	C13	116.7(3)
C30	W	P	97.13(8)	C13	C8	C7	120.9(3)
O1	Ge	O2	100.62(9)	C10	C9	C8	121.9(3)

O1	Ge	C5	107.66(15)	C11	C10	C9	120.5(3)
O1	Ge	C6	112.88(13)	C10	C11	C12	119.2(3)
O2	Ge	C5	113.23(14)	C11	C12	C13	120.5(3)
O2	Ge	C6	105.46(14)	C12	C13	C8	121.3(3)
C6	Ge	C5	116.01(18)	C15	C14	C7	122.7(2)
O1	P	W	113.93(8)	C19	C14	C7	119.7(2)
O1	P	C2	103.45(12)	C19	C14	C15	117.6(3)
O1	P	C7	101.05(11)	C16	C15	C14	120.8(3)
C2	P	W	114.23(9)	C17	C16	C15	120.5(3)
C2	P	C7	102.04(12)	C16	C17	C18	119.6(3)
C7	P	W	119.96(9)	C17	C18	C19	119.9(3)
P	O1	Ge	124.16(12)	C18	C19	C14	121.6(3)
C1	O2	Ge	128.42(18)	C21	C20	C7	122.5(2)
O2	C1	C2	116.8(2)	C21	C20	C25	118.2(3)
O2	C1	C3	107.9(2)	C25	C20	C7	119.1(2)
O2	C1	C4	104.6(2)	C20	C21	C22	120.7(3)
C3	C1	C2	108.6(3)	C23	C22	C21	120.2(3)
C4	C1	C2	110.0(2)	C22	C23	C24	119.7(3)
C4	C1	C3	108.7(3)	C25	C24	C23	120.1(3)
C1	C2	P	118.4(2)	C24	C25	C20	121.0(3)
F1	C3	F2	106.4(3)	O3	C26	W	177.0(3)
F1	C3	C1	112.9(3)	O4	C27	W	179.1(3)
F2	C3	C1	110.0(3)	O5	C28	W	171.9(3)
F3	C3	F1	107.9(3)	O6	C29	W	178.9(3)
F3	C3	F2	106.4(3)	O7	C30	W	170.0(2)
F3	C3	C1	112.9(3)				

Table 4: Torsion angles for **60.3b**.

A	B	C	D	Angle/°	A	B	C	D	Angle/°
W	P	O1	Ge	75.92(14)	C6	Ge	O2	C1	151.5(2)
W	P	C2	C1	-81.2(2)	C7	P	O1	Ge	-154.05(14)
Ge	O2	C1	C2	-40.0(3)	C7	P	C2	C1	147.8(2)
Ge	O2	C1	C3	82.6(3)	C7	C8	C9	C10	178.4(3)
Ge	O2	C1	C4	-161.8(2)	C7	C8	C13	C12	-178.4(3)
P	C7	C8	C9	51.1(3)	C7	C14	C15	C16	179.8(3)
P	C7	C8	C13	-132.0(2)	C7	C14	C19	C18	-178.8(3)
P	C7	C14	C15	-122.6(3)	C7	C20	C21	C22	-176.5(2)
P	C7	C14	C19	57.8(3)	C7	C20	C25	C24	177.2(2)
P	C7	C20	C21	-132.8(2)	C8	C7	C14	C15	-0.9(4)
P	C7	C20	C25	52.4(3)	C8	C7	C14	C19	179.5(3)
O1	Ge	O2	C1	34.0(3)	C8	C7	C20	C21	106.3(3)
O1	P	C2	C1	43.2(2)	C8	C7	C20	C25	-68.5(3)
O2	Ge	O1	P	18.41(16)	C8	C9	C10	C11	-0.2(5)
O2	C1	C2	P	-3.8(3)	C9	C8	C13	C12	-1.3(4)
O2	C1	C3	F1	178.3(2)	C9	C10	C11	C12	-1.2(5)
O2	C1	C3	F2	-63.1(3)	C10	C11	C12	C13	1.3(5)
O2	C1	C3	F3	55.6(3)	C11	C12	C13	C8	0.0(5)
O2	C1	C4	F4	-174.2(3)	C13	C8	C9	C10	1.4(4)
O2	C1	C4	F5	-53.6(4)	C14	C7	C8	C9	-67.3(3)
O2	C1	C4	F6	67.2(3)	C14	C7	C8	C13	109.6(3)
C2	P	O1	Ge	-48.67(17)	C14	C7	C20	C21	-17.3(3)

C2	C1	C3	F1	-54.2(3)	C14	C7	C20	C25	167.8(2)
C2	C1	C3	F2	64.4(3)	C14	C15	C16	C17	-0.5(5)
C2	C1	C3	F3	-176.9(3)	C15	C14	C19	C18	1.5(4)
C2	C1	C4	F4	59.7(3)	C15	C16	C17	C18	0.7(5)
C2	C1	C4	F5	-179.7(3)	C16	C17	C18	C19	0.2(5)
C2	C1	C4	F6	-59.0(3)	C17	C18	C19	C14	-1.3(5)
C3	C1	C2	P	-126.0(2)	C19	C14	C15	C16	-0.6(5)
C3	C1	C4	F4	-59.1(4)	C20	C7	C8	C9	169.7(3)
C3	C1	C4	F5	61.5(4)	C20	C7	C8	C13	-13.3(3)
C3	C1	C4	F6	-177.8(3)	C20	C7	C14	C15	120.6(3)
C4	C1	C2	P	115.1(2)	C20	C7	C14	C19	-59.0(3)
C4	C1	C3	F1	65.4(4)	C20	C21	C22	C23	0.1(4)
C4	C1	C3	F2	-176.0(3)	C21	C20	C25	C24	2.1(4)
C4	C1	C3	F3	-57.3(4)	C21	C22	C23	C24	0.9(4)
C5	Ge	O1	P	137.15(18)	C22	C23	C24	C25	-0.4(4)
C5	Ge	O2	C1	-80.6(3)	C23	C24	C25	C20	-1.1(4)
C6	Ge	O1	P	-93.51(19)	C25	C20	C21	C22	-1.6(4)

12.46 Tetrabutylammonium pentacarbonyl[(2-hydroxyethyl)methylphosphanoxido- κ P]tungsten(0) [61]

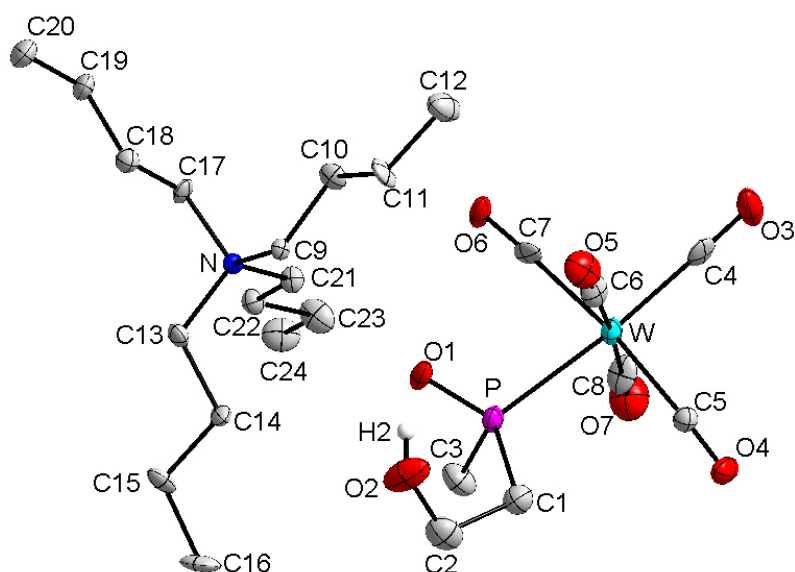


Table 1: Crystal data and structure refinement for **63**.

Identification code	GSTR545, AKY-610 // GXrayneu
Crystal Habitus	clear colourless block
Device Type	Bruker X8-KappaApexII
Empirical formula	C ₂₄ H ₄₄ NO ₇ PW
Moiety formula	C ₈ H ₈ O ₇ P W, C ₁₆ H ₃₆ N
Formula weight	673.42
Temperature/K	100
Crystal system	monoclinic
Space group	P2 ₁ /n
a/Å	11.2279(8)
b/Å	13.5773(8)
c/Å	20.1880(14)

$\alpha/^\circ$	90
$\beta/^\circ$	105.457(3)
$\gamma/^\circ$	90
Volume/Å ³	2966.2(3)
Z	4
$\rho_{\text{calc}}/\text{cm}^3$	1.508
μ/mm^{-1}	3.986
F(000)	1360.0
Crystal size/mm ³	0.2 × 0.14 × 0.1
Absorption correction	empirical
Tmin; Tmax	0.227682; 0.746070
Radiation	MoK α (λ = 0.71073)
2 θ range for data collection/ $^\circ$	3.788 to 50.052 $^\circ$
Completeness to theta	0.982
Index ranges	-14 \leq h \leq 14, -17 \leq k \leq 17, -26 \leq l \leq 26
Reflections collected	5140
Independent reflections	5140 [R _{int} = 0.0929, R _{sigma} = 0.0564]
Data/restraints/parameters	5140/30/313
Goodness-of-fit on F ²	1.070
Final R indexes [$I \geq 2\sigma(I)$]	R ₁ = 0.0730, wR ₂ = 0.1635
Final R indexes [all data]	R ₁ = 0.0944, wR ₂ = 0.1720
Largest diff. peak/hole / e Å ⁻³	10.14/-1.50

Table 2: Bond lengths for 61.

Atom	Atom	Length/Å	Atom	Atom	Length/Å
W	P	2.529(3)	N	C9	1.533(12)
W	C4	2.025(13)	N	C13	1.523(13)
W	C5	2.030(12)	N	C17	1.521(13)
W	C6	2.058(14)	N	C21	1.528(13)
W	C7	2.047(12)	C9	C10	1.501(15)
W	C8	2.027(12)	C10	C11	1.551(15)
P	O1	1.526(8)	C11	C12	1.489(16)
P	C1	1.858(13)	C13	C14	1.520(15)
P	C3	1.843(13)	C14	C15	1.518(15)
O2	C2	1.399(16)	C15	C16	1.538(17)
O3	C4	1.121(15)	C17	C18	1.507(15)
O4	C5	1.144(14)	C18	C19	1.547(16)
O5	C6	1.136(15)	C19	C20	1.516(17)
O6	C7	1.137(14)	C21	C22	1.520(15)
O7	C8	1.135(15)	C22	C23	1.502(16)
C1	C2	1.532(18)	C23	C24	1.528(17)

Table 3: Bond angles for 61.

Atom	Atom	Atom	Angle/ $^\circ$	Atom	Atom	Atom	Angle/ $^\circ$
C4	W	P	173.3(4)	O3	C4	W	178.5(12)
C4	W	C5	93.8(4)	O4	C5	W	177.5(10)
C4	W	C6	90.9(5)	O5	C6	W	178.4(11)
C4	W	C7	92.3(4)	O6	C7	W	176.8(11)
C4	W	C8	92.5(5)	O7	C8	W	178.6(12)
C5	W	P	89.4(3)	C13	N	C9	108.2(7)
C5	W	C6	91.6(5)	C13	N	C21	111.3(8)
C5	W	C7	173.5(5)	C17	N	C9	111.1(8)

C6	W	P	83.1(4)	C17	N	C13	109.6(8)
C7	W	P	84.8(3)	C17	N	C21	108.8(8)
C7	W	C6	90.8(5)	C21	N	C9	107.9(7)
C8	W	P	93.4(4)	C10	C9	N	115.4(8)
C8	W	C5	89.0(5)	C9	C10	C11	110.2(9)
C8	W	C6	176.5(5)	C12	C11	C10	111.1(10)
C8	W	C7	88.3(5)	C14	C13	N	115.1(8)
O1	P	W	114.9(3)	C15	C14	C13	110.0(9)
O1	P	C1	106.2(5)	C14	C15	C16	110.8(10)
O1	P	C3	108.4(6)	C18	C17	N	116.2(9)
C1	P	W	112.4(4)	C17	C18	C19	107.0(9)
C3	P	W	113.1(4)	C20	C19	C18	111.2(10)
C3	P	C1	100.6(6)	C22	C21	N	114.0(9)
C2	C1	P	112.5(9)	C23	C22	C21	109.4(9)
O2	C2	C1	111.0(11)	C22	C23	C24	111.4(11)
